GAC®-MAC 2021 :: London, Canada
Joint Annual Meeting

Exploring Geosciences Through Time and Space
Explorer les géosciences à travers le temps et l'espace

Abstracts :: Résumés
Volume 44

GEOLOGICAL ASSOCIATION OF CANADA
ASSOCIATION GÉOLOGIQUE DU CANADA

MINERALOGICAL ASSOCIATION OF CANADA
ASSOCIATION MINÉRALOGIQUE DU CANADA

Western UNIVERSITY · CANADA

Contents

GAC-MAC 2021
Meeting Themes :: Thèmes de reunion

Earth & Planetary Systems

Life, Climate & Environment

Tectonic Processes & Geohazards

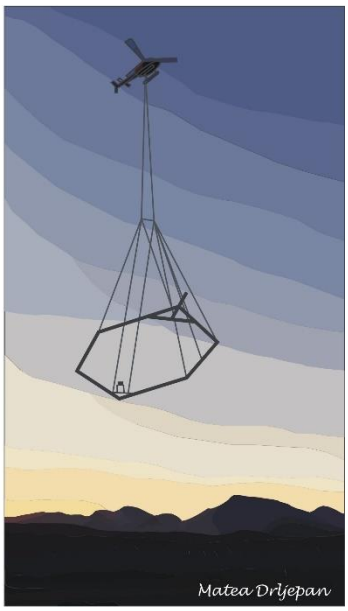

Resource Geoscience

Publisher * Éditeur: The Geological Association of Canada
c/o Dept. of Earth Sciences, Memorial University of Newfoundland St. John's, NL A1B 3X5 CANADA
Email : gac@mun.ca Website www.gac.ca

Suggested citation for abstracts within this abstract volume

Authors of abstract, Title of abstract: Geological Association of Canada-Mineralogical Association of Canada, Abstract Volume, v. 44, p. X.

Citation suggérée pour les résumés au sein de ce volume de résumés

Auteurs du résumé, Titre du résumé : Association géologique du Canada-Association minéralogique of Canada, Volume de résumés, v. 42, p. X.

GAC-MAC 2021 Sponsors :: Commanditaires

Platinum Sponsor

Gold Sponsors

GAC-MAC 2021 Sponsors :: Commanditaires

Silver Sponsors

IAMGOLD

WESDOME

Petrophysical sample measurement & analysis
magnetics :: density :: porosity
IP/resistivity :: P-wave
Western
WPPL
wppl@uwo.ca
Dr. Phil J.A. McCausland
Director
Tel: (519) 661-2111 x88008
Western Paleomagnetic & Petrophysical Laboratory

PROBE METALS INC

SOCIETY for GEOLOGY APPLIED to MINERAL DEPOSITS

Geo- and Thermochronology Lab
University of Calgary

Browse the Index of Rocks, Minerals, Fossils and Meteorites at Turnstone!
http://www.turnstone.ca/romindex.htm

The following organizations are also gratefully acknowledged for their Bronze Sponsor contributions:

APGO Education Foundation, Canadian Geoscience Education Network (CGEN), CANQUA, Canadian Science and Technology Historical Association (CSTHA), City of London, GAC Canadian Sedimentology Research Group (CSRG), GAC Canadian Tectonics Group (CTG), GAC Environmental Earth Sciences Division (EESD), GAC Geophysics Division, GAC Mineral Deposits Division (MDD), GAC Paleontology Division, GAC Planetary Science Division, GAC Precambrian Division, GAC Volcanology & Igneous Petrology Division (VIP), Geothermal Canada, International Subcommission on Quaternary Stratigraphy, Ingenium, Canada's Museums of Science and Innovation, IGCP 648 Supercontinent Cycles & Global Geodynamics, Mineralogical Association of Canada, Mining Matters, NWT & Nunavut Chamber of Mines, Oxford Instruments, Planet, Western University, Bruker, Olympus, Proto Manufacturing, Society of Economic Geologists

GAC-MAC 2021 :: Plenary Speakers

Monday Plenary, November 1, 2021 – 11:20 to 12:20

Attrition, recruitment and retention in the Geosciences: rethinking past approaches

Hendratta Ali
Fort Hays State University

Despite decades of efforts to increase interest, attract scholars and diversify the geosciences, progress continues to be slow in the recruitment and retention of young scholars into the discipline while attrition increases. Incidentally, given the central role that the geosciences play in understanding the challenges associated with the global climate crisis, technology, and energy security, geoscience academic programs should be increasing the number of students and geoscientists at institutions and professional communities. Instead, compared to other STEM disciplines fewer students know about or aspire to select the geosciences as their primary discipline; this is true for both majority and students from historically excluded communities. As a result, several geoscience programs at universities are shutting down. Though significant opportunities for recruitment from an untapped pool exist in minoritized communities, strategies to increase enrollment and retention in the geosciences must be holistic. With the high competition for students and trainees from other STEM disciplines, new efforts need to be thoughtful and target individuals from all communities, and at all levels of academic and professional attainment. By employing intentional actionable steps to address equity and embracing a braided model for academic and professional pathways, the geoscience community can turn these trends around. This talk aims to discuss some of the approaches that should be considered in addressing the challenges in recruitment and retention of current and future geoscientists.

Biography – Hendratta Ali

Dr Hendratta Ali is Associate Professor of Geosciences at Fort Hays State University. She has a master's in Soil Science and a post-graduate degree - Diplôme d'études approfondies - in Environmental Science, from the University of Yaoundé 1, in Cameroon. Her Ph.D. in Geology is from Oklahoma State University. Dr Ali conducts research in exploration geoscience, in aqueous and stable isotope geochemistry and hydro-geophysics; and on justice, equity, diversity and inclusion as well as geoscience education. She has received awards in recognition of her scholarship and leadership initiatives, including: Outstanding Graduate Advisor and Outstanding Undergraduate Research Mentor from Fort Hays State University; Outstanding Educator Award from the Society of Exploration Geophysicists; Inspirational Geoscience Educator award from the American Association of Petroleum Geologists; President's Award from the Association for Women Geoscientists; Rising Star -Distinguished Alumni Award from the College of Arts and Sciences, Oklahoma State University; Presidential Citation for Geology and Society from the American Geophysical Union; and recently, the 2021 Randolph W. "Bill" and Cecile T. Bromery Award from the Geological Society of America. She served as a faculty leader of the Early Career Geoscience Faculty workshop series run by the National Association of Geoscience Teachers that helps new faculty establish their programs, in professional geoscience organizations, led a petition for societies to engage in anti-racist actions in the geosciences that has garnered more than 26,000 signatures. She is also cofounder and organizer of *#BlackInGeoscienceWeek*. We've also learned that she used to coach soccer, is an avid book reader, coffee drinker, and dancer.

Wednesday Plenary, November 3, 2021 – 11:20 to 12:20

Seismic hazard assessment in Canada – applying science for societal relevance

John Adams
Canadian Hazards Information Service, Natural Resources Canada

Damaging earthquakes have occurred and will inevitably occur again in Canada. Correctly estimating the hazard posed by these events is important to ensure that earthquake-resistant engineering is appropriately provided across Canada. Modelling earthquake hazard through probabilistic seismic hazard assessments (PSHA) also provides a quantitative determination of likely losses, and so informs public policy and financial ventures that need to plan for future disasters.

The Government of Canada has been involved in earthquake monitoring for 125 years. The results of this long-term commitment to basic data collection – including running seismographs and strong motion instruments, collecting felt information and assembling information about historical earthquakes, as well as basic research about the nature and origins of Canada's earthquakes – have been the basis for five previous national seismic hazard maps.

Through a review of seismic hazard assessment in Canada, this presentation will explain the how Canada's latest PSHA model (CanadaSHM6) has been created to estimate where future large earthquakes are expected to occur, their rates, and the shaking they will cause. Multiple disciplines in geology and geophysics - from geochronology to geodetics - assist seismological observations in these estimates. The information is quantified (together with its uncertainties), and combined in a probabilistic framework to estimate the likelihood of future shaking events.

CanadaSHM6 incorporates recent research on the rate of great Cascadia earthquakes, includes a new potentially active fault near Victoria BC, and incorporates the latest updates of the ground motion predictions of large earthquakes. Previous models provided hazard values on a reference ground condition (firm ground) together with foundation-adjustment factors for soil or rock. Canada SHM6 will instead provide hazard for a continuous range of site conditions, expressed in Vs30, which expands the applicability and usefulness of the results. To improve access to the full suite of values, a new and improved online seismic hazard web-tool is being developed. CanadaSHM6 is currently proposed to be the basis for seismic design values in the 2020 edition of the National Building Code of Canada, and is being used for Canada's National Risk Assessment.

Biography – John Adams

John graduated with a PhD in Geology from New Zealand in 1978. His 41-year career at Natural Resources Canada has involved all aspects of the earthquake program, from running field aftershock surveys to managing the program, and from creating national seismic hazard maps to participating in post-earthquake engineering reconnaissance visits. Since 1985 John has worked to produce seismic hazard maps for the National Building Code of Canada, including those for the 2020 Code.

He became a member of the Canadian Standing Committee on Earthquake Design in 1986 and is a past member of various Canadian Standards Association committees dealing with earthquake provisions to critical structures such as nuclear power plants.

He is involved with the regulatory assessment of seismic hazard reports for important facilities, such as nuclear power plants, LNG plants, dams, and pipelines, and recently completed an updated seismic hazard screening analysis for Canadian embassies abroad.

John's research interests include the seismotectonics of Canadian earthquakes, evidence for paleo-earthquakes, and the crustal stresses driving the neotectonics and geomorphology, and how these can, and can not, be used for improving seismic hazard estimates**.**

An Evolutionary System of Mineralogy: In Search of Mineral "Natural Kinds"

Robert M. Hazen
Earth and Planets Laboratory, Carnegie Institution for Science

Minerals provide the most robust, information-rich artifacts of planetary origins and evolution. Each mineral specimen is a time capsule that preserves a record of successive chemical, physical, and ultimately biological environments. If we are to understand the 4.5-billion-year story of Earth and its neighboring planets and moons, then minerals hold the most eloquent testimony of deep time and epic change.

The universally accepted classification of minerals is provided by the rigorous protocols of the International Mineralogical Society's Commission on New Minerals, Nomenclature and Classification (IMA-CNMNC; [1]). Each mineral species owes its identity to its unique combination of idealized end-member composition and/or chemical range, plus idealized crystal structure. In this regard, the IMA-CNMNC approach employs the minimum information (i.e., data) necessary to unambiguously define each species. To date, more than 5700 species have been approved by the IMA-CNMNC, while thousands more potential species await discovery and description [2]. However, these criteria do not lend themselves to an exploration of planetary evolution, nor are the idealizations that define IMA species equivalent to mineral "natural kinds" that represent "genuine divisions of nature" [3].

We have proposed, and are now detailing in a series of papers [4-8], a complementary "evolutionary system of mineralogy" that strives to define mineral natural kinds based on: (1) their positions in the evolutionary chronology of a planet, and (2) the process by which they formed (what we term "paragenetic mode"). In this system, each mineral natural kind has a distinctive temporal and paragenetic context, as manifest in its unique combination of chemical, structural, physical, and contextual attributes. The evolutionary system is thus data intensive, embracing all of a mineral's attributes in identifying natural kinds, for example through "cluster analysis" [9,10].

Recent studies of all known minerals and their paragenetic modes suggest that more than 10,000 mineral natural kinds exist, many of which relate to IMA-approved species by lumping and/or splitting criteria [11,12]. Analytical and visualization methods applied to mineral data reveal striking temporal and spatial trends across the Mineral Kingdom.

[1] Hawthorne et al. (2021) Min. Mag. 85, 125; [2] Hystad et al. (2019) Math. Geosci. 51, 401; [3] Bird & Tobin (2018) Stanford Encyc. Phil.; [4] Hazen & Morrison (2020) Am. Mineral. 105, 627; [5] Morrison & Hazen (2020) Ibid. 105, 1508; [6] Hazen et al. (2021) Ibid. 106, 325; [7] Morrison & Hazen (2021) Ibid. 106, 730; [8] Hazen & Morrison (2021) Ibid. 106, in press; [9] Hazen (2019) Ibid. 104, 468; [10] Boujibar et al. (2021) Ap. J. Lett. 907, L39; [11] Hazen & Morrison (2022) Am. Mineral. 107, in press; [12] Hazen et al. (2022) Ibid., 107, in press.

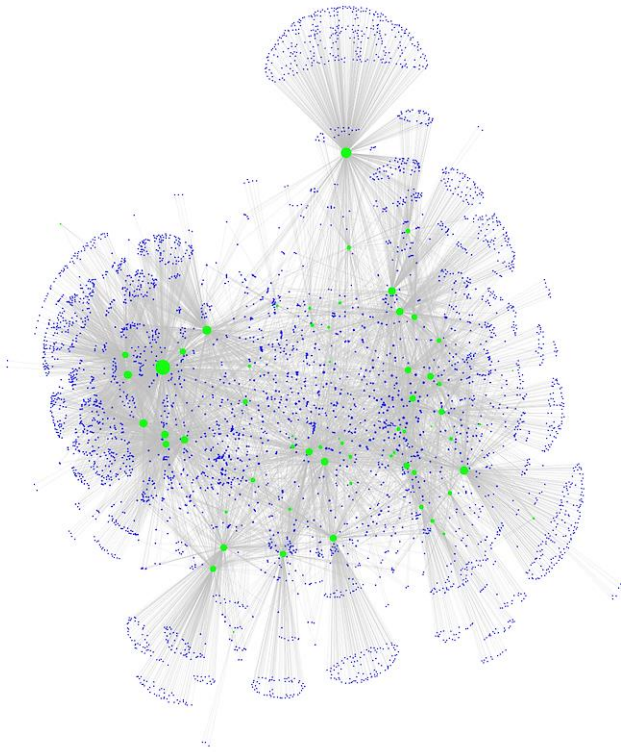

Fig. 1: A bipartite network graph displays 5659 blue nodes, each representing a mineral species, linked to 57 green nodes representing different formation processes of minerals, resulting in a total of 10,556 links. Analysis of network topologies reveal dramatic temporal trends in the physical and chemical properties of minerals.

Biography – Robert M. Hazen

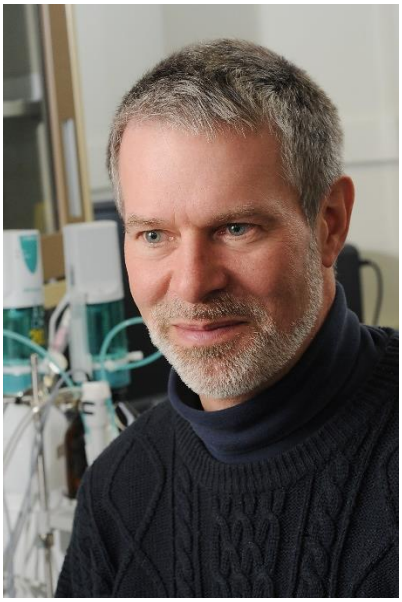

Robert M. Hazen, Senior Scientist at the Carnegie Institution for Science and Robinson Professor of Earth Science, Emeritus, at George Mason University, received degrees in geology from MIT and Harvard. Author of more than 450 articles and 25 books on science, history, and music, his recent book The Story of Earth (Viking-Penguin) was finalist in the Royal Society and Phi Beta Kappa science book competitions. Hazen has been recipient of numerous awards, including the 2021 IMA Medal, the 2016 Roebling Medal of the Mineralogical Society of America, and the 2012 Virginia Outstanding Faculty Award. In 2020 he was elected Foreign Member of the Russian National Academy of Sciences. The biomineral "hazenite" was named in his honor. Since 2008, Hazen and his colleagues have explored "mineral evolution" and "mineral ecology"—new approaches that exploit large and growing mineral data resources to understand the co-evolution of the geosphere and biosphere. In October 2016 Hazen retired from a 40-year career as a professional trumpeter, during which he performed with numerous ensembles including the Metropolitan Opera, Royal Ballet, and National Symphony.

Friday Plenary, November 5, 2021 – 11:20 to 12:20

Learning from our Grandfathers: How Indigenous Knowledge and Western Science systems come together as we select a site for the long term management of Canada's Used Nuclear Fuel

Sarah Hirschorn and Jessica Perritt
Nuclear Waste Management Organization

The Nuclear Waste Management Organization is responsible for implementing Adaptive Phased Management (APM), Canada's plan for the long-term management of its used nuclear fuel. APM has as its endpoint centralized containment and isolation of Canada's used fuel in a deep geological repository in an area with suitable geology and an informed and willing host community in partnership with Indigenous and municipal neighbours. Since 2002, NWMO sought opportunities to learn from Indigenous knowledge (IK) holders and in 2016, the NWMO finalized an Indigenous Knowledge Policy committing us to interweaving IK with western science into all aspects of work, including planning and decisions making processes. Through our practice of informing project decisions through the dual lenses of western science and Indigenous Knowledge, we note reflections that help Geoscientists embrace the sophisticated system of IK drawn on millennia of wisdom and experience. Applying Indigenous knowledge to Geoscience site characterization activities has allowed the for the expansion of thought that both knowledge systems rely on the rock (referred to as 'Grandfathers' within IK) to pass on the memories it has gathered over its lifetime. Together with Indigenous knowledge holders and scientists, NWMO is working to ensure that this combined knowledge contributes to our understanding of the geosphere, and its evolution over time (i.e. geosynthesis) for a particular site. As an organization we have come to learn that applying Indigenous Knowledge to a traditionally western science focused industry has improved the quality of our understanding, and of our project. This includes assessing worldviews and how key components of Indigenous worldview; like the practice of the Seven Grandfather Teachings; have allowed the organization to have a better understanding of what a successful partnership might look like. We have learned important lessons about relationship, land, governance, research methods, knowledge transfer and the role for technology as we implement a project that will impact current and future generations. Our work to date, and plans for the future, demonstrate NWMO's commitment to contribute to what Reconciliation could look like for corporate Canada.

Biography – Jessica Perritt

Jessica Perritt is the Section Manager of Indigenous Knowledge & Reconciliation at the Nuclear Waste Management Organization (NWMO). Jessica is member of the Chippewas of Nawash Unceded First Nation and a proud Anishnaabe-kwe (Ojibway women). She is a mother to two sons, daughter, granddaughter, wife, sister, auntie, niece and cousin. Jessica joined the NWMO in 2008 and had been instrumental in creating the NWMO's Indigenous Knowledge policy, Reconciliation Policy, and liaising with the Council of Elders and Youth. Her formal education is within western science majoring in Physics and Mathematics and has also received Indigenous education from Elders and knowledge keepers throughout her life. Jessica has brought respect for Indigenous perspectives to life at the NWMO and her next big project is helping the NWMO take further steps towards its journey in reconciliation, a true example for the rest of Corporate Canada.

Biography – Sarah Hirschorn

Sarah Hirschorn is the Director of Geoscience at the Nuclear Waste Management Organization (NWMO). In her current role, Sarah is responsible for the NWMO's geoscientific site investigations activities, as the NWMO continues to assess the suitability of potential sites for hosting a deep geological repository.

GAC-MAC 2021 :: Award Lectures

GAC Logan Medal (2020) Lecture, Monday, November 1, 2021 – 15:00 to 16:00

Tectonic history of the Canadian Rocky Mountains

Margot McMechan,
Emeritus, Geological Survey of Canada

The Canadian Rocky Mountain fold and thrust belt (RMFTB) is one of the world's classic foreland fold and thrust belts. It developed along the eastern margin of the Canadian Cordillera in the mid-Jurassic to early Eocene as a result of oblique convergence of the North American craton with terranes to the west. Major changes in stratigraphic make-up, structural style, shortening and crustal structure occur along strike north to south. These reflect changes in the importance of different tectonic events and structural features along strike. This talk reviews the tectonic record for the region of the Canadian RMFTB from when the adjacent and underlying Laurentian basement was assembled (ca 1800 Ma) to the Miocene.

Proterozoic rifting and compression events resulted in the deposition of very thick Paleoproterozoic and early Mesoproterozoic successions above thinned continental crust in the north but not in the south. The record of later Mesoproterozoic intracratonic rifting and basin infilling is only preserved in the far south. Following cryptic compressional event(s) Neoproterozoic rifting at high angle to the structural grain of the Laurentian basement established the initial proto-Pacific margin along the length of the Canadian Cordillera. An Ediacaran thermal and rifting event modified the shape of the margin and drove the subsidence of the still extending lower Paleozoic passive margin. Following a mid-Paleozoic (strike-slip?) event that resulted significant uplift and erosion of lower Paleozoic strata from 55° N south, the RMTFB area formed the east side of a back-arc basin and experienced renewed subsidence and extension. Paleozoic extensional faults are much more common in the northern Rockies and early tectonic events appear to have had a much greater effect on the final expression of the RMTFB in the north than in the south.

Triassic strata mark the start of the long and complex interaction of the RMFTB area with various terranes to its west. These predominantly east-derived sediments filled a foreland basin caused by lithospheric flexure due to crustal loading immediately west of the RMTFB area. Cordilleran compressive deformation of the RMFTB began in the Late Jurassic and occurred in a few major pulses separated by periods of relative quiescence until ca 52 Ma (early Eocene). Deformation pulses resulted in crustal loading, lithospheric flexure and the deposition of foreland basin sediments to the northeast. Deformation generally progressed from west to east and cannibalized older sediments in the western part of the Jurassic – Eocene foreland basin. Compressive deformation was concurrent with 100's of km of dextral strike-slip faulting immediately to the west. The structural style of the RMFT changes from thrust-dominated and thin-skinned in the south to fold-dominated and thick skinned in the north and aggregate shortening drops dramatically from about 200 km to 40 km in the north. Several reasons are plausible.

Extensional faulting with local associated post-orogenic sedimentation occurred in the late Eocene, Oligocene and Miocene in the southern RMTFB. Late Miocene and younger uplift renewed the topographic expression of the Canadian RMTFB and made the mountains something worth seeing.

GEOLOGICAL ASSOCIATION OF CANADA
ASSOCIATION GÉOLOGIQUE DU CANADA

The 2020 Logan Medal is awarded to
La médialle Logan 2020 est décernée à

Dr. MARGOT McMECHAN

Geological Survey of Canada
Commission géologique du Canada

"For an outstanding career of geological mapping and syntheses representing fundamental advances to understanding the tectonic evolution of the Canadian Cordillera and the Western Canada Sedimentary Basin, and their implications for hydrocarbon and mineral exploration."

Mineral Deposits Division
Geological Association of Canada

GAC – Mineral Deposits Division
William Harvey Gross Award and Lecture, Thursday, November 4, 2021 – 10:00 to 11:00

William Harvey Gross Award
The William Harvey Gross Award is bestowed annually by the Mineral Deposits Division (MDD) to a geoscientist under the age of 40 (as of December 31st of the nomination year) who has made a significant contribution to the field of economic geology in a Canadian context. The recipient may be either a Canadian or non-Canadian who has made a contribution in Canada, or one within a Canadian context. The contribution on which the award is based may relate to studies that include all aspects of what is generally referred to as economic geology, and which represents the broad spectrum of fields to which Bill Gross contributed. These include mineral exploration and development, scientific research either applied or fundamental, and field based studies.

Winner of the 2021 William Harvey Gross Award:
Dr. Pilar Lecumberri-Sanchez
The 2021 William Harvey Gross Award is awarded to Dr. Pilar Lecumberri-Sanchez of the University of Alberta. Dr. Lecumberri-Sanchez is recognized for her contributions towards understanding the geochemistry of ore-forming fluids and fluid-rock interactions with implications for a range of deposit types (e.g., W skarn, Cu porphyry, high-sulfidation epithermal, Ag-Pb-Zn, and orogenic Au deposits) and hydrothermal-magmatic systems in general.

Geochemical vectors and grade indicators of mineralization in orogenic gold deposits

Pilar Lecumberri-Sanchez
University of Alberta

Orogenic gold deposits are a major source of gold worldwide (over 30 % of historic global production). However, in many deposits, gold shows a highly heterogeneous distribution. This spatial distribution can lead to issues with assay representativity, over or underestimation of resources and misidentification of targets. In this context, finding proxies for high gold concentration or vectors towards mineralized structures would significantly facilitate exploration.
The Yellowknife Greenstone Belt has produced over 13 million ounces of gold in a belt that expands over 10s of kilometers. However, mineralization in the Yellowknife Greenstone Belt occurs in diverse lithologies, structures, and minerals. As a result, identifying a targeting strategy that is applicable broadly has presented a challenge.
In this study we evaluate the potential of whole rock compositions, mineral chemistry and fluid inclusion characteristics as indicators of grade within a given structure and as indicators of proximity to a mineralized structure and their potential implications in terms of geochemical processes.

GAC-MAC 2021 :: Abstracts

A Gravity Study of the Valentine Gold Project, West-Central Newfoundland

Stephanie Abbott[1], Alison Leitch[1]

[1]Memorial University of Newfoundland (MUN) sma504@mun.ca

The Valentine Gold Project (VGP) is located in the west-central region of the island of Newfoundland and encompasses four significant gold deposits, which are structurally controlled and of orogenic origin. These deposits, which have proven challenging targets for geophysical exploration, occur proximal to a major thrust faulted contact between the Precambrian Valentine Lake Intrusive Complex (VLIC), which houses the majority of gold mineralization, and the Silurian Rogerson Lake Conglomerate. Hosted within the silicic quartz-eye porphyry and trondhjemite phases of the VLIC, the gold concentrations are associated with extensional and shear parallel quartz-tourmaline-pyrite (QTP) veining. The VGP has undergone multiple complex stages of deformation and contains many generations of mafic dykes. While geophysical techniques are commonly used to investigate mineral prospects, their ability to delineate the ore zone at the Valentine Gold Project has met with little success. This is primarily because the gold is scattered throughout veins within the resistive, siliceous host rocks and the relationship between the mineralization and the property's mafic dykes is unclear. Consequently, the primary methods for locating the ore have been drilling and soil sampling. This study employs the gravity method, a fresh geophysical technique that has not previously been used over the property, to investigate the VGP. Although gravity methods are often used in mineral exploration, they are not typically applied to the type of gold deposits present at the Valentine Gold Project, where the density contrast between lithologies is small, the topography is rough and the overburden is thick and irregular. A 2018 proof-of-concept survey over the gold-bearing hydrothermal alteration zone, using a Scintrex CG-5 Autograv system, revealed a small but measurable negative gravity anomaly. Encouraged by this, in August 2019, a 14.2 line-kilometre broad-scale gravity survey, comprising 159 stations, was carried out over the property in an effort to map the subsurface extent of the alteration zone and delineate areas suitable for further exploratory drilling. Additional in-fill gravity stations were acquired on bogs and along lake shorelines during the winter and summer of 2020, yielding a total of 252 gravity stations throughout the property. The resulting property-wide Bouguer gravity map indicates that there is a measurable low gravity anomaly from the alteration zone. This suggests that gravity is a suitable technique for assessing the mineral prospects at the VGP, and it may be applicable over similar deposit types, which are exhibited in belts across the island of Newfoundland.

Melt evolution based on an analysis of solid mineral inclusions in Ti-andradite garnet and related co-magmatic mineral constituents in the Crowsnest Formation, Alberta

Robin Adair[1], David Lentz[1], Chris McFarlane[1]

[1]University of New Brunswick radair@osiskometals.com

Insight into magma crystallization and fractionation can be determined from a detailed investigation of mineral inclusions within phenocrysts coupled with analyses of phenocryst zonation, and crystal growth domains. The complex mineralogy of the Crowsnest Formation, Alberta provides an excellent example of this thesis using inclusion relationships within and between titanian andradite, sanidine, titanite, aegirine-augite and analcime phenocrysts. Titanian andradite is used as the benchmarking phenocryst in so far as this crystal phase exhibits pronounced zonation as well as both the highest concentration of inclusions and the widest variety of inclusions observed. The composition of the Crowsnest Formation is based on whole rock geochemistry and petrology of juvenile and cognate xenoclasts. Bulk compositions are indicative of a potassic to sodic differentiation path as follows: 1) sanidine-melanite trachyte, 2) sanidine-melanite-analcime phonolite, and 3) analcime tephriphonolite. Titanian andradite is ubiquitous in the first two compositions where it is present as a primary, micro-phenocryst phase up to 0.7mm in size. It becomes less abundant to absent in the analcime tephriphonolite where evidence of resorption of garnet can be observed. Garnet compositions suggest that the melt fluctuated between silica-saturated and silica-undersaturated composition based on aluminum - iron - titanium concentrations and overall garnet composition that ranges between grossular (silica-saturated) to morimotoite (silica-undersaturated) within single crystals. Inclusions in Ti-andradite garnet are investigated via EPMA, μXRF, SEM-BSE and petrological microscopy. Identified inclusions in garnet, in order of abundance, are aegirine-augite, sanidine, titanite, apatite, ilmenite and chalcopyrite. Aegirine-augite and garnet share an epitaxial relationship. Apatite inclusions demonstrate a complex crystallization history suggesting a precursor parental melt that evolved to sanidine-melanite trachyte. Co-magmatic crystallization of garnet, sanidine, aegirine-augite and titanite is demonstrated. Analcime is notably absent as an inclusion in garnet with the converse also being true. Evolution of the Crowsnest magma is suggested to have initiated from a parental trachybasalt and evolved to a potassic trachyte phase with the co-crystallization of sanidine, titanian andradite, aegirine-augite and titanite. Continued fractionation led to increasingly sodic compositions and silica under-saturation with the appearance of analcime in the phonolite. This further evolved to a residual sodic melt as demonstrated by crystallization of analcime with co-magmatic aegirine-augite.

Hydrothermal and structural controls on Lead-Zinc mineralization at Pine Point, NWT

Robin Adair[1], Eric Garcelon[1], Jared Hansen[1]

[1]Osisko Metals Incorporated radair@osiskometals.com

The Pine Point Lead-Zinc camp has historically been classified as "MVT-Type". Wide-spread lead and zinc mineralization is localized into some 100 deposits over a 72-kilometre trend. Data from roughly 20,000 historical drill holes (1945-2012) have been recovered and converted to a modern digital database and tied into GIS space using LiDAR and DGPS. Field observations and 1326 new drill holes are combined with new airborne gravity gradiometry and airborne magnetic surveys. Ground-based IP and gravity surveys provide further geophysical precision and petrological microscopy, pXRF and µXRF provide new mineralogical detail. These datasets have been modeled in 3D at a regional and deposit scale. Pine Point deposits are characterized as “Tabular” and “Prismatic” types. Tabular deposits are elongated, with a strata-bound preference to mineralization. Prismatic deposits are characterized by a vertical aspect, often crosscutting multiple stratigraphic units. Both types exhibit sulphide-mineral zonation. Mineralization is hosted in dolomite-altered, lower a Devonian carbonate reef with the Great Slave Shear Zone, a deep-crustal structure, obliquely transecting Pine Point. Early-stage dissolution of primary carbonates and precipitation of secondary dolomite alteration was developed by low-temperature hydrothermal fluids. Alteration shows preference for specific facies within the reef, but new evidence also suggests significant structural controls. Sphalerite, galena, and marcasite mineralization is associated with on-going dissolution and alteration. Alteration is characterized by various textures and stages of hydrothermal dolomitization, some of which are pathfinders to mineralization, and calcification. Hydrocarbons (bitumen and H2S) present during precipitation of sulphide minerals may have provided a source of sulphur and played a key role in the precipitation process. It is now demonstrated that the Tabular deposits form as discrete channel ways with significant structural influence as demonstrated by stratigraphic off-sets and vertical fracturing in drill core. These channel ways feed directly into the Prismatic-style deposits where the combination of lithology and fracturing maintained fluid focus and promoted vertical fluid flow and resultant mineralization with related alteration. On-going, paleo-dissolution and reprecipitation during the mineralizing process is demonstrated by stratified sedimentary rock consisting of non-soluble material and, locally, sulphide detritus within paleo-cavities. The system was active during and after this internal sedimentation as demonstrated by the development of colloform sphalerite growing within these internal sedimentary rocks. Recent karsting, is characterized by till-filled collapse structures unrelated to mineralization. We classify these deposits as “Carbonate Hosted Pb-Zn” demonstrating structural and stratigraphic control of low temperature hydrothermal alteration and resultant mineralization in the presence of hydrocarbons.

Development of a comprehensive regional geodatabase for seismic microzonation of Metropolitan Vancouver, Canada

Sujan Adhikari[1], Sheri Molnar[1], Jinfei Wang[1]

[1]University of Western Ontario Sadhika6@uwo.ca

Metropolitan Vancouver is situated in southwestern British Columbia over an active subduction zone. More than 400 earthquakes occur each year related to three major sources of seismicity in the shallow crust, deeper inslab, and subduction interface. Earthquake shaking is influenced by near-surface geology. Metropolitan Vancouver is geologically divided into Holocene sediments, Pleistocene glacial tills and Tertiary clastic sedimentary bedrock units. Material properties of the subsurface geology is a vital component in evaluating seismic microzonation. This work demonstrates the harmonization process and quality assessment of geodata from several different agencies to develop the most comprehensive geodatabase to date by compiling borehole records, geotechnical laboratory data and in situ geophysical tests. We identify the depth to Pleistocene and Tertiary impedance contrasts within the Metropolitan Vancouver region using the improved geodatabase and geostatistical interpolation methods. Average depth profiles of various measured material properties (e.g., shear-wave velocity, SPT blow count) are derived per geologic unit. These empirical-based average depth profiles enable improved development of the geophysical/geotechnical regional model to predict earthquake site response and seismic-triggered liquefaction and/or slope instability.

Divergent fluid evolution and dolomitization of the Palaeozoic successions, Huron Domain of southern Ontario, Canada: petrologic and geochemical evidence

Ihsan Al-Aasm[1], Richard Crowe[2], Marco Tortola[1]

[1]University of Windsor alaasm@uwindsor.ca, [2]Nuclear Waste Management Organization

Petrographic, stable and Sr isotopic composition, fluid inclusions and major, trace and rare-earth elements (REE) of core samples from deep boreholes within the Huron Domain characterize diagenetic history and fluid composition. These samples represent carbonate formations throughout the Paleozoic sequences (Cambrian to Devonian). Multiple generations of non-stochiometric dolomite have been observed. They occur as both replacement (D1 and D2) and cement (saddle dolomite; SD). Petrographic and geochemical data of dolomite types and calcite cement suggest that Cambrian and Ordovician strata have two possibly isolated diagenetic fluid systems. These are: i) an earlier fluid system that is characterized by a pronounced negative shift in oxygen and carbon isotopic composition, more radiogenic Sr isotopic ratios, warm (75-156 °C for dolomite and 85-141 °C for calcite;) and saline signatures (23.2 to 27.2 wt.% NaCl eq. for dolomite; and 23.6 wt.% NaCl eq. for calcite), higher average REE compared to warm water marine brachiopods, negative La anomaly and positive Ce anomaly; and ii) a later Ordovician system, characterized by less negative shifts in oxygen and carbon isotopes, comparable homogenization temperature (Th =66-152 °C for dolomite and 68 to 153 °C for calcite) hypersaline (20.8 to 30.5 wt.% NaCl eq. for dolomite and 24.8 to 30.3 for calcite), less radiogenic Sr isotopic ratios, less negative La anomaly and positive and negative Ce anomaly but also higher average ?REE compared to warm water marine brachiopods. Ordovician, Silurian and Devonian Sr isotopic ratios, however, show seawater composition of their respective age as the primary source of diagenetic fluids with minor rock/ water interactions. In contrast, the overlying Silurian and Devonian carbonates show overlaps between $\delta^{13}C$ and $\delta^{18}O$ values. Dolomite samples from both age groups show similar $\delta^{13}C$ values compared to those of carbonates deposited in equilibrium with seawater of their respective ages. However, $\delta^{18}O$ values show evidence of dolomite recrystallization. Replacive medium crystalline dolomite matrix (D2) shows homogenization temperatures (Th) ranges from 49.7 to 134.1 °C and salinity of 15.2 to 25.2 wt. % NaCl eq. and from 69.9 to 102.3 °C, and salinity of 18.9 to 21.8 wt. % NaCl eq. for the Silurian and Devonian samples, respectively. Higher Th (101.2-193.4 oC) and salinity (25.2-32.6 wt. % NaCl eq.) is observed in saddle dolomite (SD) in Silurian carbonates. REE shale-normalized patterns suggest that in both age groups the diagenetic fluids were originally of coeval seawater composition, subsequently modified via water-rock interaction. The different evolution of the diagenetic fluids is more prominent in REESN patterns from Silurian samples and it is possibly related to brines, which were modified by the dissolution of Silurian evaporites from the Salina series.

Geochemical and Mineralogical Characterization of Gold Mineralized Quartz Veins Contextualized by Mineralogical Cluster Analysis, Vertigo Target, White Gold District, West-Central Yukon Territory, Canada

James Alexander[1], Neil Banerjee[1], Lisa Van Loon[1]

[1]Western University alexanja1@gmail.com

The Vertigo target on the southwestern JP Ross property is a gold-mineralized showing ~70 km south of Dawson City in the White Gold district, west-central Yukon Territory, Canada. Gold-mineralized zones exhibit a strong geochemical correlation with As-Ag-Te-Pb-Bi /- Cu-Co - a unique suite of pathfinder elements in the district. This study evaluates the spatial, geochemical, and mineralogical distribution of 120 sample pulps from Vertigo target diamond drill intervals analyzed using synchrotron radiation x-ray diffraction. Mineral cluster analysis of diffractogram data reveals 6 discrete mineralogical domains that provide an objective framework to interpret sample mineralogy. Supplemented by petrography, electron probe microanalysis, and micro x-ray fluorescence on related thin sections, the clustering of diffraction patterns with a high degree of similarity has revealed characteristic signatures of Au-mineralization. Structural interpretation by means of optical televiewer imagery from drill holes, magnetic data, and lidar surveys has revealed structural geometries coincident with the mineralogical clustering. Gold at the Vertigo target occupies a principal ESE striking, SSW dipping array of en-echelon quartz veins within a 2.0 x 0.8 km sinistral jog structure. Structural geometries, alteration signatures, and gold-grain geochemistry are consistent with other mesothermal gold events in the district and indicate that the principal quartz vein mineralizing event likely formed during the Jurassic. This is demonstrated by the widespread alteration of mineralogical Domain 2 samples across the target area and supported by Au-Ag-Te pyrite inclusions found in least altered quartz veins. The sinistral pull-apart structure that defines the Vertigo target quartz vein array is bound to the east by a NE-trending normal fault coincident

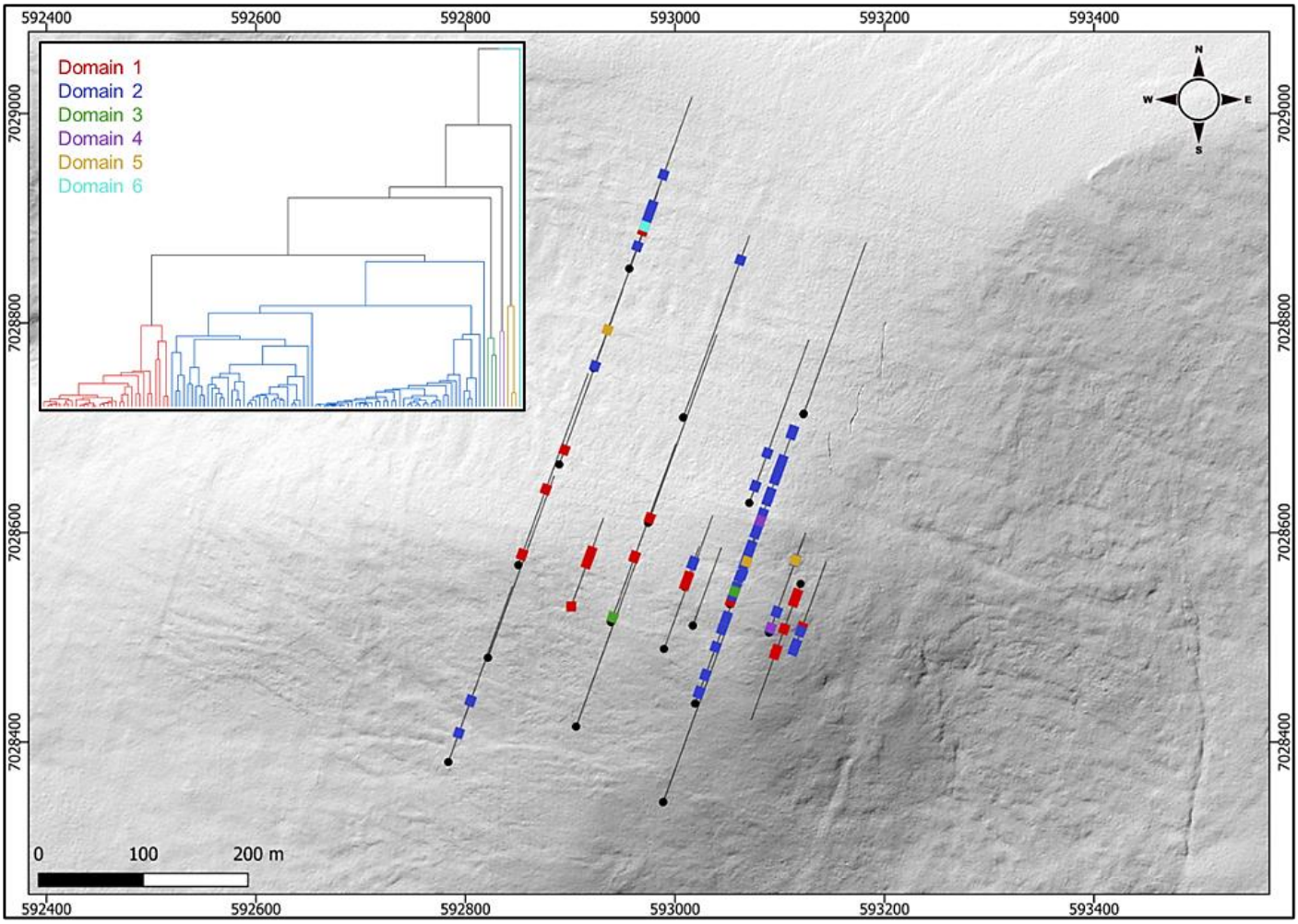

with NE- to NNE-trending sinistral faulting. These NE-trending structures are likely late-Cretaceous in age and cross-cut ESE-striking structures. Evidence of a second gold event is indicated by structural relationships, alteration mineralogy, and gold-grain geochemistry coincident with NE-trending late-Cretaceous intrusions. The Vertigo target was conceivably reactivated by NE-trending faults in the late Cretaceous, resulting in a polymetallic Au-Ag event with associated galena /- carbonate. The highest-grade gold occurs in quartz veins shallower than 30 m depth with elevated As-Ag-Te-Pb-Bi that manifest as secondary arsenates and oxides. Magnetite- and carbonate-destructive silica-sericite alteration overprints early potassic mineralogies and is confined to the upper oxidized zone. The western Yukon and eastern Alaska experienced a protracted history of fault emplacement and mineralizing events, with structural geometries prone to reactivation. The spatial distribution of mineralogical domains obtained from our objective cluster analysis provides compelling evidence for polyphase Au-mineralization at the Vertigo target.

Natural Carbon Dioxide (CO2) Sequestration by the Oman Ophiolite: Implications for Engineered CO2 Sequestration

Arshad Ali[1], Iftikhar Abbasi[1], Sobhi Nasir[1], Leonardo Nogueira[2], Mohamed El-Ghali[1], Osman Salad Hersi[3]

[1]Sultan Qaboos University arshadali@squ.edu.om, [2]Federal University of Ouro Preto, [3]University of Regina

Compared to the exchanges among geological carbon reservoirs occurring on longer timescales, the natural carbon-cycle that circulates carbon through the atmosphere, hydrosphere, and biosphere is underway at a time scale ranging from days to millennia. With the advent of the industrial revolution, the global carbon balance between emissions and sinks has been lost due to excessive use of fossil fuels, causing CO_2 to rise from 277 ppm in 1750 to 405 ppm in 2017. Several studies have been conducted on listvenite rocks (carbonated peridotite) associated with the Oman Ophiolite to better understand natural CO_2 sequestration. Fluvial sediments, termed as the Barzaman Formation (BF), first described in Oman by Maizels, are characterized by whitish-pink massive fine-grained dolomitic, calcitic, and clay mineral-rich rocks. These highly altered rocks, which often display 'ghost' textures showing the relicts of primary ophiolite clasts, were subsequently recognized in the United Arab Emirates (UAE) by the British Geological Survey. Sediments of the BF exposed along the western margin of the Hajar Mountains in the UAE may have stored an estimated ~4 years of global CO_2 emissions at the current rate. The new estimate of CO_2 stored in BF carbonates (Oman) confirms the natural sequestration of atmospheric CO_2. Based on the C-O isotope model, we estimate that atmospheric CO_2 accounts for ~78% of the carbon stored during the precipitation of a calcite sample. The remaining 22% of carbon in this sample could be attributed to DIC species derived from various sources, including different carbonate lithofacies and ophiolite-derived soil. However, the rate of natural CO_2 sequestration is relatively slow, making it difficult to effectively counteract the increasing anthropogenic CO_2 emissions in the atmosphere. Hence, a significant increase of rates of CO_2 absorption by ophiolite would be required to offset rising CO_2 levels. In the present study, we have attempted several laboratory and field experiments in order to enhance the weathering of olivine in the ultramafic rocks. This provides better understanding about engineered CO_2 sequestration as a complementary protocol in the carbon capture and storage (CCS) technology. Furthermore, the conversion rate of atmospheric CO_2 gas to stable calcite and magnesite could be improved by adopting in-situ reaction under deeper weathering horizons at higher temperatures. Thus, we envisage that natural CO_2 sequestration can be enhanced by artificial means to restore the carbon balance by executing the safest mitigation policies and utilizing the data required to resolve the potential environmental risks associated with artificial sequestration.

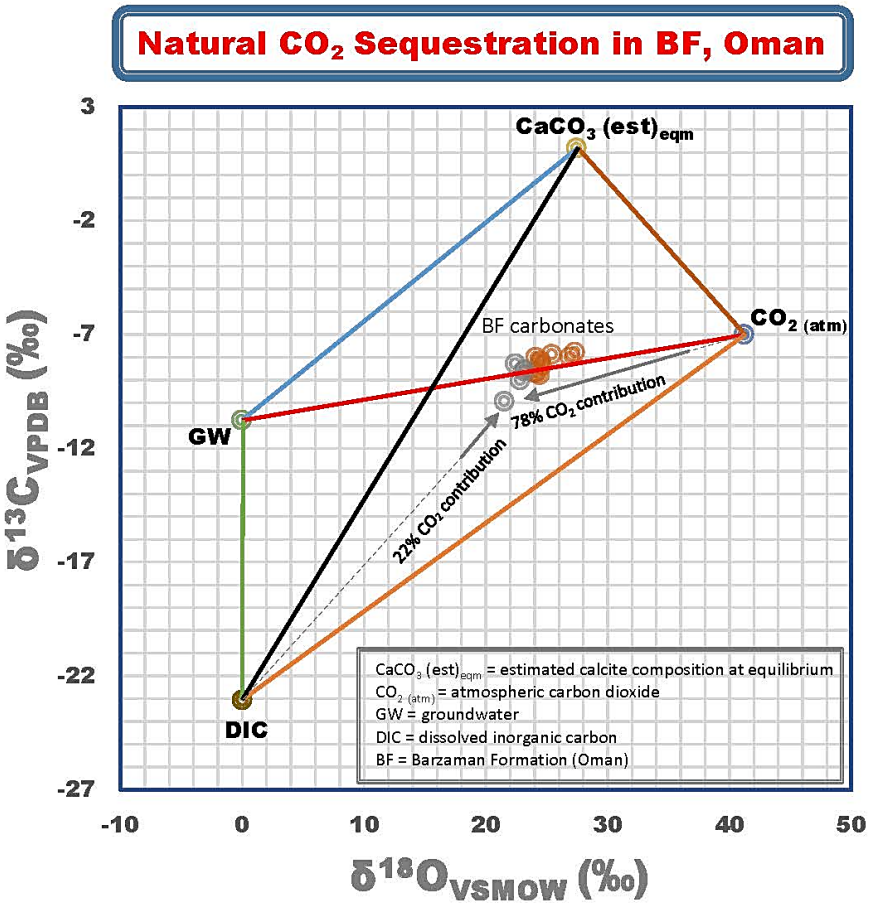

Using Computed Tomography to Assess Physical and Salinity Controls on Sedimentation in the Champlain Sea Basin, Ottawa, Canada

Omar Al-Mufti[1], William Arnott[1], Marc Hinton[2], Sam Alpay[2], Hazen Russell[2]

[1]University of Ottawa onalmufti@gmail.com , [2]NRCAN

In this study, computed tomography (CT) was used to unravel the depositional history of the Champlain Sea basin in Ottawa, Canada. CT-scan images and Hounsfield Units (HU) profiles from two continuous drill cores identified five lithologically distinct, mud-dominated stratal units. Distinctively, all strata exhibit a several cm- to few dm-thick pattern of upward increase followed by decrease in HU, suggestive of an upward increasing and then decreasing silt content, which collectively, is interpreted to reflect the annual glacigenic waxing followed by waning of flow and sediment discharge conditions. Mud rhythmites at the base of the succession (Unit 1) and beds of well-stratified mud at the top (Unit 4a), contain well-developed parallel-stratification in the lower part of each bed, and are characterized by a range of ~ 250-350 HU. This wide HU spread reflects the effective partitioning of silt-rich and clay-rich parts in each bed, and therefore bed-surface and near-bed transport processes that sorted sediment based mostly on grain size, followed by low-energy sediment fallout. The silt-rich part of each bed was deposited by glacigenic meltwater-sourced hyperpycnal flows, which due to the freshwater composition of the basin, or at least in the upper part of the water column, were able to plunge to the basin floor and sort particles along the bed. In comparison, beds of bioturbated mud (Unit 2), banded mud (Unit 3), and diffusely stratified or structureless mud (Unit 4a) have a narrower range of ~ 50-120 HU indicating poorer particle segregation. These conditions, most clearly illustrated by the bioturbation, indicate a change to a saltwater basin that caused meltwater inflows to instead form buoyant, sediment-laden hypopycnal flows, which aided by clay-silt particle flocculation and particle-settling convection, resulted in accelerated bedward transfer and deposition of suspended sediment. The uppermost part of the succession is characterized by sharply bounded interbeds of internally deformed slump-slide blocks (Unit 4b) that indicate the onset of episodic mass wasting, possibly related to local gravitational instability on the slope of a newly-developed and nearby delta. In addition to characteristic bed-scale HU values, and a distinctive assemblage of sedimentary structures and textures, beds within each unit also vary little in their thickness. However, across unit boundaries, beds abruptly and consistently thicken (doubling or tripling), in addition to typically changing in their sedimentological character. This suggests that abrupt and systemic changes in the dynamics of deglaciation, and its control on sediment supply and water chemistry, were the main factors that controlled the temporal evolution of sedimentation in the Champlain Sea basin.

Analogue models of symptomatic vs. asymptomatic lithospheric drip removal with applications to the Arizaro Basin

Julia Andersen[1], Tasca Santimano[1], Ögüz Gogus[2], Russell Pysklywec[1], Ebru Şengül[3]

[1]University of Toronto julia.andersen@mail.utoronto.ca, [2]Istanbul Technical University, [3]Çanakkale Onsekiz Mart University

Metamorphic processes such as eclogitization or tectonic processes, may increase the density of the mantle lithosphere in intraplate regions in contrast to the underlying sub-lithospheric mantle creating a gravitational instability. Inferred from geophysical interpretations of the lithosphere (i.e., seismic tomography) and geological interpretations of the upper crust (i.e., subsidence, uplift, convergence, and extension) it is suggested that the mantle lithosphere drips or sinks into the underlying mantle due to Rayleigh-Taylor (gravitational) instability. This process may be responsible for the removal or thinning of the lithosphere in intraplate (e.g., Arizaro Basin) and active orogenic (e.g., Cordilleran magmatic arcs, Anatolia) regions. A series of scaled 3D analogue experiments were conducted with quantitative analyses using the Particle Image Velocimetry (PIV) technique. The models include a sub-lithospheric mantle (Polydimethylsiloxane-PDMS), mantle lithosphere (PDMS and plasticine), and upper crust (Si spheres and e-spheres) in a Plexiglass box. The viscosity of the mantle lithosphere was varied between experiments and in some cases, a lower crust was introduced (PDMS and plasticine). Results show that not all drips will yield surficial evidence of significant crustal convergence and thickening, and we define these drips as asymptomatic due to the lack of crustal features. There may be subsidence associated with asymptomatic drips, but it is only detected with the high resolution equipment. Symptomatic drips produce subsidence followed by thickening/convergence of the upper crust. In these experiments, the drip thins and necks, and the surface topography increases as a response to the upwelling sub-lithospheric mantle. Meanwhile, regions of surface extension develop as a response to the convergence. We interpret that asymptomatic drips are not well coupled to the upper mantle lithosphere and thus do not influence horizontal convergence in the crust. Our results are applicable to areas where lithospheric drips have been postulated on Earth such as beneath the Arizaro Basin in the Altiplano-Puna Plateau, South America. The models suggest a symptomatic type of drip beneath the basin and imply possible future uplift of the basin. Importantly, the models also suggest that there may be 'undiagnosed' tectonic processes beneath the surface of Earth and other planets that may not manifest in the crust.

Cesium fractionation in miarolitic pegmatites: A reevaluation of K-feldspar data

Alan Anderson[1], Scott Ercit[2]

[1]St. Francis Xavier University aanderso@stfx.ca, [2]Canadian Museum of Nature

Crystal-lined pockets in miarolitic pegmatites are the products of late-stage melt crystallization in the presence of an exsolved magmatic volatile phase. A recent Rayleigh equation model predicts that in a volatile undersaturated silicate melt, K/Cs ratios of K-feldspar crystals decrease as crystallization proceeds from the margin to the core of the pegmatite. The model further predicts that any K-feldspar formed by simultaneous crystallization in a two-phase (melt + aqueous solution) system will be characterized by low Cs concentrations and high K/Cs ratios that increase with crystallization. Our survey of published K-feldspar compositions from 21 miarolitic pegmatites, however, shows that the Cs concentration of pocket K-feldspar crystals in 18 pegmatites exceeds the Cs concentration of non-pocket K-feldspar by as much as 93% (see e.g., Morton et al. 2018). If, instead, pocket K-feldspar crystals formed in a melt-fluid system as proposed by Jahns and Burnham (1969) and Maneta and Anderson (2018), then the observed decrease in the K/Cs ratio of pocket feldspar - and its sympathetic covariance with decreasing K/Rb - is inconsistent with the predictions of the recent Rayleigh model. A possible explanation for exceedingly high Cs concentrations in pocket K-feldspar, and their high rate of change in some pegmatites, is that unlike Rb, a significant amount of Cs may accumulate in dislocation defects (Tauson et al. 2001). Furthermore, the Rayleigh model does not account for the evolving PTX conditions during pocket formation, which affects Cs partitioning between the silicate melt and fluid and between the fluid and growing K-feldspar crystals.

Jahns RH & Burnham CW (1969) Experimental studies of pegmatite genesis. I. A model for the derivation and crystallization of granitic pegmatites. Economic Geology 64:843-864. Maneta V & Anderson, AJ (2018) Monitoring the crystallization of water-saturated granitic melts in real time using the hydrothermal diamond anvil cell. Contributions to Mineralogy and Petrology 173:83. Morton DM, Sheppard, JB, Miller, FK & Lee C-TA (2018) Petrogenesis of the cogenetic Stewart pegmatite-aplite, Pala, California: Regional implications. Lithosphere 11:91-128. Tauson VL, Taroev VK, Karimov VV, Gottlicher J, Pentinghaus H & Rocholl A (2001) New data on Cs and Rb distribution between potassium feldspar and alkaline fluid: A study of the trapping effect. Geochemistry International 39:725-731.

Exploring the influence of curved subduction margins on the structural and magmatic-hydrothermal evolution of back-arc basins

Melissa Anderson[1], Octavio Acuña-Avendano[1], Chantal Norris-Julseth[1], Mark Hannington[2], William Chadwick[3], Kenneth Rubin[4]

[1]University of Toronto melissao.anderson@utoronto.ca, [2]University of Ottawa, [3]Oregon State University/CIMRS, Hatfield Marine Science Center, [4]SOEST, University of Hawaii

Curved trenches are ubiquitous in intra-oceanic subduction zones. While many studies explore the influence of curved margins on processes related to the down-going slab, few explore the consequences for the upper plate. Here, we will address the fundamental question: How does curved trench geometry influence the structural and magmatic-hydrothermal evolution of the back-arc region? To answer this, we explore the geology and geodynamics of two key subduction zones--the Marianas and northern Tonga--using morphotectonic analysis (remote-predictive geologic mapping), fault kinematics interpreted from multibeam bathymetry and CMT data, and regional magnetic and gravity data. We find that arc-orthogonal structures directly control differences in the siting, style, and intensity of magmatic-hydrothermal systems in the back-arc regions of these two sites. This indicates that arc-parallel extension alone may not be enough to produce large mineral resources. The Mariana subduction zone is characterized by a westward-convex trench bound by two large oceanic plateaus in the north and south. In the southern and central back-arc region, we distinguish four types of segments based on their morphology: (i) magmatic segments; (ii) tectonic segments; (iii) magmatic segments currently undergoing tectonic extension; and (iv) tectonic segments currently undergoing magmatic extension. These morphologies reflect variable magma supply and processes of crustal accretion. Notably, there are several arc-orthogonal structures with active seismicity that extend from the arc into the back-arc, resulting from arc-parallel extension during asymmetric slab rollback along a curved margin. Importantly, these structures provide conduits for magma, producing cross-arc volcanic chains and enhanced magmatism and hydrothermal activity in the associated back-arc segments. In the northern Tonga subduction zone, there is a sharp bend in the trench with a transition from subduction to transform motion, resulting in tearing of the subducting slab. Our results highlight two notable features within the associated NE Lau back-arc basin: (1) the occurrence of widely distributed off-axis volcanism, in contrast to typical ridge-centered back-arc volcanism, and (2) fault kinematics dominated by shallow-crustal strike slip-faulting (rather than normal faulting) extending over ~120 km from the transform boundary. The orientations of these strike-slip faults are consistent with reactivation of earlier-formed normal faults in a sinistral megashear zone. Notably, two distinct sets of Riedel megashears are identified, indicating a recent counter-clockwise rotation of part of the stress field in the back-arc region closest to the arc. Importantly, these Riedel structures directly control the development of complex volcanic-compositional provinces, which are characterized by variably-oriented spreading centers, off-axis volcanic ridges, extensive lava flows, and point-source rear-arc volcanoes.

Student-led virtual field trips using Google Earth: Increasing accessibility of geoscience programs through innovative assignments

Melissa Anderson[1]

[1]University of Toronto melissao.anderson@utoronto.ca

Field trips are an essential component of geoscience education, allowing students to apply what they have been taught in the classroom. However, there are many circumstances where in-person field trips are not feasible due to travel restrictions or cost. Classic field trips may also be a barrier for students with accessibility considerations. In this presentation, I outline a virtual approach to simulating a field trip through an innovative student-led assignment to different "Geologic Wonders" around the world (e.g., different volcanoes, sedimentary environments, impact craters, etc.) using Google Earth. The purpose of this assignment is for students to become familiar with geological processes, educate others about these processes (peer instruction), and reinforce oral and written communication skills, with an emphasis on engaging scientific writing with the use of appropriate citations. It also serves to increase excitement about future opportunities within geoscience fields, which may help recruit students into our programs. The assignment includes: (1) an introductory stop with a short video embedded within (2) intermediate stops featuring place markers with different Google Earth perspectives (e.g., panoramas, street view), relevant figures, paragraph text, educational resources, and appropriate citations, and (3) a final stop with a longer video presentation (8-10 minutes) describing the geology of the site, related processes, and geology-human interactions. Students are given the opportunity to explore virtual field trips created by their classmates, answer questions related to geologic processes within each field trip and provide feedback to the presenters. This assignment was developed for a second-year geoscience course at the University of Toronto that was taught remotely in 2020, with enrollment of 60 students, and can be modified for different levels of learners (high school to upper-year undergraduate). This virtual approach increases accessibility of geoscience education, particularly in an era of remote education. It also provides a stimulating and interactive learning environment for students, with diverse modes of communication used to reach different types of learners.

North Tibetan Plateau as an analogue for Martian environments

Angelica Angles[1]

[1]The University of Science and Technology of Macau aangles@connect.hku.hk

The surface of Mars preserves a variety of geomorphological structures formed by episodic hydrodynamic processes. The transition stage between the wetter and warmer early Mars and the hyper-arid environment that is today may have been characterized by strong chemical weathering by the long-term water rock interactions and the deposition of various salts. However, understanding the planetary images and geomorphology, dynamic evolution and chemical geodynamics of Mars in terms of properties and processes of the host rocks continues to be a challenge. Western Qaidam Basin, located in North-western Tibetan Plateau, contains many geomorphological structures that combine fluvial and glacial attributes and relic clues comparable in their dimensions to the features associated with Martian landforms. The area is characterized by its high altitude (>3000m), dramatic change of diurnal and annual temperatures and extremely low annual precipitation (~14mm). The weak hydrodynamic erosion of the compacted detrital sediments of the mountain area during the latest glaciations developed a unique geomorphology and geology. The dry lakes are mainly formed of siliciclastic deposits covered by salts, which were encrusted by the evaporation of water, forming a surface of mostly sulphates and carbonates. The geomorphology of the mountain area is characterized by its high density of small gullies and large surrounding fluvial fans, cyclic structures and catastrophic debris flow structures. Small gullies filled with white mirabilite salt strongly suggest their young age and the sapping of brine fluid confirms the interaction between the thawed ice and salts in the upper alcove in a strong evaporite environment. The geomicrobiology and adaptive mechanisms of the only observable microbial life (hypolithic cyanobacteria) to survive the environmental extremes provides a rare chance to study the living strategies of life on Mars during its habitable time window. Given the level of information that western Qaidam Basin contain about its unique dynamic evolution and microorganisms preservation potential, this site is a great terrestrial analogue to study the Martian processes and potential habitability, and likewise can be treated as an important site for future Mars sample return missions.

Methanogenesis and sulfur-cycling in Eocene phosphatic carbonate lacustrine oil shale

Alex Ani[1], Dave Keighley[1]

[1]University of New Brunswick aani@unb.ca

The precipitation of microcrystalline phosphate is linked directly to the preservation of microfossils, in carbonate oil shale from the Uinta formation of the Eocene Green River Formation. Sampled intervals of this organic-rich carbonate mudrock contain elevated concentrations of carbon and phosphorus (e.g. Keighley, 2018), within which phosphatized microfossils occur. The origins of the hypersaline bottom waters which facilitated the preservation of elevated concentrations of organic matter (OM) in the lake sediments is not universally agreed upon, and numerous sources have been proposed (Lowenstein et al., 2017). Analysis of laser-ablation inductively-coupled-plasma mass-spectrometry (LA-ICP-MS) data provides insights into a confluence of biogeochemical cycling, and inorganic precipitation of distinct mineral phases related to the accumulation of organic matter in the ancient lake sediments. Variations in elemental abundance and distribution(s) suggest changes in the dominant system of biological autotrophic carbon fixation in the OM-rich anoxic lake bottom sediments, during burial and early diagenesis.

Constraining the role of poorly crystalline Mg-silicates in carbonate precipitation in lacustrine environments

Maria Arizaleta[1], Nina Zeyen[1], Maija Raudsepp[1], Siobhan Wilson[1]

[1]University of Alberta arizalet@ualberta.ca

Authigenic Al-poor Mg-silicates (e.g., stevensite, sepiolite, kerolite) are important components of a wide array of environments, such as alkaline lakes and submarine hydrothermal vents. Mg-silicates are also observed in the geologic record as part of ancient evaporite deposits from lakes or seawater, and they are associated with carbonate minerals, such as calcite, aragonite, dolomite and magnesite. Diagenetic replacement of Mg-silicates by carbonate minerals has been observed in lake sediments and microbialites. For this reason, it has been hypothesized that poorly crystalline Mg-silicates can serve as a precursor for carbonate precipitation in alkaline lakes1. The presence of specific microbial groups and metabolic processes has also been hypothesized to impact the transformation between Mg-silicates and carbonates by generating alkalinity and promoting cation availability1. However, the precise geochemical conditions in which this transformation can happen, and the mineral phases involved, are poorly understood. Here, we present the results of a series of bench-top batch experiments designed to study the reaction between poorly crystalline Mg-silicates and alkaline waters. The first set of experiments reacted a synthetic, poorly crystalline stevensite/kerolite with synthetic lake water solutions whereas the second set of experiments used natural samples of alkaline lake water and sediments from lakes in the Cariboo Plateau, British Columbia. In particular, we tested the effect of alkalinity, pH, and the presence of microbes on the rate of carbonate mineral precipitation and final mineral products for these batch experiments. The mineralogy and structure of the synthesized poorly crystalline Mg-silicate was analyzed using scanning electron microscopy (SEM), powder X-ray diffraction (pXRD), and Fourier-transform infrared spectroscopy (FTIR). Secondly, sediment samples from the Cariboo Plateau were micronized followed by a clay separation procedure in order to isolate the clay fraction. This clay fraction was then analyzed with SEM and pXRD to identify amorphous and crystalline phases present. Findings from this study will be used to produce better quantitative geochemical models to predict the behaviour of Mg-silicates and carbonates in natural systems and their use for carbon sequestration.

References:

[1] Pace A., et al. 2016. Microbial and diagenetic steps leading to the mineralisation of Great Salt Lake microbialites. Scientific Reports. 6, 31495.

[2] Tosca, N. J. 2015. Geochemical pathways to Mg-clay formation. In: Magnesian Clays: Characterization, Origins and Applications (Eds M. Pozo and E. Galan). AIPEA Special Publications, 2, 283-329.

Pb isotope variability in the Archean: insights from the Superior Province, Canada

Sheree Armistead[1], Bruce Eglington[2], Sally Pehrsson[3], David Huston[4]

[1]Laurentian University & the Geological Survey of Canada sheree.armistead@gmail.com, [2]University of Saskatchewan, [3]Geological Survey of Canada, [4]Geoscience Australia

Isotopic proxies are widely used to understand the evolution of Earth's crust and mantle. Of these, Pb isotopes are used extensively in studies of ore deposit geology, which has resulted in large quantities of data being available on a global scale. We present a global Pb isotope compilation that comprises over 25,000 analyses. Like other Pb isotope studies, we have focussed on data from VMS and Lode Gold deposits for several reasons, but most importantly because they occur throughout most of Earth's history from 3.5 Ga to present, allowing us to assess long-term secular and cyclical changes. In this study we focus on model source μ values (238U/204Pb), which allow us to compare samples and deposits through time. Model source μ values for VMS and Lode Gold deposits that formed from 1000 Ma to present have a relatively restricted range, with the majority plotting close to the Stacey and Kramers (1975) second stage average ore lead model, or slightly lower near to mantle values. This is consistent with our understanding of VMS deposit formation on the sea floor or in back-arc basins, with relatively average Pb signatures with some input of mantle fluids. This is in marked contrast to the wider range of model source μ identified further back in time. For the Archean, model source ? ranges between ~7 and ~12.5, with the first occurrence of low μ values occurring at c. 3.2 Ga. Importantly, at the terrane scale, the range in model source ? is relatively restricted, indicating that the processes driving the Pb isotope signatures are large scale. We show how the relationship between model source μ and time-integrated μ (232Th/238U) at a global scale changes through time. This may indicate that fundamental tectonic processes driving the Pb isotopes in these deposits have changed over time. Using the Superior Province as a case study, we also consider published Nd and Hf isotope data (e.g. Vervoort et al., 1994; Mole et al., 2021), which indicate dominantly juvenile sources for the Abitibi sector of the Superior Province. This juvenile signature contrasts with its low model source μ signature, which requires several hundred million years to evolve. We propose that this requires an old, low μ source that mixes with juvenile material at c. 2700 Ma. Similar, but more muted, Pb, Nd and Hf systematics occur during younger major global magmatic episodes, such as the Birimian and Trans-Hudson, suggesting the presence of a long-lasting low μ source region, presumably in the mantle.

3-D geophysical modelling of a deeply buried, simple impact crater: Holleford impact structure, Ontario, Canada

Mary-Helen Armour[1], Joseph Boyce[1], Zack Shulman[1], David Zilkey[1]

[1]McMaster University armourm@mcmaster.ca

Holleford Crater, located in southeastern Ontario, Canada, was identified in 1960 as a simple (~2.4 km diameter) impact crater in Late Proterozoic target rocks. An impact origin was confirmed through gravity surveys, deep drilling, and recovery of impact breccias but the structure depth and geometry were not determined. Ground-based geophysical surveys (magnetics , microgravity) and 3-D potential field modelling were conducted to investigate the impact basin geometry and depth. Surveys revealed a small (< 20 nT) residual magnetic anomaly and ~2-3 mGal Bouguer anomaly over the crater basin. The lack of a well-defined magnetic anomaly is due to the low magnetic contrast between metasedimentary target rocks and crater infill sediments. 3-D gravity models indicate a heavily eroded impact crater that is slightly elliptical in shape with a maximum diameter ~2 km and a depth to basement of ~550 m, The crater infill consists of ~580 m Cambrian-Ordovician sandstones and carbonate strata overlying breccias. The sandstone isochore thickness indicates the presence of an erosional channel in the upper surface of the breccia. A rim breach, marking a possible outflow channel, is present in the southeast corner of the crater. The channel feature is up to 150 m depth, 400 m in width, and is similar to outlet channels produced by fluvial rim dissection of terrestrial and Martian 'polywog' craters (e.g. 2.3 km diameter Arabia Terra).

Petrogenesis of Pleasant Ridge topaz granite: a highly differentiated, fluorite-bearing hybrid I-type granite, New Brunswick, Canada

Zeinab Azadbakht[1], David Lentz[2], Chris McFarlane[2]

[1]Ontario Geological Survey Zeinab.azadbakht@ontario.ca, [2]University of New Brunswick

The Late Devonian (362 Ma) topaz-bearing Pleasant Ridge Granite (PRG) and its associated Sn-bearing cupola at Kedron Granite (KG) are situated in southwestern New Brunswick, Canada. These intrusions are highly evolved granites that are characterized by high SiO2 (> 75 wt.%), Gottini index (?) >227, K/Rb < 41, Li (951± 133 ppm), and low P2O5 (<0.02 wt.%), Zr/Hf (<14), Nb/Ta (3), La/Sm (2.7-3.9), and Eu/Eu* (< 0.01) values. Both examined intrusions possess high total rare earth element (REE) abundances (REE from 247 to 281 ppm) and an apparent M-type tetrad effect. Higher first tetrad effect (average of 1.39±0.04) in comparison with the third tetrad effect (average of 1.10±0.21), suggest crystallization of the LREE minerals like monazite or fluorite may played an important role in the genesis of these intrusions. It may also indicate selective complexation of REE during the interaction of granitic melts with halogen-enriched aqueous fluids. PRG and KG are suggested to be generated by extreme fractional crystallization of feldespars, lithium-siderophyllite, and some accessory phases including fluorite from the Mount Douglas Granite (MDG). In addition, the cogenetic mafic rocks associated with the Saint George Batholith may have enhanced the thermal gradient in the region, which would allow slow cooling and the extended fractional crystallization in these intrusions. Also, the presence of halogen complexes, such as HF-KF would flux the melt and enable it to fractionate to lower temperatures. These intrusions have crustal A-type affinities, although they have much higher Rb/Sr and Rb/Ba ratios than typical A-type granites. Consequently, they are believed to be highly evolved hybrid I-type granites formed by flat-slab subduction of Meguma under composite Laurentia during the Neoacadian Orogeny. Whole-rock $\delta^{18}O$ values of about +8.1?, high initial $^{87}Sr/^{86}Sr$ ratios of 0.712, slightly positive εNd (+0.7), and Pb isotopic data indicate that the granite was derived dominantly from high temperature granulite partial melting of Avalonian crust, contaminated by supracrustal rocks. Close geochemical affinities and temporal relationship between these intrusions and the most fractionated phases of the MDG (Dmd2, Dmd3) and Mount Pleasant Granites may indicate their association through extreme fractional crystallization, fluorite melt immiscibility, and fluid exsolution. Exsolution of volatiles from the crystallizing highly evolved magma played a major role in the generation of associated Sn-Li-In mineralization in the region, analogous to the North Zone Sn-Zn-In deposits at Mount Pleasant. The estimated zircon saturation temperatures resulted in average of 673±5 ºC for PRG and 687 ºC for KG that is slightly higher than the expected temperatures for such evolved systems. The crystallization pressure of the systems was estimated at 1.8±0.4 kb and 1.7 kb using PQz for PRG and KG, respectively.

A review of Archean to Paleoproterozoic surface weathering trends from the perspective of paleosols and chemical weathering proxies: best practices, limitations of existing data, and new directions

Michael Babechuk[1]

[1]Memorial University mbabechuk@mun.ca

One of Grant M. Young's career legacies is the detailed body of research produced with collaborators into modern and ancient surface weathering processes. The hallmarks of this research include, but are not limited to: its comprehensive examination of weathering from thermodynamic, geochemical, stratigraphic, and sedimentological perspectives; its derivation of the chemical index of alteration (CIA); its novel reconstruction of key differences between modern and ancient weathering profiles (i.e. paleosols); and, its wider contributions towards understanding major transitions in Precambrian Earth surface conditions, especially Proterozoic climate and atmospheric redox variations. Firstly, this contribution will provide an overview of typical Precambrian chemical weathering trends through the lens of paleosols and applying the CIA, mafic index of alteration (MIA), and the molar oxide ternary plots (Al_2O_3, CaO, Na_2O, K_2O ± MgO, Fe_2O_3(T)) accompanying these chemical indices. An outline of best practices in applying chemical indices to study weathering under variable redox conditions will be included, as well as an account of the limitations imposed by some elemental datasets in the literature. Secondly, this contribution will provide a summary of recent research into 3 paleosols developed on fine-grained mafic rock that collectively capture intervals of weathering from the Neoarchean into the Paleoproterozoic (ca. 2.77 Ga Mt. Roe, ca. 2.45 Ga Cooper Lake, and ca. 1.85 Ga Flin Flon). This summary permits more in-depth consideration of the weathering trends recorded at different spatial scales in saprolith of the paleosols and examples of the new insights into ancient Earth surface conditions offered by the combined application of major element weathering indices with high-precision trace element and stable metal isotope geochemistry.

Seismic structure of the lithosphere across SE Canada and the NE USA

Omid Bagherpur Mojaver[1], Fiona Darbyshire[1]

[1]University of Quebec at Montreal (UQAM) omid.bagherpur@gmail.com

Eastern North America is shaped through the occurrence of many Wilson cycles, and includes terranes that experienced formation and break-up of two supercontinents since ~1 Ga. Studying the lithospheric structure beneath this region will shed light into our understanding of evolution of the continental lithosphere. Our study area includes Proterozoic easternmost Grenville and the Phanerozoic northern Appalachian provinces in southeastern Canada and the NE USA. This region includes oceanic/continental terranes with different heritage that accreted during various orogenic episodes. We used distant earthquakes recorded by 71 broadband stations between 2013 and 2015 in a surface wave tomography technique, and modelled shear velocity variations at depths from the Moho to ~200 km. Our resolution analysis suggests that the resolving power of our model is sufficient to describe velocity variations at the scale of individual domains, enabling us to discuss tectonic implications. The crustal and lithospheric thicknesses vary significantly across the study area but show no simple relation to the age of the surface tectonic divisions. Adding to the complexity of the lithospheric seismic structure, we observe a region of unusually thicker lithosphere beneath southern New Brunswick that we interpret as resulting from a "slab-stacking" process which occurred after flat-slab subduction at ~430 Ma. This interpretation is also supported by previous geochemical and paleomagnetic evidence.

GeoExplore Saskatchewan: A New Virtual Geoscience Tool for Teaching and Exploration

Emily Bamforth[1], Ralf Maxeiner[2], Kevin Ansdell[3], Janis Dale[4], Michelle Hanson[2], Thomas Love[2], Kate MacLachlan[5], Sam Narimani[4], Erik Nickel[6], Pam Schwann[7]

[1]Royal Saskatchewan Museum emily.bamforth@gov.sk.ca, [2]Saskatchewan Geological Survey, [3]University of Saskatchewan, [4]University of Regina, [5]Association of Professional Engineers and Geoscientists of Saskatchewan, [6]Petroleum Technology Research Centre, [7]Saskatchewan Mining Association

GeoExplore Saskatchewan is a new website designed for teachers, students, and anyone interested in exploring the geoscience of the province. Launched in 2020, the website is a digital redesign of the 2002 Geological Highway Map of Saskatchewan. GeoExplore Saskatchewan allows visitors to virtually explore the province's landscape and geology through photographs and accompanying explanations in language accessible to a broad audience. The website helps raise awareness of Saskatchewan's numerous geoscience treasures, from the Cypress Hills in the south to the Athabasca Sand Dunes in the far north, from an underground potash mine in south-central Saskatchewan to uranium exploration in the north; from the world's largest T. rex in the Frenchman River valley to the complexly deformed metamorphic rocks of the Canadian Shield, and much, much more. The website is built using ESRI's StoryMap online tool. More than 110 geoscience points of interest are superimposed on a digital road map of the province, with the interactive map displayed on the right-hand side and points linked to "story boards" on the left-hand side providing photos and information about each. Additional thematic panels further explain basic geological concepts (e.g. plate tectonics, the rock cycle), economic resources, fossils, mass extinctions, the ice age, landforms and much more. The Association of Professional Engineers and Geoscientists of Saskatchewan (APEGS) and the Saskatchewan Geological Society spearheaded the initiative. Other collaborators who contributed photographs, expertise, and/or time are the Saskatchewan Geological Survey, the Saskatchewan Mining Association, Tourism Saskatchewan and the Royal Saskatchewan Museum. The working committee is comprised of volunteers who are geoscience professionals from the above organizations, as well as from the University of Regina and the University of Saskatchewan.

[Fig. 1 next page]

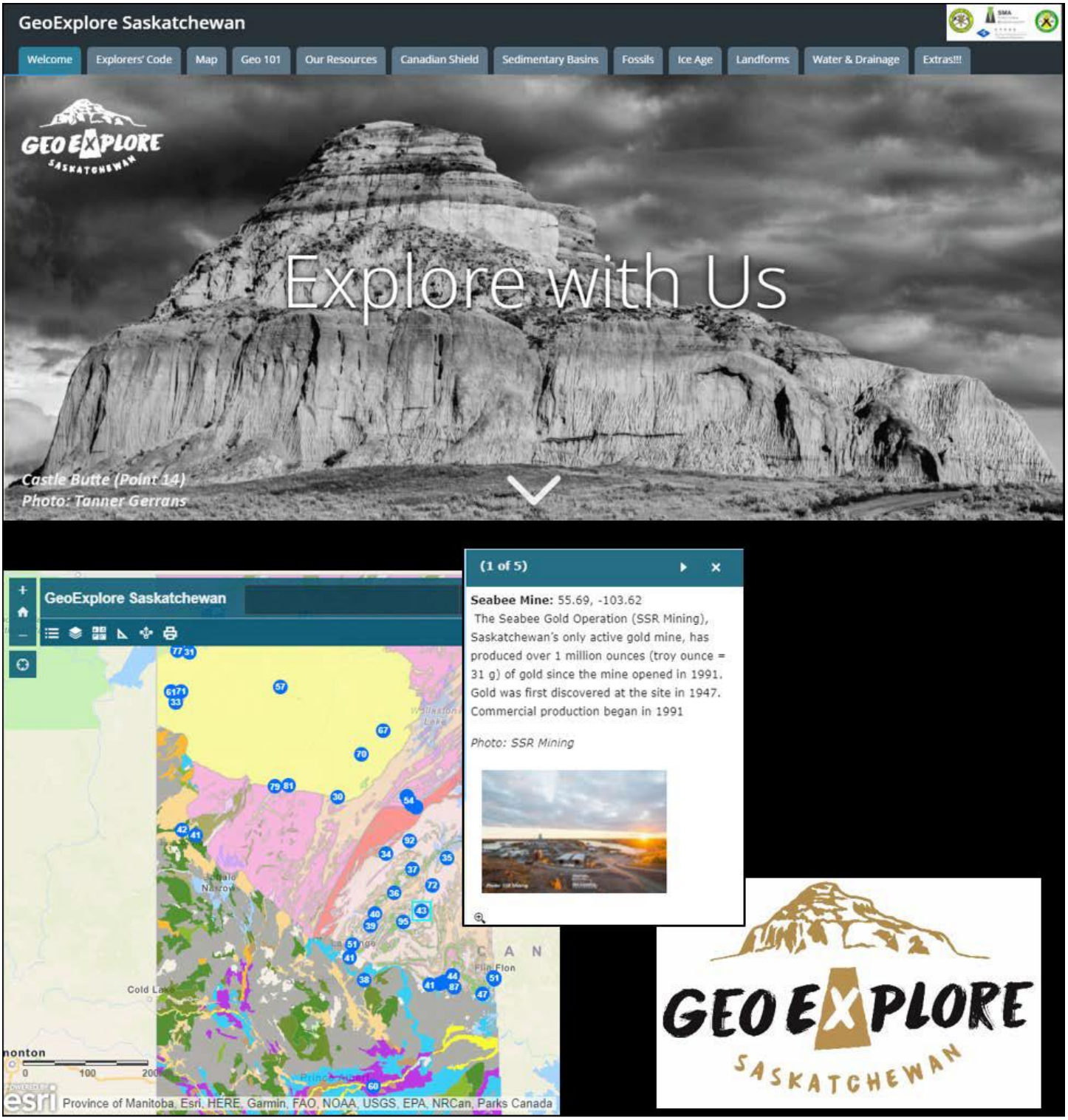

Fig. 1: Screen captures from the GeoExplore Saskatchewan website

Cold and fast hypabyssal kimberlite emplacement within the upper crust demonstrated using cold seal experiments

Roy Bassoo[1], Kenneth Befus[1]

[1]Baylor University Roy_Bassoo1@baylor.edu

Syn- to post-emplacement alteration of hypabyssal kimberlite may represent an overlooked opportunity to better understand kimberlite volcanism and diamond preservation potential. To learn more about these effects, we conducted a series of short duration (0.25 - 4 h), high-temperature (300 - 900 °C) cold seal experiments designed to test mineral abundances and textures in the hypabyssal environment. A combined approach of petrography, Raman spectroscopy, SEM, and optical cathodoluminescence demonstrates that both calcite and olivine are sensitive to temperature in the hypabyssal environment. Primary calcite and olivine are pervasive hypabyssal kimberlite minerals but they will react in a decarbonation reaction to produce monticellite when exposed to elevated temperatures. Monticellite is an indicator of decarbonation and elevated temperature. Decarbonation rates vary directly with temperature and indirectly with CO2 in the fluid, with +12 wt.% CO2 increasing the stability range of calcite by 100 °C. Decarbonation rates are relatively fast, ranging from 1 to 6 area% h-1. To replicate the observed mineral assemblage and textures in natural hypabyssal kimberlites, the rocks could only be exposed to elevated temperatures by syn- to post-emplacement processes with timescales ranging from hours to days. Additionally, calcite preservation in hypabyssal kimberlite provides an observational constraint that diamond grade has not been diminished by post-emplacement conditions. Hypabyssal kimberlites may record other post-emplacement alteration features, which lead to the exsolution of unaccounted for volatiles.

Biostratigraphie et paléoenvironnement de l'intervalle Cenomanien-Senonien inférieur dans le puits KES-1 de la marge d'Abidjan (Côté d'Ivoire)

BEHI ZOH DERRICK AURELIEN[1], KESSE Touvalé Marcel[2], YAO N'goran Jean-Paul[1], GBANGBOT Kouadio Jean-Michel[3], DIGBEHI Zéli Bruno[1]

[1]UNIVERSITE FELIX HOUPHOUET BOIGNY aurelienzoh@gmail.com, [2]Institut National Polytechnique de Yamoussoukro, [3]Université Jean Lorougnon Guédé

Treize échantillons (13) de déblais de forage allant des côtes 2630 m à 2400 m ont fait l'objet d'analyse biostratigraphique afin de déterminer l'âge et l'environnement de dépôt des sédiments provenant du forage KES-1. Ce dernier est situé dans la partie immergée (offshore) du bassin sédimentaire de la Côte d'Ivoire. Le tri a révélé la présence de 1003 individus dont 831 foraminifères planctoniques soit 82,85%, 98 foraminifères benthiques agglutinés soit 9,77% et 74 foraminifères benthiques calcaires soit 7,38%. Ces foraminifères ont été identifiés et utilisés pour la datation des formations traversées par le forage. Ainsi sur la base des premières ou des dernières apparitions de foraminifères planctoniques et des associations microfaunistiques, les âges déterminés sont le Cénomanien, le Turonien et le Sénonien inférieur (Coniacien). La diversité des foraminifères planctoniques et la présence de foraminifères benthiques ont permis la reconstitution du paléoenvironnement des fonds marins qui vont du néritique interne au type bathyal inférieur.

Mots clés: Analyse biostratigraphique, Paléoenvironnement, Cénomanien, Turonien, Sénonien.

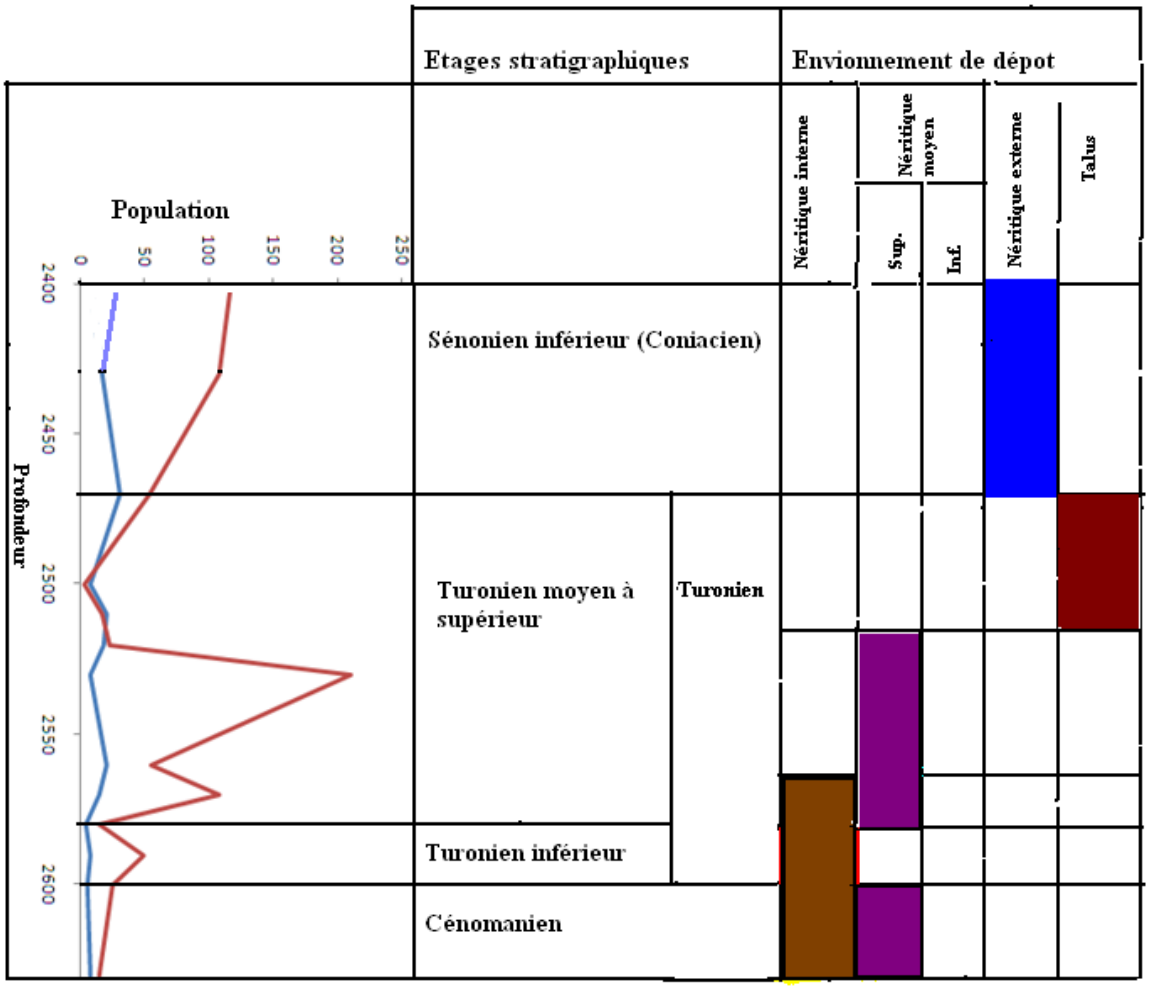

Figure 1: Courbe d'évolution des foraminifères et évolution paléoenvironnementale de l'intervalle Cénomanien-Sénonien inférieur (Coniacien) dans le puits KES-1

New insights to early Paleoproterozoic paleogeography of Superia supercraton from U-Pb zircon geochronology of mafic sills, dikes, and volcanics and detrital zircons from supracrustal successions of southern margin of Wyoming craton

Andrey Bekker[1], Nicholas Mammone[1], Kevin Chamberlain[2]

[1]University of California, Riverside andreyb@ucr.edu, [2]University of Wyoming

Paleogeography is a critical component in providing a backdrop for environmental changes, yet the early Paleoproterozoic reconstructions are still poorly resolved. The Snowy Pass Supergroup (SPS), a Paleoproterozoic supracrustal succession on the SE Wyoming craton (Medicine Bow Mountains - MBM), has been historically correlated with the Huronian Supergroup (HS) of the Superior craton based on similar lithostratigraphic patterns, suggesting deposition in the same basin between ca. 2.45 and 2.31 Ga, and indicating that these cratons were adjoined in the Paleoproterozoic Superia supercraton. The Phantom Lake Metamorphic Suite, underlying the SPS and SPG, contains a significant mode of ca. 2.45 Ga zircon ages. The mafic phase of the Baggot Rocks granite and Colberg Metavolcanics of the same suite also yielded the ca. 2.45 Ga ages, indicating the early Paleoproterozoic age for this suite and the ca. 2.45 Ga extensive, rift-related mafic magmatism on the southern margin of the Wyoming craton, correlative to that recorded by the basal HS units. Zircon age spectra for lithostratigraphically correlative units on the southern Wyoming and Superior cratons show strikingly similar, primarily Archean patterns, which, along with paleocurrent directions, establish provenance of both cratons for the shared basin. Most units of the SPS and Snowy Pass Group (SPG; Sierra Madre - SM) have detrital zircon age peaks at ca. 2.85 and 2.7 Ga, ca. 2.55 and 2.3 Ga modes are common for the uppermost formations, and five units throughout both successions contain minor peaks at ca. 2.45 Ga. Mafic sills in the MBM yielded CA-ID-TIMS U-Pb zircon ages of 2220 ± 8 Ma and 2094.3 ± 1.6 Ma that closely correspond to the ages of the Nipissing mafic intrusions in the HS and the Cauchon Lake dikes in NW Superior craton. Correlation between the HS and SPS breaks down in the upper SPS at the Nash Fork Formation, which bears unique detrital zircon age modes at ca. 2.2 and 2.1 Ga, whereas deposition of the HS was terminated before ca. 2.22 Ga when the Nipissing dikes intruded and shortly after a ca. 2.31 Ga volcanic event recorded by tuffs and volcaniclastic sediments of the Gordon Lake and Bar River formations. The matching detrital zircon ages to, globally unique, ca. 2.3 Ga mode recorded by these two units of the HS first appeared in the Lookout Schist of the SPS and steadily decreased upsection through the upper SPS, pointing to a similar, volcanic source. Maximum depositional ages for the uppermost formations of the SPS and SPG, the purportedly correlative Nash Fork and Slaughterhouse formations, are at 2081 ± 10 Ma and 2334 ± 20 Ma, respectively. The maximum depositional age and the youngest (2066 ± 9 Ma) concordant zircon age for the upper Nash Fork Formation correspond to that of the basal Animikie basin units (Denham Formation of the Mille Lacs Group in MN and East Branch Arkose of the Dickinson Group, MI) that have been linked to rifting, breakup, and ultimate separation of the Wyoming and Superior cratons at ca. 2075 Ma.

Multi-element paleoredox evaluation of the Kettle Point Formation: Comparison of thallium with the molybdenum and uranium redox proxies

Natasha Bell[1], Brian Kendall[1]

[1]University of Waterloo ncbell@uwaterloo.ca

Thallium (Tl) is a novel paleoproxy that is utilized to estimate global redox conditions during the deposition of ancient black shales. More specifically, stratigraphic decreases and increases in the Tl isotopic compositions of black shales indirectly records the surface area expansion and contraction of Fe-Mn crusts in oxic sediments, which reflects globally higher and lower dissolved oxygen within marine waters, respectively. However, the Tl redox proxy has not been thoroughly studied in relation to local depositional influences, such as local water column redox and sea-level fluctuations. The Gore of Chatham (GoC) core of the Late Famennian Kettle Point Formation was previously studied in regard to local depositional factors. An inverse correlation between molybdenum (Mo) and uranium (U) isotope ratios, and together with stratigraphic trends, indicate the local water column evolved from strongly euxinic to weakly euxinic moving stratigraphically upsection (Kendall et al., 2020). The uppermost Kettle Point shales from this core have low Mo isotope ratios and high Mo and vanadium (V) concentrations, which suggest a local Fe-Mn particulate shuttle influence (Kendall et al., 2020).

In this study, the same Kettle Point black shale powders from the GoC core were leached with 2M nitric acid (HNO3) to obtain authigenic concentrations of Tl and other trace metals, including Mo, U, V, rhenium (Re), and selenium (Se). The authigenic fractions were measured using a triple quadrupole inductively coupled plasma mass spectrometer (QQQ-ICP--MS). Authigenic Tl concentrations increase from moderately low (1 – 4 ppm) to high (4 – 14 ppm) moving stratigraphically upsection. Thallium has strong positive covariations with authigenic Re and Se concentrations, but weak correlation with total organic carbon and aluminum, suggesting that authigenic Tl is primarily located in early diagenetic pyrite, which is in agreement with previous studies. In addition, a moderate positive covariation of Tl concentrations with authigenic Mo and U concentrations, and with U isotope ratios, suggests a relationship between authigenic accumulation of Tl and the local extent of primary productivity, organic carbon burial, and sedimentary pyrite formation. However, a moderate inverse correlation between authigenic Tl concentrations and Mo isotope ratios also suggests that high Tl concentrations in the uppermost Kettle Point Formation arose from a Mn-oxide shuttle that delivered Tl and isotopically light Mo to euxinic sediments. The Tl isotope ratios of the GoC core will be measured to test these hypotheses, and to further explore local and global effects on Tl concentrations and isotope ratios in black shales.

Authigenic Clay Mineral Formation in Sulfate-Rich Saline Lakes

Jennifer Bentz[1], Ronald Peterson[2]

[1]Syncrude Canada Ltd-Research jennifer.bentz@queensu.ca, [2]Queen's University

Saline lakes are important for understanding authigenic clay mineral formation at surface temperature and pressure due to their fluctuating wet/dry cycles, variable redox conditions, and the high ionic strength of their solutions driven by evaporative concentration. Given their abundance, chemical variation, and sensitivity to the geochemical environment, authigenic minerals can be used to characterize the specific geochemical limits of the paleoenvironment they formed in and reconstruct past climates, but only after present day investigations of modern systems are well understood. To date, the majority of research has focused on large (>100 km^2) basins where concentric zonation of the sediments helps delineate detrital minerals near the basin's edge from authigenic minerals near the center. However, most of these large basins are dominated by bicarbonate-rich systems and little research has focused on sulfate-rich lakes due to the relative scarcity of large sulfate-rich basins, the small size of the basins that are present, and detritus rich sediments, all of which complicate their analysis and interpretation. Yet the number and diversity of these small endorheic basins makes them important for understanding clay mineral formation in sulfate-rich systems on Earth and on Mars--where an episodically dry lake has been identified in Gale crater with Mg-rich clay minerals and Ca-sulfates. This research summarizes the findings of micro-scale investigations of transects across the mudflats of 23 sulfate-rich saline lakes and salars from the Great Plains Region of Saskatchewan, Canada and the Sur Lipez Region of the Andean Plateau, Bolivia outlining the mineral assemblages present in the sediments and modes of authigenic clay formation. In the Great Plains region of Saskatchewan the lakes exhibit considerable variation in their size, chemistry, and heterogeneity of their sediments. Despite their extreme diversity however, similarities can still be found between the mudflat sediment layers when grouped into sediment class based on texture (clay-rich, till-rich, and sand-rich) and specific layers of authigenic clay formation can be identified. On the Bolivian Altiplano, the majority of the salars exhibit silicate-rich, brackish environments expected to favour sepiolite formation, yet any evidence of sepiolite was absent in the samples analyzed. Instead, the authigenic mineral assemblages were dominated by Mg-smectite and a hydrated and highly disordered variety of talc (aka “kerolite”) due to the unique biogeochemical conditions present. The results from both of these regions highlight the importance of understanding clay mineral formation in modern sediments in order to use these assemblages to reconstruct past environments on Earth and Mars.

Early Paleozoic magmatism, tectonics, and establishment of the western Laurentian passive margin: evidence of an ancient magma-poor rift system?

Luke Beranek[1]

[1]Memorial University of Newfoundland lberanek@mun.ca

Tonian to Cambrian rift processes that fragmented supercontinent Rodinia resulted in lithospheric breakup, thermal subsidence, and establishment of the Cordilleran passive margin system along the western edge of Laurentia. Although the early Paleozoic platformal successions of western North America are typically characterized in the literature by tectonically quiescent conditions, coeval basinal assemblages from northwestern Canada to the southwestern United States contain late Cambrian and Ordovician igneous rocks and extension-related base metal occurrences that are not easily reconciled with published models for Ediacaran to early Cambrian passive margin formation. A number of research groups have recently used zircon CA-TIMS geochronology, stable and radiogenic isotope geochemistry, paleontology, and field stratigraphic studies to revise these models and better resolve the timing and spatial patterns of syn- to late-rift and post-breakup tectonism along western Laurentia. The establishment of the Cordilleran passive margin was diachronous, with the timing of lithospheric breakup or the rift to post-rift transition ~530 Ma (late Fortunian) in parts of the western United States, ~520 Ma (early Stage 3) in the southern Canadian Cordillera, and ~500 Ma (Drumian-Guzhangian) in the northern Canadian Cordillera. Late Cambrian to Early Ordovician alkaline mafic rocks along the western Laurentian margin, including recently studied 488-483 Ma and 473 Ma intrusions, submarine lava flows, and related volcaniclastic facies in central Yukon, were generated during regional- to plate-scale extension that continued at least 20 Myr after breakup. The timing and geochemical fingerprints of post-breakup magmatism in northwest Laurentia are analogous to those recognized along the modern Newfoundland (SE Grand Banks)-Iberia conjugate margins and provide compelling evidence for the Cordilleran margin to represent an ancient, North Atlantic-type magma-poor rift system. Post-breakup, off-axis magmatism in northwest Laurentia was apparently driven by release of tensile stresses during the prolonged initiation of seafloor spreading. Mesozoic plate convergence has obscured most distal elements of the ancient magma-poor rift system in the Cordilleran orogen, but slivers of serpentinized ultramafic rocks outboard of the Laurentian shelf-slope transition in central Yukon and northern Nevada may represent exhumed mantle domains that similarly characterize the distal regions of the modern Newfoundland-Iberia margins. 3D gravity modeling studies have furthermore interpreted these key lithospheric elements beneath accreted terranes in Yukon and eastern Alaska. Future research opportunities on early Paleozoic tectonics and magmatism are plentiful; examples include the significance of NE-trending lineaments (e.g., Liard and Fort Norman lines, St. Mary-Moyie and Snake River transfer zones) on magmatism and base-metal mineralization in western Canada and western United States.

Mercury Heat Flow in an Fe-Si and Fe-Ni-Si Core

Meryem Berrada[1], Richard Secco[1], Wenjun Yong[1]

[1]University of Western Ontario mberrada@uwo.ca

It has been suggested that Mercury's magnetic field may be generated by either a thin shell dynamo or a deep core dynamo, where the dynamo is operating at depth under a stably stratified liquid outer core. Thermal evolution models adopting the second scenario suggest the heat flow through the core-mantle boundary (CMB) becomes sub-adiabatic within 1 Gyr after formation. A sub-adiabatic Fe-Si core has been shown to stimulate inner core solidification and consequently magnetic field generation. We calculate the adiabatic heat flow at the top of the core in two scenarios, from direct measurements of electrical resistivity on potential core compositions in the Fe-Ni-Si system. The main core composition is in the Fe-Si system (2-17 wt%Si) in the first scenario and Fe-10wt%Ni-10wt%Si in the second scenario. Measurements of electrical resistivity were carried out at 3-24 GPa and at temperatures in the liquid state in a 1000 ton and 3000 ton multi-anvil press using a 4-wire method with two Type-C thermocouples and a polarity switch. The compositional integrity of the samples was confirmed with electron-microprobe analysis of quenched samples from various pressure and temperature conditions. As the Si content increases, the change in electrical resistivity upon melting decreases until it becomes negligible. The electronic component of thermal conductivity, calculated via the Wiedemann-Franz law, of Fe-10wt%Ni-10wt%Si is similar to that of Fe-8.5wt%Si at comparable pressure and temperature conditions. The calculated adiabatic heat flow is compared to thermal evolution models in order to assess the age of Mercury's inner core, which is indicated by the beginning of a sub-adiabatic heat flow through the CMB. Our results suggest a range of values between 0.08 and 0.22 Gyr after formation, depending on the core composition and CMB temperatures.

Oxygen fugacity and volatile content of three Neoarchean alkaline intrusions potentially related to gold mineralization

Patrik Berthoty[1], Lucie Mathieu[1], Stéphane De Souza[2], Zsuzsanna Tóth[3]

[1]Université du Québec à Chicoutimi patrik.berthoty1@uqac.ca, [2]Université du Québec à Montréal, [3]Laurentian University

Intrusion-related gold systems (IRGS) are increasingly recognised in Neoarchean greenstone belts such as the Abitibi greenstone belt of the Archean Superior craton, and they correspond to polymetallic disseminated mineralisation genetically related to alkaline intrusions and other magma types. Such mineralization forms in greenstone belts during the syntectonic period, which is a time of increased tectonic activity leading to craton stabilization. The syntectonic phase corresponds to a shift in magmatism from high volume, K-poor tonalite-trondhjemite-granodiorite (TTG) suites to smaller volume, sanukitoid, high-K calc-alkaline (HKCA) and alkaline series intrusions, and includes orogenic events leading to the formation of orogenic gold deposits. The petrogenesis and gold potential of syntectonic magmatism remains debated. The objective of this study is to constrain the petrogenesis of Archean alkaline intrusions and their potential to transport gold through the crust. This contribution concentrates on magmatic systems with poorly evaluated potential, and summarizes the key factors that control gold solubility, i.e. oxygen activity and volatile content. The studied alkaline intrusions vary significantly in size and composition. They include the Dolodau and Otto stocks in the Abitibi greenstone belt, and the Jackson pluton in the eastern Wabigoon subprovince. The Dolodau stock is an example of a two-phase, small volume syenite-carbonatite complex associated with Au-Ag-W showings in a mylonitic shear, whereas the Jackson pluton and the Otto stock are unmineralized. The polyphased Otto stock syenite, however, has an unclear relationship with a pyroxenite-hornblendite unit that is associated with a Cu-Au-Pt-Pd mineralization. The Jackson pluton is a large-volume quartz-biotite monzonite intrusion.

Preliminary petrography shows that the Otto stock contains more magnetite, apatite and titanite than the Dolodau intrusion. In the Dolodau, sulphides, predominantly pyrite, are only present in the rim of the intrusion, whereas the core is devoid of sulphides and accessory phases, with the exception of minor magnetite. A small amount of sulphides, including pyrite and chalcopyrite, occurs in several phases of the Otto stock but are unrelated to gold. Ongoing mineral chemistry on trace elements in zircon, apatite and amphibole will provide insights into the oxygen fugacity and volatile contents of the melts, and enable comparison with well-documented magmatic systems. Hence, comparing the physico-chemical properties of these intrusions provides insight into their potential to generate gold mineralization and helps constraining the IRGS metallogenic models in the Superior craton.

A micromechanics-based model to determine quantitative kinematic information from flanking structures

Ankit Bhandari[1], Dazhi Jiang[1]

[1]Western University abhand3@uwo.ca

Determining quantitative information such as incremental strain and kinematic vorticity number from rocks is useful for understanding regional tectonics. Flanking structures, which are deflections in linear or planar fabric elements around a cross-cutting element such as a fracture, vein or dyke, can be used to derive such information. Previous numerical models of flanking structures are mostly limited to special cases that consider the cutting element as either a frictionless free slipping surface or a rigid material. Models with more variable rheology of the cutting element are limited to 2-D cases with low finite strains and high aspect ratios of the cutting element as well as special cutting element's initial orientations. These limitations cannot capture the realistic variability of natural flanking structures. In this work, we apply a micromechanics-based model to simulate 3-D flanking structures around cutting elements of varying rheological properties, initial orientation and shapes. We regard a cutting element as an Eshelby inclusion embedded in a viscous medium and use numerical exterior Eshelby solutions to determine velocity fields around the element. These velocity fields are then used to simulate the deflection of marker elements surrounding the cutting element, under any given macroscale flows. Our modelling reproduced all flanking structure types recognized in nature. In contrast to the previous models, our results show that all three types of flanking structures with antithetic (a-type), no- (n-type) and synthetic (s-type) displacement along the cutting element can be formed around any cutting element rheologically stronger than the embedding medium such as a dyke or a strong mineral inclusion. The a-type flanking structure may transition into an s-type depending on cutting element's viscosity and macroscale finite strain. We applied a reverse model approach to extract quantitative information such as incremental strain, kinematic vorticity number of the macroscale flow and cutting element's viscosity ratio to the surrounding medium, from a flanking structure surrounding quartz veins for some natural examples from the Cross Lake group, Cross Lake greenstone belt, Manitoba.

Early Paleozoic seas of offshore eastern Canada: insights from the lithology and palynology of lower Paleozoic strata from the Labrador margin

Nikole Bingham-Koslowski[1]

[1]Natural Resources Canada nikole.bingham-koslowski@canada.ca

The lower Paleozoic stratigraphy of the Labrador margin is poorly understood due to the scarcity of samples from the offshore, the occurrence of diagenetic alteration (dolomitization), and a lack of up-to-date biostratigraphic data. Paleozoic rocks, known from seven wells on the Labrador margin, represent erosional remnants primarily associated with Cretaceous syn-rift half grabens: the wells are Hopedale E-33, South Hopedale L-39, Tyrk P-100, Gudrid H-55, Roberval K-92, Indian Harbour M-52, and Freydis B-87. Due to limited data, it was previously unknown whether the Paleozoic strata in these seven wells could be correlated with one another, or how they relate to other Paleozoic occurrences in Davis Strait and on Baffin Island. Of the seven wells, only four contain conventional cores in the Paleozoic interval: Gudrid H-55, Roberval K-92 (cores #6 and #7), Indian Harbour M-52, and Freydis B-87 (cores #1 and #2). Of these six cores, lithological analysis shows that five are composed of carbonate rocks, with dolostones present in Gudrid H-55 and Roberval K-92 and fossiliferous limestones occur in Indian Harbour M-52 and Freydis B-87 (core #2). The sixth core, Freydis B-87 (core #1), consists of siliciclastic lithologies, including massive and laminated sandstones, siltstones, and mudstones with varying degrees of bioturbation. Similar lower Paleozoic fossil assemblages are observed in Indian Harbour M-52 and Freydis B-87 (core #2), but the pervasive dolomitization of the Gudrid H-55 and Roberval K-92 cores prevents meaningful correlations among the four wells. Previous palynological studies on the Labrador margin Paleozoic strata provide no further clarification as they report a range of ages for the seven wells, including Ordovician, Devonian, Carboniferous, and undifferentiated Paleozoic. Thus, a new palynological study was conducted on all seven wells and recorded, for the first time, consistent Ordovician ages spanning an interval from possible Middle Ordovician (Tyrk P-100, Roberval K-92, and Indian Harbour M-52) to Katian (Indian Harbour M-52). This study resulted in the Paleozoic strata in Gudrid H-55 and Roberval K-92 being reassigned to the Ordovician from the Carboniferous; to new age determinations for the Paleozoic rocks of South Hopedale L-39 and Tyrk P-100 (formerly undifferentiated Paleozoic); and to the refinement of the Paleozoic ages to stage level in Hopedale E-33, Indian Harbour M-52, and Freydis B-87. The findings of this study imply that the Paleozoic of the Labrador margin is syndepositional and therefore correlatable, and is similar in age to other lower Paleozoic strata from Canada's northern Atlantic margin.

A Complete Water-Ice Cloud Record of the Phoenix Mission Derived from Modeling the MET Temperature Record

Grace Bischof[1], Brittney Cooper[2], Haley Sapers[1], John Moores[1]

[1]York University gbischof@yorku.ca, [2]Gemini North Observatory

Water on Mars is dynamic: exchanging between subsurface ice beneath the regolith and water-vapour in Mars' atmosphere. Under certain atmospheric conditions, water vapour condenses into water-ice clouds that can provide a marked effect on local meteorology. On Mars, the thin atmosphere allows thermal infrared radiation to pass through, meaning temperatures near the surface are driven by the balance of incoming solar flux and outgoing surface longwave flux. However, when radiatively active water-ice clouds are present, longwave radiation is reflected back toward the surface, warming the near-surface environment [1]. This work investigates the amount of flux re-radiated toward the surface by water-ice clouds by modelling the thermal forcing at the Phoenix mission landing site. Phoenix, at a high latitude of 68.2ºN, studied the water cycle in the polar regions of Mars. During the mission, the Surface Stereo Imager and LIDAR onboard made many positive detections of water-ice clouds. Near the halfway point of the mission, shallow, surface-based clouds formed each night near local midnight. By 01:00 local true solar time (LTST), a second cloud base was present 4 km in the atmosphere. This cycle repeated nightly, with clouds dissipating by the late morning [2]. The flux reflected by water ice clouds, R, is calculated using an energy balance equation to model the near-surface temperature at the mission site. R varies within the model in 2-hour increments and is controlled as an independent parameter. For each sol of the mission, the modeled temperature is compared to the temperature data collected in situ by Phoenix to determine the diurnal change in R. Modelling shows that reflected flux from water-ice clouds contributed to a warming effect of the near-surface environment at the Phoenix lander. In the first third of the mission, between 0 and 10 W/m2 of reflected flux were observed throughout the night, starting no earlier than 20:00 and ending no later than 10:00 LTST. From Sol 50 to Sol 80, small R values were determined each night from the modeling, with several sols showing no reflected flux at all. A noticeable increase in reflected flux is seen throughout the night after Sol 90, with values upwards of 20 W/m2. This analysis suggests water-ice clouds were present at the site before they were observed by the lander. The decrease in R in the middle of the mission coincides with warmer diurnal temperatures a few sols after summer solstice. In turn, when diurnal temperatures decrease toward the end of the mission, this is contrasted by an increase in reflected flux.

References: 1. Wilson R.J. (2007) Geophys. Res. Lett., 34, L02710. 2. Dickinson C. et al (2010) Geophys. Res. Lett., 37, L18203.

Geophysical Imaging of a Seeping Tailings Dam in West-Central Newfoundland, Canada

Andrew Blagdon[1], Alison Leitch[1]

[1]Memorial University of Newfoundland aleitch@mun.ca

Centered over a volcanogenic massive sulfide ore deposit in west-central Newfoundland island, the abandoned Gullbridge mine produced 94,000 tonnes of copper concentrate from 2.8 million tonnes of ore from 1967 to 1972. The tailings facility employs an earth-filled dam separating a valley impoundment reservoir, containing 1.8 million m3 of subaqueously deposited copper tailings, from an adjacent wetland. Historical seepage of tailings water through the embankment is concerning as it poses a risk of seepage related erosion. This is the likely failure mechanism which, combined with a poor dam foundation, contributed to a spectacular breach in December 2012, where a 35 m long section of the embankment collapsed, casting dam material, water and tailings into the wetland. Since then, the breach has been repaired and the dam modified by lowering the crest, introducing a spillway and decreasing the downstream slopes. However, in the last few years seepage through the dam has been observed in two locations: a main area near the centre of the dam wall, and a secondary area near the northern end. As part of ongoing dam monitoring, several geophysical techniques were used to investigate the embankment structure. These were: spontaneous-potential (SP), ground-penetrating radar (GPR), magnetics, direct-current resistivity (DCR) and ground conductivity (EM31). The most useful techniques for this project were GPR and SP. SP data indicate that tailings water seepage through the embankment, at the known seep areas, is irregular in both space and time. GPR data suggest that in the main area of seepage this flow of tailings water is constrained to poorly compacted 'core' materials surrounding an historical decant structure. Magnetics was useful in confirming the location of metal-bearing structures used in the past for controlling the dam water level. DCR and EM31 surveys, which involve electrical current flow over broad volumes, were more of use in exposing the general dam structure, which includes a 1-2 m thick resistive dry layer over a damp, much more conductive layer. An embankment long DCR survey showed markedly increased resistivity over the main seep region, presumably caused by draw-down of the water table in this region. EM31 was most useful for mapping tailings distribution in the adjacent wetland, probably mostly related to the 2012 breach.

Cumulative Effects and the Impact Assessment Act

Kevin Blair[1]

[1]Impact Assessment Agency of Canada kevin.blair@canada.ca

The new Impact Assessment Act (IAA) came into force on August 28, 2019, repealing the Canadian Environmental Assessment Act, 2012 (CEAA 2012), and transforming the the Canadian Environmental Assessment Agency into the Impact Assessment Agency of Canada (the Agency). Impact assessment is a planning and decision-making tool to assist project design and to ensure appropriate measures are in place to mitigate impacts. Under this new Act, the Agency's mandate and responsibilities have been expanded as the single federal organization responsible for impact assessment and the Crown coordinator for Indigenous consultation on designated projects. In leading these assessments, the Agency is responsible for assessing the positive and negative environmental, economic, social and health effects of designated projects, including cumulative effects. The IAA calls for a broadened consideration of cumulative effects beyond environmental effects, but it also provides new tools, including regional and strategic assessment, that can help inform the understanding of cumulative effects from a broader perspective. The Agency proposes to provide a presentation outlining key aspects of the new IAA legislation, focussing on how cumulative effects are considered under the Act, how new tools under the Act can support a better understanding of cumulative effects, and opportunities for sharing results.

Halite-hosted fluid inclusion gases: a direct measurement of ancient atmospheric gases

Nigel Blamey[1], Uwe Brand[2]

[1]Western University nblamey@uwo.ca, [2]Brock University

The evolution of oxygen and its timing has influenced many factors of our planet including animal life, ore deposits, surface weathering and the chemistry of the oceans. Earth's atmosphere currently comprises ~21% oxygen but it was not always like that. It has been the desire of scientists to quantify the ancient atmospheric oxygen level, starting with modeling by Berner, followed by a variety of indirect analytical methods (including RSE's, other trace elements, and isotopes) but to date the only direct analytical approaches have been Fryer and Wagener (1970) and the Blamey group (Blamey et al., 2016; Blamey and Brand, 2019; Brand et al., 2021). The direct analytical approach analyses halite-hosted fluid inclusion gases by mass spectrometry. The advantage of halite is that it: grows at the atmosphere-brine interface or within inches of it; can easily be verified as primary; is uncontaminated; and modern samples across 4 continents give a similar oxygen value. Many indirect analytical approaches have not been validated against modern environments and in several cases, deep marine sediments have been used which are clearly disconnected from the atmosphere. The only known calibration attempt using trace elements is the study by Steadman et al. (2020). The primary halite inclusions are analysed in vacuo using incremental crushing and the released gases are analysed by quadrupole mass spectrometry. Standards take the form of calibration gas mixtures, modern atmosphere, and four in-house fluid inclusion gas standards. Halite from the 2.0 Ga Onega Basin (Russian Karelia) give O2 measurements that range from 14.2-18.4 % (68-88 % PAL), whereas Mesoproterozoic halite from the Sibley Grp. (Canada) confirms ~3.6 % oxygen (17 % PAL) at ~1.45 Ga. Neoproterozoic halite from the Browne Fmn. (Australia) confirms 10-11 % atmospheric oxygen at ~815 Ma. Approaching the Ediacaran, halite measurements give 17.3 % O2 and during the Cambrian atmospheric oxygen reached 19 %. However, by the mid- to late-Ordovician oxygen level was down to ~16%. At the Ordovician-Silurian boundary, the atmospheric oxygen was 18.8% ±1.1%. Atmospheric oxygen levels have fluctuated over the past 2 billion years and prior to that, there is a need to use approaches that are calibrated to modern geochemistry. The Neoproterozoic and Mesoproterozoic have not been anoxic as inferred by some RSE studies and since 2.0 Ga there has been adequate oxygen to support the evolution of animal life. It is the abundance of oxygen that drove animal life in the Precambrian and these data explain the presence of eukaryote life as far back as 1.65 Ga. Analysing halite-hosted fluid inclusion gases have been vital in measuring atmospheric oxygen levels in deep time but the limitation is the lack of primary halite older than 2.0 Ga. This is where indirect analytical approaches will be valuable provided that they can be calibrated against modern environments or against direct analyses.

Western- and Eastern-type ultramafic massifs of the Mirdita ophiolite, Albania: a Jurassic example of oceanic core complex and its possible links to VMS mineralisation

Adina Bogatu[1], Alain Tremblay[1], Meshi Avni[2], Jean Bédard[3], Joshua Davies[1], Giselle Sauvé[1]

[1]UQAM bogatu.adina@gmail.com, [2]Tirana University, [3]GSC

The Jurassic Mirdita ophiolite of Albania contains distinctive Eastern- and Western-type mantle and crustal rocks. Geological mapping of selected sections combined with geochemical and structural analysis suggests that the Western-type Mirdita ultramafic massifs represent a fossilized oceanic core complex (OCC). The relationship between Western and Eastern massifs, their respective crustal covers, and VMS mineralisation is still under debate, as is the position of the spreading center associated with the crustal sequence(s) and the OCC's genesis. In the crustal sequence of Eastern-type massifs, multiple VMS deposits define a north-south trend above the inferred OCC-related detachment. Studies on modern OCCs suggest that a 'locus of hydrothermal discharge' frequently occurs in the hanging wall of OCC-forming detachments (de Martin et al., 2007). Temporally linking VMS mineralisation with OCC genesis in the Mirdita ophiolite would help to clarify the position of the spreading center from which it originated. Eastern-type massifs are dominantly harzburgites with a thick arc-related IAT intrusive and extrusive crust, late gabbro dykes of boninitic affinity, and display an apparently classical Moho mantle/crust transition. At the Moho, mantle harzburgites grade through a ~2 km wide transition zone dominated by dunitic harzburgite, dunite, and chromititites, which are succeeded by layered peridotites and pyroxenites, and then by layered gabbroic cumulates. Conjugate, moderately to steeply, E-SE dipping normal faults affect both Eastern- and Western-type crustal rocks, consistent with east-west trending extension. Western-type mantle massifs are harzburgitic to lherzolitic, and have a thinner MORB-like crustal sequence of tholeiites and locally prominent isotropic gabbros. The Western-type mantle/crust transition is exposed in the Puka and Krabbi massifs. Here, the upper mantle and the lower crust display zones of lithospheric ductile flow 10s of m wide that are marked by cataclastic breccias and amphibolitized layers of crustal and mantle rocks affected by an intense NNW- to NE-dipping ductile shear fabric. Crustally-derived amphibolites contain possible igneous zircons and syn-detachment titanites. An ongoing U-Pb dating analysis of zircon and titanite should help to establish the temporal association, if any, between VMS mineralisation (Bathonian à Oxfordian) and OCC genesis. The presence of extension structures at the mantle/crust contact in the Western-type massifs, the west-to-east geochemical variations, and the thickening of the ophiolitic nappe from west to east are consistent with east-over-west emplacement of the Mirdita ophiolite. This is supported by the occurrence of VMS deposits in the hanging wall of the inferred detachment suggesting an easterly spreading center, possibly located in the Vardar zone more than 100 km away.

Distribution, Age and Duration of Volcanism of the Cheakamus Basalts, Garibaldi Volcanic Belt, British Columbia

Annie Borch[1], James Russell[1], Rene Barendregt[2], Steven Quane[3], Alex Wilson[4]

[1]University of British Columbia aborch@eoas.ubc.ca, [2]The University of Lethbridge, [3]Sea to Sky Fire & Ice Geopark, [4]Minerva Intelligence

The Cheakamus basalts comprise a group of Quaternary olivine tholeiite lavas in the Garibaldi volcanic belt of British Columbia, distributed within the Cheakamus River and Callaghan valleys 12 km SW of Whistler. The Cheakamus basalts are >26 km in length, with lateral extents of 1-2 km, reaching thicknesses of 80 m where exposed in sections through paleo-valleys. Previous studies, while asserting basic distributions and lithological, geochemical and paleoenvironmental results, do not establish the basalt's eruptive source, definitive age, distribution, or eruptive duration. Work in the 2020-2021 field seasons increased the areal extent of the lavas toward previously unmapped regions proximal to volcanic edifices of the Mount Cayley Volcanic Field. New 40Ar/39Ar dating places the stratigraphically oldest, bedrock-contact lavas at 23.9 ±15.7 Ka, tightening previous high-uncertainty ^{14}C and K-Ar ages. A paleomagnetic sampling program indicates all Cheakamus basalt lavas were emplaced within the same paleomagnetic moment, the duration of which is estimated at less than 5,000 years. The basalts record evidence for both subaerial and ice/meltwater-contact cooling surfaces, as well as syn- and post-emplacement erosional features such as glaciated interflow surfaces and incised meltwater channels. Our paleomagnetic results suggest that both the eruption and the multitude of paleoenvironments and glacial erosional events recorded by the Cheakamus basalts were not protracted but rather occurred during a rapid and dynamic moment in time.

Cumulative impacts of oil and gas development in the Fox Creek area, west-central Alberta: preliminary results and considerations from a groundwater quality study

Geneviève Bordeleau[1], Christine Rivard[2], Roxane Lavoie[3]

[1]Institut national de la recherche scientifique genevieve.bordeleau@ete.inrs.ca, [2]Natural Resources Canada, [3]Université Laval

Between 2012 and 2019, the Geological Survey of Canada (GSC) has built a strong expertise in developing and conducting state-of-the art environmental studies to evaluate the potential impacts that unconventional oil and gas (O&G) exploitation may have on shallow groundwater resources. One of the key components of these multidisciplinary studies is hydrogeochemistry, where both compositional and isotopic data from residential and monitoring water wells have been used to develop a strategic, methodical approach that allows determining the origin of dissolved hydrocarbons in shallow aquifers, with greater certainty than was possible before. This approach was first developed in eastern Canada, where unconventional O&G activities have been limited to exploration only (Québec) or moderate levels of commercial production (southern New Brunswick). In 2019, it was decided to apply this approach to a region that has been subjected to more intensive O&G production, thus presenting a higher risk of industrial contamination. In this context, it appears essential to take into account the cumulative impacts that originate from the higher number of O&G wells and their associated activities (e.g. building roads and pipelines, pumping water for hydraulic fracturing). With a 50-year history of O&G production, and currently over 775 O&G wells in a relatively small 700 km2 watershed, the Fox Creek area of west-central Alberta was considered an ideal location for such a project. For the hydrochemical component of the project, various maps were used to start planning a strategic network of monitoring wells (ideally installed upstream, mid-basin, downstream; and both near and far from O&G wells) and chemical analysis plan. However, it soon became clear that the possibility to install wells and other monitoring equipment was governed by: 1) land claims (formal agreements with companies must be signed to access roads and potential drilling sites), 2) companies being sold and bought (which often jeopardizes agreements), 3) protected land regulations (whereby permits are required to install instruments on several sites), and 4) adverse meteorological and road conditions (access roads are often closed). The scientific design of the project was thus profoundly affected by these factors, which may at term limit its ability to effectively measure cumulative impacts. This presentation outlines the hydrogeochemical results obtained so far, but perhaps most importantly, it is a tale of obstacles, incongruities, as well as unexpected collaboration and potential solutions that revolve around the assessment of cumulative environmental impacts. The specific difficulties may differ from one industrial region to another, but most large Canadian resource development areas requiring cumulative impact assessments involve similar challenges, which stresses the need to join forces and reflect about better strategies to improve and facilitate these assessments.

Petrogenesis and gold potential of sanukitoid magmatism

Esther Bou[1], Lucie Mathieu[1], Michel Jébrak[2], Jean-François Moyen[3]

[1]Université du Québec à Chicoutimi esther.bou1@uqac.ca, [2]Universté du Québec à Montréal, [3]Université de Lyon, LGL-TPE, UJM-UCLB-ENSL-CNRS

Sanukitoids are granitoids formed mainly during the Neoarchean. Some of these intrusions are associated with porphyry Au deposits (e.g., O'Brien stock of the Abitibi greenstone belt, Canada). The petrogenesis of sanukitoid magmatism and the association of such magmas with auriferous magmatic-hydrothermal mineralizing systems remain debated. The aim of this study is to evaluate the contribution of sanukitoids to the gold and base metals fertilization of the Neoarchean upper crust. Sanukitoids form intrusions emplaced at the end of the main deformation stage (syn- to post-tectonic) that led to craton stabilization. They are characterised by high contents in both compatible (high Mg#, Ni, Cr) and incompatible (LILE) elements pointing to a metasomatized mantle source. The metasomatic agent may correspond to: 1) TTG magmas derived from the partial melting of a metamorphosed hydrated basalt; 2) oceanic fluids; and 3) melts derived from sedimentary rocks of the subducted plate. The differentiation of sanukitoids (fractional crystallisation, assimilation) also impacts their capacity to transport metals through the crust and requires evaluation. Constraining the petrogenesis of these magmas will provide insights into parameters that are paramount to understand the distribution of gold and base metals in ancient magmatic systems, and these parameters are source composition, partial melting depth, oxidation state and volatile contents. This study focuses on plutons of the Abitibi greenstone belt, i.e., the Opémisca, Barlow, O'Brien, and East Sullivan pluton, and these fertile and barren intrusions will be compared to gain insights into magmatic-hydrothermal systems. The differentiation process, for these intrusions, will be documented using numerical modelling. In addition, physico-chemical parameters (fO2, S and Cl contents) will be measured using amphibole, zircon and apatite chemistry. In this contribution, preliminary results are presented. Future research will use LA-ICP-MS analysis to evaluate the gold and base metals content of mafic phase and to model the distribution of metals in sanukitoid magmatic systems.

Pressure-Temperature-time constraints for high temperature metamorphism and deformation in deep crustal shear zones: Shuswap Metamorphic Complex, British Columbia

Sarah Bowie[1], H. Daniel Gibson[1], Brendan Dyck[2], Laurent Godin[3], Kyle Larson[2]

[1]Simon Fraser University sarah_bowie@sfu.ca, [2]University of British Columbia Okanagan, [3]Queen's University

The Shuswap Metamorphic Complex (SMC) in south-central British Columbia exposes highly deformed, deeply exhumed crustal rocks. This panel of rocks is bounded by two west-dipping shear zones at its eastern and western flanks - the Monashee décollement (MD) and the Okanagan Valley-Eagle River fault system (OVF), at the basal and upper boundaries, respectively. With decreasing structural levels, rocks between these faults exhibit a kinematic reversal from top-to-the-northeast directed shear to top-to-the-west directed shear. This project aims to characterize a series of pressure-temperature-time-deformation (P-T-t-d) paths across the SMC at the latitude of the Trans-Canada highway - a transect representing a complete crustal section of the SMC. Key questions addressed include: 1) How does the timing of fabric development compare across the transect? 2) How do peak metamorphic conditions compare across the transect? 3) What do the structural and metamorphic trends observed imply about the kinematic reversal and the tectonic development of the SMC? Four metapelitic samples collected across the SMC were chosen for metamorphic phase modeling. Preliminary results and phase equilibria calculations indicate that these rocks reached peak temperatures of 750-850ºC and pressures of 8-10 kbar. In situ U-Pb-Th dating of zoned monazite grains in the same samples was completed via LA-ICP-MS. Detailed microstructural analysis and monazite petrochronology, linked with trace element analysis and garnet compositional data, indicates that high-temperature metamorphism and deformation predominantly took place between 55-45 Ma at the uppermost structural levels of the transect within the ductile portion of the OVF, and between 100-60 Ma across the transect, including at the structurally deeper levels nearest the MD. Given that the footwall rocks of the MD experienced NE-directed shearing as young as 50 Ma, our results suggest that shearing and metamorphism decrease in age with depth, except at the uppermost structural levels along the OVF where ductile deformation occurred as young as 45 Ma. Therefore, by ~50 Ma it appears that this portion of the SMC behaved as a high metamorphic-grade crystalline nappe, with opposite-sense shearing localized at the upper and lower boundaries, rather than deforming via penetrative ductile flow throughout the entire thickness of the structural panel.

3D geological-geophysical and geochemical modeling of the Russell Lake property and its uranium occurrences (Saskatchewan, Canada)

Joseph Bravo[1], Irvine Annesley[2], Zoltan Hajnal[3], Tobias Bauer[4]

[1]ESNG - Université de Lorraine jabravo1992@yahoo.com, [2]ESNG - Université de Lorraine/ Dept. Geological Science of the University of Saskatchewan, [3]University of Saskatchewan, [4]Luleå University of Technology

The Paleoproterozoic to Mesoproterozoic Athabasca Basin, northern Saskatchewan, is well known for hosting the world's highest grade uranium deposits. The basin has been widely explored, and most near-surface deposits have already been discovered. Nowadays, deeper basement-hosted U deposits are being targeted; increasing the need to develop new strategies, e.g., 3D/4D geomodeling, to reduce the time and cost of exploration at depth. By developing a comprehensive 3D geological model of the Russell Lake property, our research is adding knowledge to basement-hosted U exploration. A lengthy exploration history in the study area has provided large, freely available databases; including geological, geophysical, and structural data/maps, multi-scale edge analysis images, EM conductors, and seismic profiles. Using Emerson SKUA-GOCAD and Geoscience ANALYST Pro, two models were developed. First, a large-scale regional to district-scale model (eastern Athabasca) was built based on 3D objects; free from the Saskatchewan Geological Survey. Then, geological/geophysical maps and regional seismic reflection (Line S2B) added detail to the model. This allowed us to: 1) distinguish the regional NE trend of the Wollaston fold-thrust belt, 2) recognize lithotectonic domains and subdomains boundaries (e.g., Wollaston-Mudjatik Transition Zone (WMTZ) and its geophysical characteristics), and 3) associate the fault system generations to their respective thermotectonic stages. Secondly, a district- to property-scale model was built based on the interpretation of migrated high-resolution seismic profiles of two seismic reflection surveys (2004, 2005) on the Russell Lake Property. The modeling workflow incorporated visual inspection/interpretation of the seismic profiles and correlation with geological/geophysical maps, as well as structural lineament analysis of the study area. The seismic interpretation and handling of other geophysical data utilized additional software packages (OpendTect, SeismiGraphix, Oasis Montaj, ArcGIS, QGIS). Finally, available geochemical data was added to the 3D model to provide additional constraints. The results reveal the structural complexity of the area; related to Trans-Hudson Orogen events. The model suggests that large basement-sourced fault zones of different generations (trends and ages) interconnected (in part) through time served as pathways/precipitation sites for mineralizing fluids. The reactivations of these zones are associated with offsets in the basement-sandstone unconformity and late sub-vertical brittle events. Moreover, some large fold-and-thrust structures appear listric to a prominent seismic reflector at depth; whereby younger brittle faults intercept and offset this reflector. The latter in conjunction with basement age constraints may imply its initial age. In summary, the 3D model allows the identification of zones with favorable structural-geochemical features that can host U mineralization (e.g., the M-Zone).

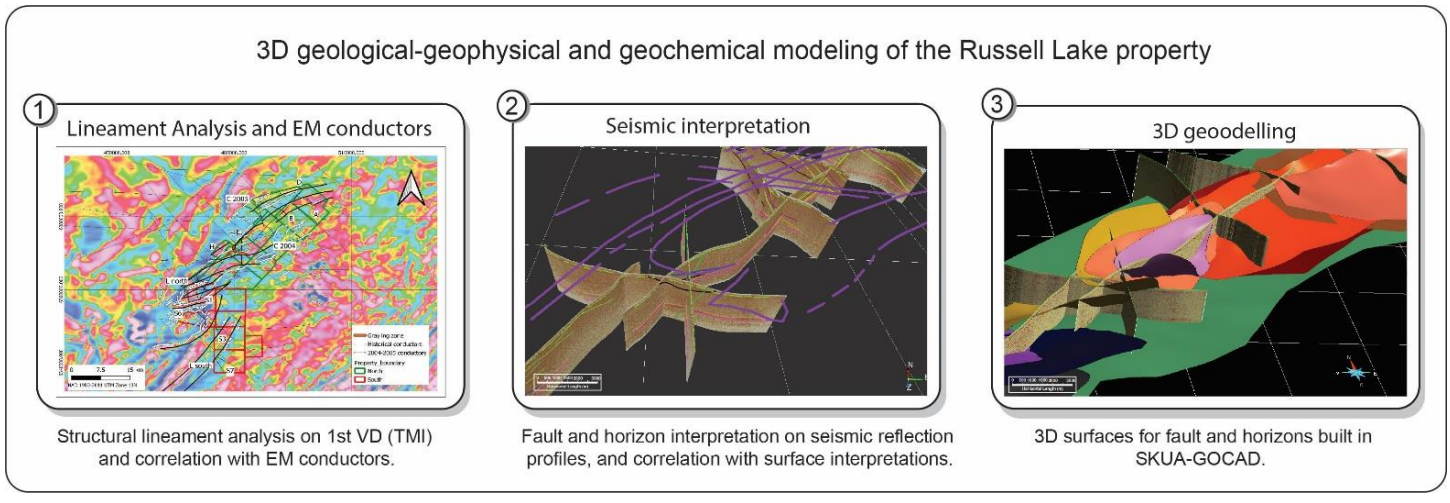

Closing the 'North American Magmatic' Gap: Crustal evolution of the Clearwater Block from multi-isotope and trace element zircon data

Daniel Brennan[1], Paul Link[2], Zheng-Xiang Li[1], Laure Martin[3], Tim Johnson[1], Noreen Evans[1], Jiangyu Li[1]

[1]Curtin University daniel.brennan1@postgrad.curtin.edu.au, [2]Idaho State University, [3]University of Western Australia

Along the west-central margin of Laurentia, within the Priest River and Clearwater metamorphic complexes, rare exposures of crystalline basement rocks of the Clearwater Block show 'North American Magmatic Gap' (NAMG, ca. 1.61-1.49 Ga) ages. Elsewhere in this region, crystalline basement rocks are buried beneath thick deposits of the overlying Mesoproterozoic Belt Supergroup and younger Neoproterozoic-Phanerozoic sequences. The unique combination of magmatic basement ages and the detrital zircon components (which also include NAMG detrital ages) within the overlying Mesoproterozoic Belt Supergroup strata, has led researchers to identify the Clearwater Block region as a key tie-point for Proterozoic paleogeographic reconstructions. Some researchers even speculate that Proterozoic supercontinent events may have stranded exotic (possibly Australia, Antarctica or South China associated) basement terranes within the Clearwater

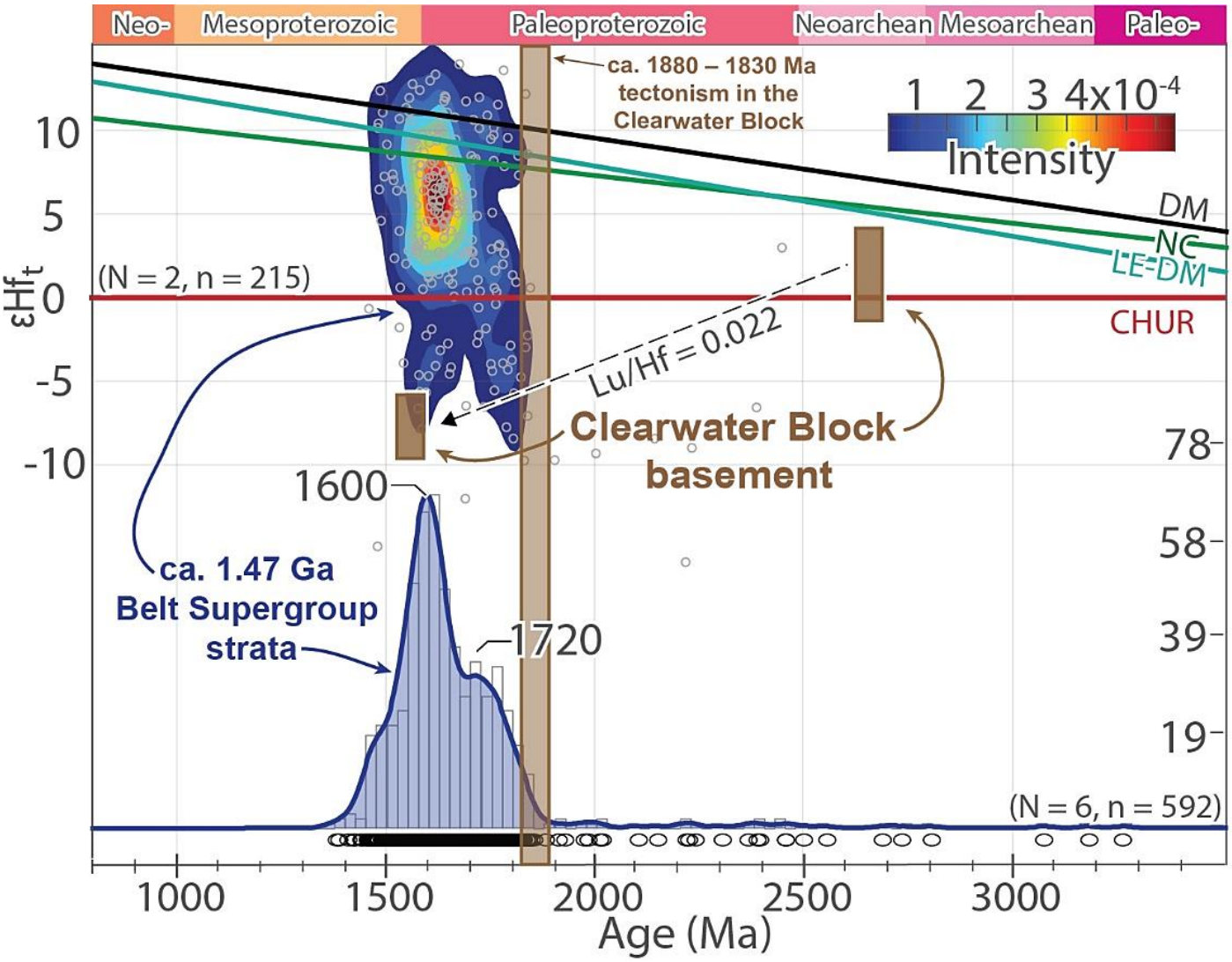

Block. However, to date, a comprehensive multi-isotopic dataset for the Clearwater Block which allows for a more conclusive interpretation of potential non-Laurentian connections has not been presented. We report new Lu-Hf and O isotope data and trace element results of zircon grains, along with new U-Pb results, for basement rocks of the Clearwater Block. Collectively, these results indicate a crustal evolution for the Clearwater Block that consists of: 1) ca. 2.67 Ga juvenile mantle-derived crustal growth as evident by mantle-

like $\delta^{18}O$ and supra-CHUR (3.5 to -0.5) εHft values, 2) complete or partial "Trans-Hudson age" resetting of some zircons within this ca. 2.67 Ga crust as recorded by ca. 1.86 Ga zircon U/Pb ages with low (< 0.1) Th/U ratios and retention of mantle-like $\delta^{18}O$ values, and 3) ca. 1.58 Ga "NAMG" magmatism that records mantle-like $\delta^{18}O$ but sub-CHUR (-5.5 to -9.7) εHft values. We interpret the ca. 1.58 Ga magmatism to be consistent with (perhaps plume-driven) reworking of the Clearwater Block's ca. 2.67 Ga lower crustal reservoir. Consequently, these results support a Laurentian origin for NAMG-age magmatism within the Clearwater Block but confirm the necessity of non-Laurentian sources for juvenile (εHft) NAMG-age detrital zircon grains in the overlying ca. 1.47 Ga lower Belt Supergroup strata. Figure 1: Igneous zircon U/Pb and Lu/Lf results for the Clearwater Block basement rocks (in brown) compared to the detrital zircon U/Pb and Lu/Hf components (in blue) found in the overlying Mesoproterozoic Belt Supergroup strata. Mantle evolution lines include: ca. 3.8 Ga late extraction (LE-DM), new crust (NC), and depleted mantle models (DM). CHUR-Chondritic Uniform Reservoir.

Microstructures and Paleopiezometry of Orogenic gold quartz veins in the Archean Abitibi Greenstone Belt

Crystal Brochard[1], Michel Jébrak[1], Stéphane De Souza[1]

[1]UQAM crystal-bro@outlook.com

Most Archean orogenic gold deposits are associated with major faults such as the Cadillac-Larder Lake fault zone (CLLFZ) in the Superior craton, and are related to second-order structures that host quartz vein systems. Quartz is commonly deformed in areas such as fault or shear zones, either at a macro- or a micro-scale. Microstructures induced by quartz deformation give indication on the P-T conditions during deformation. EBSD (electron backscatter diffraction) mapping of grain orientation is a powerful tool that has been developed more extensively since the end of the 20th century to complement the microstructural observations. It allows to measure the mean recrystallized grain size in a sample, that can be use in quartz piezometer equations to determine a flow stress. Microstructural observations and EBSD analysis are usually done on mylonite or quartzite samples from shear zones. This study tests the validity of such methods on hydrothermal auriferous quartz veins, to better constrain the conditions of quartz vein deformation along the CLLFZ and evaluate the effect of depth and host rock on the microstructures. Samples were collected from drill holes, underground mines, and outcrops in 23 gold deposits and showings from the Kirkland Lake, Rouyn-Noranda and Val d'Or

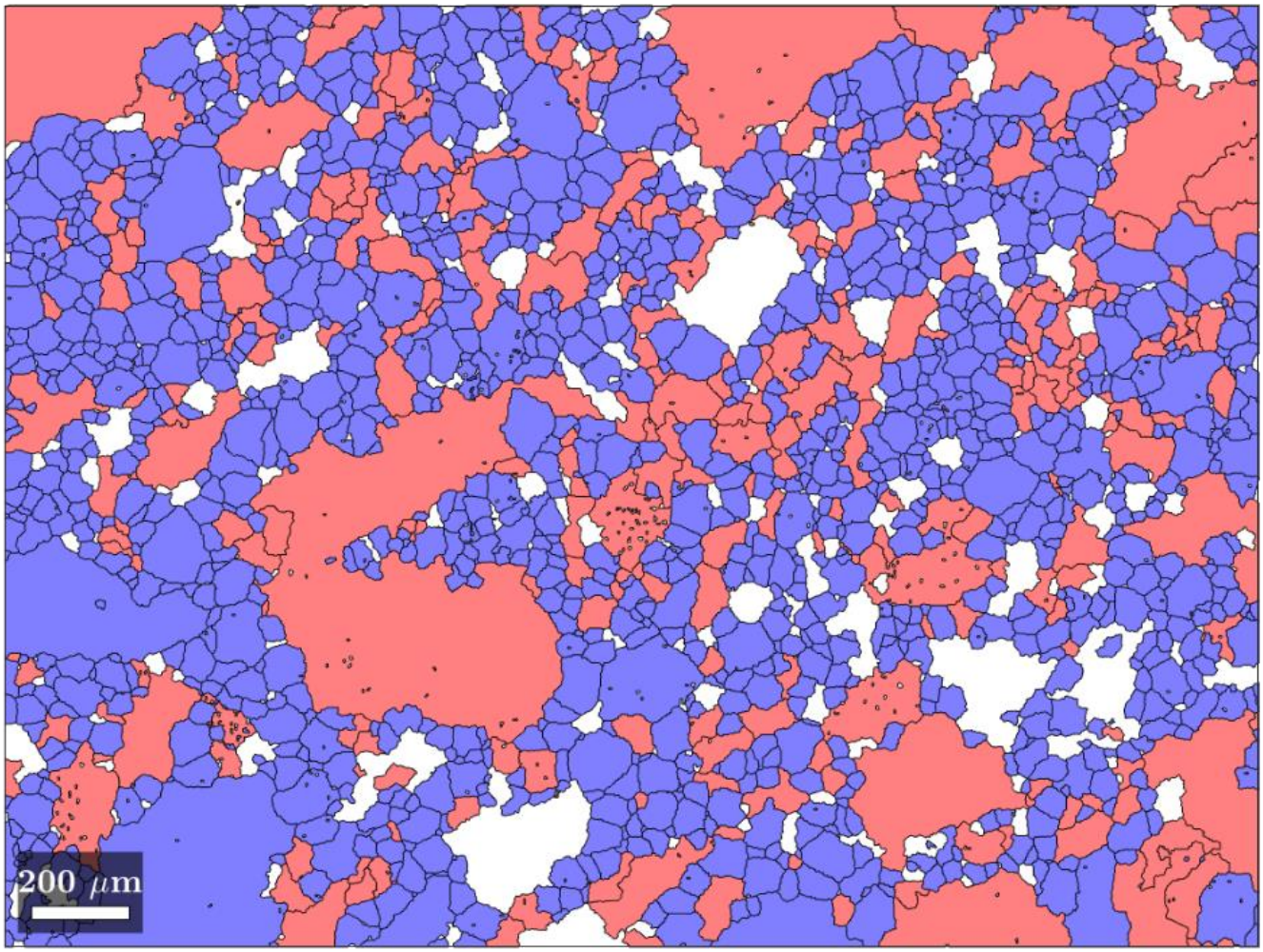

Figure: EBSD map after post-processing, sample SIL2 (Silidor deposit, Rouyn-Noranda). Red grains depict relict grains and blue ones the recrystallized grains. SRG is the dominant dynamic recrystallization mechanism.

districts. The host rock varies from intermediate plutonic rocks to mafic volcanic and sedimentary rocks. In thin sections, all these samples exhibit typical textures of recovery and dynamic recrystallization of quartz (DRX). Preliminary results demonstrate a variation of dominant DRX mechanism relative to CLLFZ segment. Bulging mechanism (BLG, low temperature-high strain rate) is predominant in the west (Kirkland Lake and Rouyn-Noranda segments), except for the Silidor deposit, which is hosted by an intrusive rock and exhibits microstructures typical of subgrain rotation (SGR, medium temperature and strain rate). SGR-dominated textures and BLG-SGR transition characterized by core-and-mantle structure are found in the Joannes and Malartic segments. Further east along the Val-d'Or segment, textures are more complex and vary relative to space and depth. Several samples show textures that might indicate multiple events of recrystallization. Dominant DRX mechanism and recrystallized grain size vary significantly between the hinge and limb of a folded vein in Dubuisson. The grain boundary migration mechanism, typical of higher-T and lower strain rate, is only found at the Nordeau deposit, which is the closest to the Grenville front, and at the Goldex mine at a depth of ~427m. Samples analyzed with EBSD display a log-normal distribution of recrystallized grain sizes that is consistent with data for natural samples such as mylonite. These data underline therefore the potential of quartz veins microstructures to contribute to the evaluation of conditions of deformation and their evolution.

Evidence of early postglacial paleoearthquakes from mass transport deposits buried within glaciolaustrine sediments in northeastern Ontario-western Quebec, Canada

Greg Brooks[1]

[1]Natural Resources Canada greg.brooks@canada.ca

Eastern Canada is a large region of recently glaciated terrain where evidence of early postglacial, glacially-induced seismic activity should be abundant, but there are no confirmed examples of early postglacial seismogenic faults. Nevertheless, research within the basin of Glacial Lake Ojibway, which persisted between 10.57-8.47 ka cal BP in northeastern Ontario-western Quebec, revealed mass transport deposits (MTDs) buried at differing stratigraphic levels within the glaciolacustrine sediments throughout the region. Detailed mapping of the sub-bottom deposits at Dasserat, Duparquet, and Dufresnoy lakes, located 24 to 38 km apart, near Rouyn-Noranda, Quebec, identified 26 MTD event horizons of which 15 contain three or more MTDs. High-resolution, relative dating control using varves indicates: that the event horizons span a period of about 450 varve years (between 9.4-8.95 ka cal BP); that one set of identically-aged event horizons is common to each lake; and another set is common to two lakes. The 15 event horizons containing three or more MTDs are interpreted to be evidence of 11 paleoearthquakes of Mw5 or larger. The confidence of each interpretation is weighted from low to high, reflecting the relative strength of the MTD signature in each event horizon (moderate (three to five MTDs) or strong (more than six MTDs)), and evidence of common- or similar-aged MTD signatures at two or more distinctly separate locations. The event horizon with the most numerous and widespread MTDs in each lake formed in the identical varve year 1483 (about 9.1 ka cal BP). These occurrences are part of a regional MTD signature present in other lakes and in subaerial exposures that enclose an area of about 14,600 km2 in northeastern Ontario and western Quebec. This signature is best explained by a strong paleoearthquake of about Mw 7.3. The interpreted paleoearthquakes occurred when early postglacial uplift had diminished moderately, but was still high, compared to mid-Holocene and late Holocene rates. This record, thus, is likely representative of a period of elevated, early postglacial seismicity associated with rapid crustal unloading from the waning of the Laurentide Ice Sheet.

Impact and Split Water

Eckart Buhlmann[1]

[1]UCN - Northern Manitoba Mining Academy ebuhlmann@ucn.ca

VMS deposits occur with iron-rich mafic to intermediate rocks of volcanic appearance. The rocks are dark grey, fine grained and chloritized. They have a Co>Ni ratio. Levels of Fe, Ti, and P values are elevated. The Co>Ni ratio is a sign of a marine impact event. The impactor will split large quantities of water into oxygen and hydrogen. The hydrogen escapes into space due to the extreme heat, leaving oxygen behind to oxidize any iron from its Fe** state to the Fe*** state. In this state iron cannot participate in the forming of olivine as olivine can only accommodate Fe** but no Fe***. As a result, the olivine will use available Mg** and Ni** to crystallize forsterite. Mg** and Ni** will form forsteritic Ni-rich olivine cumulate thereby locking up Mg**, and Ni**. The crustal abundances for cobalt (29 ppm Co) and nickel (102 ppm Ni) suggest that the ratio in rock should be similar but not the reverse. This is an important detail. The rocks have undergone a strong Ni-depletion. In the Mg and Ni rich komatiites and nearby Fe-rich tholeiitic lavas of Munro township in Ontario Olivine cumulates are common. Forsterite reaches >90% MgO and 0.5% NiO. These results indicate that the iron-rich tholeiitic lavas are a product of Mg silicate depletion rather than of iron enrichment. The reversed Co/Ni ratio in the iron-rich tholeiitic lava can be understood as the result of Ni depletion together with Mg-silicate depletion (into the olivine cumulates). The chemical data show that the SIC contains several tens of meters of 'icelandite' like rocks in the section between the norite in the footwall and the transition zone in the hanging wall. This icelandite material is chemically very similar to Carmichael's 'icelandite'. It has the typical increased levels of iron, titanium and phosphorus.

Impact Associated Distal Landscape Modifications: An Assessment of Extended Deposits and Flows on Mars

James Burley[1], Livio Tornabene[1], Gordon Osinski[1], Alfred McEwen[2], Nicolas Thomas[3], Gabriele Cremonese[4]

[1]University of Western Ontario jburley6@uwo.ca, [2]University of Arizona, [3]University of Bern, [4]National Institute of Astrophysics

Impact cratering is an important and ubiquitous process throughout our solar system, playing a significant role in the formation and evolution of planetary surfaces. The vast majority of ejecta deposition, and any landscape modification associated with them, are generally reported to occur within the range of proximal ejecta deposition (~5 crater radii) (Stoffler and Grieve 2007; Osinski et al. 2011). However, more recent observations indicate the deposition of additional continuous deposits well beyond this range on both the Moon and Mars (Ghent et al. 2010; Tornabene et al. 2019). Additionally, extensive surface modification features including dry and viscous flows have been identified thus far around one recent cluster of small impact craters (Ds < 50m; Burleigh et al. 2012) and one of the best-preserved complex craters on Mars - Hale Crater (D ~125 x 150 km) (Tornabene and McEwen 2008; Jones et al. 2011; El-Maarry et al. 2013; Grant and Wilson 2018) respectively. Using visible/near-infrared (VNIR) from HiRISE (McEwen et al. 2007), CaSSIS (Thomas et al. 2017), the Mars Reconnaissance Orbiter's Context (CTX) camera (Malin et al. 2007), and thermal infrared images from THEMIS (Christensen et al. 2004), we identify additional candidate craters that appear to possess evidence of extensive ejecta deposition and flow features that modify the surrounding landscape. Through a global survey of the best-preserved martian craters from the most up-to-date catalogue based on Tornabene et al. (2012) (n=290), 31 candidates have been identified. The objectives of our assessment focus on determining the nature, extent and origin of these modifications observed beyond the layered ejecta deposits of our candidate craters. To achieve these goals, we will morphologically and morphometrically characterize these features through detailed morphologic mapping to A; assess the geologic context and stratigraphic relations of these features to other units and features within their geologic setting, and B; determine the distribution of these features to see if they are indeed within a fixed radial distance of proposed parent craters, and thereby related to them. We will also make morphometric constraints using stereo-derived DTMs (e.g., slope information) to assess wet vs. dry mechanisms of emplacement. Here we identify two specific examples of these putative impact-related deposits and flows at craters much smaller than Hale Crater: Noord (D=7.5km) and a currently unnamed 9.5-km crater (located at -29.405°N, 351.319°E in the Noachis Terra region). Based on morphology, observed topographical interactions, and slope values, the flows appear to be viscous in nature, as the range of observed slopes (?5-25º) is inconsistent with models for martian dry flows (e.g., Kleinhans et al. 2011; Atwood-Stone and McEwen 2013). Our conference presentation will provide an update on our latest results from our detailed investigation of these two candidate craters.

MAPLE: a Simple Optical Meteorological Station for Mars

Charissa Campbell[1], Christina Smith[2], Alex Innanen[1], Jacob Kloos[1], Heather Stone[1], John Moores[1]

[1]York University ccamp93@yorku.ca, [2]Oberlin College

Earth, Mars exhibits seasonal variations that range from dust storms at perihelion to thin cirrus-like water-ice clouds at aphelion. Several orbiters and surface spacecraft have studied these atmospheric phenomena, but not enough data has been returned to fully characterize the Martian atmosphere. Of importance is the Planetary Boundary Layer (PBL) located in the lower atmosphere (2-10 km) and the most active part of the Martian atmosphere. Orbiters have the advantage of observing multiple locations but struggle with the lower atmosphere due to terrain, increased opacity and atmospheric turbulence [1]. Currently three operational surface spacecraft - Mars Science Laboratory (MSL), Perseverance, and InSight - can study the local atmospheric conditions but are limited to only a few weekly observations. It has been suggested that a minimum of 15 dedicated meteorological stations are needed to validate the Global Climate Models (GCMs) that are used to fill in the gaps in Martian atmospheric studies [2]. To achieve this, the Mars Atmospheric Panoramic camera and Laser Experiment (MAPLE) will be a small, low powered optical meteorological station dedicated to studying atmospheric aerosols.

Based on [3], it was proven with the Phoenix lander that using the Surface Stereo Imager (SSI) to observe the lidar in the atmosphere is a valid way to study the properties of aerosols within the PBL. However, only four observations were obtained as the SSI had a small field of view and using two separate instruments simultaneously made the observation prohibitively operationally complex to carry out more than a few times. Building on these limitations, MAPLE optimizes the amount of returnable science while minimizing power and cost. For example, MAPLE will have a panoramic camera, capturing the full sky. The ability to observe the full sky in a single frame reduces the operational complexity as no motion is needed. The addition of multiple low-powered lasers at different wavelengths adds the ability to study the shape and size of the aerosols. MAPLE will also investigate cloud and dust optical depth, wind direction and cloud morphology using similar techniques previously validated. Data acquired from MAPLE will help validate current Martians GCMs that use estimated parameters for particle microphysics. Increasing the accuracy of Martian climate models will both improve our understanding of Martian atmospheric dynamics and benefit future human exploration by determining if any hazards exist, especially pertaining to global dust storms.

[1] Kleinbohl A., et al., JGR"

Relict glacial terrains in west central Keewatin Sector of the Laurentide Ice Sheet, Northwest Territories and Nunavut

Janet Campbell[1], Pierre-Marc Godbout[1], Isabelle McMartin[1], Philippe Normandeau[2]

[1]Geological Survey of Canada janet.campbell3@canada.ca, [2]Northwest Territories Geological Survey

he Glacial Map of Canada portrays several regions devoid of glacial lineations and eskers, or with discordant ice-flow indicators in the Keewatin Sector of the Laurentide Ice Sheet (LIS). Such regions have been theorized to reflect relict terrains preserved under cold-based ice during all or part of the last glaciation cycle. Recent field-based work in other regions of mainland Nunavut has confirmed the presence of relict/cold-based terrains. One of the largest proposed relict landscapes lies in the largely unmapped west-central region of the Keewatin Sector. To ascertain the nature of this terrain and the adjacent glacial landscapes, targeted surficial geological studies were conducted in an area between Aylmer Lake, Northwest Territories (NWT) and the western edge of the Thelon Wildlife Sanctuary in the NWT and Nunavut. New field-based observations and striation measurements were combined with till composition data to reveal the complex glacial history of the study area. Spatial variability in the region's geomorphology, and surface material composition, thickness and degree of weathering, are the result of changes in substrate lithology, depositional environments, basal thermal conditions (warm-based to cold-based) and paleo-ice flow dynamics. Much of the landscape is warm-based to deglacial warm-based, dominated by west to northwest-trending streamlined and/or thicker drift terrains. However, the landscape of the central part of the study area is bedrock-controlled; dominated by low relief, weathered and frost-shattered outcrops, and block fields, consistent with relict terrains preserved under non-erosive, cold-based ice conditions. Relative terrestrial cosmogenic nuclide abundances confirm that this central region is a relict landscape that has been preserved under cold-based conditions during the last glacial cycle. Small patches of warm-based ice terrains with very thin, discontinuous veneers of till are interspersed throughout this central area. Rare glacially sculpted and polished outcrops record older south-southwest flow(s). The south margin of the study area is bounded by the west-northwest trending Exeter Lake esker system, a major deglacial feature. The results of this research have implications for mineral exploration in this under-explored region and will inform paleo-ice dynamic modelling of the LIS.

NRCan contribution number: 20200639

Micro X-ray diffraction characteristics of experimentally shocked andesine anorthosite

Fengke Cao[1], Roberta Flemming[1], Matthew Izawa[2], Steven Jaret[3], Jeffrey Johnson[4]

[1]Western University fcao23@uwo.ca, [2]Institute for Planetary Materials Okayama University, [3]American Museum of Natural History, [4]Johns Hopkins University Applied Physics Laboratory

Plagioclase feldspars are common rock-forming minerals that can be used to evaluate the shock pressures in impact craters, or shock stages in meteorites, by petrographic and spectroscopic methods (e.g., Raman and infrared). The deformation features of shocked plagioclase include undulatory extinction, mosaicism, and PDFs at low to moderate pressure levels and transformation to diaplectic glass at moderate to high levels, which are barometers to generally recognize different stages of shock metamorphism. Here we studied 11 experimentally-shocked intermediate composition plagioclases (andesine-rich) with different shock pressures (0-56 GPa) using in situ micro-X-ray diffraction (μXRD) techniques. These andesine samples are acquired from St. Urbain, Canada. They are monomineralic rocks that contain ~ 95% andesine (An36-46), with minor amounts of quartz and potassium feldspar, with grains < 5-10 mm. Shock recovery experiments were performed on these samples using a flat plate accelerator, with the intent to load different peak pressures from 15.8 to 56.5 GPa. Finally, thin sections were made from these experimentally shocked specimens. Their 2D XRD images display a continuous dispersion of diffracted X-ray intensity or "streaking" along the Debye rings when loaded pressure is between 0-34.5 GPa. The average streak length over the sample tends to increase with increasing pressure from 0 to 34.5 GPa. Andesine shows decreasing diffraction intensities with increasing pressure from their XRD patterns. The transition from crystalline to amorphous is gradual. Andesine starts to be partially amorphous at ~ 29 GPa and becomes almost completely amorphous (diaplectic glass) at ~ 47 GPa. The full width at half maximum ($FWHM_X$) along the Debye rings for samples, with shock pressures less than 34.5 GPa, were obtained through peak fitting and then used to calibrate the shock effects of plagioclase phases in Martian regolith breccias and Lunar samples (Apollo). The estimated maximum shock pressure of andesine grains in Martian breccias is ~ 22.4 GPa, with a maximum $FWHM_X$ of 6.59°. In summary, this work provides a quantitative approach to assessing shock metamorphism of plagioclase and will help to constrain the degree of shock in rocks containing plagioclase feldspars. In the future, micro-XRD will be used to study experimentally-shocked (0-56 GPa) albite-rich and bytownite-rich rocks as a function of pressure and composition. There will also be a detailed shape analysis of the X-ray scans.

Shock-induced deformation of pyroxene in Martian Regolith Breccias

Fengke Cao[1], Roberta Flemming[1], Matthew Izawa[2], Takuya Moriguti[2], Carl Agee[3]

[1]Western University fcao23@uwo.ca, [2]Institute for Planetary Materials Okayama University, [3]Institute of Meteoritics, University of New Mexico

Northwest Africa (NWA) 7034 and its pairings (e.g., NWA 7475, 8171, 11220) are pieces of a polymict regolith breccia representing the very ancient Martian crust. We have studied the shock effects in pyroxene minerals from these four Martian breccia pairings using in situ micro-X-ray diffraction (μXRD) and Raman techniques. Pyroxene has been identified as the second most abundant phase in crystal clasts in Martian breccias; nevertheless, no highly shocked pyroxene has been reported in Martian breccias from previous studies. Minerals show a characteristic behavior when subjected to impact shock waves. Ultra-high pressures and temperatures cause crystal deformation, which is often preserved permanently in minerals. The shock-induced metamorphism recorded in minerals is a fingerprint of impact events and can be used to retrieve information about the shock level. In the case of pyroxene in Martian breccias, both orthopyroxene (opx, including enstatite) and clinopyroxene (cpx, including augite, diopside, pigeonite) are prevalent in Martian breccias. 2D XRD images of most pyroxene crystal clasts show streaking along the Debye rings, i.e., progressive elongation of diffraction spots, caused by the strain-related mosaicity associated with shock events. The degree of the streakiness along the Debye rings – here defined by the angular parameter chi (X) and quantified as the full width at a half maximum along X ($FWHM_X$) is acquired by peak fitting using WIRE software. Preliminary results indicate a maximum average $FWHM_X$ for enstatite is ~ 8.52°. Raman spectra among the same enstatites show no systematic changes in Raman peak positions or widths. The most strained diopside grain (in NWA 7034) has an $FWHM_X$ value of 8.32°. The only observed augite crystal clast (in NWA 8171) has an $FWHM_X$ = 3.71°. In augite, the width of the Raman peak at ~ 665 cm-1 shows a distinct variation (22 cm-1) between different locations selected from this single clast. Preliminary micro-XRD studies underline that micro-scale shock-induced deformation is quantifiable in minerals, but their response may vary depending on their crystal structures and chemical compositions, as is illustrated here by comparison between enstatite, diopside, and augite. The evaluation of shock level among these pyroxene minerals will require three different calibration scenarios, with the intent to assess the cumulative shock experienced by the ancient Martian crust, as preserved in its rock-forming minerals. In the future, SEM-EDS and EPMA will be done to acquire chemical data for pyroxene, and EBSD will be performed to check the microstructural deformation features on some highly shocked grains.

Phengite and amphibole contributed to partial melting in retrogressed eclogite from the Algonquin terrane, western Grenville Province

Wentao Cao[1], Hans-Joachim Massonne[2], Hans-Joachim Massonne[3], Xiao Liang[2]

[1]State University of New York at Fredonia cao@fredonia.edu, [2]China University of Geosciences, [3]Universität Stuttgart

Retrogressed eclogites from the Algonquin terrane in western Grenville Province were studied to better understand the partial melting of metabasite. The studied samples are retrogressed eclogite with relics of a peak-pressure mineral assemblage consisting of garnet, omphacite, amphibole, phengite, biotite, and rutile. Strong retrogression produced various exhumation- and melt-related textures indicating a complex post-peak pressure history. Rutile is only found in the core of garnet, whereas ilmenite-bearing assemblages predominate in the garnet rim and the matrix. Symplectite of diopside + plagioclase + amphibole replaced former omphacite, and that of amphibole + plagioclase forms a corona around garnet.

Both mesoscopic and microscopic textures in the studied retrogressed eclogites indicate that they were partially melted. Leucocratic veins without external connection, present in the sampled mafic pod at outcrop scale, are interpreted as crystallized pockets of melt which derived internally. Polymineralic inclusions of plagioclase + K-feldspar ± ilmenite ± biotite ± amphibole ± apatite ± sulfides in garnet crystallized from melt, which was captured during garnet growth and reacted with the host. Cusps of plagioclase into the boundaries of other phases (e.g. garnet and clinopyroxene) mimic the original melt-solid interface. Neoblasts of garnet with euhedral crystal faces were formed as a peritectic phase during eclogite melting. Isochemical phase equilibrium modeling of the studied samples along with compositional isopleths of chemically zoned garnet yielded an exhumation path from 1.7 ± 0.1 GPa, 680 ±50 °C to 1.3 ± 0.1 GPa, 920 ± 50 °C. Along this path, the modal content of melt increased in response to the breakdown of phengite and amphibole along with involvement of omphacite and rutile. The melt crystallized during cooling and equilibrated at 0.6 to 0.8 GPa, 710 to 750 °C, estimated using empirical thermobarometry. This study shows that metabasite from Proterozoic collisional orogens can be partially melted on the exhumation and heating path through phengite- and amphibole-dehydration melting.

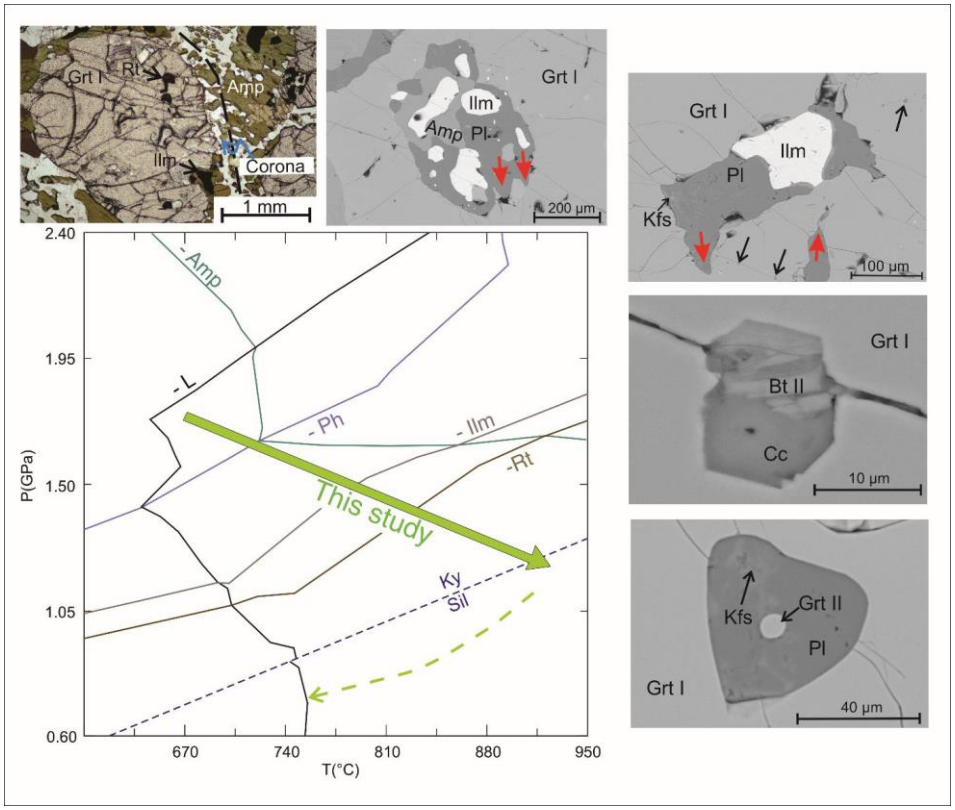

Sulfide Analysis of the Fenelon Gold Deposit, Québec

Joy Carter[1], Daniel Gregory[1]

[1]University of Toronto joy.carter@mail.utoronto.ca

The Abitibi Greenstone Belt is the most important gold-producing area in Canada and one of the most important globally. Until recently, the primary focus of exploration endeavors has been in the southern Abitibi due to abundant rock exposure at surface. Increasing effort is now being expended to explore the northern Abitibi, which has a high probability to contain undiscovered mineral wealth. The Fenelon Gold deposit, situated along the Sunday Lake Deformation Zone in the northern Abitibi, is the focus of this research project. In this presentation, we will discuss sulfide textures and chemistry related to gold mineralization at the Fenelon Property. Using a combination of reflected light microscopy, scanning electron microscopy (SEM), and Laser Ablation Inductively Coupled Plasma Mass Spectrometry (LA-ICP-MS), we establish the relationship between sulfide and gold precipitation in the Fenelon deposit. The two main areas of known gold mineralization at the Fenelon Gold Property are known as the Area 51 and Tabasco zones. Area 51 mineralization is hosted in quartz veins that crosscut the main intrusive body in the Property, the Jeremie Diorite. Tabasco mineralization is associated with a shear zone along the contact between the Jeremie Diorite and the host sediments. The textures and chemistry of sulfides from both zones reveal the relationships of the sulfides to the gold mineralization and significantly enhance the understanding of mineralization at the Fenelon deposit. This study contains the first observations of sulfide textures and chemistry at the Fenelon Property and is among the few studies that have been conducted along the Sunday Lake Deformation Zone. Its success will encourage future exploration in the northern Abitibi and generate growth for the Canadian mineral resource sector.

3-D bedrock hydrostratigraphy of southern Ontario: a regional framework for multidisciplinary subsurface management

Terry Carter[1], Charles Logan[2], Hazen Russell[2], Jordan Clark[3], Elizabeth Priebe[4], Melissa Bunn[2], Shuo Sun[5]

[1]Carter Geologic terry.carter@cartergeologic.com, [2]Geological Survey of Canada, [3]Oil Gas and Salt Resources Library, [4]Ontario Geological Survey, [5]University of Western Ontario

Southern Ontario is underlain by up to 1500 metres of sedimentary rock within the Michigan and Appalachian basins. Large volumes of groundwater occur in these rocks. Shallow bedrock aquifers, together with aquifers in the overlying surficial sediments, are important sources of potable groundwater for private water wells and municipal water supply systems, for agricultural irrigation, and as shallow energy storage-exchange systems such as heat pumps. Groundwater discharge to streams and wetlands supports surface aquatic habitats. At greater depths groundwater is increasingly saline; nevertheless, aquifers in these rocks have a variety of practical uses. Saline aquifers are utilized for disposal of saline oilfield water produced as a by-product of petroleum production operations, and, in the past, for disposal of liquid industrial wastes. In some parts of southern Ontario there is potential for CO_2 sequestration in deep brine aquifers. Hydrochemical and isotopic zonation of groundwater also provides supporting scientific knowledge to develop a safety case for long-term isolation of nuclear wastes in geological repositories in low-permeability aquitard units. At intermediate depths groundwater aquifers support a diverse but poorly understood microbial ecosystem dominated by sulphur proteobacteria and characterized by the rotten egg odour of dissolved H_2S. This "sulphur water" is a known corrosion hazard for unprotected steel and concrete in subsurface infrastructure such as tunnels, mine shafts, petroleum wells and foundations. Three-Dimensional modelling can promote and improve geological understanding of these groundwater systems by creating a spatial context that is easily viewed and understood and provides practical tools for interpretation, analysis and resource development. Digital 3-D models are also excellent tools for illustration of geological concepts for public education and outreach, and for training of the next generation of engineers and earth scientists. Two versions of a lithostratigraphic 3-D model for southern Ontario have been published, with 56 model layers covering 110,000 km^2 with a modelled volume of over 75,000 km^3. The models are based principally on data from petroleum wells. A new hydrostratigraphic model is being developed based on re-assigning lithostratigraphic model layers into 14 hydrostratigraphic layers

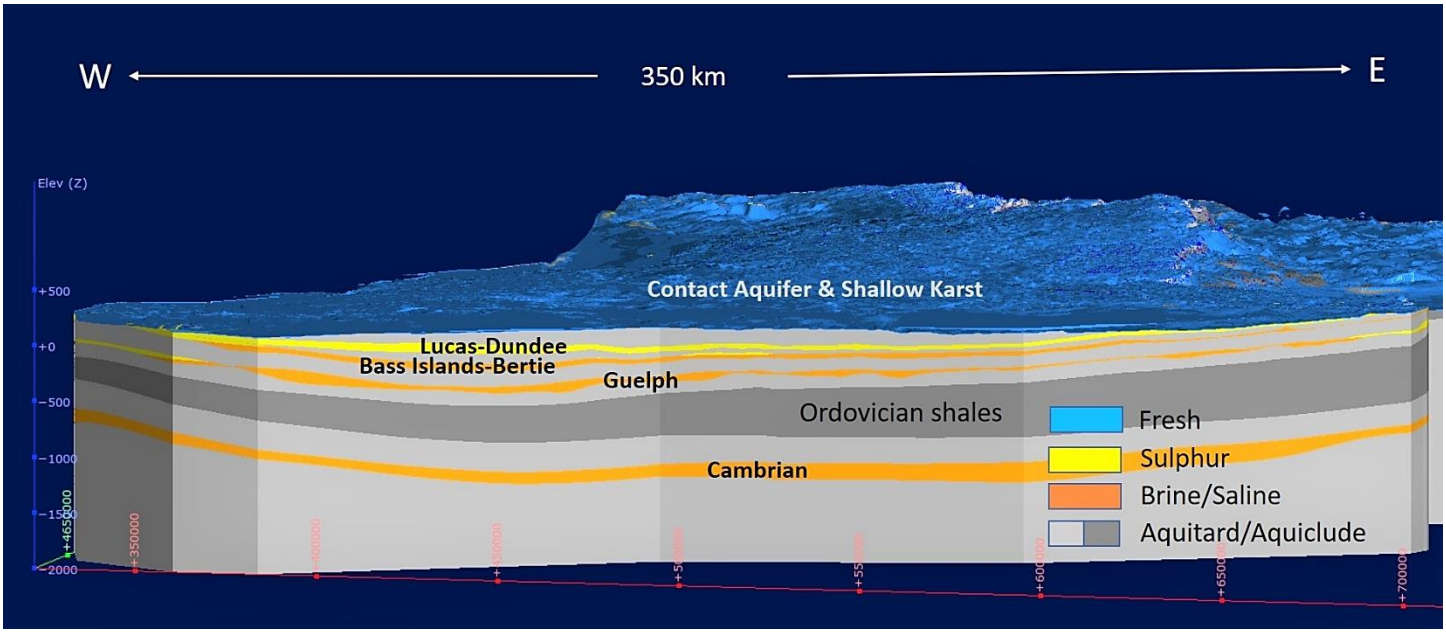

Site Classification of Mars

Paris Cassidy[1], Sheri Molnar[1], Jinfei Wang[1]

[1]Western University pcassid4@uwo.ca

Humans are intent on landing and possibly setting up habitats on Mars in the near future, e.g., NASA and China proposed Mars landings in the 2030s. The locations of future (semi)permanent habitats on Mars require comprehensive knowledge of the surface on which the mission will land and build. Site classification is used here on Earth to differentiate sites based on ground stiffness to mitigate and design for earthquake shaking. The time-averaged shear-wave velocity (Vs) of the upper 30 meters (Vs30) is the measure used to classify any location on Earth into one of six (A-F) site classes. Remote sensing Vs30 proxies have been developed for Earth based on topography (slope gradient) or its combination with surficial geology, surface roughness, or convexity. We start with only using DEM's of the Martian surface taken from the Mars Orbiter Laser Altimeter (MOLA) to create slope gradient maps. We assess two resolutions of Mars DEMs (available in pixels per degree) equivalent to 9 and 30 arcsecond DEM resolutions used for site classification on Earth. We sort 11 past and known-future Mars landing sites into three simple geologic categories (plains, valleys, or inside craters). We then generate slope gradient maps for these 11 map areas to determine site class(es) using our preferred Mars DEM resolution. Relating slope gradient to Vs30 is accomplished using an empirical relationship developed for stable craton sites on Earth as well as our own crude approximation relating Vs30 measured at basaltic sites on Earth to sites on Mars based on terrain characteristics (roughness, simple geologic category). The latter is our attempt to calibrate use of topographic slope as a Vs30 site class proxy on Mars. We predict a relatively narrow site class range will be determined on Mars corresponding to rocky conditions (classes A and B) with thin veneer (class C) on Earth."

Calcium carbonate polymorphism in fish otoliths

Bryan Chakoumakos[1], R. Wood[2], Alison Loeppky[3], Gary Anderson[3]

[1]Oak Ridge National Laboratory chakoumakobc@ornl.gov, [2]Washington University, [3]University of Manitoba

Fish otoliths, or "ear bones", are comprised of the CaCO3 polymorphs (aragonite, calcite and vaterite), which can occur either alone or in combination. Otoliths are part of a fishes auditory sensory system and also are accelerometers to determine and control the fishes orientation and motion. Otoliths are frequently used in environmental studies to infer temporally-explicit environmental conditions or fish life history events such as migrations based on concentrations of trace elements within daily-to-annual growth rings. Proper characterization of the mineralogical composition and microstructure of fish otoliths feeds into the interpretation of trace element chemistry. The polymorph phase abundance in an otolith depends on, as yet, unexplained genetic and environmental factors, particularly when multiple polymorphs are present. Most fish otoliths are comprised of the densest CaCO3 polymorph, aragonite, and concentric growth rings are the common microstructure, but these notions are potentially outdated with many recent reports showing otherwise. We have been employing a variety of materials science methods (Polarized Light Microscopy, X-ray Diffraction, Neutron Diffraction, X-ray Tomography, Raman Spectroscopy. Neutron Vibrational Spectroscopy, Synchrotron XRF, Gas Pycnometry, Crystal Growth Screens) to characterize the CaCO3 polymorph distributions and microstructures of fish otoliths to form a basis for understanding their ontogenetic, environmental, phylogenetic controls. Our work suggests that examination of the CaCO3 polymorph composition of otoliths should become more common, especially in studies where results will or may inform fisheries management decisions. Future research should work to attribute controls on otolith CaCO3 polymorph expression using a combination of -omics and material characterization approaches to enrich the life history and environmental information obtained from otoliths.

Research conducted at ORNL's High Flux Isotope Reactor and Spallation Neutron Source was sponsored by the Scientific User Facilities Division, Office of Basic Energy Sciences, U.S. Department of Energy.

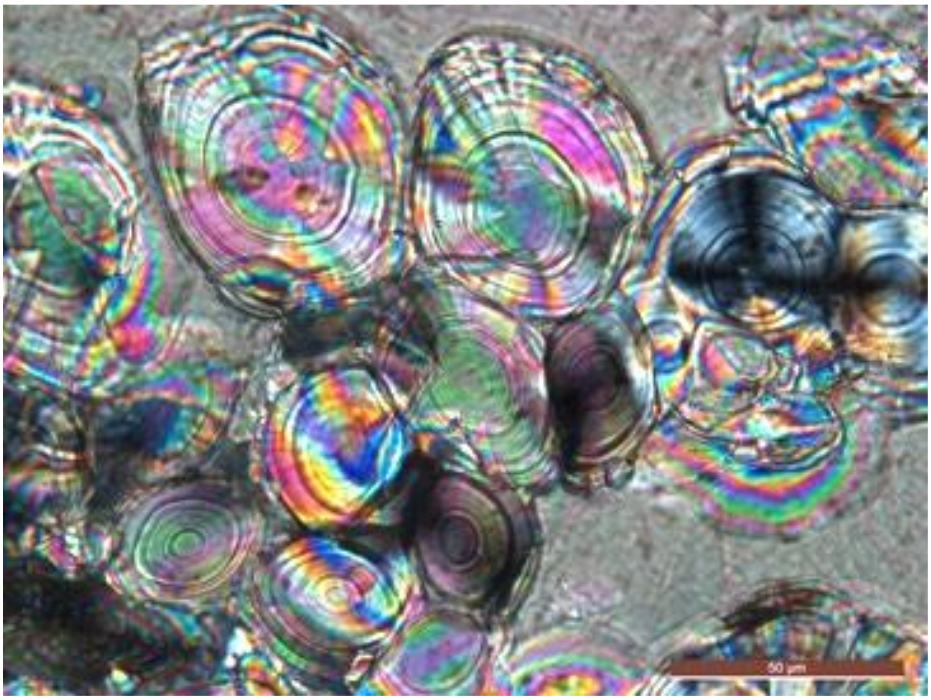

Fig. 1: Crossed-polarized optical micrograph of vaterite (spherulites) + calcite (matrix) in an otolith from a Lake Sturgeon (Acipenser fulvescens), Lake Winnebago, Wisconsin. Isogyres in spherulites indicate orientation of nearly uniaxial sheath-like crystallites, despite the onion-like daily growth rings.

Microstructures, deformation temperatures, and differential stresses from quartz-rich mylonites from the Grenville Front Tectonic Zone

XUEKE CHANG[1], Ziyan Cui[1], Janek Urbanski[1], Biwei Xiang[2], Dazhi Jiang[1], Lucy Lu[3]

[1]Western University xchang49@uwo.ca, [2]East China University of Technology, [3]Cardiff University

Quartz-rich mylonites and ultramylonites are well developed and exposed nearly continuously across a high-strain zone along the northeast striking Grenville Front Tectonic Zone (GFTZ), southeast of the township of Coniston, Ontario. Previous work suggested that the high-strain zone is a top to the NW thrusting shear zone which was formed at the end of the Grenville Orogeny ca. 1.0 Ga. These quartz-rich mylonites provide an excellent opportunity to study the rheology, deformation mechanisms of quartz in natural conditions. We have conducted systematic analysis on the microstructures and quartz c-axis fabrics to determine the deformation mechanisms. We apply the titanium-in-quartz thermometer to estimate the deformation temperature and use dynamically recrystallized quartz grainsize to constrain the level of differential stress from recent quartz piezometers. The c-axis fabrics show continuous cross girdles indicating basal <a> slip, romb <a> slip and prism <a> slip in C-foliation-parallel pure quartz bands in ultramylonite samples and discontinuous cross girdles with the romb <a> slip missing in C-parallel quartz-feldspar mixed bands of the same ultramylonite samples. We interpret this by the von Mise principle. Quartz c-axis open angle thermometer yields temperature estimate of 500 +/-75 °C. Temperature estimated from titanium in quartz thermometers fall into two groups. The temperature of first group is 430 +/-25°C or 391 +/-27°C based on two different thermometer equations at depth ~15 km; the temperature of second group is 518 +/-33°C or 463 +/-32°C, based on the same thermometers at the same depth. The mylonites and ultramylonites show typical regime 2 subgrain rotation recrystallization microstructures. Average dynamically recrystallized grain size is 14.9 (±7.4) μm, which corresponds to differential stresses of 123 +/-50 MPa based on current piezometers. We compare the microstructures and deformation mechanisms of the mylonites to other natural cases and experimental results and discuss the implications of our results for the flow laws of wet quartzites.

Fingerprinting the formation of Sn and W (±Mo) mineral systems and developing new mineral exploration tools

Yanbo Cheng[1]

[1]Norges Geologiske Undersøkelse (NGU) yanbo.cheng@ngu.no

Similar to porphyry Cu-Au (±Mo) systems, Sn and W (±Mo) mineralization are also primarily associated with magmatic rocks. Magmatic source, redox state, the degree of magma fractionation, and their tempo-spatial sequence are petrogenetic factors that control the development of metal-fertile magmas leading to magmatic-hydrothermal mineral deposits. Most previous studies on Sn and W (±Mo) genesis and exploration have focused on the ore-associated granitic rocks, whereas there has been little attention paid to explore the potentials of other rocks and minerals in these systems. This study examines the in-situ trace element composition of zircon and cassiterite, and geochronology, bulk rock geochemical and zircon Hf isotopic features of volcanic-intrusive rocks from several world's best-known Sn and W (±Mo) districts. Thereby, their potentials as new exploration tools have been revealed. Cassiterite is the most important tin ore mineral in nature, therefore the chemistry of cassiterite may returns insightful understandings on cassiterite crystallization under hydrothermal conditions, which will be helpful for developing tin ore exploration. A set of cassiterite samples from different mineralization environments were examined, and Zr/Hf and Ti/Zr ratios of cassiterite have shown potentials to be used as a broad tool for vectoring toward a tin mineralized intrusive system. This study also investigates the redox characteristics of the granites related to W and Sn mineralization, and further discusses the magmatic controls leading to Sn, W, porphyry Cu-Au, porphyry Mo and granite-related W-Mo deposits. Our new results suggest that The CeN/CeN* and EuN/EuN* ratios are useful metal discriminators for porphyry Cu-Au±Mo, via porphyry Mo, Mo-W, W-dominant, to Sn-dominant mineral deposits. When combined with Mo/W tonnage ratios, the CeN/CeN* ratio of zircon can be further employed to determine the style of Mo-W mineralization. To discern differences between "fertile" and "non-fertile" igneous rocks associated Sn and W (±Mo) mineralisation and reveal the genetic links between coeval intrusive and extrusive rocks, this study integrates multiple datasets from contemporaneous plutonic and volcanic rocks from a world-class Sn and W (±Mo) mineral field. The results indicate that magmatic province that contains Sn-rich fractionated rhyolites may be less prospective for granite-hosted Sn mineralisation, whereas the less evolved rhyolite with reduced redox state and poor fluxing component content may be more prospective for Sn exploration. Furthermore, the temporal sequence of magmatic-hydrothermal activities associated with this mineral field was updated using high precision muscovite 40Ar-39Ar, molybdenite Re-Os and LA-ICP-MS zircon U-Pb methods. Through combining these geochronological data, this study presents a framework for the temporal-spatial occurrences of deposits along with the associated magmatic rocks, to provide a basis for aiding mineral exploration in the region.

Shock metamorphism in zircon from West Clearwater Lake impact structure, Quebec, Canada

Neeraja Chinchalkar[1], Gordon Osinski[1]

[1]University of Western Ontario nchincha@uwo.ca

Meteorite impacts produce unique features in shocked rocks that can record conditions of the impact event. At high shock pressures, the post shock temperatures can be high enough to melt a significant amount of the target material. It is known from natural and experimental studies that impact melt is superheated with respect to endogenic igneous melt, but our understanding of the degree of superheating involved in the formation of impact melts is still evolving. The current work focuses on impact glass samples from West Clearwater to constrain initial pressure and temperature conditions experienced by the impact melt using zircons as extreme geothermobarometers. The West Clearwater Lake impact structure located in Quebec, Canada, is a ~286 Ma complex type crater with an apparent crater diameter of 36 km. A preserved impactite sequence in the ring of islands in the Clearwater Lake makes the crater an excellent site for studying a diverse suite of impactites. The crater-fill sequence at West Clearwater, from bottom to top, consists of fractured granodioritic basement rocks, monomict lithic breccias, impact melt-bearing breccia, clast-rich fine-grained melt, clast-poor fine-grained melt, and clast-poor coarse-grained melt. Impactite samples were collected from the ring of islands by a team led by Dr. Osinski during an expedition to the West Clearwater structure in 2014. In this work, shocked zircons from the impact glass at West Clearwater were studied in situ using polished thin sections. Backscattered electron imaging (BSE) and Zr elemental mapping were used to identify all the zircons within each thin section, followed by imaging of each individual zircon to assess the shock features in each grain. BSE imaging coupled with cathodoluminescence (CL) imaging revealed domains of zircons grains that have dissociated into zirconia, as well as zones where neoblastic zircon grains have formed within the parent crystal. Several zircons also show development of granular or vermicular rims, planar microstructures, fractures, and porosity. Figure 1 shows a partially decomposed zircon grain with a vermicular rim of zirconia with some relict zircon. Dissociation of zircon is an extreme temperature phenomenon and the products of dissociation along with other shock features are useful indicators of initial P/T conditions experienced by the melt. Future work for this study involves analyzing the zircons with Electron Backscatter Diffraction to determine the type of zirconia polymorph that is present in the zircons, as it will allow for constraining the pressure-temperature conditions using phase diagrams.

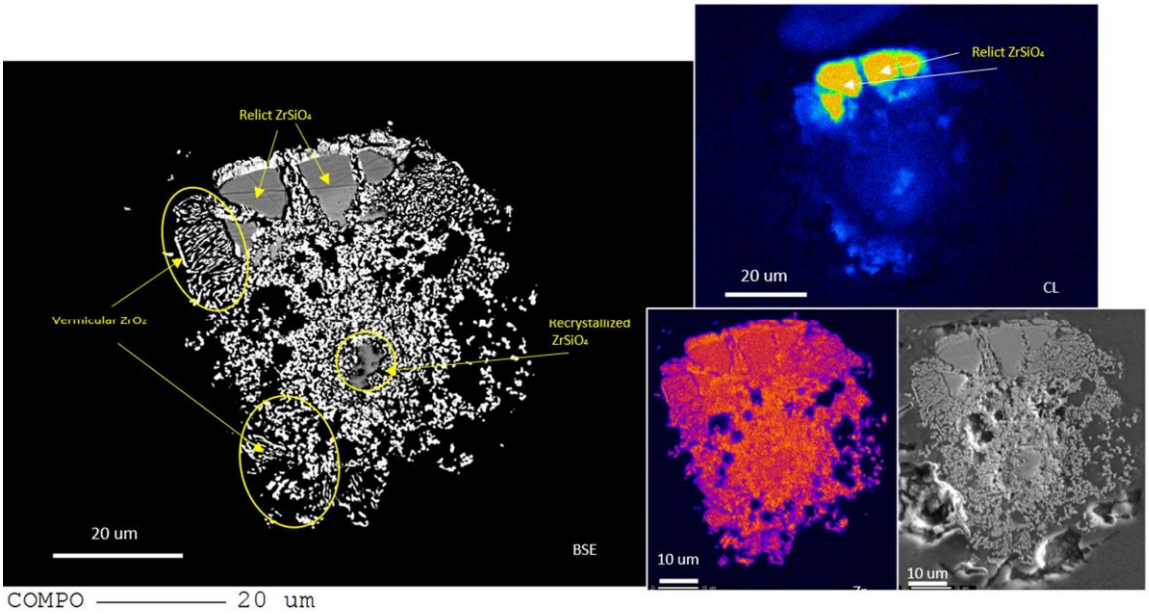

Figure 1: A shocked zircon in impact glass from West Clearwater. A: BSE image showing dissociated rim, relict, and neoblastic zircon (as evident from CL image in B). C: Elemental map showing distribution of Zr in the zircon. D: Secondary Electron image of the zircon showing the morphology of the grain.

Bayesian Updating of Seismic Microzonation for the Greater Montreal

Luc Chouinard[1], Philippe Rosset[1], Mohammad Talukder[2]

[1]McGill University luc.chouinard@mcgill.ca, [2]East West University

Since 2000, data from multiple sources have been compiled to estimate the influence of site conditions on seismic waves in the urbanized region of Montreal. Information consists of borehole data, seismic data from invasive and non-invasive methods and numerical modelling. The compiled data is used to develop seismic microzonation by integrating data on depth to bedrock, predominant frequency of resonance, and Vs30 through Bayesian updating and to estimate uncertainties on site characteristics and site characterization following the 2015 National Building Code of Canada (NBCC-2015) terminology (Figure 1). The regions identified as site classes D and E are locations where deposits of Leda clay from the Champlain Sea are predominant. Site amplification factors as a function of resonance period are obtained using 1D numerical modelling for typical soil profiles. Probabilistic microzonation maps are proposed for both site classification and site amplification. Epistemic uncertainties associated with amplification factors due to variability in soil profiles, soil properties and input seismic ground motions are also investigated. The microzonation maps are compared to felt reports from 26 recent earthquakes in the Montreal area (Did You Feel It Data by Natural Resource Canada). The spatial distribution from more than 12500 intensity reports is shown to be correlated with the site conditions.

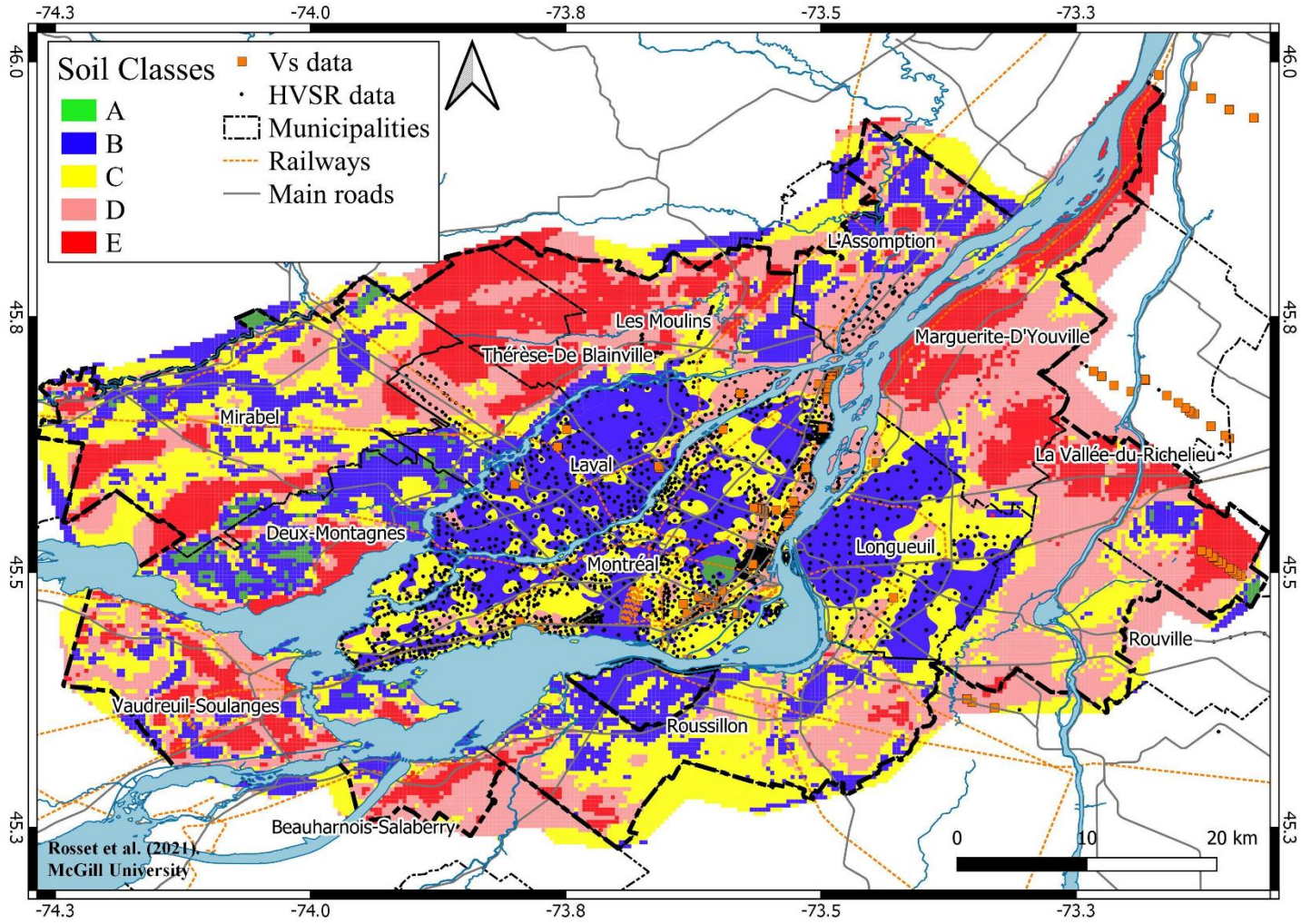

Provenance of Kimberlite Indicator Minerals from Saglek Basin, Labrador Sea, Canada

Evan Ciardullo[1], Roberta Flemming[1], Lisel Currie[2], Alejandra Duk-Rodkin[2]

[1]Western University evan.jciardullo@gmail.com, [2]Geological Survey of Canada

The Mokami and Saglek formations are comprised of Middle Eocene to Plio-Pleistocene deltaic deposits in the Labrador Sea, at the mouth of the Hudson Strait. In this study we use the provenance of KIM minerals to investigate the origin of these sediments. Fifty one mineral grains were obtained from Miocene to possibly Pliocene Mokami and Saglek formation strata by sub-sampling ocean cuttings from the Petro-Canada et al. Rut H-11 well. These grains were examined by optical methods, micro X-ray diffraction (μXRD) and Electron Probe Microanalysis (EPMA) at Western University for identification purposes, and 20 grains were determined to be of peridotitic mantle origin, based on the well-established compositional and mineral-formula discrimination criteria. The compositions of these Kimberlite Indicator Minerals (KIMs) have been compared to equivalent mineral grains from known Canadian kimberlite deposits, in a preliminary attempt to determine their provenance. Out of eleven garnets in the suite, nine garnets were classified as G9, thus establishing their lherzolitic mantle origin; one garnet was wehrlitic (G12), and one garnet was crustal (G0) (Fig 1A). The presence of G9 garnets, however, does not indicate provenance, as G9 garnets are ubiquitous in the mantle. Three Cr-diopside grains were found in the suite. They all passed compositional and mineral-formula criteria established by Ziberna et al. (2016) to be recognized as peridotitic. On Al+Cr-Na-K versus Ca/(Ca+Mg+Fe) plots (e.g. Grütter 2009, Fig. 4), these grains plotted in a region occupied by both garnet peridotite and spinel-garnet peridotite, such that formation in the presence of garnet is confirmed, but the type of peridotite is not definitive. These grains were used to calculate P-T conditions of formation using the Nimis and Taylor (2000) thermobarometer, and the Cr-diopside grains revealed P-T formation conditions ranging from 1304-1417 °C and 4.5-5.2 GPa (Fig 1B). These grains plot in the P-T region representing an extension of that occupied by both Somerset and Kirkland Lake kimberlites, however, calculated temperatures significantly above 1300 °C should be treated the caution because this has not been reported for Cr-diopside from any Canadian kimberlites. It is worth noting that the Cr-diopside grains definitively do not match those from the Chidliak kimberlites, although that kimberlite field is located geographically proximal to the Saglek deposit. Seven orthopyroxene grains found in the suite had compositions matching kimberlites from the Slave craton (Fig. 1C). This provenance agrees with the paleo-drainage pattern of the Bell River basin, which extended from the Northern Interior plains to the Sea of Labrador until the late Pleistocene.

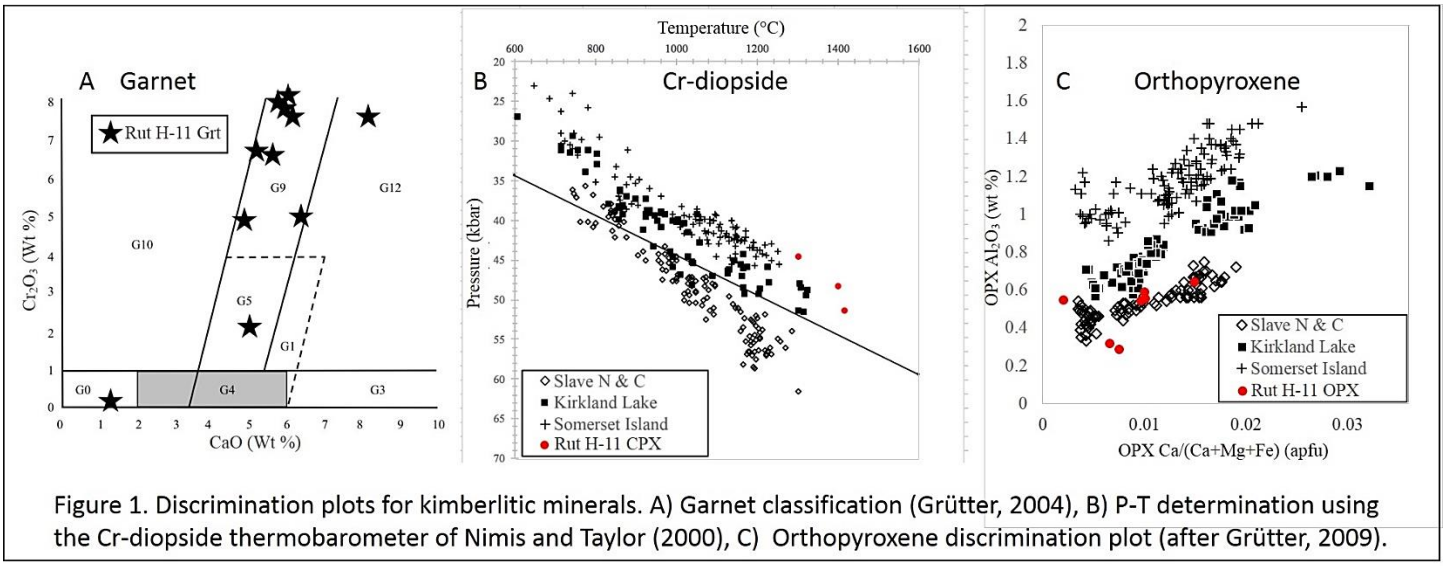

Figure 1. Discrimination plots for kimberlitic minerals. A) Garnet classification (Grütter, 2004), B) P-T determination using the Cr-diopside thermobarometer of Nimis and Taylor (2000), C) Orthopyroxene discrimination plot (after Grütter, 2009).

WEDigHistory: Case Studies in Archaeogeophysics

Maria Cioppa[1], Team WEDigHistory[1]

[1]University of Windsor mcioppa@uwindsor.ca

The WEDigHistory project was originally a Canada150 citizen science project that used geophysics, geoscience, history, and archaeology to explore Canada's history in the Windsor-Essex area. Since 2017, the project has expanded to other areas - both literally and figuratively. While the initial study area in 2017 was associated with the oldest Catholic parish west of Montreal (Our Lady of the Assumption / Notre-Dame-de-l'Assomption), later projects have included several post-colonial church cemeteries and historical sites. Ground-penetrating radar (Sensors and Software Noggin), magnetometry (Geometrics G858 cesium magnetometer) and conductivity (Dualem 2/4S conductivity meter) techniques have been used to explore and image the subsurface at these sites. Surveying of most sites was carried out with 0.5 or 1 m grid spacing on grids of varying sizes. The results of three studies will be presented. Geophysical results on several grids from the initial study site (2017 and 2018), which is currently parkland with a clay-rich soil, indicated the presence of the foundations of at least one building. The historical research suggested that these foundations could have been associated with one of several buildings on the site; however, no excavations are planned due to the presence of a conservation easement through the Ontario Heritage Trust. A preliminary GPR survey (2019) of the area around a nearby historical building revealed structures consistent with the known archaeology of the site. These multidisciplinary studies integrated historical knowledge, archaeology and geophysics. Following the initial success of the WEDigHistory project, several geophysical studies have been carried out in cemeteries in southern Ontario, primarily to search for unmarked graves and/or buried tombstones. In 2019, a very small scale GPR study of an approximately 4x4 m cemetery plot (0.25 m line spacing) investigated the difference between two burials of different ages. Evidence of an unmarked grave within this small area demonstrated the need for geophysical imaging.

What can we learn from the Greenland Ice Sheet and its surroundings for safe radioactive waste disposal?

Lillemor Claesson Liljedahl[1], Anne Kontula[2], Monique Hobbs[3]

[1]DHI Sweden lcla@dhigroup.com [2]Posiva Oy, [3]NWMO

Deep geological repositories for spent nuclear fuel use a multi-barrier principle aimed at isolating waste from the surface environment over long timescales (up to 1 million years). Over these timescales, glacial conditions are expected to reoccur in regions that were previously glaciated. Changes in hydrological, hydrogeochemical, and in-situ stress conditions are expected as ice sheets advance and retreat. Permafrost associated with glaciations will also alter the surface and sub-surface environments. These glacial processes have the potential to impact repository performance and consequently are considered in safety assessment analyses. Given the very long timescales covered by safety assessments, natural analogues are often studied to learn about features and processes over the long term. Observations from sites with currently existing continental ice sheets can help reduce uncertainties and provide a stronger scientific basis for the treatment of glaciation within safety assessments through improved process understanding. The multidisciplinary Greenland Analogue Project (GAP) was collaboratively initiated by the nuclear waste management organizations in Canada (NWMO), Sweden (SKB), and Finland (Posiva) to increase knowledge on glacial hydrological processes. Due to the size of the ice sheet and its accessibility, paired with the crystalline bedrock setting, the Greenland Ice Sheet and the Kangerlussuaq region, West Greenland, was selected as a suitable natural analogue for future glacial conditions expected in Fennoscandia and much of Canada over safety-relevant timeframes. To study ice sheet hydrology and groundwater dynamics, indirect and direct field observations were carried out on the ice sheet to study the basal system and which parts of the ice sheet contribute to groundwater infiltration. Geosphere investigations were done to study groundwater flow dynamics, composition of groundwater at depth, redox conditions, and the infiltration of glacial meltwater to bedrock. To facilitate hydrogeological and hydrogeochemical monitoring, three bedrock boreholes were drilled, instrumented, and tested. By combining the results from the field investigations, it is now possible to describe where and how groundwater is formed under an ice sheet, how water pressure under an ice sheet varies in time and space, and how an ice sheet influences the groundwater flow, all of which are relevant to groundwater models. It has also been possible to describe how deep meltwater can penetrate the bedrock and the chemical composition of this water, which is of relevance to bentonite buffer stability and canister corrosion. The output from the GAP thereby helps to ensure that assumptions in safety assessments are realistic and will strengthen future safety cases in crystalline bedrock settings. The obtained datasets and continued site monitoring provide significant input to ongoing climate research.

The Archean tonalite-diorite Chibougamau pluton and associated Cu-Au porphyry-style of mineralization

Alexandre Crépon[1], Lucie Mathieu[1], Daniel Kontak[2]

[1]UQAC alexandrecrepon.geology@gmail.com, [2]Laurentian University

Cu-Au porphyry-type deposits are among the least documented mineralizing systems in Archean greenstone belts. These porphyries are generally Au deposits with lesser Cu, e.g., the 2.74 Ga Côté-Gold Au-(Cu) deposit (~10 Moz Au) located in the southwestern part of the Abitibi greenstone belt (AGB), Canada. The Central Camp deposit, which is associated to the Chibougamau pluton in the northeastern part of the AGB, is one of a few Archean examples of Cu-rich and Au-bearing magmatic-hydrothermal system. This study focuses on the Central Camp deposit to unravel the characteristics of Archean porphyries and compares the study area with post-Archean systems to discuss mineralizing processes that evolved through time. The Neoarchean tonalite-diorite Chibougamau pluton assembled in the upper crust at ca. 2718 to 2716 Ma, towards the end of the main magmatic and volcanic stage (i.e., synvolcanic period), during which a large volume of basalt and tonalite-trondjhemite-granodiorite (TTG) suites were emplaced in the greenstone belt. Additional tonalite and leucotonalite (trondhjemite) emplaced in the pluton at ca. 2705 to 2701 Ma, during the main shortening event that lead to cratonisation (i.e., syntectonic period). Geochemical and petrological data indicates that the Chibougamau pluton is made of two main magmas and belongs to a tonalite-trondjhemite-diorite (TTD) suite. Such TTD suites are volumetrically minor but are economically significant in the AGB, as they tend to be associated with magmatic-hydrothermal systems such as Côté-Gold. Reviewing the physical characteristics of the mineralized zones in Central Camp unrevealed similarities and differences with modern porphyries. The deposit is structurally-controlled and consist of: (1) sulfide-dominated and (2) magnetite-dominated mineralization. Sulfide-rich type, such as the Lac Clark deposit, is characterized by hydrothermal breccia (1b) or Fracture-infillings (1b) displaying mineral assemblages also observed in younger porphyries. The magnetite-dominated zones (2), also known as McKenzie-type, are found in shear zones and are locally intersected by sulfide zones (1). These magnetite-dominated zones (2) formed in several stages during the synvolcanic and, possibly, syntectonic periods. Alteration assemblages are also similar to those of modern porphyry-type systems. The Central Camp mineralization is, however, less voluminous than its modern counterparts. Additional differences can be attributed to the nature of the host rock (i.e., anorthosite intrusion deformed prior the onset of mineralizing processes), the chemistry of the fluid (exsolved from the diorite and/or tonalite phases, which are magmas with moderate fO2 and low volatile contents), and the post-porphyry major deformation events (hydrothermal systems may have remobilize part of the Central Camp deposit during the syntectonic period).

A report on the Mid-Cambrian (Series 3, Guzhangian; Marjuman) trilobite Arapahoia from the Sullivan Formation, southern Rocky Mountains, Alberta and British Columbia

Michael Cuggy[1]

[1]University of Saskatchewan michael.cuggy@usask.ca

The systematics of a few of the trilobites from the Sullivan Formation of the Southern Rockies of Canada have been briefly described by Walcott (1924;1925). The trilobites were then treated in more detail by Resser (1942) who was perhaps the most notorious 'splitter' in Cambrian palaeontology. Consequently, numerous species have been named but many are likely to be synonyms. Since this previous work was based on relatively few, small collections with little stratigraphic control, a great deal of systematic description and revision is still needed. One such species is Arapahoia an abundant and species rich genus, that is poorly known from other locations across Laurentia. New collections of Arapahoia from the Sullivan Formation allow the species within this genus to be evaluated, new characteristics to be identified and hopefully for the first time allow the genus to be placed within a phylogenetic framework. Over seven species have been identified in the Sullivan, as well taxa from Montana and Wyoming have been re-evaluated. The diversity and high rate of turnover seen in Arapahoia in the Sullivan Formation makes it ideal taxa for biostratigraphy.

A statistical-based stochastic model for far-field horizontal ground motions and its validation considering nonlinear inelastic responses

X.Z. Cui[1], Y.X. Liu[1], H.P. Hong[1]

[1]Department of Civil and Environmental Engineering, University of Western Ontario xcui55@uwo.ca

The nonstationarity in the energy distribution of seismic ground motions in the time-frequency domain is well-known and has been discussed extensively in the literature. However, often only time-varying modulation is considered while the time-dependent frequency content is neglected. We provided a new statistical-based stochastic model for the strike-slip earthquake that can be used to simulate ground motions. The model was developed by analyzing the ground motions using the S-transform. Validation was carried out based on spectral acceleration for simulated and actual ground motion records. However, a comparison of the nonlinear inelastic response of the simulated records based on the proposed stochastic model to those of actual records has not been carried out. In the present study, we provide the results of such needed comparison by considering different damping ratios, soil conditions, and earthquake magnitude distance characteristics.

Generating nonstationary time- and frequency- dependent coherent ground motions at multiple sites

Xizhong Cui[1], Hanping Hong[1]

[1]University of Western Ontario xcui55@uwo.ca

Seismic ground motions at multiple sites are commonly modeled as a nonstationary gaussian stochastic processes. However, there are evidence the ground motions are non-Gaussian. The seismic ground motions vary in time and space with time-dependent coherency. Strong ground motions can cause damages to structures and infrastructure systems. Since the actual ground motion records at multiple sites that match the configuration of the multiple supports of a structure, such as a bridge or a latticed shell structure, are usually unavailable, simulated ground motions are commonly employed to assess the structural responses. In this presentation, we present an iterative power and amplitude correction algorithm to simulate the nonstationary, non-Gaussian ground motions at multiple sites with time-dependent coherency. The algorithm does not directly rely on the definition of evolutionary process or translation process theory. The algorithm is successfully validated and illustrated numerically by simulating nonstationary Gaussian and non-Gaussian vector of ground motions with prescribed coherence. The application of simulated records for assessing structural response is illustrated.

Classifying Northwest Africa ordinary chondrite `SdB-06': Possible late stage mobilization of Ni and S and metasomatic reaction of Ni-bearing minerals

Bianca Currie[1], Roberta Flemming[1], Phil McCausland[1], Alysha McNeil[2]

[1]University of Western Ontario, Institute for Earth and Space Exploration curriebianca@gmail.com, [2]University of Western Ontario

We report observations for an unclassified Northwest Africa chondrite from meteorite collector Simon de Boer (working name SdB-06) during ongoing classification. From optical microscopy, micro X-ray diffraction (μXRD) and Electron probe microanalysis (EPMA) examination of SdB-06, it is determined to be an unequilibrated ordinary chondrite (H3). X-ray fluorescence (XRF) maps were collected on a Bruker Tornado M4 at Western University and compiled for the entire thin section. Elemental maps were collected for Ca, Fe, Mg, Al, Co, Cr, Mn, Ti, P, Si, S, and Ni. The elemental maps for Ni and S show unique patterns of elemental distribution which are unusual for an ordinary chondrite (Fig 1), revealing a complex history. The Ni map shows a fluid-like distribution, an enriched "nickel front", throughout a large portion of the thin section, within which is a large zone where both Ni and S are essentially absent. Troilite and taenite are absent in the apparently altered zone. Ni and Fe in troilite, kamacite, taenite, and other oxides are concentrated in small sub mm blebs and along fractures throughout the region outside of the altered zone, found mainly in pyroxene and some olivine grains. Ni is present in many of the chondrules which were observed by EPMA and μXRD. This pervasive distribution of Ni and the unique pattern suggest late-stage aqueous alteration of troilite and metal and mobilization of Ni and S. It is not clear if this is from parent body aqueous alteration or from terrestrial weathering. There may have been a metasomatic reaction producing other Ni-bearing minerals such as pentlandite, awaruite, and trevorite.

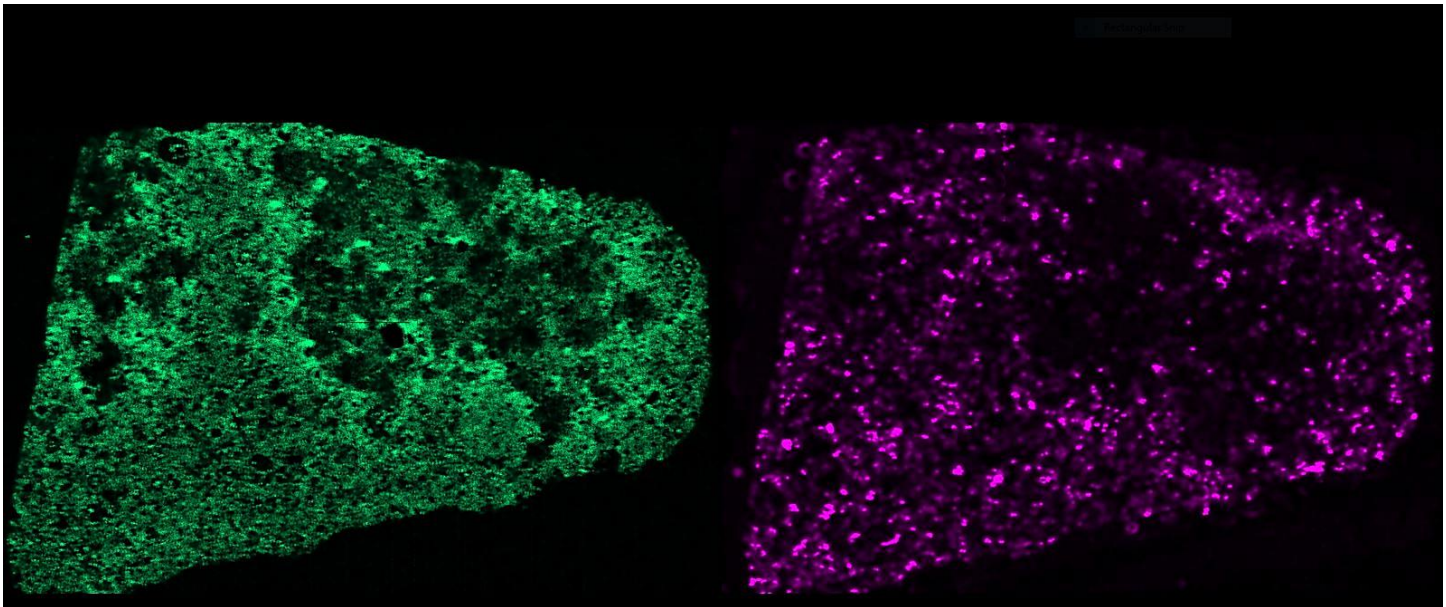

Figure 1: XRF maps of unclassified chondrite SdB-06 showing Ni distribution (left), and S distribution (right).

Teaching Rock and Mineral Identification Entirely Online: Effective or Ineffective?

Jennifer Cuthbertson[1]

[1]University of Calgary cuthberj@ucalgary.ca

In the Winter 2021 term (January-April), the decision was made to run the lectures and laboratories for second-year igneous, metamorphic, and ore rocks at the University of Calgary entirely online. This decision was made with the safety of students, teaching assistants and the instructor in mind due to the covid-19 pandemic. This course is a core component of the undergraduate geology program. In order to make the online labs as interactive and engaging as possible, the instructor utilized 3-D hand sample images from Sketchfab.com, and high-quality thin section images from VirtualMicroscope.org. Sketchfab allows users to search for images using keywords, upload their own images, rotate images, and zoom in on features. There is a wide range of igneous and metamorphic rocks available on Sketchfab for observation. VirtualMicroscope aims to broaden accessibility to thin section collections from universities and museums around the word, by providing open access to hundreds of samples that the user can explore using plane polarized light, cross-polarized light, different magnifications, and rotations. Most samples also have a description about the locality and geological history of the sample. These two websites formed the basis for many of the online labs in the igneous, metamorphic, and ore rocks course at the University of Calgary. In this presentation, the author will show examples of some of the samples used, and their associated lab questions for the students to complete. Informal feedback from students indicates that they found both websites to provide useful, high-quality images of rocks. But the question remains, were these web-based resources effective in helping students to correctly identify and name rocks and minerals? Will they be able to remember and use the knowledge gained during this course when it comes time to use a real petrographic microscope? With a return to campus planned for Fall 2021, the Department of Geoscience is providing an opportunity for students to practice with the petrographic microscope during the week before classes start. Students will be surveyed to determine how confidant they feel in identifying rocks and minerals, and how well they feel the online labs prepared them for real-life. The results of the survey will be discussed in the presentation.

Bedrock Exhumation Across the Columbia River Fault Near Revelstoke, B.C

Kade Damant[1], Eva Enkelmann[1], William Matthews[1]

[1]University of Calgary kade.damant@ucalgary.ca

In the southeastern Canadian Cordillera, Paleocene-Eocene extension exhumed metamorphic core complexes along low-angle normal detachment faults. The Columbia River Fault (CRF) is one such brittle-ductile detachment bounding the eastern margin of the Monashee Complex. Hornblende and mica 40Ar/39Ar and apatite fission track (AFT) ages suggest the CRF initiated ~56 Ma and accommodated rapid vertical displacement of the Monashee Complex from 25 km to ~2 km depth during the Eocene. Apatite (U-Th)/He (AHe) ages adjacent to the CRF suggest it may have been reactivated in the early Miocene and exhumed the Monashee Complex an additional 2 km. However, the precise timing of reactivation and amount of exhumation are unclear due to the low temperatures (~60°C) constrained by the AHe system. In this study, we quantify the upper crustal cooling history of bedrock across the CRF to determine when, and how quickly bedrock was exhumed along the fault. We use AFT and AHe thermochronology and thermal history modeling to quantify when bedrock cooled between 120-40°C. We aim to answer three questions: When and how long was the CRF reactivated? How much vertical displacement was accommodated by reactivation of the CRF? What role has erosion played in exhumation since the end of faulting? This information will help constrain models for the tectonic evolution of the southeastern cordillera and improve our understanding of the connection between tectonics and climate in forming the Columbia Mountains. We present 10 new AFT ages and 12 AHe ages from the CRF north of Revelstoke, BC. AFT ages in the footwall range from 25.5 to 17.7 Ma, and ages in the hanging wall range from 29.3 to 20.1 Ma. Mean track lengths in the footwall averaged from 13-14 µm, whereas mean track lengths in the hanging wall averaged ~12 µm. Longer mean track lengths in the footwall suggest it cooled through the apatite partial annealing zone (APAZ) (120-60°C) more rapidly than the hanging wall. Additionally, track lengths in the hanging wall form a characteristic wide distribution found after long residency in the APAZ. Inverse thermal history modelling of the AFT and AHe data indicate the footwall underwent rapid Oligocene cooling (>10°C/Myr) between 33-25 Ma. During this time, the hanging wall experienced slow cooling or steady state (~1°C/Myr) within the APAZ, suggesting the CRF was active and exhuming the footwall. Based on these results, we suggest the CRF was reactivated in the Oligocene and continued to brittlely deform and exhume the Monashee Complex an additional 2-3 km. Together with existing thermochronology data from the region we suggest 3 phases of accelerated cooling: 1) Eocene (56-40 Ma) very rapid cooling (>40°C/Myr) during core complex exhumation from >25 km depths, 2) Oligocene (33-25 Ma) rapid cooling (>10°C/Myr) and 2-3 km of exhumation during CRF reactivation, 3) Pliocene to present (<5 Ma) rapid cooling (>10°C/Myr) suggested as erosion from continental glaciation.

Identifying and measuring hydraulically closed ovoid basins using High Resolution Topographic Models visualized on Google Earth

Michael Davias[1]

[1]Cintos Research michael@cintos.org

Aerial photographs of oriented ovoid basins taken in the 1930's across Southeastern USA sparked the initial research into their geomorphology. Typically hydrologically closed, these landforms host flat-floored interiors which retain moisture as precipitation capture basins. Satellite Imagery available today expands the regions available for interrogation, but reveal only part of their unique planforms. High Resolution Topographic Models (HRTMs), generated from publicly available Light Detection And Ranging (LiDAR) remote sensing data, accentuate the visual presentation of these shallow basins by removing dense obfuscating vegetation and accentuating their subtle circumpherential rims. To support a geospatial survey of these landforms in the continental USA, 1x106 km2 of false-color encoded seamless HRTMs were rendered as KML-JPEG tile sets on 1.5 m spatial gridding using Global Mapper GIS. A perceptually uniform color palette is employed, with the palette cycling modulo 10 meters to enhance subtle elevation variations evidenced across relatively level terrain. The tile generation process and integration into Google Earth is demonstrated. The HRTMs have provided an effective visualization tool for identification of Carolina Bays, High Plains Playas and Nebraska Rainwater Basins. These landforms vary in size from 100 m to 10 km on major axis, with a mean of ~350 m. While the generic planforms are considered oval, we document subtle regional variations. Using a small set of empirically identified planform archetypes, corresponding Google Earth ground overlay images were engineered. The analysis protocol for an individual basin is demonstrated by placing an appropriate archetype onto the virtually globe, then sizing and rotating it by edit handles such that it satisfactorily represents the bay's crisply expressed rim. The overlay element's metadata is extracted from Google Earth's object directory and programmatically processed to generate metrics such as location, elevation, major and minor axis and inferred orientation. Utilizing a virtual globe facility for data capture may result in higher quality data compared to methods that reference flat maps, where geospatial shape and orientation of the basins could be skewed and distorted in the orthographic projection process. Using the methodology described, we have measured ~

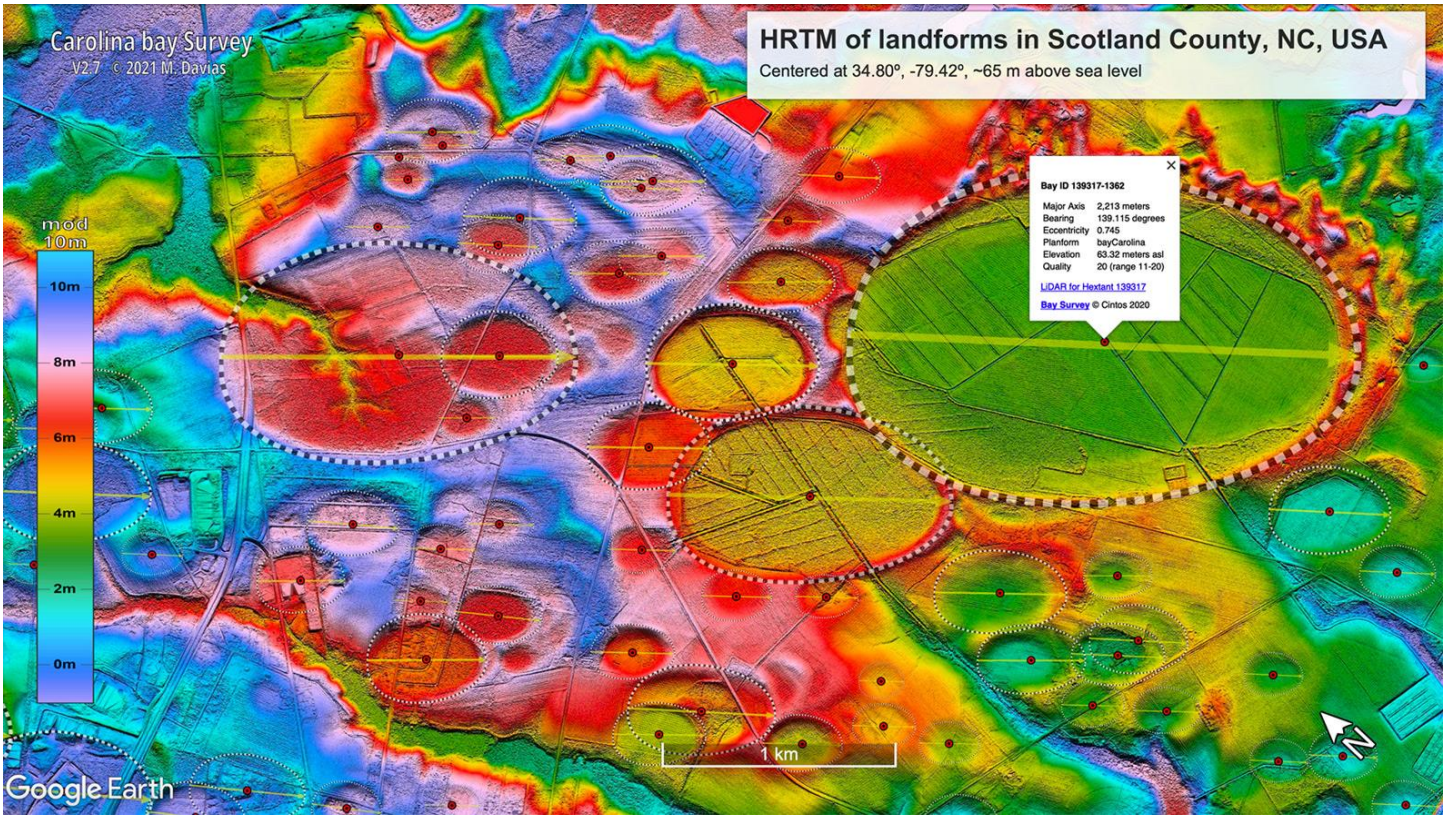

60k distinct oriented ovoid landforms. HRTM imagery and resulting landform metrics data are openly web-accessible to other researchers as a geospatially searchable facility presented on Google Earth and an Excel spreadsheet. Preliminary findings from the survey are discussed, such as how basin surface area, eccentricity and orientation vary across ~3,000 15' × 15' quadrants. While consensus opinion accepts these landforms as gradualistic in nature, such robust conformance to archetype planforms suggests they may warrant further consideration as enigmatic products of a unifying catastrophic event. Future work includes interrogation of orientation data to clarify possible systematic geospatial relationships.

Comparing student learning achievements using traditional versus virtual microscopes for Mineralogy and Petrology

Heidi Daxberger[1], Kirsten Kennedy[1], Rebecca Moumblow[2], Shane Sookhan[1]

[1]University of Toronto – Scarborough heidi.daxberger@utoronto.ca, [2]McMaster Univeristy

During the Covid 19 pandemic, instructors faced major challenges when teaching practical lab skills such as using polarizing microscopes. To overcome these challenges we developed a new web-based open educational resource of digitized thin sections and hand samples, called Virtual Petrography. The tool enabled instructors to select samples from a database of interactive virtual thin sections and accompanying 3D hand sample models, and deliver them to students as a coherent laboratory set directly within any type of Learning Management System (LMS). The interactivity of the virtual materials enabled students to simulate the use of a polarizing microscope by rotating the stage, applying a polarization filter, and changing magnification. As in previous years, the lab exercises centered on learning the optical properties of rock-forming minerals, identifying rocks, and interpreting their genetic history. To provide context we briefly summarize the features of the Virtual Petrography web tool and quantified student learning achievements by comparing outcomes of two semesters of in-person classes to one semester of fully virtual usage, wherein students were given comparable exercises and samples. Preliminary grade analyses of two instructors show that in general, grade averages of the fully online course (76-90%) did not vary significantly from the in-person course (71-92%) for selected labs. Student survey and course evaluation comments qualitatively described the overall user experience as being positive. The users mentioned the following positive aspects: the interactivity of the provided digital thin sections, the possibility to investigate 3D hand samples from all sides, confirm findings by looking at close-up sample images, use of digital diagrams that helped determine rock types and rock formation conditions, and 24/7 availability. They found that the integration of the Virtual Petrography web tool enabled them to understand concepts and let them practice mineral and rock identification. Solely, unpredictable internet connectivity was mentioned as possible drawback of the virtual labs. Though we used this system as a pandemic-era substitute for in-person training, we note that it will also be useful as a supplementary resource with large capacity for existing microscopy-based courses and as a highly accessible tool for those with difficulties using or accessing traditional microscopes. Hence, we promote the integration of virtual thin section and sample sets such as provided by the Virtual Petrography web tool, into fully online, but also in-person classes, supports learning goal achievement, helps students to get more confident in their skills (can practice at home), and can also alleviate issues such as class sizes versus equipment number, equipment set-up times, room capacities, use during lectures, accessibility, and for example one of a kind samples that could not be included in the instruction before.

Mapping Fe-Mg Phyllosilicates in northwest Noachis Terra, Mars

Anthony Dicecca[1], Livio Tornabene[1], Catherine Neish[1], Nicolas Thomas[2], Gabriele Cremonese[3], Alfred McEwen[4]

[1]University of Western Ontario adicecc@uwo.ca, [2]University of Bern, [3]National Institute for Astrophysics, [4]Arizona State University

Prominent exposures of phyllosilicate-bearing surface materials offer an important opportunity to understand the regional alteration and hydrological history of Mars from orbit. A distinct phyllosilicate-bearing layer has been identified with the Compact Reconnaissance Imaging Spectrometer for Mars (CRISM) in the Her Desher and Nirgal Valles systems in northwestern Noachis Terra (Buczkowki et al., 2010; 2014). This investigation has shown that the clay is consistent with iron-magnesium smectites. In combination with geomorphic analysis, it was posited that this layer formed by interaction with groundwater rather than surface water. However, in consideration of other working hypotheses, further work is needed to substantiate this conclusion.

In this study, exposures of the phyllosilicate layer throughout the Coprates Quadrangle are more completely mapped using an extensive suite of imagers in order to understand it's distribution and geologic setting. This investigation utilizes multispectral images from the Color and Stereo Surface Imaging System (CaSSIS) that offers high resolution (4 m/pixel) color mapping of the Martian surface (Thomas et al., 2017; Tornabene et al., 2018). CRISM provides spectral maps at 230 m/pixel of the stratigraphic layers in the area of interest. In addition, thermal infrared data (100 m/pixel) from the Thermal Emission Imaging System (THEMIS) is used to complement the CaSSIS and CRISM data (Christensen et al., 2001). Morphologic analysis is completed using digital terrain models derived from 2 m/pixel stereo image pairs from the High-Resolution Imaging System Experiment (HiRISE; McEwen et al., 2007).

Preliminary observation has shown that the phyllosilicate-bearing layer is exposed in valley incisions and in several excavated craters throughout the region. A defined stratigraphic cross section will also be developed in order to understand the broader geologic context of this layer. By mapping and analyzing the distribution of these clays, planetary scientists will have a better understanding of past alteration conditions in the region. Understanding the full extent of past water-rock interactions will inform future Martian missions in their search for where extinct life forms may have thrived.

Early Forecasting for the Probability of Large Aftershocks for the Mw 6.5 Monte Cristo Range Sequence

Elisa Dong[1], Robert Shcherbakov[1], Katsuichiro Goda[1]

[1]Western University edong2@uwo.ca

In the case of a strong earthquake, one is not only interested in the impact of the main event, but also in the subsequent triggered aftershocks. These aftershocks could cause more destruction in addition to mainshock effects. Moreover, strong aftershocks significantly increase the seismic hazard immediately after the main event and should be considered for operational earthquake forecasting and risk management. We investigate one case of the ongoing Monte Cristo Range earthquake sequence (initiated after the occurrence of the Mw=6.5 event at 11:03:27 UTC, May 15, 2020) in Nevada, which is presently taking place along a previously unmapped fault zone in the Mina Deflection in the Walker Lane. Specifically, we analyze the frequency-magnitude statistics to estimate the catalog completeness during the sequence. We then calculate the probability for the occurrence of the largest expected aftershock during prescribed future forecasting time intervals by using the Extreme Value Theory (EVD) and Bayesian Predictive Distribution (BPD). This is done by assuming that the earthquake rate can be approximated by the modified Omori Law (MOL) or the Epidemic Type Aftershock Sequence (ETAS) model. The Bayesian predictive framework combined with the ETAS model has been recently implemented for aftershock forecasting. We estimate the probabilities for the occurrence of the largest expected aftershocks during a fixed forecasting time interval by using the early events in the sequence. In addition, we include the forecast for the probability of a large aftershock (Mw=5.3) which took place half a year after the mainshock. Finally, we review the forecasting performance of the models based on the modified Omori Law, which is commonly used for early aftershock forecasting, and the ETAS model. The local earthquake catalog has enough events for reliable seismicity modelling and forecasting. This offers the rare opportunity to apply several statistical models to characterize the first few days and the subsequent evolution of the sequence. From our initial findings, there is no clear indication that one model might fit better than the other during the early sequence. We also find that the early forecasted probability of large aftershock for a range of magnitudes is similar for all methods, the MOL using EVD and BPD, and the ETAS model using EVD and BPD.

Preliminary P-T-t results from the Chesterfield Fault Zone, Baker Lake area, Nunavut

Derek Drayson[1], Alfredo Camacho[1], Sally Pehrsson[2], Jamie Cutts[3]

[1]University of Manitoba dadrayson@gmail.com, [2]Geological Survey of Canada, [3]University of British Columbia

The Chesterfield Fault Zone (CFZ) is one of the most poorly understood structures within the Churchill Province. It was originally defined by Schau (1982) as a 7-20 km wide, east trending zone of variably sheared granitoids north of Baker Lake, Nunavut. Recent geophysical surveys and geological mapping has extended the CFZ to Wager Bay, ~400 km northeast of Baker Lake (Wodicka et al. 2016; Tschirhart et al. 2016). Previous work has established that the CFZ coincides with a major change in the exposed crustal level with rocks to the north and south recording pressures of ~0.5 GPa and ~1.2 GPa, respectively (Pehrsson et al. 2013; Berman et al. 2007). In addition, the structure is speculated to have facilitated exhumation of the lower crustal rocks during the Snowbird Orogeny (Berman et al. 2007; Sanborn-Barrie et al. 2019). Reconnaissance mapping in the Baker Lake area revealed that the CFZ represents a 3 km wide zone of heterogeneously deformed granitoids with a high-strain fabric striking at ~075 and dipping 54° to the south and a mineral lineation plunging ~30° to the southwest. The footwall (rocks to the north) is dominated by tonalite gneiss that is overprinted by upper greenschist to lower amphibolite facies mineral assemblages. The hangingwall is dominated by porphyritic monzogranite that contains garnet hornblende plagioclase quartz that define the high-strain fabric. Garnet-hornblende-plagioclase thermobarometry gives pressure and temperature conditions of 0.85-1.05 GPa and 700-750°C, respectively. Garnet yields Lu-Hf ages of ca. 1868 Ma and constrains the timing of high-P mylonitization in the hangingwall of the CFZ. This age is similar to the timing of static metamorphism recorded in the Chesterfield Block (Berman et al. 2007) and slightly younger than dynamic metamorphism in the Kramanituar Complex and in the Lunan Domain (Wodicka et al. 2017; Sanborn-Barrie et al. 2001; Berman et al. 2007). Future work will assess the timing and conditions of metamorphism in the footwall of the CFZ; the cooling history across the CFZ; and Sm-Nd model ages of the protoliths. In addition, a regional synthesis of previously collected data will be integrated with these new findings. Together, this work will increase our understanding of the tectonometamorphic architecture of the Churchill Province at one of its most fundamental boundaries.

Mesozoic brittle faults of the St. Lawrence platform in the Montreal area, Canada

Thibaut Ducat[1], Alain Tremblay[1], François Hardy[1], William H Amidon[2], André Campeau[3], Michel Kuntz[4], Eric Chartier[3]

[1]UQAM ducat.thibaut@courrier.uqam.ca, [2]Middlebury College, [3]Ville de Montréal, [4]WSP

This study aims to develop a 3D model of rock basement structures of the Montreal area, in order to lower the geotechnical risks in the development of major underground infrastructures. Structural data collected from outcrops, quarries and deep excavations, and during the construction of past major underground works (i.e. subway) are combine to the stratigraphic information provided by the K-bentonite ash layers of the Trenton Group to constrain the location and mechanism of major faults and evaluate their offset. Regional faults crosscutting the Paleozoic sequence of the St. Lawrence platform (SLP) in the Montreal area show two main orientations, EW and NW-SE. The EW-trending faults are, from north to south, the Bas-Sainte-Rose (BSR), Rapide-du-Cheval-Blanc (RCB), Ile-Bizard and Sainte-Anne-de-Bellevue faults. These faults are subvertical, with an apparent normal-sense throw toward the North or the South. Fault offsets range from a few tens to several hundred of meters, up to 435 meters for the RCB fault. Some of these faults extends continuously for 30-40 km and merge westward into the Ottawa graben. The principal NW-SE faults are the Saint-Vincent-de-Paul and Duvernay faults. They occur between the BSR and RCB faults and extend along-strike for ~10 km. They are subvertical or steeply SW-dipping, and show down-dip normal-sense offsets less than a few tens of meters. On the south shore of the St. Lawrence River, the Havelock fault trends North-South and extends southward for >40 km towards the USA-Canada international border. The Havelock fault is subvertical with an east-directed normal-sense fault throw and offset of 150 meters or more. In the field, faults are poorly exposed, except for some quarries and a few outcrops. They are usually mark by a series of closely-space, discrete faults and fractures within 10 to 20 meters-wide zones in sharp contacts with the hosting carbonate rocks. Fault surfaces are frequently mark by calcite coating, deposited by fluids that circulated during faulting. When present, fault striations are slightly to moderately plunging toward the West for the EW faults, toward the NE or the SW for NW-SE trending faults and toward the S-SE for the N-S faults. Hydrothermal calcite coatings on EW, NW-SE and NS faults has been sample for U-Pb isotopic dating in three areas, Ile-Bizard (Montréal), Jesus Island (north shore), and Saint-Isidore (south shore). Three samples of the Ile-Bizard fault that were analyze yield a nearly perfect isochron age of 112 ± 2 Ma, whereas a fourth sample yields a less robust age of 102 ± 16 Ma. Such a late Early Cretaceous age is consistent with field observation suggesting that some of the EW trending faults cut across the Mt Royal intrusion, which belongs to the ca. 125 Ma Monteregian Hills igneous Suite. More samples are currently under investigation for U-Pb dating of calcite coating, and should be helpful in order to constrain the timing of the different orientation families of faults.

In situ and rapid quantitative analysis of platinum-group elements (Pd, Pt and Rh) in ores using Laser-Induced Breakdown Spectroscopy combined with laser-induced fluorescence (LIBS-LIF)

ISMAIL ELHAMDAOUI[1], Mohamad Sabsabi[2], Marc Constantin[3], François Vidal[1]

[1]INRS Ismail.ElHamdaoui@inrs.ca, [2]CNRC, [3]Université Laval

The Canadian mining industry is always looking for new technologies that meet its needs for in situ and real-time measurement of platinum group element (PGE) content during the various stages of mining exploration and production. Laser-induced breakdown spectroscopy (LIBS) is an emerging analytical tool in the field of geochemistry that has the potential to meet the needs of the mining industry for rapid quantitative measurement of PGEs. Compared to conventional methods (ICP, AAN, AAS, etc.), the advantages of LIBS are its ability to analyze rapidly and in situ with little or no sample preparation. To date, the only known in situ analysis technique for ore samples is X-ray fluorescence (XRF). However, the latter is totally unsuitable for measuring PGE concentration due to its high detection limit (LOD). This study demonstrates the potential of LIBS-LIF (laser-induced fluorescence-assisted LIBS) technology to assess the PGE content of ore samples in situ. LIBS-LIF is a selective excitation technique that improves LOD as compared to conventional LIBS and eliminates spectral interferences that prevent the use of conventional LIBS for certain chemical elements such as platinum in the presence of iron. LIBS-LIF uses a first conventional laser to ablate the sample and generate a plasma and a second laser of the optical parametric oscillator (OPO) type to selectively excite the plasma and thus intensity the emission of spectral lines of interest. Two types of reference materials, doped with 25, 50, 100, 200 and 500 ppm concentrations of Pd, Pt and Rh, were used to calibrate the LIBS instrument. Different combinations of excitation/fluorescence lines as well as plasma creation conditions were studied to optimize the PGE signal. The established calibration was used to evaluate PGE concentrations in certified materials and ore samples. The concentrations obtained on certified materials prove that the LIBS-LIF method has high sensitivity and good accuracy. On the other hand, LIBS-LIF analysis of ore samples shows a good correlation with the results of the conventional gravimetric and optical absorption methods. These results demonstrate that the LIBS-LIF technique can be used for the rapid measurement of PGE in geological exploration.

Multi-phased late Cenozoic exhumation history along the central Rocky Mountain Trench

Eva Enkelmann[1], Kelley Fraser[1], Scott Jess[1], Hersh Gilbert[1]

[1]University of Calgary eva.enkelmann@ucalgary.ca

The Rocky Mountain Trench (RMT) is an impressive long valley that stretches from Montana northwest across British Columbia and into Yukon. The length (1600 km) and continuous nature of the RMT have been interpreted to be the result of faulting and localized erosion. The location of the RMT coincides with a sharp change in crustal thickness that possibly represents the limit of an ancient continental margin. At the surface, the RMT separates the Foreland belt (Rocky Mountains) from the Omineca belt (Columbia Mountains) of the Canadian Cordillera. The kinematics of the faults underlying the RMT change from normal faulting in the south to dextral strike-slip faulting in the north. The central RMT, located near Valemount, BC, is thought to be the transition zone between strike-slip and normal faulting. This area also coincides with the Malton Gneiss Complex (MGC) that represents the northernmost exposure of Proterozoic high-grade metamorphic rocks. The MGC is bound in the east by the RMT and in the west by the North Thomson Albreda normal fault (NTAF), which merges into the RMT south of Valemount. We investigate the fault kinematics along a 130 km long stretch of the central RMT, between the town of McBride, BC and 50 km south of Valemount, BC. We use apatite fission track and (U-Th)/He analysis to investigate the cooling history of rocks across and along the RMT and the NTAF. Thermal history modelling of the thermochronology data reveals four phases of Cenozoic cooling: (1) Late Cordilleran (70-55 Ma) cooling is recorded in the Cariboo Mountains located west of the RMT and the NTAF. (2) Eocene (~45-30 Ma) cooling occurs throughout the entire study area and is associated with the well documented widespread extension in the southern Canadian Cordillera. (3) Early-mid Miocene (~20-10 Ma) cooling resulted in the rapid exhumation of the MGC as a horst structure, bounded by the NTAF in the west and the RMT in the east. This finding implies a phase of east side-down faulting along the RMT, which has not been reported before. (4) Late Miocene to present (<10 Ma) cooling is observed along the eastern side of the RMT and in the MGC. Age-elevation relationships of samples collected from both sides of the RMT suggest west-side down normal displacement starting ~12 Ma. We propose that dip-slip motion along the RMT reached at least as far north as McBride and occurred through the late Miocene, suggesting transtension much rather than pure strikes-lip motion. We suggest the high gravitational potential to be a driver for orogenic collapse that stretches the crust towards the surrounding regions. This driving force creates a stress field with vertical sigma1, which can easily reactivate steeply dipping structures such as the RMT and normal faults of the Omineca Belt. In contrast, the shallower dip of thrust faults within the Foreland Belt may be unfavourable to slip and explain the general lack of young extension and the higher topography in the Rocky Mountains.

Reaction rims on ilmenite macrocrysts from different kimberlite facies in class 1 kimberlites, Orapa kimberlite cluster, Botswana

Lydia Fairhurst[1], Yana Fedortchouk[1], Ingrid Chinn[2], Philippe Normandeau[3]

[1]Dalhousie University ly593526@dal.ca, [2]De Beers Exploration, [3]Northwest Territories Geological Survey

Kimberlites are mantle-derived igneous rocks emplaced in the upper crust. Class 1 kimberlite are multi-phase bodies consisting of coherent kimberlite (CK) and different pyroclastic facies, including diatreme Kimberley-type pyroclastic kimberlite (KPK). The composition, crystallisation conditions and emplacement processes of these multiphase kimberlites are poorly understood, especially the formation of KPK. CK facies include hypabyssal kimberlite (HK) and ambiguous partially fragmented CK. Ilmenite macrocrysts from some Orapa kimberlites show reaction rims, the composition of which correlates with kimberlite facies. The goal of this study is to document the reaction products on ilmenite from different kimberlite facies and to use them to determine crystallisation temperature (T) and oxygen fugacity (fO_2). Obtaining a better understanding of fO_2 is important not only scientifically, but also for economic reasons, because highly oxidising conditions would have promoted resorption of diamonds in the kimberlite. This study used thin sections taken in well constrained depth intervals from drillholes in AK15 and BK1 kimberlites from the Orapa kimberlite cluster (Botswana). The AK15 intrusion consists of a single phase of CK facies. The BK1 pipe consists of two CK facies (CK-A and CK-B) and one KPK facies. CK-B is a HK and CK-A shows areas of partial fragmentation. Kimberlite textures were examined with a petrographic microscope. Ilmenite reaction rims were identified with SEM. EMP analyses were performed on perovskite, ilmenite and magnetite grains for T and fO_2 calculation. We found that ilmenite macrocrysts in CK-A develop rims composed of magnetite and rutile. The reaction rims on ilmenite macrocrysts in KPK are highly variable and are distinguished by the presence of titanite. In CK-B, ilmenite macrocrysts are replaced by a symplectic intergrowth of magnetite and perovskite. In AK15, ilmenite macrocrysts consist of magnetite rims. fO_2 estimated using ferric iron content in $CaTiO_3$ perovskite varies from NNO -5.74 to -1.30 showing progressive oxidation upwards and within KPK facies. Such fO_2 conditions require T during perovskite crystallisation between 560 and 700 °C. The observed textures suggest that BK1 ilmenite macrocrysts reacted with the melt to produce magnetite and perovskite rims followed by full ilmenite replacement by symplectic intergrowth of perovskite and magnetite in CK-B and replacement of perovskite with TiO_2 oxide in CK-A. Development of titanite in KPK indicates assimilation of crustal xenoliths, while variability of reaction rims and fO_2 estimates within the same sample confirm the high degree of material mixing in KPK. Similarities of ilmenite rims in CK-A and KPK indicate similarity in the process of their formation.

Re:Presenting the History and Culture of Geology in Nova Scotia 1910-1914

Tim Fedak[1]

[1]Nova Scotia Museum tim.fedak@novascotia.ca

New historical research was initiated to understand the context of the Nova Scotia Museum's geology collection in relation to the past two hundred years of geoscience in Nova Scotia. The Nova Scotia Museum was established in 1868 from collections dating back to the Halifax Mechanics' Institute of 1830, while the earliest description of Nova Scotia mineral sites can be traced to New England geologists visiting the region in 1820s. Using historical publications and reports, biographies, and newspaper articles, a two-hundred-year timeline has been developed. While the recent decade is framed within my personal research network, the older portions of the timeline provide a framework to explore social aspects of geology within a larger historical perspective. Three examples from the history of geology are provided to demonstrate the value of widening the perspective of geoscience to highlight cultural and social history. In 1914, Eleanor T. Long (1880-1922) was a trailblazing woman who studied the rocks and fossils of Nova Scotia. After her tragic death in 1922, Eleanor's Nova Scotia studies were completed by Walter Bell. Charles S. Fletcher (1896-1970) was an African Nova Scotian man who was born in Newport Station and worked as a laborer in the gypsum quarries as a young boy. In 1928, Fletcher began working in the Laboratory of Mining Geology at Harvard University and for twenty-five years was an international expert on preparing polished ore samples. William F. Jennison (1858-1936) was a Nova Scotian born and educated geologist that documented the gypsum deposits of Nova Scotia with detailed descriptions and photographs in a report published in 1911. These three histories coalesce around the culture of geology that was present in Nova Scotia from 1910-1914, a time that saw an influx of geologists from New England and the Geological Survey of Canada working with local geologists - as well as

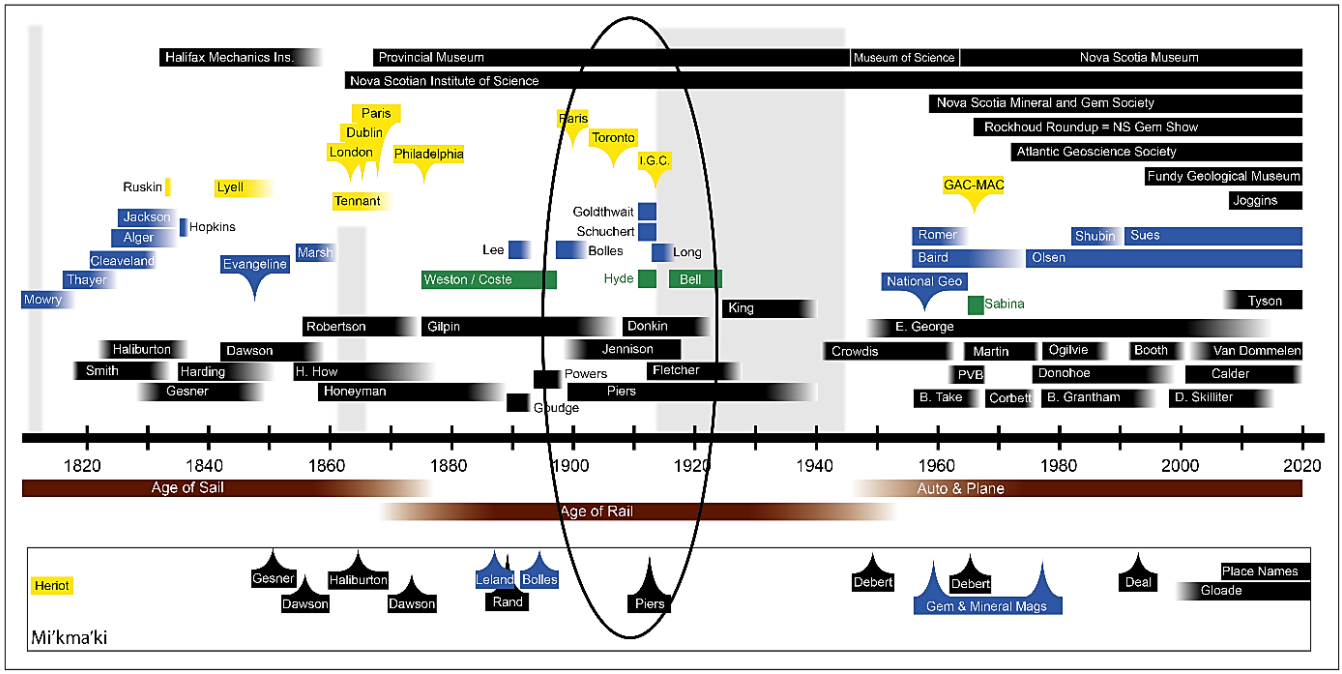

the hosting of a field trip to the Atlantic Provinces during the International Geological Congress in July of 1913. The ICG field trip is well documented with official published guide and itinerary, as well as hand-written notebooks and photographs of Charles Schuchert. Prior to the start of WWI, women were explicitly excluded from university training in mining geology and faced hostile environments in field experiences. African Nova Scotians also faced barriers to education and limited work opportunities. Therefore, the early contributions of women and an African Nova Scotian working at Harvard University are significant histories to represent. Local geologists worked with international collaborators to promote economic minerals and are also linked to social justice movements of the post-war periods. The International Geological Congress in 1913 was a significant milestone for the history and culture of geology in Nova Scotia.

Exploration of chemical weathering and diagenesis in weathering profiles, paleosols, and sedimentary rocks in 3-D compositional space

Christopher Fedo[1]

[1]University of Tennessee cfedo@utk.edu

Since the original introduction of the chemical index of alteration (CIA) by Wayne Nesbitt and Grant Young in 1982, there has been rising interest in quantitatively determining the extent of chemical weathering in weathering profiles and derived sediments in order to evaluate contemporary (paleo)climate conditions. CIA values document the proportion of immobile to mobile cations during hydrolysis of silicate mineral phases. Application of the CIA has spanned from the Holocene to the Archean and even forms a fundamental approach to examining sedimentary rocks on Mars. With thousands of citations to the original and derivative studies, the importance of determining CIA is clear. Yet, because CIA values essentially condense the geochemistry into a 1-dimensional value, the application needs to be approached cautiously in paleosols and sedimentary rocks where diagenesis can add elements used in determining CIA. By converting the components of the CIA expression into a triangular plot (Al2O3 - CaO*+Na2O - K2O; A-CN-K), increasing weathering intensity (conversion of plagioclase and K-feldspar to clays), as well as addition of K+, can be portrayed as a 2-dimensional pathway. Because the CIA expression does not include FeO and MgO, a second triangular space that adds FeO (F) and MgO (M) (A-CNK-FM) permits the tracking of mafic phases, although at the expense of combining plagioclase and K-feldspar into the CNK term. As a way to incorporate all the elements that go into the two triangular projections, I combine all of the terms into 3-dimensional (3D) tetrahedral space with Al2O3, CaO*+Na2O, K2O, and FeO+MgO (A-CN-K-FM) as apices; advancing this approach, combining CN and K allows for Si (S) to be added to generate an A-CNK-FM-S tetrahedron. Plotting Quaternary weathering profiles of different compositions shows that the positions observed in A-CN-K and A-CNK-FM plots represent face projections from inside the 3D tetrahedron. As a result, the data in 2D plots have an imposed flattening effect, which is particularly serious for rocks of mafic composition on the A-CN-K triangle. Plotting data in tetrahedral space from Precambrian paleosols and sedimentary rocks, along with rocks from Mars, reveals otherwise unrecognized fine textures in weathering pathways, as well as subsequent modifications formed during diagenesis. Approaching the study of major-element distribution using 3D space expands the region on a plot where different aspects of interest (source, weathering intensity, sorting, diagenesis) might cluster, which in some cases might overlap because of data flattening using more conventional 2D plots.

Mapping seismic hazard for selected regions in Canada using adaptive kernel smoothing approach

C Feng[1], H.P. Hong[2]

[1]Chang'an University cfeng@chd.edu.cn, [2]University of Western Ontario

The probabilistic seismic hazard analysis based on the assigned seismicity model is adopted by NRCan to estimate and map the seismic hazard. The mapped hazard and obtained uniform hazard spectra are used as the basis to suggested seismic design loads in the structural design code (National Building Code of Canada (NBCC 2020). The seismicity model consists of well-defined seismic source zones, magnitude-recurrence relations, and ground motion prediction models. The assignment of the seismic source zones is based on seismo-tectonic information, which depends on the historical earthquake catalog. In the present study, we apply an adaptive kernel smoothing approach to assess the seismic source model for regions in Canada based on the historical earthquake catalog. We then use the develop smoothed seismic source model to evaluate the seismic hazard and uniform hazard spectra. We compare the obtained results with those reported in NRCan. We discuss the results and their implication in seismic design.

Rock magnetic and stable isotopic constraints on paleoenvironmental and diagenetic interpretation of a Frasnian carbonate platform, Canning Basin, Australia

Ian Ferguson[1], Anne-Christine Da Silva[2], Nancy Chow[1], Annette George[3]

[1]University of Manitoba ij_ferguson@umanitoba.ca, [2]Liège University, [3]University of Western Australia

Stable isotope and rock magnetic analyses of data from two sections 1.5 km apart in the South Hull Range (SHR) and Guppy Hills (GH), and paleomagnetic and isotopic results from previous studies, are used to provide investigate deposition and diagenesis of Late Devonian carbonate rocks of the Hull platform in the Lennard Shelf, Canning Basin. Biostratigraphic evidence constrains the Hull Platform to be early to middle Frasnian (M.N. Conodant Zone 2-6), an interpretation supported by identification of the punctata excursion in the $\delta^{13}C$ record from both sections as a positive 2 ppt excursion that can be correlated to a similar response elsewhere in the Canning Basin and globally. Comparison of stable isotope results from microdrilled micrite samples with those from CBCP coarsely-drilled bulk-rock samples shows the micrite yields the Late Devonian marine $\delta^{13}C$ signature while bulk-rock samples record significant diagenetic events. Diagenetic studies from the Lennard Shelf have defined events including (1) early marine diagenesis, (2) late Devonian-Carboniferous burial diagenesis and dolomitization, and (3) Carboniferous meteoric diagenesis. In the GH section, diagenetic features include localized late Devonian meteoric diagenesis at a subaerial exposure surface at 70 m height, and extensive Carboniferous diagenesis in a 50 m thick zone in relatively deeper-water facies surrounding the exposure surface. Initial magnetic susceptibility for the SHR and GH sections is characterized by small positive and negative background values indicating relatively pure (diamagnetic) carbonates, interrupted by sparsely-spaced small positive peaks, due to intermittent increases in abundance of paramagnetic minerals, most likely pyrite and clay, associated with sea-level change and local tectonic events. Hysteresis results show the magnetic mineralogy is related to the initial input of detrital magnetite. Increases in high field remanence at, and above, 70 m height, and at other exposure surfaces, indicate oxidation of the magnetite to form hematite (and possibly goethite), and subsequent erosion and redeposition of this mineral. Correlations with isotopic responses show early marine diagenesis involved additional oxidation of magnetite to form hematite. The Carboniferous meteoric diagenesis, is interpreted to have included partial bacterial reduction of hematite to form superparamagnetic magnetite producing an isothermal remanant magnetization loss response that is proportional to both hematite abundance and the $\delta^{13}C$ response. The meteoric diagenesis was spatially- and stratigraphically-localized to relatively deeper water facies and did not reset either the primary paleomagnetic signature or micirtic $\delta^{13}C$ response.

In Situ X-ray Diffraction (ISXRD) for Exploring Mineralogy and Geology on Mars

Roberta Flemming[1], Jayshri Sabarinathan[1], Eric Pilles[1], Stanislav Veinberg[2], Phil McCausland[1], Ken McIsaac[1], Gordon Osinski[1], Livio Tornabene[1], Mariek Schmidt[3], Ralf Gellert[4], Michael McCraig[4], David Armstrong[1], Dana Beaton[1], Daliah Bibas[1], Fengke Cao[1], Yaozhu Li[1], Catheryn Ryan[1], Matthew Svensson[1], Gregory Schmidt[2]

[1]Western University rflemmin@uwo.ca, [2]Proto Manufacturing Ltd., [3]Brock University, [4]University of Guelph

The geologic history, impact history, paleoclimate, and habitability of Mars are recorded in its minerals. To understand the evolution of Mars, we need to study its mineralogical record. Rover-based instruments on the Mars Exploration Rovers (MER) and Mars Science Laboratory (MSL) have measured elemental information from the surface of Mars, but elemental composition alone does not provide a complete analysis of which minerals are present. X-Ray Diffraction (XRD) is the primary technique to determine the mineralogy of geologic materials. An XRD is currently deployed on Mars with the CheMin instrument on MSL; however, CheMin requires a fine-grained sample from scooping or drilling, and retains limited context regarding the inter-relationships between the minerals in the rock. It also has a limited capacity to handle samples. A Canadian Space Agency (CSA)-funded team from Western University, Brock University, University of Guelph, and Proto Manufacturing are developing a miniaturized in situ XRD (ISXRD) contact instrument which will analyze minerals directly on the martian surface. We are assembling a set of Mars analogue rocks, minerals, and meteorites, for which we are comparing XRD results from laboratory-based µXRD at Western University with results obtained using various candidate miniaturized X-ray components and geometries tested by Proto. Our growing set of Mars-related samples for XRD analysis includes minerals and rock types known to occur on Mars (igneous and sedimentary, shocked and unshocked), as well as simulants, Alpha Particle X-ray Spectrometer (APXS) calibration materials, and martian meteorites. XRD results are reported for selected martian analogue rocks, minerals, simulants, and meteorites. The example pictured in Fig. 1 is a whole-rock specimen from the Moenkopi formation, which is primarily gypsum. Our XRD results compare well between the laboratory and prototype instruments for this fine-grained sample. Various sulfates have been documented on Mars, like Ca-sulfates from CheMin and jarosite from Mössbauer. But many martian samples with elevated sulfur content are still a mystery, as either no XRD instrument was on the payload or the sulfur-rich phase was amorphous. XRD patterns compare excellently when the material is naturally fine-grained, like the majority of the rocks investigated thus far on the surface of Mars, because polycrystalline samples contain all lattice planes in diffraction condition simultaneously, and all lattice planes in the ICDD reference pattern are present in the observed XRD pattern. Coarse-grained samples contain fewer diffraction lines and non-representative intensities (preferred orientation), making phase identification less definitive. Amorphous material (e.g. glass) decreases X-ray intensity. These are among the challenges going forward. This work lays the foundation for an in situ XRD instrument to be used in future Mars exploration, or anywhere a remotely-operated robotic rover might be deployed, including remote regions of Earth for environmental science or resource prospecting.

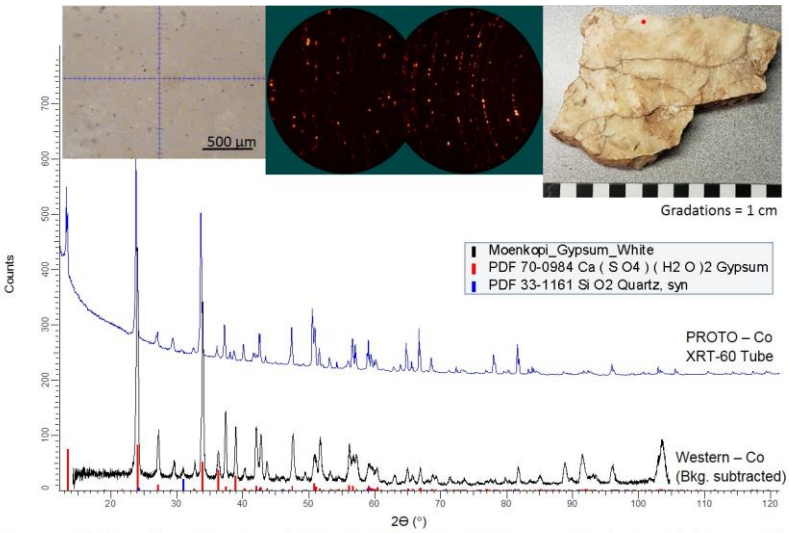

Figure 1. Whole-rock specimen from the Moenkopi formation, St. George, Utah, (upper right) is primarily gypsum, a hydrated calcium sulfate. Our XRD results compare well between the laboratory (black diffraction pattern) and prototype instrument (blue diffraction pattern) for this relatively fine-grained sample. ICDD patterns are shown for gypsum (red sticks) and minor quartz (blue sticks). The grain size is estimated to be 15-50 µm from the spotty rings in the 2D image (upper middle). Upper left: Context image for lab XRD target.

Using X-ray Diffraction to Quantify Strain in Solids

Roberta Flemming[1], Phil McCausland[1], Fengke Cao[1], Yaozhu Li[1], Laura Jenkins[1], Jennifer Newman[1]

[1]Western University rflemmin@uwo.ca

The crystalline nature of solids can be examined by X-ray diffraction (XRD) of polycrystalline as well as coarsely crystalline materials. This can provide crystal structural parameters and also crystallite size and strain parameters. Our group is at the forefront of observing, quantifying, and calibrating size and strain in minerals (naturally-occurring crystalline solids) using various XRD techniques. For fine-grained polycrystalline samples, such as calcite and dolomite in carbonate rocks, crystal lattice strain (micro-strain) can be measured by examining line shape variation as a function of diffraction angle (2θ), using Rietveld refinement of powder-XRD data. In this case, broadening due to size and strain are distinguishable as line broadening (βε) due to strain increases with tanθ: $\beta\varepsilon = 4\varepsilon\tan\theta$, whereas line broadening with diminished grain size varies inversely with cosθ: $\beta_D = \lambda/D_V\cos\theta$, by rearranging the Scherrer equation. For coarse-grained samples, lattice strain in crystals such as olivine, pyroxene or feldspar can be measured using the Williamson-Hall plotting method using in situ micro-XRD data (Fig. 1). Line broadening (βε) due to strain increases with tanθ: $\beta\varepsilon = 4\varepsilon\tan\theta + \beta o$. Plots of βε vs tanθ yield slope 4ε (ε is % lattice strain) and intercept βo (a term related to crystallite size and instrument parameters). Plastic deformation or non-uniform strain in minerals can be measured by analyzing textural diffraction information obtained using a two-dimensional (2D) area detector. 2D textures contain size and strain information: Polycrystalline samples (crystallite size <5 μm) exhibit complete Debye rings (X dimension), whereas large unstrained crystals (>50 μm) exhibit single diffraction spots. Plastically-deformed large crystals exhibit elongate spots or streaks along X due to a mosaic spread of subdomain orientations upon bending or disruption of the crystal. Analysis of the line shape along X enables measurement of crystallite misorientation or strain-related mosaicity (SRM). SRM has been quantified by measuring Full Width at Half Maximum along X ($FWHM_X$) for several rock-forming minerals (olivine, pyroxene, plagioclase, quartz). We are also calibrating lattice strain and SRM by analyzing experimentally shocked mineral samples with known peak shock pressures. Methods for Lorentzian-Gaussian fitting and assessment of complex diffraction peaks are also being developed (e.g. Best Fit for Complex Peaks - BFCP). XRD is complementary with other techniques such as optical microscopy, Raman spectroscopy, and Electron Backscatter Diffraction (EBSD); these observations are often made in tandem, representing different scales of strain observation. Recent measurements of shocked or tectonically strained Earth and planetary materials will be highlighted.

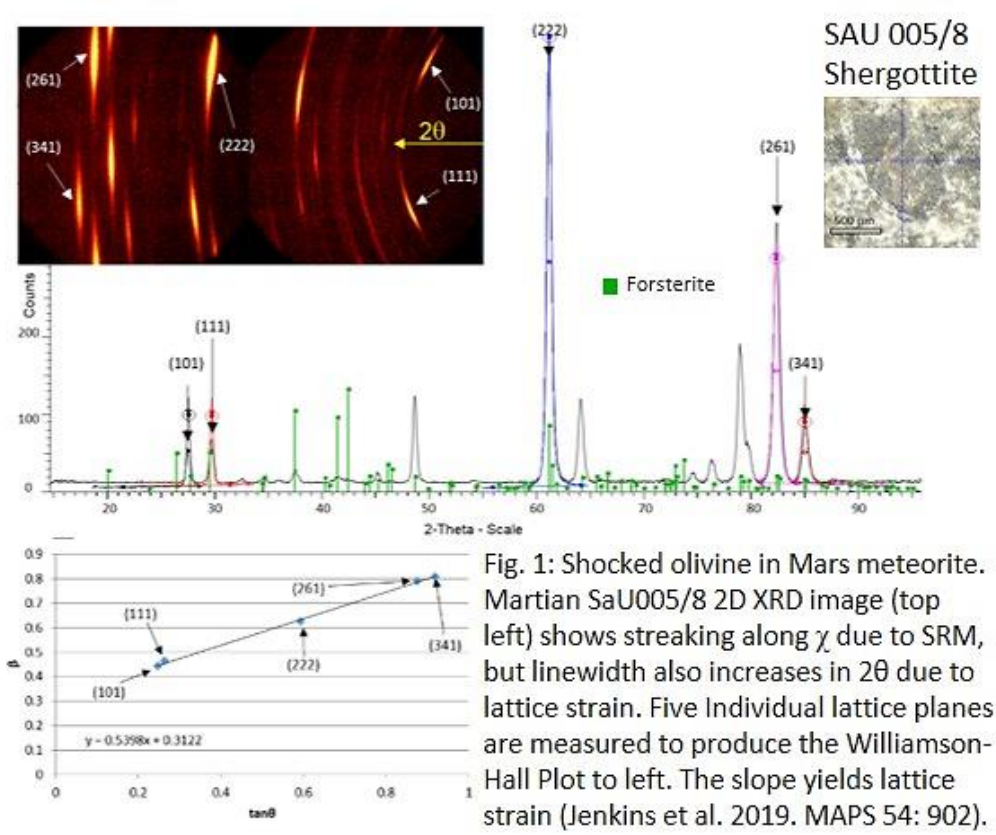

Fig. 1: Shocked olivine in Mars meteorite. Martian SaU005/8 2D XRD image (top left) shows streaking along χ due to SRM, but linewidth also increases in 2θ due to lattice strain. Five Individual lattice planes are measured to produce the Williamson-Hall Plot to left. The slope yields lattice strain (Jenkins et al. 2019. MAPS 54: 902).

Long ago and (not so) far away - Spinel cation ordering as a record of temperature in the early solar system

Roberta Flemming[1], Victoria Houde[1]

[1]Western University rflemmin@uwo.ca

On a human time scale, long ago, when I was an M.Sc. student with Ron Peterson, he suggested using Magic Angle Spinning Nuclear Magnetic Resonance (MAS NMR) spectroscopy to measure cation ordering in $MgAl_2O_4$ spinel as a function of temperature. I took on that challenge and we synthesized spinel (1300 °C in air for 129 h with three regrindings), equilibrated and drop quenched samples at various temperatures (700 - 1400 °C), and measured the octahedral/tetrahedral Al ratio by ^{27}Al MAS NMR (at 9.4 Tesla) to directly determine x in the structural formula $(Mg_{(1-x)}Al_{(x)})[Al_{(2-x)}Mg_{(x)}]O_4$, where x = 2/(1+Al(oct)/Al(tet)). Thus, we contributed our calibration curve (Millard, Peterson & Hunter, 1992, Am. Min. 77: 44-52) to what is now a considerable body of literature, as spinel is an important rock forming mineral on Earth and other rocky bodies across the solar system. On a deep time scale, spinel is among the early forming refractory minerals in the solar nebula and it is a common constituent of the earliest condensed solids, Calcium Aluminum-rich Inclusions (CAIs). CAIs are common constituents of carbonaceous chondrite meteorites, and the spinel contained within them has a cation distribution which has the potential to have remained frozen in place since its early formation, or it may have re-equilibrated during subsequent heating on carbonaceous chondrite parent bodies. This early-formed cation distribution in spinel, and the formation or equilibration temperature it recorded, has been preserved for billions of years. Recently, my former M.Sc. student Victoria Houde took on the challenge of measuring cation ordering in spinel in these early solar system materials by ^{27}Al NMR. We obtained CAIs from several CV3 chondrites (NWA 2364, NWA 6991, Allende, and NWA 6603). We used micro X-ray diffraction to identify spinel-containing CAIs, and used ^{27}Al MAS NMR and ^{27}Al Triple Quantum (3Q) MAS NMR (at 21.1 Tesla) of bulk CAI material to evaluate the cation ordering in spinel (Fig. 1). Temperature estimates were calculated for spinel in each CAI using several spinel thermometers. NWA 2364 and NWA 6991 yielded temperatures of 520-710 K and 360-610 K, respectively, depending on the calibration curve used. These temperatures likely represent parent body processing. Challenges to quantifying the temperature recorded by Allende and NWA 6603 will be discussed. Our results are preliminary and more work needs to be done, such as Rietveld modal analyses of the sample mineralogy to support the ratios obtained by peak fitting of the NMR spectra, and further development of 'NMR standard samples' of the common refractory CAI minerals fassaite, gehlenite, anorthite, and grossular. But we are not so far away from getting reliable temperatures for these materials! I want to thank Ron Peterson for unlocking the power of mineralogy for me long ago, and for starting me on this mineralogical journey - an enjoyable journey indeed!

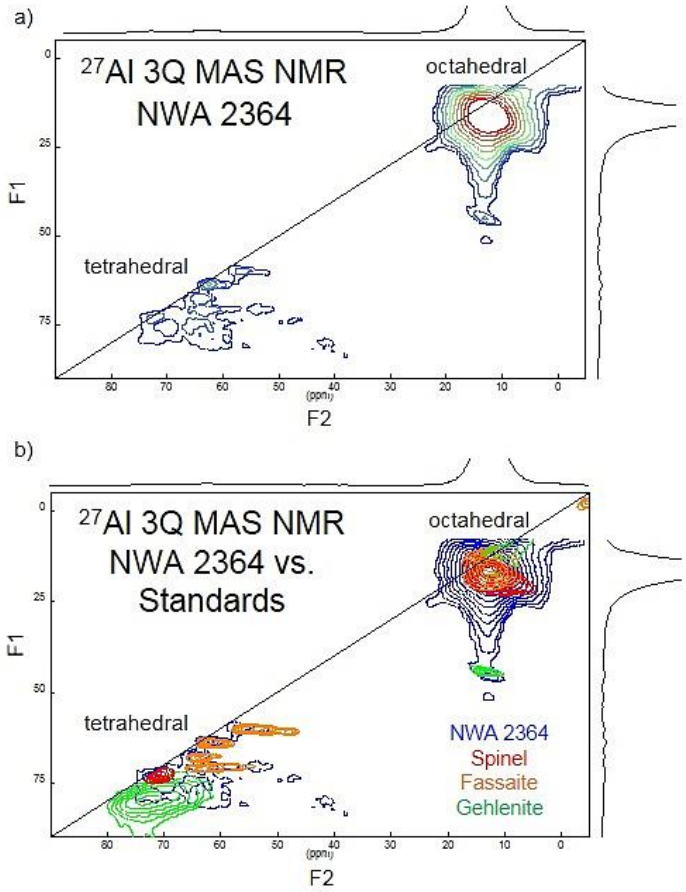

Fig. 1. a) ^{27}Al 3Q MAS NMR spectrum of NWA 2364 (multicoloured) b) ^{27}Al 3Q MAS NMR spectrum of NWA 2364 (blue) overlain by spinel standard (red) [Syn, MEQ-003], gehlenite standard (green) [Crestmore, CA, Dana 3461], and fassaite standard (orange) [Allende CAI TS62B], showing the overlap of the spinel standard with the spinel peak from NWA 2364. (From Houde et al. (2018) 49th Lunar and Planetary Science Conference, Abs. # 2673.)

The link between Archean climate change and gold metallogeny

Hartwig Frimmel[1]

[1]University of Würzburg hartwig.frimmel@uni-wuerzburg.de

The first large-scale concentration of gold took place c. 2.9 Ga ago in fluvial conglomerates. Endogeneous gold deposits, such as in porphyry and epithermal systems or orogenic-type deposits only start to play a significant role from c. 2.75 Ga onwards when plate tectonic processes began to operate. The gold mega-event at 2.9 Ga has been explained by a higher Au run-off from the Mesoarchean land surface promoted by deep chemical weathering under a reducing acidic atmosphere and effective trapping of Au dissolved in river water and shallow seawater by microbial colonies. Remnants of microbially fixed gold are preserved in kerogen layers in the lower Central Rand Group of the Mesoarchean Witwatersrand Basin in the Kaapvaal Craton. Most of that gold became mechanically reworked to form rich gold-bearing conglomerates, mainly between 2.9 and 2.8 Ga. The postulated gold mega-event is, however, at odds with our understanding of the Archaean atmosphere and biosphere. The atmospheric composition prior to 2.9 Ga should not have been significantly different to that after 2.9 Ga, and mounting evidence exists that photosynthesizing microbes thrived, at least locally, as early as 3.2 Ga. This raises the question as to the determining factor that controlled the leaching of Au background concentrations from the granitoid-greenstone-dominated Archean land surface. The answer is: climate! At least for the Kaapvaal Craton, a drastic change from cold to warm climate is postulated at around 2.9 Ga. This is indicated by the occurrence of diamictite in the 2.99-2.91 Ga West Rand Group (Witwatersrand Supergroup) and its stratigraphic equivalents in the 2.99-2.95 Ga Mozaan Group (Pongola Supergroup), first recognized as the oldest known glaciogenic deposits by G. Young. In the various goldfields across the Witwatersrand, glaciogenic diamictite has been identified in up to three stratigraphic positions. They are overlain by littoral sandstone, shallow marine ferruginous shale and locally iron formation in the form of finely laminated magnetite-silicate rhythmite, resembling typical glacial and post-glacial deposits known from Paleo- and Neoproterozoic successions elsewhere. Further evidence of cold climate at that time comes from the abundance of detrital feldspar in sandstone, reflecting low degrees of chemical weathering. In contrast the dominant sandstones and in many places gold-bearing conglomerates in the 2.90-2.79 Ga Central Rand Group are conspicuously devoid of feldspar. That group is marked by generally high chemical index of alteration, especially below erosional unconformities. Local diamictite in that group represents debris flow and not glaciogenic deposits. All in all, geological, petrological and geochemical evidence speaks for a major climatic shift at around 2.90 Ga to warm conditions that facilitated leaching of Au from the hinterland, thus triggering the first major concentration of gold in Earth's history.

Shock metamorphism in nature and experiment

Jörg Fritz[1], Vera Assis Fernandes[2]

[1]Rieskratermuseum joerg.fritz@kino-heppenheim.de, [2]Museum für Naturkunde

Meteorites are collisionally derived fragments from various planetary bodies. In space, collisions between a smaller projectile and a larger target typically occur at velocities exceeding several km/s. These impacts drive shock waves through the lithologies in the target area. Minerals constituting the rocks develop characteristic modifications collectively called "shock metamorphic effects". The shock metamorphic record allows quantifying the pressure (P), temperature (T) and time (t) induced by the passing shock wave. Shock metamorphism typically involves increase in P by 10's GPa, induce T increase from few degrees up to the rock's melting point, and typically lasting tens to hundreds of microseconds. Three different types of shock metamorphic effects are discriminated: 1) in the main mass of the meteorite, most minerals develop destructive shock effects where lattice order and density decrease. Examples are mosaicism and planar deformation features (PDF) in olivine and pyroxene or formation of diaplectic glasses of quartz and/or plagioclase; 2) some minerals within the main mass of the rock develop constructive shock effects characterized by an increase in lattice order and density; e.g., the diffusionless transformation of graphite to diamond, cristobalite to seifertite and zircon to reidite. Additionally, specific shock effects are restricted to petrographically atypical regions of the rock; 3) in localized zones of shock melt, specific high-P phases crystallize from the melt or form by coherent and incoherent solid-state transformation processes. These high-P/T phases include ringwoodite, bridgmanite and donwilhelmsite. It has been problematic to develop a self-consistent thermo-barometric interpretation of the complex mineralogical record in meteorites including all types of shock effects. Especially the presence of high-P phases sparked a long lasting discussion regarding the application of dynamic shock versus static high-P experimental data for shock thermo-barometry of naturally shocked meteorites, and correlate it to the mineralogical record with the magnitude and scale of the impact event. Despite the controversy, many impact shock researchers agreed that the natural shock metamorphism preserved in rocks is in conflict with experimental results obtained by the different types of high-P experiments, with different authors favoring results from either one or the other. Here, it is argued that the shock metamorphism changes in meteorites are consistent with results obtained by both shock and static pressure experiments. Characteristic shock deformation effects develop in shock reverberation experiments and hydrostatic pressure experiments as long as both types of experiments achieved the same P and T conditions and the samples are studied in decompressed state. Hence, material behavior during shock compression can be studied "in-situ" using static pressure experiments. A revised shock classification scheme for rocks is presented.

Observations and Projections of Thermal Factors Affecting Weathering of Fractured Sedimentary Rocks of the Niagara Escarpment

Henry Gage[1], Carolyn Eyles[1], Rebecca Lee[1], Alexander Peace[1]

[1]McMaster University gageh@mcmaster.ca

Little research has been conducted into the processes, extent, or factors involved in weathering and erosion of the Niagara Escarpment, particularly those caused by thermal mechanisms. The findings of a preliminary study of temperature changes in fractured sedimentary rocks exposed along the escarpment in Hamilton, Ontario during the winter, spring and summer of 2021 are reported here. The objective of the study was to examine factors promoting freeze-thaw and/or thermal stress during the coldest months, and to identify thermal processes affecting the rocks during the summer. Three field sites along the escarpment were selected for study and at each site temperature probes were affixed to the exposed rock surface and inserted into a nearby fracture. Site characteristics varied in terms of aspect, lithology, vegetation cover, and water seepage. Field observations were supplemented with recordings of rock surface and interior temperature from four dolostone blocks of the Lockport Formation located in an exterior, but protected, location in Hamilton. In all cases, a sampling interval of one minute was used to provide sufficient data resolution for the examination of rapid temperature changes that may lead to thermal fatigue and shock. Preliminary results indicate that recorded temperatures on escarpment rocks follow diurnal trends in insolation and air temperature; however, differences in temperature of several degrees were recorded between the rock surface and fracture interior. Temperatures recorded in the Lockport dolostone blocks showed similar diurnal trends but with smaller differences between the rock surface and interior values. Analysis of field site characteristics suggests that aspect and exposure to direct sunlight play a significant role in determining whether the rock surface is warmer or cooler than the fracture. The influence of changing atmospheric temperature also appears to be weaker in the fracture, which experiences smaller magnitude changes with a lag time. Nevertheless, frequent, rapid shifts from warm to subzero temperatures were recorded at all sites throughout the winter months. Gradients of 1°C per minute or greater, considered necessary for thermal shock, were seldom recorded from either the escarpment face or dolostone blocks during cold periods, but were common during the summer months. This suggests that thermal stress plays a more important role in weathering of the escarpment during the summer, whereas temperature fluctuations around the freezing mark that could stimulate freeze-thaw weathering processes predominate during winter months. Climate modelling suggests that the magnitude of thermal stresses will increase over the next century, potentially leading to increased fracturing of the escarpment rocks and decreasing their resilience to weathering and erosion. Evaluation of the influence of climate change on weathering is an important topic for further research.

Mapping Ejecta Diversity of Young Lunar Craters with Thermal Infrared Imaging

Cailin Gallinger[1], Jean-Pierre Williams[2], Paul Hayne[3], Rebecca Ghent[4], Catherine Neish[1]

[1]University of Western Ontario cgallin4@uwo.ca, [2]University of California, [3]University of Colorado Boulder, [4]Planetary Science Institute

The process of impact cratering creates a wide diversity of ejecta with different geological and physical properties, including particulate/clastic debris, large excavated rocks, and impact melt. Here we fit surface temperature data from the Diviner Lunar Radiometer instrument onboard the Lunar Reconnaissance Orbiter with a modified version of the 1-D lunar regolith thermal model from Hayne et al. (2017), in order to distinguish ejecta types by their variation in thermal inertia (TI), an intrinsic property related to a material's density and thermal conductivity. Specifically, we account for densities in our model beyond standard "regolith" values (~1100-1800 kg/m3), up to the density of basaltic rock (~2940 kg/m3). By simultaneously fitting both the model bottom density and the depth at which the density increases by 1/e of its surface value (the "H-parameter") to night-time surface temperatures, we find that we are better able to match these temperatures than with a single-parameter model. We also find that we can readily distinguish different types of ejecta based on these two parameters and their corresponding thermal inertia-depth profiles for the first time, and that the resulting categories correspond well to observed morphology in high-resolution images. To accomplish this, we map the difference in temperature from early in the lunar night to just before sunrise (Tbol) in red, the best-fit model bottom thermal inertia (TId,T=273K) in green, and the best-fit model H-parameter (H) in blue, creating an RGB map of variations in these parameters across the crater ejecta blanket. Impact melts primarily show up as cyan or green in colour, indicating both high thermal inertia at depth as well as a thick covering of regolith-like material on top, leading to rapid cooling early in the night followed by steady maintenance of temperature once the thermal wave reaches the buried high-TI material. Impact melt flows often have irregular surfaces and cracks that emit at higher surface temperatures than their regolith cover, making them appear green (high TId,T=273K, low H, low Tbol), while impact melt ponds disrupt this layer less, and so appear cyan (high TId,T=273K, high H, low Tbol). Areas with a high concentration of "boulders" (rocks >1 m in diameter) show up as yellow (high TId,T=273K, high Tbol, H=0), indicating high-thermal inertia material with no covering layer of regolith, and show a large change in temperature through the lunar night due to their large emission surface area. Particulate (μm-cm scale) impact ejecta range from red to deep purple (low TId,T=273K, mid-high H, mid-high Tbol) depending on the degree to which they have been resurfaced by mass wasting on sloped surfaces or gardened by self-secondaries and/or minimal disruption of the mature background regolith, respectively.

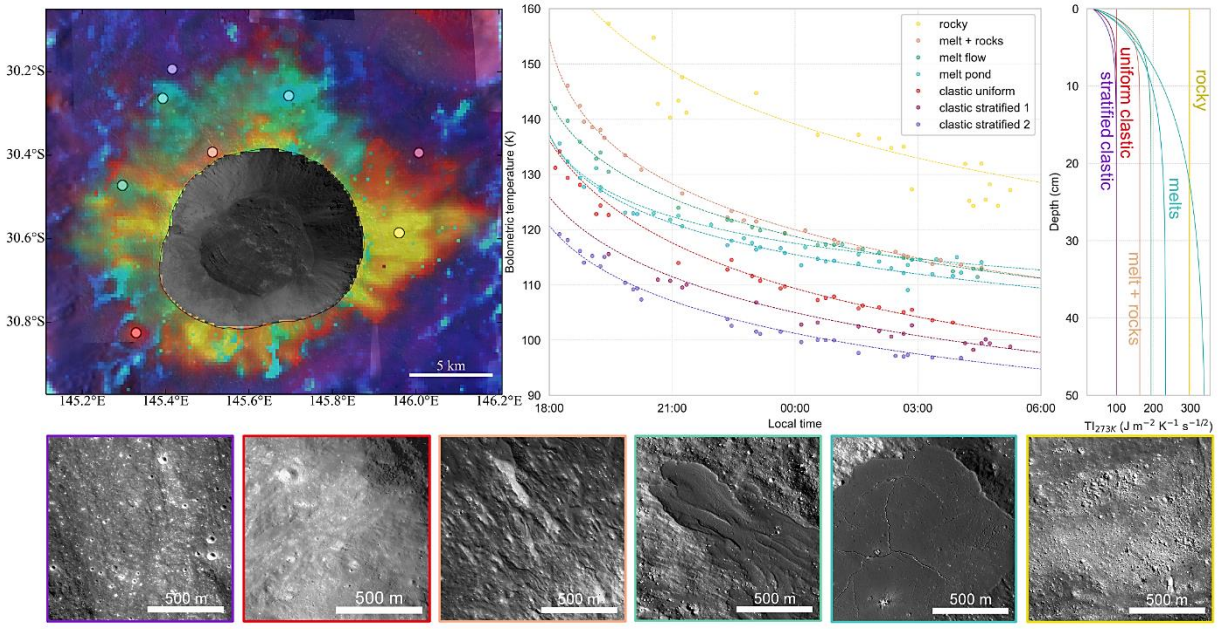

Characterizing zinc-bearing chromite cores in uvarovite garnets from the Pikoo diamondiferous kimberlite field, central eastern Saskatchewan, Canada

Song Gao[1], Kerri Campbell[2], Roberta Flemming[1], Barb Kupsch[3], Ken Armstrong[3]

[1]Western University sgao289@uwo.ca, [2]HighGold Mining Inc., [3]North Arrow Minerals Inc.

Zinc-rich chromite [(Fe,Zn)Cr2O4] is an important repository for chromium (Cr) that has been observed sporadically in kimberlite-bearing deposits worldwide. As another source reservoir for Cr, the green uvarovite garnet [ideally Ca3Cr2(SiO4)3] is the rarest variety among anhydrous garnets. Despite being reported from a wide range of localities, the occurrences of uvarovite are predominately restricted to hydrothermal and metamorphic settings rarely associated with kimberlite. Here, we present a detailed petrographic, mineralogical, and geochemical characterization of 71 uvarovite garnets with zinc-bearing chromite cores recovered from the Pikoo Property (central eastern Saskatchewan), which also hosts recently discovered kimberlites proven to be diamondiferous. In this work, euhedral to anhedral unzoned chromite occurs as kernels or cores and, in some cases, as irregular inclusions enclosed by uvarovite mantles. They contain moderate to high Cr [41.63-66.70 wt.% Cr2O3; Cr/(Cr+Al) = 0.64-0.99], Fe2+ (16.71-28.67 wt.% FeO) and Zn (1.64-15.52 wt.% ZnO) contents (Fig. 1), accompanied by an appreciable amount of Mn (0.63-2.32 wt.% MnO). The core with the highest Zn content gave structural formula $(Zn_{0.409}Fe^{2+}_{0.555}Mg_{0.018}Mn_{0.019})_{1.00}(Cr_{1.174}Al_{0.674}Fe^{3+}_{0.152})_{2.00}O_4$, which corresponds to Zn-rich chromite with a minor proportion of other end-members (e.g., hercynite, FeAl2O4). The garnets are compositionally zoned and occasionally devoid of inclusions. Formula calculations indicate that they are mainly members of the uvarovite-grossular series (up to 93% mol.% Uv) enriched in Ca (22.99-35.57 wt.% CaO) and Cr (up to 28.10 wt.% Cr2O3), but consistently depleted in Mg (mean = 0.10 wt.% MgO) and Ti (mean = 0.26 wt.% TiO2). Most garnets exhibit a core-rim zoning pattern, whereas the remainder are irregularly zoned and show evidence of resorption. The core to rim trend is characterized by an increase in grossular proportion at the expense of the uvarovite component. Morphological characteristics, textural interrelations, and compositional trends suggest that uvarovite garnet formed through interaction of Zn-rich chromite with late metasomatic (Ca,Al)-enriched hydrothermal fluids capable of precipitating secondary grossular.

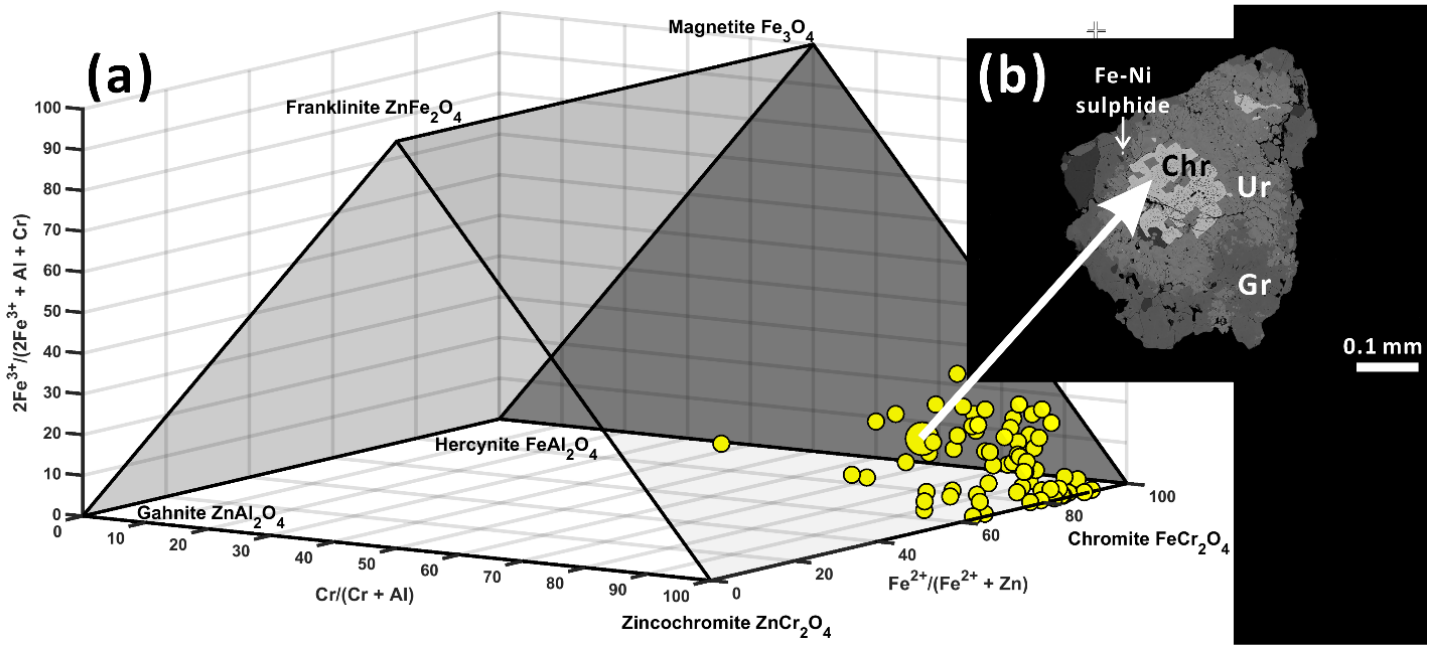

Figure 1. (a) Spinel-group mineral prism showing compositional variation of zinc-rich chromites from the Pikoo Property; (b) Back-scattered electron (BSE) image showing zinc-rich chromite core enclosed by uvarovite-grossular mantle. Chr = chromite; Ur = uvarovite; Gr = Grossular.

The origin of carbonates from well M0077A at the Chicxulub impact crater, Mexico

Nicolas Garroni[1], Gordon Osinski[1]

[1]University of Western Ontario ngarroni@uwo.ca

Despite there being a presence of carbonate lithologies in the target rocks of ~40% of all confirmed impact craters on Earth, how carbonates react during impact events remains debated. Contention remains as to whether carbonate rocks melt or devolatilize and release CO2 gas, or both. The Chicxulub impact crater in Mexico is ~180 km in diameter and it is calculated that approximately 425 gigatons of CO2 was released into the atmosphere from devolatilization, contributing to the subsequent K-Pg mass extinction event at ~66 Ma. However, carbonate melt discovered in several core sections across the crater alternatively suggests less CO2 than calculated managed to escape. In this contribution, core from the 2016 offshore IODP/ICDP Expedition 364 containing impact melt-bearing breccia was analyzed to further understand the effects of hypervelocity impacts into carbonate rocks. From 41 thin sections, calcite was the only carbonate present and was classified petrographically and geochemically into five morphological types: two types of clasts (A-class and B-class), matrix, void fill and flow. The A-class clasts are typically composed of featureless crystalline calcite, yet occasionally show sedimentary and biological features; they are also slightly elevated in MgO. The B-class clasts are also featureless crystalline calcite and are slightly elevated in MgO and MnO; however, these clast types include one or more rims of clay/calcite enveloping the clasts. The matrix calcite is crystalline and found interspersed with varying amounts of SiO2, feldspar, clay and zeolites, and is similarly elevated in MgO and MnO. The void fill calcite is coarse crystalline and the most elevated in MnO. Finally, the flow calcite is the purest form without any elevated concentrations of minor oxides. Here, it is suggested that the B-class clasts were a product of melted carbonate rock explosively interacting with resurging seawater shortly after impact, and that the mineralized rim and elevated concentration of MnO were the result of later hydrothermal activity, as is the MnO concentrations in the other calcite varieties. Large quantities of carbonate melt would likely have been present at this time in order to produce the numerous rimmed clasts in the breccia; however, significant layers of carbonate melt rock have yet to be discovered. Nevertheless, the small amount of flow calcite, here interpreted as carbonate melt rock, which is located directly above the contact with the underlying silicate-rich melt rock, may be the missing-link to the prior existence of a larger quantity of carbonate melt.

Ice-margin reconstruction during MIS 2 deglaciation in Manitoba, Canada

Michelle Gauthier[1], Andrew Breckenridge[2], Tyler Hodder[1]

[1]Manitoba Geological Survey michelle.gauthier@gov.mb.ca, [2]University of Wisconsin - Superior

Reconstruction of deglacial ice margins provide insights into the demise of past ice sheets and help to understand how former ice sheets responded to climate change. Here, we reconstruct deglacial Laurentide Ice Sheet margins across Manitoba (Canada), a dynamic region that in MIS 2 spanned from an inner core region of the Keewatin Sector to a periphery ~900 km north of the Late Glacial Maximum limit. The area was also overrun by ice flowing from both the Quebec-Labrador dispersal centre and the Hudson Bay Ice Saddle. Complicating reconstruction, the surficial landscape of Manitoba contains inherited relict and palimpsest glacial landscapes, which need to be separated from landscapes formed during deglaciation. We first compile deglacial data using newly-digitized geomorphology, simplified surficial geology mapping and the youngest-mapped (relative age) ice-flow orientations. Then, we incorporate local and regional field studies to assess relative timing and evidence that deglacial features are ice-marginal (e.g. end moraine vs interlobate moraine). An attempt is made here to assign vetted and updated calibrated radiocarbon ages to deglacial isochrones.

Petrogenesis and mode of emplacement of the Neoarchean Round Lake Batholith, Kirkland Lake, Ontario

Catherine Gavaris[1], Matthew Leybourne[1], Lucie Mathieu[2], Kate Rubingh[3]

[1]Queen's University 16ceg@queensu.ca, [2]Université du Québec à Chicoutimi, [3]Laurentian University

The petrogenesis of Archean synvolcanic intrusions of the Abitibi greenstone belt (AGB) can provide essential constraints on Archean mantle conditions and on the geodynamic and metallogenic evolution of the AGB. During the synvolcanic period, which is the main phase of construction and maturation of the AGB, large-volume tonalite-trondhjemite-granordiorite (TTG) intrusive suites formed. A part of these suites is genetically associated with Au and Cu-Au magmatic-hydrothermal mineralisation. These TTG suites can provide essential constraints on the geodynamic and metallogenic evolution of the AGB, and most intrusions remain poorly documented. This study aims at unravelling the petrogenesis of one of these TTG suites, the Round Lake Batholith, in order to better understand the geodynamic and economic significance of TTG suites, and to better constrain Archean mantle conditions. The Round Lake Batholith is an example of a southern Abitibi TTG magmatism and could be one of the youngest TTG suites of the AGB. According to field relationships, the Round Lake Batholith consists of two distinct intrusive phases: 1) the outer rim, which displays a strong foliation and is made of quartz, feldspar, ± amphibole and biotite; and 2) the inner section, which is massive to weakly foliated and made of amphibole or biotite, quartz and feldspar. These magmatic phases have distinct chemistries, with REE profiles that are more fractionated for the inner phase than for the outer (La/Yb= 12.17 to 60.00 for the outer phase and La/Yb= 28.18 to 184.00 for the inner phase). The outer rim is more HREE-rich than the inner section (i.e., Yb = 0.25 to 0.46 ppm versus 0.05 to 0.22 ppm). Geothermobarometry using amphibole chemistry will determine depth, pressure, and temperature conditions of emplacement of the intrusive phases and isotopic analyses will determine source and partial melting conditions. Furthermore, in-situ U-Pb ages determined from zircons observed in thin sections indicate that the outer rim (2720.65 ± 17.7 Ma) is older than the inner portion (2691.15 ± 22.1 Ma). In addition to showing that the Round Lake Batholith has the typical geochemical signature of a TTG suite, its geochemistry supports field observations and initial U-Pb geochronology that show that the batholith is composed of two distinct magmatic phases. Due to the current pandemic procedures, this study is on hold and additional geochronological data will be obtained using zircon separates, while additional geothermobarometry and isotopic analysis will be performed using amphibole.

The Path from Raw Data to Robust Data Analysis: The Significance of Data Treatment to Geochemical Interpretation

Zohreh Ghorbani[1], Neil Banerjee[1], Lisa Van Loon[1]

[1]Western University zghorba@uwo.ca

One of the most important objectives in conducting geochemical surveys, from mineral exploration to environmental assessment, is to identify thresholds and evaluate multi-element interrelationships and correlations. Therefore, it is of utmost importance to validate data before statistical analysis and interpretation. Data validation helps deal with missing values and outliers. Many studies have indicated that fabrication or data substitution by a fraction of the detection limit for each undetected value causes bias and poor correlation. Hence, robust data analysis has been developed to maintain the quality of data proactively without reporting bias, artificial anomalies, contaminations, or correlations. Maximum likelihood estimation (MLE) and Kaplan-Meier are commonly used as the most robust approaches to deal with missing values in geochemical data. Besides, geochemical data are most commonly compositional and do not follow a normal distribution. Therefore, the next step is to normalize data using a suitable transformation method such as log-ratio, robust Z-score, or power Box-Cox to overcome the potential for closure and the skewed nature of geochemical data. Finally, to reveal the complex and hidden interrelationships and correlations between elements and associated samples, simultaneously, robust multivariate statistical analyses can be applied. M-estimation or Fast minimum covariance determination (Fast-MCD) principal component analysis (PCA) is a well-known robust multivariate technique used to complement the limitations of the graphical and classical methods of geochemical processes interpretation. This study aims to demonstrate the path from raw data toward robust data analysis and attest to the robustness of the results. To illustrate the point, a comparison between raw data statistics and robust data analysis at each step is provided using ioGAS (geochemical analysis software). These approaches assist geochemists to reliably discover a wide range of elemental interrelationships, vectors toward mineralization, or sources of contamination.

Taphonomy and Depositional History of the Southfork Quarry (Cypress Hills Formation) in southwestern Saskatchewan, Canada

Meagan Gilbert[1], Frank McDougall[2]

[1]Government of Saskatchewan meagan.gilbert@gov.sk.ca, [2]Saskatchewan Archaeological Society

The Eocene to Miocene Cypress Hills Formation (CHF) spans 28 million years, and forms the conglomeratic caprock of the Cypress Hills plateau in southwestern Saskatchewan. The formation records one of the last major sedimentation events in the western plains of North America at a time when the world was undergoing major climate fluctuations. As well, the CHF contains the only high latitude, non-polar mammalian fossil assemblage known (Uintan to Hemingfordian land mammal stages) in North America. The Southfork Quarry is Late Eocene in age and was originally discovered in 1962 after bones were discovered at the base of a road cut on the southeastern flanks of the Cypress Hills. Numerous field campaigns (e.g. 1962, 1970, 1971, 1999, 2000, and 2001) by staff of both the Royal Saskatchewan Museum and the Royal Ontario Museum have resulted in the collection of numerous fossil elements from a multitaxonomic bonebed. This includes a dog-like carnivore (Hyaenodon horridus), early horses and tapirs (Mesohippus westoni, Colodon occidentalis), small rhinos and deer (Hyracodon petersoni, Leptomeryx yoderi.), Megacerops coloradensis and freshwater fish (i.e. Astephus sp.). Detailed sedimentologic, paleontologic, and taphonomic studies have been conducted to establish a depositional environment framework of the Southfork Quarry. The datasets reveal a complex depositional history consisting of a number of stages of stream channel evolution over geologic time. This small site reveals basal coarse cobble conglomerates sequentially replaced by sandstone and claystone deposited by meandering channel systems in a semi-arid riparian biome. Numerous studies of this kind are ongoing to established a detailed regional framework to help unravel the notorious complexity of the CHF, which hosts one of the most significant Cenozoic mammalian faunas in Canada.

Thermal Conductivity of Geologic Material at Cryogenic Temperatures

Cosette Gilmour[1], James Freemantle[1], Michael Daly[1]

[1]York University cgilmour@yorku.ca

There are many thermal conductivity investigations of geologic material available [1-10]; however, these studies focus on atmospheric and mantle conditions (T ~ 300 K; P ~ 1 atm). For temperatures < 300 K, there are very few studies [e.g., 11,12] indicating a need to improve our understanding of how thermal properties of geological material behave at low temperatures. Thermal conductivity is a complex property to measure at any temperature given that the physical properties of minerals are determined by their crystallographic structure and symmetry [13]. As such, thermal conductivity varies in anisotropic minerals based on the direction of heat flow relative to the crystallographic axes. Porosity of a rock sample can also influence the thermal conductivity as pore spaces act as barriers for heat flow (thermal conductivity ≈ 1/porosity) [11]. Beyond physical properties, a mineral's composition is also important to consider as elemental variations (i.e., solid solution) result in thermal conductivity variations [e.g., 5,7,8]. Other properties that influence the thermal conductivity of a given rock sample are density, mineral distribution, water content, grain size, sample locality, and experimental conditions [7,9-11,14].

To overcome the challenges of measuring the thermal conductivity of geologic material, we have developed an analytical procedure that considers the composition, porosity, and bulk density of a given sample to aid in interpreting the thermal conductivity at cryogenic temperatures. Our study uses a Cryogen Free Measurement System to measure the thermal conductivity of geologic material between 5 and 300 K under vacuum (10-4 hPa). Completing thermal conductivity measurements under vacuum removes the effect of the thermal conductivity of the surrounding gas, thus effectively measuring the true thermal conductivity of a given sample. Measuring thermal conductivity at cryogenic temperatures offers novel insight into the behaviour of thermal properties of geologic material at low temperatures which also has implications for extraterrestrial studies.

1Birch F. & Clark H. 1940. Am. J. Sci, 238:529-558.
2Birch F. 1942. Handbook of Physical Constants, pp. 243-266.
3Clark S. 1966. Handbook of Physical Constants, pp. 459-482.
4Horai K. & Simmons G. 1969. EPSL, 6:359-368.
5Horai K. 1971. J. Geophys. Res., 76:1278-1308.
6Beck A. et al. 1978. Phys. Earth. Planet. Int., 17:35-53.
7Čermák V. & Rybach L. 1982. Landolt-Börnstein, Vol. 1a. pp. 305-343.
8Diment W. & Pratt H. 1988. USGS, Report 88-690, p. 15.
9Robertson E. 1988. USGS, Report-88-441, p. 106.
10Clauser C. & Huenges E. 1995. Rock Physics & Phase Relations, Vol. 3, pp. 105-126.
11Opeil C. et al. 2012. M&P

The Fåvne vent field: an active iron-rich hydrothermal deposit at the termination of the axial valley bounding fault on the Mohns ridge

Caroline Gini[1], John Jamieson[1], Katleen Robert[1], Thibaut Barreyre[2], Eoghan Reeves[2], Steffen Jorgensen[2], Amy Gartman[3]

[1]Memorial University of Newfoundland cgini@mun.ca, [2]University of Bergen, [3]USGS

Each new discovery of a seafloor hydrothermal deposit along the global mid-ocean ridge system improves our understanding of the diversity of composition, morphology and geological setting of these often metal-rich deposits, and provides important comparisons for understanding ancient analogues. Fluid pathways are poorly constrained due to the complexity and diversity of hydrothermal systems, and the challenges associated with collecting data from the sub-seafloor. Here we present results from exploration and sampling of the Fåvne vent field, a hydrothermally active field discovered in 2018, and located at a depth of 3000 m on the Mohns Ridge, in the Greenland Sea, northwest of Norway. The vent field is located on the hanging wall at the termination of a 2 km high normal fault scarp that forms the western bounding wall of the ridge axial valley. The roughly 200 m diameter circular vent field consists of clusters of sulfide- and oxide-rich mounds with some active chimneys. In addition, inactive hydrothermal deposits were also discovered on the footwall fault scarp directly across from the main field, and weathered sulfide-rich talus was discovered at the base of the fault scarp 500 m to the southwest of the main field. Within the main vent field, the deposits are arranged in 15-60 m diameter and 5-20 m high mounds with needle-like chimneys at their summits and broken pieces of chimneys at their bases. On the outskirts of the field to the east, mounds are less than 5 m high. The deposits are primarily composed of pyrrhotite, sphalerite, chalcopyrite, Fe-oxides, pyrite, marcasite, galena. A unique feature of this vent field is the relatively Fe-oxide-rich, S-poor composition of the deposits. We investigate the origin of this high Fe/S ratio, as well as the unique tectonic setting of the vent field at the termination of a major fault scarp, away from the supposed heat source associated with the axial volcanic ridge.

SEM-Based automated petrography: Applications to mineral exploration

Rejean Girard[1], Jonathan Tremblay[1]

[1]IOS Services Géoscientifiques rejeang@iosgeo.com

Petrography in an intrinsic part of a geologist training, so its value remains undisputed as part of most comprehensive studies. However, petrography remains a descriptive and interpretative procedure the quality and accuracy of which is heavily dependent on petrograph's experience and skills. Recent advances in performances of fast EDS detectors enabled the capacity of an automated SEM to scan the entire surface of a thin section with a few micrometers resolution within an hour, work that can be automated for overnight acquisitions. Aside of conventional secondary and back scattered electrons or cathodoluminesence image, X-ray maps are simultaneously acquired for most elements, which spectrums can be deconvoluted into chemical analyses for each pixels. Crystal orientation and fabrics can even be simultaneously acquired with adjunction of EBSD detectors. Chemical analysis can then be clustered into mineral species, and an accurate mineral map is computed. Aside of this stack of maps, minerals species are quantified both in abundance and chemistry. Then, with the use of image processing software, the maps can be segmented into individual minerals grains or aggregates, with their individual size measurement, axis ratio, orientation, rugosity, and neighboring or association relations with other mineral. All this information is quantitative, replicable and certified, and mineral species are properly identified as far as their size exceeds the resolution of the image. Then, this information can be provided to the petrograph so he can complete its interpretation with conventional optical microscope verifications. Identifying and estimating the abundance and size of the mineral is a tedious task with an optical microscope, with time consuming measurement of various crystallographic parameters (ex: conoscopic observations). These tasks typically consume most of the petrograph efforts to acquire incomplete or inaccurate mineral species identification. Consequently, the effort and times saved by the petrograph amply compensates for the SEM acquisitions cost. A seamless and cost effective workflow will be presented. A case study will be presented where alteration facies within a volcanic hosted orogenic gold deposit were reconstructed in conciliation of their chemistry and norms. The use of the method for vectoring alterations, geometallurgical domaining and eventual mine residues management will be addressed.

Gold assaying, grains size distribution and probability laws: Dealing with the nugget effect

Rejean Girard[1]

[1]IOS Services Géoscientifiques rejeang@iosgeo.com

Gold is notoriously nuggetty in any mineralized deposit, and this heterogeneity at the sample scale is the cause of a plethora of issues in determining a sample grade. These issues are well known to gold explorationists and are the cause of severe uncertainties in deposit evaluation or resource estimation. Since gold is malleable, its grain size cannot be reduced by milling, and representativeness cannot be maintained through conventional pulverization and aliquoting. Hence, the traditional approach to evaluate the grade of coarse gold samples is to increase the weight of the aliquot submitted for assaying, which faces practical limitation. Even using 1 kg aliquots, replicate assays remain plagued with variance that exceeds what can be tolerated for deposit evaluation. Gold weight contribution of a grain in a sample is a nearly cubic function of its diameter, and the distribution of large grain in assaying aliquots is more or less random causing this variance. Automated SEM technologies currently enable measuring the size of thousands of gold grains in samples in efficient and accurate manner. Such measurements indicate that gold grain size, as for most minerals in rocks, follows a log-normal distribution, typically slightly asymmetric and leptokurtic on the log-scale. From the statistical estimators of these distribution, a rate of occurrence of grains of specific size can be computed, including the rate of occurrence of abnormally large grains. Furthermore, the probabilities of obtaining a grain from a sub-population with a rare characteristic, such as a grain of a specific size, are dictated by a Poisson probability law. From these, the probability of occurrence of grains of specific size in an aliquot of limited representativeness can be estimated. Integration of the probabilities of occurrence of grains over the spectrum of size can hence be converted into a grade distribution, hence a probability of grade and a variance in the assaying aliquots. Although theexact grade of a specific sample cannot be forecast, the biais caused by the presence of coarse grains on a large set of assays can be estimated. The method can be used to detect sampling or assaying flaws in resource definition projects.

Geology and geochemistry of the Elsie Mountain and Stobie formations, Huronian Supergroup: Developing a chemostratigraphy to address challenges with the current subdivision

Caroline Gordon[1]

[1]Ontario Geological Survey caroline.gordon@ontario.ca

The Paleoproterozoic Huronian Supergroup (HSG) is a well-preserved package of supracrustal rocks deposited along the southern margin of the Superior Province between ~2.5 and 2.2 Ga. Volcanic rocks occur in the lower part of the HSG succession. In the Sudbury area, the volcanic rocks are subdivided into the Elsie Mountain Fm (mafic metavolcanic rocks with minor felsic metavolcanic and metasedimentary rocks), Stobie Fm (mafic to felsic metavolcanic rocks with metasedimentary rocks), and Copper Cliff Fm (felsic metavolcanic rocks). The criterion historically used to differentiate between the Elsie Mountain and Stobie fms is the percentage of intercalated metasedimentary rocks (Elsie Mountain <15%: Stobie >15%). This presents challenges in identifying and correlating the volcanic units, especially where the Elsie Mountain and Stobie fms are interlayered with overlying metasedimentary rocks of the Matinenda or McKim fms; intruded by mafic rocks; and/or have undergone multiple deformation events. Based on recent mapping in the Sudbury area, a preliminary geochemical characterization of the mafic volcanic rocks of the Elsie Mountain and Stobie fms is presented. Mafic volcanic rocks of the Elsie Mountain Fm are divided into EMF-1 and EMF-2, which are geochemically distinct from each other and mafic rocks of the Stobie Fm. Mafic rocks of EMF-1, along with Stobie Fm, are high-Fe tholeiitic basalts. EMF-1 represent the basal lavas, but they are not the most primitive lavas as they have lower MgO, Ni and Cr and higher SiO2 compared to the overlying Stobie Fm. Mafic rocks of EMF-1 and Stobie Fm exhibit similar primitive mantle-normalized trace element profiles characterized by LREE enrichment relative to HREE and negative Nb-Ta-Ti anomalies. EMF-2 mafic volcanic rocks are tholeiitic andesites with distinct primitive mantle-normalized REE profiles characterized by strongly depleted HREE. EMF-2 mafic rocks also have higher Ni and lower V contents compared to EMF-1. On a Nb/Yb versus Th/Yb diagram (Pearce element diagram), the EMF-2 mafic rocks define a distinct trend separate to that of the EMF-1 and Stobie Fm mafic rocks. Comparing data from this study with HSG volcanic rocks in the Thessalon area (~200 km to the west), the mafic rocks of EMF-1 and Stobie Fm are comparable to an upper basalt-basaltic andesite Thessalon unit. The rocks of EMF-2 closely resemble a stratigraphically lower basalt-andesite Thessalon unit. Based on the geochemical similarity with the Thessalon volcanic rocks, similar magmatic processes were likely responsible for the generation of the Thessalon, Elsie Mountain and Stobie fm mafic volcanic rocks. Results from this study highlight: 1) there are at least 3 geochemically distinct mafic lava sequences within the Stobie and Elsie Mountain fms, and 2) the need for detailed geochemical characterization of volcanic units in the Sudbury area to aid in mapping and correlation.

The Chapel Island Formation and the Cambrian GSSP in Newfoundland, Canada: A view from unexplored sections

Romain Gougeon[1], Gabriela Mángano[1], Luis Buatois[1], Guy Narbonne[2], Brittany Laing[1], Maximiliano Paz[1]

[1]University of Saskatchewan gougeon.romain@gmail.com, [2]Queen's University

The Chapel Island Formation (CIF) of Newfoundland, Canada, is a 1000+ m-thick siliciclastic succession that hosts the Cambrian GSSP (ca. 541 Ma) 2.4 m above the base of its member 2 (M2) in Fortune Head. Although the first appearance of Treptichnus pedum was considered as the marker of the base of the Cambrian, other burrows typical of the Fortunian (e.g. Bergaueria, Gyrolithes) made their first appearance close to the base of M2 as well. Fortune Head has been the focus of most studies in the area, but Ediacaran and Cambrian strata are also recorded in three additional sections of the CIF. Grand Bank Head, located ? 6 km northeast of Fortune Head, consists of a thick Ediacaran interval (member 1, or M1), and a good exposure of M2; however, the beginning of the Fortunian is located on a faulted zone with difficult access. The succession at Lewin's Cove, located ~45 km east of Fortune Head, includes strata from M1 up to the middle of M2; however, rock exposure is hampered by discontinuities and vegetation cover. Finally, Point May is located ~17 km southwest of Fortune Head and holds a record of the top of M1 to M2 with a fault affecting the M1/M2 contact. Detailed information on sedimentary facies and trace fossils, the latter including trace fossil occurrences, trace fossil sizes and depths, and bioturbation intensities [Bioturbation Index (BI) and Bedding Plane Bioturbation Index (BPBI)], has been collected from Fortune Head, Grand Bank Head, Lewin's Cove, and Point May. At the former three sections, the Ediacaran is dominated by low ichnodiversity, mm-scale burrow size and depth, and low bioturbation intensities (BI = 0-1, BPBI = 1-2). Conversely, the basal Fortunian is marked by a burst in ichnodiversity and ichnodisparity, the appearance of cm-scale burrow size and depth, and a slight increase in bioturbation intensities (BI = 0-2, BPBI = 1-4). However, a different situation is apparent at Point May, with trace fossil diversity and bioturbation intensities remaining relatively low through M2. Facies analysis at Point May shows that depositional environments fluctuated between the lower and upper offshore, which are also common at the three other localities. However, the paucity of bedding plane exposures, which are the most favorable setting to detect predominantly horizontal Cambrian trace fossils (e.g. Psammichnites, Rusophycus, Treptichnus), may have impacted negatively on trace fossil identification. This may be the reason why the Point May section does not provide confident examples of Treptichnus pedum. Therefore, other ichnologic criteria had to be employed to delineate the basal Fortunian, such as the first appearance of vertical burrowing (Bergaueria, Gyrolithes) and slightly higher bioturbation intensities (BI = 2). These results demonstrate that robust sedimentological analyses coupled with an assessment of outcrop quality are essential procedures for any ichnological studies focussing on this critical time of the history of life.

Expression of the Middle Devonian Kačák Episode in the Mackenzie Mountains, Northwest Territories, Canada

Sofie Gouwy[1]

[1]Geological Survey of Canada sofie.gouwy@canada.ca

In the Mackenzie Mountains (NW Territories, Canada), the Kačák Episode interval situated close to the Late Eifelian-Early Givetian boundary is characterized by a sharp facies change due to a hypoxic perturbation. The open-shelf limestone of the Hume Formation is overlain by the fine black calcareous shales of the Bluefish Member (Hare Indian Formation). This interval was studied in 6 sections along the northern Mackenzie Mountain front. Conodont faunas from the Hume Formation place its main part in the Eifelian kockelianus Zone. The initial onset of the black shales took place in the Eifelian ensensis Zone, suggested by the appearance of the brachiopod Eliorhynchus castanea in the uppermost 3 meters of the Hume Formation. The first Givetian conodont fauna was identified at 7.5m above the base of the Bluefish Member. The global Ka?ák Episode represents a polyphased biotic crisis, usually associated with a transgression, with a first phase indicated by a sharp turnover in conodont fauna and facies: a sudden onset of dark otomari shales in the hemipelagic to pelagic realms (otomari event), and a second phase (Kačák event s.s.) coinciding with the Eifelian-Givetian boundary. The Hume-Hare Indian formation transition is generally interpreted as a deepening event and the sharp contact between the two formations as a drowning surface. Nowakia sp. cf. otomari appears in the uppermost meter of the Hume Formation. This otomari event coincides here with an innovation in conodont fauna: new taxa and new morphotypes appear in the top of the Hume Formation, right below the onset of the black shales. The Eifelian-Givetian boundary (and the Kačák event s.s.) cannot be accurately situated in the sections, due to the lack of the index taxon Polygnathus hemiansatus. Based on stable oxygen isotope analysis on conodont apatite of monogeneric assemblages, this innovation coincides with a significant decrease of $\delta^{18}O$ values from 18.1 -18.2‰ in the Hume Formation to 16-17.2‰ in the uppermost meter of the Hume Formation and lowermost few meters of the Bluefish Member. If no change in salinity were assumed, this shift would suggest a warming of the paleo-ocean surface waters that might have promoted the innovation and could have induced a reduction in oxygenation of the water column in combination with a sea-level rise.

Impactites on Earth and the Moon: Examining Impact Melt Rocks and Assessing their Link to Volcanic Deposits on Earth and other Planetary Bodies

Jamie Graff[1], Gordon Osinski[1]

[1]University of Western Ontario

Impact cratering is a fundamental process affecting nearly all terrestrial planetary bodies in the Solar System. Understanding the cratering process and resultant ejecta deposits is crucial for characterizing planetary surface geology on terrestrial bodies. Impact cratering events are complex processes that yield a wide variety of ejecta and melt products during their emplacement phases, while volcanic processes and pyroclastic flows also create vast areas of ejecta deposition. Both impact and volcanic processes often produce rock types and ejecta deposits that feature similar morphology, in the form of heterogenous rock formations interspersed with glass, fractured rock fragments, and mineral clasts produced by either the eruption of ash or lava (volcanic origin) or from meteorite impact into planetary crusts (impact origin). Many impact deposits on Earth are not well preserved, nor has anyone directly witnessed the process of impact crater formation, and so narrowing down the exact process(es) of formation of impact craters remains a difficult task. Further examination and understanding of impactite and volcanic rock characteristics will help to provide connections between these two depositional events and to better classify impactites using modern and consistent naming conventions. In this study we aim to assess the similarities and differences in textural and petrographic characteristics between impactites and pyroclastic ash flow tuffs from a variety of locales. These locales include pyroclastic rocks from the Lake Taupo Volcanic Zone in New Zealand and the Joe Lott Tuff in Utah, and impactites from the Popigai Impact Crater in Siberia and a suite of lunar rocks obtained during the Apollo missions. The main objective of this research is to investigate the nomenclature currently in use to describe both pyroclastic rocks and impactites to lay the groundwork for revisiting and updating the previously established, yet archaic, nomenclature of impactites to more modern and descriptive naming conventions. Preliminary results from the analysis of Lake Taupo volcanic rocks and Popigai impactites have shown that both suites of rocks exhibit similarities in overall mineralogy and texture, notably among the presence of dominant rock-forming minerals, flow textures, crystal fracturing, grain size variability, and poor sorting. Regarding nomenclature, the Lake Taupo volcanic rocks exhibit characteristics most indicative of unwelded ash tuffs, while the Popigai impactites contain samples - previously characterized as 'suevites' - that are more accurately described as impact melt-bearing breccias and lithic impact breccias.

Geothermal Energy Resources of the Garibaldi Volcanic Belt

Stephen Grasby[1]

[1]Geological Survey of Canada steve.grasby@canada.ca

Canada stated goal of achieving net zero emissions by 2050 requires a significant transition to renewable energy resources. While wind and solar power have been a primary focus, their intermittent generation creates challenges to support a grid. Geothermal energy has many benefits compared with other renewables, principally it provides a highly stable, reliable, and dispatchable power supply. The reliability of geothermal energy is countered by the high exploration risk associated with drilling deep exploration wells to discover hot, and more critically, permeable reservoirs. Reducing these exploration risks requires novel geoscience tools. Mount Meager is the only active volcano in Canada, last erupting about 2400 years ago, and today being characterised by fumaroles and numerous thermal springs. During the energy crises of the late 70's and early 80's the federal government initiated a Geothermal Energy Program, responsible for collecting much of the geothermal data that exists today. As part of this now defunct program an exploration well was drilled on Mount Meager, this and subsequent wells defined the highest temperature thermal resource known in Canada, with 250 °C waters discovered at about 2 km depth. This is a world class thermal resource - that has never been developed. Initial attempts at power generation were marginally successful and it was determined that despite the high temperature, flow rate was insufficient to produce sufficient power. Permeability became the limiting factor for the project success. New ideas and methods for the prediction of high-permeability zones at depth are required. To this end the Geological Survey of Canada assembled a team assembled comprised of 34 researchers from a total of seven universities and government agencies. The research program is supported by Geoscience BC and the Natural Resources Canada Emerging Renewable Power Program. Researchers with expertise in geological and structural mapping, volcanology, geophysics (especially gravity, magnetotelluric, and passive seismic surveying), geochemistry, regional stress field analyses, and hydrogeology were brought together into one coherent research project starting in July 2019. The goal is to use an integrated approach to see into the heart of the mountain and enable clearer identification of high-permeability zones within the known thermal anomaly. The research is ongoing and this presentation will highlight the challenges of running a geothermal field program on a crumbly volcano, current findings of the research team, and future work.

Late Paleoproterozoic lower crustal nappe stacking in Rae craton continental margin, Athabasca mylonite triangle, Snowbird tectonic zone

Riccardo Graziani[1], Kyle Larson[1], Jaida Lamming[1], Nicolas Piette-Lauziere[1]

[1]University of British Columbia riccardo.graziani@alumni.ubc.ca

The assembly of Laurentia is characterized by a series of orogenic events that occurred in the late Paleoproterozoic era. One such is the Snowbird Orogeny, caused by the collision between Rae and Hearne cratons. A portion of Rae affinity lower crust is exposed in the Athabasca Mylonite Triangle (AMT) of Northern Saskatchewan where three structurally separated tectonic units, the Upper Deck, NW domain, and Chipman Domain, offer a unique window into lower crustal processes not typically available in younger orogens. Here we present a detailed, multidisciplinary investigation of the tectonic evolution of the Intra Tantato Shear Zone (ITSZ), which separates the Upper Deck and NW domain. The ITSZ is a low to high angle, curvy planar kilometer-thick mylonite zone hosted within granulite-facies orthogneiss and paragneiss. Kinematic indicators and quartz crystallographic preferred orientations outline two distinct deformation events characterized by opposite sense shear: (1) a top-to-the-ENE thrusting of the Upper Deck over the NW domain (D1) and (2) a later normal-sense top-to-the-WSW kinematics reactivation (D2). The shape and the opening angle of D1 quartz c-axis fabrics indicate constrictional kinematics at temperatures ranging between 750±50 °C and 550±50 °C while D2 c-axis fabrics indicate plane strain deformation at 550±50 °C. Monazite and garnet geochronology from the Upper Deck returns a variety of dates spread between 2.6-2.3 Ga, broadly coincident with the Arrowsmith orogeny. Europium-rich monazite overgrowths in Upper Deck specimens indicate a metamorphic peak at ~1.915 Ga, slightly older than garnet nucleation (Lu-Hf) dates in the NW domain at ~ 1.905 Ga. This contrast in dates is interpreted to reflect post-peak metamorphism Upper Deck overthrusting and burial of the NW domain. Monazite rims on specimens that record D2 reactivation yield dates of ~ 1.860-1.830 Ga, contemporaneous with the oldest activity recorded in the nearby Grease River Shear Zone, part of the main Snowbird system. We interpret early deformation (1.905 Ga) within the ITSZ (D1) to reflect nappe stacking during the collisional stage of the Snowbird orogeny while its reactivation (D2) is interpreted to record the transition to a regional strike-slip dominated regime. Our results indicate that the Snowbird Orogeny records a similar tectonic evolution to that found in more recent collisional belts such as the Variscan orogen with early shortening accommodated by crustal thickening and dip-slip shear zones and late lateral drift dominated by strike-slip shear zones.

A tectonostratigraphic framework for the late Mesoproterozoic Bylot basins of Laurentia

Wilder Greenman[1], Angelo dos Santos[1], Mollie Patzke[2], Timothy Gibson[3], Alessandro Ielpi[4], Galen Halverson[1]

[1]McGill University wilder.greenman@mcgill.ca, [2]Laurentian Unviersity, [3]Yale University, [4]Laurentian University

The Bylot basins of northeastern Canada and northwestern Greenland comprise the Borden, Hunting-Aston, Fury and Hecla, and Thule basins. This system of late Mesoproterozoic (ca. 1.27-1.0 Ga) sedimentary basins preserves an important stratigraphic record of northeastern Laurentia whose deposition overlapped with the emplacement of the Mackenzie Large Igneous Province, the Shawinigan and Ottawan phases of the Grenville orogeny, and the development of the Midcontinent Rift. However, establishing correlations between the sedimentary successions of the Bylot basins has been hindered by the absence of robust chronostratigraphic constraints. As a result, the degree that these basins were interconnected, whether they share a common tectonostratigraphic history, and how their sedimentary patterns relate to regional tectonic events remain open questions. Recent Re-Os geochronology from organic-rich strata from the Borden and Fury and Hecla basins has yielded depositional ages of ca. 1050 Ma and ca. 1090 Ma, which we integrate with existing models for the depositional history of the Fury and Hecla and Borden basins. We interpret three tectonostratigraphic assemblages for the Bylot basins in the Borden and Fury and Hecla successions and project this interpretation to northeastern Greenland to establish a testable hypothesis for how the Thule Supergroup fits into this tectonostratigraphic picture.

How Does As redox state affect the incorporation of other trace elements?

Daniel Gregory[1], Anthony Chappaz[2], Nicole Atienza[1], Daniel Perea[3], Sandra Taylor[3], John Cliff[3]

[1]University of Toronto daniel.gregory@utoronto.ca, [2]Central Michigan University, [3]Pacific Northwest National Laboratory

Arsenic is a common element in many ore systems, especially gold deposits. It has been argued that the amount and redox state of As can enhance incorporation of several elements in pyrite. When As- substitutes for S in pyrite it may enhance the incorporation of cations similar to Fe2+, such as, Ni2+, Co2+ etc. Whereas when As3+ substitutes for Fe2+ to maintain charge balance it causes a void in the pyrite structure. These voids can then enhance the incorporation of large cations like Pb or Au. In this study we examine in detail the spatial relationship between trace elements from different pyrite samples from two localities. These are the Leicester pyrite member, New York (medium trace element content) and the Black Bute SEDEX deposit, Montana (high trace element content). In this study we examine trace element concentration and variation from the mm to nm scale using a combination of LA-ICPMS mapping, nanoSIMS trace element mapping and atom probe tomography. Additionally, we examined the redox state of the As in the samples use synchrotron based XANES analysis. The trace element mapping at all scales (mm to nm) showed significant variability in As and other trace element content throughout the samples, often without direct correlation between concentration of As and other trace elements. In the XANES analyses it was found that there is a significant component of both As3+and As- in pyrite from both locations. If the As redox state was the most significant factor in trace element enrichment then it would be expected that two trace element vs As trends would be observed, one for As- and another for As3+. This is not the case, instead we observe a moderate correlation between As with most trace elements in LA-ICPMS spot data. Thus, we conclude that in our samples As redox state does not significantly affect which trace elements are enriched in the pyrite.

Prediction of structural parameters and physical properties of beryl from compositional data

Lee Groat[1], Rhiana Henry[1], R. James Evans[1]

[1]University of British Columbia groat@mail.ubc.ca

Beryl is a common rock-forming mineral with general formula Be3Al2Si6O18. The crystal structure (space group P6/m2/c2/c) is composed of SiO4 tetrahedra that share two corners to form Si6O18 rings; these rings are stacked and connected via BeO4 tetrahedra and AlO6 octahedra. The rings form channels parallel to c. In an ideal beryl the channel sites are vacant, but in practice they are commonly occupied by alkali cations and water molecules; Na can occupy the 2b (Na) site (0 0 0), and H2O or larger alkali cations can occupy the 2a (OW) site (0 0 ¼). The availability of Na+ in the structural channels makes it possible to charge balance heterovalent coupled substitutions. Two types of this substitution can occur in beryl: divalent substitutions of Al ("octahedral" substitutions) and monovalent substitutions of Be ("tetrahedral" substitutions); octahedral substitutions take the form VIAl3+ + Cvac <=> VIM2+ + CNa+, and tetrahedral substitutions take the form IVBe2+ + Cvac <=> IVLi+ + CNa+. In addition to these, most beryl coloration is caused by homovalent substitutions of transition metal cations at the Al site via the simple substitution VIAl3+ <=> VIM3+. The beryl structure responds responds predictably to these substitutions because it is subject to several structural constraints. All of the atoms in the beryl structure except O2 are at special positions and the only refineable positional parameters are x and y for Si and O1 and x, y, and z for O2. All six Al-O2 and four Be-O2 distances are constrained to be the same, and there are two different Si-O bonds (two to O1 and two to O2) and two Na-anion (six bonds to O1 and two to OW) distances. We have investigated beryl's structural responses using crystal structure and compositional data for more than 75 samples from different geological environments. The results show that it is possible to predict structural parameters (unit cell dimensions, atomic positions, bond distances) and physical properties (colour) from compositional data, for example electron microprobe analyses.

Profound ~ 1075 Ma (re)fertilization of the central Superior craton lithosphere, based on composition and Pb-isotope data for clinopyroxenes from the Victor mine, Ontario, Canada

Herman Grutter[1], Thomas Stachel[2], Chiranjeeb Sarkar[2], Graham Pearson[2]

[1]SRK Consulting (Canada) Inc. herman.grutter@outlook.com, [2]University of Alberta

The Victor diamond mine in Ontario, Canada opened in 2008 and ceased operations in June 2019. Previous researchers documented that Victor diamonds are unusually young (~ 720 Ma, Aulbach et al., 2018) and grew predominantly in unusually fertile peridotite substrates, specifically garnet lherzolite and garnet wehrlite (Stachel et al., 2018).

Our recent work on n=157 lherzolitic clinopyroxene (Cpx) xenocrysts from the Victor mine reveals profound major- and trace-element (re)fertilization of the deepest 1/3rd of the central Superior craton lithosphere. For example, Cpx Mg/(Mg+Fe) of 0.93 in shallow peridotite decreases across a steep gradient to Mg/(Mg+Fe) of 0.89 at depths of 4.2 to 5.6 GPa. We document marked compositional gradients over a similar depth range for certain minor (Ti, Mn, Ni) and trace elements (LREE and HREE) and attribute the gradients to chromatographic and/or crystal-chemical fractionation effects.

We carefully categorized the Victor cpx xenocrysts in nine depth-composition classes and determined Pb-isotope ratios for representative grains from each class in a bold experiment aimed at capturing geochronological data from mantle Cpx. A resultant 207Pb/206Pb secondary isochron array at ~ 1075 Ma identifies craton-scale events related to the Mid-Continent Rift as the source of fluids and/or melts that (re)fertilized the central Superior craton at depth, some 355 Ma prior to diamond growth.

Coordinated, systematic major- and trace-element relationships in clinopyroxene permit compositional discrimination of mantle (re)fertilization at ~1075 Ma from fluid-metasomatism attending diamond growth at ~ 720 Ma. Roughly 10% of the clinopyroxene xenocrysts analyzed in this work exhibit diamond-associated compositions.

References:

Aulbach S, Creaser RA, Stachel T, Heaman LM, Chinn IL, Kong J (2018) Diamond ages from Victor (Superior Craton): Intra-mantle cycling of volatiles (C, N, S) during supercontinent reorganisation. Earth Planet Sci Lett 490:77-87

Stachel, T., Banas, A., Aulbach, S. et al. The Victor Mine (Superior Craton, Canada): Neoproterozoic lherzolitic diamonds from a thermally-modified cratonic root. Miner Petrol 112, 325-336 (2018). https://doi.org/10.1007/s00710-018-0574-y

The Subduction Pulley: The role of Oceanic Slab on the Pre-Collisional Extension of Microcontinents

Erkan Gun[1], Russell Pyskylwec[1], Oguz Gogus[2], Gultekin Topuz[2]

[1]University of Toronto erkan.gun@mail.utoronto.ca, [2]Istanbul Technical University

Plate tectonics is a well-recognized and accepted theory that provides rather simple explanations to many geodynamics problems. The theory depends on rifting and drifting continental plates, creating new oceanic lithosphere along the mid-ocean ridges which later sinks into the asthenosphere along the convergent subduction plate boundaries. Oceanic lithosphere plays a key role in this theory by transporting continental material, such as microcontinents, to their final destinations at the subduction zones where they are either going to accrete to the overriding plate or sink into the mantle. Essentially, the plate tectonics theory assumes that the drifting continental or ocean lithosphere is rigid and not deformed throughout this process. Here we provide a new perspective suggesting that microcontinents can undergo significant extensional deformation during their drift to subduction zones that is supported by geological evidence from Tethyan belts--the Western Alps and eastern Anatolia--and numerical geodynamic experiments. This type of pre-collisional extension of the continental terranes on the pro-plate side has not been recognized earlier and differs from the well known post-collisional terrane extension at the retro-plate of convergent plate boundaries. Numerical models demonstrate that the pull of the sinking oceanic slab, essentially the tensile stress, is transmitted to the horizontal oceanic lithosphere at the subduction trench, similar to a mechanical analogue of a “pulley” mechanism. This tensile stress acts foremost on the embedded weak continental terrane inside the strong ocean lithosphere, and yields major extension of the microcontinent long before it arrives to the subduction plate boundary.

Understanding the Triple Oxygen Isotope Variability of Soil Water in London, ON

Minger Guo[1], Anne Alexandre[2], Christine Vallet-Coulomb[2], Elizabeth Webb[1]

[1]University of Western Ontario mguo85@uwo.ca, [2]Aix-Marseille Université

Triple oxygen isotopes of fossilized bio-minerals (such as phytoliths) formed in equilibrium with partially evaporated waters (such as leaf water undergoing transpiration) has good potential to be used as an accurate proxy for changes in ancient continental relative humidity (RH). The ^{17}O-excess is the small deviation of the $\delta^{17}O$ of a sample from the Global Meteoric Water Line, and it is complementary to the d-excess parameter for indicating RH during water evaporation. In contrast to d-excess, ^{17}O-excess is measurable in minerals and is temperature insensitive. Recent calibration studies in climate chambers, using irrigation water with constant 17O-excess, show a clear relationship between ^{17}O -excess of leaf phytoliths and controlled RH. However, this relationship will be complicated in natural systems because of many variables, one of which is the oxygen-isotope variability of the Soil Water (SW) that feeds the plant during phytolith formation. SW might experience recharge, mixing, and evaporation, which can change its ^{18}O and ^{17}O -excess values. Understanding what controls the triple oxygen isotope compositions of SW and whether it affects the isotopic composition of phytoliths is required if the ^{17}O -excess values of phytoliths are to be developed as a proxy for ancient terrestrial RH.

In this study, the triple oxygen isotope composition of precipitation and one meter depth profiles of SW were determined monthly in 2018-2019 near London, Ontario. The SW Line is $2H=7.48* \delta^{18}O +4.8$, which is very close to the Local Meteoric Water Line. The $\delta^{18}O$ and ^{17}O -excess versus soil depth plotted did not show any evaporation signal. The trend in $\delta^{18}O$ of the weighted average SW over the year is consistent with but smaller in magnitude than the $\delta^{18}O$ of monthly precipitation. The difference between ^{17}O -excess of SW and monthly precipitation is less than 30 per meg. The $\delta^{18}O$ and ^{17}O -excess signals indicate that using precipitation oxygen-isotope composition to represent SW is appropriate in southwestern Ontario. Each month the SW content was higher near the surface and continuously decreased until around 60 cm depth and the sign of piston flow process can only be observed after September. This indicates that the shallow soils do not drain water very quickly, and frequent rain events during the growing season will become mixed and taken up by plants. SW absorbed by roots should be close to the monthly average rainwater triple-oxygen isotope composition without evaporation. However, in different environments, such as drier climates, different soil porosity, or different plant coverage, whether the SW evaporation signal will interfere with the phytolith triple oxygen isotope composition should be studied.

Tectonic geomorphology of the western Quebec seismic zone (WQSZ), Eastern Canada: implications for regional uplift and intraplate seismicity using GIS

Ugi Gusti[1], Alexander Peace[1], Jeremy Rimando[1]

[1]McMaster University gustiu@mcmaster.ca

In intraplate areas regional strain may be accommodated by pre-existing structures such as failed rift zones. In such settings, geomorphic and paleoseismic characterization of faults may be challenging due to poor surface expression of low displacement faults, scattered seismicity, and long earthquake recurrence intervals. In eastern Canada, the cause of intraplate seismicity remains unresolved. This is partially because faults have been eroded by glaciation and in many cases are undetectable until a seismic event. To estimate the relative tectonic uplift rate and its patterns, 131 drainage basins along 629 km of the Ottawa River were analysed using geomorphic indices. The aim of this was to: (1) identify late Quaternary deformation along with presumed tectonic structures; (2) recognize uplift or subsidence along the catchment areas; and (3) test the application of geomorphic indices in low relief and low-moderate late Quaternary deformation rate environments, and (4) identify potential sites for future more detailed field observation and quantitative slip-rate studies. In this study, we measured mountain-front sinuosity (Smf), valley-floor-width-to--height ratio (Vf), basin elongation ratio (Re), basin hypsometric integral (HI), and normalized channel steepness index (ksn) along 8 nearly W-E striking, bedrock escarpment faults that span the Ottawa-Bonnechere Graben. Cross-correlation between several geomorphic indices suggests uplift rates for the 7 range-bounding faults display changing trend along west-east profiles that are associated with the pre-existing structures and regional seismicity. The results show that eastern Gatineau and Saint-Jerome City characterized as high relative uplift rates areas. Although valley height-width ratio, mountain front sinuosity and channel steepness index show that relative uplift rates are higher in the eastern and western segments of Ottawa-Bonnechere Graben, seismicity in this area isstill relatively low compared to seismicity on plate tectonic boundary areas.

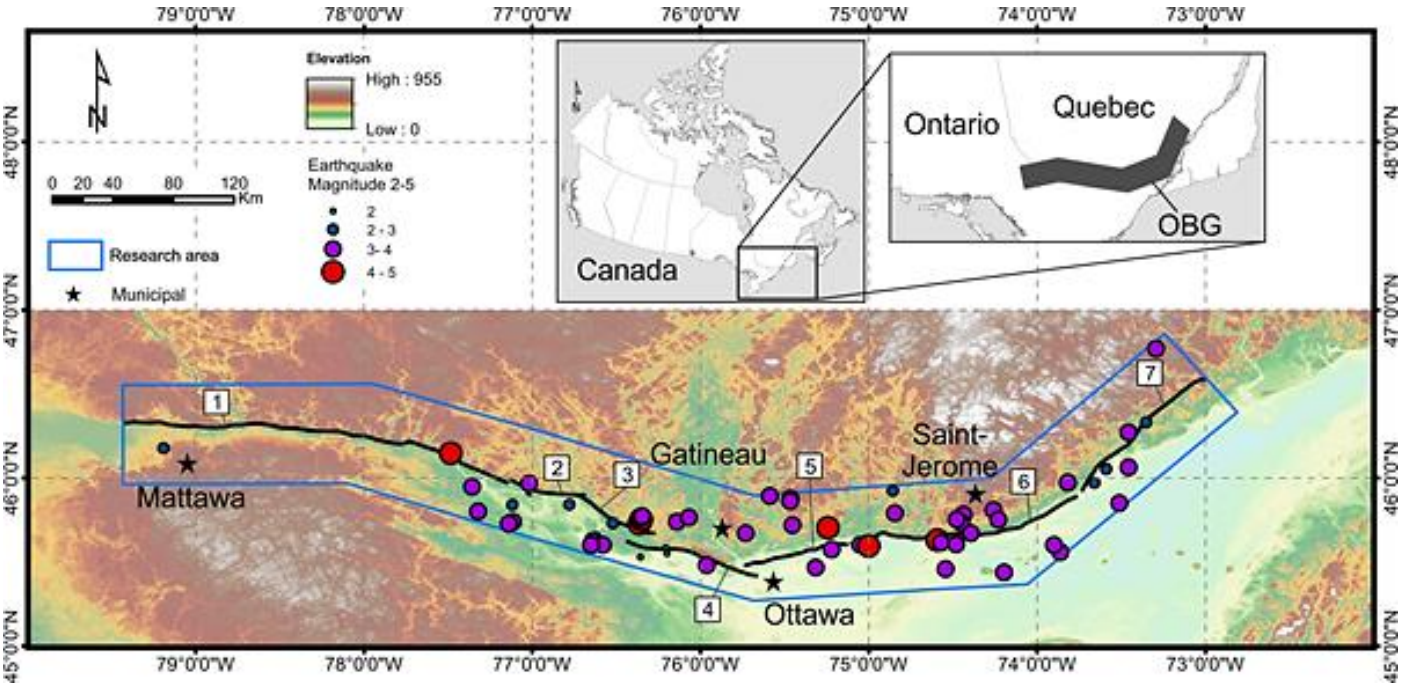

Ice-flow history and Regional stratigraphy of the northwestern Laurentide Ice Sheet, evidence from the Great Slave Lake area

Grant Hagedorn[1], Martin Ross[1], Roger Paulen[2], Rod Smith[2]

[1]University of Waterloo gw2hagedorn@uwaterloo.ca, [2]Natural Resources Canada

Reconstructing the evolution of past ice sheets and understanding their net effect on landscapes and surficial sediments provide important insights into long-term glacial processes, as well as useful knowledge for mineral exploration in glaciated terrains. The evolution of the northwestern Laurentide Ice Sheet is poorly understood due to a limited number of field-based studies. Our research addresses this knowledge gap around the southwestern shore of Great Slave Lake. Our goal is to reconstruct the ice flow chronology of this region and trace the dominant provenance of subglacial tills to improve our understanding of past ice-sheet configuration and subglacial sedimentary processes. Relative ice-flow chronology is established using glacial landforms, outcrop-scale ice-flow indicators, as well as till stratigraphic and provenance analyses. Outcrop-scale indicators show a shift in ice flow direction from an oldest southwestern (230°) flow, to a western (250°) flow, to a final northwestern (305°) flow. Lodged boulders and till clast fabrics from till stratigraphic sections across the study area are broadly consistent with the clockwise ice flow shift. Indicators of northeast provenance include Canadian Shield clasts and certain major oxides (e.g. Cr2O3, Fe2O3) that are considered enriched in northeast bedrock sources relative to local bedrock. At least one till unit is associated with the southwest ice-flow phase based on landforms, till clast macro-fabrics, and a discernible northeast provenance (Canadian Shield) signature. Younger tills were deposited during the clockwise ice flow shift. These tills are located in lower elevation areas of the study area and their composition has an increased Paleozoic (local bedrock) signature, but also includes input from Paleozoic strata to the east. The integrated ice flow records from this study, along with previous studies from the Pine Point mining district, show compelling evidence for major shifts in ice sheet configuration and flow dynamics, as well as related subglacial conditions (e.g. changes in subglacial sediment entrainment) during the last glaciation."

Application of Bayesian Modelling to Age Calibration of Stenian to Tonian Strata in Northern Laurentia

Galen Halverson[1], Elizabeth Sullivan[1], J. Wilder Greenman[1], Morgann Perrot[1], Joshua H.F.L. Davies[2]

[1]McGill University galen.halverson@mcgill.ca, [2]Université du Québec à Montréal

A steady stream of new U-Pb and Re-Os radiometric dates on Stenian to Tonian (1200-720 Ma) strata in northern Laurentia has dramatically improved the chronologies for these rocks, with major implications for the tectonic evolution of Rodinia, the tempo of Proterozoic oxygenation, and the timeframe of early eukaryotic evolution. However, while immensely valuable, these scattered age constraints have not been unified into coherent age models for these stratigraphic successions. Here we explore probabilistic techniques that exploit Bayesian statistics to refine ages based on geological constraints, such as the principle of superposition. With the addition of models for sediment accumulation rates, this approach can be used to generate stratigraphic ages that explicitly include uncertainty. Such models are increasingly applied to younger, relatively short-duration and well-dated stratigraphic successions, but questions remain about how to apply these models to older successions with few direct dates. Here we demonstrate that in the Stenian Borden Basin of northeastern Canada and the late Stenian to Tonian Amundsen basin of north-central Canada, even simple modelling approaches that incorporate prior geological information provide more realistic and precise ages than the radiometric dates alone. Correlation between basins further improves these age models, and importantly, the models can easily be updated and re-run with newly obtained radiometric dates.

Magnetotelluric Exploration at Mount Meager, Southwestern BC: An integrated study of the hydrothermal and magmatic system beneath the geothermal prospect

Cedar Hanneson[1], Martyn Unsworth[1]

[1]University of Alberta cedar@ualberta.ca

The Garibaldi volcanic belt in northwestern North America is part of the ring of fire, a belt of volcanic activity that surrounds the Pacific Ocean. Many countries in this region produce electricity from hot water extracted from geothermal reservoirs found beneath these volcanoes, and Canada could do the same. The most recent volcanic activity in the Canadian Garibaldi belt occurred around 350 BC at Mount Meager. Steam vents on this volcano have become emergent in recent years due to glacial recession and major landslides have occurred, including an event in 2010 that remains Canada's largest recorded landslide. Geothermal research has taken place at Mount Meager since the 1970s and early work included geothermometry, DC resistivity, diamond drilling and heat flow measurements. To reduce the economic risks of development, additional information

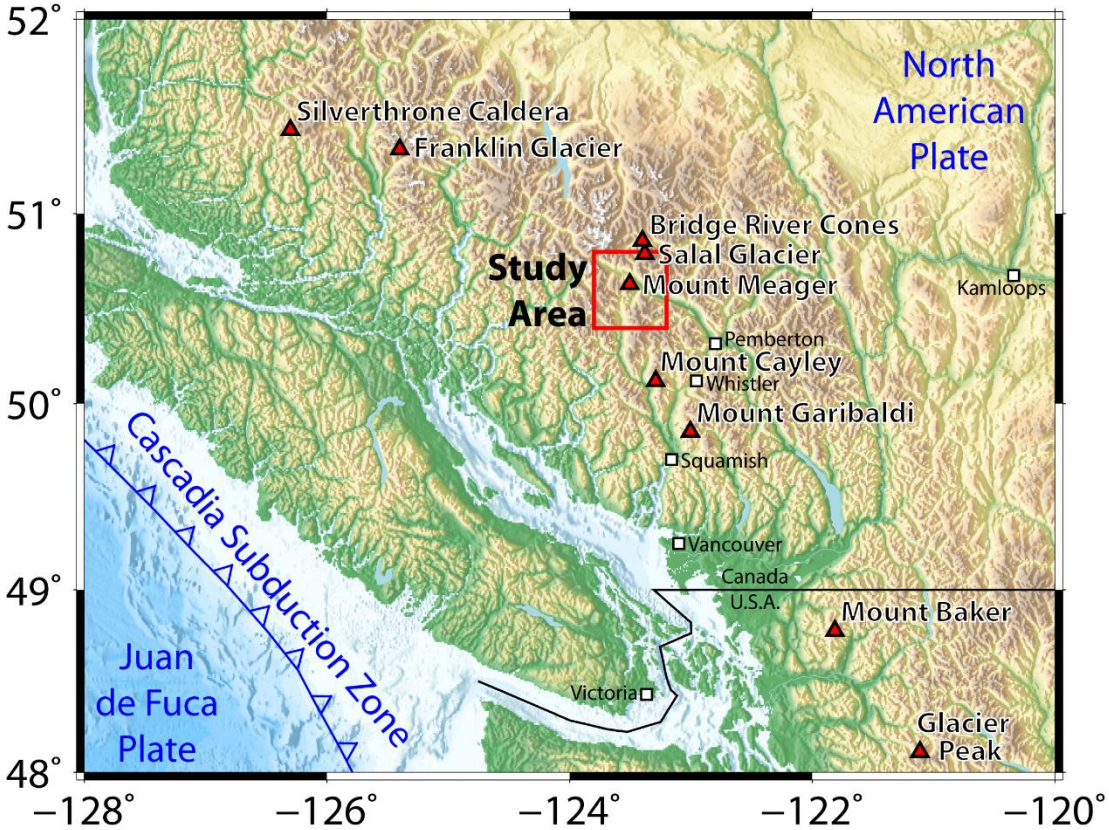

about the geothermal reservoir and natural hazards is needed. Geophysical studies of the subsurface are part of the required data collection and a recent multidisciplinary research program included magnetotellurics, passive seismic, gravity, bedrock mapping, fracture analysis and thermal-spring geochemistry. In 2019 and 2020, broadband magnetotelluric data were collected in the region around Mount Meager. They were used to generate a 3-D model of electrical resistivity, a property that is sensitive to the presence of fluids. This model gives valuable information about the size and location of potential geothermal reservoirs and magma body beneath this active volcano. The uppermost kilometre of the Mount Meager massif is characterized by low resistivity, likely caused by saline aqueous fluids (brines) and hydrothermally altered rocks. There is likely a magma body beneath the Mount Meager massif in the depth range 7-10 km, associated with a conductor that is more than 10 km long, more than 7 km wide, and more than 3 km thick. The inferred magma body has a resistivity in the range 0.1-1 Ωm. To reduce the uncertainty in interpreting the resistivity values, petrological data are being used to estimate the melt fraction and melt composition of the magma body.

Explosive Glaciovolcanism at Cracked Mountain Volcano, Garibaldi Volcanic Belt, Canada

Martin Harris[1], James Russell[1], Rene Barendregt[2], Alex Wilson[3]

[1]University of British Columbia mharris@eoas.ubc.ca, [2]University of Lethbridge, [3]Minerva Intelligence

Cracked Mountain (CM) is a basaltic volcano in the Mount Meager volcanic complex, Southwest, British Columbia, Canada (i.e. Garibaldi Volcanic Belt). The edifice is dated at 401 ± 38 ka (40Ar/39Ar), has an area of ~1.1 km2, a volume of 0.25 km3, and relief of ~250 m (1,650 m a.s.l) relative to the basement rocks. The main morphological features for CM include steep margins and a gentle sloping, highly eroded top. CM contains abundant N-S and E-W trending, 30x20 m (width/depth) cracks that expose the volcanic stratigraphy. The edifice is dominated by massive to poorly stratified, moderately to pervasively palagonitized lapilli tuffs, comprised of vitric fine ash to lapilli sized components with blocky to highly vesiculated shapes. These deposit characteristics indicate a phreatomagmatic (i.e. explosive) origin. The lapilli tuffs are extensively mingled with coherent to disaggregated lobes of pillowed lavas. We find soft-sediment deformation and in-situ quench-fragmentation along lapilli tuffs and pillowed lava contacts. These findings show the tephra was both unconsolidated and water-saturated at the time of magma intrusion (i.e. peperitic). Effusive lavas exist at the edifice margins as stacked pillows, and near the summit as highly eroded remnant sheets. Over fifty dykes cut through the CM stratigraphy, range from 0.5 to 3 m thick and up to 200 m long, and display both pillowed and columnar-jointed margins. A glaciovolcanic origin is indicated by the abundance of subaqueously erupted volcanic lithofacies (i.e. palagonitized tephra, pillows, peperites) where no physical barrier other than ice confinement could have sustained a closed catchment paleolake. There are no stratigraphic indicators of significant time breaks between the individual lithofacies, and paleomagnetic signatures of all CM lithofacies overlap within uncertainty (i.e. monogenetic). The elevation of CM and depth of surrounding valleys require that a ~850 m thick ice sheet must have existed at the time of the eruption. The physiography of CM indicates that a paleolake could have sustained ~0.36 km3 of water. The minimum thickness of ice (850 m) and the edifice geometry (thickness and diameter) suggest melting of ~ 2.8 km3 of ice producing ~2.5 km3 of water. Calorimetric calculations, assuming 60% efficiency, show sufficient heat within the volcanic pile to melt this volume of ice and potentially heat the water to temperatures of >10 °C. Thus, a 'leaky' lake system was likely. Therefore, the absolute (40Ar/39Ar) age of CM is an important climate proxy for the Cordilleran Ice sheet (CIS) reconstruction during the mid-Pleistocene.

Evaluating marine genetic resources associated with seafloor massive sulphide deposits: combining photogrammetric reconstruction and molecular diversity surveys

Moronke Harris[1], Sheryl Murdock[1], S. Kim Juniper[1]

[1]University of Victoria moronke.harris@gmail.com

Seafloor massive sulphides (SMS) represent both prospects and challenges for environmental management of deep-sea mining. We are exploring approaches for addressing potential use conflict between mineral and microbial resource extraction. Marine microorganisms are frequently overlooked in environmental impact assessments and conservation strategies despite their critical role in ecosystem function and mostly unexplored potential as a source of genetic novelty for bioprospecting. Our work is focused on the highly diverse microbes that colonize sulphide mineral deposits, from actively discharging hydrothermal chimneys through to inactive, weathering mounds. We are developing a 'microbial landscape modelling' methodology for the evaluation of genetic resources associated with SMS deposits. We will report on results from a small-scale study on an active sulphide edifice known as Grotto, located within the Main Endeavour vent field on the Juan de Fuca Ridge, in the northeast Pacific. This pilot study is aimed at developing a remote-sensing approach that combines photogrammetric reconstruction of the edifice and visible habitat features, with existing microbial gene sequence data from samples collected from these habitats. The gene sequence data are allowing us to 'ground truth' the distribution of microbial diversity and genetic novelty on the edifice. We are focussing on microbial assemblages associated with two of the common habitats colonized by the hydrothermal vent tubeworm *Ridgeia piscesae*. These tubeworms colonize areas of high-low and low-flow hydrothermal discharge that are easily distinguished in imagery used for photogrammetric reconstruction. Our sample data reveal a robust distinction in microbial diversity and genetic novelty that is related to the high-flow and low-flow discharge regimes. Based on 16S rRNA sequence data, specific to the two principal communities, we have assigned scores for genetic diversity and novelty to the microbes associated with the two assemblages. Our next step will be to scale up this approach to enable comparison of the microbial resource potential of entire hydrothermal vent fields and extinct deposits. SMS deposits go through a cycle of growth, inactivity, and slow erosion that parallels the lifetime of hydrothermal vent fields. There is evidence in the literature for shifts in the composition of vent microbial communities that can be linked to stages of deposit growth and weathering. Yet, this knowledge has not been systematically applied at a landscape scale for genetic resource evaluation. Combining seafloor habitat mapping and existing knowledge of microbial diversity, genetic novelty, and economic biodiversity valuation to develop comparative genetic resource maps for different stages of the life cycle of SMS deposits: (i) enables quantification of associated uncertainty and loss of genetic resources resulting from mining deposits of different ages; (ii) leads to an increased understanding of the interaction between the weathering of deep-sea mineral deposits and biological processes.

Petrological and geochemical study of the active volcanic ridge of Mayotte (Mozambique Channel)

Théo Hassen Ali[1], Carole Berthod[2], Etienne Médard[2], Lucia Gurioli[2], Andrea Di Muro[3], Pascale Besson[4], Patrick Bachélery[2]

[1]Université du Québec à Chicoutimi thassenali3@gmail.com, [2]Laboratoire Magmas et Volcans, [3]Observatoire volcanologique du Piton de la Fournaise, [4]Institut de physique du globe de Paris

Comoros Archipelago is a volcanic complex located at the northern end of the Mozambique Channel. Volcanic activity seemed to have migrated from east (Mayotte Island being the oldest island at 20 Ma) to west (active Karthala volcano on Grande Comore Island). However, renewed activity started offshore Mayotte in May 2018: a volcano-tectonic crisis resulted in the formation of an 800 m high submarine volcano on the distal part of a NW-SE volcanic ridge east of the island (Feuillet et al., submitted). Initial petrologic study of erupted lavas demonstrated that the eruptive site is fed by a deep mantle reservoir (> 35 km), from which magma ascend rapidly with little to no shallower storage (Berthod et al., submitted). The goal of this study is to characterize the older eruptive products of the ridge, compare them to the active volcano and sketch the shape of the magmatic system. In order to image the magmatic system of the entire volcanic ridge, we realized a petrological and geochemical study of samples dredged during three oceanographic campaigns (MAYOBS 1, 2 and 4). The volcanic ridge is characterized by a bimodal volcanism with basanites (3.1 - 5.7 wt.% MgO) containing olivine (Fo 64-87) + clinopyroxene (Mg# 64-84) + apatite + titanomagnetite (FeO <74 wt%) and phonolites (< 0.5 wt.% MgO) containing alkali feldspar (CaO 2,56-4,06 wt%) + olivine (Fo 13-29) + apatite + spinel (Cr2O3 <0.68 wt%). Phonolites contain mantellic xenoliths with olivine (Fo 89-94) + orthopyroxene (Mg# 83-87) + clinopyroxene (Mg#> 85) + spinel (Cr2O3 > 30 wt%) indicating that differentiation from basanite to phonolite takes place in the mantle. Barometric calculations on zoned clinopyroxene phenocrysts from basanitic samples allowed us to identify two magma storage levels. A deeper level over 30 km and a shallower level located between 15 and 20 km near the MOHO. These results are coherent with regional magneto-telluric and seismic studies. MELTS models show that phonolites are derived from basanites by approximately 80% of crystallization, probably in the shallower reservoirs at the MOHO interface. Magmatic temperatures vary between 900-1073°C for basanites, 859-1012°C for phonolite and 933-1008 °C for mantle xenoliths. Based on these results, we propose three scenarios following intrusion of basanitic magmas in this volcanic ridge:1. Fast magma ascent resulting in the eruption of aphyric basanites (currently happening on the active volcano)2. Quick stalling at 15-20 km resulting in the eruption of basanites with zoned clinopyroxene phenocrysts.3. Longer stalling at 15-20 km inducing a significant differentiation and eruption of phonolites.

Gold Fingerprinting: Project overview and method development

Evan Hastie[1], Joseph Petrus[2], Harold Gibson[2], Kim Tait[3], Julian Melo-Gomez[2], Dave Crabtree[1]

[1]Ontario Geological Survey evan.hastie@ontario.ca, [2]Laurentian University, [3]Royal Ontario Museum

Many proxies for gold have been used to help understand gold-forming processes, deposit types, and the differential gold endowment among similar geologic terranes. These proxies (e.g., quartz, sulfides, etc.) are problematic in terms of definitively showing their genetic relationship to high-grade visible gold and this has resulted in an incomplete understanding of the critical elements involved in the formation of gold deposits. Advances in laser ablation inductively-coupled plasma mass spectrometry (LA-ICP-MS) and atom probe tomography (APT), along with sample characterization by scanning electron microscopy using energy-dispersive spectrometry (SEM-EDS) and electron microprobe analysis (EMPA) now offer an opportunity to comprehensively analyze gold directly, from which, direct evidence for Au-elemental associations or "fingerprints" can be truly characterized. "Gold Fingerprinting" is a collaborative project involving the Ontario Geological Survey (OGS), the Royal Ontario Museum (ROM) and the Metal Earth Initiative at Laurentian University. This project is developing a rigorous in-situ methodology to geochemically characterize gold, spanning sample preparation to innovative analysis, and assessment of the elemental associations contained within native gold samples from significant deposits across Ontario, Canada, and the world. Data obtained from this project will be used to create a global gold database that is freely available to all, and digital map data for the province of Ontario. Herein, we present an overview of the project and preliminary results, with the latter indicating best practice sample preparation, optimal operating conditions for analysis, ablation characteristics, in-house and international reference materials, and possible metallogenic differences by region in Ontario of gold major and trace element chemistry. The gold database will provide a baseline to assess the critical processes related to gold endowment, deposit formation and provenance, and improve our understanding of gold for exploration, metallurgy, archeology, and forensic science.

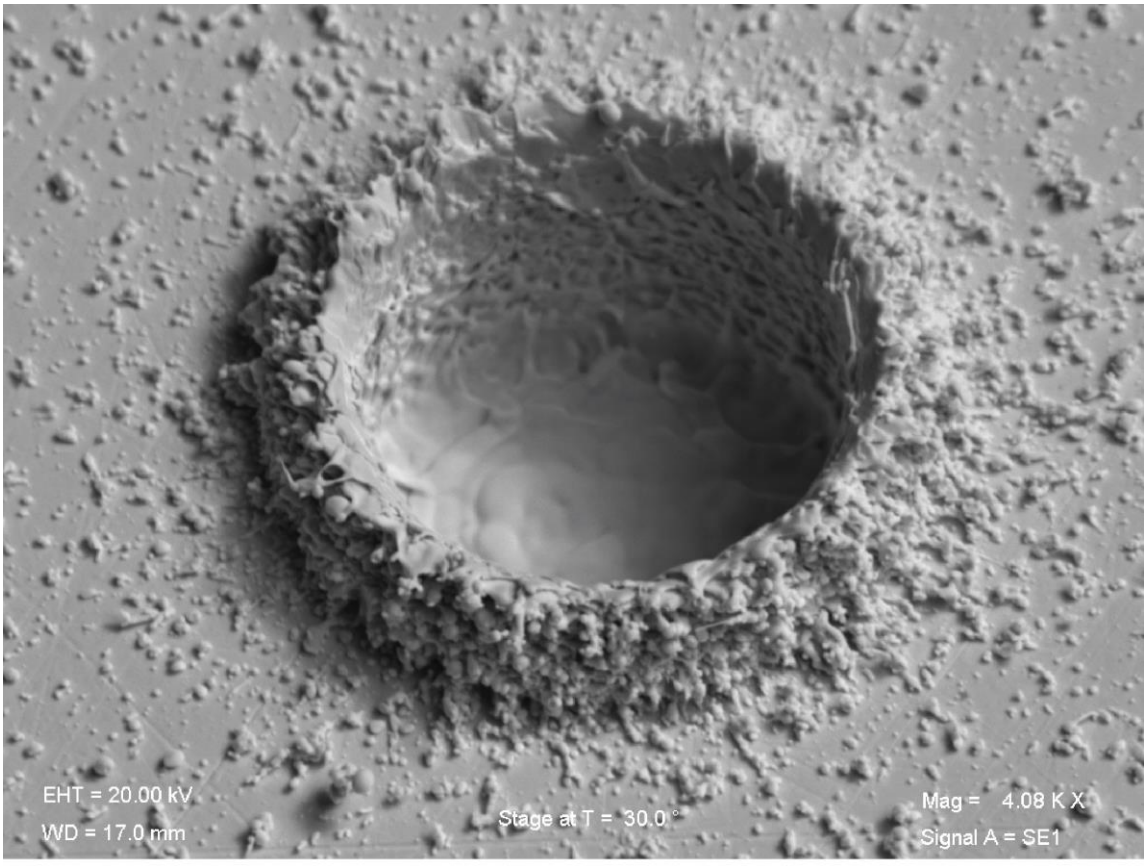

Figure 1. Tilted Secondary Electron image of a laser ablation test pit in native gold.

Small-scale topography and the temperature distribution of permanently shadowed regions on the Moon

Conor Hayes[1], Jacob Kloos[1], John Moores[1]

[1]York University hayes954@yorku.ca

The potential distribution of volatile materials at or near the lunar surface is strongly dependent on temperature. For this reason, large permanently shadowed regions (PSRs) present at both of the Moon's poles have garnered attention for their ability to act as volatile traps due to their consistently low temperatures. Furthermore, because sublimation rates increase rapidly beyond a certain critical stability threshold, determined primarily by a substance's vapor pressure, temperature maps can serve as a first-order estimation of where volatiles may be present. Currently, the best temperature data available comes from the Diviner Lunar Radiometer Experiment onboard the Lunar Reconnaissance Orbiter. These data suggest that while many PSRs are cold enough to trap water, there is very little area available for the cold trapping of other volatile species like carbon dioxide, methane, and ammonia, all of which require much lower temperatures to remain stable over long timescales. In this work, we will examine the extent to which these results are limited by the 240 metre per pixel resolution of the Diviner data. Although PSRs are protected from direct sunlight, they are still subject to a number of alternate illumination sources, the most substantial of which is sunlight scattered off of nearby terrain. Much like how the large-scale features of the surface create PSRs, small-scale features below the Diviner resolution may create doubly-shadowed areas within PSRs that are shielded from both direct and singly-scattered solar illumination. In the absence of both major sources of illumination, these areas would be significantly colder than the temperatures measured by Diviner. Although we cannot directly map volatile stability in the absence of higher-resolution terrain data, we aim to produce a realistic estimate of how obtaining higher-resolution data might expand the ultra-cold trapping area within PSRs by using 240 metre per pixel digital elevation models (DEMs) produced by the Lunar Orbiter Laser Altimeter (LOLA). The LOLA DEMs will be interpolated before having a Gaussian rough surface overlaid on top of them to simulate the small-scale roughness of the lunar surface. This will allow us to model real-world illumination conditions and produce more accurate estimates than a model based on entirely synthetic terrain data.

On the paragenetic modes of minerals: A mineral evolution perspective

Robert Hazen[1], Shaunna Morrison[1], Anirudh Prabhu[2], Jason Williams[1]

[1]Carnegie Institution for Science rhazen@ciw.edu, [2]Rensselaer Polytechnic Institute

A systematic survey of 57 paragenetic modes distributed among 5659 mineral species reveals patterns in the diversity and distribution of minerals related to their evolving formational environments. The earliest minerals in stellar, nebular, asteroidal, and primitive Earth contexts were dominated by relatively abundant elements, notably H, C, O, Mg, Al, Si, S, Ca, Ti, Cr, and Fe. Significant mineral diversification subsequently occurred first through gradual selection and concentration of rarer elements by fluid-rock interactions (for example, in hydrothermal metal deposits, complex granite pegmatites, and agpaitic rocks), and then through near-surface biologically-mediated oxidation and weathering. We find that 3349 mineral species (59.2 %) are known from only one paragenetic context, whereas another 1372 species (24.2 %) are associated with two paragenetic modes. Among the most genetically varied minerals are pyrite, albite, hornblende, corundum, magnetite, calcite, hematite, rutile, and baryte, each with 15 or more known modes of formation. Common paragenetic modes of minerals include near-surface weathering/oxidation (1998 species), subsurface hydrothermal deposition (859), and condensation at volcanic fumaroles (459). In addition, many species are associated with compositionally extreme environments of highly differentiated agpaitic rocks (726 species), complex granite pegmatites (564), and carbonatites and related magmas (291). Biological processes lead to at least 2707 mineral species, primarily as a consequence of oxidative weathering but also through coal-related and taphonomic minerals (597 species), as well as anthropogenic minerals (603). However, contrary to previous estimates, we find that only ~34% of mineral species form exclusively as a consequence of biological processes. By far the most significant factor in enhancing Earth's mineral diversity has been its dynamic hydrological cycle. At least 4583 minerals - 81 % of all species - arise through water-rock interactions. We find that 41 rare chemical elements, which collectively account for only 1 in every 10,000 crustal atoms, are essential constituents of 42% of known minerals; i.e., rare elements play a disproportionate role in Earth's mineral diversity. A timeline for mineral-forming events suggests that much of Earth's mineral diversity was established within the first 250 Mya. If life is rare in the universe, then this view of a mineralogically diverse early Earth provides many more plausible reactive pathways over a longer timespan than prior models. If, however, life is a cosmic imperative that emerges on any mineral- and water-rich world, then these findings support the hypothesis that life on Earth developed rapidly in the early stages of planetary evolution. FIG: A bipartite network graph links 5659 blue mineral node to 57 green paragenetic nodes. Minerals with many formation modes lie near the center; minerals with one mode surround the periphery.

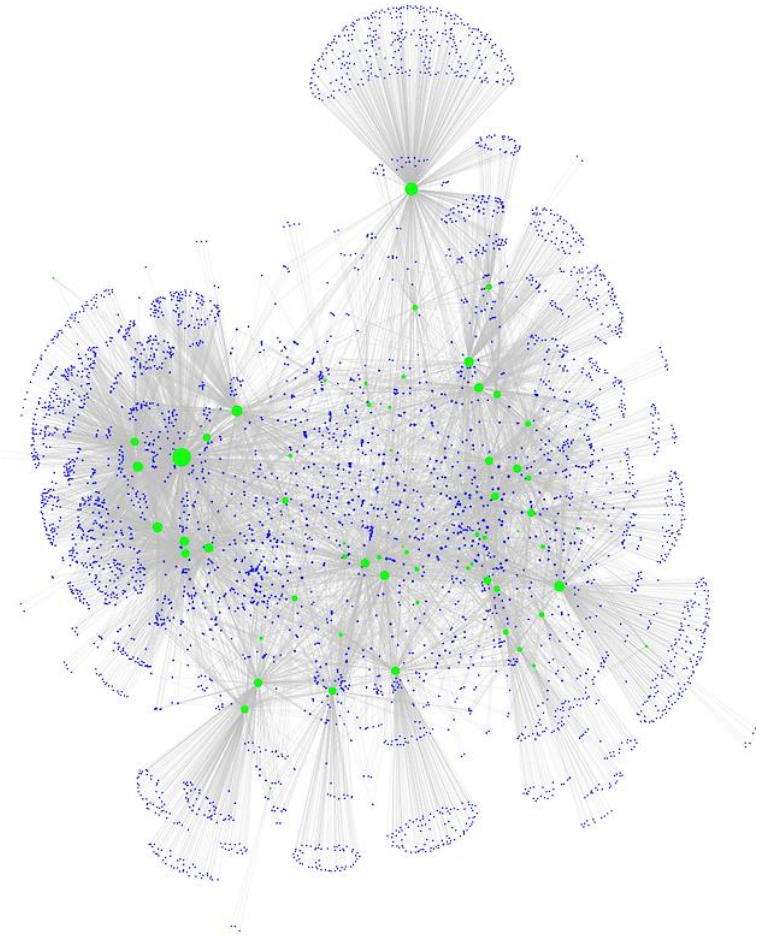

Integrated Geophysics for Three-dimensional Modelling of Mine Waste

Wei Xuen Heng[1], Olivia Wilson[1], Eliza Fisher[1], Michael Roach[1], Clare Miller[1], Matthew Cracknell[1]

[1]University of Tasmania wxheng@utas.edu.au

The Endurance mine site is a legacy alluvial cassiterite (SnO_2) mine in northeast Tasmania, Australia. The mine operated for over a century, from 1874 until 1982, producing up to 50 t of tin per year at its height in 1952. During this time, quartz-rich sandy gravel mine waste was discharged into Ringarooma River and disposed of across the site. Almost four decades from closure, Acid and Metalliferous Drainage (AMD) generated from the mine waste continues to impact the local environment and pose challenges to remediation. Through the combination of several near-surface geophysical methods, such as DC resistivity, ground penetrating radar (GPR) and seismic refraction tomography, this project aims to define and characterise the thickness and internal structure of mine wastes across the Endurance site.

Three primary hydrogeological units within the mine wastes were identified by integrating inverted DC resistivity, seismic refraction models, GPR radargrams and confirmed through drilling: (1) unsaturated or saturated mine waste to ~1-17 m depth (2000-20,000 Ohm.m, 300-1300 m/s); (2) kaolinitic clay layer to ~2-18 m depth (1-100 Ohm.m); and (3) weathered or unweathered granite to ~20-30 m depth (70-120 Ohm.m, >1500 m/s). GPR was most useful for detecting the boundary between the kaolinitic clay layer and quartz-rich mine waste, as well as defining the water table to depths of ~15 m. Beyond GPR depths of investigation, DC resistivity and seismic refraction models indicated the base of the mine waste and a boundary interpreted to represent a transition from weathered to unweathered Devonian alkali-feldspar granite basement.

A three-dimensional (3D) model of depth to the base of mine waste, the water table and granitic basement was developed by integrating inverted geophysical models. The 3D model, combined with borehole observations, was used to constrain a hydrological model of the Endurance site and was instrumental in defining granitic basement topographic controls on groundwater flow paths. Furthermore, the 3D model was used to estimate the volume of mine waste at ~2.7 hm^3; and the total mass of mine waste at ~4 Mt.

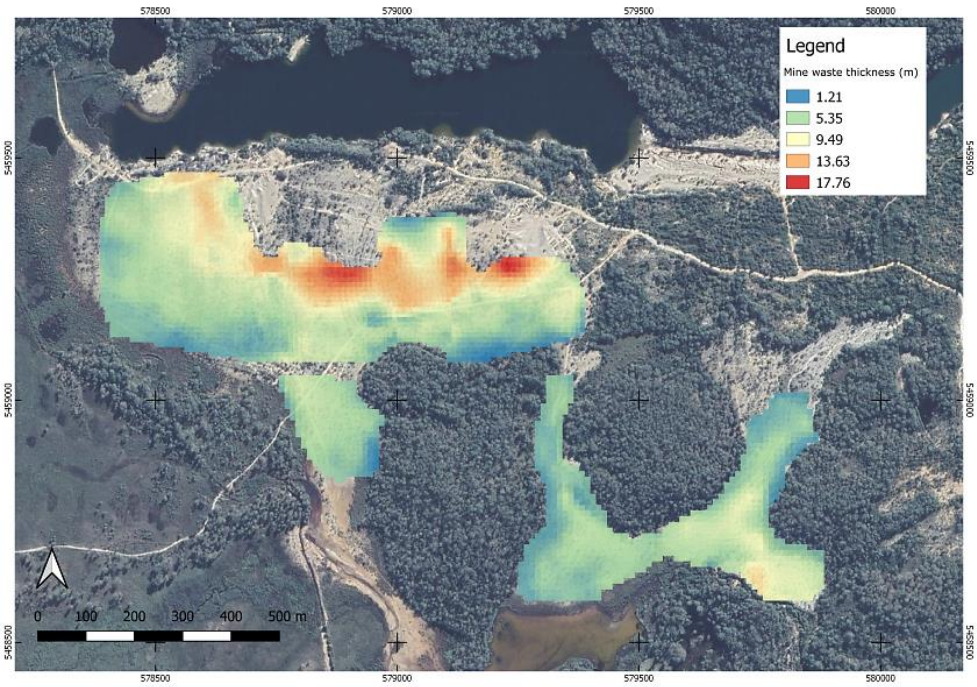

Knowledge generated in this study provided essential information on the thickness and internal structure of mine wastes across the Endurance site. This information assisted concurrent hydrogeological and sediment geochemical projects to inform future rehabilitation strategies.

Locating the Source Craters of the Martian Meteorites: An Integrated Approach

Christopher Herd[1], Jarret Hamilton[1], Erin Walton[2], Livio Tornabene[3]

[1]University of Alberta herd@ualberta.ca, [2]MacEwan University, [3]University of Western Ontario

Martian meteorites are currently the only samples available for laboratory study on Earth, and provide important insights into the formation, differentiation, and geologic evolution of Mars [1]. Spallation is a logical delivery mechanism, which favors the launch of low-shock competent rock; this ejection mechanism is consistent with the fact that >80% of the meteorites are coherent igneous rocks, all formed within the past 2400 Ma [1, 2]. Ejection ages, derived from cosmic ray exposure geochronology, indicate that the meteorites were produced by ~10 distinct impact events between 0.7 and 20 Ma [3, 4]. Therefore, the martian meteorites are derived from a relatively small number of the youngest impact craters formed into Amazonian (<~3400 Ma) igneous terrain, likely in the Tharsis or Elysium volcanic regions. While this conclusion is not novel [5, 6], advances in modeling of the meteorite impact and delivery process [7] and the availability of high-resolution imagery of Mars provides an opportunity to make further constraints on candidate craters for the martian meteorites. Our approach uses these advances to narrow the number of potential candidate craters, with the goal of matching individual craters to specific martian meteorites (or suites of meteorites).

Initial results of our approach are presented in [8]. In summary, we constrained the range of possible crater diameters from modeling [7] applied to four martian meteorites having distinct crystallization and ejection ages. We then cross-referenced these crater diameters with a database of the best-preserved impact craters on Mars, generally ranked according to the preservation of the pitted impact melt deposits [9]. This process resulted in 52 craters (out of 279) that are candidates for at least one of the four meteorites. A subset of 8 craters was chosen for detailed mapping, on the basis that any of these 8 candidates could be the source of any of the four meteorites. Mapping of these craters is now complete [10] and provide an additional constraint towards determining possible sources of martian meteorites.

Our approach enables the linking of meteorites with known crystallization ages to a specific volcanic surface unit, potentially contributing to one of the main goals of a Mars Sample Return campaign: to quantitatively determine the evolutionary timeline of Mars [11].

[1] Udry A. et al. (2020) JGR-Planets, je006523. [2] Walton E.L. et al. (2008) GCA, 72, 5819-5837. [3] Nyquist L.E. et al. (2001) Space Science Reviews, 96, 105-164. [4] McSween H.Y. (2015) Am. Min., 100, 2380-2395. [5] Mouginis-Mark P.J. et al. (1992) JGR-Planets, 97, 10213-10225. [6] Tornabene L.L. et al. (2006) JGR: Planets, 111. [7] Bowling T.J. et al. (2020) Icarus, 113689. [8] Herd C.D.K. et al. (2018) LPSC, 48, Abstr. #2266. [9] Tornabene L.L. et al. (2012) Icarus, 220, 348-368. [10] Hamilton J.S. (2020) University of Alberta M.Sc. Thesis, 142 p. [11] Beaty D.W. et al. (2019) M&PS, 54, S3-S152.

The Plan for Sampling: Perseverance Rover Notional Caches for Mars Sample Return

Christopher Herd[1], Justin Simon[2], Kathleen Benison[3], Kathryn Stack[4], Vivian Sun[4], Sanjeev Gupta[5], Tanja Bosak[6], Kenneth Williford[4], Kenneth Farley[4]

[1]University of Alberta herd@ualberta.ca, [2]ARES, NASA Johnson Space Center, [3]West Virginia University, [4]JPL/Caltech, [5]Imperial College London, [6]Massachusetts Institute of Technology

A central objective of the NASA Mars 2020 Perseverance rover mission is to collect a suite of scientifically compelling samples for return to Earth by a subsequent mission [1]. The Mars 2020 Science Team identified a set of notional sample caches via strategic planning carried out prior to landing. We describe notional sample caches that have been defined for the prime mission within Jezero crater, and an extended mission outside Jezero crater. The types of samples identified through this process align well with the list of desired samples prioritized by the broader Mars science community [2, 3]. Important scientific questions that can be addressed through Earth-based analysis of these samples are listed in [3].

The prime mission notional cache. The geology of Jezero crater consists of well-preserved, Hesperian deltaic and lacustrine deposits sourced from a river system that drained Noachian terrain [e.g., 4]. The crater floor is characterized by at least two distinct units, of sedimentary or volcanic origin; the relationship of these units to the deltaic deposits is unclear [4]; however, remotely sensed data contain signatures of carbonate and clay minerals within several of the units, including the crater floor and near the crater margin [e.g., 5]. Samples from within Jezero that comprise the prime mission notional cache thus include: fine- and coarse-grained delta facies, the former with a high potential to preserve organic matter, the latter to better understand the geology and constrain the timing of the watershed from analyses of detrital mineral grains; carbonate-bearing and/or chemical sediments with the potential to preserve biosignatures; crater floor units; a sample of the crater rim; and at least one sample of regolith.

The extended mission notional cache. The region of southern Nili Planum, directly outside the western rim of Jezero crater, is geologically distinct from Jezero crater, and contains diverse rock types as old as the Early or even Pre-Noachian. The notional cache from this region includes: layered and other basement rocks; megabreccias, which may represent blocks of (pre-)Noachian crust excavated by the Isidis and/or Jezero impact events; fractures cross-cutting basement; olivine- and carbonate-bearing rocks that are regionally significant and may be related to units within Jezero crater; and a mafic cap.</p> At the current time, the mission is embarking on the Green Zone Campaign to explore - and sample - crater floor units. The decisions involved in the collection of these first samples will provide insights into the process by which the prime and extended mission caches will be established.

Note: Please see [3] for complete author list.

[1] Farley K.A. et al. (2020) SSR, 216. [2] Beaty D.W. et al. (2019) M&PS, 54, S3-S152. [3] Herd C.D.K. et al. (2021) 52nd LPSC, #1987. [4] Stack K.M. et al. (2020) SSR, 216. [5] Horgan B.H.N. et al. (2020) Icarus, 339, 113526.

Continental fragment formation by rifting of orogenic belts

Phil Heron[1], Russell Pysklywec[2], Ken McCaffrey[3], Alex Peace[4]

[1]University of Toronto Scarborough philip.heron@utoronto.ca, [2]University of Toronto, [3]Durham University, [4]McMaster University

Continental 'slivers', 'ribbons', and 'flakes' are small fragments of the Earth's continents that become isolated from their principal domain during plate tectonic movements. Examples of which are the Cordilleran terranes in western North America, the Lewisian of North West Scotland, present-day New Zealand (which rifted from Gondwana), and the Nain Province in Labrador, Eastern Canada. Given the variety of isolated continents that exist, the processes involved in the generation and structure of such fragments are not well understood. Inherited structures from previous tectonic activity can control first-order deformation during rifting, and potentially generate continental slivers. Specifically, rifting impacted by mantle sutures (inherited from ancient orogenesis) have been indicated to play a role in the development of margin architecture (e.g., Heron et al., 2019). In this submission, we present numerical models analyzing the potential impact of mantle sutures in the generation of continental fragments during rifting. The results of our models are compared with the Nain Province in Labrador, where a fragment of the North Atlantic Craton became separated from Greenland during the formation of the Labrador Sea. We hypothesize that a Palaeoproterozoic collision, which featured the North Atlantic Craton and produced the Nagssugtoqidian Orogen, would have left mantle lithosphere scarring during the continental suturing. Here, we present simulations that implement continental extension in the presence of a modelled mantle lithosphere suture and vary the geometry of scarring to understand the impact of inheritance reactivation in the production of continental slivers.

Building confidence in students: lessons from teaching (geo)science in prison

Phil Heron[1], Jamie Williams[2]

[1]University of Toronto Scarborough philip.heron@utoronto.ca, [2]Spectrum First Education

'Think Like A Scientist' is a course designed to improve critical thinking and encourage independent thought for people in prison. The program uses short, impactful talks on science topics to bring new information to the class and promote open discussion. Through dialogic teaching methods and guided by a critical thinking framework, the students are taught to analyse research and feel connected to the outside world through learning about earthquakes, volcanoes, plate tectonics, and climate change (alongside other science topics). For this GAC MAC submission, we will describe a typical Think Like A Scientist session and outline practical advice when dealing with students who have had difficulty accessing (or being engaged by) formal education - specifically those who have no confidence in themselves or the education system. Based on our experience in teaching, we will focus on how to create a classroom dynamic that is accessible, inclusive, and relatable to students from all backgrounds. By taking into consideration these key aspects, Think Like A Scientist works to remove often unaddressed barriers to a student's education pathway. Despite mainly running education courses in prisons, Think Like A Scientist has been taught in varied settings (including to young people experiencing homelessness). In our experience, the lesson learned from teaching in restrictive environments to diverse students can be applied to wide range of audiences and settings, and therefore may be of interest to the geoscience community.

The UNFC, A Science Based Geothermal Resource Estimation Framework for use in Canada

Catherine Hickson[1], Yannick Champollion[1]

[1]Alberta No. 1 c.hickson@albertano1.ca

Basins, in particular the Western Canada Sedimentary Basin, have significant potential for extraction and development of warm fluids. The importance of extraction and use of these fluids for electrical generation and thermal applications (space heating, agriculture, and forestry, etc.) is growing as the world grapples with trying to achieve net zero in carbon emissions by mid-century. Geothermal projects are both carbon neutral, and when combined with carbon sequestration, carbon negative. Financing these projects continues to be a challenge. Significant capital has been raised on the Toronto Stock Exchange (TSX) by publicly traded companies seeking financing for renewable energy and resource projects. In 2002, the TSX adopted the National Instrument 43-101 for mineral and mining development and NI51-101 for the oil and gas industry to prevent misleading, erroneous or fraudulent information relating to mineral properties. As Canada begins to establish a geothermal industry to help it meet its climate change goals, it needs to adopt a reporting standard for geothermal projects. The United Nations Economic Commission for Europe (UNECE) published a comparison between fossil energy, mineral reserves and geothermal energy in 2016 (UNECE 2016). This classification is evolving and provides a science-based resource classification and estimation framework. The framework also includes important cultural and social values that have entered the arena and are changing the landscape of international financing. The UNECE has continued to push ahead on updating and refining the resource framework. In 2019 they released an updated framework called United Nations Framework for Classification for Resources (UNFC) (UNECE 2019). The importance of this update is its full alignment with the UN sustainable resource management goals, referred to as ?2030 Agenda for Sustainable Management?. In doing so, there is a heavy emphasis on the environmental-socio-economic viability as well as the technical feasibility of projects. This growing trend is parallel with significantly increasing interest in geothermal projects in Canada and across the globe.

Advancing the Curation of Aldehydes and Ketones for Applications to Carbonaceous Chondrites and Cometary Nucleus Sample Return

Patrick Hill[1], Madison Chevalier[1], Chris Herd[1], Robert Hilts[2]

[1]University of Alberta pjhill@ualberta.ca, [2]MacEwan University

The presence of abiogenic organic compounds in carbonaceous chondrites and cometary material marks an important starting point for investigations examining the processes that led to the origin of life. Of particular interest are the aldehydes and ketones, commonly known as "carbonyl compounds", which play an important role in the synthesis of a range of organic compounds, including amino acids [1-3]. With ongoing sample return missions from asteroids, proposed future sample return missions from comets, and the continual arrival of carbonaceous chondrites to the Earth's surface via meteorites, constraining the ideal curation conditions for the preservation of extraterrestrial organic compounds that proactively prevent terrestrial reactions is essential for ongoing research. Given the importance of carbonyl compounds in the production of organic compounds required for early biogenic processes, the aim of this study is to examine the reactivity of carbonyl compounds under a variety of conditions to provide insight into the curation and handling requirements of organic-rich materials. To this end, several carbonyl compounds will be added to a powdered mixture of the Allende meteorite and consequentially stored under various curation conditions to investigate the reactivity of the compounds. Two procedural blanks are utilized in this study to act as controls and for points of reference. The first blank is pure, crushed silica which will undergo all the same experimental conditions as the Allende-carbonyl mixture. This will provide insight into the reactivity of meteorite medium as silica should be inert. The second blank is powdered Allende meteorite, with no extra carbonyl compounds added. This blank will be exposed to all the same experimental conditions, in order to constrain background levels of carbonyl compounds and their reactivity. Three environments (a class 1000 cleanroom at 25°; a class 1000 cleanroom at -15°; and a -15°-Ar atmosphere glove box) will assess how the carbonyl compounds react with Allende over a period of time at different temperatures and under different atmospheric conditions. To test what affects the availability of water has on any reactions, a fixed volume of water will be added to a subset of samples. The ammonia scenario follows a similar procedure: a known volume of ammonia will be added to each sample to see how ammonia interacts. Five main variables are assessed through this study: meteoritic material as a reactive medium; temperature effects; argon atmosphere vs. ambient air; the presence of water; and the presence of ammonia. Results are anticipated to confirm that the best environment in which to store the volatile organic compounds found in cometary material is an oxygen-free atmosphere at subzero temperatures.

[1] Peltzer E. T. and Bada J. L. (1978) Nature, 272, 443-444. [2] Peltzer E. T. et al. (1984) Adv. Space. Res. 4, 69-74. [3] Simkus D. N. et al. (2019) Meteorit. Planet. Sci. 54, 142-156.

Advancing Sample Return Curation using the Bruderheim Meteorite as an Analogue

Patrick Hill[1], Christopher Herd[1], Libby Tunney[1]

[1]University of Alberta pjhill@ualberta.ca

The L6 ordinary chondrite, Bruderheim, fell on March 4, 1960, at 01:06 MST near the town of Bruderheim, Alberta. Shortly after the recovery of over 300 kg of material, two large specimens (1.4 kg and 1.2 kg) were sealed under vacuum conditions in glass capsules. These preserved samples, part of the University of Alberta Meteorite Collection, provide a unique opportunity to not only investigate how vacuum conditions preserve meteoritic material but also to advance handling and curation techniques by treating the specimens as an analogue for sample return capsules. Here we outline a proposed procedure for the extraction of one of the specimens from its capsule for community feedback and provide an update on ongoing curation efforts. The curation process for removing this specimen can be divided into two main efforts: headspace gas extraction and solid sample processing. The composition of the gas within the headspace of the capsule is important to better understand both the outgassing of the meteorite over the past seven decades and to quantify the amount of air that may have been ingassed. To this end, a stainless-steel vessel, capable of being taken to vacuum conditions, has been designed. Once at vacuum, the vessel will crack the gas capsule and any escaping gas will be transferred to a metal gas cylinder using a liquid nitrogen cold trap. Following the transfer, the vessel and cylinder will be sealed. The cylinder will be analyzed and the vessel containing the cracked capsule will be transferred to an argon glovebox for solid sample processing. All solid sample processing will be conducted at the University of Alberta's Subzero Facility for the Curation of Astromaterials. The facility's argon glovebox will ensure that the specimen is not exposed to an oxidizing environment during further processing. All tools and materials that will be utilized in the processing of the specimen will be sterilized to remove any potential contamination. All metal and glass materials will be combusted at 450°C for a minimum of 4 hours and Teflon materials will be rinsed with HPLC-grade dichloromethane and then sterilized within an autoclave. To quantify both the degree of contamination during the processing and the pristine nature of the glass sealed specimens, several reference materials will be processed alongside the specimen. Sterilized quartz beads will be utilized as a procedural blank to identify any phases that are introduced during the processing. Two additional specimens of Bruderheim, stored in standard collection conditions, will also be examined as points of reference to identify how the glass capsule has preserved the meteorite. Thin sections, cut faces, mineral separates, and surface analysis will be conducted to quantify the chemical differences between specimens. This work will advance our understanding of how to ensure extraterrestrial material is handled properly and develop the methodologies for processing sample return material.

Applications of using complementary advanced analytical techniques to address the needs of the mining and mineral processing industries

Carolyn Hill-Svehla[1], Ivan Barker[1], Stamen Dimov[1]

[1]Western University chill59@uwo.ca

Several advanced analytical techniques, such as SEM/EDX and Dynamic SIMS, are often used as benchmark tools to address problems that can arise in the mining and mineral processing industries. Issues such as characterizing ores, optimizing metallurgical operations, and improving recovery of precious metals, can be investigated and explored using these techniques. These advanced analytical techniques are used due to their low detection limits, ability to spatially target and analyze individual mineral grains, and their ability to measure and quantify, or semi-quantify, chemical components of minerals. A variety of complementary and supporting analytical techniques (e.g. Raman spectroscopy and ToF-SIMS), are often also applied in order to obtain a comprehensive understanding of the ore or process stream samples collected from various points throughout the mineral recovery process, and to thoroughly address the issue at hand. This presentation outlines case studies where multiple analytical techniques were utilized as diagnostic and predictive tools, demonstrating the benefits of using a variety of instrumentation to decipher the characteristics and chemistries of geological samples, and unravel a multitude of mining and mineral processing issues.

Understanding the Cryogenian

Paul Hoffman[1]

[1]University of Victoria paulfhoffman@gmail.com

The Cryogenian period (717 - 635 Ma) included the Sturtian and Marinoan glaciations and a brief nonglacial interlude. Both glaciations were long-lived, started and ended abruptly, and extended to sea level even at low paleomagnetic latitudes. Long-lived shallow-marine carbonate platforms residing in the warmest climatic zone were glaciated. Cryogenian glacial terminations are marked by strange 'cap-carbonate' sequences that distinguish them from all younger glacial epochs and one from the other. Consilient U-Pb zircon and Re-Os isochron dating (of volcanic ash and sedimentary organic matter) indicates that both glaciations ended synchronously on multiple cratons. Sturtian glaciation lasted 56 Myr, from 717 to 661 Ma. Its onset coincided with equatorial emplacement of the S-rich Franklin large-igneous province, in a climate pre-cooled by Rodinia breakup. Molecular biomarkers record a step-rise in algal over bacterial primary production during the nonglacial interlude. Marinoan glaciation began at ~651 Ma and ended at 635 Ma. Average sediment accumulation rates for both glacial epochs were ten times slower than for any younger glaciation, scaled for duration. The glacial inceptions and terminations caused large eustatic falls and rises, respectively, but net subsidence during the glacial epochs reduced the relative sea-level falls and boosted the rises. Synglacial ironstones formed where oxygenated subglacial meltwater was discharged from ice grounding lines into a well-mixed ferruginous Sturtian but not Marinoan ocean. Sulfate with large $\delta^{17}O$ anomalies was deposited during the Marinoan glaciation and its aftermath, consistent with high pCO2, low productivity, and synchronous deglaciation on a time scale below radiometric resolution. Ba isotopes fingerprint the global ocean as the Ba source for Marinoan cap barite. All these observations can be understood in terms of a self-reversing climate bistability, driven by ice-albedo feedback and extreme pCO2 hysteresis--the 'snowball Earth' hypothesis. Progressive synglacial ocean acidification stored massive amounts of dissolved (CaMg)CO3, which precipitated as cap carbonate in response deglacial warming, shelf flooding, pH rise, and intense weathering of loess and fresh bedrock as ice sheets receded. The small thermal inertia of the frozen snowball surface accounts for evidence of strong seasonality at low paleolatitudes, especially during regular periods of large orbital eccentricity (but low obliquity). During snowball epochs, preexisting polar-alpine ecosystems expanded into the equatorial ablation zone, establishing supraglacial cryoconite meltwater ecosystems on the oceans, and equatorial dry-valley habitats under thin ice covers of salinity-stratified (meromictic) lakes and hotsprings. These hardy and diverse biotic assemblages, after navigating the global meltdown floodings and torrid aftermaths, provided the genetic codes and metabolic passwords for the Ediacaran and Phanerozoic radiations to come.

Was snowball ocean water 18O-enriched or depleted?

Paul Hoffman[1]

[1]University of Victoria paulfhoffman@gmail.com

In the late Pleistocene, benthic foraminiferal aragonite was ^{18}O-enriched by 1.5‰ at glacial maxima relative to interglacials. About half of this difference is attributed to seawater compositional change due to sequestering in ^{18}O -depleted ice sheets. It is commonly assumed that snowball ocean water would have been even more enriched, due to a larger volume of meteoric ice if most continental areas were glaciated, as models and geology suggest, and up to half the volume of the km-thick sea-glacier consisted of depleted meteoric ice as well. Here it is suggested from a first-principles approach that the assumption may not be correct in the snowball case. When the ocean first freezes over and the ice cover rapidly thickens by freezing from below, equilibrium fractionation should yield ice that is ~30 heavier than the water. If one-third of the ocean was directly frozen, the ice would be +20 and the water -10, assuming unfrozen nonglacial ocean water (UNOW) was 0.00. In a snowball climate, the hydrologic cycle is driven by sublimation of equatorial sea ice and causes net snowfall elsewhere. The rate of hydrologic cycling rises as atmospheric CO2 accumulates, but the spatial pattern of the surface moisture balance remains unchanged so long as the tropical ocean is ice covered. Sublimation produces water vapour that is little fractionated (~30) because of slow diffusion in ice. Precipitation in cold air produces snow that is strongly fractionated (+150). The initial water vapour composition then would be -10 UNOW and the first snowfall would be +140. Strong Rayleigh distillation would yield water vapour and snowfall that become increasingly more ^{18}O-depleted with distance from equatorial vapour sources, but which in aggregate should be -10 UNOW in steady state, similar to snowball seawater. Models suggest that the snowball meteoric ice-vapour cycle and marine ice-seawater cycle are nearly decoupled. However, a small flux of meteoric subglacial meltwater returns to the liquid ocean as groundwater, recharged by basal melting of large ice sheets, and as direct injections of subglacial meltwater at tidewater ice grounding lines. These meltwaters would mainly derive from ice accumulated near the centers of ice sheets and would be strongly 18O-depleted. Their influx should tend to drive the (well-mixed) ocean water lighter than its starting composition of -10 UNOW. However, isotopic reequilibration of snowball ocean water by low- and high-temperature seawater-silicate exchange at mid-ocean ridges (Defliese, EPSL 554:116661, 2021) might offset this tendency, shifting UNOW itself heavier over snowball epochs. Sturtian iron-formations provide $\delta^{18}O$ proxy records from a snowball ocean, but represent mixing zones between ferruginous snowball ocean water and oxygenated meteoric meltwaters that could in principle range from heavily enriched (+140 UNOW) to highly depleted, depending on sites of snow accumulation. Snowballs were not simply colder Pleistocenes.

Structural, geochronological and metamorphic characterization of the Monashee décollement and its role in the tectonic evolution of the Canadian Cordillera

Katharina Holt[1], Kyle Larson[1]

[1]The University of British Columbia – Okanagan kah24@student.ubc.ca

The Monashee décollement (MD) is a crustal-scale shear zone within the southern Omineca belt of the Canadian Cordillera. The MD marks the contact between the autochthonous Precambrian basement core rocks of the Monashee metamorphic complex and the allochthonous rocks of the Selkirk allochthon. Both packages were metamorphosed at mid-crustal depths but are now exposed at ~ 2200 m elevation. The timing and style of deformation along the MD are disputed. Studies have proposed that the MD is: 1) the base of a mid-crustal ductile "channel"; 2) a complex normal-sense (top-to-the-west) extensional shear zone; or 3) a major reverse-sense (top-to-the-east) contractional shear zone that possibly forms the basal detachment of the Rocky Mountain thrust and fold belt. This project aims to test those different interpretations through characterizing the detailed temperature-time-deformation histories of the rocks within and adjacent to the MD at the Probity Peak field site, ~ 50 km northwest of Revelstoke, British Columbia. Fieldwork during the summers of 2019 and 2020 served as the basis for new 1:10,000 scale lithological and structural maps and facilitated the sampling of targeted rock specimens. Laboratory analyses of selected rock specimens were conducted in the Fipke Laboratory for Trace Element Research (FiLTER) at the University of British Columbia, Okanagan. This work involved microstructural analyses of thin sections to determine shear sense, quartz c-axis crystallographic preferred orientations (CPO), titanium-in-biotite (Ti-in-Bt) and zirconium-in-titanite (Zr-in-Ttn) geothermometry, as well as titanite and monazite petrochronology. The rocks affected by deformation along the MD have a SSW-striking, moderately-dipping tectonic foliation with a near down-dip quartz-biotite elongation lineation. Brittle top-down-to-the-WSW microfaults generally crosscut ductile top-up-to-the-ENE kinematic indicators. Deformation temperatures returned are ~ 465-683 ± 50 °C (CPO opening angle) and ~ 670-720 ± 23 °C (Ti-in-Bt), whereas titanite growth temperatures are ~ 740-775 ± 20 °C (Zr-in-Ttn). Monazite dated in 7 different metapelitic specimens returned five distinct Th-Pb age populations: 158.7 ± 1.2 Ma, 120.2 ± 0.5 Ma, 97.0 ± 0.3 Ma, 78.0 ± 0.3 Ma and 64.5 ± 0.2 Ma. Titanite in one calc-silicate specimen returned three distinct age populations: 59.3 ± 1.2 Ma (cores), 52.6 ± 1.1 Ma (mantles), and 49.7 ± 0.8 Ma (rims). We suggest that the rocks within/adjacent to the MD were deformed in two distinct, closely timed, phases of deformation of opposite shear sense. Continued work aims to determine the detailed sequence of structural events related to the MD and tie them directly to temperature-time-deformation data. Ultimately, this work will contribute to a larger-scale initiative that aims to create a universal model for how shear zones develop in collisional tectonic regimes and understand the complex roles they play in orogenesis.

Fe-Ni Sulfide Mineralogy of Tagish Lake and Other Carbonaceous Chondrites

Miranda Holt[1], Christopher Herd[1]

[1]University of Alberta holt@ualberta.ca

CM and CI carbonaceous chondrites have experienced extensive aqueous alteration resulting in significant changes to their primary mineralogy [1]. Here we report on the textures of sulfides in Tagish Lake (TL), an ungrouped C2 chondrite [2] and Aguas Zarcas (AZ), a CM2 chondrite, to gain insights into the role of alteration on their asteroidal parent bodies.

As a result of such alteration -likely on the asteroid parent body [1] - it has been argued that any Fe-Ni sulfide minerals within these groups must have a secondary origin. However, more recent studies have noted widespread occurrences of primary sulfides which retain textures that can only form at high temperatures, such as in the solar nebula [3]. We examined 10 polished fragments of TL and 5 of AZ using scanning electron microscopy to characterize the mineralogy and textures of their Fe-Ni sulfide grains and constrain their potential origins.

TL samples contain sulfides with a variety of textures, indicating formation by multiple mechanisms. Some pyrrhotite grains exhibit pentlandite exsolution, indicating formation at high temperatures [3], at odds with conditions of alteration on the TL parent body. These grains are common components within chondrules containing relatively Fe-rich olivine and are also found as isolated grains within the matrix. Also present are numerous grains which lack pentlandite exsolution, including a previously described "bull's-eye" morphology consisting of separate inner core and outer rings of sulfide grains interpreted to be secondary in origin [4]. This morphology is more abundant in sample TL1, along with an increased abundance of magnetite, suggesting the formation of this morphology may be related to an increase in oxygen fugacity.

AZ samples contain chondrule-rich, chondrule-poor, and metal-rich lithologies. A mixture of sulfide morphologies was observed, similar to that in TL, including some as chondrule components or rims and scattered within the matrix. The chondrule-rich and chondrule-poor lithologies contain numerous pyrrhotite grains exhibiting submicron pentlandite exsolution. The metal-rich lithology contained a lower abundance of sulfides. Pentlandite exsolution was observed in only two grains.
Together, these observations suggest that it is common for these groups of carbonaceous chondrites to contain multiple generations of sulfides, with distinct formation mechanisms. Recently obtained compositional data will provide further constraints on the origin of sulfides in these important samples.

[1] Brearley A. J. (2006) The action of water. In Meteorites and the early solar system II, 587-624. [2] Zolensky M. E. et al (2002) Meteorit. Planet. Sci. 37, 737-761. [3] Schrader D. L. et al. (2016) Geochim. Cosmochim. Acta. 189, 359-376 [4] Blinova A. I. (2014) Meteorit. Planet. Sci. 49, 473-502.

Transition Metal Mobility and Recovery from Weathered Serpentinite and Serpentinite Skarn Tailings from Lord Brassey Mine, Australia and Record Ridge, British Columbia, Canada

Makoto Honda-McNeil[1], Siobhan Wilson[1], Ben Mililli[2], Nina Zeyen[1], Baolin Wang[1], Connor Turvey[3], Colton Vessey[1], Avni Patel[1], Andrew Locock[1], Jessica Hamilton[4], David Paterson[4], Gordon Southam[5], Jordan Poitras[5], Thomas Jones[5], Simon Jowitt[6]

[1]University of Alberta hondamcn@ualberta.ca, [2]BHP, [3]University of British Columbia, [4]Australian Synchrotron, [5]University of Queensland, [6]University of Nevada, Las Vegas

As mineral resources become scarcer, companies are lowering their ore cut-off grades and resorting to exploring deeper underground and in more isolated areas. Incorporating tailings storage facilities and tailings reprocessing as part of the ore processing circuit can potentially extend the lives of mines and save on future exploration costs. Ultramafic and mafic mine tailings host resources including first and second row transition metals, such as nickel (Ni), cobalt (Co), and platinum group elements (PGE), whose high value and recovery could serve as a motivator for existing mines to reprocess their tailings. Many of these target metals are initially hosted by olivine, are repartitioned during serpentinization to form sulfides, oxides and alloys, and then are remobilized during weathering to form authigenic carbonates, sulfates and oxyhydroxides. Reprocessing tailings may further provide environmental benefits, including a reduction in waste output and the ability to offset greenhouse gas emissions by enhanced silicate-weathering and carbonation reactions. Here we use powder X-ray diffraction, scanning electron microscopy, electron probe micro-analysis and synchrotron X-ray fluorescence mapping to demonstrate how first and second row transition metals are mobilized to their final sinks. Samples of serpentinite, skarn and weathered tailings from the historical Lord Brassey nickel mine in Tasmania, Australia and weathered outcrops of serpentinite ore from the proposed magnesium mine in Record Ridge, BC, Canada are analyzed and compared. Preliminary results from these climatically similar localities indicate clear transition metal dissemination patterns across alteration zones and distinct partitioning behavior (ex. homogenous distribution of Ni within sulfides) in weathering products. By developing an understanding of the sinks for metals across the mining lifecycle, we aim to cultivate an economically viable framework for tailings reprocessing that capitalizes on metal mobility during tailings weathering.

Metamorphism through time: A bigger data approach to improve temporal, spatial and P-T data representivity.

Peter Hone[1], Sally Pehrsson[2], Bruce Eglington[1]

[1]University of Saskatchewan peh585@usask.ca, [2]Geological Survey of Canada

Metamorphic conditions in orogens are strongly influenced by geodynamic setting and are a key component when evaluating secular tectonic change. Average geotherm (dT/dP) through time has been a focal point, however trends such as late onset of cool subduction (low dT/dP) in previous compilations are not reflected in other geodynamic markers. Moreover, significant over-sampling of individual orogens and undersampling through geologic time hampers robust analysis. European Alps data density is an order of magnitude greater (0.983 versus 0.031 samples per 10k sq km) than any other setting, modern or ancient. We present a quantitative relational database of nearly a thousand samples that enables enhanced data assessment and spatial analysis and minimizes sample bias seen in more limited data sets. Temporal and spatial gaps were addressed by expanded literature reviews with emphasis on Precambrian terranes and non-Alpine modern orogens. Over-sampling was corrected by normalization of Alpine samples into spatial groupings and the addition of xenolith data from older terranes. Geotherms are classified holistically with averages defined by facies zones instead of linear fits to °C/GPa that can excise sections of characteristic data. Preliminary findings show that lower, 'blueschist' geotherms are common since the Ediacaran, but have been present in the rock record since the Eoarchean. There is a significant gap between field classification of metamorphic rocks by index assemblage and averaged P/T condition. Distinct differences in dT/dP conditions often reflect upper or lower plate settings. The extended dataset also emphasizes the punctuated nature of global metamorphism associated with the supercontinent cycle.

Audio-magnetotelluric measurements for geothermal exploration in Mt. Meager, BC, Canada

Fateme Hormozzade Ghalati[1], James A. Craven[2], Dariush Motazedian[3], Stephen E. Grasby[2], Eric Roots[4], Vicki Tschirhart[2], SeyedMasoud Ansari[2], Jon Liu[2]

[1]Carleton University, Geological Survey of Canada fatemehormozzadeghal@cmail.carleton.ca, [2]Geological Survey of Canada, [3]Carleton University, [4]Laurentian University, Geological Survey of Canada

The potential of geothermal reservoirs as a clean energy generation source in Canada remains to be evaluated. Mount Meager is located ~150 km north of Vancouver, British Columbia Canada, and is a part of the Garibaldi volcanic belt. Exploration at Mount Meager for geothermal energy resources has been underway using different exploration techniques since the 1970s. Well data has shown that there is a permeable zone at a depth of 1200-1600 m and that the reservoir has a temperature of 270 °C near 2500 m depth.

In this study, we have utilized recordings and related information from a new network of 84 audio-magnetotelluric (AMT) stations collected during the summer of 2019 plus 37 stations from previous studies to investigate the geothermal potential of the area around Mount Meager and Pylon peak. We used Phoenix Geophysics' MTU-5C recording equipment and their proprietary software for data processing, separating extensive noise from the signal, to calculate the components of the natural electrical and magnetic signals in the frequency domain. After manual processing and editing, the data showed good quality in the frequency range of 1 to 1000 Hz. Modelling started using a coarse grid mesh with different starting resistivities, and then a finer grid size and topography was added to refine the model. The preliminary result of this 3D inversion defines the shape and location of conductors in the study area. The results show a conductor at a depth 2000 m located to the southwest of Mount Meager. Comparison of the 3D model and the geological setting of the area demonstrated that this conductor shallows toward the southern portion of the No-good Fault. The model will be further interpreted at shallow depths in terms of relationships to known hot spring occurrences, fault zones and regions of enhanced temperature and porosity within the geothermal reservoir.

Geomechanical modelling of a seismogenic fault during fluid injection operations

Charles Hulls[1]

[1]University of Western Ontario chulls@uwo.ca

Earthquakes caused by human activity such as oil/gas exploitation of the unconventional reservoirs is a relatively new phenomenon. Several processes can induce seismicity, including the injection of fluids into underground reservoirs. Injection processes can themselves vary, as do their effects. For example, hydraulic fracturing (fracking) operations involve higher pressures and lower injection volumes compared to other processes. It is important to perform geomechanical and statistical modelling to assess suitability of sites for exploitation. In this respect, the geomechanical models are useful due to their low cost and computational efficiency compared to experimental results. Underground rock formations are characterized by the stresses acting on them, and by their ability to hold and transfer fluid. Several different processes related to the injection of fluid, including powerful but short-range direct pressure changes, localized poroelastic deformation, and force transfer via aseismic slip, alter this stress state, or cause the rock formation to fracture. Direct pressure contributions dominate when there is a channel between the injection site and seismogenic faults that fluid can flow through. Poroelastic effects are more impactful at longer distances where fluid pathways are less likely to be present. For several injection processes such as wastewater disposal, the magnitude of the largest induced events is strongly tied to the total injected volume. It has been noted that fault movement produced by hydrofracturing is aseismic on the connected faults, which means that the larger earthquakes related to these operations are likely triggered by this movement causing stress change on nearby unconnected faults. We examine a computational model of a fluid injection process into a realistic rock formation including a permeable reservoir and impermeable basement formation. A single large fault connected to the reservoir is also included in the model and is assumed to be capable of slipping under the right conditions. The pore pressure propagation from the injection and resultant poroelastic stress changes are examined for the potential to trigger earthquakes on the model fault. We also investigate changes in the stress field surrounding the fault due to poroelastic stress changes and slippage of the fault. Finally, we examine the geomechanical properties of the fault and the impact of several slip models. This analysis is important in terms of assessing of the potential of the rock formations to produce sequences of earthquakes related to the hydraulic fracturing operations.

Mining Matters and the Transition from Hands-on to Virtual Education Program Delivery

Lesley Hymers[1]

[1]Mining Matters lhymers@miningmatters.ca

Mining Matters is a charitable organization dedicated to educating young people to develop knowledge and awareness of Earth sciences, the minerals industry, and their roles in society. The organization provides information about rocks, minerals, metals, mining and career opportunities available in the industry. It offers educational resources that meet curriculum expectations, created by educators and Earth science experts. Since 1994, Mining Matters has reached an estimated 780,000 teachers, students and members of the public. Mining Matters offers three core areas of programming. Teacher Training and School Programs support educators with professional learning opportunities, resources and curriculum-linked classroom workshops. Public Outreach Programs provide foundational information through interactive activities at community, education and industry events. Indigenous Community Education and Outreach Programs build mineral literacy, raise awareness of the importance of education, and highlight the range of career opportunities. With sensitivity to the importance Indigenous communities play in resource stewardship, management and development, the program includes summer camps, school programs, professional learning workshops for educators, and community events. Traditionally, Mining Matters focuses on hands-on and experiential learning, providing in-person professional learning workshops, in-classroom programming and in-community education. The recent transition to virtual delivery required the adoption of new practices, including redeveloping activities, rethinking approaches to program delivery, and identifying new partners in STEM education. New initiatives include a collection of DIY GEMS (geology, engineering, mining, sustainability) activities, synchronous learning workshops, participation in virtual outreach events, and instructional videos with accompanying hands-on resource kits shipped to communities across Canada.

Possible Atmospheric Water Vapour Contribution from Martian Swiss Cheese Terrain

Alex Innanen[1], Margaret Landis[2], Paul Hayne[2], John Moores[1]

[1]York University ainnanen@yorku.ca, [2]University of Colorado Boulder

The CO2-ice South Polar Residual Cap (SPRC) of Mars show a variety of morphologies including linear ridges, raised scalloped mesas and quasi circular depressions known as 'Swiss cheese' features. These Swiss cheese features are characterised by flat floors and steep sides that grow outwards at a rate of several metres per year, potentially exposing underlying water ice. Based on this growth rate, a total resurfacing of the cap could occur every ~100 years [1]. Our work determines the potential water vapour release from temporary removal of the surface CO2 ice.

This work is motivated by the 1969 observation by Barker et al of an unusually high amount of water vapour above the SPRC in southern summer [2]. One potential source of water vapour is water ice exposed by Swiss cheese terrain removal of CO2 ice, if water ice immediately underlies the SPRC. We present work examining if the Swiss cheese features have any substantial contribution to atmospheric water vapour, and under what conditions it could be possible to recreate the 1969 observation through Swiss cheese feature growth. Our study can help to understand whether observed erosion of the SPRC is driven by an unstable climate regime, or if this is part of a cyclical process of loss and replenishment.

We used images from the Context Camera (CTX) aboard the Mars Reconnaissance Orbiter (MRO) to map individual Swiss cheese pits to determine an approximate amount of the SPRC carved out by Swiss cheese features. We use retrieved brightness temperatures from the Mars Climate Sounder (MCS) with a linear sub-pixel temperature mixing model to determine the likely water ice temperature in the scene, assuming a fraction of the scene is composed of exposed water ice. An upper bound on this fraction is given by the mapped fraction of Swiss cheese pits to higher standing terrain. This water ice temperature can be used to determine the rate of water sublimation, and whether the water-vapour quantities are sufficient to explain the 1969 phenomenon.

[1] Byrne, S. et al (2015) LPI XLVI, Abstract #1657.

[2] Barker, E.S. et al. (1970) Science, 170, 1308-1310.

Environmental Risk Associated with Modern and Historic Dispersal of Arsenic-Bearing Dust from the Giant Gold mine, Yellowknife, Canada

Heather Jamieson[1], Alexandra Bailey[1], Kirsten Maitland[1], Jon Oliver[1], Michael Palmer[2]

[1]Queen's University jamieson@queensu.ca, [2]Aurora College

Large, long-lived mines that began operation before emission regulations existed leave complicated environmental legacies. We have used multiple methods, with an emphasis on mineralogical characterization, to distinguish historic contamination from modern tailings dust dispersal and to estimate the natural geochemical background applicable to the Yellowknife region. This area has been exposed to more than 60 years (1938-1999) of arsenic (As)-rich atmospheric mining emissions. Windblown dust from the uncovered tailings has been a recent concern among residents including the Yellowknife Dene First Nation. Detailed mineralogical characterization of dust confirms that there is no arsenic trioxide, the most toxic and bioaccessible form of arsenic, in the tailings dust. Arsenopyrite associated with the gold ore was converted to arsenic trioxide and iron oxides when the refractory ore was roasted as a pre-cyanidation step. More than 20,000 tonnes of arsenic were released from the roaster stacks, most of it during the early years of operation. Most of the arsenic in the surface tailings and windblown dust is hosted in arsenopyrite and roaster-generated iron oxides as in the later years of operation, the arsenic trioxide was collected and stored in underground chambers. However, soils within 30 km of the former Giant mine roaster do contain arsenic trioxide, suggesting that these may present a higher risk than the tailings themselves. More than 400 near-surface soil samples collected from undisturbed areas indicated arsenic concentration ranges from near zero to 4700 mg/kg. There is a strong relationship between arsenic and distance from the main emission source which has persisted in surface soils and soils at depth in the soil profile decades after the bulk of mining emissions were released Mineralogical analysis was conducted on almost 100 soil samples and, of these, 80% contained arsenic trioxide, indicative of roaster stack emissions. Even where concentrations were relatively low, most arsenic in surface soils within 15 km of Yellowknife is hosted as anthropogenic arsenic trioxide. Statistical protocols for the estimation of geochemical background were applied to an existing database of till geochemistry (N = 1490) after removing samples from mining impacted areas including those near Yellowknife. Our results suggest geochemical background for the Slave province is 0.25 - 15 mg kg-1 As. This is well below previous estimates for the area, which were based on mining-impacted soils, and below the current residential (160 mg kg?1) and industrial (340 mg kg?1) environmental remediation guidelines in the Northwest Territories, but is close to global averages and Canadian federal guidelines.

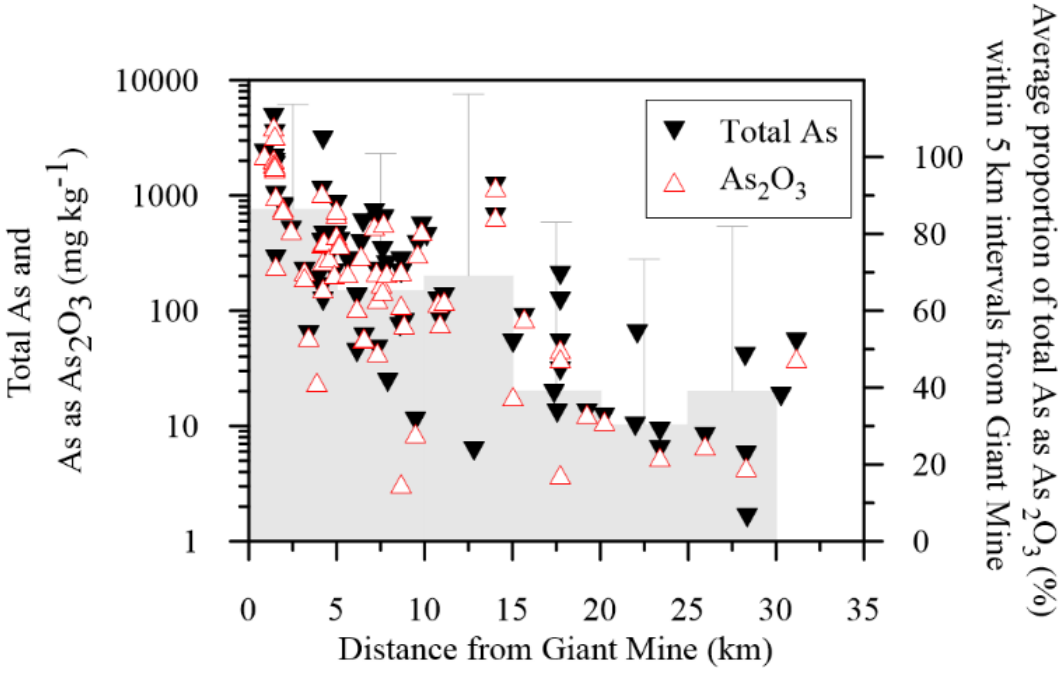

Using Synchrotron-based Microanalysis to Identify Mystery Minerals in Mine Waste

Heather Jamieson[1], Anezka Borcina Radkova[1], Amy Cleaver[1], Ron Peterson[1]

[1]Queen's University jamieson@queensu.ca

Grain-scale microanalysis of minerals provides important insight into the mineralogical hosting of potentially toxic metals and helps to predict whether metals are released through weathering or attenuated in secondary phases. These secondary minerals are usually rare, small and poorly crystalline. We have used microfocused synchrotron beams to combine microXRF (element mapping), microXRD (crystal structure identification) and microXANES (oxidation state, bonding environment) to identify solid phases formed from ore processing and weathering. Major and trace elements can be mapped simultaneously with femtogram absolute detection sensitivities, allowing metals sorbed or bound on minerals to be characterized, and the nature of this association investigated with absorption spectroscopy. Poorly crystalline minerals such as iron oxyhydroxides and rare, fine-grained contaminant-bearing weathering products that are difficult to differentiate using other techniques may be distinguished using synchrotron-based microXRD. The examples described in this presentation include roaster-generated iron oxide from tailings from the Giant Mine, Yellowknife. Synchrotron microanalysis showed that maghemite, identified by microdiffraction, contains both As3+ and As5+, determined by microXANES. This defect structure likely incorporates the As3+ within the crystal framework as trigonal bridging complexes, explaining the persistence of trivalent arsenic in tailings exposed to the atmosphere for more than 50 years. These roaster-generated iron oxides are the major host of arsenic in many tailing samples and are present in regional soils and lake sediments. A combination of synchrotron and conventional microanalysis was used to identify secondary antimony minerals that are relatively insoluble (tripuhyite FeSbO4) and soluble (brandholzite (Mg[Sb(OH)6]2*6(H2O)). Antimony is a critical mineral meaning that there is likely to be increased mining but it is also an environmental hazard and considered carcinogenic. Zinc, lead and copper sulfides are expected to oxidize in exposed mine tailings but the secondary products depend on host rock geochemistry and weathering conditions. For deposits hosted by carbonate rocks, microdiffraction has shown that sphalerite oxidizes to smithsonite (ZnCO3) and hydrohetaerolite (ZnMn2O4*H2O), galena to cerussite (PbCO3) and chalcopyrite to aurichalcite ((Zn,Cu)5(CO3)2(OH)6). The nature of these secondary minerals influences their tendency to dissolve in surface water if introduce in windblown tailings dust. The fine spatial resolution and ability to combine multiple near-simultaneous analytical techniques including X-ray fluorescence, diffraction and absorption spectroscopy makes synchrotron microanalysis a powerful characterization tool for those secondary phases that usually prove difficult to identify. This provides an opportunity to characterize the most reactive and bioavailable of the contaminant-hosting phases.

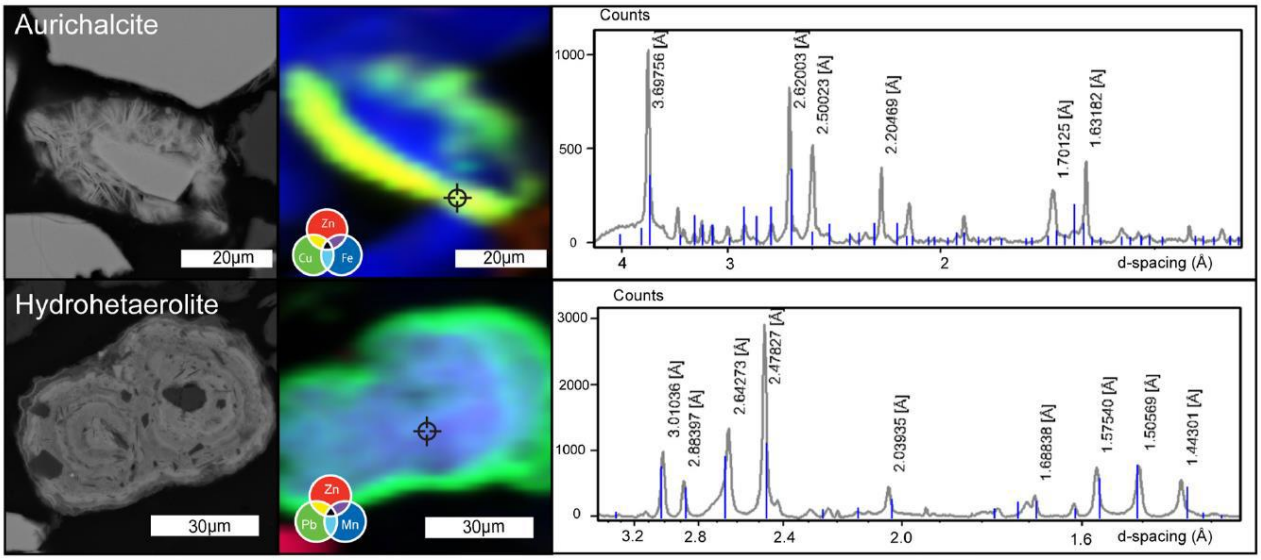

Regional liquefaction susceptibility mapping in Greater Vancouver based on surficial geology

Alireza Javanbakht[1], Sheri Molnar[1], Abouzar Sadrekarimi[1], Sujan Adhikari[1]

[1]University of Western Ontario ajavanba@uwo.ca

Soil liquefaction could be one of the most destructive consequences to occur in the saturated sands of the Fraser River delta in southern Great Vancouver, British Columbia from future strong earthquake shaking. Liquefaction hazard maps increasingly are being incorporated into earthquake risk mitigation practice and are used for site selection and planning stages for urban settlement areas and engineering structures. Soil liquefaction susceptibility is investigated based on regional surficial geology. For the 32 surficial geology units in the region, we assign a liquefaction susceptibility ranking, six rankings between none to very high, based on sediment material type, depositional environment, distribution, and age according to liquefaction susceptibility of sedimentary deposits proposed by Youd and Perkins (1978). We explain the reasons for considering liquefaction rating of each surficial geology. We compare our map with previous liquefaction hazard maps in Greater Vancouver area and state differences and similarities comparing each surficial geology unit. Holocene deposits show higher hazard of liquefaction while Pleistocene deposits and pre-Pleistocene have rarely been affected by liquefaction. Deltaic deposits and poorly compacted artificial sand fills show a considerable hazard during liquefaction. Our regional liquefaction susceptibility map of Greater Vancouver informs where to evaluate liquefaction severity as part of a Metro Vancouver seismic hazard mapping project and can be used to improve mitigation and planning in the region.

Stratigraphy, structure, correlations and uranium metallogeny of the Paleoproterozoic Amer Group, Amer Fold Belt, Nunavut

Charles Jefferson[1], Robert Rainbird[1], Grant Young[2], Sunil Gandhi[1], Joseph White[3], Victoria Tschirhart[1], Lydia Calhoun[3], Deborah Lemkow[1]

[1]Geological Survey of Canada charlie.jefferson49@gmail.com, [2]Western University, [3]University of New Brunswick

Uranium metallogenic study of the Amer Fold Belt in the Central Rae craton of the western Churchill Province in Nunavut employed high-resolution aeromagnetic data, gravity transects and structural-stratigraphic knowledge gained through detailed mapping of sparse good outcrops. The Amer Belt provides type and reference sections for revisions of four regionally mappable Paleoproterozoic (Ps1-Ps4) sequences that have similar lateral and vertical facies changes but distinct differences in the Ketyet River and Montresor belts. In the latter, more complete geochronology partly compensates for structurally dismembered stratigraphy. Ps1 is quartzarenite with polymict conglomerate at base and top, resting on paleoweathered Neoarchean volcanic and granitic rocks. Ps2 comprises gossanous and recessive, carbonaceous-sulphidic-metalliferous mudstone grading up to cherty tan dolostone. Lower Ps3 is either calcareous tholeiitic basalt (strong linear aeromagnetic markers; absent from the Montresor), or laterally equivalent fine clastic rocks. Only in the Amer Belt, the upper fine clastic rocks of Ps3 contain a strong linear aeromagnetic marker, topped by calcareous arkosic quartzarenite, then alternating shallow subaqueous calcareous arkose and mudstone with stratabound sandstone-hosted uranium occurrences coincident with two linear aeromagnetic highs. Ps4, rhythmically interbedded arkosic-lithic arenite and siltstone, has an internal orthoconglomerate but no basal conglomerate in all three belts. In Ps2-Ps3 of the Amer and Ketyet River belts, linear, discontinuous basalt and carbonate units, and local thinning of the Ps1 quartzite suggest the effects of northeast-trending, syn-depositional faulting. Lateral changes at the Ps1-Ps2 sequence boundary from orthoconglomerate to graded rhythmites of fine quartzarenite to black shale suggest overall deepening toward the southwest and across sub-basins. The ca. 1.9-1.865 Ga Snowbird orogeny (DP1) generated diversely vergent isoclinal folds and refolds of Ps1-Ps3, and basement-involved imbricate thrusts, all with weak metamorphism. Post-orogenic regional erosion cut to basement in places. Ps4 draped this erosional surface with no evidence of initial local faulting. Ps4 detrital zircon includes a 2.03-1.90 Ga population representative of the south Rae craton and Taltson-Thelon magmatic zone. Mid-sequence conglomerate comprises locally derived intraclasts and pre-deformed Ps1 quartzite + 2.6 Ga granite. The Hudsonian orogeny (DP2) produced first-generation northwest-vergent folds in Ps4, basement-involved refolds and thrusts in Ps1-Ps3, anchizone to upper amphibolite grade metamorphism, and ca. 1.85-1.81 Ga granite and ultrapotassic dykes. This Geomapping for Energy and Minerals project validated detailed mapping of the Amer Belt by Grant Young, Alex Knox and Judith Patterson, and filled gaps framed by Subhas Tella regionally. A uranium geodatabase by S.S. Gandhi and an eight-member industry partnership contributed key data.

Geological and uranium metallogenic comparisons of the Thelon and Athabasca basins

Charles Jefferson[1], Eric Potter[1], Robert Rainbird[2], William Davis[1], Colin Card[3], Sean Bosman[3], Paul Ramaekers[4]

[1]Geological Survey of Canada charlie.jefferson49@gmail.com, [2]Retired GSC, [3]Saskatchewan Geological Survey, [4]MF Resources Inc.

New and compiled data in the Thelon and Athabasca basin regions enhance comparisons of their respective uranium metallogenies. The Athabasca Supergroup overlaps the Rae and Hearne cratons of the western Churchill Province, whereas the Dubawnt Supergroup of Nunavut and the eastern NWT rests entirely within the Rae craton, west of the Snowbird Tectonic Zone cratonic boundary. The Athabasca Supergroup fills the Martin and Athabasca basins whereas the Dubawnt Supergroup fills the Baker Lake and Thelon basins. The Athabasca Supergroup comprises five, unconformity-bounded, second-order clastic sequences in the Martin, Jackfish, Cree and Mirror basins. The Martin and Jackfish sequences roughly correspond to the lower (Baker) and middle (Whart) sequences of the Dubawnt Supergroup. Three more sequences filled the Cree and Mirror basins while two more of the Barrensland Group filled the upper Baker Lake and most of the Thelon basins, completing the Dubawnt Supergroup. The Thelon Formation (lower Barrensland Group) comprises three, third-order, upward-fining, siliciclastic sequences. Limited facies and paleocurrent data suggest a single, "big river" system axial to the Thelon Basin. The upper Barrensland Group comprises Kuungmi Formation ultrapotassic mafic tuff and flows (1.54 Ga) in contrast to 1.54 Ga black shale of the Douglas Formation, and the Lookout Point Formation carbonate, much like the Carswell Formation atop the Athabasca Supergroup. The two supergroups have similar but distinct crustal settings, paleocurrents, facies changes, provenance, igneous components, geochronology and tectonic histories. Beneath the Athabasca Basin, granulite- to amphibolite-facies, conductive-graphitic-pyritic deformation zones are spatially associated with known major deposits. Conductive temporal analogues below the Thelon Basin are barren, impermeable, albeit sheared, black pyritic phyllite of anchizone to epizone facies. Instead, hosts of the smaller Thelon uranium deposits are Neoarchean pyritic greywacke and epiclastic rocks that range in metamorphic grade from lower to upper amphibolite, including partially melted paragneiss. The basins developed independently but broadly contemporaneously, possibly bridged at times by since-eroded, more extensive upper units. Pre-ore fluorapatite cements of the Athabasca and Thelon basins are 1.64 vs. 1.69-1.67 Ga respectively. The Thelon Formation and deposits lack hydrothermal tourmaline. Similarities include uranium sources in surrounding terranes and the basin fills, sodic brine transport, diagenetic and hydrothermal alteration of basement and basin-fill (hematite, clay and chlorite minerals, aluminum phosphate sulphate minerals, fluid inclusion data, silicification [before, during and after mineralization] and dequartzification), and reactivated faults that focused alteration and mineralization. Such cumulative knowledge supports adaptive exploration strategies between these prospective regions.

Comparison of the impact histories of carbonaceous chondrites Murray and MCY 05230

Laura Jenkins[1], Martin Lee[1], Luke Daly[1], Ashley King[2]

[1]University of Glasgow ljenkin9@uwo.ca, [2]Natural History Museum

Carbonaceous chondrite (CC) meteorites often show little to no evidence of shock deformation [1], though the process is poorly constrained in this group. What is known is that CCs display chondrule flattening and alignment among mineral shock effects [2,3]. Understanding shock metamorphism in CCs is important as it may have caused aqueous alteration and/or post-hydration heating of their parent asteroids [3,4]. We compare strain, chondrule flattening and alignment for two CCs, Murray and MacKay Glacier (MCY) 05230. To study strain, electron backscatter diffraction (EBSD) was used to measure mean grain orientation spread (mGOS) and to create grain reference orientation difference (GROD) maps. To study chondrule flattening and alignment, back-scattered electron images were collected by scanning electron microscopy, which were input into ImageJ to determine the aspect ratio (AR) and azimuthal angle (AA) of chondrules >150 μm in size with their fine-grained rims. Unaltered chondrules have an AR of 1.2>[2]. Murray is an aqueously altered breccia of petrologic type [5] of 2.4-2.5 [3]. Most clasts are unheated, but a few likely experienced mild heating [4]. Olivine has mGOS 1°> and GROD maps of olivine indicate low internal misorientation (straight extinction in optical microscopy). Pyroxene has a GROD map showing moderate internal misorientation and crystal plastic deformation (undulatory extinction), and it has mGOS of up to 5.7°. This corresponds to ~5 GPa of peak shock pressure [6]. 33 chondrules were measured. They had an average AR of 1.47±0.31 and 6% were within 10° of the median AA. Murray's chondrules are flattened, but not aligned. MCY 05230 is more altered than Murray, having a petrologic type [5] of 2.3. This sample shows no signs of brecciation or heating. Olivine and pyroxene have GROD maps indicating undulatory extinction, and have mGOS up to 7.4° and 4.7°, respectively. This corresponds to 5-20 GPa of peak shock pressure [6]. 23 chondrules were measured and had an average AR of 1.48±0.37. None of them had AAs within 10° of the median AA. MCY 05320's chondrules are flattened, but not aligned. MCY 05230 is more strained than Murray and experienced >5; GPa of peak shock pressure. This may have led MCY 053420 to be more altered, if impacts were responsible. Both meteorites show similar degrees of chondrule flattening but given the lack of alignment and the low shock pressures experienced by Murray, this and any heating experienced is likely not shock-related. Chondrule flattening could be due to aqueous alteration changing chondrule shapes or due to lithostatic compaction. References: [1] Scott et al. (1992) Geochim. Cosmochim. Acta, 56: 4281-4293. [2] Tomeoka et al. (1999) Geochim. Cosmochim. Acta, 63: 3683-3703. [3] Lindgren et al. (2015) Geochim. Cosmochim. Acta, 148: 159-178. [4] Quirico et al. (2018) Geochim. Comsmochim. Acta, 241: 17-37. [5] Rubin (2007) Geochim. Cosmochim. Acta, 71: 2361-2382. [6] Stöffler et al. (2018)MAPS, 53, 5-49.

Identifying Waste from Historical Gold Mines Via Supervised Classification of Remote Sensing Imagery

Daniel Jewell[1], Linda Campbell[1], Peter White[2]

[1]Saint Mary's University daniel.jewell@smu.ca, [2]Natural Resources Canada

In the mid-19th to the early 20th centuries, multiple gold rushes took place in Nova Scotia. More than 60 gold mining districts were created, comprising over 300 individual mines. Gold was mined primarily from quartz veins found throughout the Meguma terrane, made up of several groups of sedimentary and metasedimentary rocks. In addition to gold, these host rocks invariably contain high levels of arsenic-bearing sulphide minerals such as arsenopyrite. To extract gold, host rock was crushed in stamp mills and processed either by mercury amalgamation or, in later years, cyanidation. Waste rock, as well as the fine material called tailings was discarded in nearby streams, wetlands, or natural depressions. With few exceptions, these mine sites have been left mostly untouched since the mines were closed, up to a century ago. By increasing the surface area of arsenic-bearing minerals and exposing them to oxygen, water, and bacterial activity, these mine waste areas are often conducive to the production of acid mine drainage. If mercury was used in processing, this may also be present. These un-remediated mine sites may pose a threat to human and ecological health. Several have been slated for cleanup, though the vast majority have not been studied in detail. The exact location and current extent of tailings is not known at every site. Modern maps are often based on historical records - records which may include under-reporting of waste, or which may no longer be accurate due to transport of tailings via streams or wind. In order to prioritize research and remediation efforts, a rapid method of assessment is required. Remote sensing analysis has been used successfully around the world to provide such initial assessments. In this study, Google Earth Engine has been used to access Sentinel-2 multispectral satellite images. Models have been created using multiple supervised classification methods, including random forest and support vector machines, and various inputs. These models are compared by a statistical assessment of accuracy metrics. Once trained, classifiers may be able to indicate presence of tailings, even if sediment has been moved from its historical area of deposition by streams or wind. The maps resulting from this study may help guide cleanup efforts by highlighting priority areas requiring immediate research. It may also help us to understand the way that tailings are transported from historical mine sites, both near the sites and across long distances.

Research-creation to expand the conversation on geoethical training

Sandra Johnstone[1]

[1]Lakehead University johnstones@lakeheadu.ca / Vancouver Island University

Geoethics is an emerging field of discourse which aims to improve both the ethical practices of geoscientists and the ethical applications of geoscientific knowledge, drawing together perspectives from geoscience, philosophy, economics, and sociology. Proponents of improving geoethical practice for geoscientists have identified post-secondary educational settings as essential sites of exposure to geoethical thinking. Here I use my own experiences as a geologist and geoscience educator as data, applying a critical lens to illustrate the ways that stories and epistemic allegiances may limit access to diverse geoethical perspectives on complex socioenvironmental issues. Through this work I consider ethical frictions in three narratives about the professional roles of geoscientists that are common in the geoethics literature: 1) Geoscientists as environmental stewards, 2) Geoscientists as providers of raw materials essential to society, and 3) Geoscientists on a journey of scientific discovery. I apply arts-integrated research methods, informed by the interdisciplinary methodological models of parallaxic praxis and research-creation, to think differently about these three stories. Innocent representations of geoscientists as ethical actors break apart as the stories move across knowledge paradigms and are situated in local histories. Preliminary results from this study suggests that when critical perspectives on geoethical issues are engaged, both geoscience educators and students may find themselves implicated in uncomfortable ways. Here I contend that these unsettling experiences are necessary to move beyond performative conversations on geoethics, and that arts-integrated research has the potential to make visible affective nuances that are difficult to capture using more traditional methods of educational research.

Detrital zircon geochronology of Paleoproterozoic strata in northern Michigan: new insights into the age, provenance, and regional correlation of the ca. 2.3-2.1 Ga Chocolay and Dickinson Groups

James Jones III[1], William Cannon[1], Benjamin Drenth[1], Amanda Souders[1], Klaus Schulz[1], Paul O'Sullivan[2]

[1]U.S. Geological Survey jvjones@usgs.gov, [2]GeoSep Services

Detrital zircon U-Pb data from ca. 2.3-2.1 Ga metasedimentary successions in northern Michigan provide a test of regional to global stratigraphic correlations and yield key insights into provenance patterns along the Proterozoic margin of the Superior craton. Two units of the ca. 2.3-2.2 Ga Chocolay Group--the glaciogenic Fern Creek Formation and Mesnard quartzite--have unimodal age spectra with prominent ca. 2.7-2.6 Ga age populations. The Mesnard quartzite also contains a small population of ca. 2.3 Ga zircon, but grains of this age are absent in the Fern Creek Formation sample. Our findings are similar to previously published Chocolay Group data from the same region, and ca. 2.3 Ga detrital zircon are recognized in all other units except for the Sunday quartzite. Collectively, Chocolay Group detrital zircon data correlate well with published age spectra for parts of the Huronian Supergroup to the east, and they have age populations in common with other global ca. 2.3-2.2 Ga glaciogenic successions. The ca. 2.1 Ga Dickinson Group is interpreted to unconformably overlie the Chocolay Group, and it comprises three units--the East Branch Arkose, Solberg Schist, and Six Mile Lake Amphibolite. Two samples from the East Branch Arkose have prominent age populations of ca. 2.9 and 2.7 Ga, and one sample has some ca. 2.1 Ga grains. The youngest ages are consistent with previously published data from the same unit and suggest local derivation from ca. 2.1 Ga porphyritic red granite exposed nearby. However, the bimodal Archean age populations in our data are distinct, suggesting derivation from a broader region and, likely, recycling of Chocolay Group strata. Detrital zircon from one sample of the Solberg Schist define a broad age spectrum that has a dominant ca. 2.3 Ga age population and a small ca. 3.6 Ga age population. The youngest individual grains were ca. 2.1 Ga, consistent with the underlying East Branch Arkose. Globally rare ca. 2.3 Ga detrital zircon are present in both the Chocolay and Dickinson Groups, and they are also present in coeval strata in Ontario to the east and Wyoming to the west. These distinctive grains raise the possibility of a common, unique source and provide a means of correlating these successions across hundreds to thousands of kilometers along the margin of the Kenorland supercontinent. Dickinson Group detrital zircon age spectra are similar to the older Chocolay Group but also include additional age populations, indicating that new source regions in the southern Superior craton were being integrated while older strata were also being recycled ca. 2.1 Ga. These patterns are consistent with regional uplift of the southern Superior craton ca. 2.1 Ga that culminated in dismemberment of the Kenorland or Superia supercontinent and the beginning of a profound depositional hiatus that lasted until onset of Penokean orogenesis ca. 1.89 Ga.

Investigating the Formation Conditions of High-Temperature Breccias at the Steen River Impact Structure (Alberta, Canada): An Experimental Approach

Haley Jurak[1], Erin Walton[2], Cliff Shaw[1]

[1]University of New Brunswick hjurak@unb.ca, [2]MacEwan University

The Steen River impact structure (SRIS) is a buried, 25 km-diameter, complex crater located in Alberta, Canada. The impact event occurred ~141 Ma in mixed target rocks, comprising ~1.3 km of Devonian shales, carbonates, and evaporites, overlying Proterozoic granites. In 2017, an ~128 m-thick unit of impact melt-bearing, clast-rich impactite was identified in drill core. The breccia matrix is defined by a suite of high-temperature minerals (diopside > sanidine > magnesioferrite), hypothesized to have grown in the solid state from an initially clastic matrix, in response high post-shock temperatures. In this study, we test the hypothesis that SRIS breccias were deposited at temperatures >800°, resulting in decomposition of CaCO3-bearing rocks to form Ca-rich minerals (diopside), through a series of sintering experiments. The goal is to constrain the temperature at which the thermally-metamorphosed breccias were deposited, and the amount of CaCO3-bearing rocks originally present in the matrix. Experiments were performed at the University of New Brunswick. Shocked SRIS granite and limestone were crushed to powders (<100 µm grain size). Mixtures of granite and limestone were loaded into a three-zone Lindberg furnace and sintered at constant pressure (1 atm), temperatures (800, 900, & 1000°), and oxygen fugacity (fO2 = QFM + 2) for 6 months. Experiments were extracted from the furnace, then prepared for scanning electron microscopy and Raman spectroscopy. The impactite mineralogy was reproduced in 800, 900, and 1000° experiments. Ca-rich minerals (diopside & wollastonite) occurred as fine-grained rims with vermicular textures on quartz and feldspar grains (800, 900, & 1000°); as patchy, poorly-formed grains within clastic textures (900 & 1000°); and as laths within melt textures (900 & 1000°). Since the breccia matrix was sintered, but not melted, we suggest SRIS breccias were deposited at ~800°. This constraint is supported by U-Pb dating of accessory phases within SRIS breccias, which limit the temperature of sintering to 450° < T < 800°. Wollastonite lining quartz and feldspar grains was observed in 800? runs containing >25% limestone, but <50% granite. While these experiments lack diopside, we suggest that the size of starting materials was too coarse to facilitate the growth of this mineral at low temperature. We hypothesize that, by decreasing the size of our starting materials, pyroxene will form at ~800°. Our experiments demonstrate that, prior to deposition, SRIS breccias comprised >25% carbonate but <50% crystalline rocks. The observed breccia matrix mineralogy is the result of recrystallization, driven by the acceleration of hot gases from volatilized sedimentary cover mixed with shocked crystalline basement. These findings will inform a series of experiments that investigate the run products of fine-grained (<1 µm) starting materials, sintered to 450° < T < 800°.

Recent progress in the experimental studies on deformation of minerals and rocks

Shun-ichiro Karato[1]

[1]Yale University shun-ichiro.karato@yale.edu

Although laboratory studies are key to the understanding of deformation in Earth's interior, laboratory studies are challenging, and until recently only reliable data on rock deformation are from the studies using the gas-medium deformation apparatus (the Paterson apparatus) that can be operated only at low pressures (less than ~300 MPa (~10 km depth)). However, much of plastic deformation in Earth occurs not in the shallow part, but in the hot deep part. Consequently, we had very limited data set to understand plastic deformation of Earth's interior including the relatively shallow part (e.g., the upper mantle). The situation has dramatically changed during the last ~20 years due to the progress of a new experimental approach using synchrotron X-ray facilities. In the classic deformation experiment, one places a sample in high pressure, temperature environment and applies deviatoric stress, and measure the stress and strain based on the measurement of force and displacement outside of a sample. Such a technique cannot be applied under high-pressure (and temperature) conditions where a small sample is surrounded by several materials. Weidner developed new technique of measuring stress and strain of a sample using high intensity X-ray from the synchrotron radiation [Weidner et al., 1998]. In this new approach, a sample is located in a new type of deformation apparatus (DDIA (deformation DIA; [Wang et al., 2003]), RDA (rotational Drickamer apparatus; [Yamazaki and Karato, 2001])), and X-ray penetrates through the sample. This provides the information on the shape change of a sample (strain) by X-ray absorption imaging, but X-ray diffracted by a specimen also provides a data set to determine stress acting on the sample. This stress measurement uses the elastic strain of grains determined by X-ray diffraction and provides a constraint on the stress acting on grains. [Karato, 2009] developed a theory that includes the influence of plastic. Using these approaches, one can determine strain and stress of a sample in-situ during deformation under high-pressure, temperature conditions providing an important data set on plastic flow of materials. Advantages of this approach include (i) quantitative deformation experiments can be conducted under much higher pressure and temperature conditions (so far to ~30 GPa, ~2200 K), than the conventional approach (<0.3 GPa, <1550 K), (ii) in a sample made of multiple phases, one can determine the flow properties of each material, (iii) using the influence of diffraction planes ((hkl)) on lattice strain, one can infer plastic anisotropy and also deformation mechanisms (dislocation creep versus diffusion creep), and finally (iv) since all measurements are in-situ measurements, one study the evolution of mechanical properties of a rock including the processes of shear localization and the evolution from transient to steady-state creep. Some representative results will be presented with some geodynamic implications.

Intrabasinal sediments and tectonostratigraphy of the Lau Basin: Assessing linear vs diachronous models for the opening of the Lau back-arc basin

Jessie Kehew[1], Mark Hannington[1], Alan Baxter[1], Michael Riedel[2], David Diekrup[1], Sven Petersen[2]

[1]University of Ottawa jkehe018@uottawa.ca, [2]GEOMAR Helmholtz Center for Ocean Research Kiel

The Lau Basin, located in the SW Pacific, is a type-example of a back-arc basin that is actively undergoing extension. Small sub-basins have opened across the backarc to accommodate this extension, but little is known about how, and in what order they formed. We investigate and reconstruct the sedimentary and structural history of the sub-basins by analysing and interpreting both seismic reflection and high-resolution sub-bottom profiling ('parasound') data along four transects. The transects are oriented East-West at 17°20'S, 17°48'S, 18°12'S and 18°44'S and are 290 km, 100 km, 200 km and 125 km long, respectively. Large (km-scale) features, related to volcanism or faulting, are visible in the seismic profiles, while smaller (m-scale) features such as sedimentary structures and minor faults are visible in the parasound data. Attributes such as sub-basin width, sediment thickness, sediment facies and the number of sedimentary units were compiled in a sub-basin database, with >45 sub-basins identified in the four transects. The longest transect (at 17°20'S), which extends from the center of the back-arc basin to the Tonga forearc, comprises 24 sub-basins that are an average of 6 km wide, with an average sediment thickness of 50 m. This analysis enables the construction of an extensional model, outlining the sequence and timing of sub-basin development. The sub-basins were first organized into five groups, based on the character of the underlying crust and the sedimentary facies, and each group was subsequently correlated to a distinct phase of basin opening. The results of this study suggest that the locus of extension in the Lau Basin jumped to different areas over time (a diachronous model), rather than extending uniformly from the center of the basin (a linear model). Additionally, there are anomalous acoustic signatures that may indicate hydrothermal fluids are actively exploiting faults as fluid pathways in some of the sub-basins. This detailed, high-resolution investigation of modern back-arc basin sedimentation can be used as an analogue for ancient back-arc systems, which are difficult to study at the same scale as they are often poorly preserved and fragmented in the rock record.

Optimal Solar Panel Positioning for Mars Surface Missions

Justin Kerr[1], Christina Smith[2], John Moores[1]

[1]York University jkerr@yorku.ca, [2]Oberlin College

Solar panels are commonly used on Mars surface missions for power generation, but solar energy generation potential is typically not considered until after a landing site has been selected. While solar energy potential for a flat panel that is parallel to the surface has been previously calculated for the entire globe, other orientations have not been considered. Solar energy generation potential for a panel at any orientation can be calculated with a computational model of radiative transfer in the atmosphere including scattered light. By modelling available energy for a variety of panel orientations, we compare the effectiveness of static panels to that of sun-tracking and previously modelled horizontal panels across all Martian latitudes throughout the year. The loss in power generation of a static panel can then be weighed against the increased engineering and mass budget costs associated with a tracking panel during mission planning. We also provide estimates of available energy across the entire surface of Mars for both types of solar panel. While this data does not consider terrain features, it will provide the ability for preliminary consideration of power availability alongside science value during site selection for future Mars missions. Our analysis utilizes data from a 1-dimensional radiative transfer model for solar radiation entering the Martian atmosphere. The model considers solar radiation levels for all combinations of Martian latitude and solar position. It builds upon a doubling and adding code previously developed for Titan's atmosphere by implementing wavelength ranges and absorption parameters to fit the Martian atmosphere. We use this model to obtain a full hemispherical angular grid of radiances containing values from scattered flux, surface reflection, and direct flux. Using this data, fluxes for each desired panel type and orientation are calculated for a wavelength range of 200-1800nm to fit the collection range of triple-junction solar panels. The model includes Rayleigh scattering for the major atmospheric gases, absorption by CO2 and O2, and Mie scattering from aerosols. Absorption for wavelengths outside of 400-1000nm for CO2 and 650-880nm for O2 were ignored due to negligible contributions. After computing fluxes for both static panels at a variety of angles, we adjust for solar panel energy collection efficiencies at each wavelength band to determine total available solar energy as a function of panel angle, solar longitude, and Martian latitude before comparing these results to that of a tracking panel under the same conditions. This data can be used for estimation of available solar energy during mission planning and will be particularly relevant for missions seeking to use solar panels at latitudes far from the equator where horizontal panels are much less effective.

Marine Vertebrate Diversity during Late Cretaceous Western Interior Seaway Cyclothems: Insights from the Manitoba Escarpment

Aaron Kilmury[1], Kirstin Brink[1]

[1]University of Manitoba kilmurya@myumanitoba.ca

Fossil remains collected from Late Cretaceous deposits of the Manitoba Escarpment provide excellent opportunities to study the marine life of the Late Cretaceous Western Interior Seaway (WIS) because they represent communities from one of the northernmost localities over a broad temporal range (Cenomanian-Maastrichtian). Faunal occurrences of vertebrates including diving birds, bony and cartilaginous fish, and marine reptiles were examined by constructing a biostratigraphic chart using data collected from museum collection surveys and the literature. Taxonomic data were analyzed at the genus level and stratigraphic data was mostly limited to lithostratigraphic member (with the exceptions of fossiliferous stratigraphic marker beds), thus most faunal assemblages are time-averaged per member and accompanied by age estimates for lower and upper contacts. Comparison of faunal occurrences with lithologic units indicates vertebrate diversity was highest during transgressive phases of major marine cyclothems, with peaks of diversity co-occurring with the transgressive phases of the Belle Fourche, Greenhorn, Carlile, and Claggett WIS marine cycles. Comparisons of apparent diversity between traditional taxonomic groups from the most sampled stratigraphic intervals also suggest significant changes in community structure between higher-level taxa occupying similar ecomorphotypic spaces over time, with bony and cartilaginous fish being the most abundant and diverse groups in Cenomanian and Turonian assemblages, and marine reptiles and bony fish the most abundant and diverse in the Early Campanian, time-averaged assemblage. This study shows that the vertebrate faunal assemblages of the Manitoba Escarpment provide valuable insight into broad temporal changes of diversity, community structure, and composition of WIS marine life from a biogeographically important, central location of North America.

Magmatic push or tectonic pull? The 4D-evolution of a dike-induced graben

Stephan Kolzenburg[1], Julia Kubanek[2], Mariel Dirscherl[3], Christopher Hamilton[4], Ernst Hauber[5], Stephen Scheidt[6], Ulrich Münzer[7]

[1]University at Buffalo stephank@buffalo.edu, [2]European Space Research and Technology Centre (ESTEC), [3]DLR Deutsches Fernerkundungsdatenzentrum,, [4]University of Arizona, [5]DLS Institut für Planetenforschung, [6]Howard University, [7]Ludwig-Maximilians-University

The 2014-2015 rift event associated with the Bárðarbunga eruption at Holuhraun, Iceland, offers a unique opportunity to study the spatial and temporal evolution of a rift graben. The graben can be traced from the toe of Dyngjujökull outlet glacier to the Holuhraun eruption site (NNE) for a distance of ~5 km. Over the course of the eruption, this structure served as the plumbing system for a bulk erupted lava volume of 1.44 km3, covering 84 km2 between 29.8.2014 and 27.2.2015. Rift activity and subsurface magma transport started days before lava reached the surface. We present the first 4D-monitoring of a graben during active magma transport using a time series of digital elevation models (DEMs). These integrate TanDEM-X DEMs, airborne high-resolution UltraCam images and derived DEMs, oblique aerial views and unmanned aerial vehicle (UAV)-derived structure-from-motion DEMs. They cover a period from shortly before the eruption throughout the six months of magma transport and up to 4.5 years after the eruption. This multidisciplinary and multi-scale dataset enables investigations of how magma supply and eruption dynamics affect the tectonic structure through which the eruption was fed and allows to include observations on locations that were subsequently covered by lava. We perform detailed spatial and temporal monitoring of the graben structure and construct topographic cross sections. We find that after its rapid formation (timescale of days), the graben is remarkably stable throughout the eruption and years beyond. It is unaffected by large changes in eruptive activity, effusion-, and seismicity-rates within the plumbing system. The data document that: (1) there was no direct feedback between eruptive dynamics and graben topography; and (2) on tectonic timescales, graben formation is near instantaneous. These results challenge the overarching role ascribed to magma transport in recent studies of tectonomagmatic relationships in rift events, favoring regional tectonics as the fundamental driving force.

2D forward modeling of multiduplex emplacement in the Cate Creek window, southern Canadian Rocky Mountains: interaction of erosion and tectonic underplating in thrust wedges with décollements

Elena Konstantinovskaya[1], Peter Fermor[2], Jacques Malavieille[3]

[1]University of Alberta konstant@ualberta.ca, [2]retired, [3]CNRS-University of Montpellier

Interaction between tectonic underplating and surface erosion in thrust wedges with multiple décollements may result in strain partitioning with the development of multiduplex antiformal stacking, strong uplift, and synchronous normal faulting within discrete areas. These processes are studied through 2D numerical simulations and compared to the results of analog sandbox modeling. Fault propagation and structural evolution of multiduplex structure at the base of the Lewis Thrust is studied through the real-size flexural-slip restoration and forward modeling along a 115-km long 2D cross-section in the area of the Cate Creek window, southern Canadian Rocky Mountains. The thrust wedge is underlain by the Precambrian basement dipping at ~1° to the SW. The 4-5 km-thick tectonic slices of Precambrian rocks in the SW are emplaced along the Lewis Thrust to the NE over Cretaceous clastic deposits that are exposed in the Cate Creek tectonic window (Fig. 1). The multiduplex structure is composed of imbricate NE-vergent sigmoidal thrust slices of 200-400 m to 1200-1400 m thick that form a series of antiformal stacks below the roof décollement along the Jurassic Fernie shale (Fig. 1). The duplexes are composed of Upper Devonian - Mississippian carbonate rocks. The basal detachment is located in Cambrian carbonate-shale succession in the SW and it ramps up forward to the upper Devonian-lower Mississippian strata. There are several culminations in antiformal stacks distributed over 67-km segment. The highest cumulative thickness of stacked horses of 5.7 km below the Cate Creek window gradually decreases forward to 1.4 km. The low-angle Flathead normal fault and minor normal faults record the extension at the rear side of the most prominent antiformal stack. The Eocene - Oligocene clastic deposits of the Flathead Valley Graben have preserved thickness of 700-900 m. 2D numerical simulations included steps of restoration and forward modeling to reproduce and validate the horizon geometry in the original interpretation (Fig. 1). The restored length of the cross section is ~261 km. Multiduplex stacks form above the

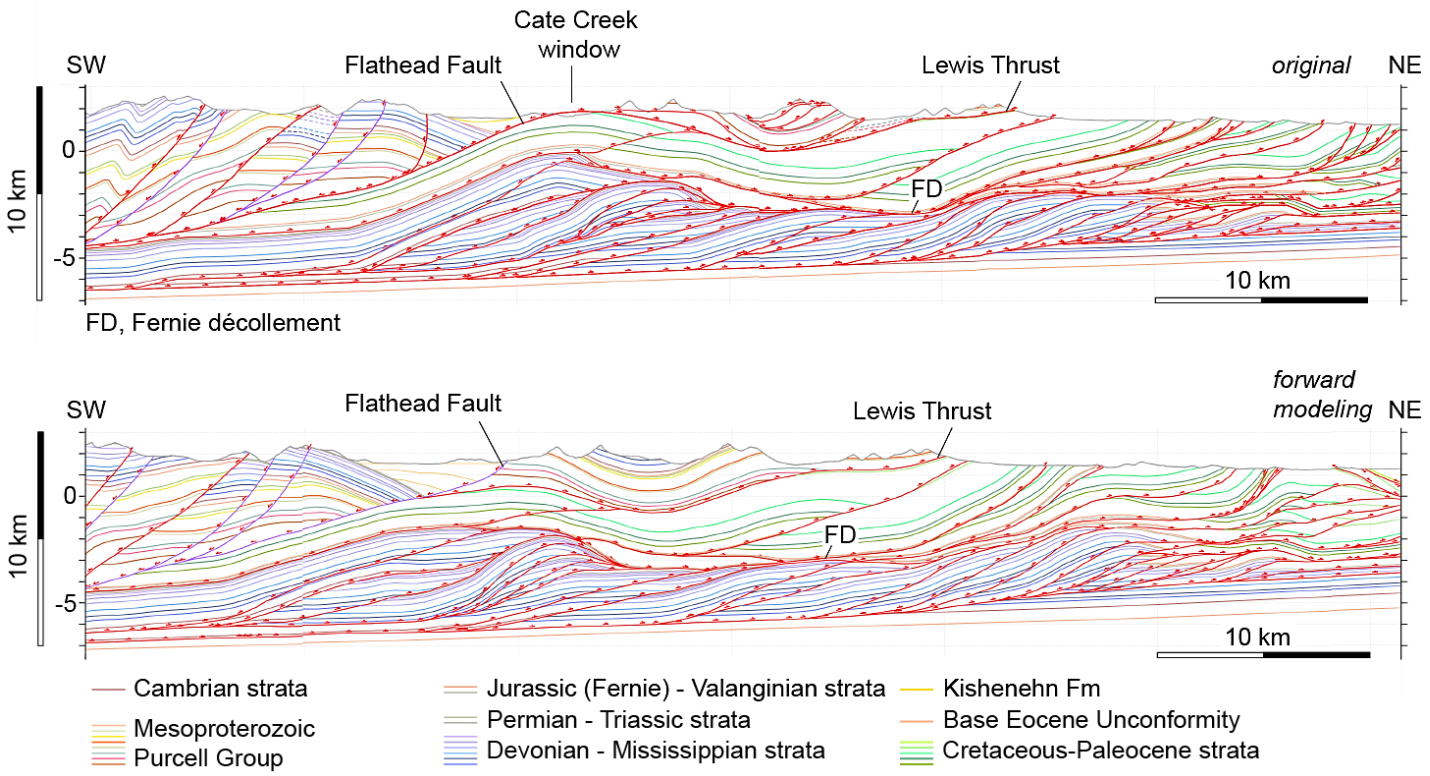

Fig. 1. The central part of the original and modeled cross-sections, southern Canadian Rocky Mountains.

ramps in the basal detachment and below the Fernie décollement. Thicker (1200-1400 m) tectonic slices are transported over a shorter distance (300-900 m) than thinner (200-400 m) slices (1600-5000 m). Erosion stimulated vertical duplex stacking and uplift. Normal faults develop during the convergence on the rear side of the most prominent antiformal stack as a result of vertical strain partitioning and upward material transfer across the wedge. The overall geometry of the multiduplex structures numerically simulated in this study is similar to the structure of antiformal stacks obtained by analog sand-box modeling for thrust wedges with one or two decollement levels. This work was funded by NSERC through grants RGPIN 2019 04397 and DGECR 2019 00186. Authors thank Petroleum Experts for donation of MOVE license to the University of Alberta.

Carbonated cratonic mantle without carbonate

Maya Kopylova[1]

[1]University of British Columbia mkopylov@eos.ubc.ca

Petrologists all agree that the "carbonated mantle", i. e. peridotite with accessory carbonate, is necessary to generate CO2-bearing melts. Carbonated peridotite is also a useful theoretical concept for geochemists seeking to explain trace element enrichment of the lithospheric mantle. Melting of peridotite with addition of carbonate has been the subject of hundreds of experimental studies. Yet mantle samples from below cratons do not contain carbonate. Our work tries to reconcile the theoretical view of the carbonated mantle with the empirical observations on cratonic mantle xenoliths. Peridotite xenoliths from the Chidliak kimberlite province (SE Baffin Island, Canada) suggest that the natural carbonated mantle are peridotites with elevated modes of clinopyroxene, garnet and olivine, and with thin rims of calcic silicate minerals. Observations on Chidliak peridotites provide an excellent "reality check" for theoretical mobility models of the carbonate-rich melts in the mantle. The "carbonation freezing front" is often theoretically imagined as the solidus of mantle peridotites infiltrated by CO2-rich melts. Our observations suggest that melting is not necessary for immobilization of carbonatitic metasomatic agent. The latter is highly reactive, readily giving away Ca to silicate minerals and exsolving CO2. At Chidliak, clinopyroxene and monticellite rims produced by carbonation do not show signs of partial melting during their formation; moreover, thicker mantles of clinopyroxene in Chidliak peridotites are equilibrated at P-Ts below the CO2- saturated peridotite solidus. Petrography of Chidliak peridotites also constrains the melt flux in the carbonation freezing model. At melt fluxes >10%, the model predicts elevated fractions of the reacted melt in comparison with the reacting melt. This should lead to loss of Ca. Natural samples, on the contrary, demonstrate addition of Ca; this is observed from quantification of compositional fluxes at Chidliak and in temporal trends of mineral and bulk compositions of the cratonic mantle. This suggests that the carbonatitic fluxes are always below 10%, and the carbonate-rich melt always "freezes in" in peridotites. We further submit that CO2-rich magmas on cratons are byproducts of carbonate metasomatism, since deep decarbonation is a necessary prerequisite to generation of CO2-rich melts. Theoretically, carbonate-rich fluids should be able to traverse the peridotitic mantle in the reacted channels where the fluids overcome the limits of the mineralogical, thermal and redox instability in deep peridotites. This study suggests the channels can be made of garnet or clinopyroxene, as only these initial products of reactive decarbonation of the deep peridotitic mantle are observed to contain fluid microinclusions and modal macro- grains of carbonates. Future research will better recognize stealth signs of carbonatitic metasomatism under cratons and enable us to better document its extent and localization.

Were Microaerophilic Iron-Oxidizing Bacteria responsible for the deposition of ca. 1.88 Ga Granular Iron Formations?

Alex Kovalick[1], Andrey Bekker[1], Andrew Heard[2], Aleisha Johnson[2], Nicolas Dauphas[2], Clara Chan[1], Luke Ootes[3]

[1]University of California, Riverside fkova001@ucr.edu, [2]The University of Chicago, [3]British Columbia Geological Survey

Granular Iron Formations (GIFs) are iron-rich sedimentary rocks, predominantly Proterozoic in age and deposited in shallow-marine, oxygenated nearshore environments where anoxic, ferruginous deep-waters upwelled. At ca. 1.88 Ga, GIFs were deposited on several active continental margins of paleogeographically distinct cratons. The synchronous deposition of these sediments suggests a global driving mechanism. Previous arguments have related these GIFs to either increased iron flux from large igneous provinces (LIPs) or change in seawater composition and redox. Iron-oxyhydroxide precipitation at the redoxcline in these basins is thought to be due to either oxygen production via photosynthesis or iron oxidation by microaerophilic iron-oxidizing bacteria (IOB). Microfossils identified in the ca. 1.88 Ga Gunflint GIF of the Superior craton have been linked to these biological processes. In the ca. 1.88 Ga Gibraltar GIFs from the Slave craton, we found microfossils in stromatolites exhibiting twisted-stalk morphology like that observed in modern IOB. Iron isotope composition of these GIFs supports oxidation at the redoxcline, and weak positive Eu anomalies might indicate high submarine hydrothermal activity associated with contemporaneous LIPs. REE data exhibit a significant MREE-arch indicating an influence of riverine waters capable of overprinting typical hydrothermal REE signatures. Therefore, rather than invoking a non-hydrothermal iron source, we relate this signature to deposition distally to, but in connection with, the global ocean in an estuary-like setting. The Gibraltar and other contemporaneous GIFs indicate that global redox conditions and deep-ocean iron supply to shallow-marine settings at ca. 1.88 Ga generated an ideal habitat for IOB to thrive in and play an essential role in deposition of GIFs.

Magmatic hydrothermal mineral systems of Alaska: An evolving understanding of porphyry system formation from the Paleozoic to present

Douglas Kreiner[1]

[1]U.S. Geological Survey dkreiner@usgs.gov

A mineral system is a conceptual framework relating deposits to the geologic environments in which they form. They consist of five critical components: 1) an energy drive (topography, geothermal gradient, magma), 2) a source of components (metals, ions), 3) transport media (melts, aqueous fluids, ligands), 4) transport pathways (permeability), and 5) traps (physical, chemical). These five components occur across multiple scales, from the tectonic setting (1,000's of linear kms), geologic environment (100's-1,000's of linear kms), mineral system (10-100's linear kms) to the deposit (1-100's linear kms) scale. They form over 10,000 to a few million years. One significant mineral system, magmatic hydrothermal, form along convergent plate margins. The process of melt generation and subsequent evolution as magma ascends and is emplaced provides the energy driver, a source of fluids and components, permeability, and the inherent traps necessary for a mineral deposit. Porphyry deposits are one manifestation of magmatic hydrothermal mineral systems and span in age from the Silurian to Pleistocene in Alaska. Older porphyry deposits formed in pre-accretionary arcs whereas most Mesozoic and younger porphyry systems formed during or after accretion of their host terranes. Magmatic compositions vary through time and space as a function of geologic setting (continental versus island). A case study in eastern interior Alaska illustrates the geologic and tectonic controls on porphyry-style magmatic hydrothermal mineralization. South of the Denali fault, the Chistochina district contains Pennsylvanian porphyry occurrences formed in the Skolai arc. These small Cu-Mo porphyry systems were formed prior to accretion of the Wrangellia-Alexander terranes. Early Cretaceous (~130 Ma) porphyry Cu-Au(-Mo) systems formed after accretion as a younger arc sequence that was superimposed on the Skolai arc. On the north side of the Denali fault in the Yukon-Tanana upland, mid-Cretaceous porphyry systems are Mo-W occurrences that likely formed during orogenic collapse following collisional orogenesis. Superimposed Late Cretaceous (~70 Ma) porphyry systems exhibit more classic calc-alkaline, near-arc, Cu-Mo-Au metallogenic signatures. Spatial zoning in metallogenic signatures correlates with pluton geochemistry and reflects variations in the underlying basement. Late Cretaceous systems hosted in Paleozoic continental margin strata exhibit more-reduced, As-Bi-Au signatures, whereas those hosted in the allochthonous arc terrane exhibit more-oxidized Cu-Mo, As-Au-poor signatures. Systematic characterization of large-scale geologic environments that host mineralization is vital for adequately determining key influences on metal enrichments and the observed and predicted diversity in magmatic hydrothermal mineral systems.

Global change in ocean redox structure at 1.84 Ga captured in ^{238}U from Rove Formation (Ontario, Canada) black shales

Alexandra Kunert[1], Simon Poulton[2], Brian Kendall[1]

[1]University of Waterloo akunert@uwaterloo.ca, [2]University of Leeds

The late Paleoproterozoic Rove Fm (1.84 Ga) captures a shift from mainly ferruginous to stratified oceans with euxinic mid-depths and ferruginous deep waters. Marine euxinia may have stunted eukaryotic evolution during the mid-Proterozoic, so quantifying its extent is essential. Molybdenum concentration and isotope data previously obtained for Rove Fm euxinic black shales suggest <10% of the seafloor was overlain by euxinic waters. Some marine carbonates provide estimates for mid-Proterozoic seawater uranium isotope values ($^{238}U_{SW}$) of -0.43 to -0.73‰, suggesting <7% mid-Proterozoic seafloor euxinia. Others suggest that U reduction into anoxic sediments in the Precambrian did not impart isotope fractionation since many carbonates have ^{238}U near average upper crust. This raises concern on using ^{238}U to estimate anoxic seafloor area as redox systematics form the basis of the U mass balance. Constraints on $^{238}U_{SW}$ for specific temporal intervals are needed to resolve redox variation and the utility of the ^{238}U proxy through these "boring billion".

We present new ^{238}U data for Rove Fm black shales in core 89-MC-1 to pinpoint $^{238}U_{SW}$ at 1.84 Ga. Iron speciation (highly reactive vs total Fe for oxic and anoxic conditions, FeHR/FeT; pyrite Fe vs FeHR for ferruginous and euxinic conditions) and Mo-U enrichments constrain local bottom water redox. Our samples show a positive ^{238}U-FeHR/FeT trend: older ferruginous shales have lighter ^{238}U (-0.48 to 0.11‰) and younger euxinic shales have heavier ^{238}U (-0.04 to 0.27‰). This is expected given larger fractionations between SW and modern euxinic sediments compared to ferruginous sediments. An intervening layer with coarse pyrite, indicating a transition from ferruginous to euxinic conditions or a fluctuating chemocline, has ^{238}U from -0.09 to 0.38‰. Heavy ^{238}U in the euxinic and pyrite-bearing intervals are 0.4 to 0.6‰ above average upper crust and modern rivers, contrary to the hypothesis of limited U isotope fractionation in Precambrian oceans. Known isotopic fractionation factors between SW and each setting (SW-sed) are used to determine plausible $^{238}U_{SW}$. Most ferruginous samples have ^{238}U of -0.2 to 0.1‰. Modern and ancient ferruginous SW-sed varies widely (0.0±0.4‰). We suggest $^{238}U_{SW}$ was near the modern crustal/riverine flux (-0.3‰) during deposition of the ferruginous interval. Euxinic sediments in modern unrestricted basins incur SW-sed ~0.6 to 0.8‰, so the $^{238}U_{SW}$ at 1.84 Ga may range from -0.8 to -0.4‰. Our data suggests a transition from ferruginous global oceans with minimal $^{238}U_{SW}$ fractionation from river flux to an ocean with expanded euxinic areas, shifting $^{238}U_{SW}$ to lighter values.

Geological Mapping of Interior Layered Deposits Within Ophir, East Candor, and West Candor Chasmata, Valles Marineris, Mars

Josh Labrie[1], Frank Fueten[1], Amanda Burden[1], Ariel van Patter[1], Jessica Flahaut[2], Robert Stesky[3], Ernst Hauber[4]

[1]Brock University jlabrie@brocku.ca, [2]CNRS-UL, [3]Pangaea Scientific, [4]German Aerospace Center (DLR)

Valles Marineris is a roughly 4000 km long network of interconnected chasmata in Mars' Tharsis region. Reaching depths of up to 11 km, these chasmata provide unique insight into Mars' crustal geology and geological history. Large, enigmatic deposits of layered material known as interior layered deposits (ILDs) can be found within many chasmata and present an opportunity to investigate some of the surficial processes that have shaped Martian geomorphology. The goal of this study is to produce geological maps of the interiors of three chasmata in central Valles Marineris: Ophir Chasma, and East and West Candor Chasmata. ILDs were categorized into distinct units based on their appearance in CTX satellite imagery, which is the only available imagery to cover each chasma in its entirety. Following the mapping of each chasm, DEMs were used to collect elevation data for the contacts between different unit types to gain a better understanding the spatial relationships between units. The results of this study show that the ILDs in these three regions share a very similar stratigraphic sequence and hence a shared geological history. The base of the stratigraphy is a massive unit which appears to be devoid of any layering in CTX imagery. The massive unit is overlain by two different layered units, the first featuring thicker layering and benches, and the second featuring thinner layering. Layered units that have been deformed by late faulting and folding appear to be near the top of the stratigraphy as do thin mesas, a late featureless cover. Work to confirm this stratigraphy is currently ongoing, and involves further mapping and mineralogical analysis.

A new predictive remote mapping method applied to volcanic terrain of the High Arctic Large Igneous Province, Nunavut, Canada

Stephanie Lachance[1], Myriam Lemelin[1], Marie-Claude Williamson[2]

[1]Université de Sherbrooke stephanie.lachance6@usherbrooke.ca, [2]Natural Resources Canada

Thematic geological maps are produced using geospatial data in a process referred to as remote predictive mapping (RPM). RPM is a tool that either helps geologists to identify regions of interest for their field campaigns or serves to fill knowledge gaps in frontier regions. Remote predictive maps are usually derived from supervised classifications performed on multispectral satellite images acquired in the visible, near infrared and shortwave infrared. However, a better spectral resolution is often sought to highlight the absorption and emission peaks that are characteristic of different minerals and rock types. Moreover, the use of a supervised classification requires a priori knowledge thus contradicting the underlying objective of predictive mapping. The objectives of the research project are to (1) generate a remote predictive geological map using emerging satellite imagery and classification methods (i.e., PRISMA hyperspectral satellite images and the self-organizing maps method), and (2) compare our results with those obtained using traditional approaches (e.g., multispectral imagery and Random Forest). The study area is located at the head of Expedition Fiord, on central Axel Heiberg Island, in Nunavut. This part of the Sverdrup Basin is characterized by the emplacement of the High Arctic Large Igneous Province (HALIP) in the Late Cretaceous. We carry out a preliminary validation of the classifications using the available 1:100 000 scale map of the bedrock with the objective of ground truthing the results during field work planned for July 2022. Firstly, field and laboratory measurements using hyperspectral and X-ray spectrometers will be used to validate the RPM tool for mapping in volcanic terrain. Secondly, digital field mapping at a 1:10 000 scale will provide a better resolution of geological units in the vicinity of the McGill Arctic Research Station. In this presentation, we introduce the methods, geological context and preliminary results associated with the two classification methods.

High-resolution photography as a tool to detect climate trends and cycles archived in a 500-year annually deposited varve record from Crawford Lake, Ontario, Canada

Krysten Lafond[1], R. Timothy Patterson[1], Francine McCarthy[2], Carling Walsh[1], Nawaf Nasser[1]

[1]Carleton University krystenserack@cmail.carleton.ca, [2]Brock University

In May 2019, the Anthropocene Working Group of the Sub commission on Quaternary Stratigraphy voted in favour of defining a new series/epoch whose base would terminate the Holocene Series/ Epoch. The beginning of the epoch, defined as the interval in geologic deposition where changes to Earth's systems driven by human impacts have left a permanent geological record, would be in the mid-20th century. Work is underway to identify a GSSP from amongst eleven potential candidate localities from around the world and spanning a variety of geologic settings, one of which is a meromictic lake within the protected Crawford Lake Conservation Area, Milton, Ontario, Canada. The undisturbed accumulation below the chemocline of this deep karstic basin of exceptionally preserved dark-coloured organic matter capped by light-coloured calcite crystals precipitated each summer records both natural and anthropogenic change at sub-annual resolution over the past several centuries. This is of interest in the search for a geologic record of the 'Great Acceleration' of population growth, industrialization and globalization that followed the Second World War. A novel high-resolution imaging protocol was used to photograph freeze core CRW19-2FT-B2, collected in February 2019, from the deepest part (23 m) of the lake. Individual images were stitched into one cohesive image using Adobe Photoshop that was subsequently used to: 1) characterize varve couplets deposited between AD 1496 and 2000, identifying the coherent pattern of varves that allow correlation across the deep basin ; 2) measure the thickness of individual varves using pixel counting, which were found to vary between 0.111 and 9.667 pixels, with a mean annual thickness 2.135 pixels; and 3) carry out wavelet and spectral time series analysis using varve thickness data to identify cyclic depositional patterns and relate them to changes in climate and lake productivity that would affect the thickness of the light- and dark-coloured laminae. Wavelet and spectral time series analysis resulted in identification of cycles with statistically significant periodicities that correlate with the Quasi-biennial Oscillation (2.3years), El Nino Southern Oscillation (2-7 years), the 11-year Schwabe sunspot cycle and Pacific Decadal Oscillation (50-70 years). This research provides baseline data on the nature of annual deposition in the lake, as well as time series analysis results that provide an improved discrimination of the natural drivers in the preserved Anthropocene depositional record.

Impact of the mineralogical variability on the lithium content of the Whabouchi pegmatite

Claude Lamy Morissette[1], Jean-François Blais[1], Emmanuelle Cecchi[2]

[1]Institut national de la recherche scientifique claude.lamy_morissette@ete.inrs.ca, [2]Université du Québec en Abitibi-Témiscamingue

Lithium continues to be a highly demanded commodity and is considered a critical element in most developed countries due to its use in batteries for electric vehicle. In Canada, lithium resources are primarily found in pegmatites in the mineral spodumene, and at least six lithium-rich pegmatite deposits are currently known in Québec. Among these, the Whabouchi Pegmatite is a spodumene deposit located in the James Bay area of northern Québec and within the Superior Province. While the overall mineralogy of the deposit is known, the mineralogical variability is poorly understood, and its impact on the eventual production of lithium is unknown. In this research we will present the relationships between the main mineralogical and the geochemical components of the Whabouchi pegmatite. Based on these relationships, a predictive model is being developed that will potentially allow for an estimation of the lithium content of the pegmatite samples. Those results were obtained by randomly selecting 25 suites of samples throughout the deposit, each suite corresponding to a different zone and depth. Whole rock chemistry using ICP-OES and quantitative X-ray diffraction were performed on selected samples. Microprobe analyses were also conducted on selected thin sections. The results from the analysed samples show an average Li2O concentration of 1.53 % with a standard deviation of 0.81 %, confirming the representativity of the subset relative to the overall deposit (average Li2O of 1.49 %, standard deviation of 0.78 %). Normative mineralogy was calculated based on the principles of the CIPW norm and compared to the X-Ray diffraction data to ensure the accuracy of the results. We will show that the mineralogy is generally homogeneous, being composed of quartz, albite, spodumene, K-feldspar and muscovite, with minor amounts of garnet, apatite and petalite, and trace amounts of beryl and tourmaline. This mineralogy is characteristic of the Albite-Spodumene type of rare-element pegmatite of the Lithium Cesium Tantalum (LCT) family. The variability lies in the proportions of each mineral. Based on this variability and the predictive model, it becomes possible to rapidly evaluate the lithium concentration of the rock in the field.

Integrating non-destructive electron and X-ray microscopy to characterize corrosion of ~ 1 billion year old copper from different settings in the Lake Superior region

Emilie Landry[1], Desmond Moser[1], Ivan Barker[1], James Noël[1]

[1]University of Western Ontario elandry5@uwo.ca

A method for isolating used nuclear fuel rods proposed by Canada's Nuclear Waste Management Organization is to place them ~500 metres underground in a deep geological repository (DGR) in copper-coated steel used-fuel containers (UFCs) encased by bentonite to create a physical barrier to mass transport for more than one million years. To date, models informed by the results of laboratory scale experiments indicate that the UFCs will remain intact long enough that the bulk of the radioactive fission products, such as 137Cs, will have decayed. As laboratory corrosion experiments on copper at geologic time scales are not feasible, we are looking to ancient natural copper from the Lake Superior region which has survived for almost one billion years under conditions that have similarities to those predicted in a DGR. Where copper is most abundant in the Keweenaw Peninsula of Michigan, USA, it occurs as veins and pore-fillings within volcanic and sedimentary lithologies. The copper from this region is of great cultural and spiritual value to North American Indigenous peoples (e.g. Redix, 2017). The purpose of this research is to characterize the texture, mineralogical associations, and strain history of the copper and its corroded contacts in different lithologic settings while searching for U-bearing accessory phases that will be used to provide accurate and precise dates for the corrosion mineral assemblage(s), and to do this with minimal damage/effects to the materials. The initial focus will be on a representative suite of cm-scale specimens from a mineral collection at Western University. The methodology will include a mix of optical, electron (e.g. EDS, EBSD) and X-ray microscopy. The field emission scanning electron microscope (FE-SEM) is a Hitachi SU6600 variable pressure Field Emission Gun instrument at the ZAPLab, and MicroCT analyses will be performed with a Zeiss Xradia 410 Versa at Surface Science Western. By utilizing the FE-SEM, major and minor element chemistry will be determined and mapped, along with the determination of the texture and strain of the copper and associated minerals. This data will be spatially correlated with non-destructive X-ray micro-computed tomography (microCT) analyses to characterize the copper corrosion interfaces within the 3D volume. In addition to using it for proxy mineral identification, microCT will also be used to measure porosity characteristics. This characterized suite of specimens will set the stage for micro- and nano-analysis techniques and electrochemical (corrosion) analysis for comparison with engineered copper coatings for UFCs. In this way we hope to learn from geological corrosion behaviour to inform and improve DGR multi-barrier design.

Redix, E. M., 2017. "Our Hope and Our Protection": Misko-biiwaabik (Copper) and Tribal Sovereignty in Michigan. American Indian Quarterly, Vol. 41, No. 3, pp 224-249"

Don't put your phones away: Development of an interactive geoscience teaching application using a commercial game engine

Kyle Laporte[1], Rob Harrap[1], Nicholas Graham[1]

[1]Queen's University kyle.laporte@queensu.ca

Interactive simulation tools developed using a game engine offer a way to teach geological processes that are currently poorly addressed by educational tools. Game engines are built to support dynamic processes, visualize real world settings with high fidelity, and provide intuitive interfaces for new users to interact with the simulated environment, all of which support geological processes at different scales. In contrast, many of the visualization techniques currently employed in geoscience education are static, 2D, and not interactive; examples include standard geological or topographic maps, precomputed grid-based flow simulations, and cartographic animations. These techniques do not encourage students to ask and answer their own questions, allowing them to build intuition by exploring processes and relationships between various simulation parameters. Game engine-based teaching tools address this problem, albeit at the cost of requiring the introduction of computers and software into the teaching environment. Using desktop or mobile computers, tools can be constructed that take advantage of the dynamic, 3D, interactive nature of modern games to show processes and promote student engagement and exploration. These tools involve taking a geological system of interest and allowing students to repeatedly interact with and manipulate it in a game environment, exploring the impact of different parameters as they interact. This study focuses on simulating erosion processes on landscapes using a tablet and touch-based interaction. Our goal is that by allowing students to change the terrain, save the current topography, erode the terrain, and visualize the resulting changes, students are able to develop an intuitive sense of how surface processes work. Interacting with the model with the current interface involves using buttons and sliders to change view or editing states, as well as intuitive orbital camera controls. Our key research question is whether this interface indeed leads to exploration of geological processes when deployed with undergraduate geography and geology students. Evaluating the effectiveness of such a tool requires qualitative analysis methods widely used in human-computer interaction studies. Working with a small cohort of volunteers as test subjects, we examine the effectiveness of an erosion tool on tablets. These trials result in a series of recordings and transcripts of user experience that capture both the interaction aspects of student use and their thoughts on the effectiveness of the method at teaching its concepts overall. The results of analyzing these study outcomes will allow refinement of the tool and recommendations for the design of future interactive geological simulation tools.

Neoarchean-Paleoproterozoic geology of the Dundas Harbour area, Devon Island, Nunavut: Implications on the Neoarchean-Paleoproterozoic framework of the Canadian Arctic and Northern Greenland

Joshua Laughton[1], Gordon Osinski[1], Chris Yakymchuk[2]

[1]University of Western Ontario jlaught2@uwo.ca, [2]University of Waterloo

The Canadian Shield extends from Southern Ontario all the way north into the Canadian Arctic Archipelago and then into Northern Greenland. The northernmost exposures of the Canadian Shield outcrop on Devon and Ellesmere islands, positioned near the northwestern margin of the Rae Province and associated Neoarchean-Paleoproterozoic terranes. Previous work in the Devon-Ellesmere region has been primarily limited to reconnaissance studies during the 1960-1980s. Here, we present the results of the first detailed investigation of the Precambrian geology on Devon Island in over thirty years, based on field mapping of the Dundas Harbour area on southern Devon Island to establish the geodynamic setting of the Devon-Ellesmere region within the Neoarchean-Paleoproterozoic tectonic framework of the Arctic. We carried out EPMA monazite petrochronology, LA-ICP-MS zircon geochronology, thermobarometry, and phase equilibrium modelling. Our observations reveal that the Dundas Harbour area is a late Neoarchean (ca. 2.56-2.50 Ga), polymetamorphic terrane of lower to middle crustal, granulite facies rocks with pervasive ductile fabrics (augen porphyroclasts, quartz ribbons, extreme flattening). Protoliths of clinopyroxene-garnet quartzofeldspathic gneiss, orthopyroxene quartzofeldspathic gneiss, two-pyroxene metabasite and biotite granite gneiss were emplaced between ca. 2.56-2.50 Ga, and the sedimentary protolith for rutile-garnet metasedimentary rocks was deposited between ca. 2.54-2.47 Ga. Possible metamorphic events are recorded at ca. 2.47, 2.30, 2.15 and/or 1.91 Ga. The most recent metamorphic event obtained peak P-T conditions of 8-10 kbar and 875-950 ºC during at ca. 1.91 Ga. This late Neoarchean Devon Island terrane may be linked with other late Neoarchean terranes in the Arctic such as on Boothia Peninsula, Somerset Island, and/or the Prudhoe Land area of Northern Greenland.

Assessment of socio-cultural cumulative effects: development of a co-constructive methodology with First Nations in Quebec

Roxane Lavoie[1], Isabelle Rancourt[1], Vanessa Dube-Moar[1]

[1]Université Laval roxane.lavoie@esad.ulaval.ca

Research on cumulative effects assessment has in the past decades focussed mainly on the development of analysis methods for biophysical components. Only recently have we started to really grasp the tremendous significance of the effects of industrial activity on nearby communities. Indeed, empirical data shows that this development can have effects on social and cultural components such as land usage, connection to the land, language, knowledge transmission or the practice of traditional activities. Few methods currently allow for an effective and holistic assessment of cumulative effects of industrial activities on human communities. As part of the Oceans Protection Plan, Transport Canada has launched a cumulative effects assessment initiative in six areas on the three coasts of the country. In the Province of Quebec, the initiative aims at assessing cumulative effect of the intensification of marine vessel activity on the St. Lawrence and Saguenay Rivers. Participating First Nations have stressed the importance of evaluating socio-cultural cumulative effects on indigenous communities. They are worried, more specifically, about the permanence of traditional, spiritual, and cultural activities, about safe access to resources as well as about land usage by First Nations. This project consists of a collaborative enterprise between Transport Canada, Laval University and five First Nations to develop a methodology for the assessment of socio-cultural cumulative effects of marine vessel activities in the St. Lawrence and Saguenay Rivers on coastal indigenous communities. During participative workshops, valued environmental components have been identified, and a methodology for socio-cultural cumulative effects assessment has been co-constructed. It includes the selection of specific data collection and analysis methodologies, as well as reflections on the sharing of indigenous knowledge and communication of cumulative effects to a broad and diversified audience. Through the workshops, a dynamic socio-cultural cumulative effects assessment framework has been developed. It focusses on supporting First Nation communities in the various steps of the complex evaluation of cumulative effects and aims at building research capacity and autonomy in those communities. This presentation will emphasise the specificities of socio-cultural cumulative effects assessments, and the preliminary methodology for assessing socio-cultural cumulative effects.

Integration of Electromagnetics in Potash Mining Geohazard Analysis

Todd LeBlanc[1]

[1]University of Saskatchewan todd.leblanc@usask.ca

Potash mining in Saskatchewan has made extensive use of geophysics for a variety of engineering and environmental purposes since the first mines were built. One of the applications for geophysics in potash mining is the location and quantification of near mine geohazards associated with possible inflow sources. The source of these water inflows are anomalously porous sedimentary formations located either above the potash evaporate layer or within the salt itself (Gendzwill and Stead, 1992). The use of surface 3D seismic has proven to be a highly effective tool in identifying many geohazards; however, to better quantify these features other geophysical tools have been brought into use. These tools have ranged from DC resistivity (Eso, 2006) to frequency- and time-domain electromagnetics (Duckworth, 1992). This project focuses on the application of multiple types of transient (TEM) and frequency-domain (FDEM) electromagnetics systems over several different mine locations to delineate areas with suspicious geophysical signatures; this effort will be pursued through both analysis of survey data and computer modelling. Different locations for these targeted surveys will include both north and south Saskatchewan mines. Each of these large areas have distinctly different near-mine geological features. These surveys have been sponsored by Nutrien Ltd. through a Ph.D. Mitacs Accelerate project with the author. They will consist largely of in-mine surveys. These types of electromagnetic surveys suffer from certain restrictions related to low magnetic moment and high infrastructure noise, though through a combination of joint geophysical investigation and computer modeling such limitations are greatly alleviated. Some in-mine TEM and FDEM survey data has already been collected in areas of concern. For details of this work, see Funk, Isbister, LeBlanc, and Brehm (2019), and LeBlanc (2020). Computer modelling for this project requires a full-space environment to account for the diffusion of current in both directions above and below the transmitter. Forward modelling for this project has been performed in COMSOL Multiphysics.

References: Eso, R. A., & D. W. Oldenburg (2006). Application of 3D electrical resistivity imaging in an underground potash mine. SEG Technical Program Expanded Abstracts 2006. Funk, C., J. Isbister, T. LeBlanc, R. Brehm, (2019). Mapping How Geophysics is Used to Understand Geohazards in Potash Mines. CSEG recorder, 44(6). Duckworth, K. (1992). Detection Of Brine Layers Overlaying Potash Mine Operations. Canadian Journal of Exploration Geophysics, 28(2), 109-116. Gendzwill, D. and D. Stead (1992), Rock mass characterization around Saskatchewan potash mine openings using geophysical techniques: a review, Canadian Geotechnical Journal, 29 (4), 666-674.

Assessment of cumulative effects in Canada within environmental assessments: What can be done to improve the practice?

Philippe Leblanc-Rochette[1], Roxane Lavoie[1], Christine Rivard[2], Scott Heckbert[3]

[1]Université Laval philippe.leblanc-rochette.1@ulaval.ca, [2]Natural Resources Canada, [3]Alberta Energy Regulator

It is now well known that impacts of industrial activities are cumulative and that cumulative effects often result in greater impacts than those resulting from actions taken individually. Despite the importance of cumulative effects assessments for the environment and the population and even though they have been required since 1995 within the Canadian Environmental Assessment Act, several scientific studies over the years have highlighted shortcomings and significant knowledge gaps that are still present and that affect the assessment of cumulative effects, notably in Canada. Although a practitioner's methodological guide was developed in Canada in 1999, there are still many obstacles that currently make this very complex and ambitious assessment an almost unachievable task for practitioners, leading to a sense of dissatisfaction on the part of the government and the people living in the study area. The main objective of this research project is to identify the obstacles and difficulties currently encountered by the various actors, as well as their concerns, in the cumulative effects assessment process in Canada and to propose concrete and realistic recommendations in order to develop a strategy to improve this process. In order to achieve this objective, this project was divided into three parts: 1) a comprehensive literature review of what has been done to date on cumulative effects worldwide, 2) the conduct of five focus groups via videoconference with First Nations communities and Indigenous organizations across Canada, and 3) the conduct of 15 semi-structured interviews via videoconference with environmental assessment practitioners and federal government staff. The aim of the second and third parts of the project was to obtain the views, concerns and recommendations of people who must live with the consequences of cumulative effects on a day-to-day basis, mainly First Nations communities, and of practitioners or federal employees who work directly or indirectly in the cumulative effects assessment process. The presentation will discuss the context and the history of the research problem, the project rationale, the research methodology and the results that are currently being analyzed. The main themes discussed during the interviews with practitioners and governmental staff were: 1) the concept of cumulative effects, 2) the tools and documents available for cumulative effects assessment, 3) Canadian government requirements, 4) the barriers in practice and recommendations, 5) valued ecosystem components (VECs), 6) indicators for VECs, 7) spatial boundaries, and 8) temporal boundaries. During the focus groups with First Nations communities and Indigenous organizations, the three main themes discussed were: 1) cumulative effects on VECs across time and space in their territories, 2) First Nations participation in cumulative effects assessments, and 3) the conduct of cumulative effects assessments by consulting firms.

Investigating Water Ice Detections in Lunar Permanently Shaded Regions using the Kaguya Spectral Profiler Data

Myriam Lemelin[1], Alex Camon[1], Shuai Li[2]

[1]Université de Sherbrooke Myriam.Lemelin@USherbrooke.ca, [2]University of Hawaii at Manoa

The first direct evidence of exposed water ice in some permanently shaded regions (PSRs) of the Moon was derived using hyperspectral data from the Moon Mineralogy Mapper (M3). Li et al. (2018) investigated light reflected from PSRs indirectly illuminated by nearby terrain (e.g., crater walls). The spectral signature of pixels displaying the three overtone and combination mode vi-brations for H2O ice near 1.3, 1.5 and 2.0 µm were investigated further using the spectral angle (SA) mapping method. A SA '<'30° between an M3 spectrum and the spectrum of pure water ice was considered consistent with the presence of some water ice. This analysis revealed that water ice is present at the optical surface in many PSRs within 20° of both poles. However, some questions remain. For example, no surficial detection was found in some of the large current cold traps such as Amundsen, Hedervari, Idel'son L and Wiechert. Is it because there is no surficial water ice (assuming most water ice has been delivered prior to the true polar wander) or is it be-cause the M3 data did not detect it? The M3 data used in this analysis was acquired during a rela-tively short timeframe (optical period 2C: May to August 2009), and perhaps the illumination conditions were not ideal. While more clues will arise from upcoming orbital (e.g., Trailblazer) and landed (e.g., VIPER) missions, data acquired by another past mission can currently be used. We use data acquired by the Kaguya Spectral Profiler (SP) between November 2007 and June 2009 as an independent dataset to search for the presence of water ice in PSRs using the same method as Li et al. (2018). SP is a point spectrometer that acquired data using three detectors: VIS (0.5-1.0 µm), NIR1 (0.9-1.7 µm) and NIR2 (1.7-2.6 µm), at a spatial resolution of 500 m per pixel. Through its lifespan, the SP acquired over 7000 orbits of data which translates into millions of reflectance measurements in each polar region. We analyze the SP data acquired within 65-90°S/N to search for water ice. We use the location of PSRs to determine if points fall within PSRs or not. For points in PSRs, we extract their radi-ance and calculate their true reflectance (RT). For points outside PSRs, we simply calculate their reflectance. We then smooth all spectra, calculate their SA and correlation with respect to pure water ice, and calculate their 1.3 and 1.5 µm band depth. The SP data near 2.0 µm is currently too noisy to be used. We find that SP points outside PSRs have SA '>'30°, which suggest that SP points with SA '>'30° cannot host surface ice. We thus investigate the SP points in PSRs with SA '<'30. These points generally contain well-defined 1.3 and 1.5 µm absorption bands and will be investigated further. Potential new detections of surficial water ice are found in Amundsen, Hedervari, Idel'son L and Wiechert.

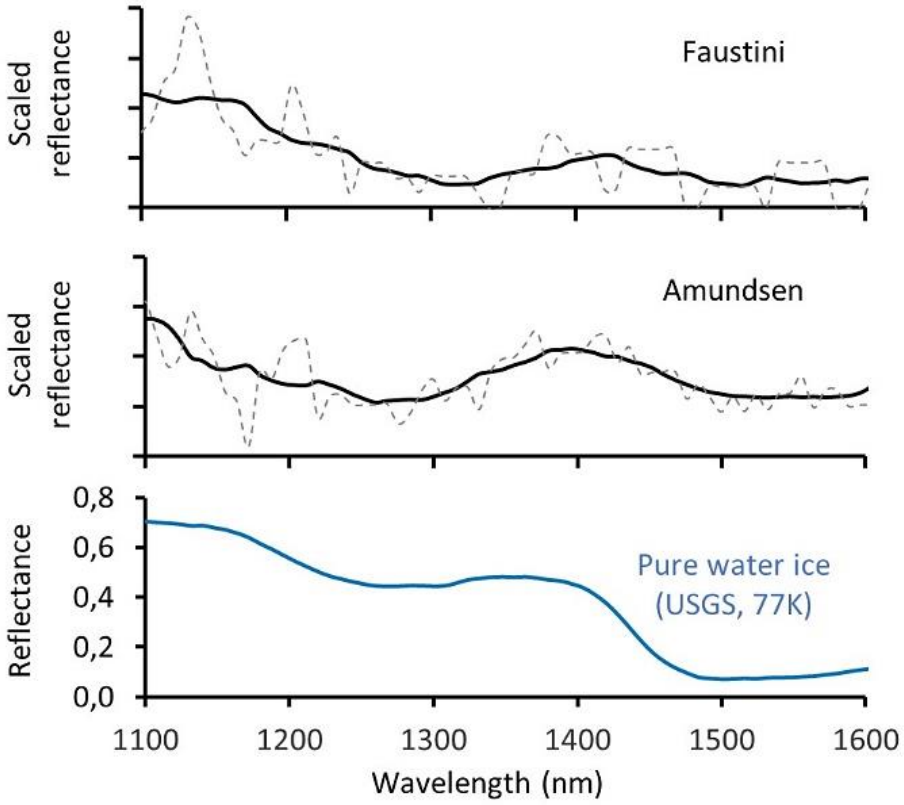

Electrical Resistivity of Liquid Fe10wt%Ni at High Pressures and Implications for the Energy Source for an Early Dynamo in Vesta

Eric Lenhart[1]

[1]University of Western Ontario elenhart@uwo.ca

The electrical resistivity of Fe?10wt%Ni was measured at pressures 2-5 GPa at temperatures into the liquid state and compared to results of previous studies of pure Fe and pure Ni. Thermal conductivity was calculated from electrical resistivity to determine adiabatic core heat flux. The results are applied to determine whether thermal convection could be responsible for the putative dynamo in early Vesta's core. An adiabatic core heat flux of ~300 MW at the top of Vesta's core is estimated from this study and compared to a range of estimates of heat flux through the CMB of 1.5-78 GW. We conclude that thermal convection would have played an important role as an energy source of dynamo action that generated a surface magnetic field for tens of millions of years in Vesta's early history.

Some ideas of online delivery of geological labs and geological mapping courses

Changcheng Li[1]

[1]University of Waterloo c293li@uwaterloo.ca

Hands-on learning is essential in some lab and some field mapping courses. These courses generally require intense interaction between instructors/TA's and students, and quite often students need some extra time to meet their instructors' expectation. It is quite challenge, especially during the pandemic, for instructors to deliver the courses in a way such that students can learn effectively. Here I present some ideas of geological lab and field mapping course delivery. In courses with the hands-on learning, interaction is the key and should be given priority in terms of limited class time. Pre-recorded videos and reading can be prepared for students to study in their spare time so such limited class time can be used for interaction. Embrace new technology when making videos or design online interactive quizzes. Block diagrams and animations can be created to help students understand the materials in online learning. Flipped classroom approach, when possible to adopt, works well for these courses. For an online geological mapping course, the main challenge is to design exercises for students to practice in different stages of geological mapping. In the fieldwork preparation stage, an exercise can be designed for students to make a base map for field mapping and to make a logistics plan, such as where to accommodate themselves and how to get to the mapping area. If there are outcrops accessible, an exercise can be designed for students to practice how to take field notes, how to identity rocks/minerals, how to measure orientations, and how to sketch or draw a block diagram to show structures. Digital mapping techniques (e.g., using ArcGIS collector or SW Maps on cell phones) can be introduced to students for them to collect data in the field mapping exercise. Geologic maps can be used to design a data analysis exercise. Hide some areas on the map for students to make interpretations to complete the map. Structural analysis using equal-area projection can be added to the exercise if there are accurate and enough orientation data. After the analysis, students can make a geologic map and draw cross sections and tell a geological history from the map. Although the online courses are temporary solutions, some practices in the online courses benefit students even in courses taught in person. Students benefit from watching again and again videos of difficult lab techniques. Data used for the data analysis exercise can be chosen from the area with best geology, whereas in a field school they are limited to the mapping area and are collected by students and may not be accurate or enough for structural analysis to make a good interpretation or to make sense. The data analysis exercise can better prepare students for their actual field mapping.

The first occurrence of Borealosuchus (Crocodyliformes: Eusuchia) from the Lower Ravenscrag Formation (Earliest Paleocene) of Saskatchewan: implications for range and diversity

Kaitlin Lindblad[1], Jorge Moreno-Bernal[2], Ryan McKellar[3], Maria Velez[1]

[1]University of Regina kaitlinlindblad@hotmail.com, [2]Universidad del Norte, [3]Royal Saskatchewan Museum

Borealosuchus is among the best known early crocodylian genera from the latest Cretaceous/early Cenozoic terrestrial fossil assemblages of continental North America. The record of Borealosuchus in the Canadian Provinces is nearly nonexistent compared with coeval units in North Dakota, South Dakota, Montana, and Wyoming. In this study we present the description and classification of three crocodylian specimens, collected from the earliest Paleocene strata of the Ravenscrag Formation near Big Muddy Lake, and now stored in the collections of the Royal Saskatchewan Museum in Regina. Our results confirm the earliest occurrence of Borealosuchus in Saskatchewan. One of the specimens, a partial skeleton with a partial skull and mandible, can be unambiguously assigned to *B. griffithi*. Another specimen includes skull fragments and partial postcranial elements, is referred to *B. sternbergii*. A final third specimen, represented by fragmentary postcranial elements, cannot be referred beyond the genus level. These specimens expand the known stratigraphic and geographic range of their respective species. The presence of *B. griffithi* and *B. sternbergii* in the same deposits in proximity to each other suggests the possibility of a range overlap in the Big Muddy area during the earliest Paleocene, implying possible niche partitioning or competition between members of the same genus.

Groundwater and surface water interaction across time and spatial scales

Emma Lindborg[1]

[1]Blackthorn Science AB emma@blackthornscience.se

The distribution, storage and movement of water across the landscape is a result of a complex system of integrated processes between surface- and groundwater and the atmosphere. One such process is the exchange of deep and shallow groundwater, and its interaction with surface waters, which is of high interest in safety assessments (SA) of nuclear waste repositories. In case of a release, water will be the main carrier of radionuclides from the geosphere towards and in the biosphere. The surface- and groundwater system is often seen as separate entities. However, to follow a radionuclide through different domains from its source to sink, an integrated approach is needed. Large scale groundwater models in the bedrock, with temporal scales from years to decades, need to be linked to local scale hydrological models on daily scale. Different temporal and spatial scales along the flow paths implies that the integrated approach of the conceptual models, need to be applied to different numerical tools in order to quantify water fluxes within and between the different domains. A useful approach applied by SKB in Sweden was the site descriptive modelling (SDM) strategy. An integrated SDM describing the present day conditions of the whole natural system at a site constitutes the platform for both the SA, repository design and the EIA. Due to the long time frames, up to a million years, that has to be taken into consideration in the SA, the climate and landscape development need to be handled. By using the models describing present conditions as a platform, future scenarios with different climate and landscape can be studied in the SA in order to quantify the influence from long term change on the site hydrology. The impact on the hydrological system from operation of the repository are studied in models tailor-made for the environmental impact assessment (EIA), but still with the SDM as a platform. By using the same conceptual model, based on and verified by site specific data, for all end users the credibility of the models capability to make predictions increases. One should be humble to model results due to the fact that models are an interpretation of the natural system. However, they represent the best understanding of the natural system and can be used as a tool to reduce the uncertainties in the scenarios describing the future. Historically, more focus has been laid on the deep than on the shallow groundwater. However, to describe the flow paths from repository to the surface, and vice versa, characterisation of the surface system has the same importance. Additionally, if we cannot understand and explain the hydrological system we can see with our own eyes (lakes, streams, wetlands), how then to argue for understanding on deep groundwater processes? Therefore, and to build confidence and trust, the nuclear waste organizations are recommended to apply an integrated approach in their site characterization as part of system understanding.

Integrated system understanding as a support in radiological and environmental assessments of geological disposal facilities of radiological waste

Tobias Lindborg[1]

[1]Blackthorn Science AB tobias@blackthornscience.se

Lessons learned from ongoing national programmes and international agencies show that the understanding on the natural system and its interactions on the designed parts needs to be treated in a common way when planning and executing a radiological waste management programme. The facility design and construction, geosphere and biosphere characterisation, safety assessment, research and environmental impact should all base their work on, and feed results into, a common system understanding structure. By this, these above typical individual functions within a disposal programme can optimise the tasks and at the same time support the overall confidence in the arguments in the safety case. This strategy fosters a culture of curiosity and responsibility on solving issues at hand as well as a, during the programme steps, general evolving and enhanced conceptual knowledge on the overall disposal system with its functions. Also, to support claims of site-specific properties or processes used in safety assessments, multiple lines of evidence gained from integrating different scientific disciplines into a common site model is needed. The overall geological disposal system can be divided into three interconnected parts, the designed facility with engineered barriers, the geosphere, and the biosphere. These parts constitute the system that needs to be understood and, over the programme stages, increasingly more enhanced towards an application to construct and operate. At the same time, the understanding should be linked to programme requirements and stakeholder expectations that may change during the programme timeframe. Step one is to produce a generic conceptual model describing the

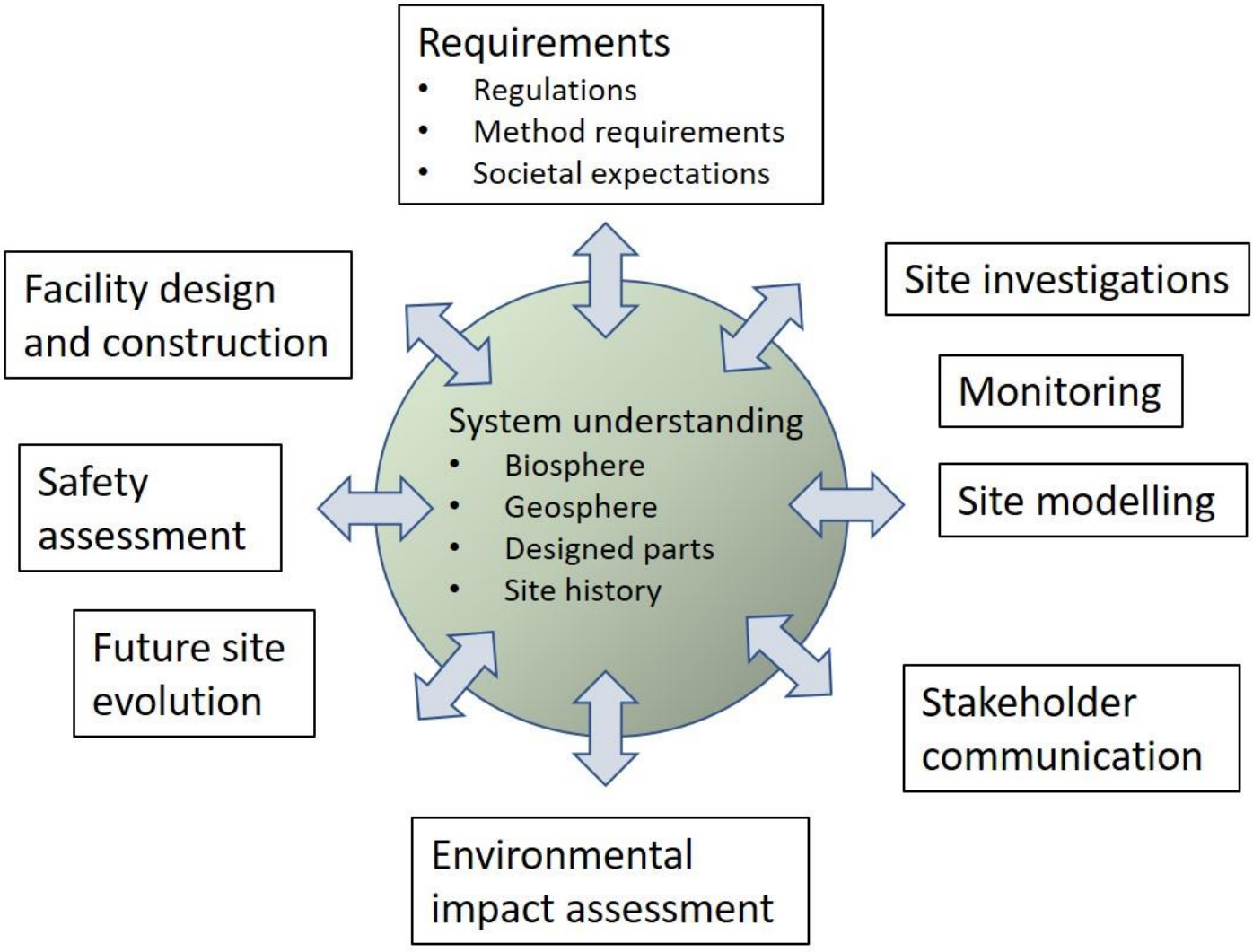

system with its features. For each programme function the conceptual model is used to identify common and individual needs. The conceptual model is then used by all programme functions as a basis for concept development, planning and to find knowledge gaps, linkages and mutual questions between disciplines. Site investigations and site modelling produce data and distributed models that fill information gaps and ongoing safety assessments uses the results and provides feedback on further site characterisation needs. The conceptual site model is enhanced for each iterative cycle together with a more and more detailed and site adapted facility design. The system understanding should have a function as a central hub in the knowledge management system that keep track of programme requirements as well as issues and questions to be handled to move forward in the waste management programme. The key aspects of this strategy, and the lessons learned from other programmes, are the importance of foster and maintain a philosophy within the radiological waste management programme that promotes a broad scientific approach and develop a culture of constant integration and interaction between programme functions.

Time-frequency representation model for near-fault vertical ground motions

Y.X. Liu[1], X.Z. Cui[1], H.P. Hong[1]

[1]Department of Civil and Environmental Engineering, University of Western Ontario yliu3863@uwo.ca

Seismic near-fault ground motions have different characteristics than those of the far-field ground motions. The vertical near-fault seismic ground motion component could also cause significant structural deformation and damage, which could be evaluated from time history analysis using actual or synthetic ground motion records. The vertical near-fault ground motion component can be viewed as the combination of pulse-like and non-pulse-like components. Both short-time Fourier transform and S-transform are used to decompose the records in the time-frequency domain. It is shown that with appropriate selected time-frequency decomposition parameters, the power distribution of the records in the time-frequency domain obtained by using the short-time Fourier transform and the S-transform could be very consistent. A new analytical function is used to fit the pulse-like component, and the non-pulse-like component is modeled based on the time-frequency representation. A comparison of the responses calculated based on simulated and actual records is given.

Shocked crystal misorientation quantified by 2D XRD strain-related mosaicity and EBSD unit segment length

Yaozhu Li[1], Phil McCausland[1], Roberta Flemming[1], Callum Hetherington[2]

[1]Western University yli2889@uwo.ca, [2]Texas Tech University

Shock metamorphism is observed as deconstructive deformation of crystals, and results from hyper-velocity impacts with an extremely high strain rate (up to 10e6/s). Petrographic shock features in olivine include reduction rims, irregular fractures, undulatory extinction, mosaicism, and recrystallization. We study and seek to quantify shock effects in olivine crystals by examining different shocked meteorite samples, NWA 2221 (ureilite with shock stage S3-S4) and NWA 2737 (Martian chassignite with shock stage S5-S6), using in-situ micro-X-ray diffraction (μXRD) and electron backscatter diffraction (EBSD). The representative 2D XRD patterns for olivine grains from both meteorites show streaks spreading along the Debye rings, indicating strain-related mosaicity (SRM) produced by non-uniform strain across the crystal. Incident X rays are diffracted from small misoriented subdomains (<10 μm) which produce streaks. Quantitative SRM analysis measures the sum of full-width-half-maximum ($\sum(FWHM_X)$) of peaks integrated from 2D XRD patterns along the Debye rings (in degrees X). For NWA 2221, the mean of $\sum(FWHM_X)$ is 4.9°± 2.1° (N = 40) with the top 25% having a mean peak shock measurement of 7.9°± 1.2° (N = 10). For NWA 2737, the mean of $\sum(FWHM_X)$ is 11.22°± 2.89° (N = 40), with the top 25% having a mean of 15.7°± 1.18° (N = 10). The strain in the olivine crystals found by SRM analysis is likely distributed by geometrically necessary dislocations (GNDs), that have migrated to form subdomain walls and boundaries. EBSD crystal orientation maps offer an opportunity to locate and quantify crystal subdomains and their boundary types. We introduce a quantity, unit segment length (USL), that is the measurement of the apparent subdomain boundary density contributed by GNDs on 2D EBSD orientation maps, where subdomains are defined by observed misorientation angle smaller than 15°. The USL developed in this work does not distinguish between "twisted" and "tilted" wall types, but is a robust way to quantify the subdomain walls that are created by shear stress during shock deformation. We observe that the USL found in shocked olivine in this work is much greater than that of unshocked olivine distorted by low-strain-rate terrestrial plastic deformation (from published terrestrial olivine data[1]). We observe that NWA 2737 has a higher shock level and produces a larger USL measurement (5.4 ± 1.1 *10-2 /μm (N=3)) than NWA 2221 (USL = 3.6 ± 0.5 *10-2 /μm (N=3)); terrestrial olivine has USL = 0.36*10-2 /μm (N=1). Observations of both shocked samples show that shock deformation strongly distorts the crystal by migrating dislocations and forming GNDs. Together, SRM and USL techniques provide a quantitative measure and spatial representation of shock-related distortion of olivine crystals. This work further demonstrates that it may be possible to not only quantify shock level in meteorites and impact rocks, but also understand the mechanisms and conditions under which natural samples have accumulated shock damage.

[1] Wieser et al. (2020). Nature communications, 11(1), 1-14.

Preservation of Varved Couplets in the Oxygenated Monimolimnion of Crawford Lake: Implications for defining the Anthropocene Epoch

Brendan Llew-Williams[1], Autumn Heyde[1], Krysten Lafond[2], Francine McCarthy[1], Mike MacKinnon[1], Uwe Brand[1], Tim Patterson[2], Martin Head[1]

[1]Brock University bl14jo@brocku.ca, [2]Carleton University

The varved sequence of Crawford Lake in a small, deep karstic basin near the Niagara Escarpment in Southern Ontario, is being investigated as a potential GSSP for the proposed Anthropocene Epoch. The dense, highly conductive, alkaline, and slightly saline water chemistry found below the permanent chemocline resembles regional groundwater confirming that the monimolimnion is groundwater sourced. Water recharged into exposed calcareous aquifers ~ 1 km east at the nearby Nassagaweya Canyon, transports oxygenated groundwater into the monimolimnion at concentrations that allow eukaryotic microorganisms to flourish, particularly in winter, when the relatively warm and very nutrient-rich waters provide a refuge. The unique preservation of seasonally laminated couplets in a well-oxygenated setting is of particular interest since the primary marker favoured by the Anthropocene Working Group to define the beginning of this epoch is plutonium fallout from atmospheric thermonuclear testing that is readily mobilized in the anoxic settings that typically allow undisturbed varved sediment accumulation. Above the ~ 15-meter chemocline, the groundwater fed mixolimnion experiences surface water dilution, and substantial seasonal variation with mixing to the chemocline in spring and fall. Although concentrations of Ca+2 and CO3-2 are lower in the mixolimnion, LSI calculations (Feb 2019 – Oct 2020) indicate that calcite crystals precipitate from solution in the slightly basic waters of the epilimnion (~ 0-6 meters) when water temperature exceed ~ 15.2 °C, forming the light-coloured couplet layers on the lakebed. Climate affects the thickness of the light layer, as well as the dark-coloured layers composed primarily of the organic remains of plankton, since it reflects productivity in the lake ecosystem. Productivity is strongly impacted by human activity in the watershed, so the thickness of the dark layer increased dramatically at times of Iroquoian and Colonial settlement, allowing precise and accurate varve-counting (and thus chronological resolution) through the past few centuries. Anoxic bottom waters were assumed essential for the preservation of seasonal laminae, but water column monitoring over the past few years reveals dissolved oxygen measurements sufficient for aerobic respiration. The largest benthic colonizer of the monimolimnion is the nektobenthic ostracod Notodromas monacha which is commonly found in caves and aquifers and appears to have migrated through groundwater flow. The highest hydraulic conductivity, and amount of karstic dissolution, is along the Gasport/Goat Island Fm contact that intersects the basin of Crawford Lake between ~ 16 and 19 m. Crawford Lake is protected by Conservation Halton providing easy access to visitors, interpretive displays on the unique study site, and reconstructed longhouses built by the Iroquoians who farmed the land in the middle of the last millennium, allowing the varves to first become discernible.

Orogenic unroofing in the Rae Craton recorded by U-Pb geochronology of the Paleoproterozoic Nonacho Group, Northwest Territories, Arctic Canada

Jade Lockie[1], Alessandro Ielpi[1], Joshua Davies[2], Edith Martel[3], Beth Fischer[3], Sally Pehrsson[4]

[1]Laurentian University jlockie@laurentian.ca, [2]Université du Québec à Montréal / GEOTOP, [3]Northwest Territories Geological Survey, [4]Geological Survey of Canada

Investigating the depositional age and provenance of clastic sedimentary rocks is key to unravelling the relationship between orogenic unroofing and the development of nearby coeval basins. The Paleoproterozoic Nonacho Group (Northwest Territories, Canada) records alluvial, fluvial, and marine sedimentation as part of a basin system that developed longitudinally atop the Rae Craton. Despite its importance to the reconstruction of the ancestral Canadian Shield, the Nonacho Group's origin has remained enigmatic. Updated detrital zircon geochronology data analyzed with Laser Ablation Inductively Coupled Plasma Mass Spectrometry provides a new Maximum Depositional Age (MDA) and supports provenance from the southern Rae plutonic domains, the nearby Taltson Orogen and unrecorded exotic sources possibly related to the Snowbird Tectonic Zone. Previous hypotheses related the Nonacho Basin to strike-slip kinematics and unroofing of the Taltson-Thelon Tectonic Zone alone; however, the updated provenance data and new MDA, coupled with new preliminary field examination, support a mechanism of crustal relaxation punctuated by a flexural episode. More broadly, the new data presented here contributes to craton-scale basin correlations and to recent reconstructions of the orogenic unroofing in interior Laurentia following its initial Paleoproterozoic assembly.

Revisiting Huronian paleoslopes

Darrel Long[1]

[1]Laurentian University dlong@laurentian.ca

Statistical relationships between average bankfull channel depth, thalweg depth, bankfull discharge, bankfull channel width, slope and drainage area based on a database of >4000 Modern rivers, in multiple climatic zones, provide a basis for paleohydrological reconstruction of ancient river systems. Dune height (Hd) is equal to Cf x 2.52 times the average height of trough crossbeds (Hx) where Cf is a compaction factor equal to 100/(100-% compaction). Thalweg depth (dmax) is calculated as 6.5058 x Hd1.111. From this, average bankfull channel depth (dbf) is calculated as = 0.6095 x dmax0.973. Bankfull channel width (wbf) is calculated as 16.293 dmax1.198 for rivers with low sinuosity (P < 1.3), or wbf = 17.338 dmax1.168 for rivers with intermediate sinuosity (1.3 < P < 1.7), and 17.458 dmax1.230 for high sinuosity rivers (P > 1.7). Bankfull discharge (Qbf) can be calculated as Qbf = 17.359 dmax1.270. Slope (S) can then be calculated from bankfull channel width as S = 0.0341 wbf-0.7430. Drainage basin area (DA) can be calculated from bankfull channel depth as = 241 dbf2.17. On this basis, the average slope of Mississagi Formation rivers within the depositional basin, after correction for 36 % compaction, was = 0.0013 m/m (0.0005 to 0.0026), with an average bankfull channel depth of 2.67 m. The slope of Serpent Formation rivers, after correction for 33.5 % compaction, averaged 0.0007 (0.0003 to 0.0016), with an average bankfull channel depth of 5.85 m. Calculation of slopes using this approach on these and other Precambrian systems indicate that paleoslopes were well below the "depositional gap" from 0.007 to 0.026 between modern rivers and arid region fans suggested by Blair and McPherson in 1994, negating the idea that pre-vegetation rivers had higher slopes than their modern counterparts.

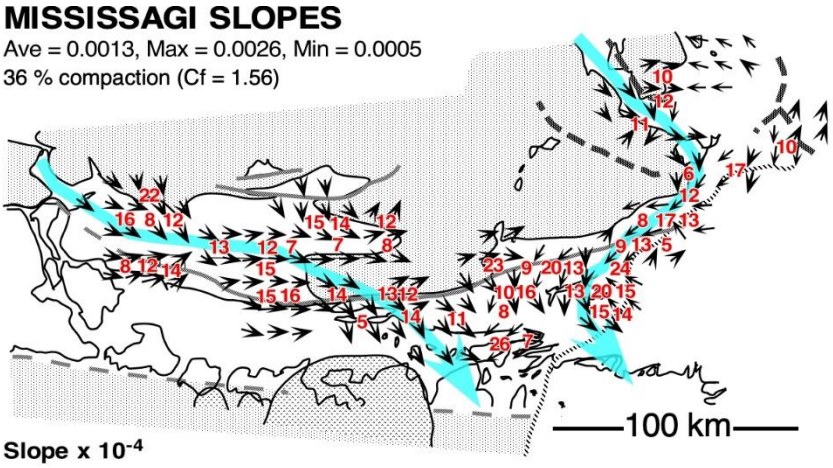

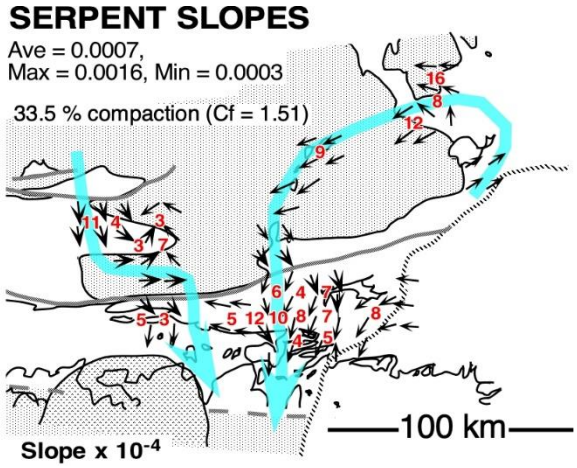

Clay Mineral-Porewater Oxygen and Hydrogen Isotope Interaction in Ordovician Shales, Southern Ontario

Fred Longstaffe[1], Skylar Chauvin[1], Ian Clark[2], Laura Kennell-Morrison[3]

[1]The University of Western Ontario flongsta@uwo.ca, [2]University of Ottawa, [3]Nuclear Waste Management Organization

Porewater H and O isotope compositions are commonly used to fingerprint past and present subsurface water movement at potential deep geological repository sites. Host rock-porewater interaction, however, can modify original porewater O and H isotope compositions. This study examines whether clay minerals in Ordovician shales from southern Ontario played a role in changing the isotopic composition of porewater in these low water content and low permeability units. We investigated whether hydrogen (H) and oxygen (O) isotope exchange has occurred between the clay minerals and porewater, and whether partitioning between water adsorbed on clay minerals and mobile porewater, has affected porewater isotopic compositions. The Queenston Formation, Georgian Bay Formation, Blue Mountain Formation and Collingwood Member of the Cobourg Formation examined at the Bruce Site (Bruce Nuclear Power Generating Station) have similar clay mineralogy, as determined by X-ray diffraction. Their <2µm size-fraction is dominated by illite, with lower amounts of kaolinite and then chlorite. Discrete swelling clay minerals were not detected. Thermogravimetric analysis of the <2µm size-fractions yielded broadly similar dehydration and dehydroxylation patterns for all samples, with some variability depending on the exchangeable cation (Na, Ca, K) on clay mineral surfaces. This behaviour underscores the complexity of clay mineral-water interactions, which depend on clay mineral type, chemistry, crystallinity, and formation water chemistry, in addition to temperature and effective rock/water ratio. Retention of residual adsorbed water at higher-than-expected temperatures, and possible cross-contamination between adsorbed water and hydroxyl group water can affect the measured isotopic results. We hypothesized that the O and H isotope compositions of the clay minerals would reflect weathering conditions and track isotopic 'weathering lines' that run near-parallel to the Global Meteoric Water Line. The results, however, do not plot on or near such 'weathering lines'. Instead, there is a match between water in isotopic equilibrium at 90°C (maximum burial temperature at the Bruce Site) with clay mineral O and H isotope compositions. Measured porewater isotopic compositions for these shales have very similar isotopic compositions to those calculated for 90°C. This scenario suggests that the porewater and clay mineral isotope compositions have shifted from original values. Whether this shift resulted from re-equilibration during diagenesis or proton-only exchange reactions remains to be determined. Experiments using <2µm size-fractions from the Bruce Site plus a standard illite (IMt-1) demonstrate the potential for hydrogen-isotope exchange in as little as ten weeks at 68°C.

Student response to the use of digital models of rocks and minerals in introductory geology labs: Lessons from a year online

Jason Loxton[1]

[1]Cape Breton University jason_loxton@cbu.ca

Free digitized versions of materials used in geology labs have become widely available, but little data is available on their utility in teaching. The shift to online only delivery of courses during the 2020-2021 academic year at Cape Breton University presented an opportunity to test the effectiveness of these technologies. Virtual rock and mineral specimens were used exclusively in labs for two introductory geology courses. In a third course, students learned on virtual specimens, but were provided with a rock kit for the final lab and exam. Students in all three courses were given an anonymous end of term survey focusing on two technologies: 3D digital models and zoomable gigapixel images of specimens and outcrop. In total, 61 students responded (58-82% response rate). Feedback on both technologies was positive in all three courses, despite different emphasis and student demographics, with >90% at least somewhat agreeing--and 50-67% strongly agreeing--that they helped their learning. Students also generally agreed that these technologies "replicated the experience of interacting with physical specimens or environments." This was true even in the course that had access to both digital and physical specimens, where 60-70% agreed or strongly agreed that the two technologies replicated physical specimens. Open ended written comments were overall positive, with emphasis on realism, variety, and interactivity, but some respondents noted missing the tactile aspect of physical specimens, limitations of digital quality (resolution, lighting or contrast), or issues getting the models to load. This latter problem was likely exacerbated by the fact that a substantial number of students were accessing the course from areas with poor internet connections and/or were completing it using a smartphone or tablet. Students were split on whether physical kits should be sent during distance learning. Among the two courses using only digital specimens, the fall class would have moderately preferred receiving physical kits and the winter class keeping digital only. In contrast, 90% of students in the course who used both physical and digital specimens believed it was "very important" that students be given access to physical specimens--although they also agreed that learning on digital specimens prepared them to identify real specimens. Students in the dual modality course were asked how digital specimens might feature in future in-person learning: 90% disagreed that they should replace physical specimens in a lab setting, but there was strong support for their use in quizzes, as study aids, and to augment physical materials in lab; only 10% saw no role for these technologies. Taken together, responses from the three courses support the use of digital specimens for teaching physical geology in an online setting and point to a role outside of distance education.

Flow laws of wet quartzite: some insights from experimental and field observations

Lucy Lu[1], Dazhi Jiang[2]

[1]Cardiff University LuX30@cardiff.ac.uk, [2]Western University

Current understanding of quartz flow laws is mainly based on high-temperature and high-pressure creep experiments on natural quartzite samples or synthetic specimens. Despite many decades of effort, an accurate flow law for quartz dislocation creep is still missing. A major difficulty lies in addressing adequately the water effect, known as "hydrolytic weakening", since 1965. To account for the water effect, a water fugacity term was phenomenologically incorporated into the quartz flow law in 1995. However, considering water fugacity alone still cannot reconcile huge discrepancies in quartz flow laws parameters derived from different experiments. Recent proposals for the effect of activation volume and the stress exponent variation with dominant slip systems are yet to be tested. Although there have been a few attempts to constrain quartz flow laws based on estimates of strain rate, stress, and deformation temperature from natural mylonites, we believe that these estimates have errors too large to produce accurate flow laws. We quantitatively investigated the effects of activation volume and slip systems on quartz rheology and determined quartz flow law parameters thoroughly rely on experimental data. From a data set of critically-selected 19 creep experiments of wet quartzite with microstructures and c-axis fabrics suggesting steady-state dislocation creep and building on previous work, and we determine flow law parameters corresponding, respectively, to dominant prism <a> slip and dominant basal <a> slip systems, using an iterative approach. We then use the above determined flow laws to extrapolate experimental data to geological PT conditions. Combining with quartz c-axis data, we propose that in natural deformation, the two flow laws do not represent two competing mechanisms. Rather, the dislocation creep of wet quartzites is defined by a piecewise function with the basal <a> dominant creep at low temperatures (< 400°C) and prism <a> dominant creep at higher temperature (> 400°C). Our results reconcile the large discrepancies in flow law parameters for wet quartzite derived from different creep experiments and are consistent with c-axis fabrics from nature and experiments.

An episode of progressively oxygenated Katian ocean during the Taconic Orogeny: evidence from uranium isotope compositions of organic-rich sedimentary rocks in southern Ontario, Canada

Xinze Lu[1], Geoffrey Gilleaudeau[2], Brian Kendall[1]

[1]University of Waterloo xlv@uwaterloo.ca, [2]George Mason University

The Late Ordovician Taconic Orogeny had a profound effect on climate and global seawater chemistry, but its influence on ocean redox conditions remains uncertain. This orogeny was coeval with deposition of the calcareous Collingwood Member (CM) of the upper Lindsay Formation and the overlying siliciclastic Rouge River Member (RRM) of the lower Blue Mountain Formation in southern Ontario. Both units are Katian-aged fine-grained organic-rich sedimentary rocks deposited in the Appalachian Basin (AB) and Michigan Basin (MB). Here, we present elemental proxies to constrain local depositional environment and uranium isotope compositions ($\delta^{238}U$, relative to CRM145, unit in ‰) to reconstruct global ocean redox conditions at the time.

Local depositional conditions are revealed by paleosalinity and paleoredox proxies. Paleosalinity proxies (Sr/Ba and S/TOC) of the CM and RRM consistently suggest brackish/marine conditions during deposition. Paleoredox conditions are inferred from Mo/U EF (enrichment factor) ratios and Fe speciation data. Covariation patterns of Mo-U EF suggests the operation of a Fe-Mn particulate shuttle for both units. Spatially, the CM from the AB and MB were mostly deposited under oxygen-deficient and anoxic environments (non-euxinic), whereas predominantly oxic/suboxic conditions are inferred for the CM near the Algonquin Arch (AA). In contrast, the RRM was deposited under oxic/suboxic and sporadic anoxic conditions.

Uranium isotope compositions were obtained for some bulk CM and RRM samples with U EF > 2 and for carbonate fractions of the CM near the AA (leached with 1M HCl). Strong positive correlations between $\delta^{238}U_{non\text{-}det}$ (non-detrital, corrected from the bulk $\delta^{238}U$) and several redox proxies are observed for the CM, suggesting a local redox control of the magnitude of U isotope offsets between sediments and water columns. The lowest $\delta^{238}U_{non\text{-}det}$ (?0.64) of the CM represents a maximum estimate of coeval seawater $\delta^{238}U$. Carbonate ?238U of the CM from the Collingwood core increases upward from ?0.63 to ?0.52. The CM from the Mount Forest core shows more fluctuations in carbonate $\delta^{238}U$ (between ?0.85 and ?0.56) but has an overall upward increasing trend. These trends suggest an episode of increasing ocean oxygenation during CM deposition. The ?238Unon-det of the overlying RRM has a narrow range (0.37 to 0.11, average = 0.25) and does not covary with redox proxies. Considering a small U isotope offset (0.15 ± 0.10) in modern suboxic settings, the coeval seawater $\delta^{238}U$ could be from 0.52 ± 0.10 to 0.26 ± 0.10 (variable seawater $\delta^{238}U$) or around 0.40 ± 0.10 (constant seawater $\delta^{238}U$), both of which are similar to modern seawater $\delta^{238}U$ (?0.39 ± 0.04). This episode of Katian ocean oxygenation may be driven by the concurrent Taconic Orogeny, because the enhanced exhumation of mafic/ultramafic rocks could consume carbon dioxide and provide nutrients to stimulate primary productivity for photosynthesis.

Identifying Potential Mineralogical Sources for Elevated Arsenic in Groundwater Associated to Granites from Southwest Nova Scotia

Bryan Maciag[1], James Brenan[1]

[1]Dalhousie University bmaciag@dal.ca

Arsenic levels in Nova Scotian well water is strongly dependent on the geogenic sources, and thus depends upon the bedrock lithologies. However, not all lithologies of similar composition behave the same, as is the case with the Devonian granitoids of southwestern Nova Scotia. Groundwater associated with the Musquodoboit Pluton (MP) and the South Mountain Batholith (SMB), both predominantly granodiorite to monzogranite, have arsenic concentrations that exceed the Health Canada maximum acceptable concentration of 10 µg/l in 80% and 60% of samples measured, respectively. However, none of the groundwater samples related to the Port Muton Pluton (PMP), comprised of tonalite to monzogranite, exceed 5 µg/l. This study seeks to identify the origin(s) of this discrepancy by considering the mineralogical controls on arsenic and the susceptibility of these phases to weathering and leaching by local groundwater. We examined over 300 accessory mineral grains (primarily apatite) and 250 rock forming minerals (primarily biotite), distributed amongst 47 SMB samples, 2 MP samples and, 3 PMP samples. Backscatter electron imaging and energy dispersive spectroscopy aided in phase identification, while Laser ablation ICP-MS determined arsenic (and a number of other trace elements) concentrations. Major rock-forming silicates yielded arsenic concentrations typically below detection limits (~1 µg/g). Apatite on average contains 3-5 µg/g arsenic; however, several samples from the SMB contain arsenic concentrations of 30-70 µg/g. Samples from the SMB and the MP contain rare grains of allanite which has an arsenic concentration of 250 µg/g and 500 µg/g, respectively. Monazite is found in all three granitic systems and contains between 380-650 µg/g arsenic. The SMB, MP and PMP also contain Fe-sulfides. The sulfide grains analyzed from the SMB have an average arsenic content of 500 µg/g, similar to a single grain analyzed from the PMP. A sulfide grain from the MP contains 2600 µg/g arsenic. Some of the sulfide grains in the SMB and MP samples are partially to completely replaced by iron oxyhydr(oxides), which themselves contain 90-950 µg/g in the SMB, and 400 µg/g in the MP. As iron sulfides constitute the most arsenic-rich phase common to all three granitic bedrock lithologies, we hypothesize that the presence of Fe-oxyhydr(oxides) in the MP and SMB but not in the PMP relates to the elevated arsenic levels in related groundwaters. The presence of oxidative weathering products could be related to differences in the host rock permeability. Higher permeability would allow groundwater to penetrate the bedrock to interact with the sulfides and leach arsenic during oxidation breakdown. The quantity of arsenic released depends upon the amount of arsenic retained by the Fe-oxyhydr(oxides), which varies between the SMB and MP.

Late Cretaceous to Cenozoic exhumation of the Purcell Mountains, southeastern British Columbia

Douglas MacLeod[1], David Pattison[1], Collin Kehler[1]

[1]University of Calgary dougrmacleod@gmail.com

The Purcell Mountains of western British Columbia form part of the Omineca belt of the Canadian Cordillera. This region records a protracted history of spatially overlapping tectonic events including two phases of rifting in the Proterozoic, orogenesis in the Mesozoic, and uplift and extension in the Eocene. Despite the importance of the Purcell Mountains to the tectonic evolution of the southeastern Canadian Cordillera, the Late Cretaceous and younger (<100 Ma) exhumation history remains enigmatic and understudied. This study examines the extent and timing of the Late Cretaceous and Cenozoic rock uplift of the Purcell Mountains, the adjacent Selkirk Mountains to the west, and the western Rocky Mountains to the east by utilizing metamorphic petrology and low temperature thermochronology. The Purcell Anticlinorium hosts numerous Late Cretaceous granitic intrusions including two major intrusive bodies, the White Creek and Fry Creek batholiths. Petrographic analysis has revealed the sequence of mineral assemblages in the contact aureoles surrounding the two batholiths. Phase equilibrium modeling constrains the pressure of contact metamorphism to 2.5-3.5 kilobars. The age of intrusion of the White Creek batholith has been dated to 97.9 ± 0.29 Ma using U/Pb zircon geochronology. Together, these data provide a point in depth and time upon which the low to mid-temperature thermochronology can be built. Three sample transects for thermochronology were collected across the Purcell Anticlinorium from the Western Rocky Mountains to the Selkirk Mountains in order to elucidate the Late Cretaceous to Cenozoic exhumation history following the emplacement of the Fry Creek and White Creek batholiths. The low-temperature T-t paths for these regions will be constrained by the apatite (U-Th)/He and zircon (U-Th)/He thermochronometers, the results of which are still in progress. When combined, the petrologic and thermochronological data will inform tectonic models for the timing and extent of Late Cretaceous to Eocene exhumation of the Purcell and Rocky Mountains.

Investigating sources of induced seismicity in west-central Alberta

Kienan Marion[1], David Eaton[1], Rebecca Salvage[1]

[1]University of Calgary kienan.marion1@ucalgary.ca

The Western Canada Sedimentary Basin (WCSB) is tectonically quiescent because of its stable intraplate tectonic setting, other than shallow crustal faulting linked to Laramide-aged thrusts in the foreland belt. There are, however, some notable exceptions. This work aims to shed light on several such clusters of induced seismicity in west-central Alberta that are currently not well understood. We report initial results from the first 17 months of monitoring using a temporary broadband seismograph array installed above a prototype geothermal pilot in west-central Alberta (Clearwater County). This array can detect regional seismic events as well as microearthquakes and fills in a gap in the public seismograph network. One such cluster is the Rocky Mountain House Seismogenic Zone (RMHSZ), a long-lived (1970's-present) cluster of earthquakes located approximately 35 km southwest of the town of Rocky Mountain House in west-central Alberta. The RMHSZ now accounts for 5 of the 10 largest earthquakes in Alberta's recorded history: as an example, a ML 4.3 event in the RMHSZ on 2014-08-09 15:28:49 UTC caused a power outage that lasted several hours. These events are well-constrained spatially to a northwest-southeast oriented region centered in T37 R9W5 (52.21ºN, 115.25ºW) spanning 26.5 km² that overlies the Devonian-aged (Frasnian) Strachan D3-A Leduc reef sour gas pool. Seismic activity in RMHSZ has historically been associated with gas production and secondary recovery. A recent (post-2012) uptick in earthquake activity, particularly as gas production and injection ceased in 2013, brings this mechanism into question. We review leading theories in light of several years' worth of new

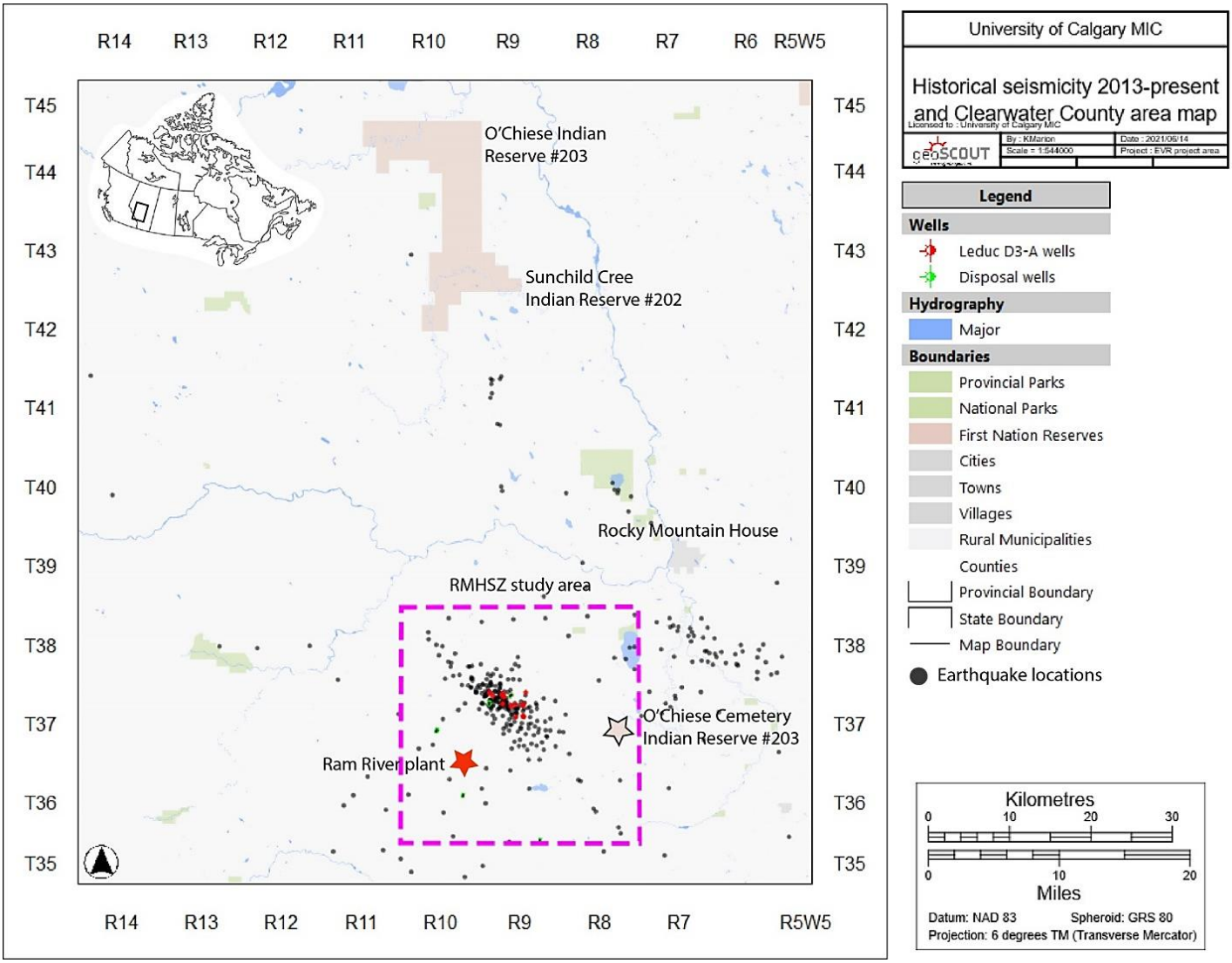

seismicity data and integrated them with production data. Wastewater injection into the Devonian Wabamun Group initiated in March 2012 may be the culprit behind felt ground motions post-2013, especially if the Wabamun is naturally fractured. This has not been previously recognized. Further analysis of the data collected by our broadband array in Clearwater County is ongoing using the open-source software packages ObsPy and REDPy, and will consider nearby seismicity clusters associated with active targets for industry in the Duvernay Formation: the East Shale Basin and Willesden Green regions.

Impact of the mid-20th century Great Acceleration on Chrysophyte (golden-brown algae) community structure in Crawford Lake, Ontario, Canada- implications for the search for an Anthropocene GSSP

Matthew Marshall[1], Krysten Lafond[1], R. Timothy Patterson[1], Francine McCarthy[2]

[1]Carleton University matthewmarshall3@cmail.carleton.ca, [2]Brock University

Crawford Lake, situated within the Crawford Lake Conservation Area near Milton, Ontario, Canada, has unique characteristics that make it ideally suited to high-resolution paleoecological studies. The seasonally deposited varved sediments in the deep basin of this meromictic lake are currently being considered as a potential Global Boundary Stratotype Section and Point (GSSP) to mark the lower boundary of the proposed Anthropocene Epoch. Golden-Brown Algae (Chrysophyte) communities were examined at annual resolution in varves spanning 1930-1990 CE from freeze core collected from Crawford Lake in February 2019. Stratigraphically constrained cluster analysis showed major assemblage changes within this interval, with one of the highest magnitude changes occurring between varves deposited in 1952 and 1953, coinciding with the first marked increased in 239Pu in sediments due to atmospheric testing of thermonuclear weapons, one of the key markers of the proposed Holocene- Anthropocene boundary. The post-1953 species assemblages within this lake were novel and differed greatly in composition compared to those examined from earlier in the 20th century. These changes in assemblage are attributed to increased industrial emissions and related effects of acid deposition on the lake's catchment, related to the Great Acceleration - the massive economic, industrial and demographic expansion beginning in the mid-20th century. The findings reported here provide support for the laminated sedimentary sequence from Crawford Lake as a potential Anthropocene GSSP.

The flash melting of scapolite and plagioclase in the Olot suite, Catalan volcanic zone, northeastern Spain

Robert MARTIN[1], Dirk Schumann[2], Lisard Torro[3], Joan Carles Melgarejo?

[1]McGill University robert.martin@mcgill.ca, [2]Fibics, [3]Pontifical Catholic University of Peru, ?Universitat de Barcelona

The flash melting of a mineral involves its disequilibrium fusion upon explosive eruption at a lava fountain. We have investigated the fate of megacrysts of scapolite and plagioclase from the Pomareda and Roca Negra monogenetic cones in the Olot suite, Catalan Volcanic Zone, northeastern Spain. The affected crystals of scapolite have a prominent white rim 1 mm or so across, easily spotted in the volcanic ejecta although they are uncommon; in the plagioclase megacrysts, the rim is sieve-textured. Ronald C. Peterson wrote his M.Sc. thesis (McGill, 1977) on scapolite from a similar occurrence at Chuquet Genestoux, Massif Central, France, using crystals supplied by RFM. He established that the mantle-derived scapolite is sulfatic, and crystallized in space group I4/m instead of the expected P42/n because of disorder in the orientation of the sulfate tetrahedra. A combined SEM-EDS study of the Olot samples using the ZEISS Atlas-5 software reveals clear evidence of disequilibrium melting. The meionitic scapolite contains roughly 35% of the silvialite (sulfatic) component; it has melted incongruently along its rim. The melt crystallized to fan-shaped skeletal plagioclase of equivalent An content, riddled with wollastonite + silvialite and vacuoles, an expression of degassing. The plagioclase megacryst, roughly An32, is far from equilibrium with the basanitic magma. Its margin melted incongruently to plagioclase An70 + glass + some form of silica. Movies will be presented to show details of the rims. The melting reactions were arrested by thermal quench upon eruption. Further details are available in Eur. J. Mineral. 30, 45-59 (2018).

LEFT
A megacryst of sulfatic meionite in its basanitic groundmass, Roca Negra volcanic center, Olot suite, Catalan volcanic zone, Spain. Incongruent melting has occurred around the periphery and along cracks.
RIGHT
A megacryst of plagioclase (andesine) in its basanitic groundmass, Pomareda volcanic center, Olot suite, Catalan volcanic zone, Spain. Incongruent melting to a more calcic plagioclase + melt is restricted to the periphery of the crystal.

Interpretation of regional gravity data acquired at the Bathurst mining camp, Canada

Juan Martínez[1], Bogdan Nitescu[1]

[1]Universidad de los Andes ji.martinez11@uniandes.edu.co

The Bathrust Mining Camp (BMC) is a metal mining district in Canada and was a focus area of the Geological Survey of Canada's Targeted Geoscience Initiative Phase 3 project (TGI3). As part of that project, the Geological Survey of Canada (GSC) conducted a new gravity survey in 2006 that led to the acquisition of over 3500 new gravity data with an average spacing of 1-2 km. In this project, analysis and modeling of the upper crustal structure of this area were performed using the gravity data set acquired by the GSC. This was done to contribute to the geological understanding of the main features of the upper crust. All the datasets used are available in the Geoscience Data Repository (GSC webserver). The gravity data were reduced to sea level following the Geomatics Canada protocol, using an average crustal density of 2.77 g/cm3 to produce the Bouguer anomaly, which was analyzed and used for 2.5D modeling of five transects over the BMC using the GM-SYS tool of the Oasis Montaj - Educational software edition version 9.7.1 of Geosoft. As a result of the project, a three-dimensional perspective of the general geometry of the main geological groups of the BMC (Fournier, California Lake, Tetagouche, and Miramichi) was obtained in which the following can be appreciated: the Nine Mile Syncline is an open fold and the Tetagouche Anticline is a gentle fold. Both folds are noncylindrical and inclined and their axial planes dip in a 295° N direction; the vergence angle of the folds tends to increase towards the northeast of their axes as do the deformation effects caused by the folds. The structures modeled under the Tetagouche Anticline axis gradually deepen to the northeast reaching a maximum depth of 4 km. The depth of the structures modeled under the Nine Mile Syncline axis varies between 2 and 9 km with the deepest part being towards the center of the BMC; towards the northeast of its axis, the modeled structures reach an intermediate depth of 4 km while towards the southeast they are 2 km deep on average. The deepest part of the entire modeled structure is beneath the Nine Mile Syncline towards the center of the BMC.

Stochastic source modeling and tsunami analysis of the 2012 Haida Gwaii Earthquake

Karina Martinez Alcala[1], Katsuichiro Goda[1], Jinhui Qin[1]

[1]University of Western Ontario kmart94@uwo.ca

The Queen Charlotte Fault is the most seismically active zone in Canada. The two largest instrumentally recorded earthquakes in Canadian history occurred along this fault. The Mw 7.8 2012 Haida Gwaii Earthquake was the second largest of those events. The tsunami that was triggered, highlighted the importance of tsunami hazard assessment in Canada's Pacific coast. Stochastic source modeling serves as a useful method to assess future tsunami hazard. The source models characterize the uncertainty of earthquake ruptures by considering variability in fault geometry and slip heterogeneity, which, in turn, allows the consideration of a wide range of tsunami scenarios in the Haida Gwaii region. The model predictions are constrained by observational data such as tidal gauges, run-up measurements in Moresby Island, and DART buoys, as well as past source inversion studies. 1000 stochastic tsunami scenarios are generated using the stochastic source modeling method to assess tsunami hazard via tsunami inundation simulations of the target region and to conduct sensitivity analyses of tsunami height variability. The resulting models, can be used to provide tools for better informed risk management decisions and future development of probabilistic tsunami hazard analysis.

Prolonged oceanic oxygenation and transient deep-ocean anoxia led to Paleozoic ironstone deposition and extinctions

Edward Matheson[1], Peir Pufahl[1], J. Brendan Murphy[2]

[1]Queen's University edward.matheson@queensu.ca, [2]St. Francis Xavier University

The timing and nature of the transition from anoxic oceans that existed at the onset of the Proterozoic to fully oxygenated modern oceans is a profound and enduring controversy. The traditional consensus that modern-like ventilated conditions were achieved by the earliest Phanerozoic has been challenged by new early Paleozoic redox proxy records. Here, we present novel geochemical data from ironstone that support the emerging view that full ventilation did not occur until well into the Paleozoic. Ironstone is a marine sedimentary rock with abundant syndepositional Fe. Many Paleozoic ironstones formed through continental margin upwelling of deep-ocean ferruginous water and the authigenic growth of Fe minerals in neritic settings. We present in situ laser ablation ICP-MS 87Sr/86Sr and rare earth element data from Ordovician-Silurian upwelling-related ironstone in the Floian Wabana Gp (Newfoundland), Darriwilian Ogwen Gp (Wales), Sandbian Fombuena Fm. (Spain), Hirnantian Neda Fm. (Wisconsin), and Telychian Clinton Gp (New York). For the first time, we document anomalously low 87Sr/86Sr values and well-defined Eu anomalies in Phanerozoic ironstone. These independent datasets provide robust evidence that continental margin ironstone formed from seawater admixed with mid-ocean ridge ferruginous hydrothermal fluid, a scenario that is not viable in oxic oceans. Thus, we interpret that Paleozoic oceanic redox dynamics differed from the modern in that the deep oceans must have been at times anoxic. Transient oceanic redox stratification persisted further into the Paleozoic than previously recognized, with anoxic deep water below a redoxcline and oxygenated surface ocean. The factors that led to the poorly ventilated deep oceans might have included lower than present

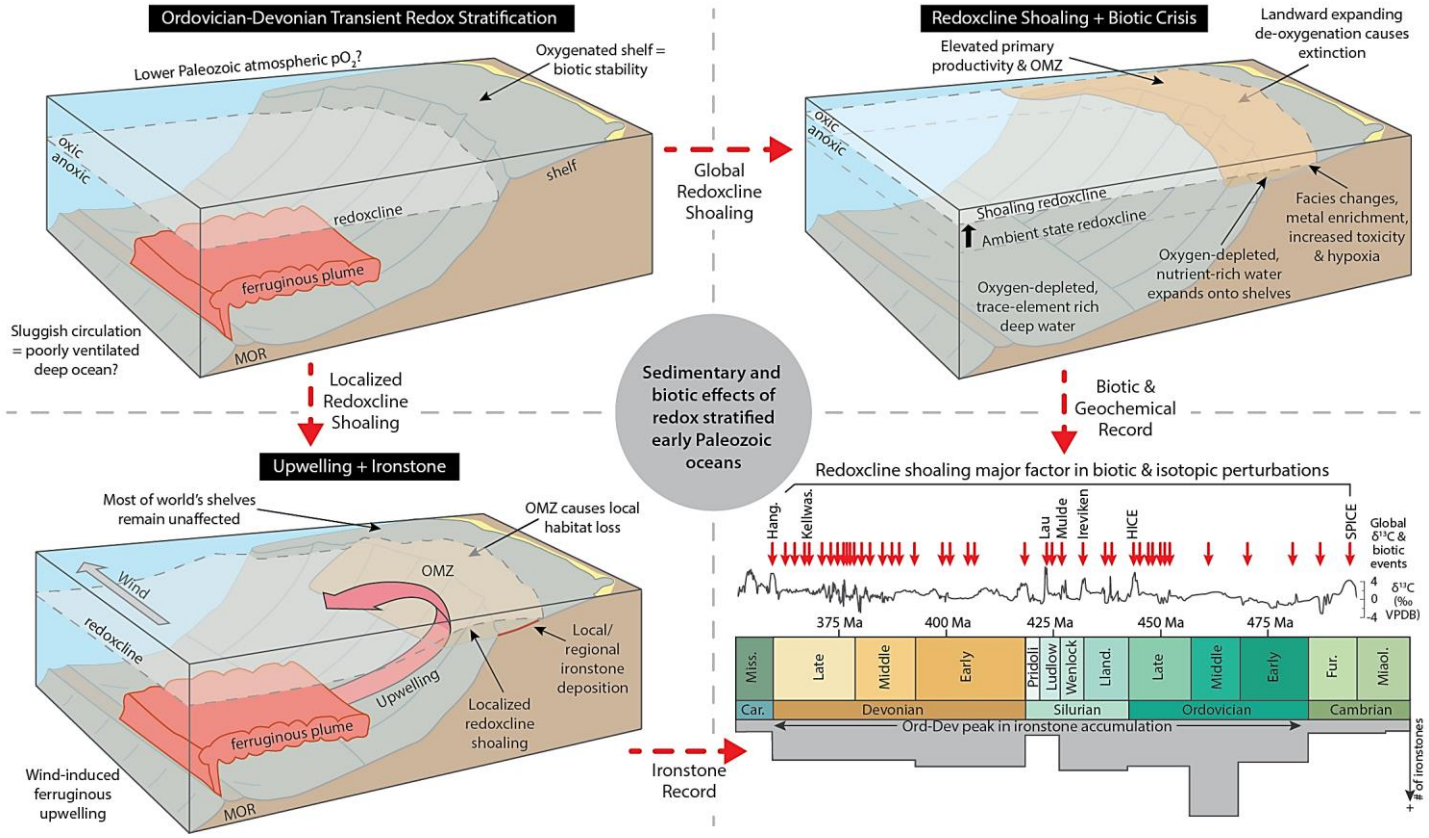

atmospheric oxygen or tectonic- and climate-induced sluggish circulation. This model provides critical new evidence regarding the recurrent extinction events and isotopic excursions that are widely associated with poorly understood neritic anoxic events in the Cambrian to Devonian. The spread of sub-redoxcline anoxic water onto shelves is a previously unrecognized trigger for these global biotic and geochemical perturbations. Thus, our data indicate that ironstone is a new proxy of Paleozoic oceanic oxygenation. The temporal

distribution of ironstone suggests global shifts in the Devonian led to the demise of redox stratification and ferruginous upwelling at that time. As such, our data support models advocating for a continuation of the oceanic oxygenation that began in the Proterozoic through at least the Devonian when modern levels were finally attained. As a result, the Cambrian-Devonian was a unique interval in which metazoan life on oxygenated continental shelves was at least transiently juxtaposed against anoxic deep waters, a delicate balance that made the oceans prone to repeated extinctions.

Magmatic-hydrothermal gold systems and multistage metallogenic processes in the Neoarchean Abitibi greenstone belt

Lucie Mathieu[1]

[1]Université du Québec à Chicoutimi (UQAC) lucie1.mathieu@uqac.ca

In Neoarchean greenstone belts, gold deposits generally correspond to orogenic gold systems (OGS) formed during the main deformation stage that led to craton stabilization. Most OGS deposits postdate and locally overprint magmatic-hydrothermal systems such as Au-Cu porphyry and polymetallic intrusion-related gold systems (IRGS). Porphyries are associated with tonalite-dominated and sanukitoid plutons, while most IRGS are related to alkaline magmatism. In addition, intrusion-associated mineralization, in the Abitibi greenstone belt, can result from complex and locally multistage metallogenic processes. In most cases, however, metallogenic models remain debated and the aim of this review is to provide an overview of gold mineralizing processes in the Abitibi belt. A new classification is proposed, which includes: 1) OGS and OGS-like deposits dominated by metamorphic and magmatic fluids, respectively; 2) porphyry and IRGS, that may contain gold remobilized during subsequent deformation episodes; and 3) multistage systems that correspond to porphyry or IRGS overprinted by OGS. Some porphyry, such as the Côté-Gold deposit, demonstrate that magmatic systems can generate economically significant gold mineralization. Other pre-deformation magmatic-hydrothermal systems post-date or are coeval with Au-bearing volcanogenic massive sulfide (VMS) mineralization. As well, many deposits display evidences for multistage processes and the source of gold remains debated. Whether magmatic activity was essential or marginal to fertilize the upper crust during the Neoarchean era remains a major topic for future researches and petrogenetic investigations may be paramount to distinguish gold-endowed from less-endowed greenstone belts. It is also suggested that prolonged magmatic activity during the main deformation stage, especially in the southern part of the studied belt, may explain part of the gold-endowment of the Abitibi greenstone belt.

[Fig. 1: next page]

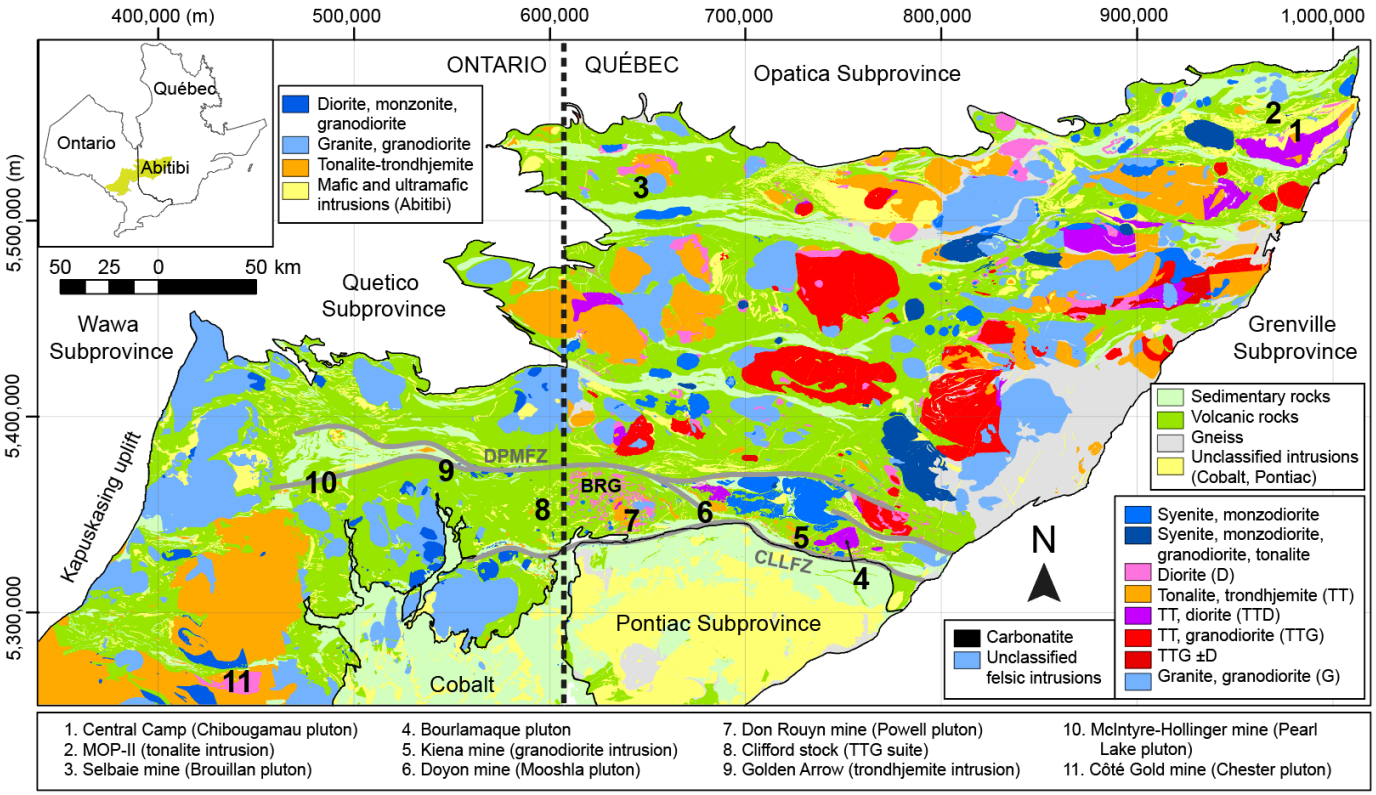

1. Central Camp (Chibougamau pluton)
2. MOP-II (tonalite intrusion)
3. Selbaie mine (Brouillan pluton)
4. Bourlamaque pluton
5. Kiena mine (granodiorite intrusion)
6. Doyon mine (Mooshla pluton)
7. Don Rouyn mine (Powell pluton)
8. Clifford stock (TTG suite)
9. Golden Arrow (trondhjemite intrusion)
10. McIntyre-Hollinger mine (Pearl Lake pluton)
11. Côté Gold mine (Chester pluton)

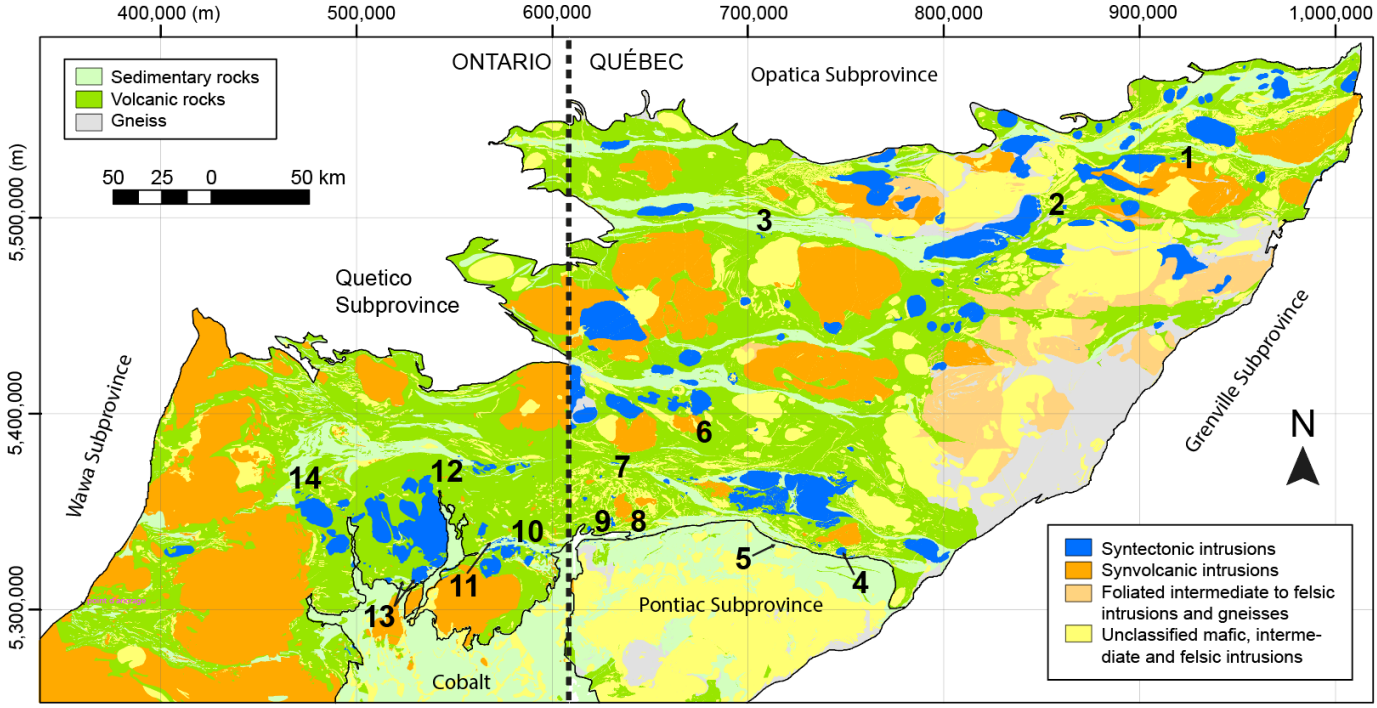

1. Dolodeau project
2. Lac Shortt; Boyvinet stock; Bachelor mine (O'Brien pluton)
3. Douay (syenite)
4. East Sullivan pluton
5. Canadian Malartic mine
6. Launay pluton
7. Beattie mine (syenite)
8. Silidor mine (Powell pluton)
9. Wasamac mine (syenite)
10. Upper Beaver
11. Lake Shore mine (syenite); Macassa mine (syenite); Kirkland Lake mine (syenite)
12. Ross and Kelore mines
13. Young-Davidson (syenite); Matachewan Consolidated; Cairo stock (syenite)
14. Hwy-44 property (syenite); Thunder Creek (syenite)

Mineralogical and geochemical characterisation of the Kipawa peralkaline complex: implications for rare-earth element deposits in peralkaline complex

Simon Matte[1], Ross Stevenson[2], Marc Constantin[1]

[1]Université Laval simon.matte.2@ulaval.ca, [2]Université du Québec à Montréal

The Kipawa rare-earth element (REE) deposit is located in the Parautochton zone of the Grenville Province 55 km south of the boundary with the Superior Province. The deposit consists of 10.2Mt proven reserves (0.44% total Rare Earth oxides - TREO) and 9.6Mt probable reserves (0.38% TREO). The deposit is part of the Kipawa syenite complex of peralkaline syenites, gneisses, and amphibolites that are intercalated with calc-silicate rocks and marbles overlain by a peralkaline gneissic granite. The Kipawa Complex outcrops as a series of thin, folded sheet imbricates located between Kikwissi Suite rocks, McKillop Lake sequence and Red Pine Chute gneiss, suggesting a regional tectonic control. A number of hypotheses for the origin of the complex have been suggested: crustal contamination, dominant crustal origin, fluid alteration, metamorphism, and hydrothermal activity. Our objective is to characterize the mineralogical, geochemical and isotopic composition of the Kipawa complex in order to improve our understanding of the formation, the post-formation processes, and the age of the complex. The REE deposit is principally composed of eudialyte, mosandrite and britholite, and less abundant minerals such as xenotime, monazite, chondrodite or euxenite are also present. Complex silicates rich in REE-HFSE, such as eudialyte and mosandrite, are present in syenites and amphibolite, whereas REE-HFSE oxide, phosphate and britholite was observed in marbles and calc-silicate rocks. We have identified three types of mosandrite which we characterized by electron microprobe. The three species belong to the seidozerite supergroup and are: 1) mosandrites poor in Na and rich in H2O, 2) Rinkite-Ce, rich in Na and REE and 3) Hainite-Y, rich in Na and Y. REE and F-rich minerals identified as belonging to the apatite family include fluorapatite, rich in P, Ca, F and REE, fluorbritholite, rich in Si, REE and F, fluorcalciobritholite, an intermediate mineral species between fluorbritholite and fluoapatite, rich in P, Si, F, Ca and REE, and britholite-Ce, rich in LREE and Si. Major and trace element geochemistry obtained by ICP-MS suggest the granitoids of the complex are within plate A2 type anorogenic granites, and our analyses indicate a strong crustal signature based on TIMS whole rock Nd isotopes (εNd = -8.7). We have analyzed crystals of zircon by SEM, EPMA, ICP-MS and MC-ICP-MS coupled with laser ablation (Lu-Hf). Initial isotopic results also yield strong crustal signatures with εHf values of -23 to -32. The Kipawa complex differs geochemically and petrologically from other well-know peralkaline complex. Classic peralkaline complexes such as the Illimaussaq, Lovozero, Khibiny and Thor Lake complexes have isotopic signatures reflecting a mantle origin with different degrees of crustal contamination and assimilation (e.g., Illimaussaq has εNd values of 0.4 to -5.7) and are largely circular igneous complexes.

GOLD-SULFIDE MINERALIZATION OF THE MANITANYRD REGION, POLAR URALS, RUSSIA

Tatyana Mayorova[1], Sergey Kuznetsov[2], Ludmila Efanova[2], Natalia Sokerina[2]

[1]Institute of geology FRC Komi SC UB RAS, Syktyvkar, Russia, mayorova@geo.komisc.ru, [2]P. Sorokin Syktyvkar State University

The Manitanyrd gold ore region, located on the western slope of the Polar Urals, is one of the industrially promising and interesting because of finding evolutionary laws of hydrothermal ore formation. Geologically the Manitanyrd region is NE oriented anticline. The area is composed of Late Riphean-Vendian volcanic rocks and Late Vendian-Early Cambrian volcanic-sedimentary deposits crossbedding by Late Cambrian-Early Ordovician sedimentary rocks. Intrusive rocks are represented by Early Ordovician gabbrodolerites. The Niyayu ore zone stretches NE-SW across the entire region. Structurally, this is a zone of close tectonic dislocations of NNE strike and characterized by a high rock fracturing, widespread shistosity zones, metasomatic changes (chloritization, epidotization, silicification, pyritization). All major gold occurrences are located within the Niyayu ore zone. Gold-sulfide and gold-sulfide-quartz vein and vein-disseminated mineralization is localized in Pre-Ordovician volcanic and volcanic-sedimentary rocks and controlled by faults. The gold sulfide ores are predominantly arsenopyrite-pyrite by the mineral compostion. Chalcopyrite, sphalerite, galena are abundant. Secondary minerals include pentlandite, tetrahedrite, tennantite, aurostibite, native bismuth, and rare minerals sulfosalts (hysenite, aikinite, boulangerite), sulfoantimonides (ulmanite). Gold is observed as the smallest isometric inclusions of 1-5 microns in size in arsenopyrite, less often in pyrite. At the same time, we noted both small and relatively large (up to 10-50 microns) elongated, irregular gold particles located in microfractures in pyrite and arsenopyrite, often together with chalcopyrite, galena, sphalerite. The main elements-impurities in gold are silver, mercury and copper. The formation of gold-sulfide and gold-sulfide-quartz mineralization, associated with hydrothermal processes, was staged. First, the gold-pyrite-arsenopyrite stage occurred. Then, after a pause and tectonic movements, the gold-galena-chalcopyrite-sphalerite stage with larger gold took place. According to the study of fluid inclusions, mineral formation occurred within 400-70º C. The sulfur isotopic composition ?34S varies within -0.5 to -8.0 ‰. Values close to -0.5 ‰ correspond to the meteorite standard, which testifies to the participation of hydrothermal-magmatogenic fluids in the ore formation. The processes of regional metamorphism of the greenschist facies, which affected all rocks of the region in the Paleozoic and could also initiate hydrothermal flows, mobilization and deposition of various components, very likely played an important role.

The reported study was funded by RFBR and Government of the Komi Republic, project number 20-45-110006.

Paleoarchean sedimentation and volcanism on Singhbhum craton, India: insights from the Iron Ore Group of rocks

Rajat Mazumder[1], Trisrota Chaudhuri[2]

[1]German University of Technology in Oman rajat.mazumder@gutech.edu.om, [2]University of Calcutta

The Singhbhum craton in eastern India and bears geological record from Paleoarchean to Neoproterozoic. The Paleoarchean Iron Ore Group (IOG) of rocks of low metamorphic grade (greenschist facies) are distributed in three distinct belts encircling the Singhbhum granitoid batholith (the eastern (EIOG), the western (WIOG) and the southern (SIOG) belts) and contain banded iron formation as one of the most important lithologies. While the SIOG succession contains deeper water turbidites, deictic volcaniclastics and mafic-ultramafic associations, the WIOG succession is characterized by terrestrial (alluvial fan-fluvial) to shallow marine largely siliciclastics (with minor dolomite)-mafic (minor felsic) volcanic association. The EIOG succession bears both terrestrial to shallow marine sediments as well as relatively deeper water turbidites. The komatiite-basalt association of the EIOG belt has petrological and geochemical similarities with the Barberton greenstone ultramafic-mafic volcanic associations. Paleoarchean sedimentary record is very limited and fluvial interpretation of a few Paleoarchean successions is highly ambiguous (Long, 2019). In contrast, the IOG fluvial successions have the potentiality to undertake the architectural analysis of early river systems. Although preliminary sandstone petrography reveal a tectonically stable depositional setting during the WIOG sedimentation, detailed provenance studies of the three IOG successions is essential to infer the source rock, paleoclimate and tectonic setting during early history of earth and the extant crust-mantle interactions.

The palynological record of Crawford Lake (Ontario, Canada) and its application to the stratigraphic definition of the Anthropocene Epoch

Francine McCarthy[1], Autumn Heyde[1], Paul Michael Pilkington[1], Andrea Krueger[1], John McAndrews[2], Charles Turton[2], William Finlayson[3], Nicholas Riddick[1]

[1]Brock University fmccarthy@brocku.can [2]University of Toronto, [3]Wilfrid Laurier University

Varves provide an annually resolvable record of Earth history in the deep karstic basin of Crawford Lake on the Niagara Escarpment. Samples processed for palynological analysis without the use of harsh oxidants contain a rich, diverse assemblage of non-pollen palynomorphs that provide insights into this highly unusual meromictic lake ecosystem as well as pollen that records changes in vegetation resulting from climate and land use changes. This natural archive records the response of this small, deep naturally oligotrophic lake to settlement in its watershed, initially by Iroquoian people who grew maize, sunflower, and other crops (known from their pollen and from the spores of fungal pathogens that affected them) and subsequently by colonial settlers who cleared land and milled lumber in the late 19th - early 20th century. The varved sequence is currently under investigation as a potential GSSP to define the proposed Anthropocene Epoch. In addition to the unusual accumulation of varves in an oxygenated environment (see Llew-Williams et al., this session) the clear evidence of anthropogenic impact in the well-dated record that can be correlated with archeological and historic records is an attractive feature, illustrating the difference between anthropogenic impact at a local scale and at a global scale, associated with the Great Acceleration, which is recorded by many proxies in the varved sequence of Crawford Lake.

Will the real Ediacaran paleopole please stand?

Phil McCausland[1]

[1]Western University pmccausl@uwo.ca

Despite its many successes as a primary tool for determining paleogeography and the past behaviour of the geodynamo, paleomagnetism has proven to be more difficult for some periods of Earth's history. The Ediacaran (635-539 Ma) has perhaps been the most resistant to paleomagnetic analysis, featuring puzzlingly discordant and inconsistent directional results from within a number of cratons involved in the dispersal of the supercontinent Rodinia, making paleogeographic reconstructions hard to resolve. Many workers have invoked nonuniformitarian solutions to explain apparent ~90° shifts in locally-observed paleomagnetic directions and between paleopoles, including episodes of large scale true polar wander or the existence of a dominantly non-axial (equatorial) dipole geomagnetic field. That this problem still defies resolution after more than two decades of dedicated attention suggests that the Ediacaran Period truly does represent an unusual, and potentially informative, part of the secular evolution of Earth's geodynamo and thermophysical regime. Recently published paleointensity and paleomagnetic results suggest that the Earth's paleofield had extraordinarily low intensity during the mid-Ediacaran, perhaps representing a near collapse of the dipole and/or an unusually rapid reversal rate. Apparently primary and nearly coeval discordant paleomagnetic directions mark shifts that may be too rapid to explain by true polar wander, which is rate-limited by relaxation of the Earth's equatorial bulge. It is therefore useful to consider what might be observed for weak geocentric axial dipole (GAD) or possibly non-GAD paleofield geometry during the Ediacaran. Examining the mid-Ediacaran directional record of Laurentia and Baltica paleomagnetic results, some useful collective features emerge: 1) After removing steep present-day viscous remanence overprints, most paleomagnetic results still have sites which display well-defined steep directions, some with reverse polarity, which -assuming GAD- place Laurentia and Baltica at high paleolatitudes. 2) Many results also have much lower inclination site mean directions with some scatter lying in the SE quadrant, or NW reversed; these have often been taken to represent the `true' GAD result, placing Laurentia and Baltica at low paleolatitudes. 3) Some results show distinct high- and low-inclination site groupings, whereas others show streaking of directions from high to low inclination, even within sites. Considering what would be recorded during a mid-Ediacaran weak or non-existent GAD paleofield, it is possible that results from slow-cooling intrusions with long (myr) integration times may record the dipole poorly or not at all, and be prone to recording standing non-dipole components such as steep regional octupolar flux, or even crustal fields. Results from much faster-cooling dykes may represent switching between a reversing dipolar paleofield and snapshots of other components in the relative absence of a dipole. The real Ediacaran paleofield may be stranger, but more understandable, than expected!

Tectonometamorphic evolution of the Kluane basin, Northern Canadian Cordillera

Will Mckenzie[1], Brendan Dyck[2], H. Daniel Gibson[1]

[1]Simon Fraser University wmckenzi@sfu.ca, [2]UBC Okanagan

A wealth of information related to the disputed Mesozoic configuration of the Northern Cordillera is held within a series of inverted Jura-Cretaceous basins. The structural and metamorphic evolution of these basins may prove key to understanding the timing and style of Insular terrane accretion. Two competing models accounting for the development and tectonic significance of these basins are: 1) these basins were all interconnected and part of a larger 2000-4000 km wide ocean that closed through west-dipping subduction during the latest Jurassic to Early Cretaceous, or 2) these basins represent a series of en echelon pull-apart basins that developed along a strike-slip fault system at the interface between the previously accreted Insular and Intermontane terranes. The Kluane Metamorphic Assemblage (KMA), SW Yukon, represents the remnants one of these inverted Jura-Cretaceous basins. Comprised of variably metamorphosed and deformed pelitic and psammitic units that were intruded by granodioritic plutons of the Paleogene Ruby Range Batholith (RRB), the KMA preserves a complex metamorphic history of both regional and contact events. Previous work documented a large thermal aureole related to the RRB emplacement. Our work, however, indicates that the KMA reflects an oblique section through a prograde Buchan-style metamorphic sequence with static recrystallization associated with the RRB restricted to < 1km of its intrusive contact. Detailed petrographic analysis suggests that the KMA represents a single lithological package which experienced two distinct phases of deformation and metamorphism: an early greenschist-facies phase that resulted in the development of a bedding-parallel chlorite-epidote fabric, and a later amphibolite-facies phase that demonstrates a progressive transposition of an oblique chlorite-muscovite fabric to a biotite-sillimanite-K-feldspar-melt gneissosity. Isograds relating to this second event show continuity across the KMA with monazite petrochronology suggesting protracted amphibolitefacies metamorphism coeval with intense coaxial flattening and tops to the WSW shear from 90-55 Ma. This aligns with previous zircon geochronology concluding the KMA was deposited after 94 Ma and experienced two significant metamorphic events at 82 Ma and 70 Ma. We aim to build on current KMA petrochronology, increasing the resolution of zircon datasets and investigating titanite, found abundantly within lower-grade samples. The preservation of a single Buchan-style field gradient, tops to the WSW shearing and distinct lithological homogeneity across the KMA are at odds with the basin representing an extensive 2000-4000km wide ocean that closed though west-dipping subduction. Our results are more consistent with a model of post-accretionary back-arc spreading, developing a basin of limited width, atop an already thermally matured pre-mid-Cretaceous magmatic arc.

Geoheritage Day 2021: how a pandemic brought a local initiative across Canada

Beth McLarty Halfkenny[1]

[1]Carleton University beth.mclartyhalfkenny@carleton.ca

Geoheritage Day 2021: how a pandemic brought a local initiative across Canada Geoheritage Day is an initiative began as a way for the Carleton University's Earth Sciences Department to engage with the public at some of the wonderful local parks and green spaces to highlight the local geological history. It began as a big idea, in partnership with the Ottawa-Gatineau Geoheritage Project in 2008, and has occurred annually since. Our undergraduate and graduate students, staff, faculty and retired geoscientists play host at various geologically significant locations around the region for 5 hours on a sunny Saturday in October, to speak to the public and explain how geological processes have shaped the regional landscape, given us a glimpse into past environments and life forms and provided resources for our use. In pre-COVID times, this event was in-person, place-based inquiry learning at its best, with 25 volunteer experts and aspiring experts bringing their knowledge and enthusiasm to the event. Each group was provided with volunteer t-shirts, rock, mineral and fossil specimens that might help illustrate the features on outcrop, as well as maps and diagrams. Visitors were encouraged to visit more than three of up to nine locations across the National Capital Region for a chance to win a Quentin Gall's Ottawa Building Stones book. This also gave our students an opportunity to speak about their subject of study, pass along their passions, and build a love for service to their community. As has been the case with other such in-person events, it was not possible to run Geoheritage Day in the same way in 2020. It did however give us an opportunity to imagine what we could do in a digital environment. After some experimentation last October, we were able to come up with a formula that we think will both enhance our future in-person event, and expand the possibilities for other communities across Canada to join us. Geoheritage Day 2021 was a virtual event based around a new Geoheritage Day website, complete with the usual Google map of publicly accessible interesting geological sites in the National Capital Region, expanded to include geosites all over the Canada. Canada's Geoparks Network, University Earth Science Departments and other geoheritage enthusiasts have provided images and information for their favourite spots to add to the map. We have also discovered wonderful virtual field trips and built our own Google Earth Virtual Tour of the sites in the Ottawa/Gatineau Region. We feel the potential for this initiative is unlimited. Local groups can highlight interesting geology of their area and Canada's publicly accessible geosites can be documented creating a National register. We are excited by the possibility of combining this effort with the soon to be approved UNESCO International Geodiversity Day connecting more people to the geology around them, ultimately improving Earth Science literacy. We hope you will join in this exciting initiative.

The Canadian Geoscience Education Network at 25: Who we are and what's next

Beth McLarty Halfkenny[1]

[1]Canadian Geoscience Education Network beth.mclartyhalfkenny@carleton.ca

The Canadian Geoscience Education Network (CGEN) celebrates its 25th anniversary in 2022. Founded to increase public awareness of Earth Science, CGEN is the education arm of the Canadian Federation of Earth Sciences (CFES). Powered by enthusiastic volunteers from all sectors of geoscience, CGEN's initiatives seek to improve Earth Science literacy by promoting and supporting the teaching of Earth Sciences at all levels of education across Canada, to encourage Earth scientists to be involved in education and outreach, and to encourage and support activities that increase public appreciation of the study of our planet. The organization is open to anyone interested in forwarding these goals in Canada. Membership has included those working in industry, academia, government, education and communication. CGEN provides a forum for information exchange, a place to share ideas and challenges within a coordinated network of like-minded individuals and groups. EdGEO Canadian Earth Science Teacher Workshop Program is a principle activity of CGEN, supporting teacher professional development workshops, providing funding and teaching resources for locally organized, curriculum-specific teacher training. Since 1976, EdGEO funding has allowed teachers to gain knowledge, resources and confidence to teach Earth science components of their curriculum. EdGEO grants are awarded annually to Local Organizing Committees for workshops and field trips associated with the GAC-MAC conferences, designed for teachers in the region, like the one taking place at GAC-MAC London 2021. The Geoscientists in Canadian National Parks is a new initiative, in partnership with Parks Canada, to place geoscience expertise within our National Parks. As you are all aware, Canada's National Parks were chosen and inscribed in most cases, due to their exceptional geology, and it is important to help Park Interpreters bring this key aspect back to public attention. The first pilot project will take place during two weeks in August of 2022 at Pukaskwa National Park in Ontario. The successful applicant will assist the Park staff in identifying and interpreting the geological assets of the Park. Volunteer expenses are funded by a generous grant from the Association of Professional Geologists of Ontario Education Foundation. We anticipate the successful pilot will encourage other National Parks to adopt this program at their sites. A call for applications will take place in February. We are currently undertaking a Strategic Planning Exercise that will inform the way forward for CGEN into the next quarter century. At a time when geoscience faces a crisis in public perception, and geoscientists are needed to support Canada's response to global challenges, Earth science communication, education and outreach are needed more than ever. A special session at GAC-MAC 2022 in Halifax will include talks related to the history of geoscience education and outreach in Canada, the presentation of the new CGEN Strategic Plan, and time to workshop an actionable plan. We hope you will join us.

The CIA goes to Mars

Scott McLennan[1], Christopher Fedo[2], Kirsten Siebach[3]

[1]Stony Brook University Scott.McLennan@stonybrook.edu, [2]University of Tennessee, [3]Rice University

The actions of sedimentary processes have been observed on the surface of Mars since return of the first high resolution images (e.g., Mariner-9), but the presence of an ancient (Noachian/Early Amazonian ~ Late Hadean/Early Proterozoic) lithified sedimentary rock record has been recognized only for the past two decades. In that short time, this record has been shown to include a variety of subaqueous and subaerial depositional environments (fluvio-deltaic-lacustrine; wet and dry aeolian), exhibiting varying degrees of groundwater-mediated diagenesis and influenced by variable and likely cyclical climatic conditions. The so-called CIA (Chemical Index of Alteration) concepts (e.g., A-CN-K and A-CNK-FM diagrams), pioneered by Wayne Nesbitt and Grant Young have not only revolutionized our ability to understand the terrestrial sedimentary record, they have also proven to be of great value in interpreting this Martian sedimentary rock record. The provenance of Martian sedimentary rocks is variable in detail but fundamentally basaltic in character. Among the consequences of this is that sedimentary sorting processes are far more important in governing major element compositions. Unlike Earth, where common framework detrital grains (quartz, K-feldspar, plagioclase) differ in density by only a few percent, common basaltic detrital grains (olivine, plagioclase, pyroxene, Fe-Ti-oxides) may differ in density by nearly a factor of two, leading to distinctive "unmixing" trends on A-CNK-FM and other geochemical diagrams due to framework mineral sorting. Evaluating chemical weathering processes in Martian rocks using CIA concepts presents special challenges. In terrestrial sedimentary rocks, chemically precipitated constituents are dominated by carbonate (calcite, dolomite) and minor phosphate (apatite) and the necessary corrections for non-siliciclastic components are relatively straight-forward. In stark contrast, for Mars, carbonates appear to be rare and phosphates are more abundant but their mineralogical character is poorly characterized. Instead, Martian sedimentary rocks contain a wide variety of highly variable chemical constituents, including Fe-, Mg- and Ca-sulfates, perchlorates, chlorides and Fe(-Mn_x)-oxides. In addition, Martian sedimentary rocks typically contain 25-40% of compositionally variable and S-bearing amorphous components whose phase relationships and origins are complex and poorly understood. Accordingly, strategies have been developed to characterize A-CN-K and A-CNK-FM relationships by focusing on low-S samples or systematically applying non-siliciclastic corrections where mineralogy is quantitatively characterized independently. It appears that the Martian sedimentary record has been influenced by relatively modest (by terrestrial standards) but variable degrees of chemical weathering indicating climate variability that occurred on timescales broadly comparable to the cyclical timescales observed on Earth.

New insights into Keewatin glacial landsystems

Isabelle McMartin[1]

[1]Geological Survey of Canada isabelle.mcmartin@canada.ca

In the former glaciated areas of central mainland Nunavut west of Hudson Bay, large volumes of ground-based datasets and high-resolution remote sensing imagery were recently integrated to allow interpretation of glacial landsystems. This central part of the Laurentide Ice Sheet (LIS) holds the key to accurate paleo-ice sheet reconstructions due to its sheer size, presence of the Keewatin Dome and its effects on modelling glacio-isostatic adjustments (GIA), and diversity of glacial landform assemblages and patterns. From the early field observations of Tyrrell suggesting a "Keewatin Glacier" to the remote compilations of cross-cutting glacial lineations, and the recognition of important glacial landmark features such as the Keewatin Ice Divide, the Dubawnt dispersal train and the Dubawnt Lake Ice Stream, the recent history of this region has always fascinated glacial geologists and generated important discussions. Debates on the stability of the Wisconsinan ice cover in Hudson Bay, the location of ice divides and saddles radiating from a central dome, the timing of the giant radial esker system and the style of deglaciation still continue today. Recently, increased field-based research on glacial dynamics, relative sea level variations and chronology, and glacial sediment provenance, have contributed to refining the configuration and paleoglaciological evolution of the Keewatin Sector of the LIS. The advent of high-resolution digital elevation models such as ArcticDEM (2 m) and the development of innovative techniques for dating glaciated terrains provide a timely opportunity to synthesize previous work, produce new maps of glacigenic features and interpretations of glacial landsystems, and identify gaps in knowledge and outstanding issues. This presentation will briefly review the development of mapping approaches and concepts in Keewatin, and summarize the latest identification of various glacial landsystems, including ice streams, palimpsest streamlined landscapes, and terrains where basal ice thermal regimes fluctuated between cold-based and warm-based, in an effort to provide constraints on the glacial history of Keewatin and numerical modelling of the LIS.

GEOCHRONOLOGY OF SEAFLOOR HYDROTHERMAL SULFIDES FROM MID-OCEAN RIDGES

Natalie McNeil[1], John Jamieson[1], Jenny Maccali[2], Desiree Roerdink[2]

[1]Memorial University of Newfoundland ncmcneil@mun.ca, [2]Universitetet i Bergen

Submarine hydrothermal systems are host to accumulations of metal-rich sulfide deposits on the seafloor. The rate of formation and temporal evolution of these deposits can be investigated by determining the ages of the deposits. The 230Th/234U dating technique is the most commonly applied chronometer for determining the ages of accumulations of submarine sulfide minerals. Here, we will present results of 1) 230Th/234U dating of samples collected from several seafloor vent fields for which no age data is yet available; and 2) results of comparisons of 230Th/234U ages to ages already obtained using other radioisotope dating techniques (e.g., 226Ra/Ba). Three locations have been chosen for dating using the 230Th/234U dating method; Endeavour, on the Juan de Fuca Ridge; 9°50'N, on the East Pacific Rise; and Loki's Castle, on the Arctic Mid-ocean Ridge system. Ages determined from the 230Th/234U dating method: i) provide insights into the longevity of hydrothermal systems, ii) test the hypothesis that hydrothermal systems turn on and off over time, iii) provide data to assess the metal fluxes to the ocean, and associated sulfide mass accumulation rates, iv) link hydrothermal venting to tectonic and volcanic process at MORs, and v) help evaluate the sustainability of seafloor mining.

Reactive and Non-Reactive Components of Classic Alkali-Silica Reactive Concrete Aggregate Differentiated using ^{29}Si MAS NMR

Deborah McPhedran[1], Roberta Flemming[2]

[1]Sci-Tech Translations deborah.mcphedran@gmail.com, [2]University of Western Ontario

Alkali-silica reactivity is a deleterious expansive reaction sometimes seen in Portland cement concrete, that can occur between the high alkali pore solution of the concrete and certain aggregates. This expansion can lead to consequences that can be tolerated under some circumstances, such as in temporary structures with design lifespan under five years, but can not be tolerated in the case of significant concrete infrastructure projects such as major bridges, dams, tunnels, or nuclear power plants. One of the three ways to prevent ASR deterioration in concrete structures is to avoid using reactive aggregate. Since the approved standard concrete prism test for ASR takes a year to complete, quicker methods for characterizing ASR reactive aggregate and ultimately assessing aggregate materials are still needed. This is a contribution to the existing methods for differentiating between ASR reactive and non-reactive aggregate. Six samples representing standards and concentrates derived from concrete aggregate materials of known alkali silica reactivity (ASR) behaviour in concrete were selected for ^{29}Si MAS NMR spectroscopic investigation. Three samples represented spectacularly ASR reactive aggregates, the Potsdam Sandstone (quartz cement) (Chateauguay, QC), the Adam's Mine Taconite (chert) (Kirkland Lake, ON) and the Spratt Limestone (siliceous fossil fragments) (Carp, ON), with the last having the distinction of being a Ministry of Transportation Ontario (MTO) reactive standard used in ASR research. Two samples were suspected or known to be non-reactive aggregates, the Potsdam Sandstone (quartz grains) (Chateauguay, QC), and the Charlevoix Quartzite (La Malbaie, QC), the latter having the distinction of being a Université Laval non-reactive standard used in ASR research. We ran a sixth sample comprised of fine sand-sized detrital materials stemming from sample preparation of the Spratt Limestone. ^{29}Si MAS NMR spectra for all six samples produced a single peak at -107.3 ppm. Full Width at Half Maximum (FWHM) of these peaks can be divided into two groups: ASR reactive aggregates exhibited wide FWHM, of 60-68 Hz for Potsdam cement, 63-64 Hz for Taconite chert and 75 Hz for Spratt coarse fragments, while ASR non-reactive aggregates exhibited narrow FWHM of 17 Hz for the Quartzite, and 25 Hz for Potsdam grains. The results for the sixth sample, Spratt fine sand-sized detritals, fell into the mid-range of observed FWHM at 55 Hz.

Glacial Microsedimentology - a new lens to investigate Glacial Sediments - a review

John Menzies[1]

[1]Brock Univeristy jmenzies@brocku.ca

Studying sediment thin sections began in the early 20th century. The critical issue was in making viable thin sections. Production techniques are no longer an obstacle. Work with glacial sediments began post-World War II. With new epoxy resins etc., glacial micromorphology began to evolve in the 1970s. Glacial microsedimentology seeks to examine sediments at the microscopic level to derive insights into the processes of glacial erosion, transport, and deposition. Two issues are (1) the inability of some to recognize and utilize the microstructures in thin sections through possibly a lack of effort; and (2) an absence of quantitative data that makes reproduction of data difficult. (1) The result of non-recognition is largely the need to a re-assess new techniques often never been applied to sediments during training - a kind of 'tunnel vision'. Only when the value of these studies can be demonstrated will the 'effort' be made. The lack of quantitative data acquisition (2) is a much harder issue to resolve as a more sophisticated methods need to be applied to thin sections. This requires image capture and software methodologies that are now becoming available at reasonable costs. Thin sections are two-dimensional sections through three-dimensional objects, and this must be remembered when measurements, fabrics and other data are assessed. Research into the micro-aspects of glacial sediments followed a typical scientific trajectory. First, thin sections were described with little uniformity, with no common 'language' for observed structures. Secondly, the need for standardization developed allowing comparison between different sediments. Thirdly, with standardization, came the need to classify what was observed. Any classification or taxonomic framework must be open-ended as more structures are observed. Fourthly, the need for cross-comparison with multiple thin sections of similar sediments demands a quantitative means of study. Rather than simply a study of the relationship between individual components in thin section, it became apparent that the basic principles of structural geology had to be applied. Thus, micromorphology has subsumed into a microsedimentological study of glacial sediments where stress parameters, structural fabrics and the mapping of deformation structures and contextual integration allows an understanding of how these sediments have been formed. Microsedimentology is increasingly being used as a primary tool for analyses of glacial sediments. The technique provides far greater detail on depositional and deformation histories of these sediments than obtained from macroscale studies alone in unravelling deformation histories of glacigenic sequences. Examples of the development stages of glacial micromorphology / sedimentology are presented here as well as discussion of future avenues of study.

A micromorphological perspective on Neoproterozoic diamictites, Neoproterozoic?Tremadocian sequence of the Gaissa Basin, Varangerfjord, Norway

John Menzies[1]

[1]Brock Univeristy jmenzies@brocku.ca

There is an accumulating weight of evidence that supports the concept that many Neo-Proterozoic diamictites in both the Northern and Southern Hemispheres are glacial in origin (Young, 2018). However, many diamictites are thought to be mass movement deposits either on land or submarine are non-glacial. Part of the discussion on the nature of Neoproterozoic climate change has been, and continues to be, focused on the controversial origin of diamictite-bearing strata and the criteria used to determine the extent and nature of glacial influence on their deposition. On a macroscale, sediments (diamictons/diamictites) deposited beneath palaeo-ice masses are massive, lacking few, if any, visible signs of stratification or glacially applied deformation signatures. The use of microscopic investigations has resulted in specific structures and sedimentary structures indicative of the impact of glacial stress during and following glacial deposition. Case examples derived from diamictites of the Neoproterozoic in Varangerfjord, Norway have been investigated. Analyses of these diamictites provide strain signatures of 'unique sequences' of microstructures imparted by the palaeo-ice flow. This technique, relatively new to Precambrian research, can deliver far greater detail on the depositional and deformation histories recorded by these diamictites than obtained from macroscale studies. The technique allows the unscrambling of composite deformation histories of potential glacigenic and non-glacigenic sequences. Many, if not all, of these microstructures can be observed within most diamictons/diamictites. However, it has also been demonstrated that diamictons /diamictites, both glacigenic and non-glacigenic, contain these microstructures and can be statistically segregated based on a specific 'set' of summative structures present in any individual sediment. At Varangerfjord 5 thin sections were analyzed and presented here such that each provided a slightly different perspective on the diamictites from this area. The thin sections were examined using combination of quantitative methods.

A revised shock history for the youngest unbrecciated lunar basalt Northwest Africa 032 and paired meteorites

Tatiana Mijajlovic[1], Xie Xue[2], Erin Walton[2]

[1]University of Alberta tkopchuk@ualberta.ca, [2]MacEwan University

Northwest Africa (NWA) 032 is an unbrecciated porphyritic basalt found in the Moroccan desert in 1999 [1]. Constituent igneous minerals--olivine, pyroxene, and plagioclase--exhibit shock deformation and transformation effects. NWA 032 is among the youngest radiometrically dated sample from the Moon, with concordant Sm-Nd and Rb-Sr ages of 2.947 ± 0.016 Ga and 2.931 ± 0.092 Ga, respectively, representing the timing of igneous crystallization [2]. We present the first comprehensive study of shock metamorphism in NWA 032, with a focus on the structural state of fine-grained plagioclase feldspar, shock deformation in olivine and pyroxene, and the microtexture and mineralogy of shock melts. Micro-Raman spectroscopy, optical properties, and electron imaging confirm that plagioclase in this meteorite has been shock amorphized, which, for calcic plagioclase (An80-90), requires shock pressures on the order of ~25-27 GPa. Shock pressures in this range are accompanied by a postshock temperature increase <200 °C [3]. Shock deformation in olivine and pyroxene phenocrysts comprises undulose extinction to weak mosaicism, irregular fractures, polysynthetic mechanical twinning in pyroxene, and development of planar fractures in olivine. The shock effects in mafic minerals constrain the upper limit of shock in NWA 032 to have been <30 GPa [3]. Shock melt in NWA 032 has quenched to glass of basaltic composition, representing localized in situ melting of igneous minerals by shearing along lithological boundaries to form shock veins and shock impedance contrasts to form isolated pockets of shock melt. These melts quench-crystallized olivine and pyroxene during the pressure release (<14 GPa) [4]. Using recent experimental data on shock amorphization of feldspars, coupled with constraints on the formation of metastable minerals associated with shock melt [5, 6], we have revised the shock pressure experienced by paired meteorites NWA 10597, NWA 4734, and LaPaz Icefield 02205/02224/0226/02436/03632/04841. These largely unbrecciated, basaltic meteorites experienced an equilibration shock pressure on the order of ~22-25 GPa, constrained by partial amorphization of precursor igneous bytownite. Our results are consistent with crater pairing and ejection in a single impact cratering event.

References: [1] Fagan et al. 2002. MAPS 37 (3): 371-94. [2] Borg et al., 2009. Geochimica et Cosmochimica Acta 73 (13): 3963-80. [3] Stöffler et al., 2018. MAPS 53 (1): 5-49. [4] Herzberg C., and Zhang J. 1996. Journal of Geophysical Research 101:8271-8295. [5] Rubin, A. E. 2015. Icarus 257: 221-29. [6] Miyahara et al. 2013. Nature Communications 4:737."

Post-depositional mobility of arsenic in a changing climate: implications for cumulative effects assessments at northern mine sites

Clare Miller[1], Michael Parsons[2], Heather Jamieson[3], Omid Ardakani[2], Nawaf Nasser[4], Braden Gregory[5], Timothy Patterson[4], Jennifer Galloway[2]

[1]University of Tasmania clare.miller@utas.edu.au, [2]Natural Resources Canada, [3]Queen's University, [4]Carleton University, [5]University of Ottawa

Climate change is affecting the seasonality, biological productivity, and hydrology of lakes in high northern latitudes. These changes may affect the cycling of naturally occurring metal(loid)s and long-term stability of mining-derived contaminants. In mineralized regions, where concentrations of naturally occurring metal(loids) are commonly above environmental quality guidelines, understanding the transport and fate of elements and the drivers of chemical change is especially relevant to guide cumulative effects assessments at past, present and future mine sites. This study integrates arsenic geochemistry, organic petrography, multivariate analysis of climate proxies (particle size, organic matter type and quantity), and radiometric dating (14C and 210Pb) to determine the influence of modern and late-Holocene (5,000 yr cal BP to present) warming episodes on the loading and cycling of arsenic in lake sediments. Integrated paleoclimate and sediment geochemistry reconstructions of two sediment cores collected from mining-impacted lakes in the Courageous Lake Greenstone Belt, Northwest Territories, Canada, document increases in sediment and porewater arsenic

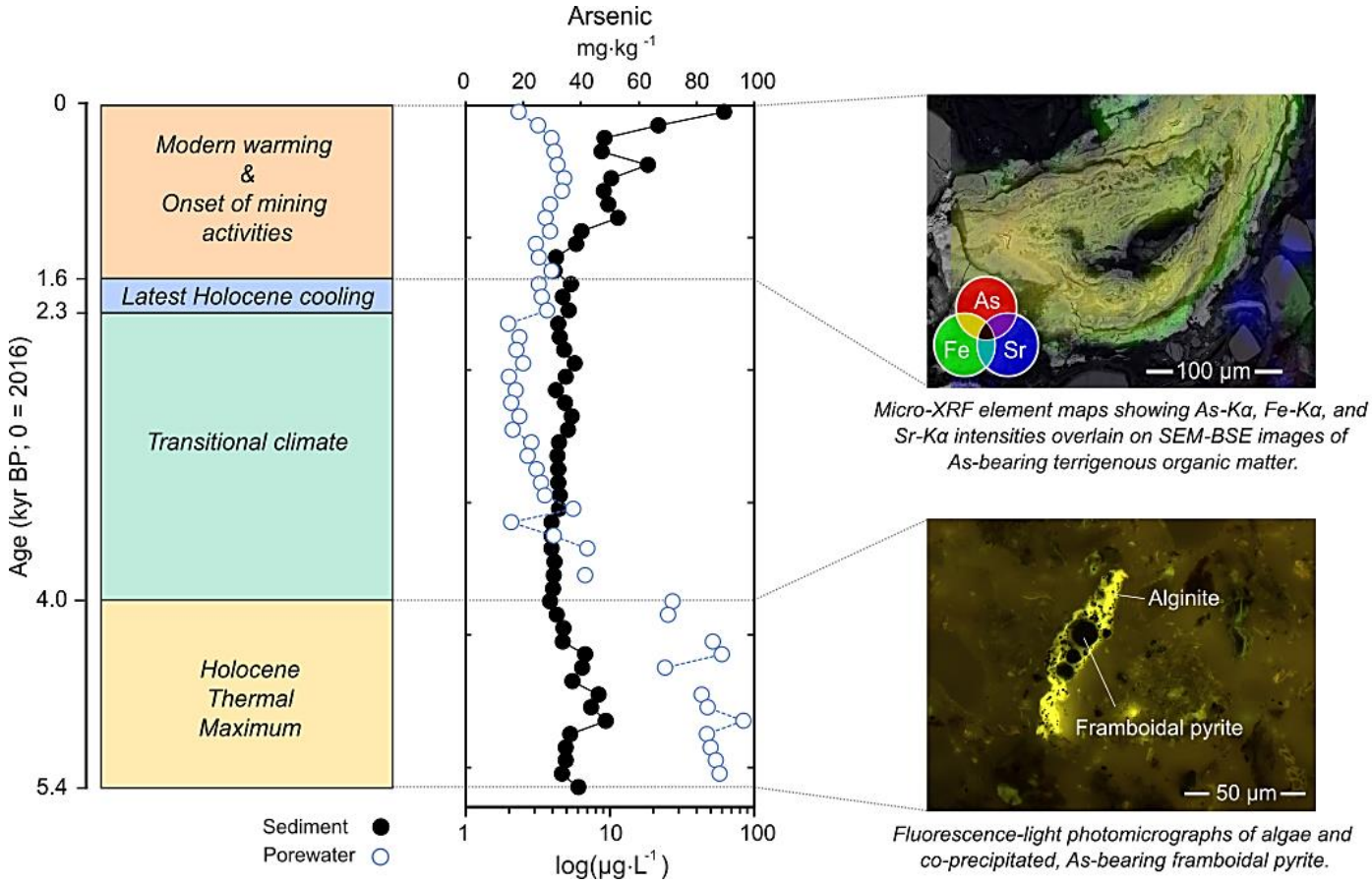

Increased aquatic production and growth of terrestrial vegetation in catchments will enhance the mobility of arsenic in near-surface sediment.

concentrations coincident with periods of climate warming. The presence of both primary arsenopyrite and secondary, authigenic arsenic-bearing minerals (framboidal pyrite and Fe-oxyhydroxides; determined by SEM, EMPA and synchrotron-based bulk-XANES) suggests that enhanced weathering and active remobilization of geogenic arsenic occurred in lake catchments during past warming intervals. Detailed characterization of the solid-phase speciation of arsenic and its association with organic matter shows that organic material plays an important role in stabilizing redox-sensitive authigenic minerals (i.e., sulphides and Fe-oxyhydroxides) in lake sediments. Based on the results of this study, we expect that increased concentrations of aquatic- and terrestrially-derived labile organic matter will drive the redistribution of arsenic in shallow lake sediments and result in surface-enrichment of arsenic. These findings are relevant for predicting future climate change-driven variations in metal(loid) cycling in sub-Arctic lakes. Knowledge from this study can be used to improve environmental monitoring and remediation strategies at northern metal mines.

Using models to understand Earth's oxygenation

Benjamin Mills[1]

[1]University of Leeds b.mills@leeds.ac.uk

Computer models are useful tools for understanding why something happens. My group builds models of Earth's global biogeochemistry and climate, and one of our main focuses is understanding what has driven the rise of oxygen on Earth. It is also possible to use modelling approaches to estimate paleo-atmospheric oxygen levels by leveraging large and detailed datasets that are only indirectly linked to the oxygen cycle. I will discuss both of these approaches and our latest results.

A novel robotic technology for surveying flooded underground mines

Zorana Milosevic[1], Richard Zoltan Papp[1]

[1]UNEXMIN GeoRobotics Ltd. zorana@unexmin-georobotics.com

Increasing interest in reopening abandoned mine sites faces two severe problems: lack of reliable, recent information about the mines' status; and flooding. Initial surveys must be carried out to acquire the topological, structural, and geoscientific data needed for making decisions about reopening. However, a complex network of flooded tunnels is an extremely hazardous environment which makes conventional methods such as human exploration impossible.

A new company UNEXMIN GeoRobotics (UGR) was formed to answer these challenges. UGR's robot, named UX-1, has a spherical shape with a diameter of 0.8 m, an approximate weight of 95 kg, and it can operate at 500 meters depth. It carries various scientific instrumentation, such as multispectral camera; sub-bottom profiler; magnetic field, conductivity, pH, temperature, and pressure measuring units; and water sampler. It is equipped with navigational sensors which enable semi-autonomous surveys. Six cameras give a full 360 degrees high-quality perception of the environment. Furthermore, using photogrammetry techniques, we can produce 3D models of the explored areas. In addition to the cameras, the UX-1 robot has mapping sensors, such as sonar and lidar units, that can create a high-resolution point cloud of the environment and build an accurate 3D map with a few cm resolution.

The UX-1 robot has demonstrated its capabilities in seven different sites: Kaatiala pegmatite mine in Finland, Idrija mercury mine in Slovenia, Urgeirica uranium mine in Portugal, Ecton Cu-Zn-Pb mine in the UK which has been flooded for over 160 years, Molnar Janos cave system in Hungary, Csor water well in Hungary, and Solotvyno salt mine in Ukraine. The most challenging environment was the Solotvyno salt mine, where the robot operated in saturated brine, in a partially collapsed shaft, and with very low visibility. However, it successfully explored a 300 meters deep shaft and built a 3D map.

The completed field trials proved that the UX-1 robot could be used for various applications, such as mineral exploration, geological studies, and surveying different underwater structures. The UX-1 robotic platform can gather high-quality and high-resolution geological, mineralogical, and topological data from inaccessible sites without human risks or environmental impacts.

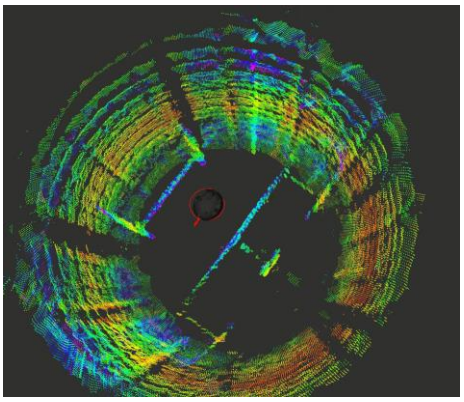

The next generation of the robot, the UX-2, is currently being developed. It will have similar dimensions to the UX-1, but an increased depth rating of 1500 meters, a rock sampler unit, and improved navigational and geoscientific instruments to address even more challenging scenarios.

Acknowledgements: UGR is supported by the UNEXUP project which is funded by EIT RawMaterials, project number 19160.

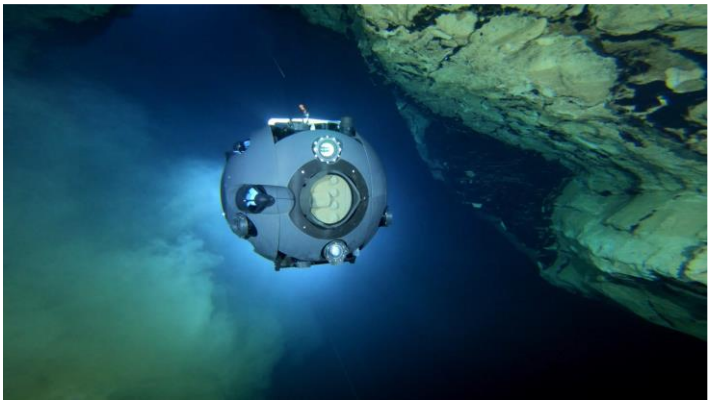

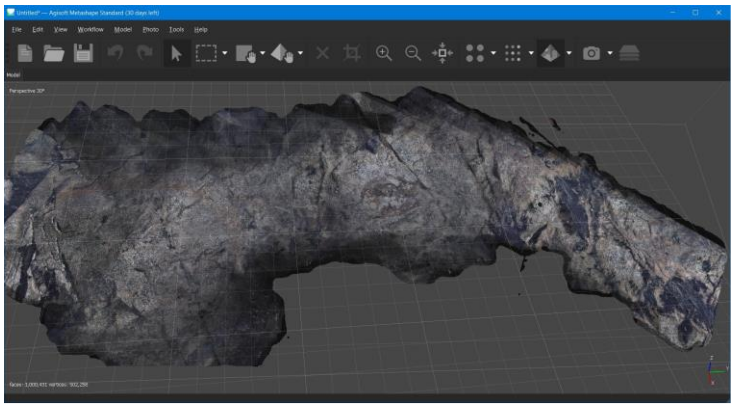

Mineralogical mapping of ore samples and the implementation of qualitative and quantitative analysis of Pd and Pt contents using Laser-Induced Breakdown Spectroscopy and µ-XRF

Nessrine Mohamed[1], Kheireddine Rifai[2], Samira Selmani[3], Marc Constantin[1], François Doucet[2], Lütf ü Özcan[2], Mohamed Sabsabi[4], François Vidal[3]

[1]Université Laval nessrine.mohamed.1@ulaval.ca, [2]Elemission Inc, [3]INRS-EMT, [4]National Research Council Canada

Laser-Induced Breakdown Spectroscopy (LIBS) is an emerging technique in the field of analytical geochemistry. It clearly stands out for its rapidity and high sensitivity which allows the detection of trace elements up to concentrations of ppm and even ppb on heterogeneous rock surfaces. This research demonstrates the potential of LIBS in the mineralogical characterization of PGEs ore samples from Lac des Îles mine (LDI; Ontario, Canada). It also demonstrates the capability of LIBS in the quantitative evaluation of Pd contents within core samples. In this perspective, TESCAN Integrated Mineral Analyzer (TIMA) and Scanning Electron Microscopy (SEM) analyses were used to calibrate the LIBS instrument for the mineralogical characterization of PGEs ore samples whereas micro-X-ray fluorescence (µ-XRF) mapping was independently achieved to evaluate the LIBS mapping results. For Pd and Pt quantitative analyses, the LIBS instrument was calibrated with reference materials whose chemical composition is similar to that of LDI samples. Two rock types were scanned by LIBS for their mineralogical characterization: pyroxenite and gabbronorite. Through LIBS mineralogical mapping, four major silicate phases (chlorite, plagioclase, actinolite and hornblende) and five minor sulfide and oxide phases (Pd-bearing pentlandite, chalcopyrite, pyrrhotite, pyrite and ilmenite) were identified. The LIBS mineralogical maps display not only the distribution of the identified mineral phases but also their abundances along the scanned surfaces of samples. The mineral phases identified by LIBS and by µ-XRF were in very good agreement for their compositions, abundances and distributions. Further, this study revealed a noteworthy potential of µ-XRF chemical mapping in identifying areas of interest for PGMs (Platinum Group Minerals). These results provide good insight for a higher-resolution characterization of PGMs within ore samples. LIBS mapping also allowed to display the distribution map of Pd. By comparison to LIBS mineralogical map, Pd exhibited similar distribution to that of pentlandite. Overall, these results show the ability of LIBS to perform rapid high-resolution mapping of the mineralogical composition of PGEs ore samples. LIBS is significantly faster and more sensitive to trace and light elements than µ-XRF. In addition, this study is the first of its kind allowing the establishment of calibration curves for measuring Pt and Pd contents at low concentrations up to ppm level within PGEs ore samples. Further investigations are underway to validate the calibration and to optimize LIBS sampling on core samples. At this stage of research, it is possible to claim that in the near future the LIBS technique can be remarkably valuable for fast characterization of ore samples.

[Fig. 1 next page]

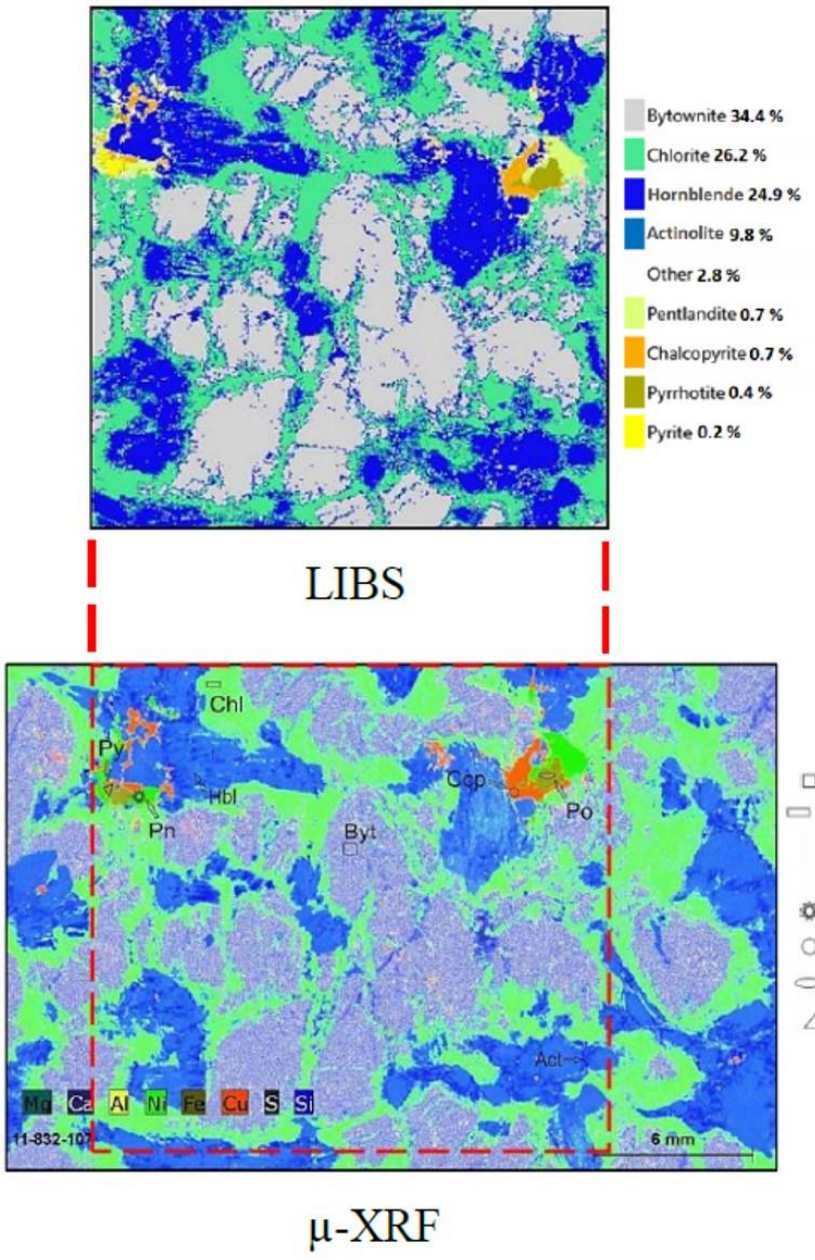

Key Points

- 8 mineral phases were identified automatically by laser-induced breakdown spectroscopy (LIBS) on PGE ore samples.
- The main mineral phases were corroborated by µ-XRF.
- Mineral maps generated by both methods are in excellent agreement (LIBS acquisition speed is 1000 spectra per second).

Disseminated molybdenite within hidden highly fractionated granitic intrusions, northeastern New Brunswick, Canada

Nadia Mohammadi[1], David Lentz[2], Brian Cousens[1], James Walker[3], Christopher R.M. McFarlane[2], Neil Rogers[3]

[1]Carleton University Nadia.mohammadi@unb.ca, [2]University of New Brunswick, [3]New Brunswick Geological Surveys North, [3]Geological Survey of Canada

Late Silurian to Late Devonian intrusions in the New Brunswick segment of the Canadian Appalachians host multiple Mo±Sn±W±Bi±Li mineral occurrences/deposits. Although the Pabineau Falls Granite (PFG) and Nicholas-Denys Granodiorite of northeastern New Brunswick have been known to contain molybdenite mineralization since 1905, they remain for the most part poorly understood. The largest known mineral occurrence in the PFG, the Pabineau Lake Mo occurrence (PLM), consists of high-grade (up to 5.02% MoS2) disseminated molybdenite-bearing granitic rocks. Combined U-Pb zircon geochronology, whole-rock geochemistry (major- and trace-elements) and radiogenic (Sr, Nd, Hf, and Pb) isotopes analyses of the PML host granite are deployed to constrain the evolution of this mineralization. Geochemical characteristics together with a new laser ablation ICP-MS zircon crystallization age (390 ± 1 Ma; MSWD = 1.1; n = 15) of the granite hosting the PLM occurrence argues against its direct relationship with the distinctly older (397.2 ± 1.9 Ma) and less evolved PFG. The PLM host granite is more fractionated than typical PFG, with higher SiO2 (78.93 wt.%), incompatible elements (e.g. Rb, Y, Th, and U) and Mo (100 ppm) contents, but lower MgO, CaO, TiO2, Sr, Ba, K/Rb, Zr/Hf and Nb/Ta. Although it remains a possibility, there is no direct evidence of the PLM host granite being the product of continuous fractional crystallization processes within the PFG. The high initial 87Sr/86Sr of 0.71268, negative εNd of -1.28 and high Pb isotope data together with trace- and major- element

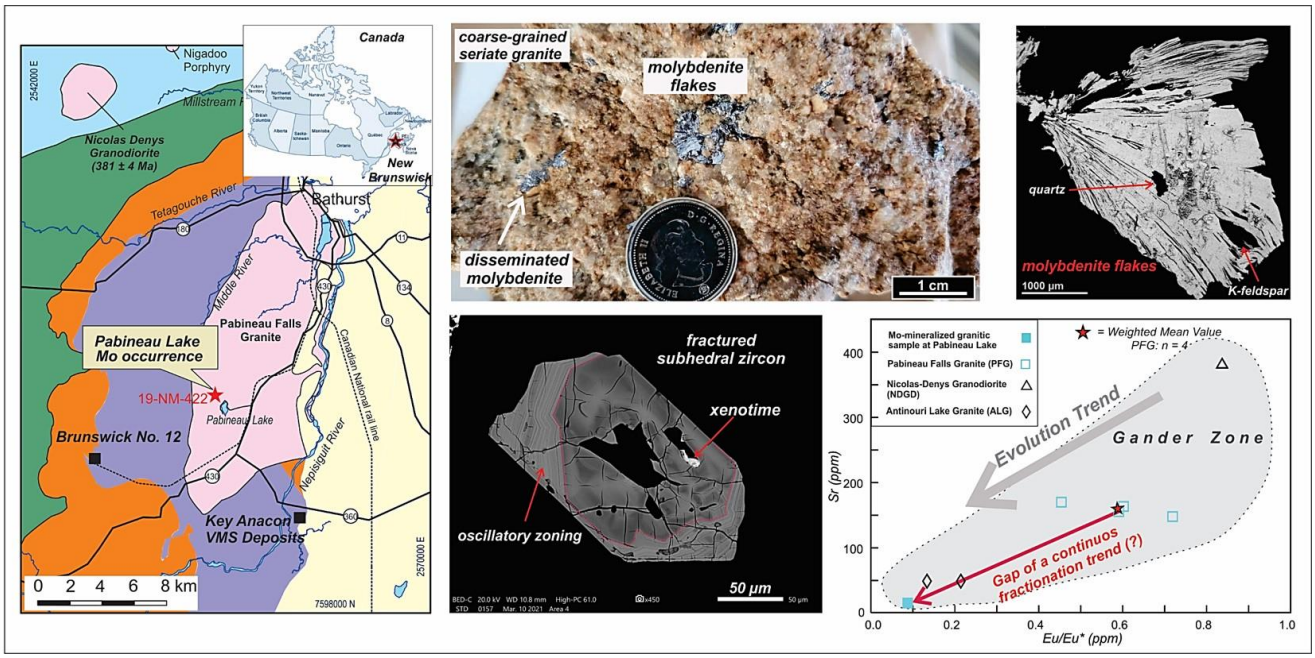

concentrations indicate a moderately to highly radiogenic source, and derivation from a significant amount of supracrustal materials, with a contribution from the upper mantle. Such a source corresponds to that proposed for Gander Zone Siluro-Devonian granitic bodies. A positive εHf (+1.34) also suggests involvement of sedimentary components. These data indicate that a previously unrecognized mineralized intrusion is nested within the PFG. Failure to recognize this intrusion previously is likely due to the extensive glacio-fluvial cover and very limited bedrock exposures in the area. This interpretation is further supported by recent regional-scale geophysical surveys that demonstrate that the PFG is a composite intrusion and substantially larger than mapped as it extends unconformably beneath Carboniferous sedimentary rocks. Consequently, further mapping and investigation, including geochemical analyses would ideally be integrated with geophysical data to constrain the extent of this igneous body/pluton within the larger PFG, and to identify other Middle to Late Devonian intrusions in the area.

ORIGIN OF THE VANADIFEROUS TITANOMAGNETITE-BEARING LAYERED ZONE, LAC DORÉ COMPLEX, CHIBOUGAMAU

Nesrine Mokchah[1], Lucie Mathieu[1,2]

[1]Centre d'Étude sur les Ressources Minérales (CERM), Département des Sciences Appliquées (DSA), Université du Québec à Chicoutimi (UQAC) nesrine.mokchah1@uqac.ca, [2]Chaire institutionnelle UQAC sur les Processus Métallogéniques Archéens, Centre d'Étude sur les Ressources Minérales (CERM), Département des Sciences Appliquées (DSA), Université du Québec à Chicoutimi (UQAC)

The origin of the titanomagnetite-rich units, in layered intrusions, and associated V mineralization, remains debated. This study focuses on the Neoarchean (ca. 2728 Ma) tholeiitic Lac Dore Complex (LDC), a layered intrusion located in the northeastern corner of the Abitibi greenstone belt, Chibougamau, Quebec. The LDC is intruded into felsic to mafic volcanic rocks, as well as sedimentary units that may have been assimilated by the mafic magma. The upper part of the LDC also contains Fe-Ti-V mineralization explored for V, a strategic element for green energies of the future. The LDC offers a unique opportunity to evaluate the impact of the assimilation of volcanic and sedimentary rocks on the oxygen fugacity parameter and on the distribution of V. This study aims at proposing a new metallogenic and petrogenetic model for the accumulation of vanadiferous titanomagnetite in the layered zone of the LDC. This project also aims at explaining the heterogeneous distribution of Fe-Ti-oxides in the layered zone, using field observations, detailed mineralogical and textural examination, whole rock analysis and mineral chemistry. In the south limb of the LDC, the layered zone is in contact with felsic volcanic units and is characterized by alternating and laterally continuous magnetitite and meta-anorthosite layers. In the northeastern limb, the layered zone is in contact with carbonate-rich mafic units and is dominated by discontinuous serpentine-magnetite rocks. The LDC have been affected by greenschist facies metamorphism that induced extensive recrystallisation of the Fe-Ti-oxides. Plagioclases and pyroxene are pseudomorphed by aggregates of epidote (clinozoisite) and albite, and ferrochlorite, actinote, hornblende and pargasite, respectively. In addition, olivines are replaced by serpentine and talc. Petrographic study also indicate that magnetite contains a large amount of ilmenite exsolutions (oxy-exsolution of ulvospinel followed by metamorphic recrystallisation) and chlorite inclusions. Despite metamorphism, V, Cr and Ti remain valid petrogenetic tracers are used to identify stratigraphic reversals. Mineral chemistry analyses have been delayed and preliminary field and petrographic results indicate that the layered zone may be a stack of sills and that minerals may have been transported by gravity currents. Mineral chemistry will be used to comment on the oxygen fugacity parameter and its impact on the distribution of V in the layered zone of the LDC.

Studying the Martian Atmosphere above Gale Crater with Cameras

John Moores[1], Charissa Campbell[1], Alex Innanen[1], Haley Sapers[1], Grace Bischof[1], Conor Hayes[1], Christina Smith[2], Brittney Cooper[3], Casey Moore[1], Jacob Kloos[4], Paul Godin[5], Raymond Francis[6]

[1]York University jmoores@yorku.ca, [2]now at: Oberlin College, [3]now at: Gemini North Observatory, [4]now at: University of Maryland, [5]now at: University of Waterloo, [6]Jet Propulsion Laboratory

For the past nine years, the Mars Science Laboratory (MSL) Rover has been making observations of the atmosphere above its Gale Crater landing site using all onboard cameras. Though captured relatively infrequently, these images and movies are revealing in the aggregate, illuminating processes that evolve on diurnal and seasonal scales. Notably, this rich dataset provides atmospheric conditions at a distance from the rover; important context for in-situ measurements made by the Rover Environmental Monitoring Station (REMS) as well as measurements of atmospheric composition made by the Sample Analysis at Mars (SAM) Quadrupole Mass Spectrometer (QMS) and Tunable Laser Spectrometer (TLS). By making movies above the rover, we can reveal the motion of clouds, which in turn provides wind direction and transport at altitude. Examining the radiance variations in those same images provides cloud thickness, which provides clues to the magnitude of the water cycle at Gale. For instance, before the mission orbital data disagreed as to whether most clouds formed in the afternoon or in the early morning - our observations were able to show that peaks exist at both times of the day due to different mechanisms. Meanwhile the shadow of those clouds cast can be tracked along the landscape, revealing their altitude via simple geometry. Meanwhile, the crater rim provides the perfect backdrop for images designed to examine atmospheric dust loading within the crater and to separate the dust in the lower atmosphere from dust lofted higher. These images reveal that at most times of the year, the air nearest to the surface is relatively dust free. Prior to the mission, numerical atmospheric models predicted this condition as the result of reduced mixing within the crater. Through our observations we have been able to map out when this effect is most pronounced and when dust is mixed into the crater from external sources. We have even been able to observe structure within the clearing of dust from the lower atmosphere following a global dust storm (GDS) event. Even though we cannot see a single cloud or dust particle with any of the cameras, examining them in the bulk gives us critical information about the size and shape of these particles. Examining clouds at different angles to the sun can be used to derive the microstructure of the icy particles out of which they are composed. Though much has been accomplished over the last decade, many fascinating problems remain. We look forward to MSL's next nine years of observations at Gale crater.

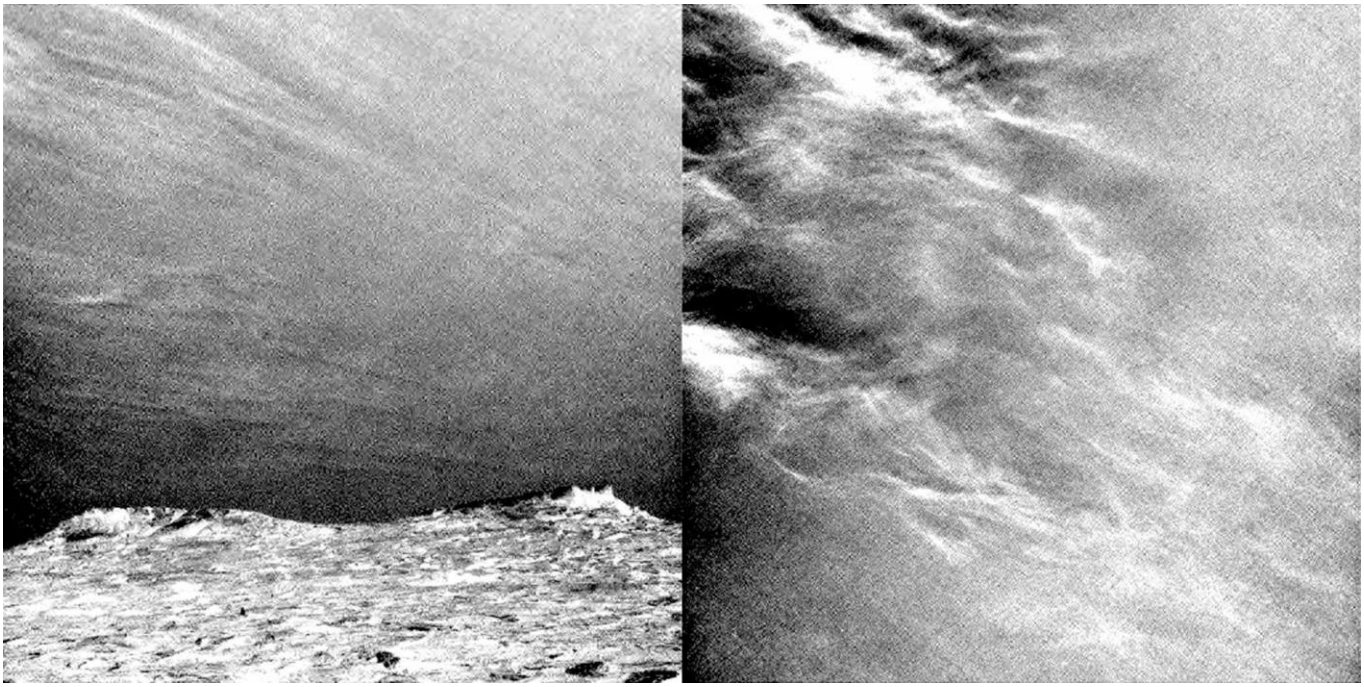

A Transformer-Based Classification System for Volcanic Seismic Signals

CINDY MORA-STOCK[1], Alexander Hemming[1], Cristian Bravo-Roman[1]

[1]University of Western Ontario cmorasto@uwo.ca

Volcanic seismic signals are a key element in volcano monitoring to assess the state of unrest and a possible eruption style and timing. Different sources such as brittle fracture (volcano-tectonic - VT) or fluid movement (long period - LP) generate signals with distinct characteristics in frequency content and shape, but site effects such as attenuation or background noise make their determination difficult to the untrained eye. In cases of unrest or an eminent eruption, the amount of data would require a fast and reliable source of pre-classification to classify and catalogue to aid in the job usually done by a human. To model the problem, we will develop a custom-made Transformer model. Transformers are state-of-the-art deep learning methodologies that work with sequence-based data such as audio, text or, in this case, volcanic signals. The power of transformers lies in their ability to identify complex, disconnected patterns and then use them to identify phenomena in a very effective manner. We will be building the model architecture in TensorFlow and will be running them through SHARCNET. Villarica and Llaima volcanoes are the first and second volcanoes on the list of specific risk for hazardous volcanoes in Chile, respectively. Llaima is a close vent edifice with some fumarolic activity, and presented its last strombolian eruption in 2007-2009, remaining since then seismically active. Villarrica is an open vent stratovolcano with an active lava lake and constant fumarolic activity; its last eruption in 2015 has increased its background tremor and seismic activity. Both pose great risk to people living at their flanks, as lahars, lava flows, and ash fallout are the direct hazards linked to their eruptions. Filtered data from Llaima volcano will be used to train the model and generate a benchmark with previous studies. Unfiltered continuous data from seismic stations in Villarrica volcano will be used as a second train dataset and catalogued from at least these two types of events (VT and LP). The model will be then tested with a different set of stations to assess changes in the signal due to attenuation at the site. This will allow to discriminate the same event in different stations. It is expected this model will serve as a first step towards automatic event recognition and event classification, test and validate the model for different stratovolcanoes, and hopefully to aid in easing the monitoring workload for volcano observatories.

Volcano-Seismology in Chile: developments and advances in the last 20 years

Cindy Mora-Stock[1]

[1] University of Western Ontario cmorasto@uwo.ca

Volcanic seismic events are standard in real-time volcano monitoring to assess the state of unrest and the possible style and timing of an eruption. The different characteristics in frequency content and shape of the signal provide information on the generating source of the events, whether brittle failure occurring as the magma breaks a new pathway towards the surface, or the movement of such magma and its gases ascending through conduits. In time, different methodologies beyond monitoring have been used to move forward and make use of the signals to study temporal changes to the volcanic structure and the faults around them. Chile has one of the most active volcanoes in South America, and about 90 potentially active volcanoes in its territory. With the creation of the National Volcanic Network, 45 of them are monitored in real-time through the Volcanic Observatory of the Southern Andes (OVDAS, acronym in Spanish). This review is made in the context of the Symposium Update on the Chilean Geology (SAGChi, acronym in Spanish), 2021. In this work, I go over the studies on Chilean volcanoes generated with seismic signals, with a focus on those from volcanoes, their developments and different techniques used through time. Focus is taken on the integration of multidisciplinary work, advances in relation with other volcanic areas in the South American Andes, as well as a personal view for future work in the area.

Whitefish Falls ?Breccia?: Spatial, sedimentological, and structural evidence for a pre-Sudbury impact tectono-magmatic origin

William Morris[1]

[1]McMaster University morriswa@mcmaster.ca

Locally, argillites within the Huronian Gowganda sequence near Whitefish Falls, Ontario, are mapped as Sudbury Breccia implying their formation was associated with the Sudbury meteorite impact event. Attention to detail and integration of all sources of information, a Grant Young characteristic, indicates these breccias are the result of a local tectono-magmatic event. Soft sediment deformation of breccia clasts and differential lithification of sandstones versus silts indicates the breccia formed long while these units were still sediments. That is this deformation occurred long before the meteorite impact. Magmatic textures indicate that diabase was intruded prior to folding of the sediments. Yet, paleomagnetic evidence proves regional scale folding pre-dated emplacement of most Nipissing Diabase intrusions. There was more than one period of diabase emplacement in the Whitefish Falls area. But all of them again predated the meteorite impact. On a more regional scale the distribution of known breccia bodies does not show any direct association with presence of Nipissing Diabase intrusions. Using gravity and magnetic anomaly imagery to provide an outline of the regional geological structure it becomes apparent that the so-called Sudbury Breccia occurs in two types of association. First, as expected there is a direct increase in the frequency of true Sudbury Breccia with increased proximity to the margins of the Sudbury Impact crater. Second, what we refer to as Whitefish Falls "Breccia" is most strongly associated with regional scale fault structures. It is postulated that this Breccia was generated because of tectonic (fault) adjustments to the Huronian sedimentary basin during sedimentation of the Gowganda argillites.

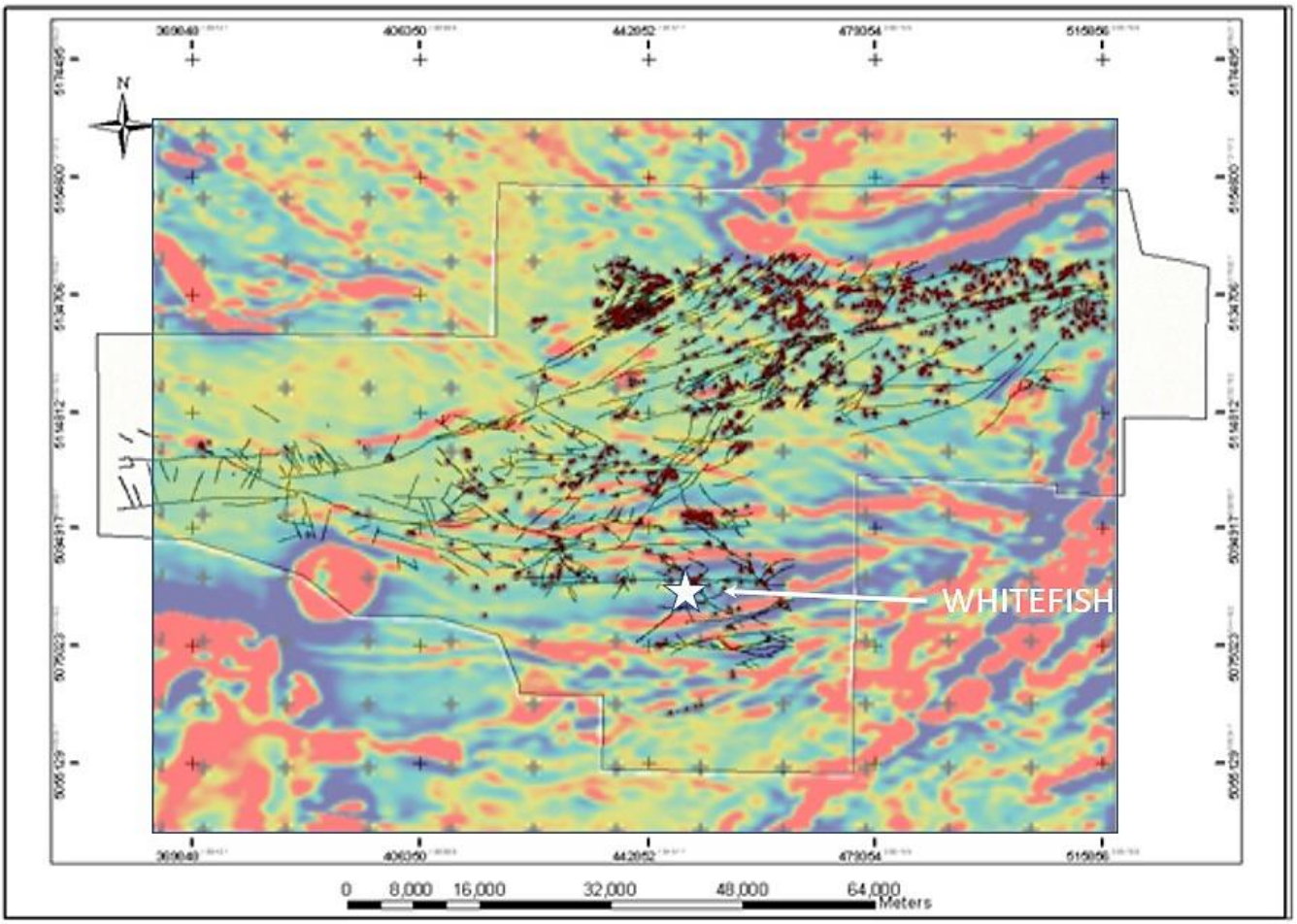

Electron and atom probe microscopy of 1 billion-year-old copper; first results

Desmond Moser[1], Jamie Noël[1], Anna Dobkowska[2], Emilie Landry[1], Dmitrij Zagidulin[1], Gabriel Arcuri[1], Brian Langelier[3]

[1]University of Western Ontario desmond.moser@uwo.ca, [2]Warsaw University of Technology, [3]McMaster University

Veins and pods of natural copper have long been known to occur in the upper crust of the Lake Superior region of North America, where copper has been culturally, politically and spiritually significant to Indigenous peoples for millennia (e.g., Redix, 2017). The source copper deposits were emplaced close to one-billion-years ago in lithosphere, which has since experienced a protracted history of glacially and tectonically driven isostatic adjustment events. In light of this longevity, structural history, and related exposure to crustal fluids, copper has the potential to hold many lessons for deep geological repository (DGR) specialists in corrosion engineering and society in general. We will present our early findings on the grain size, texture, and growth mechanisms of copper in different lithologic settings, the nature and distribution of impurities in the copper, the relict, cumulative strain, if any, in the copper crystals, and whether there are co-existing uranium-bearing mineral phases that can be used to date past fluid activity. Techniques in the analytical workflow include electron microscopy using energy dispersive X-ray spectroscopy (EDS) and electron backscatter diffraction (EBSD) to identify phases, and map impurities, and microstructure, followed by atom probe tomography (APT) to measure chemical nanostructure. These will be compared to the properties of manufactured wrought copper (phosphorus-doped oxygen-free). Initial BSE grey-scale imaging of vein copper indicates a heterogenous texture of mm-scale, ovoid, featureless, bright domains surrounded by arcuate zones, in which ~50% of the surface area is composed of randomly distributed, 50 µm-diameter, dark ovoids. EDS analysis indicates that all are dominantly copper composition. Atom probe analysis indicates trace elements including Ag and Si distributed homogeneously in a single crystal, and that other trace elements such as S may be present. These results will eventually be integrated with electrochemical analyses such as corrosion potential measurements and potentiodynamic polarization scans on the same sample in order to probe the corrosion performance of natural copper. Early results suggest that the natural copper corrosion performance is slightly lower than that for fabricated used nuclear fuel container material. These measurements may inform container design aspects such as optimal fabrication and the role of impurities in corrosion behaviour of fabricated copper components compared to those of aspects of natural copper which may have allowed it to exist for a time span of three orders of magnitude greater than the DGR design requirements.

Redix, E.M., 2017; "Our Hope and Our Protection": Misko-biiwaabik (Copper) and Tribal Sovereignty in Michigan. American Indian Quarterly , Vol. 41, No. 3, pp. 224-249

Searching for Ontario's 'missing' ice streams

Riley Mulligan[1], Andrea Marich[1], Roger Paulen[2]

[1]Ontario Geological Survey riley.mulligan@ontario.ca, [2]Geological Survey of Canada

The advance and retreat of the Laurentide Ice Sheet (LIS) across Ontario extensively modified the landscape through erosion of bedrock and pre-existing sediment, and deposition of thick sediment sequences along the margins of ice lobes during deglaciation. The recent release of high-resolution (<2 m) LiDAR and other digital terrain data for large areas of Ontario enables improved mapping of glacial landforms at regional scales. Increasingly, over the last decade, the existence - and influence - of paleo-ice streams on the landscape has been recognized. Mega-scale glacial lineations (MSGL), a landform assemblage diagnostic of paleo-ice streams, can be difficult to identify from the ground, but are readily visible on these high resolution digital elevation model datasets and hold significant implications for paleoglaciological reconstructions. Developing an understanding of the onset, evolution, timing, and interactions between paleo-ice streams and their beds is critical to understanding ice sheet evolution and provides important constraint to models of ice sheet response to climate changes. As glacial morphotypes, MSGL in Ontario occur in clusters, in areas mapped as coarse-grained till in Canadian Shield terrain, as isolated till mounds surrounded by streamlined bedrock, and in larger swarms in thicker (>40 m) unconsolidated sediment zones. Commonly, larger clusters of MSGL occur within or along the margins of large topographic lowlands, and in many cases, MSGL long-axes are parallel to the lows, or diverge from or converge towards the central portions of low-lying terrain. The downflow extents of numerous clusters are commonly marked by large moraine complexes, representing clear flow sets. Within each flowset, a wide variety of sediment-cored, mixed, and bedrock-cored bedforms exist. Low-relief (<6 m high) MSGL are also observed across regional bedrock highs separating lowland flowsets. Small (<3 m high) recessional moraines overlie the MSGL across portions of the exposed beds. Large areas of iceberg scouring are observed downflow of the MSGL clusters in areas inundated by proglacial lakes during deglaciation. The abundance of MSGL suggest a larger proportion of the LIS margin developed ice streams than previously recognized, particularly in hard-bedded Canadian Shield areas. MSGL distribution and relationships with local to regional topography and antecedent bedforms suggest several ice streams were initiated within topographic lows as the ice sheet thinned during deglaciation. Ice stream propagation was likely enhanced in many areas due to the existence of deep proglacial lakes fronting the ice margin. Future work involves field-mapping the surficial geology of several parts of the exposed beds of these inferred paleo-ice streams to refine understanding of sediment-landform assemblages and collect samples to improve knowledge on the timing of ice stream activity in the region.

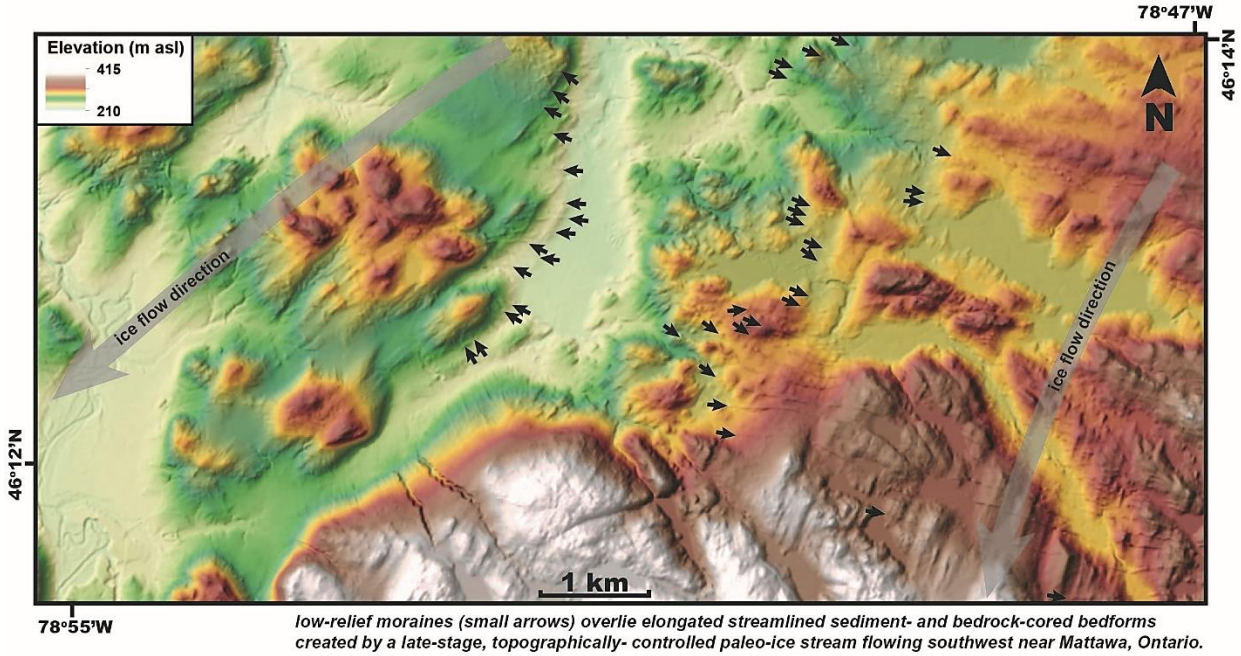

low-relief moraines (small arrows) overlie elongated streamlined sediment- and bedrock-cored bedforms created by a late-stage, topographically- controlled paleo-ice stream flowing southwest near Mattawa, Ontario.

Method Development & Benchmarking: Crystalline Rock Porewater Extraction Using Vacuum Distillation

Tarek Najem[1], David Zal[1], Oliver Blume[1], Michelle Landry[1], Jeremy Potvin[1], Ian D. Clark[1]

[1]Department of Earth and Environmental Sciences, University of Ottawa tnaje098@uottawa.ca

Knowledge of the geochemical and isotopic composition of groundwater and porewater residing in the inter- and intragranular pore-space is important for determining potential flow pathways, origins, and evolution of fluids, as well as estimates of residence time. Within the context of the deep geological repository (DGR) for hosting radioactive waste, such information is important for assessing the suitability of the proposed host media from a safety perspective. Therefore, developing and demonstrating reliable methods to extract and characterize porewaters from different media is of critical importance. Vacuum-distillation is a method demonstrated to have the ability to extract porewaters from low water content and low permeability materials, and to have produced useful stable isotope and geochemical data. With R&D support from the Nuclear Waste Management Organization (NWMO), a new approach to extract porewater from crystalline whole-core samples was developed at the University of Ottawa. As part of this program, stainless-steel chambers were constructed to house and seal whole crystalline cores and fitted to a vacuum line for porewater extraction. The methodology was bench-marked using crystalline cores re-saturated with water of known isotopic and chemical composition using various saturation methodologies. Full recovery of the porewater was possible within an extraction period of 7 hours over 2-days using a temperature of either of 120°C or 150°C. We show that the stable isotopic composition (18O and 2H) of the recovered porewater was, within error, equivalent to that of the saturating water. In addition, for cores saturated with an artificial saltwater (1M NaCl and 0.05M KBr), we show that leaching of post-extraction cores and normalizing to the amount of porewater extracted provided interpretable concentration data of the conservative solutes Na, Cl, K and Br. Taken together, the development of a new chamber extends the applicability of vacuum distillation to extract and characterize porewater from intact crystalline drill-cores.

The first record of impact crater in the desert of Oman

Sobhi Nasir[1], Brian Spratley[2], Sue Spratley[2]

[1]Sultan Qaboos University sobhi@squ.edu.om, [2]Kinghtsbay Exploration Company

Oman contributed around 14 % of all the world's meteorite finds. However, no surface impact craters were yet recorded from Oman. This work report for the first-time evidence for impact cratering in Oman. The newly found crater is a simple impact crater located near the city of Mahoot in the central desert. The impact crater consists of an elliptical ridge about 770 m in length and 550 m in width and aligned roughly NNE to SSW (Fig. 1). The crater has been preserved in a nearly pristine state due to the dry climate of the Oman desert, and the lithology of the target rocks. The perfect preservation of the crater shape and ejecta pattern indicates that the crater formed through an impact from a northeastern direction during Cenozoic. Formations penetrated by this impact include the local Late Proterozoic Masirah Bay sandstone Formation, and the underlying dolomitic and acidic volcanic and volcaniclastic of the Halfayn Formation and the Pre-Cambrian basement rock. The central peaks contain breccia that is pushed upward from the deepest levels excavated by the crater. The rim of the basin, which rises to a maximum of 15 to 20 meters above the floor is composed of shocked siliceous breccia. Preliminary gravity and geomagnetic data reveal a buried large individual impactor body. The centre splays off a dyke with an NNE-SSW trend and occupied by low outcrops of suevite, polymictic impact breccia and melt. All clasts show irregular fractures, planar deformation features and diaplectic glass melt, indicating different shock stage which ranges from moderately shocked to whole rock melting. Lithic breccia consists of a matrix and clasts of carbonate, quartz, feldspar, coesite, apatite and glass. Carbonate spherules, globules, liquid immiscible and quench textures, as well as euhedral calcite crystals within impact glass clasts, are very common within the breccia. Highly deformed carbonate and feldspar grains are the main components of suevite. Quartz grains show 1-4 sets of PDFs. Most of the melted glass and clasts shows obvious flow texture. The glass occurs as ovoid, droplet, ribbon, or irregular fragments of different size. The melt origin for carbonates and feldspars includes carbonate spherules, euhedral carbonate and feldspar grains within impact glass, calcite intergrown with feldspar and liquid immiscible textures.

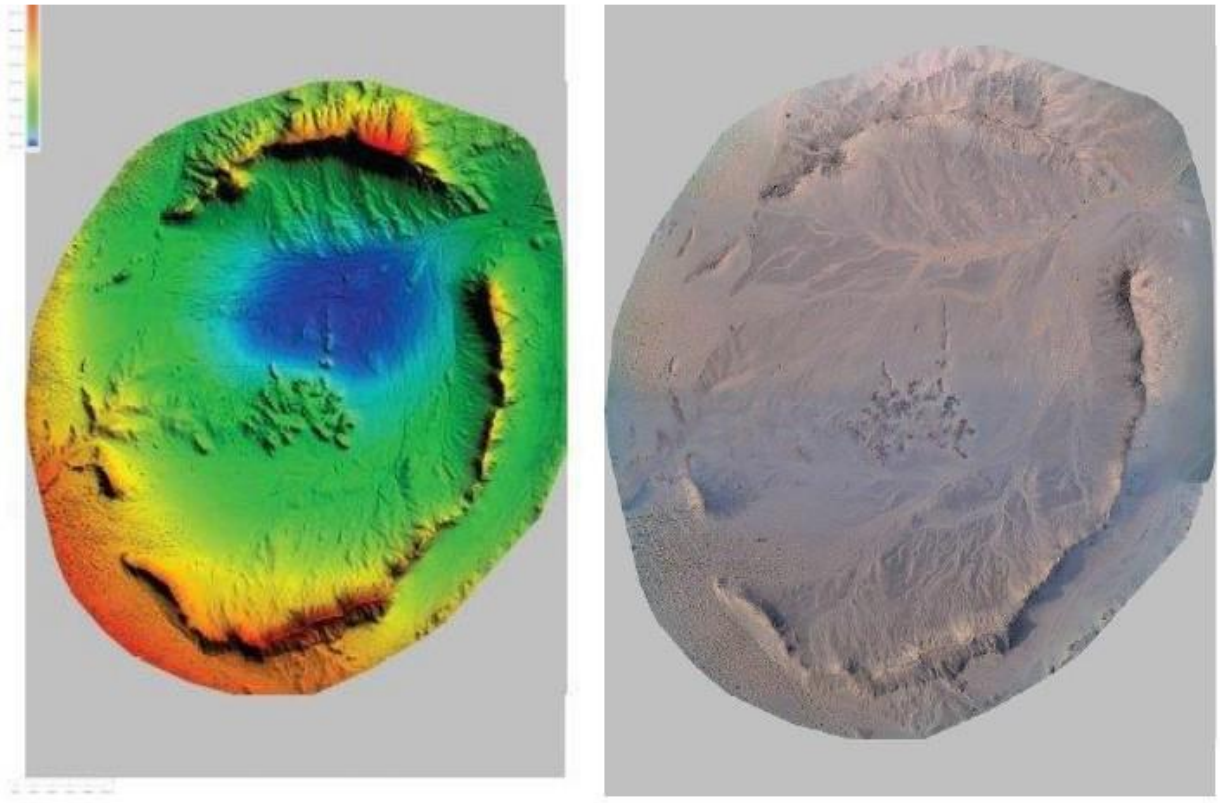

Fig 1. Elevation and 3D model of the crater

Using COVID19 as an Opportunity to Measure Seismic Silences and Bring Geoscience Projects to Students in Canada

Artash Nath[1]

[1]HotPopRobot artash.nath@gmail.com

On 11 March 2020, the World Health Organization declared Covid19 a pandemic. Countries around the world rushed to declare various states of emergencies. Canada also implemented emergency measures to restrict the movements of people including the closure of borders, non-essential services, and schools, restaurants, and offices. I used this opportunity to measure changes in seismic vibrations registered in Canada before, during, and after the lockdown due to the slowdown in transportation, economic, and construction activities. I analyzed continuous seismic data for 6 Canadian cities: Calgary and Edmonton (Alberta), Montreal (Quebec), Ottawa, and Toronto (Ontario), and Yellowknife (Northwest Territories). These cities represented the wide geographical spread of Canada. The source of data was seismic stations run by the Canadian National Seismograph Network (CNSN). Python and ObSpy libraries were used to convert raw data into probabilistic power spectral densities. The seismic vibrations in the PPSDs that fell between 4 Hz and 20 Hz were extracted and averaged for every two weeks period to determine the trend of seismic vibrations. The lockdown had an impact on seismic vibrations in almost all the cities analyzed. The seismic vibrations decreased between 14% - 44% with the biggest decrease in Yellowknife in the Northwest Territories. In the 3 densely populated cities with a population of over 1 million - Toronto, Montreal, and Calgary, the vibrations dropped by over 30%. To enable students at home to undertake similar projects for their cities, I created an online training module with custom Python functions using Jupyter notebooks available on my Github. Students are able to learn about seismic vibrations, gather live data directly from the seismic stations, and analyze and interpret seismic vibrations during different lockdown periods. They can share their findings with local policymakers so that they become aware of the effectiveness of the lockdown imposed and are better prepared for lockdowns in the future. When we make data and technology accessible, then lockdowns because of pandemics can be an opportunity for students to take up practical geoscience projects from home or in virtual classrooms.

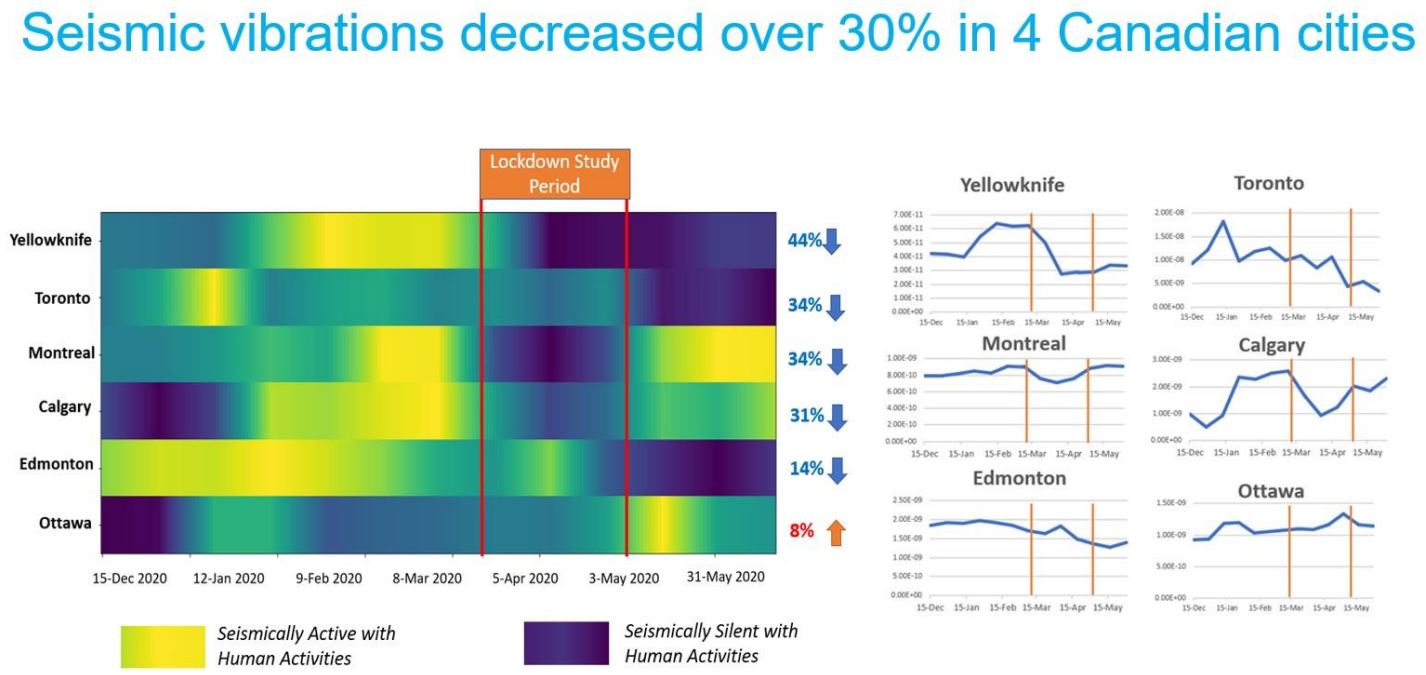

Physical properties of lunar impact melt deposits

Catherine Neish[1], Emilie Lafleche[2]

[1] University of Western Ontario cneish@uwo.ca, [2]Purdue University

Lunar impact melt deposits are common features on the Moon, often seen around young, fresh craters. They take a variety of different forms, including veneers and lobate flows, and show evidence for past molten behavior, such as cooling cracks and leveed channels. Data from the Lunar Reconnaissance Orbiter (LRO) has revealed a number of previously unknown melt deposits that are exterior to their crater rims. Many of these were identified using LRO's Mini-RF radar, because they appear remarkably rough at the dm-scale. Despite their dm-scale roughness, lunar impact melt deposits appear smooth when viewed at the meter-scale with LRO Narrow Angle Camera images and digital elevation maps. The reason for this discrepancy remains unclear, although it may relate to their unique cooling conditions. To help us better understand the physical properties of impact melt deposits, we examined LRO Diviner thermal infrared data. Specifically, we examined the Diviner rock abundance (RA) data set, which provides a measure of the number of meter-scale boulders on the surface of the Moon. Past work has found a general correlation between areas of high radar circular polarization ratio (CPR) data and high Diviner RA values. Here, we focus specifically on exterior melt deposits for craters of a variety of ages. We seek to use this data to make inferences about the formation and degradation of lunar impact melt deposits. We identified melt deposits around 17 lunar craters ranging in age from ~4 Ma to ~3.6 Gyr. We outlined a section of the melt deposit for each crater in ArcGIS, and extracted mean values for CPR and RA in those regions. We focused specifically on melt deposits that were clearly separable from their blocky ejecta blankets, so as to exclusively target the physical properties of melt deposits. In general, we found that the CPR of impact melt deposits tends to increase as RA increases, up to a value of ~ 2%. At that point, further increases in rock abundance show no corresponding increase in CPR. We also found that the highest RA and CPR values belonged to the impact melt deposits of the youngest craters, while older craters had correspondingly lower values. This finding is consistent with past work suggesting that the rock abundance of lunar ejecta can be used to date craters, since blocks will break down over time. However, we find that the melt deposits have consistently higher rock abundance values than those of the blocky ejecta from the same crater. This suggests that either (1) the melt deposits initially formed with more coherent sections of rock exposed, (2) that melt deposits take longer to degrade to background levels, and/or (3) that coherent melt deposits produce more meter-sized blocks over time, as small impacts disrupt the surface. Over time, the melt deposits will also break down, creating a similar downward trend in RA with time as observed by Ghent et al. (2014). However, since these deposits take longer to erode to the background levels, they will be easier to identify around older craters than their corresponding blocky ejecta.

A fresh approach to increase the sensitivity of SEM-based automated indicator mineral detection

Alexandre Néron[1], Rejean Girard[1]

[1]IOS Services Géoscientifiques neron.alex@iosgeo.com

Study of indicator Minerals (IM) in glacial sediments is a well established technique for mining exploration, assuming that IM satisfies three essential criteria. 1) IM has a sufficiently distinguishable and unique appearance for visual discrimination, 2) IM can be easily concentrated, and 3) IM is specific and exclusive for a metallogenic environment. Each of these three criteria must be fulfilled in order to guarantee the effectiveness of the conventional IM visual sorting. However, this approach is dependent on the experience and skills of the professional and severely constrained by any of the three essential criteria. Automated SEM routine for IM sorting are currently being tested by various research groups. Traditional sample scanning techniques are based on particle segmentation from BSE image mosaics prior to EDS analysis. Although powerful, the technique has inherent speed limitation. An approach based on particle segmentation directly from X-ray maps has been developed, reducing significantly acquisition time, to less than an hour per samples. Then, particle segmentation can be conducted as post-processing, not slowing SEM operations. Particle segmentation form X-ray maps is not available in commercial EDS operating package and EDS spectrum deconvolution codes are not publically available. So, an AI-based algorithm has been developed which enables such particle segmentation and estimation of their individual chemical composition. Stoichiometry of the mineral can be computed, and mineral species classification based on IMA database. Although still under testing, the effectiveness of this approach will be demonstrated and its ability to circumvent the aforementioned limitations will be discussed. As chemical analysis can be computed on individual minerals directly from X-ray maps, a chemical classification can be performed even if based upon low abundance elements. As sensitivity is increased, so is the capability to detect rare minerals with subtle signature. Given a lower detection limit and increased precision, the cost-effectiveness of the overall survey can be improved. Finally, working with an universal mineral library enables the detection of minerals species from deposit type that were not specifically targeted, leading to a true multi-commodity approach. Circumventing the restrictive criteria for indicator minerals thus significantly increase the potentiality of the methods to detect characteristic signatures of exploration targets.

Modelling the silicate atmosphere of lava planet K2-141b and implication for observations

Tue Giang Nguyen[1], Nicolas Cowan[2], Raymond Pierrehumbert[3], John Moores[1]

[1]York University giang@yorku.ca, [2]McGill University, [3]University of Oxford

Lava planets are tidally-locked rocky planets that orbit very close to their star - their surfaces are covered by in giant magma oceans. Surface temperatures on these planets are hot enough to vapourize rocks which generate a thin mineral atmosphere. Due to their extreme orbital configurations, lava planets are currently the best target for observing a rocky exoplanet's atmosphere, and K2-141b is the best lava planet to do so. We model K2-141b's atmosphere and improved upon previous works by implementing ultraviolet and infrared radiation. The results show that the silicate-dominant atmosphere is significantly warmer than the surface below it due to UV heating. By calculating the expected emission spectra at secondary eclipses, we can detect the silicate atmosphere by analyzing the emission at silicate's spectral features (e.g 4.5 or 9 micron). This can be compared with observations from the upcoming James Webb Space Telescope. As K2-141b is a highly valued target, it will be one of the first exoplanets to be observed extensively by James Webb in 2022.

Surficial geology and glacial history of the Birch Lake area, in the Dessert Lake drumlin field, Northwest Territories

Philippe Normandeau[1], Gideon Lambiv Dzemua[1]

[1]Northwest Territories Geological Survey, GNWT philippe_normandeau@gov.nt.ca

Surficial geology mapping and glacial history reconstruction are essential to drift prospecting, infrastructure development, terrain sensitivity characterization, and baseline geochemical data interpretation. Previous surficial geological work by industry and remote mapping by the Geological Survey of Canada in the 85K NTS map sheet identified the Dessert Lake drumlin field and enhanced a preliminary understanding of the regional distribution of surficial material. This knowledge is being extended with a multi-year initiative by the Northwest Territories Geological Survey to better understand the variability and suitability of the surficial material as geochemical and indicator minerals sampling media, as well as to evaluate the presence of dispersal patterns associated with known geophysical anomalies in the area. The first field season of the project was completed in the summer of 2020 and included the collection of 60 till indicator minerals and geochemistry samples as well as a preliminary evaluation of the industrial minerals (silica sand, gypsum, barite, carbonate, and shale/slate) potential of the area. The industrial mineral potential of the area is enhanced by the road infrastructure and proximity to Yellowknife. Based on our field observations, the distribution and thickness of surficial material in the area is mainly controlled by bedrock geology and post-glacial processes. Most of the map sheet is covered by thin reworked till and fine-grained glaciolacustrine sediments overlying low relief drumlinoids, forming a poorly drained streamlined landscape. A 15-25 km wide band of thicker till runs from the southeast to the northwest of the map sheet. The band of thicker till is bordered on the northeast side by drift-poor areas including narrow locally derived boulder fields, clast-dominated thin till, and northeast facing limestone cliffs associated with the contact between the Chinchanga and Lonely Bay formations. On the southwest side, the thicker till transitions gradually to a thin reworked till and fine-grained glaciolacustrine sediments. High relief, pristine drumlins are present in the southwest portion of the area, east of Birch Lake.

A Review of Geoscience Communication Resources in British Columbia & Opportunity for Discussion

Courtney Onstad[1], Eileen van der Flier-Keller[1]

[1]Simon Fraser University courtney_onstad@sfu.ca

Geoscience Communication in formal and informal educational settings in British Columbia has been strengthened thanks to the dedication and passion put forward by various organizations (not-for-profits, universities, community groups) and individuals. While significant Earth science educational opportunities and resources have been developed in British Columbia, no research has tried to summarize these efforts. Without knowing what opportunities and resources are available, how can we coordinate our communication and expect non-earth scientists to be receptive to Earth science ideas and content? This research aims to address this question by constructing and analyzing a database reviewing all earth science communication, education, and outreach initiatives across British Columbia. Web searches were used to identify organizations and individuals who communicate the Earth sciences. Websites, social media platforms, travel blogs and tourism resources were used to gather data. This database includes information such as target audience, venue, societal relevance, resource types, social media platforms, location of services offered and more. Preliminary research has identified plentiful educational resources and programming related to the mineral and mining industries, but lesser resources focusing on environmental impacts/climate change, natural hazards, and water systems. Educational outreach programming for the formal education sector is abundant in the B.C. lower mainland, but less options exist in other parts of B.C., including the north, making a well-rounded earth science education inaccessible to many communities and especially Indigenous communities. In informal educational settings, B.C. has museums, heritage sites, science centers, geotours, hobbyist/enthusiast activities, and more. A significant gap, however, has been identified based on the lack of educational resources available in B.C. national and provincial parks. Indigenous ways of knowing are also either absent or inauthentically merged with earth science information, presenting an area for significant improvement. Continued research will focus on increasing accessibility to educational resources, and understanding how to weave Indigenous perspectives, beliefs, and stories with traditional earth science. Following the presentation on database results, there will be an opportunity for discussion with participants regarding their insights on gaps in the Canadian geoscience communication space based on their experiences and knowledge.

The Canadian International Geological Congresses: Toronto 1913, Montreal 1972

David Orenstein[1]

[1]Danforth CTI david.orenstein@utoronto.ca

Canada has hosted two International Geological Congresses: Toronto in 1913 and Montreal in 1972. They brought the Geological world to Canada, not just to share their research and to socialise among themselves, but also to study Canadian geology first hand in a vast array of field trips from coast to coast to coast. Using primary sources such as the published Proceedings, field trip guidebooks, news reports, contemporary photographs and scrapbooks, this talk will focus on a comparison of Tectonics, Pre-Cambrian Geology and Paleonotlgy at the two Congresses.

Review of historical valued components and indicators in the Lower James Bay Region of Ontario and Quebec Canada to organize cumulative effects science at Natural Resources Canada

Camille Ouellet-Dallaire[1], Anica Madzarevic[2], Sara Ryan[2]

[1]Memorial University cdallaire@grenfell.mun.ca, [2]Natural Resources Canada

Regional Assessments (RA) are "studies conducted in areas of existing projects or anticipated development to inform planning and management of cumulative effects and inform project impact assessments" (Government of Canada 2019). On February 10, 2020, the Minister of Environment and Climate Change announced that the Impact Assessment Agency of Canada (IAAC) would conduct a RA in Ontario's Ring of Fire in collaboration with the federal and provincial governments Indigenous groups and non-governmental organizations. Valued Components (VC) are defined as "environmental, health, social, economic or additional elements or conditions of the natural and human environment that may be impacted by a proposed project and are of concern or value to the public, Indigenous peoples, federal authorities and interested parties" (IAAC 2020). Indicators are parameters or metrics used to measure and report on the condition and trend of a VC (BC 2013). Project-level assessments focus on VCs to evaluate impacts and inform decisions. To organize and connect Natural Resources Canada's cumulative effect science efforts, we compiled historical VCs and indicators from previous and on-going environmental and impact assessment related work in the James Bay Lowlands, and used language consistent with IAAC's Tailored Impact Statement Guidelines (TISG). In our analysis, we refer to historical VCs as assessment priorities (APs). The reviewed work provides information on trends associated with APs and indicators, while the TISG connects this work to project-level assessments, which RAs intend to inform. From the reviewed work, we analyzed 34 APs and 172 indicators. In the review work, we found strong commonalities; indicators measuring multiple APs; and a lack of socio-economic APs and indicators. Our findings support the need for multidisciplinary integration in RAs and we use this analysis to propose a conceptual approach that could organize this integration.

The continuing volcanic and structural evolution of the southern Reykjanes Ridge: A remote-predictive geologic mapping study of a dynamic slow-spreading ridge

Sofia Panasiuk[1], Melissa Anderson[1], Ármann Höskuldsson[2], Fernando Martinez[3], Dominik Palgan[4]

[1]University of Toronto, Toronto, Canada panasiuk.sofia@gmail.com, [2]University of Iceland, Reykjavik, Iceland, [3]SOEST, University of Hawai'i at Manoa, Hawaii, USA, [4]Institute of Oceanography, University of Gdańsk, Poland

The Reykjanes Ridge is a spreading center that presents an opportunity to track the dynamic formation of structural and volcanic features at an asymmetric slow-spreading plate boundary. The ridge spans the northern ~1000 km of the Mid Atlantic Ridge and has been spreading at a full spreading rate of ~20 mm/year [1]. The characteristic along-ridge basement depth, crustal thickness, and chemical gradient have been variably attributed to an active mantle plume beneath Iceland, or a passive mantle anomaly pre-dating the rifting [1]. A unique feature of the ridge is that it spreads obliquely to the spreading axis: a consequence of the change in spreading direction from ~125 to ~100 degrees due to the failure of the triple junction between the Greenland, Eurasian, and North American plates 37 Mya [2]. Following the failure, disjunct ridge segments were formed and separated by transform faults which have been consistently eliminating from north to south, thereby re-establishing the original linear geometry of the ridge [1]. Despite the termination of strike-slip motion along previous transform faults, the ridge remains in a state of active tectonic deformation as demonstrated by the rotation of linear structures, lengths of spreading segments, migration of non-transform discontinuities (NTOs), and deviation from the previously asserted linear continuity of the ridge. Investigating the relationship between structures, volcanism, and regional geodynamics will characterize the evolution of the ridge for the past 10 Mya based on the extent of newly acquired high resolution bathymetric and acoustic backscatter data. The novel remote-predictive geological mapping method is used to map the neovolcanic terrain on-axis and older time-correlated crust off-axis. This analysis will produce new insight into the on-going first and second-order deformation of the Reykjanes Ridge, its controls, and its effects on diffuse low-temperature vs. focused high-temperature hydrothermal venting.

[1] Martinez et al., 2020. Reykjanes Ridge evolution: Effects of plate kinematics, small-scale upper mantle convection and a regional mantle gradient. Earth-Science Reviews. [2] Jones, Stephen M., 2003. Test of a ridge-plume interaction model using oceanic crustal structure around Iceland. Earth and Planetary Science Letters.

Are supercontinents really super?

Daniel Pastor-Galán[1], J. Brendan Murphy[2], R. Damian Nance[3], Christopher Spencer?

[1]Universidad de Granada dpastorgalan@gmail.com, [2]St. Francis Xavier University, [3]Ohio University, ?Queen's University

There is an emerging agreement that Earth's landmasses amalgamate every now and then into supercontinents, many times interpreted to be rigid super-plates essentially lacking tectonically active inner boundaries and showing little internal lithosphere-mantle interactions. The formation and disruption of supercontinents it is thought to be somewhat periodical and have been linked to changes in sea-level, biogeochemical cycles, global climate change, continental margin sedimentation, large igneous provinces, deep mantle circulation, outer core dynamics, Earth's magnetic field, and roughly any other long term secular variation observable in Earth. If these hypotheses are correct, long-term mantle dynamics and much of the geological record, including the distribution of natural resources, may be largely controlled by these cycles. Despite their potential importance, many of these proposed links are, to date, permissive rather than proven. Sufficient data are not yet available to verify or fully understand the implications of the supercontinent cycle. In this virtual talk we will explore the definitions of a supercontinent and the implications on Earth's geodynamics of each definition, the involved forming mechanisms and the prospective consequences. Finally we will use what we think it is a well known example, the case of Pangea, to assess how super are supercontinents.

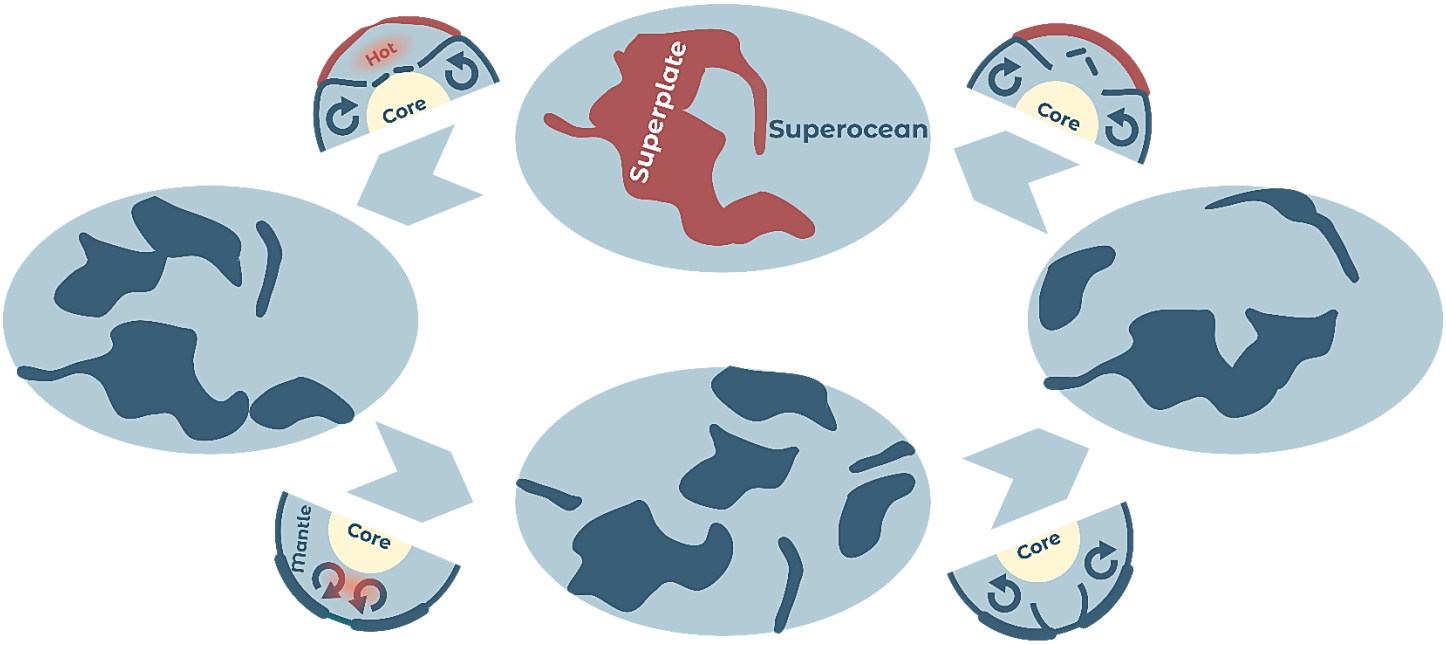

The effect of relative humidity on phase transformations of amorphous Ca-Mg-carbonate minerals

Avni Patel[1], Siobhan Wilson[1], Maija Raudsepp[1], Anna Harrison[2]

[1]University of Alberta avni1@ualberta.ca, [2]CNRS

Ca- and Mg-carbonate minerals are pervasive in the geological record and represent important paleoarchives and vast reservoirs for long-term CO2 storage. Amorphous Ca-, Ca-Mg- and Mg-carbonate (ACC, ACMC, and AMC; respectively) are important precursors to crystalline carbonate minerals in low-temperature environments where formation of carbonate minerals may be kinetically inhibited. These amorphous phases precipitate more readily than crystalline carbonate minerals due to the lower free energy requirements associated with their formation and undergo stepwise re-crystallization until the most stable crystalline phase is reached. The crystallization pathways of amorphous Ca- and Mg-carbonates typically comprise several metastable intermediates occurring in multi-phase assemblages. It is known that the lifetime of the amorphous precursors and the phases forming along these pathways are controlled by: [Mg], pH, temperature and alkalinity. However, few studies have considered the effect of water activity on crystallization rates and pathways. In this study, we synthesized amorphous Ca(1-x)Mg(x)CO3nH2O (ACMC) with variable compositions (0 ? x ? 1) at 21.0 ± 0.8 ?. The dry amorphous solids were then placed under relative humidity (RH) conditions of 2, 29, 53, 75 and 100 ± 2% and analyzed for up to 210 days. Results from X-ray Diffraction analysis show preservation of the amorphous precursor phase for compositions 20% < MgCO3 ?100% at RH ? 53% for the duration of the experiment. At 75% RH, the amorphous-crystalline transformation occurs within 210 days for both Mg-rich and Mg-poor ACMC; however, ACMCs with intermediate compositions of 30% < MgCO3 <80% show enhanced stability and do not transform over the experimental duration. At 100% RH crystallization is observed within 14 days of reaction, thus indicating that crystallization is significantly accelerated at RH >75%. The first phases to crystallize at 100% RH are highly hydrated Ca- and Mg-carbonates and very high Mg-carbonate (VHMC). These hydrated carbonate phases gradually transform into aragonite, dypingite and hydromagnesite. Notably, we also observe distinct spatial segregation on the micrometre scale of Ca-rich and Mg-rich phases at 100% RH. These findings offer important insights on cation transport and mineral phase transitions mediated by adsorbed water films. These thin film reactions are key to understanding mineralogy and element cycling in important water-undersaturated systems including carbonate deposits on Earth and Mars, CO2 sequestration projects, and cement and concrete infrastructure.

Detrital zircon provenance of the Mesoproterozoic Fury and Hecla Group: Refining a tectono-depositional model for the Bylot basins (Arctic Laurentia)

Mollie Patzke[1], John Wilder Greenman[2], Galen Halverson[2], Robert Rainbird[3], Alessandro Ielpi[1]

[1]Laurentian University mpatzke@laurentian.ca, [2]McGill University, [3]Geological Survey of Canada

Extensive Proterozoic intracontinental basins developed during supercontinent amalgamation of Nuna and Rodinia. This is evident across arctic Canada and Greenland, including in the Bylot basin group, which is made up of the Thule, Borden, Hunting-Aston and Fury, and Hecla basins (from north to south, present coordinates). The Fury and Hecla Group is a generally fining upward sequence of proximal terrigenous rocks to fine-grained marine rocks. We provide a first complete detrital-zircon provenance study of the Fury and Hecla Basin, the southernmost among the Bylot basins (in present coordinates). Seven samples spanning the Fury and Hecla Group were analyzed on the Sensitive High-Resolution Ion Microprobe (SHRIMP) at the Geological Survey of Canada (Ottawa). Detrital zircon U-Pb ages range from ~3350 to ~1695 Ma and display bimodal distributions with dominant peaks at ~2700 and ~1900 Ma. Archean peaks are prominent in basal samples but diminish up-section relative to Paleoproterozoic peaks, which become more prominent. Although the importance of sedimentary recycling from Paleoproterozoic supracrustal successions of the Rae Craton must be accounted for, provenance from local sources supports a recently proposed half-graben interpretation for the lower part of the Fury and Hecla Group. Late Paleoproterozoic zircon age modes suggest that during deposition of the middle/upper stratigraphy, the Fury and Hecla Basin acted as a sink for terrigenous detritus sourced from the unroofing of orogenic topography bounding the Rae Craton to the south (present coordinates). This hypothesis potentially reconciles the lack of thick carbonate accumulations in the Fury and Hecla Basin when compared to other Bylot basins. This detrital geochronology dataset supplements recently published absolute geochronology for the Fury and Hecla Group to differentiate otherwise monotonous sandstone units based on changes in provenance and generally furthers our understanding of intracratonic basin development leading up to the amalgamation of supercontinent Rodinia.

Quaternary stratigraphy and glacial history at Peace River, Alberta

Roger Paulen[1], Alwynne Beaudoin[2], Martin Ross[3], Scott Botterill?

[1]Natural Resources Canada roger.paulen@canada.ca, [2]Royal Alberta Museum, [3]University of Waterloo, ?Alberta Geological Survey

The Quaternary stratigraphy documented in Alberta's Peace River lowlands has been subject to many conflicting interpretations. This is probably due to the lack of a complete stratigraphic sequence preserved at a single section because of extensive landsliding along the Peace River valley, as well as a lack of chronologic control for lower parts of the sequence. There is ongoing debate over the number and style of Laurentide glacial advances in the Peace River district of western Alberta and eastern British Columbia. Given its northern Alberta location, resolving the glacial record of this area has important implications for understanding the evolution of the Laurentide Ice Sheet. The valley-fill sediments located at the confluence of the Heart and Peace rivers, at the town of Peace River, Alberta, provide perhaps the best record in western Canada of a continuum of Quaternary sedimentation from the preglacial bedrock surface to present. The composite stratigraphy of the Peace River valley (Fig. 1), which is 187 m thick, records the transition from preglacial fluvial sedimentation (unit 1), to a penultimate proglacial sedimentary sequence (units 2 and 3) conformably overlain by interstadial fluvial sediments (unit 4) of possible MIS-3 age, or older (based on radiocarbon). In turn, these are overlain by a Late Wisconsin ice advance/retreat cycle of sedimentation from the Laurentide Ice Sheet (units 5-8). The sequence is capped with Holocene cliff-top loess with paleosols, yielding mollusc and plant macrofossils. The only till unit in the stratigraphy (Unit 7) is from the Late Wisconsin glacial advance. The Canadian Shield lithologies in the lower fluvial sediments are from westward draining catchments, derived from the Buffalo Head Hills, where multiple, older glacial sediments have been documented. Consequently, there is evidence for only a single Laurentide glaciation in the eastern Peace River district, similar to what is defined to the southwest in other exposures on the Smoky River. Figure 1. Composite stratigraphy at the confluence of the Heart and Peace rivers. The Quaternary sediments overlie Early Cretaceous (Albian) Shaftesbury Formation shale, and consist of nine major units, approximately 187 m thick.

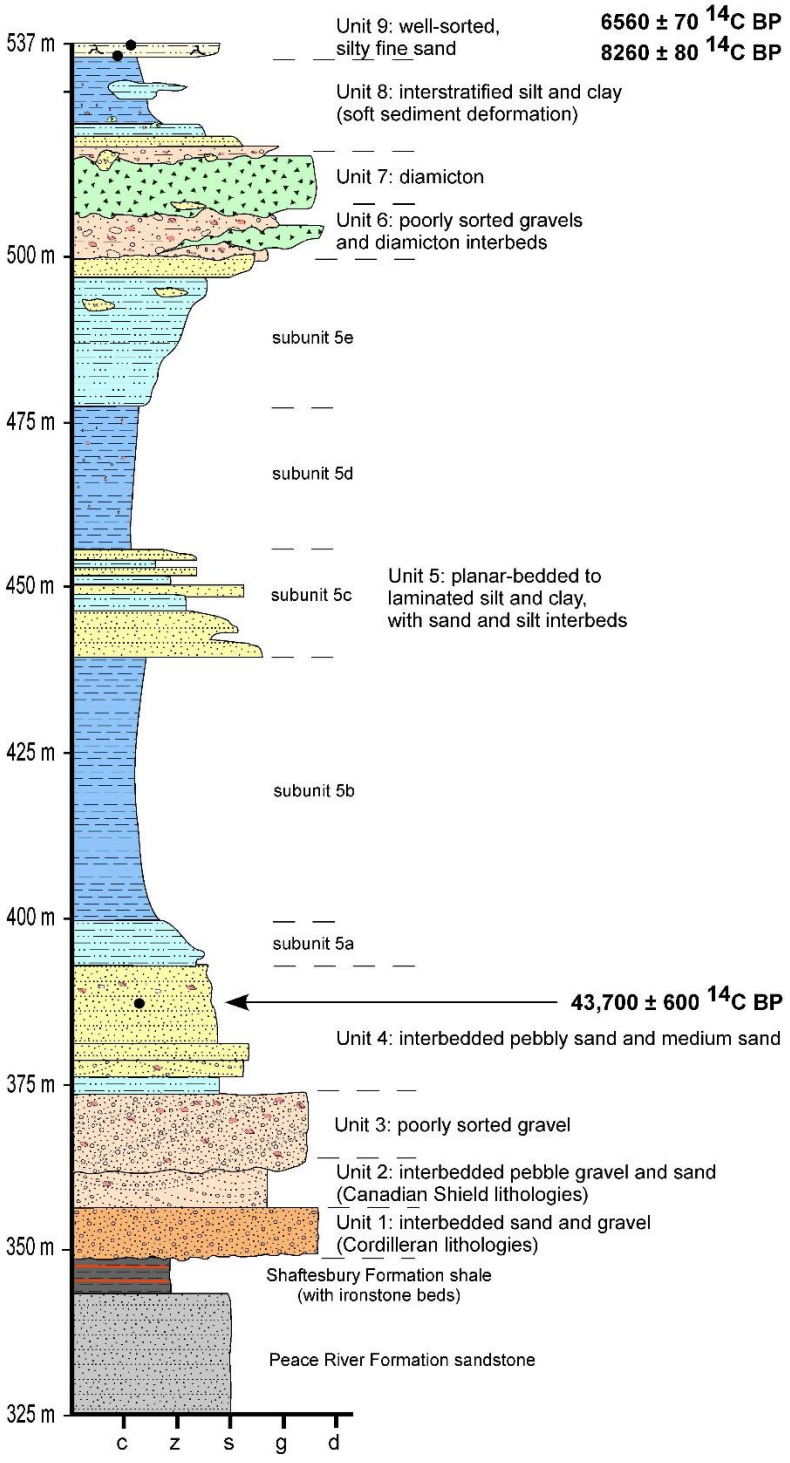

Revisiting the craton concept and its relevance for diamond exploration

Graham Pearson[1], Andrew Schaeffer[2], Thomas Stachel[1], Bruce Kjarsgaard[3], Herman Grütter[4], James Scott[5], Jingao Liu[6], Thomas Chacko[1], Karen Smit[1]

[1]University of Alberta gdpearso@ualberta.ca, [2]Geological Survey of Canada, Natural Resources Canada, [3]Geological Survey of Canada, [4]SRK, [5]University of Otago, [6]China University of Geosciences

The term craton has a complex and confused etymology. Despite originally specifying only strength and stability - of the crust - the term craton, within the context of diamond exploration, has widely come to refer to a region characterised by crustal basement older than 2.5 Ga, despite the fact that some such "cratons" no longer possess their deep lithospheric root. This definition often precluded regions with deep lithospheric roots but basement younger than 2-2.5 Ga. Viscous, buoyant lithospheric mantle roots are key to the survival and stability of continental crust. Here we use a revised craton definition (Pearson et al., 2021, in press), that includes the requirement of a deep (~150 km or greater) and intact lithospheric root, to re-examine the link between cratons and diamonds. The revised definition has a nominal requirement for tectonic stability since ~ 1 Ga and recognises that some regions are "modified cratons" - having lost their deep roots, i.e., they may have behaved like cratons for an extended period but subsequently lost much of their stabilising mantle roots during major tectono-thermal events. In other words, despite being long-lived features, cratons are not all permanent. The 150 km lithospheric thickness cut-off provides an optimal match to crustal terranes with 1 Ga timescale stability. In terms of regional diamond exploration, for a given area, the crucial criterion is when a deep mantle root was extant, i.e., over what period was the lithospheric geotherm suitable for diamond formation, stability and sampling? A thick lithospheric root is key to the formation of deep-seated magmas such as olivine lamproites and to the evolution of sub-lithospheric sourced proto-kimberlites, all capable of carrying and preserving diamonds to Earth's surface. This criterion appears essential even for sub-lithospheric diamonds, that still require a diamond transport mechanism capable of preserving the high-pressure carbon polymorph via facilitating rapid transport of volatile-charged magma to the surface, without dilution from additional melting that takes place beneath thinner (<120 km) lithospheric "lids". Seismology can help to define the lateral extent of today's cratons, but a detailed understanding of the regional geological history, kimberlite eruption ages and geothermal conditions is required to evaluate periods of past diamond potential, no-longer evident today. This revised craton concept broadens the target terranes for diamond exploration away from only the Archean cores of cratons and an associated mentality that "the exception proves the rule". The revised definition is compatible with numerous occurrences of diamond in Proterozoic terranes or Archean terranes underpinned by Proterozoic mantle.

Pearson, D.G., Scott, J.M., Liu, J., Schaeffer, A., Wang, L.H., van Hunen, J., Szilas, K., Chacko, T., Kelemen, P.B. (2021 - in press. Deep continental roots and cratons. Nature. https://doi.org/10.1038/s41586-021-03600-5)

Structural and metamorphic evolution of the Nemiscau subprovince, Superior Province, Quebec: long-lasting extrusion and lateral flow of the middle-lower crust?

Rocio Pedreira Perez[1], Alain Tremblay[1], Yannick Daoudene[2], Jean David[2], Gilles Ruffet[3], Daniel Bandyayera[2]

[1]Université du Québec à Montréal pedreira_perez.rocio@courrier.uqam.ca, [2]Ministère de l'Énergie et des Ressources naturelles, [3]Université de Rennes 1

The Nemiscau subprovince is a metasedimentary rocks-dominated terrane of the Archean Superior Province. North and south, it is bounded by plutonic terranes of the La Grande and Opatica subprovinces, respectively. The Nemiscau consists mostly of more-or-less migmatized metasedimentary rocks and felsic orthogneisses making up a dome-and-basin map pattern. Mafic-to-ultramafic metavolcanic rocks occur along its northern and southern boundaries. Previous studies of its structural and metamorphic evolution suggested that it was the result of subduction-related, accretionary and collisional tectonics with adjacent plutonic terranes during the Kenorean orogeny. The integration of geological mapping and various sets of structural and geochronological data acquired during this study indicates that the Nemiscau had a long-lasting tectonic evolution between ~2.80 and 2.50 Ga. The structural architecture of the Nemiscau subprovince and adjacent subprovinces is consistent with a N-S crustal shortening event recognized elsewhere in the Superior Province. Geochronological data suggest that the basal volcanic sequences of the Nemiscau formed between ca. 2755 and 2710 Ma, with oldest volcanic sequence exhibiting D1-related folded foliation. Shear-sense indicators related to major shear zones bordering the Nemiscau suggest the sinking of the volcanic and sedimentary rocks as compared to the adjacent TTG-rich terranes during a regional D2 deformational event around 2700 Ma. U-Pb zircon geochronology reveals that the associated granulite facies metamorphism, peaked at ca. 2695 Ma, and crustal anatexis of metasedimentary and TTG rocks from the Nemiscau progressively developed from 2700 to 2680 Ma. Later, strike-slip shear zones attributed to D3 accommodated the exhumation of mid-crustal rocks between ca. 2650 and 2640 Ma. 40Ar/39Ar amphibole cooling ages in the innermost part of the Nemiscau moreover suggest slow cooling of the high-grade rocks between ca. 2600 and 2575 Ma, prior to the formation of late-stage (D4) conjugated dextral and sinistral shear zones. Our field results and geochronological analyses suggest that the Nemiscau and adjacent La Grande and Opatica subprovinces most likely represent a single composite tectono-metamorphic terrane, and that the contacts between these three subprovinces should not be interpret as "collisional sutures" of distinct crustal blocks or microcontinents. The Nemiscau subprovince is rather interpreted as a supracrustal sedimentary sequence unconformably overlying a TTG-rich basement that is represented by both the La Grande and Opatica orthogneisses. In terms of tectonic evolution, the overall architecture of the Nemiscau, La Grande and Opatica subprovinces is compatible with a «hot orogen» model, in which the lower crust is usually characterize by channel-flowage and/or the lateral extrusion of the crustal material at high temperature.

Geological mapping of the SE Futuna Volcanic Zone, Lau Basin: tectonics and off-axis magmatism in modern back-arc systems

Ryley Penner[1], Margaret Stewart[1], Mark Hannington[2]

[1]Mount Royal University ryleypenner96@gmail.com, [2]University of Ottawa

Complex tectonism in the Lau Basin reflected by the interplay between extension and strike-slip faulting produces diverse fabrics along microplate boundaries. The Lau Basin is a type-example of a back-arc basin with well-documented hydrothermal venting, creating a natural laboratory for studying-ore forming processes. Crustal-scale structures, particularly those with a nearby heat source, act as pathways for hydrothermal fluids to reach the surface, and potentially form seafloor massive sulfides (SMS). Most hydrothermal studies have focused on spreading centres; therefore, our understanding of off-axes hydrothermal systems is less clear. The volcanic architecture off-axis of spreading centres in the SE Futuna Volcanic Zone (SEFVZ) suggests that the magmatic output may be partly controlled by the structural regime. We explore volcano-tectonic dynamics at a regional scale (1:200 000) using remote-predictive seafloor geological mapping techniques, to better understand the structural controls on the distribution of hydrothermal systems. To provide a picture of off-axis

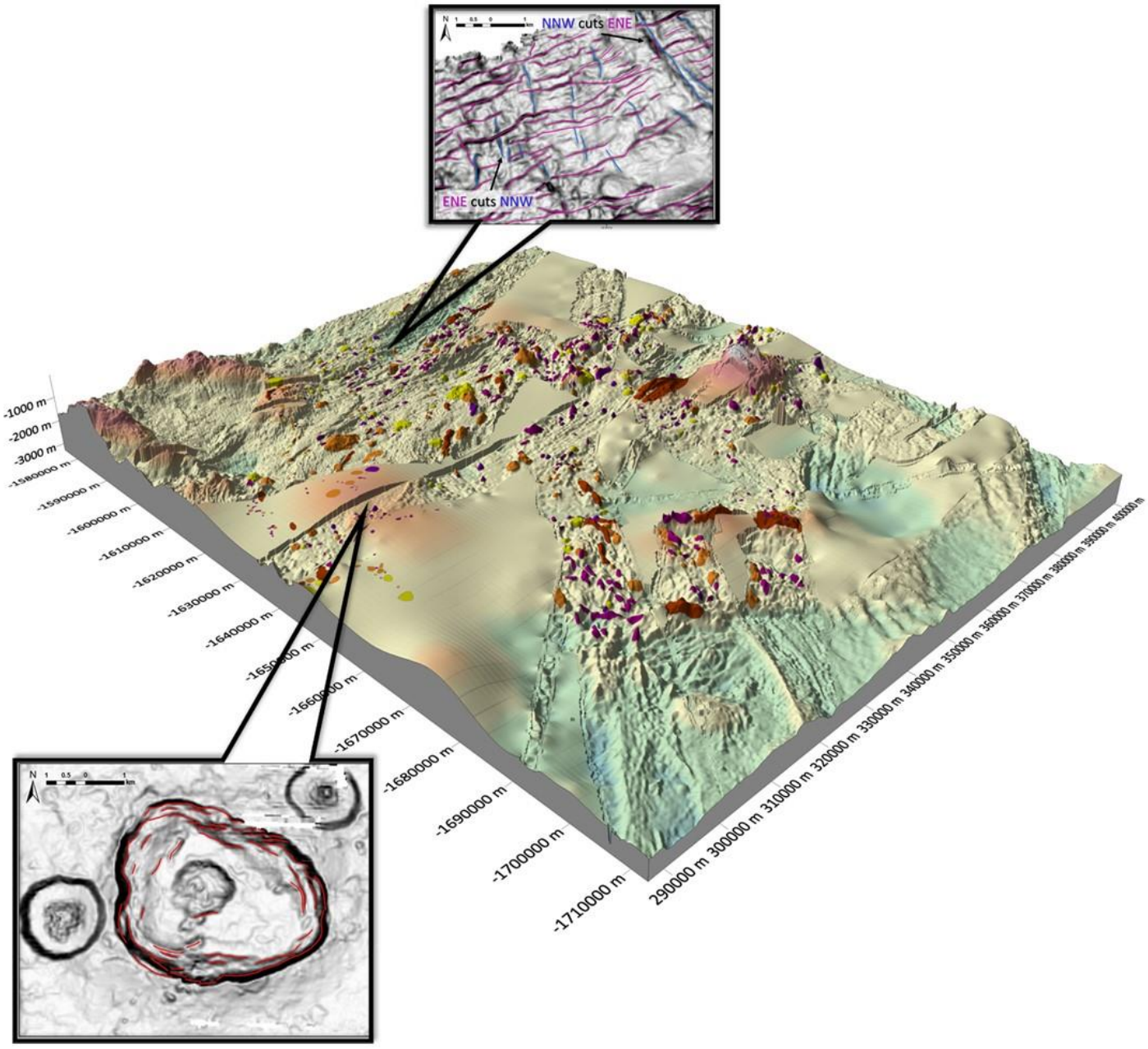

mechanisms for melt source and availability to form the large Kulo Lasi shield volcano, which is distil to any known plate boundaries, we compared the influence of local stress regimes on major structures and the geochemical affinity of samples collected along these structures. Lineament orientations and volcano morphologies were mapped using high-resolution ship-based multibeam bathymetry. Centroid moment tensor groupings are interpreted with stress vector addition of the local tectonic regimes to gain a sense of motion of the previously unresolved SE Futuna Deformation Zone (SEFDZ). The mapped features highlight intricate changes in tectonic fabric. Variations in volcanic morphology and volume indicate magmatic supply is locally enhanced by strike-slip faulting along the SEFDZ. We propose the SEFDZ represents an early, crustal-scale structure that was reactivated by transpression. Normal faulting combined with left-lateral strike-slip stress from the local regimes likely caused oblique compression to sufficiently reactivate an old spreading centre as a strike-slip deformation zone. Geochemical signatures of the SEFVZ compare closely to the affinity of Rochambeau Rifts (RR), suggesting the regimes are a part of one structural system tapping melt from the same mantle source. This evidence supports our interpretation that local stress re-activated pre-existing extensional features as R-shears. Kulo Lasi extruded proximal to the RR arm and the coincident intersection is interpreted to form a triple junction that increased crustal permeability and melt availability. Additionally, lineaments mapped along the rim of the Kulo Lasi caldera are suggested as synvolcanic reverse faults that may be prospective for SMS deposits. Off-axis settings can potentially host giant ore bodies due to the decreased rate of plate motion that may sustain long-lived hydrothermal systems for concentrating metals.

Cumulative Effects and Mining Legacies: Identifying Past, Present, and Future Impacts

Jeanne Percival[1], Michael Parsons[1], Alexandre Desbarats[1]

[1]Geological Survey of Canada Jeanne.Percival@Canada.ca

As former mining districts across Canada see increasing exploration for critical metals, impact assessment studies become more complicated. Distinguishing the environmental effects of legacy mining activity from the effects of new exploration and development requires improved geoscience tools and approaches. Renewed interest in the historical mining district of Cobalt, Ontario for cobalt metal, an essential component of rechargeable batteries, continues to make the news. The environmental legacy of mining in Cobalt spans over 100 years and is becoming increasingly complex because of ongoing remediation activities, natural recovery of local ecosystems, and exploration activities in impacted watersheds. Ongoing research at the Geological Survey of Canada is examining how best to unravel the history of polymetallic contamination from multiple sources over time and distinguish between mining impacts, naturally elevated background concentrations, and the effects of climate change and non-mining activities in the region (e.g. wastewater treatment). Mineralogical and geochemical data from mine tailings and lake sediments collected over the last several decades are being used to assess recent changes in the loading of metals and metalloids throughout the district. Surface water samples collected in June 2019 from various sites between Cobalt Lake and the Farr Creek Wetland have dissolved arsenic concentrations much lower than samples collected in the mid-1990s (e.g., 500 vs. 1000 µg/L for Cobalt Lake). Core samples from tailings sites along the drainage system show comparable changes. A push core from Cobalt Lake in 2019 shows a surface concentration of arsenic of 1500 mg/kg vs. ~3000 mg/kg from the north basin and up to 8000 mg/kg from the south basin, proximal to the high-grade mill runoff, in the older cores. These preliminary results demonstrate that natural recovery and local remediation efforts over this time have been successful in reducing the flux of arsenic into the receiving environment. The question remains, what effects will renewed mining activity pose in the coming years? The information arising from this new study and approach will help inform future cumulative impact assessments in the Cobalt mining camp and will be summarized in a geo-environmental model for Ag-Co-Ni-As vein-type deposits.

Impact spherules in ca. 2.1 Ga black shale of the Montresor belt, Nunavut: significance in early Paleoproterozoic history

John Percival[1], William Davis[1], Robert Berman[1], Duane Petts[1], Simon Jackson[1], Mark Harrison[2], Elizabeth Bell[2]

[1]Natural Resources Canada johnpercival@rogers.com, [2]University of California, Los Angeles

G.M. Young's 2013 Geoscience Frontiers review paper drew attention to extreme climatic and atmospheric change during the early Paleoproterozoic, and the complex interactions among Earth systems and early biota. Significantly, he related an abrupt decline in atmospheric oxygen, termination of the Lomagundi-Jatuli carbon isotopic excursion (LJE) and widespread deposition of organic-rich sediments (Shunga event) to near-extinction of life caused by the 2023 Ma Vredefort impact. Recent geochronology brackets the LJE to 2220-2060 Ma, suggesting additional complexity. New data from the Rae cover sequence (Nunavut) provide evidence of a previously unrecognized, ca. 2.1 Ga impact event. A crudely layered, 7-cm-thick bed within black shale of the Montresor belt (depositional bracket 2194-2045 Ma) contains white, mm-scale spherules. Despite a weak foliation and greenschist-facies metamorphism, imposed at ca. 1850 Ma during the Trans-Hudson orogeny, some primary textural, mineralogical and compositional features appear well preserved, including whole-rock (0.5 ppb) and spherule (1-70 ppb) Ir anomalies. SEM, TEM and LA-ICP-MS maps show K-rich cores and Ca-rich mantles in very fine-grained (<1-100 μm) assemblages of phengite-Kspar-muscovite-quartz-chlorite-prehnite. Phengite is amorphous and displays nm-scale lamellae, consistent with shock effects. Its composition resembles that of phengite from UHP terranes and its origin remains enigmatic. The spherules have high Nb contents (avg. 40 ppm) and anomalously high Nb/Ta (avg. 30), suggesting unusual impactor or target composition. Small zircons (1-30 μm) show truncated zonation overgrown by 1-5 μm-thick rims. Small spots (5-10 μm) on zircon interiors using UCLA's ion probe with a Hyperion-II RF source yielded 207Pb/206Pb ages between 2827 and 1736 Ma. Notably, two homogeneous, luminescent grains gave relatively concordant ages of 2088 ± 48 and 2203 ± 47 Ma. Assuming that the zircons are derived from the target rocks and were not reset during the impact, the bracket on depositional age is reduced to ca. 2100-2045 Ma. Although no impact event has previously been recognized within this time window, the occurrence of thin, distal spherule deposits is significant, because large (e.g., Chixculub-sized) impactors are required to generate these rare, globe-enveloping vapour clouds and consequent effects on the atmosphere and biosphere, including mass extinction events related to Phanerozoic impacts (Glass and Simonson, 2012, Distal Impact Ejecta Layers, Springer). Effects of large impacts on Paleoproterozoic biota are speculative; however, proxy evidence suggests abrupt declines in bioproductivity associated with the end of the Great Oxidation Event. This biological set-back, which heralded the "boring billion", may have resulted from repeated atmospheric disturbances related to a cluster of large impact events: Yarabubba (2229 Ma); Montresor (ca. 2100 Ma); Vredefort (2023 Ma); and Sudbury (1850 Ma).

Strategic Environmental Assessments to inform decision-making on potential oil and gas activities in Canada's Arctic offshore waters

Filip Petrovic[1], Martin Tremblay[1], Daniel Van Vliet[1], Emily Thorne[1], Joelle Crook[1]

[1]Crown-Indigenous Relations and Northern Affairs Canada filip.petrovic@canada.ca

The Arctic is a vast and dynamic ecosystem as well as a place of natural resource potential upon which northern communities rely for their livelihoods. The Government is committed to early engagement of Inuit and Inuvialuit on potential offshore oil and gas activity in the Arctic and to ensuring that decision-making on resource management is evidence-based and considers possible impacts to the unique environment and wildlife. Crown-Indigenous Relations and Northern Affairs Canada (CIRNAC) is responsible for the management of oil and gas resources in Canada's Arctic offshore waters, under the Canada Petroleum Resources Act. In partnership with Inuit and land-claim organizations, CIRNAC advanced two Strategic Environmental Assessments (SEAs) in the Beaufort Sea and Baffin Bay and Davis Strait regions to examine the risks and benefits of resource development and consider the potential interactions with the natural and social environments in these regions. This work aimed to respectfully and meaningfully gather available Indigenous Knowledge, scientific information, and community input. These components are the evidence base that decision-makers will use to guide the future of these offshore regions, and of the communities that depend on the environment. These SEAs also represent key contributions to informing the five-year review of the moratorium on oil and gas activities in Canada's Arctic offshore waters, announced in the United States-Canada Joint Arctic Leaders' Statement in December 2016.

The Dawn of the Anthropocene and the Rise of the Green Algae

Paul Pilkington[1], Francine McCarthy[2], Martin Head[2], Nicholas Riddick[2], Olena Volik[3]

[1]Brock Univeristy ppilkington@brocku.ca, [2]Brock University, [3]University Of Waterloo

In May 2021, the Anthropocene Working Group voted to treat the Anthropocene as a formal chronostratigraphic/ geochronologic unit defined by a GSSP, and that one of the stratigraphic signals around the mid-twentieth century of the Common Era serve as the primary guide for the base of this series, defining the beginning of the epoch. In addition to radioisotopes associated with the nuclear fallout from atmospheric thermonuclear testing, several proxies associated with the Great Acceleration that followed the Second World War record the unprecedented anthropogenic impact on Earth systems. These include a rapid increase in spheroidal carbonaceous particles resulting from the burning of fossil fuels and microplastics reflected the flourishing petrochemicals industry and increased rate of per capita consumption of manufactured goods. The best-known impact has been on the concentration of greenhouse gases in our atmosphere which can be measured directly in ice cores. The increase in atmospheric CO2 impacts the global climate (and many related phenomena), but it also affects the pH of water bodies (increasing the production of carbonic acid) and makes carbon more readily available to primary producers. Green algae, the earliest known eukaryotes, are less efficient at capturing CO2 than cyanobacteria or chlorophyll c-hosting eukaryotic algae (diatoms and dinoflagellates), so green algae have proliferated since the mid-20th century. A relative increase in the acid-resistant remains of green algae in slides processed for pollen analysis has been reported in lake sediments from North America, South America, and Eurasia, suggesting that this could be a useful palynological marker of the base of the Anthropocene. The increased frequency of cyanobacterial harmful algal blooms (cHABs) in recent decades, as freshwater ecosystems respond to warmer climates and continued influx of limiting nutrients, may prove to be a useful signal for subsequent decades of the proposed Anthropocene Epoch. Because many green algal palynomorphs and cyanobacterial remains are destroyed by conventional processing techniques employed by pollen analysts, avoiding the use of strong oxidants is recommended to allow this potentially important signal to be observed.

Recent Advances in Mineral Liberation Simulation and Modelling

Andriy Plugatyr[1]

[1]National Research Council of Canada andriy.plugatyr@nrc-cnrc.gc.ca

The growing need to improve energy efficiency and reduce environmental footprint of mining operations is the driving force behind efforts to develop and adopt more selective approaches in mining and mineral processing. Practical implementation of these methods requires an understanding of spatially-resolved geometallurgical attributes which, in turn, presents a challenge from the sampling, sample characterization and metallurgical testing point of view. It is envisioned that advances in geosensing techniques will soon be able to extend the application of quantitative mineralogical analysis (QMA) to spatial scales relevant to ore pre-concentration technologies (e.g. sensor-based particle sorting, Grade Engineering®, coarse particle flotation, etc.). In this regard, the development of methods for inference of geometallurgical attributes based on rock image analysis is of great practical importance for devising robust sampling and metallurgical testing campaigns. The paper highlights recent advances in mineral liberation simulation and modelling, and presents examples of practical implementations. A generalized approach for simulating mineral liberation based image analysis using the Voronoi tessellation technique is discussed in detail. The method, applicable to both 2D (e.g. QMA tiles) and 3D (e.g. µCT) image processing, can be adapted to simulate both random and non-random breakage. Examples of application of the technique for predicting grade-by-size distribution profiles based on QMA image analysis and estimating optimal particle size for liberation are provided.

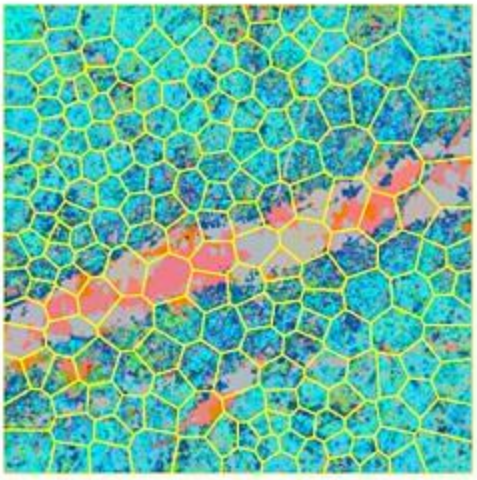

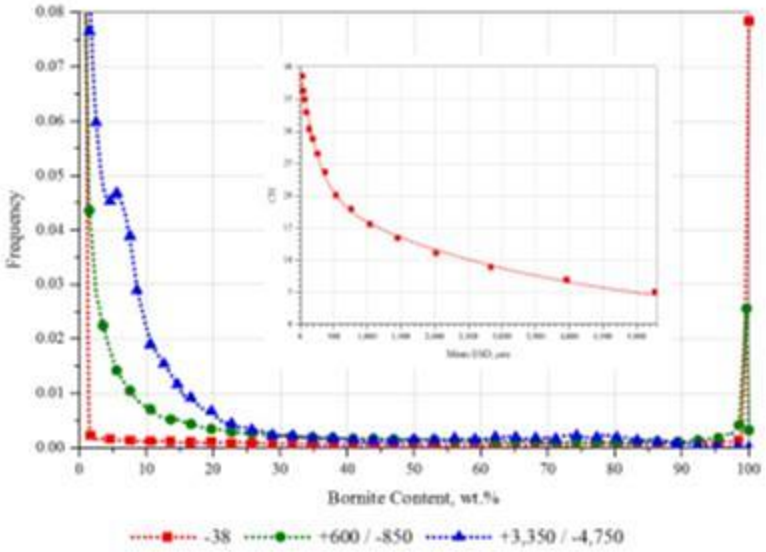

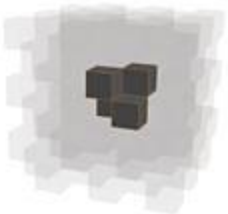

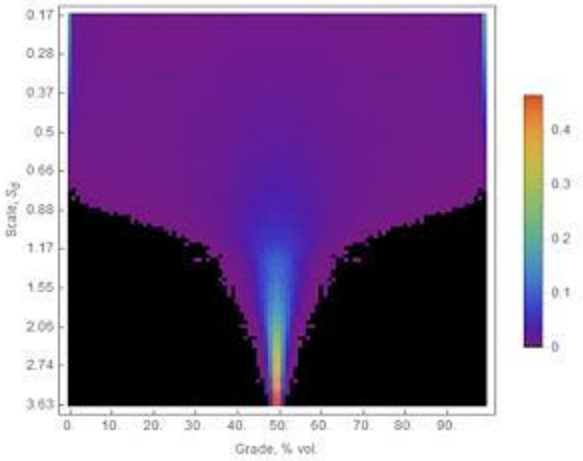

WHAT IS A PRIMARY ROCK HOSTED DIAMOND DEPOSIT, RESOURCE AND RESERVE? DESKTOP TO FEASIBILITY STUDY GOVERNANCE EXAMPLE UNDER CIM AND NI 43-101 GUIDELINES AND DEFINITION STANDARDS AND DE BEERS SCORECARD CLASSIFICATION, GAHCHO KUÉ MINE, NORTHWEST TERRITORIES

Martin Podolsky[1]

[1]SRK Consulting (Canada) Inc. mpodolsky@srk.com

A primary Rock Hosted Diamond Deposit, Resource and Reserve Asset Development Standard (ADS) model governed under the 2014 Canadian Institute of Mining, Metallurgy and Petroleum (CIM) Definition Standards on Mineral Resources and Reserves and 2016 Toronto Stock Exchange National Instrument 43-101 - Standards of Disclosure for Mineral Projects (NI 43-101), is presented. The De Beers Canada - Mountain Province Diamonds joint venture Gahcho Kué Project roadmap from exploration commencing in 1992, reporting of initial Desktop Study in 2000 to definitive Feasibility Study in 2010 and 2014 Study update is reviewed under the incorporated 2003 Guidelines for the Reporting of Diamond Exploration Results and 2008 Estimation of Mineral Resources and Mineral Reserves Best Practices Guidelines for Rock Hosted Diamonds. A published De Beers system of diamond Deposit to Resource geo-scientific scorecard classification is summarized and compared against the CIM and NI 43-101 Definition Standards and reporting guidelines. The ADS governance model utilizes the De Beers classification system, that is aligned with reporting of Desktop, Conceptual and Pre-Feasibility to Feasibility Studies.

Geophysical and structural modeling of selected REE-Th-U deposit areas within the Canadian and Ukrainian Shields

Kateryna Poliakovska[1], Irvine Annesley[2], James Sykes[3], Olena Ivanik[4], Akira Otsuki[1], Nicolas Guest[3]

[1]Université de Lorraine - École Nationale Supérieure de Géologie (ENSG), GeoRessources kateryna.poliakovska@gmail.com, [2]ENSG - Universite de Lorraine / Dept. Geological Sciences - University of Saskatchewan, [3]Appia Energy Corp., [4]Taras Shevchenko National University of Kyiv - Institute of Geology

Structural mapping and geological terrain analysis, including lineament analysis, are considered important geological tools for identifying the prevailing tectonic trends within a study area. Lineaments are straight to curvilinear landforms of the Earth's surface that are closely related to underground concealed structures, such as faults, shear zones, and folds, but also to geomorphological or man-made features and can provide valuable information related to geological structures, tectonics, hazard assessment, and natural resource availability. One of our research objectives was to establish a methodology for automatic/digital and manual lineament analysis of potential field geophysical data sets combined with aerial photography/Landsat data that would be suitable for the two selected study areas - i.e., within the Canadian (Alces Lake area) and Ukrainian (West Azov area) Shields. The first area, the Alces Lake area, contains the highest-grade REE occurrences in Canada, with the mineralized zones hosted by REE-rich abyssal pegmatites. The REEs are found mainly in monazites within granitic to biotite-garnet-rich residual melt pegmatites, which are inferred to be associated spatially with regional fold, shear, and fault structures in deformed paragneiss and orthogneiss. The second chosen area is located within the West Azov block of the Ukrainian Shield, where several REE deposit types (rare metal-rare earth granite pegmatites, rare earth granites and rare earth metasomatites) were identified,

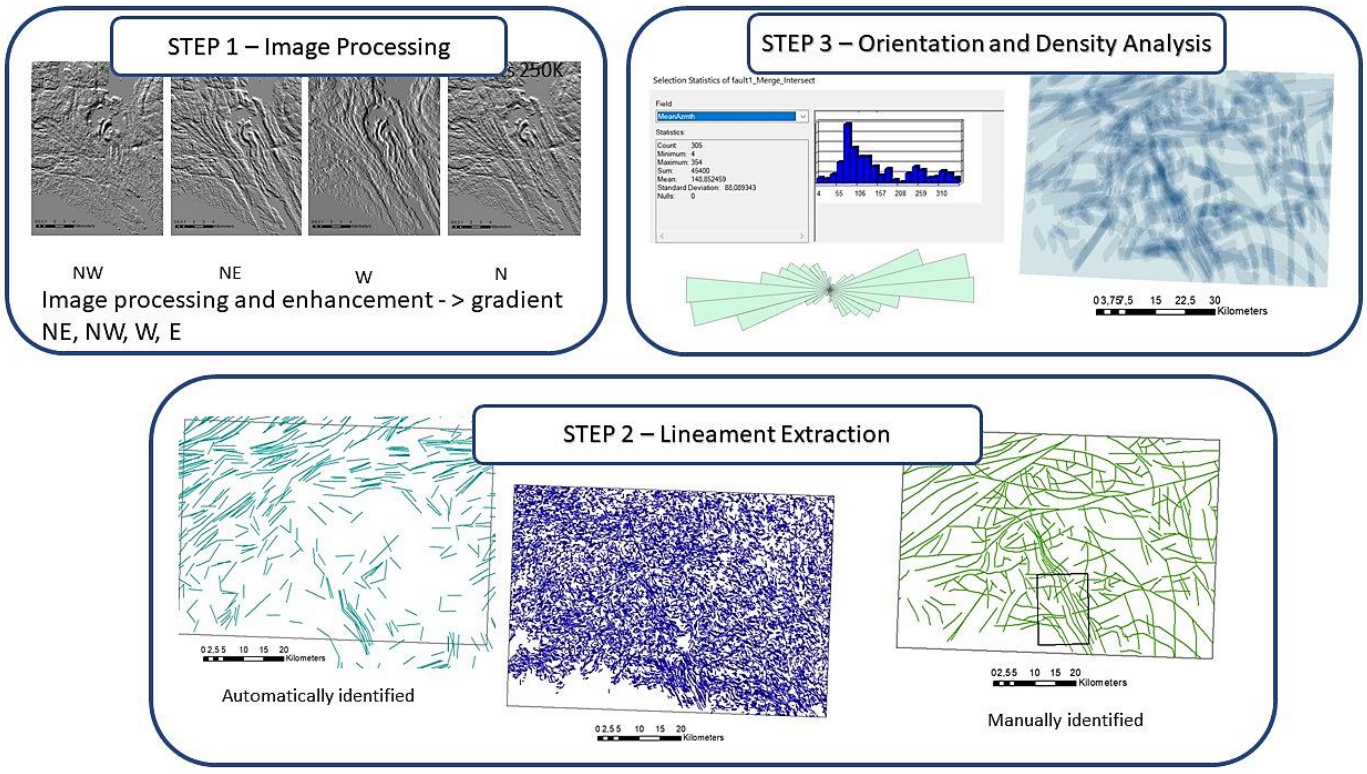

with the most favorable locations/conditions for the occurrence of mineralization linked to polydeformed and folded gneissic rocks. In our research, we created several structural geophysical models using both topographic (SRTM, DEM, Landsat 8) and geophysical data (magnetic & gravity). The modeling process utilized several geomodeling software packages (Geosoft Oasis Montaj, ArcGIS, and Python API library of Geoscience Analyst). Remote sensing and GIS techniques were applied as well for the orientation and density analysis. The obtained results indicate that both automatic and manual methods were able to correctly identify some

geological structures and have different reliability and accuracy (which depends also on the characteristics of the terrain). Thus, it is recommended by the authors to utilize the combined manual and automated approach to achieve the most reliable results. Mineralization is related mainly to the following lineament features: 1) NNW-SSE and E-W - oriented structural elements within the Alces Lake area and 2) NW-SE, E-W and NNE - ones within the West Azov area, which can be tracked using lineament analysis. This gives some new insight to the REE-Th-U mineral systems of the two shield areas and provides vectoring guidelines for new discoveries by identifying major intersection zones of possible fault dilation with associated fluid/heat flow; i.e., where structural geochemical traps are sited for precipitating metal-rich fluids (melts).

The epidemiology of landslide disasters with reference to the 2014 Hiroshima debris flows

Kevin Potoczny[1], Stephen Evans[1]

[1]University of Waterloo kpotoczny@uwaterloo.ca

As highlighted by the recent (July 3, 2021) debris flow disaster at Atami (Shizuoka Prefecture), destructive rainfall-related debris flow events are a relatively common occurrence in Japan. In Hiroshima City (Hiroshima Prefecture), historical records indicate that the city has suffered extensively from debris flows triggered by high-magnitude precipitation events (Chigira, 2000; Wang, 2015; Hashimoto et al., 2020). Since 1945, there have been five damaging debris flow episodes that have caused approximately 1,500 fatalities, the most recent occurring in 2018 (Hashimoto et al., 2020). In 2014 debris flows struck the wards of Asaminamai and Asakita, in the northern part of Hiroshima City, after experiencing 220 mm and 300 mm of rainfall respectively over a span of three hours (Wang et al., 2015; Tsuchida et al., 2019). 2015 Census data from the Statistics Bureau of Japan shows a total population of 238,763 in Asaminami (population density of 2,072 p/km2) and 151,218 in Asakita (population density of 410 p/km2). Debris flows destroyed 132 houses and partially destroyed another 122. With an occupancy rate of 2.45 persons/household (Statistics Bureau of Japan data) the estimate of the exposed population in the two wards (defined here as the number of people present in destroyed and partially destroyed houses) is thus a total of 622 (160/100,000 affected population for both wards). Debris flows left 74 killed and injured 44 for a total of 118 casualties (Fatality Ratio of 63%) equivalent to 12% of the exposed population (defined above) killed and 19% of the exposed population as casualties in both wards. Comparative data for the 2011 Great East Japan Earthquake and Tsunami in Miyagi Prefecture indicate that 72% of casualties were fatal (a similar Fatality Ratio to that obtained in Hiroshima) but only ~2% of the exposed population, as defined here, were killed (National Police Agency data); this suggests that catastrophic landslides result in high casualty rates in the population exposed to landslide impact. We also found that death/exposed population at both the societal and individual scale scales directly with population density in the Hiroshima debris flows. These data raise the question of how to define exposed population in disaster studies when not all of the population of a given administrative unit are exposed to a particular hazard. By viewing landslide disasters as a public health issue epidemiological analysis can provide comparative data for enhanced landslide risk assessment and gives insight into the elements of disaster risk.

Magnesium carbonate formation at Earth's surface: Implications for biosignature preservation on Mars

Ian Power[1], Teanna Burnie[1], Anna Harrison[2], Vasileios Mavromatis[2], Hülya Alçiçek[3], Luisa Falcón[4]

[1]Trent University ianpower@trentu.ca, [2]CNRS, [3]Pamukkale University, [4]Universidad Nacional Autónoma de Mexico

Jezero Crater, the landing site for NASA's Mars 2020 Perseverance Rover mission, is a paleolacustrine environment where magnesium carbonate minerals have been detected and may contain evidence of past life [1]. As such, Mg-carbonate environments on Earth are of renewed interest as terrestrial analogues. The depositional environment along with precipitation rates and mineral transformations for Mg-carbonate minerals will greatly influence biosignature preservation. Hydromagnesite-magnesite playas near Atlin, British Columbia, Canada host a complex assemblage of carbonate minerals including abundant magnesite (MgCO3), the most stable form of Mg-carbonate [2]. Stable, radiogenic, and clumped isotope data in concert with electron microscopy demonstrate that magnesite forms by direct precipitation from pore waters in the shallow subsurface (~3^{-10} °C) [3, 4]. Using particle size and surface area data as well as mineral abundances, we determined magnesite formation rates to be in the range of 10^{-17} to 10^{-16} mol/cm^2/s. These slow precipitation rates require ~100-1000s of years to grow micron-scale crystals. Hydromagnesite [Mg5(CO3)4(OH)2·4H2O] precipitation is also generally slow under Earth's surface conditions with its formation in the playas likely being a combination of mineral transformations and direct precipitation. The sluggish rates of magnesite and hydromagnesite precipitation lead to the formation of a variety of other metastable hydrated Mg-carbonates that generally precipitate subaerially under highly evaporative conditions. These minerals easily transform to less hydrated, more stable phases (lansfordite > nesquehonite > dypingite > hydromagnesite) through coupled dissolution-precipitation reactions that occur at the mineral-water interface. The unconsolidated Mg-carbonate sediments lack substantial biomass and there is little to no evidence that biosignatures are preserved for long periods. Other natural analogues to Jezero Crater include the lacustrine environments of Lake Salda, Turkey and Lake Alchichica, Mexico, where hydromagnesite is also the dominant Mg-carbonate mineral. Like the Atlin playas, hydromagnesite from these sites was generally devoid of morphological biosignatures. The evaporative conditions for which hydrated Mg-carbonates form are not ideal for the proliferation of microbial life in comparison to subaqueous environments and transformation reactions may destroy biosignatures. These factors along with slow magnesite precipitation rates that are unlikely to entomb microbial cells will all reduce the likelihood of biosignature preservation within Mg-carbonate environments.

1. Horgan, B.H.N. et al., 2020. Icarus, 339:34. 2. Power, I.M. et al., 2014. Sedimentology, 61:1701-1733. 3. Power, I.M. et al., 2019. Geochim. Cosmochim. Acta, 255:1-24. 4. Mavromatis, V. et al., 2021. Chem. Geol., 579:120325.

Analysis and tectonic implications of multiscale structures in the east segment of the Shangdan Tectonic zone of the Central China Orogenic Belt

Mengmeng Qu[1], Lucy Lu[2], Dazhi Jiang[3]

[1]East China University of Technology qumengmeng@ecut.edu.cn, [2]Cardiff University, [3]Western University

The Shangdan Tectonic Zone (SDTZ) is one of the most significant features in the Central China Orogenic Belt (CCOB) which separates the North China Block (NCB) from the South China Block (SCB). It is widely accepted that the SDTZ was inherited from a Paleozoic suture, but the significant tectonic deformation in the zone was due to the Triassic essentially orthogonal collision between the NCB and the SCB. However, a long unresolved issue is that the structural association in the SDTZ is not consistent with orthogonal collision. Throughout the east segment of the SDTZ where the zone is best exposed, a sub-vertical transposition foliation and sub-horizontal stretching lineations are well developed, and sinistral kinematic indicators are best observed on sub-horizontal exposures. This suggests that strike-slip motion is significant for the SDTZ and must be considered in the tectonic model of the CCOB. In this work, we conduct multiscale structural analyses in the east segment of the SDTZ and the country rock (Liuling Group). The latter has two generations of deformation. D1 consists of down-dip stretching lineations, orogen-parallel isoclinal folds, and sub-vertical transposition/axial plane foliations. We also compile previous geochronologic data and conduct zircon U-Pb dating analysis to constrain the deformation time. To quantify the significance of strike-slip motion, we use a micromechanics-based multiscale approach to relate the structures within the SDTZ with the tectonic boundary conditions. As the SDTZ was an inherited feature, we regard it as a pre-existing weak flat inclusion in the lithosphere during the Triassic convergence between the NCB and the SCB. The structural associations in the SDTZ and that D1 structures in the Liuling Group are interpreted as a strain field due to sinistral transpression between ca. 246 Ma - 201 Ma constrained from geochronological data. Modeling results show that the boundary convergence angle is in the range of 40° - 60°. The shortening across the orogen caused by the convergence was accommodated by 40% along-orogen extension and 60% vertical thickening. We discuss the tectonic implications of our results and propose a scissor-like convergence combined with previous magmatism, metamorphic and paleomagnetic studies.

Compositional and thermal variations of uranium-mineralizing fluids along the Patterson Lake corridor in the Athabasca Basin, northern Saskatchewan

Morteza Rabiei[1], Guoxiang Chi[1], Eric Potter[2], Feiyue Wang[3]

[1]University of Regina morteza.rabiei2m@gmail.com, [2]Geological Survey of Canada, [3]University of Manitoba

The high-grade unconformity-related uranium (URU) deposits in the Athabasca Basin are located within permeable corridors developed along intersections between reactivated basement-rooted reverse faults and the basal unconformity. Although URU deposits are related to these structural corridors, only small segments of them are mineralized. Previous geochemical studies suggested that either the presence or absence of reducing or uranium-rich oxidizing fluids along certain segments of the faults were the major factors in localizing ore zones. However, few studies have examined compositional changes in syn-ore fluids between areas distal and proximal to the mineralizations along these corridors. In order to determine ore-localizing factors, microthermometric and ICP-MS bulk fluid inclusion analyses were conducted and changes in the composition of the mineralizing fluids were examined along the Patterson Lake corridor (PLC) in the western Athabasca Basin. Fluid inclusion analyses along the PLC indicate that salinities of the syn-ore fluids range from 8.8 to 33.8 wt.% NaCl + CaCl2 (avg. 25.4 wt.%) and total homogenization temperatures (Th) from 64 ° to 248 °C (avg. 128 °C). The spatial distribution of both salinity and Th values does not systematically vary along strike or depth. Bulk fluid inclusion analyses support the microthermometric data and indicate elevated concentrations of uranium in syn-ore fluids from both mineralized zones (0.39 to 93.6 ppm U) and distal areas (0.12 to 1.5 ppm U). These results suggest the presence of uraniferous fluids with similar thermal and compositional characteristics along the entire PLC. Therefore, localization of ore zone is more likely controlled by the rate of fluid flow and/or timing of fluids carrying reducing agents, both of which are enhanced by late brittle fracturing.

Young et al. 1979. Middle and late Proterozoic evolution of the northern Canadian Cordillera and Shield, Geology: a retrospective and update

Robert Rainbird[1], Thomas Hadlari[2], Charles Jefferson[2], Galen Halverson[3], Elizabeth Turner[4]

[1]Geological Survey of Canada/Carleton University rob.rainbird@canada.ca, [2]Natural Resources Canada, [3]McGill University, [4]Laurentian University

Since the publication of this seminal paper, more than 40 years ago, an immense amount of research has been conducted on Proterozoic sedimentary successions exposed in the northern Canadian Cordillera and their stratigraphic equivalents in cratonic basins to the east. This work was initiated by Grant Young and his students at the University of Western Ontario as well as by Jim Aitken and Gary Eisbacher from the Geological Survey of Canada (GSC). Subsequent studies by the GSC, Yukon Geological Survey and academic researchers based at Carleton, Simon Fraser, Laurentian, McGill and Harvard universities have revolutionized our understanding of these rocks. In the original paper, these successions were subdivided into three sequences, A (~1.7-1.2 Ga), B (1.2-0.8 Ga), and C (0.8-0.57 Ga) separated by unconformities that represented deformation and uplift accompanying regional-scale orogenesis. These subdivisions have served as a robust lithostratigraphic framework for local and regional stratigraphic studies, and are still valid today, although correlations, particularly between the cordillera and craton, have been significantly modified. One of the most significant advances made over this time is better age constraints. These have refined correlations and allowed researchers to further subdivide the sequences. The advent of U-Pb detrital zircon geochronology has allowed us to establish maximum depositional ages and age "bar-codes" for clastic strata and facilitated correlation and paleogeographic interpretations derived from provenance analysis. Re-Os geochronology of carbonaceous shales has permitted direct dating of otherwise undateable strata for calibration of stable isotope curves and for identifying significant lacunae in the sedimentary record. Equally important are the detailed stratigraphic, sedimentological, paleontological and geochemical studies that have improved our understanding of depositional environments and how these vary stratigraphically and regionally as a function of the differing tectonic settings of the basins in which they were deposited. In this presentation, we highlight specific examples of where progress has been made and present an updated regional sequence stratigraphic correlation scheme.

Plausibility Milankovitch Cycles in a Super Greenhouse World

Nicolas Randazzo[1], Nicolas Randazzo[1], Janok Bhattacharya[1], Sang-Tae Kim[1], Monica Walecki[1]

[1]McMaster University randazn@mcmaster.ca

The Turonian Age (93.9 ± 0.8 Ma and 89.8 ± 1 Ma) marks a peak greenhouse in the Late Cretaceous, during which average global sea-surface temperatures are estimated to be ~35°C. High resolution sequence stratigraphic analysis shows a dominance of low amplitude, Milankovitch cycles but there is debate as to whether Earth was ice free, which would require steric effects or aquifer eustasy as the driving mechanism versus growth and decay of ephemeral Antarctica ice sheets. The presence of polar ice during a super greenhouse period, may also explain water column oxygenation and nutrient upwelling in coastal environments. In this study, we applied back-stripping analysis on multiple formations within the Cretaceous Western Interior Seaway (KWIS) to estimate the influence of sediment compaction and tectonic subsidence to deduce the magnitude of changes in sea-level and test the possibility of glacio-eustatic control. We performed this analysis on multiple sections such as the Cardium Formation in the Alberta Basin, the Last Chance and Notom Delta complex of the Ferron sandstone in the Uinta Basin, Utah and the Gallup Formation and Juana Lopez Member of the Carlisle Formation in the San Juan Basin, New Mexico. The timing of eustatic cycles was constrained by high resolution age dates from detrital zircons and sanidines in bentonites correlated to biostratigraphy. We subsequently reconstructed and correlated sea level curves to evaluate the magnitude and synchroneity of eustatic cycles within the KWIS. Our back-stripping results show sea level changes ranging in magnitude from 10-60 m. Alternate causes of sea-level change, such as steric effects and aquifer-eustasy, can only explain up to 10 m and 5 m of sea level change, respectively. Additionally, aquifer- and glacio-eustasy cannot influence sea-level at the same time. As such, any sea-level change above 15 m at the very least suggests an influence of both thermo- and glacio-eustatic effects, with the influence of glacio-eustasy increasing with increasing sea-level rise. Our observations through back-stripping calculations illustrate a plausible influence of glacio-eustasy in multiple areas in the KWIS. Consequently, our reconstructed sea-level curves based upon the timing of the parasequences in our studied locations provide evidence of glacio-eustatic cycles as a significant driver of sequence-scale sea level change in the KWIS and support the hypothesis that ephemeral ice sheets were present within Antarctica during the Turonian.

Change detection and monitoring with the Colour and Stereo Surface Imaging System onboard the ExoMars Trace Gas Orbiter

Vidhya Ganesh Rangarajan[1], Livio Tornabene[1], Gordon Osinski[1], Susan Conway[2], Nicolas Thomas[3], Gabriele Cremonese[4]

[1]University of Western Ontario vrangara@uwo.ca, [2]Université de Nantes, [3]University of Bern, [4]INAF-Osservatorio Astronomico di Padova

Mars is host to a variety of past and present active processes caused by changes in wind, seasonal ice/frost, and processes related to liquid water. Resultant surface features display distinctive morphologic or sometimes spectral changes between time periods, that provide insights into both present and past climates that may have influenced their formation and evolution. The Mars Reconnaissance Orbiter (MRO) has been tracking most of these recent changes from 2006, through temporal High Resolution Imaging Science Experiment (HiRISE) and Context Camera (CTX) images. Since MRO operates in a sun-synchronous orbit, multiple images over the same area are acquired at similar local times. Hence, qualitative methods involving visual comparisons of successive time-series images at similar lighting conditions, by looking at variations in surface brightness and/or distinct alterations in surface morphology, are sufficient. While CTX is a fully monochromatic imager, HiRISE additionally provides spatially and spectrally limited colour information as a narrow colour strip along the image centre. The higher spatial scale of HiRISE permits tracking of finer morphologic changes, but the narrow colour strip (~20% of the full image width) often fails to cover the entire region of interest (ROI), thus reducing our ability to characterise most colour-associated surface changes. Since 2018, the Colour and Stereo Surface Imaging System (CaSSIS) onboard the ExoMars Trace Gas Orbiter (TGO) has been acquiring more extensive coverage and better calibrated 4-band VNIR colour data at a spatial scale of ~4m/px. TGO operates in a non-sun-synchronous orbit, making CaSSIS the only orbiting sensor to image Mars at multiple times of day, potentially allowing us to even track diurnal processes in colour. However, this configuration also means that qualitative change detection methods may not be suitable for CaSSIS-based change detection campaigns, as variable image acquisition parameters, resulting as a combination of different atmospheric and geometric conditions between successive images may significantly impact interpretations. With MRO's operational capability reducing with time, shifting to a CaSSIS-based change detection process is even more crucial and thus, a layout of optimal methods to pursue change monitoring from CaSSIS observations is necessary. Our work presents a set of additional semi-quantitative colour-based techniques, that can be used in concert with visual comparisons to aid reliable change detection. It is observed that inter-image variations in spectral band ratios, aimed to enhance absorptions due to ferrous/ferric bearing surface morphologies significantly help in characterising newer changes. This is supplemented by distinct changes seen while comparing in-scene spectra, between ROIs inside and outside the change area. These additional methods have since then been tested and found to be useful to track newer changes across a variety of surface settings.

Modelling Canada's deep geological repository throughout space and time

Tarek Rashwan[1], Md Asad[1], Sarah Couillard[1], Ian Molnar[2], Peter Keech[3], Mehran Behazin[3], Magdalena Krol[1]

[1]York University trashwan@yorku.ca, [2]University of Edinburgh, [3]Nuclear Waste Management Organization

Nuclear waste management is a major global issue and nuclear safety agencies around the world agree that deep geological repositories (DGRs) are viable end-of-life solutions. DGRs consist of multibarrier systems and are designed to safely isolate hazardous nuclear waste in used fuel containers (UFCs) surrounded by highly compacted bentonite within stable host-rock formations. The Nuclear Waste Management Organization (NWMO) is responsible for the design and execution of Canada's DGR. However, as the lifespan for DGRs far exceeds the timescales of practical experimentation, there is a need for robust numerical models to support long-term predictions. One of the concerns with the long-term integrity of Canada's DGR is the potential for microbiologically-influenced corrosion (MIC) of the UFCs. Current NWMO's UFC design involves using copper coating, due to its corrosion-resistant properties. Although the bentonite acts as a barrier to bisulfide (HS-) transport, as HS- could be produced from sulfate-reducing bacteria at the host rock/bentonite interface, the HS- could slowly diffuse through the bentonite and corrode the copper surface. To support Canada's proposed DGR design, a multidimensional numerical model was developed using COMSOL. This model couples the chemical HS- transport, bentonite saturation, and energy transport to understand the physics relevant to MIC in two potential Canadian host-rocks. The simulations show that, although saturation delayed and heating accelerated HS- transport over the first 100's and 10 000's of years, respectively, these times of influence are negligible compared to the long lifespan of the DGR (i.e., 1 000 000 years). In addition, these modelling efforts have informed which transport parameters need to be accurately measured and validated in laboratory experiments to reliably forecast the evolution of MIC. Therefore, this presentation provides an overview of the ongoing progress in modelling DGR dynamics, which bolsters confidence in the model's capabilities and provides improved flexibility to account for new site-specific information as it becomes available (e.g., specific host-rock thermal, hydraulic, and geochemical properties). Altogether, this work supports the broader effort in addressing the evolving needs of the Canadian DGR and other international nuclear waste agencies.

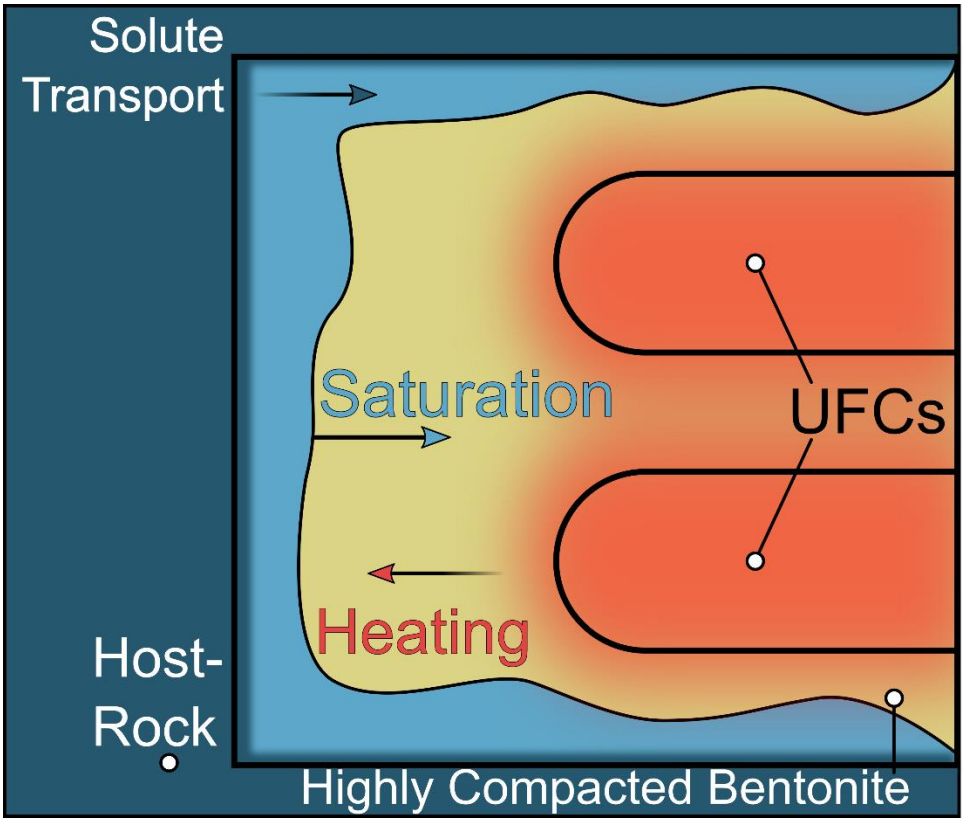

Formation of biogenic magnetite and fougèrite by anaerobic methanotrophy coupled to iron reduction

Maija Raudsepp[1], Siobhan Wilson[1], Helen Brand[2], Anita D'Angelo[2], Gordon Southam[3]

[1]University of Alberta raudsepp@ualberta.ca, [2]Australian Synchrotron, [3]University of Queensland

Microbially mediated iron reduction is an important control on the mineralogy and redox state of iron in shallow subsurface environments. In dissimilatory iron reduction, the oxidation of organics is coupled to the reduction of iron. Methanotrophy is only facilitated by a few select microbial groups, however it is major control on the global biogeochemical cycle of methane. Recently, anaerobic methane oxidation coupled to iron reduction (AOM-Fe) was demonstrated as a possible microbial metabolic process (Beal et al., 2009). This is a very specialized metabolic process and we currently only know of one microbial group, an Archaea in the family 'Ca. Methanoperedenaceae' (previously ANME-2d), that is able to use AOM-Fe.

We tested an enrichment culture of 'Ca. Methanoperedenaceae' sourced from the groundwater of an Australian coal mine on a variety iron minerals to the determine what minerals are produced by AOM-Fe. In six months of incubation, the enrichment culture of 'Ca. Methanoperedenaceae' was able to reduce a poorly crystalline synthesized ferric hydroxide but was not able to reduce goethite, hematite or magnetite. Difficulty in reducing more crystalline iron minerals has been observed in other iron reducing microorganisms, such as Shewenalla and Geobacter. The minerals produced by the enrichment culture were identified using X-ray diffraction (XRD) on the Powder Diffraction beamline at the Australian Synchrotron. Using ferric hydroxides, the AOM-Fe enrichment culture formed fougèrite (green rust) and magnetite. The biogenic fougèrite has a d(003) value of 7.556 Å, which is consistent with intercalated CO32- anions within the interlayer space [i.e., (CO3)(OH)12 * 3H2O]. Rietveld refinement using XRD data give a crystallite size of 111 nm for fougèrite and differing crystallite sizes for two distinct populations of magnetite (average of 56 nm and 2.2 nm). This study demonstrates that AOM-Fe has the potential to reduce poorly crystalline ferric iron in simulated shallow subsurface environments with high iron and methane. Although the range of this microbial metabolic process is likely restricted today, AOM-Fe may have been an important microbial metabolic process.

Chronological records of the unique angrite meteorite Northwest Africa 10463

Philip Reger[1], Bidong Zhang[2], Abdelmouhcine Gannoun[3], Marcel Regelous[4], Carl Agee[5], Audrey Bouvier[6]

[1]University of Western Ontario preger@uwo.ca, [2]University of California Los Angeles, [3]Université Clermont-AuvergneUniversit, [4]Friedrich-Alexander-Universität, [5]University of New Mexico, [6]Universität Bayreuth

Angrites are a group of basaltic achondrite meteorites which have played an important role in establishing the chronology of planetesimal formation and differentiation in the early Solar System. Not only do they record some of the earliest evidence of volcanic activity in the Solar System, members of the angrite group have been used as reference points for anchoring short-lived chronometers like ^{26}Al-^{26}Mg (half-life ~ 0.73 Myr) to absolute ^{207}Pb-^{206}Pb dates, and to evaluate the degree of homogeneity of ^{26}Al within the protoplanetary disk. Angrites are subdivided according to their petrology into the (quenched) volcanic angrites (~ 4564 Ma) and the (coarse-grained) plutonic angrites (~ 4557 Ma). Northwest Africa (NWA) 10463 represents a new type of cumulative angrite. Its texture is similar to those of plutonic angrites, however, the presence of ~ 30% olivine as well as chemical zoning and exsolution lamellae in some olivines suggest a different petrogenesis. To constrain its petrogenesis and the evolution of the angrite parent body, we investigated the 207Pb-206Pb and ^{26}Al-^{26}Mg radiogenic system records in NWA 10463. Pyroxene, olivine and plagioclase mineral separates, and a whole-rock powder were prepared for analyses. For Pb, both a hand-picked pyroxene fraction and a WR fraction were leached in progressively stronger acids, before Pb was separated from the dissolved leachates and residues by ion-exchange chromatography at UWO. The Pb isotope compositions were determined using a Tl-doping method by multi-collector ICP-MS at UCA. A York regression of the most-radiogenic Px leachates and residue results in an absolute age of 4560.6 ± 1.1 Ma using the average 238U/235U of plutonic angrites (^{238}U/^{235}U = 137.771). Magnesium isotope analyses by MC-ICPMS at FAU on unleached olivine, pyroxene and plagioclase fractions of NWA 10463 indicate radiogenic ^{26}Mg excesses for some, but not all, of the plagioclase fractions with comparable or higher 27Al/24Mg ratios. Those with resolvable ^{26}Mg excesses (0.11 ± 0.01 to 0.39 ± 0.04 ‰) define an isotopic relationship against their corresponding Al/Mg indicating a possible crystallization ~ 3 Ma earlier than the Pb-Pb pyroxene age when anchored to the D'Orbigny angrite. These isotopic regressions could also reflect the mixture of source components and have no chronological meaning. The Al-Mg andPb-Pb records therefore indicate a complex petrogenesis from possibly different sources and/or thermal history for NWA 10463. The Pb-Pb age is consistent with formation of NWA 10463 as an intermediate lithology between the younger plutonic angrites and the older volcanic angrites, and matches within errors reported Pb-Pb and model Hf-W ages for NWA 6291 and NWA 2999, two paired plutonic angrites with unusually high abundances of metal, likely influenced by an impact event.

Glacial dispersal from a migrating Laurentide Ice Sheet ice divide in northeastern Quebec

Jessey Rice[1], Heather Campbell[2], Martin Ross[3], Roger Paulen[1], Beth McClenaghan[1]

[1]Geological Survey of Canada jesseymurray.rice@canada.ca, [2]Geological Survey of Newfoundland and Labrador, [3]University of Waterloo

Complex ice-flow records are documented for major ice-divide regions of the Laurentide Ice Sheet, including areas where previous empirical work and numerical models indicate a low probability of warm-based subglacial conditions and concomitant low-erosion rates during the last glaciation. Growing evidence of widespread, shifting subglacial warm-based erosion demonstrates that these inner-ice sheet regions had dynamic polythermal subglacial conditions. However, the effect of a polythermal regime under migrating ice divides on subglacial sediment production and dispersal is poorly documented. Here we reconstruct the evolution of glacial sediment dispersal across a large area (~ 20 000 km²) in northeastern Quebec where the ice flow history, including an ice-divide migration, is well constrained. Dispersal patterns are assessed using geochemistry, indicator mineral, clast lithology data, and principal component analysis of till matrix geochemistry. Our results first improve the characterization of the Labrador Trough iron formation clast dispersal, which now extends to the northeast up to 120 km from its source. This relatively long northeast dispersal pattern, which is correlated to the oldest ice-flow phase characterized by wide-spread, warm-based subglacial conditions, formed prior to the development of the regional Ancestral Labrador ice divide. Results also show that this regional pattern is overprinted by several shorter but more complex dispersal patterns (e.g. amoeboid shapes), such as the dispersal of orthopyroxene grains from the western half of the De Pas Batholith in the centre of the study area in multiple directions. These modified dispersal patterns are greatest in the directions of the Cabot Lake and Ungava Bay ice streams which influenced ice flow within the study area. This suggests that the ice flow phases that followed the regional northeast ice flow phase strongly modified and/or overprinted pre-existing patterns due to ice divide formation and migration, as well as due to the development of late glacial ice streams. This work brings new evidence for warm-based subglacial erosion, transport, and deposition in relatively close proximity to a contemporaneous ice divide, a situation that has yet to be captured by ice sheet models. These findings also provide important insights for future mineral exploration programs within inner ice sheet regions.

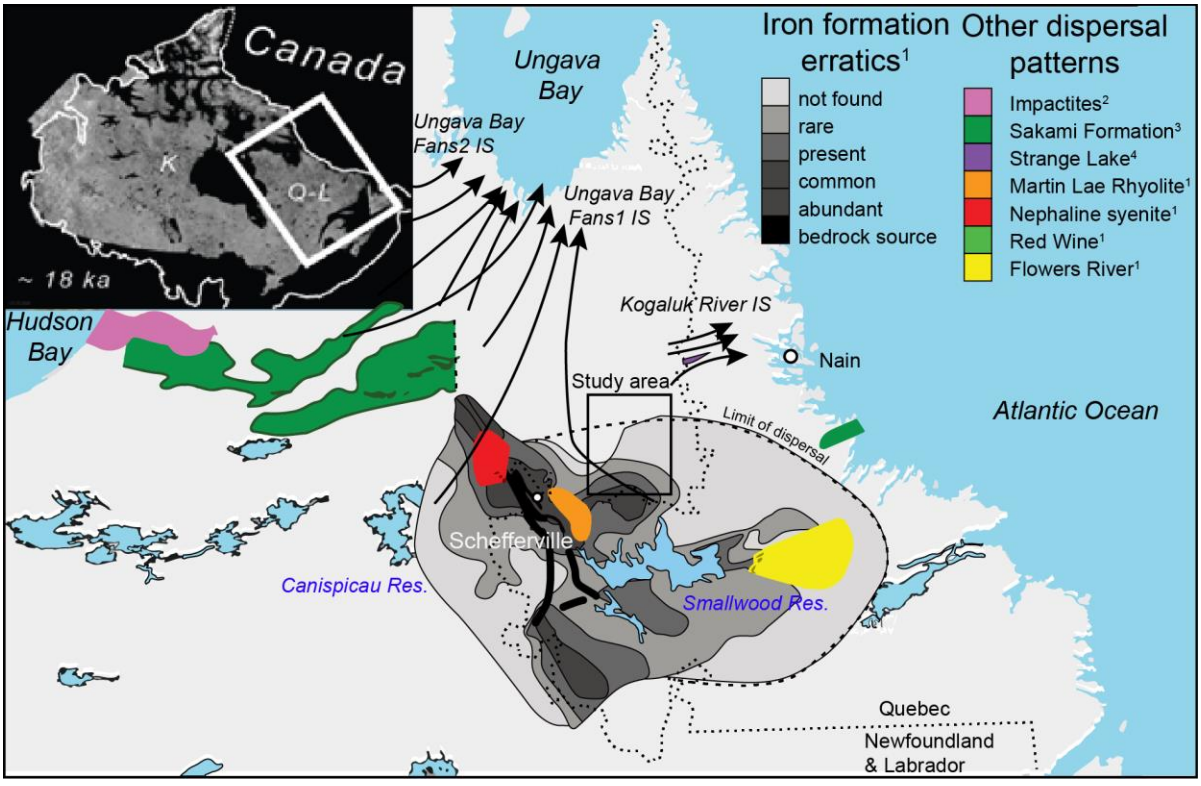

Assessment of cumulative effects in an oil and gas production region: the Fox Creek area in west-central Alberta

Christine Rivard[1], Claudio Paniconi[2], Denis Lavoie[3], Elena Konstantinovskaya[4], Omid Haeri Ardakani[5], Heather Crow[5], Geneviève Bordeleau[6], Philippe Leblanc-Rochette[7], Roxane Lavoie[7], Julie Lovitt[1], Laura Isabel Guarin Martinez[6], Barbara Javiera Meneses Vega[2], Brian Smerdon[8], Rick Chalaturnyk[4], Dan Alessi[4], Bin Xu[9], Honn Kao[5], Scott Heckbert[10], Bernard Giroux[6], Isabelle Aubin[1], Dani Degenhardt[1]

[1]Natural Resources Canada christine.rivard@canada.ca, [2]INRS, [3]Consultant, [4]University of Alberta, [5]Natural Resources Canada / Geological Survey of Canada, [6]INRS-ETE, [7]Université Laval, [8]Alberta Geological Survey, [9]Northern Alberta Institute of Technology (NAIT), [10]Alberta Energy Regulator

Environmental concerns related to unconventional resource development have arisen in the last decade. The Fox Creek area in Alberta was selected for an environmental project because it has been one of the most active regions for resource production in Canada over the last 50 years. This region comprises numerous recent unconventional condensate-gas wells and older conventional oil wells. The initial objective was to study potential impacts of oil and gas activities on shallow aquifers. However, in autumn 2019, different sectors within Natural Resources Canada identified the Fox Creek area as a region of interest for developing regional cumulative effects evaluation methods in support of the new impact assessment legislation (Bill C-69). Therefore, the project scope has widened and now includes, or will include, many other environmental components. The objectives of this project are hence multifold: 1) to characterize the shallow bedrock aquifer, including a study of surface water/groundwater interactions and a study on atmospheric processes and their linkages to surface/subsurface processes; 2) to carry out a geochemical study to identify the origin of hydrocarbons in groundwater, when present, based on rock and groundwater sample analyses; 3) to study the intermediate zone integrity and the mechanisms that could affect pressures in shallow aquifers during hydraulic fracturing and reinjection using geomechanics, borehole geophysics, petrophysics and seismicity; 4) to study and map the impact of the heavy forest fragmentation that this region has undergone on ecosystem services at the landscape scale; 5) to study the functional and structural recovery of the forest subsequent to these industrial activities; 6) to evaluate potential ecological stress and the assessment of landscape changes over time using satellite imagery; and 7) to characterize shallow freshwater bodies (e.g., wetlands) over time to monitor for changes to these environments using spectral imagery. This project includes a combination of fieldwork (including the drilling of several monitoring wells and their geophysical logging), laboratory analyses, interpretation and analysis of existing and newly acquired data, as well as numerical modeling. The different models that are currently being developed include: a coupled surface water / groundwater model, an ecohydrological model, a velocity model and a geomechanical model of the entire sedimentary succession. A somewhat separate component of the project also aims to provide recommendations for the assessment of cumulative effects related to industrial activities on the environment to help project proponents and consultants better assess them. Interviews and discussions with indigenous communities and consultants conducting environmental assessments are being carried out to have their views, opinions and perspectives on cumulative effects, in general and more specifically on hurdles and obstacles encountered during such studies.

Correlation between different pyrite LA-ICP-MS maps using unsupervised clustering

Nelson Román[1], Daniel Gregory[1], Simon Jackson[2], Jean-Luc Pilote[2]

[1]University of Toronto nelson.roman@mail.utoronto.ca, [2]Geological Survey of Canada

Pyrite LA-ICP-MS mapping has become a common technique for the study of pyrite in ore deposits, since pyrite texture and trace element composition provide unique insights into the evolution of these systems. However, their interpretation is still challenging, especially when comparing pyrite generations from the same deposit that have similar textures, intricate paragenesis, or absence of cross-cutting relationships. In this study, we aim to develop a statistically robust approach to identify chemical zones associated with different pyrite generations, such that they allow confident comparison of pyrite from different parts of a deposit. For this purpose, we applied unsupervised clustering for the examination of pyrite LA-ICP-MS maps from the Colosseum Au mine, southern California. Gold mineralization here is closely associated with pyrite. We used five pyrite LA-ICP-MS maps, representative of the two main pyrite generations in the Colosseum mine, which are (1) early pyrite, characterized by coarse, euhedral crystals (>500 µm); and (2) late pyrite, characterized by

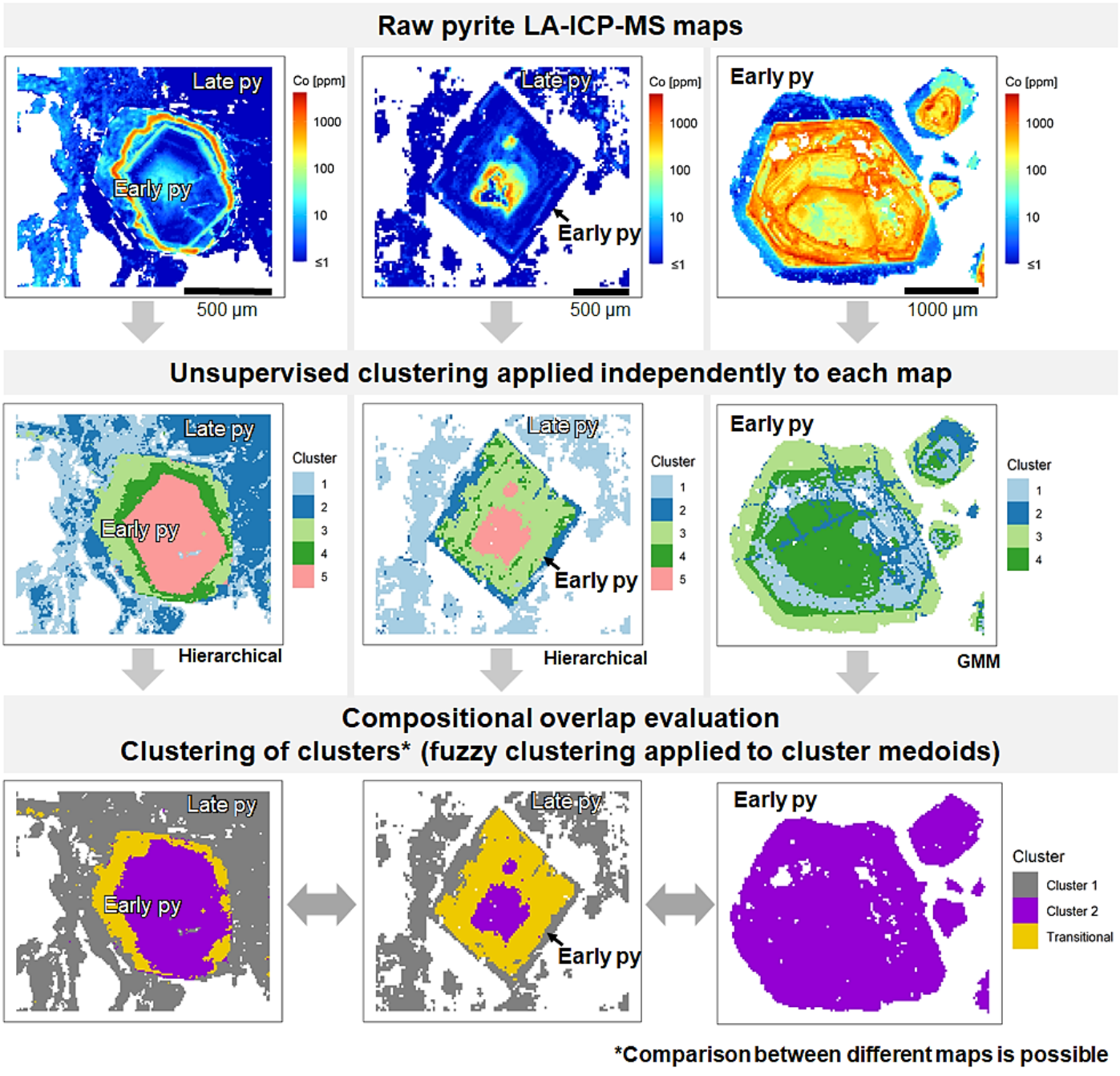

aggregates of finer-grained euhedral crystals (<150 µm). First, unsupervised clustering was applied independently to each map. The techniques used were K-means, Clustering Large Applications (CLARA), Hierarchical clustering, Hierarchical K-means, and Gaussian Mixture Models (GMM). Results were validated using clustered maps and biplots of compositional data. The best results were achieved by different methods in each map. Ward's hierarchical clustering, CLARA and GMM yielded the best results. In each map, between four to five clusters were identified, which correctly differentiated between early pyrite, fractures in early pyrite, and late pyrite, matching petrographic observation. Second, the compositional overlap between these clusters was examined using Isolation Forests, One-Class Support Vector Machines and Convex Hulls. This procedure showed that most clusters do not significantly overlap in compositional space. Finally, a second clustering step was applied to all previously found clusters, with the objective of grouping them by compositional similarity. This was done through Fuzzy Clustering applied to the medoids of the clusters. This procedure allows the definition of "transitional" groups for clusters that cannot be confidently assigned to a group. Moreover, this approach preserves the petrographic consistency of the previously obtained clusters and simplifies result inspection. Three groups of clusters were identified, including a transitional one, which allow direct comparison between maps. These results show that clustering techniques applied to pyrite LA-ICP-MS maps ease chemical zone identification in pyrite grains and allow direct comparison between maps, highlighting their potential as a tool for improved interpretation of the paragenetic context of pyrite and associated mineralization.

Recruiting geoscience students with memorable learning events

Tobias Roth[1]

[1]Laurentian University tm_roth@laurentian.ca

Relatively few high school students are exposed to the geosciences and their career opportunities while pursuing their secondary education. It often lies in the hands of post-secondary geoscience departments to attract secondary students to their respective geoscience BSc programs. Hosting outreach events may benefit post-secondary geoscience units with direct recruitment, however also help secondary students identify their own interests and career preferences, while becoming acquainted with the culture of the geoscience community. To support such outreach efforts, geoscience events used over the past 5 years are showcased here to help spark your own ideas on how to engage secondary students and create memorable geoscience events, to recruit students for BSc programs in environmental geoscience, Earth sciences or geophysics. The proposed events are hosted by a panel of geoscience workers and involve smartphone/computer technology, such that secondary students may readily interact with us hosts and provide feedback to us via their fingertips; example events include Instagram lives, virtual hands-on workshops, field trips, digital scavenger hunts. The wider the spectrum of digital ways geoscience departments offer in such events, the better we can customize our events and engage with new generations of students. Furthermore, surveys and analytics integrated in our geoscience events will help track recruitment success and improve our respective recruitment strategies. Surveys may include what students want to pursue in their careers (Earth science, environmental geoscience, or geophysics), how many students are considering vs will be applying to our BSc programs, or how many would like another presentation on Earth science. Analytics may be used to gauge the level of participation in our interactions, in order to improve targetting our geoscience events to specific audiences."

Putative microbial ichnofossils in mafic phreatomagmatic glass from a Mars-analogue environment: Fort Rock Volcanic Field, Oregon, USA

Catheryn Ryan[1], Mariek Schmidt[2], Roberta Flemming[1]

[1]Western University cryan73@uwo.ca, [2]Brock University

Early planetary habitability research is crucial to guiding investigations of the potential for life's existence beyond Earth. To that end, the study of traces of microbial life in geologic environments that mimic early (>3.5 Ga) Earth and Mars is a key tool to constraining the conditions best suited to promoting habitability under primordial conditions. These life traces, or biosignatures, can be contextualized within a geochemical and mineralogical micro-environment in a rock, providing clues for which conditions within a rock support life and which do not. We studied Pleistocene-aged mafic tuff samples from the Fort Rock Volcanic Field in Oregon, United States of America, the site of a pluvial alkaline lake during this time period. These samples were collected from tuff cones and tuff rings, structures that form during phreatomagmatic eruptions near the water's surface. Orbital imagery and in situ sample analyses by rovers have indicated the likelihood of this type of environment existing on Mars during its highly dynamic first billion years. Samples are glass-rich and hydrothermally-altered to varying degrees, containing palagonite, calcite, and zeolites as secondary products. Many samples contain microscopic tubule structures within the glass (see accompanying figure), the morphologies of which are consistent with biotically-generated structures found in numerous ocean floor basalt glasses and other mafic tuff glasses. We are working to analyze the mineralogy and trace-element geochemistry found both near these microtubules, and in samples collected from the same outcrops that do not contain microtubules. We also are conducting morphological analyses of these microtubules. We believe that there are correlations between tubule morphology, fluid and glass composition, and temperature that can be used to constrain the ideal conditions for tubule proliferation - and thus, microbial colonization - in this environment. Such constraints will be used to develop a set of exploration criteria for future Mars astrobiological investigations.

[Fig. 1 next page]

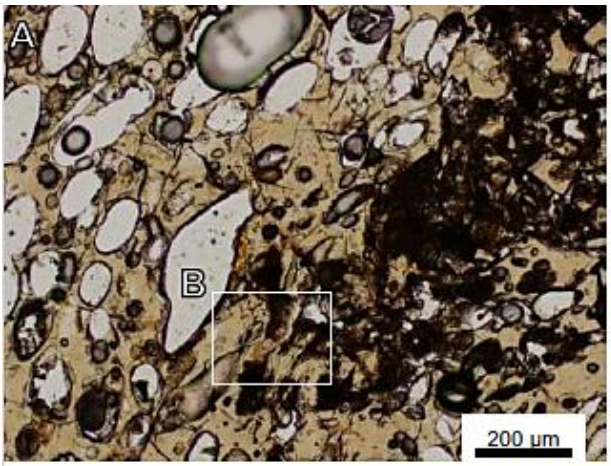

Abstract Figure: *A) Contextual microscopic image of palagonitized, vesiculated tuff glass. B) Focus-merged microscopic image stack of microtubules (identified with arrows) in altered glass. Black arrows denote microtubules with more complex morphologies such as interior septae or ovoid bodies, or terminal enlargements. White arrows denote simple, curvilinear, empty tubules. Many tubules originate at the boundaries between granular palagonite and glass, or from vesicles. The glass contains plagioclase microphenocrysts (lower right corner). One vesicle (lower left corner) is rimmed with granular palagonite and calcite crystals.*

Distinguishing and quantifying on- vs. off-axis volcanism using remote predictive mapping techniques in the Rochambeau Rifts, northern Lau back-arc Basin

Michael Ryan[1], Mark Hannington[1], Alan Baxter[1], Margaret Stewart[2], Kaitlyn Breker[1]

[1]University of Ottawa mryan093@uottawa.ca, [2]Mount Royal University

The Rochambeau Rifts (RR) are a series of 'en echelon' back-arc spreading segments in the northern Lau Basin, characterised by fast spreading rates (~110 mm/yr) and effusive volcanism. Recent marine expeditions to the region have mapped a prominent axial volcanic high in the southern segment ('Lobster Caldera'), and rift segments in the north, with possible evidence for significant intraplate volcanism represented by the dense array of volcanoes observed in the off-axis regions. The elevated levels of volcanism throughout the region may be influenced by the nearby Samoan Plume, as is suggested by high 3He/4He values observed at the RR. To quantify the area and volume of volcanism and crustal accretion in this region, and to estimate the amount of on- vs. off-axis magmatism, we produced a geological map at 1:200,000 using high-resolution acoustic and geophysical data. Over 2600 volcanoes were mapped, in addition to several formation types, assigned based on crustal type, structure, composition and age. Less than half of the mapped volcanoes are constructed on the axial ridge or inner rift valley of active spreading segments, with the remaining volcanoes located on off-axis crust. Additionally, most volcanoes are flanked by volcanic and volcaniclastic material, such as flow fields and breccias, which comprise about 45% (3655 km2) of the total area of RR (8155 km2). To distinguish off-axis volcanic products from those originally formed at spreading axes and subsequently moved off-axis, the amount of sediment cover, inferred from backscatter intensity, was used as a proxy for the age of the volcanic products. This was compared to the mapped formations and volcanoes to calculate the volume of intraplate volcanism. Interpretations for the evolution of the Rochambeau Rifts using high-resolution maps may help to determine some of the factors controlling the elevated volcanic productivity levels observed in the region. Furthermore, the results of this study may help to contribute towards a better understanding of the regional geodynamic evolution of the Lau Basin.

Canyon Formation from Similarities Between Tethys and Charon

Leah Sacks[1], Catherine Neish[1], Alyssa Rhoden[2]

[1]University of Western Ontario lsacks4@uwo.ca, [2]Southwest Research Institute

The ocean worlds of the outer solar system are some of the foci for the search for water, and consequently the search for life. Studies suggest the presence of global subsurface water oceans on these bodies, either currently or in the past. Many of these worlds are moons of the large gas giants or dwarf planets. As a result, they have been subject to various forces related to their formation and their interactions with other moons as well as their parent planet. Tidal forces, changes in eccentricity, changes in rotation, internal processes, and impact cratering influence the surface features of these bodies. The surfaces of both Charon and Tethys, moons of Pluto and Saturn respectively, are marked by distinct linear features. Serenity Chasma on Charon and Ithaca Chasma on Tethys are large canyons that show characteristics suggesting they are rift zones, areas where the crust has thinned and stretched in response to stress. Linear features, both fractures and ridges, on Charon and Tethys have been interpreted as tensile features formed from the same types of stresses assumed to have formed the canyons. The current formation theories for these surface features, including the canyons, involve expansion from a frozen ocean. Water expands volumetrically as it freezes, thus the overlying icy crust would have to thin to accommodate the larger volumes of subsurface ice in the mantle. From this type of extensional stress, we expect to see rift zones in the crust, oriented isotropically (randomly and evenly). Instead, the canyons and tensile fractures on Charon and Tethys both show preferential directions of stress. Previously mapped features on Charon (Beyer et al., 2017; Robbins et al., 2019) will be compared against new results from Tethys. This study will map the orientation, distribution, and other characteristics of linear features on Tethys, in Cassini spacecraft images. By comparing the two sets of features, we seek to understand which factors may have contributed to the formation of the canyons on Charon and Tethys that resulted in such concentrations of stress. Tidal forces have been eliminated as a possible formation mechanism for tensile fractures on Charon (Rhoden et al., 2020). Thus, differences between the planets may be able to be attributed to the viability of formation mechanisms that have been eliminated for Charon, while similarities may suggest possible common forces on both planets.

Detection of Early Aragonite to Calcite Diagenesis in a Modern Inner Carbonate Ramp

Radhika Saini[1], Hilary Corlett[1]

[1]Macewan University sainir26@mymacewan.ca

Early diagenetic replacement of aragonite by the more stable calcite mineral is not well documented in modern carbonate environments. Understanding the timing of these early diagenetic transitions is critical to our reliance on geochemical signatures in carbonates as paleoenvironmental proxies. Depositional features and early diagenetic alterations are often overprinted and challenging to recognize once sediments are lithified and buried, where pressure, temperature, and subsurface fluids impart further diagenesis. Whole-rock x-ray diffraction (XRD) is traditionally used to distinguish between calcite and aragonite minerals, but this technique cannot map these transitions on a grain-by-grain scale. Raman spectroscopy is also practical for distinguishing between carbonate minerals, and it is non-destructive. Though similar, the Raman spectra of aragonite and calcite display subtle differences in peak positions, which are ideal for differentiating these minerals within a single grain that may have experienced early diagenetic alteration. The main objective of this study was to use Raman spectroscopy to identify early diagenesis, in the form of aragonite-to-calcite transition, in inner ramp carbonate sediments from Abu Dhabi, United Arab Emirates. Additional XRD and petrographic data were used to document changes through the 26 cm section of cored sediment. XRD of unconsolidated sediment revealed a downward decrease in aragonite to calcite content (80:4 top 12 cm and 61:8 bottom 12 cm). Polished thin sections from the sediment core were used to create 2D Raman maps of grains subjected to early diagenesis. The Raman 2D maps depict an explicit transition between aragonite and calcite as the corresponding Raman spectra contain both calcite (280 cm-1; 714 cm-1) and aragonite (203 cm-1; 704 cm-1) peaks. In some of the mapped grains, the internal modes of aragonite and calcite Raman spectra at ~703 cm-1 and ~713 cm-1 are too close and blend, resulting in one band. A blended aragonite-calcite spectrum that has the internal mode shifted toward 703 cm-1 suggests that the grain mainly contains aragonite with minor calcite, whereas if the internal mode that shifts toward 713 cm-1 suggests that the aragonite-to-calcite transition is nearly complete. Optical microscopy confirmed aragonite-to-calcite alteration along the edges of grains that have experienced mechanical boring. Cathodoluminescence (CL) revealed luminescence only in detrital calcite grains, proposing that the early diagenesis mapped by Raman spectroscopy is linked to seawater. These findings illustrate the need for further investigation into the timing and controls on early diagenesis. Aragonite that has been altered to calcite in the upper 25 cm of the sedimentary column may still record primary marine signatures. However, without further mapping and geochemical characterization of altered sediments, we cannot be confident in paleoenvironmental proxy data extracted from the carbonate record.

Ordovician K-bentonites of the St. Lawrence platform in the Montréal area, Canada: stratigraphic markers for the Trenton Group limestone formations

Vanessa Sanchez[1], François Hardy[1], Joshua Davies[1], Thibaut Ducat[1], Alain Tremblay[1], Michel Kuntz[2], André Campeau[3], Eric Chartier[3]

[1]Université du Québec à Montréal vanessa4425@hotmail.com, [2]WSP, [3]Division expertise et soutien technique, Ville de Montréal

During the Middle to Late Ordovician, the eastern continental margin of Laurentia was exposed to multiple explosive island-arc volcanic events associated with ongoing Iapetus subduction. These volcanic ash deposits are known as K-bentonite beds within the St. Lawrence platform (SLP). They usually consist of volcanic glass altered into an assemblage of kaolinite and/or illite-smectite. Due to their wide dispersion, K-bentonite beds represent excellent stratigraphic markers. In North America, two important marker horizons are the Millbrig ash, a sequence of multiple ash beds, and the Deicke ash bed. Previous 39Ar-40Ar and U-Pb geochronology on these units has produced an array of ages most of which suggest eruption in the Late Ordovician (i.e., 458 to 443 Ma). In the area of Hawkesbury (Ontario), ash beds attributed to the Millbrig horizon yielded a U-Pb zircon age of 453.36 ± 0.38 Ma (Oruche et al., 2018). In the Montreal area of the SLP, two ash beds have been identified in the Ordovician Chazy Group (Laval Formation), and seven beds in the Trenton Group (Tétreauville and Rosemont formations). In the Chazy Group, a yellow-to-orange sandy layer is associated with one of the ash beds. In the field, these beds display a high gamma-ray activity, commonly attributed to their K content, but also to the presence of Th and U. Laboratory gamma-ray spectral analyses can quantify these radionuclides. The results indicate that K-bentonites of the Trenton Group are enriched in Th (mean value of 27.5 ± 0.7 ppm) when compared to the Chazy Group (mean value of 11.9 ± 0.3 ppm). XRD analyses indicate that kaolinite is the main clay mineral (22 %), with a lesser amount of illite-smectite (11%) for both groups of K-bentonites. Primary crystals, such as microcline, albite, apatite, and zircons are also present in some samples. Major and trace element analyses indicate that the ashes have a rhyodacite/dacite to trachyandesite composition. Principal component analysis of the geochemical data is successful to distinguish the Chazy- from the Trenton-hosted beds, as well as similar-looking lithologies such as shales beds and altered Cretaceous sills. U-Pb data from zircon extracted from the two ash layers compares well with new analysis from the Millbrig and Deicke ashes from Kentucky and Tennessee in the United States. Our new data suggest that the Montreal ashes might be equivalent to the Millbrig and Deicke horizons, which has major implications for regional stratigraphic correlations within the eastern Ordovician basin e.g., eastern part of the United States, New York state, Southern Ontario, Ottawa embayment and Quebec basin.

The Permian Liuyuan Complex, NW China: a back-arc basin ophiolitic complex and implications for the late evolution of the Beishan Orogen

Gabriel Santos[1]

[1]University of Waterloo gabriel.santos@uwaterloo.ca

Located at the southern edge of the Beishan Orogen, NW China, the Liuyuan Complex is an ophiolitic complex with a length of approximately 90 Km and a maximum exposed width of 9 Km. There is intense debate in the literature whether the Complex formed as continental rift or a forearc ophiolite. A major goal of this study is to contribute to this debate. The lower stratigraphy of the base of Complex is dominated by plagioclase-olivine cumulates, with varying degrees of interstitial and poikilitic clinopyroxene, forming troctolite and olivine gabbro. Measured olivine and plagioclase compositions ranges between Fo85.2 - Fo73.3 and An83.2 - An54.2. The cumulate troctolite and olivine gabbro grades into varitextured olivine gabbro, with textures including poikilitic, ophitic, and equigranular. The varitextured olivine gabbro is intruded by plagiogranite and diabase, typically forming composite dykes and locally magmatic breccias. Diabase intrusions increase in volume towards the top of the varitextured gabbro, forming a sheeted dyke complex. The sheeted dyke complex ranges in thickness from a few to more than 100 meters and can be continuously traced along the contract between the lower gabbro and the overlying basalt. These basalts, preserving pillow structures and locally lava tubes are the dominant lithology of the Liuyuan Complex, representing more than 90% of its outcrop area. Locally chert and dacite beds are interlayered with the basalts. A liquid line of descent was calculated for the basalts using the modelling software rhyolite MELTS. A pressure of 1 kbar was kept constant during fractionation, and the initial water content that provided the best fit for the collected samples was 0.5 wt%. The model predicts the crystallization of olivine at 1215 °C, followed by plagioclase at 1201 °C and clinopyroxene 1181 °C. The calculated mineral compositions are in good agreement with the measured compositions in the cumulate gabbro. Trace element inversions further indicate the lower gabbroic complex formed in a liquid with similar trace element composition as the overlying basalts. The most primitive basalts from the suite were produced by 10-17% partial melting of a spinel peridotite source, in a suprasubduction zone setting. The Th/Yb vs. Nb/Yb (Pearce 2008) and V vs. Ti (Shervais 1982, Pearce 2014) projections were used to classify these basalts as slab-distal back-arc basin. Further evidence for a back-arc basin formation includes the high initial water content of the parental melt.

No evidence of saltation-mediated triboluminescence at Gale crater, Mars

Haley Sapers[1], Mariah Baker[2], Ken Edgett[3], Deirdra Fey[3], Hemani Kalucha[4], Jacob Kloos[1], Mark Lemmon[5], Claire Newman[6], John Moores[1]

[1]York University haley.sapers@gmail.com. [2]Smithsonian Institution, [3]Malin Space Science Systems, [4]California Institute of Technology, [5]Space Science Institute, [6]Aeolis research

Triboelectric discharge produced as a result of saltating sand grains has been demonstrated to ionize Ar under simulated Martian atmospheric conditions1. Given the low ionization energies of CH4 and O2, it was postulated that saltation-mediated triboelectric discharge could ionize CH4 and O2 on Mars1, creating a previously unrecognized destruction mechanism for both atmospheric components. This could explain the enigmatic decline in CH4 and O2 during the dust storm season in the planet's southern spring and summer. The empirical study demonstrated that saltating grains could produce a discharge flux of 10 μW/m2 attributed to the ionization of Ar1. This flux is of the same order of magnitude as the detection limit of the Mars Hand Lens Imager (MAHLI) camera onboard the Curiosity rover operating in Gale crater, Mars. On 31 Jan. 2021 we performed a directed observation to capture evidence of saltation-mediated triboelectric discharge-driven ionization of the near-surface Martian atmosphere at an aeolian sand sheet called the Sands of Forvie during late southern summer (Ls 356°). Triboluminescence is a poorly understood phenomenon whereby solid materials emit radiation in response to mechanical stress-induced perturbation of their electron distribution, such as during collisions between saltating sand grains. The MAHLI triboelectric observations consisted of seventeen 60-second exposures captured at night (beginning at 21:03 LMST) on mission Sol 3017 in the absence of light reflected from the Martian moons. Four targeted regions were masked based on a pre-pointed daylight image: sky, foreground, background, and a portion of the sand sheet, where, if occurring, triboluminescence was expected to be observed. We found no significant difference in signal between the regions, suggesting that if triboluminescence occurred that night, it produced a flux below the camera detection limit. Triboelectric discharge at or below this level would not have a measurable effect on the volume mixing ratios of CH4 or O2 in the near surface atmosphere. We can conclude that saltation-mediated triboluminescence does not constitute a continuous viable methane sink in Gale crater. Additional observations with seasonal and geographic variation could further constrain the influence of electrochemical phenomena on the composition of the near-surface Martian atmosphere.

1Thøgersen, J. 2019. Icarus 332: 14-18. https://doi.org/10.1016/j.icarus.2019.06.025

Analysis and Interpretation of Regional Geophysical Data in the Swayze Greenstone Belt of the Superior Province, Canada

Daniel Satizabal[1], Bogdan Nitescu[1]

[1]University of Los Andes dm.satizabal10@uniandes.edu.co

The Swayze Greenstone Belt (SGB) is an Archean granitoid-greenstone terrain located in the central part of the Superior Province in Canada. In this region, a number of geophysical projects have been recently completed by MERC (Mineral Exploration Research Centre, Laurentian University, Sudbury), using various methods. In addition, the Geological Survey of Canada has been collecting regional geophysical data (gravity and aeromagnetic data) that is publicly available. Nevertheless, there are not many projects that have performed a geophysical investigation using regional gravity data to determine the geometry and estimated depth extent of the Swayze Greenstone Belt. The main objective of this project consisted in doing an analysis and the modelling of public regional gravity and aeromagnetic data of the Swayze Greenstone Belt with the aim of examining the geometry and depth extent of the geological bodies that occur in the area of the belt. Gravity data from the Geophysical Data Repository of Natural Resources Canada was used, with the GM-SYS tool extension of the Oasis montaj - Educational software version 9.10 to obtain forward 2.75D gravity models along five profiles, three transversal and two longitudinal to the geological structures of the Swayze Greenstone Belt. As a result of the project, a general perspective of the geometry and depth extent of the formations and groups of the SGB (Newton, October Lake, Brett Lake, Heenan formations; Marion and Chester groups), which were grouped in three different types of rock (mafic, intermediate and felsic metavolcanic) was obtained, being concluded that: - The Brett Lake Syncline appears to extend between 4 km and 7 km. - The Woman River Anticline appears to extend up to 4 km. - The deepest parts in the greenstone rocks are located in the central-southern area of the SGB. - The surrounding and intruding tonalite-granodiorite plutons appear to extend in depth up to 20 km (e.g. the Kenogamissi granitoid complex). In general, these bodies extend to a greater depth than the metavolcanic rocks. - The geometry of the SGB and the surrounding and intruding tonalite-granodiorite plutons form a typical Archean keel-and-dome pattern.

Exploring mechanisms of Mo(VI) sequestration by ferrihydrite transformation products

Valerie Schoepfer[1], Jullieta Lum[1], Matthew Lindsay[1]

[1]University of Saskatchewan valerie.schoepfer@usask.ca

Metastable Fe(III) (oxyhydr)oxides are important metal(loid)s sinks in soils, sediments, and aquifers but are susceptible to recrystallization, transformation, and dissolution during oxic–anoxic transitions. Electron transfer can promote phase transformations and adsorbed and co-precipitated metal(loid) repartitioning. Complex reaction pathways may include metal(loid) release or incorporation into neoformed phases.

Molybdenum enzymes play central roles in global biogeochemical cycles, and biosynthesis is dependent upon cellular uptake of aqueous molybdate (MoO42-). Processes controlling MoO42- may therefore have implications for both modern and ancient environments. Nevertheless, MoO42- repartitioning during Fe(III) (oxyhydr)oxide transformations is not fully understood. Previous repartitioning research during ferrihydrite transformation is limited to alkaline pH (i.e., 8, 10) with transformation induced by Fe(II) or heating, but reaction mechanisms remain enigmatic.

Recent studies under varied redox and temperature conditions report MoO42- retention during Fe(III) (oxyhydr)oxide transformations coupled with a tetrahedral to octahedral Mo(VI) coordination change through an unknown pathway. One hypothesis is that bamfordite [FeMo2O6(OH)3•H2O] precipitation following Mo(VI) adsorption onto goethite at pH < 4 may change Mo coordination. However, this contribution to Mo retention during Fe(III) (oxyhydr)oxide transformation remains unclear.

Here, we test the hypothesis that bamfordite precipitation contributes to MoO42- retention and Mo coordination changes during Fe(II)-induced ferrihydrite transformation. We conducted batch experiments under varied pH0 conditions (5.0, 6.5), MoO42- loading (0, 25, 100 µmol Mo g-1 ferrihydrite), and MoO42- uptake mechanisms (sorption, co-precipitation). We examined initial and reacted solids using X-ray diffraction (XRD), transmission electron microscopy-selected area electron diffraction (TEM-SAED), and X-ray absorption spectroscopy (XAS) to identify phase transformations and determine Mo coordination and bonding.

Combined XRD and TEM-SAED analyses reveal phase transformation limited to ferrihydrite surfaces except under pH0 6.5 co-precipitation, where more extensive transformation occurred. TEM-SAED analysis confirmed nanoscale bamfordite formed in reacted solids and Mo K-edge EXAFS modelling supports Mo(VI) coordination and bonding consistent with bamfordite and Mo incorporation into Fe(III) (oxyhydr)oxides. Our results support earlier hypotheses and indicate that bamfordite precipitation contributes to MoO42- retention during Fe(II)-induced ferrihydrite transformation and may explain observed coordination changes."

Late-orogenic extensional collapse and incipient megaboudinage in the Ottawa River Gneiss Complex, western Grenville Province

Walfried Schwerdtner[1], Toby Rivers[2]

[1]University of Toronto fried.schwerdtner@utoronto.ca, [2]Memorial University of Newfoundland

Extensional collapse of the western Grenville Orogen and exhumation of the Ottawa River Gneiss Complex (ORGC), the metamorphic core of a large metamorphic core complex, in the mid- to late-Ottawan (ca. 1050-1020 Ma), involved two sequential kinematic mechanisms: (i) orogen-perpendicular, disharmonic, transtensional cross-folding (mode-1 extension), and (ii) orogen-perpendicular and orogen-parallel bulk extension that resulted in incipient megaboudins (mode-2 extension). The incipient megaboudins are asymmetrical structures consisting of weakly strained granulite-facies cores and intensely strained margins and tails composed of amphibolite-facies banded gneiss. This contribution focusses on mode-2 extension and highlights a cluster of incipient megaboudins comprising more than 60% of the allochthonous part of the ORGC (Ontario portion), specifically within the Parry Sound, Muskoka and Algonquin domains. The bulk configuration of the megaboudin cluster was governed by an early-Ottawan (ca. 1090-1050 Ma) system of anastomosing shear zones comprising strain-weakened banded gneisses at the base of large fold nappes and thrust sheets, and their contained structures including cut-offs, tight to isoclinal asymmetrical folds and relict S-Z structures. These features imparted rheological heterogeneity to the gneiss complex that was exploited during mode-2 extension, localizing fluid ingress and strain, and leading to formation of the incipient megaboudins. At the mesoscopic scale, mode-2 extension culminated in brittle-ductile extensional faulting and associated fault-propagation folding, and injection of cross-cutting pegmatite dikes.

[Fig. 1 next page]

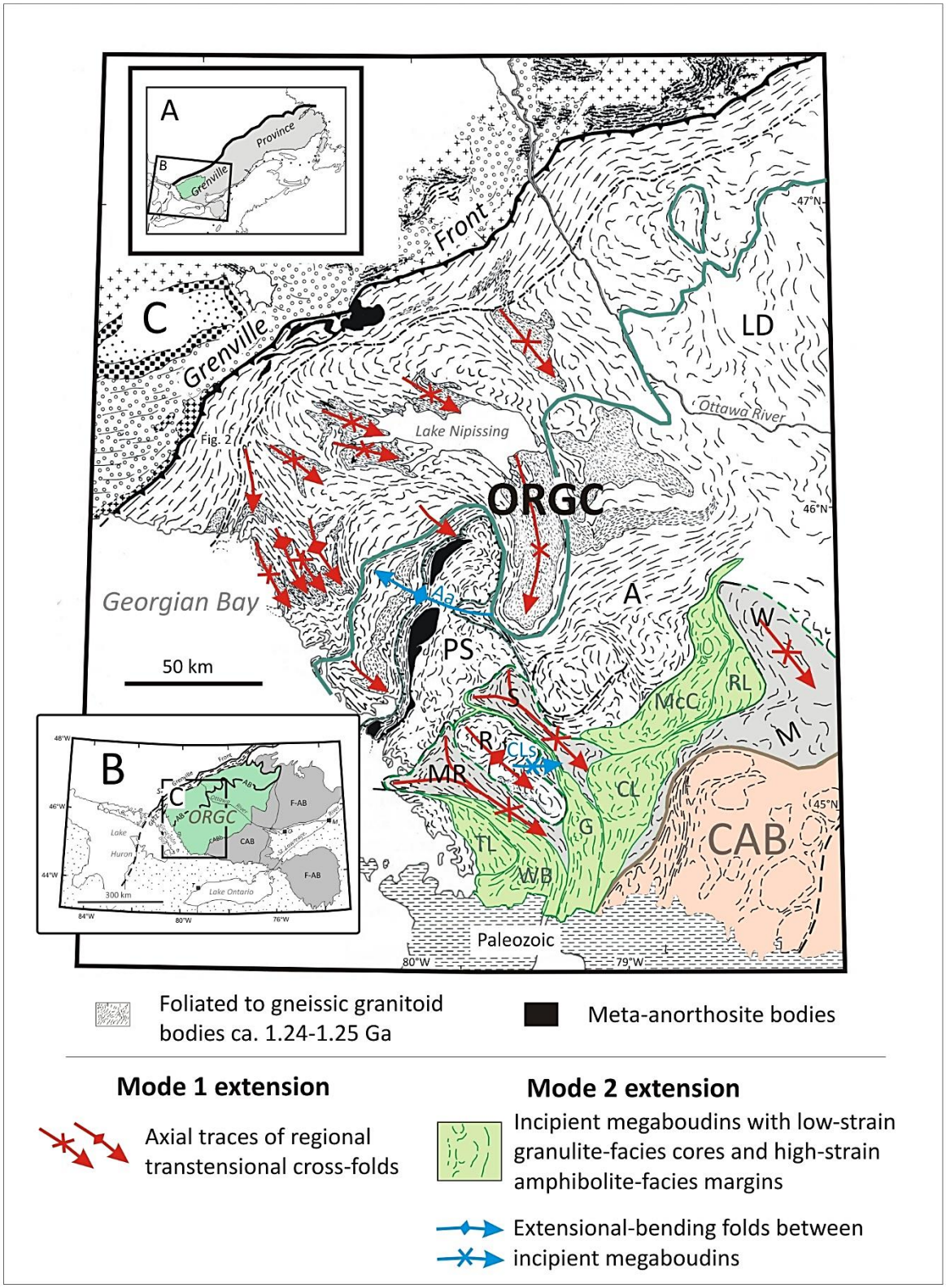

Extensional modes during orogenic collapse and formation of the Ottawa River gneiss complex (ORGC), the metamorphic core of a large metamorphic core complex (LMCC). The detachment zone of the LMCC, the Muskoka domain (M), is grey, its cover, the Composite Arc Belt (CAB), is brown. ***Mode 1 extension:*** orogen-perpendicular transtensional cross-folding; ***Mode 2 extension:*** Orogen-perpendicular and orogen-parallel bulk extension, including formation of crustal-scale incipient megaboudins (light green) and extensional-bending folds in necks between megaboudins. A, LD, PS - Algonquin, Lac Dumoine and Parry Sound domains; MR, S, W - Moon River, Seguin and Wallace subdomains of the Muskoka domain. *Megaboudins:* CL - Clear Lake, G - Germania, McC - McClintock, RL - Rockaway Lake, TL - Tea Lake, WB - West Bay. *Extensional bending folds:* Aa - Ahmic antiform, CLs - Camel Lake synform. *[Based on a figure by Davidson 1984.]*

The Analysis of the Aftershock Sequences of the Recent Mainshocks in Alaska

Mohammadamin Sedghizadeh[1], Robert Shcherbakov[1]

[1]University of Western Ontario msedghiz@uwo.ca

The forecasting of the evolution of natural hazards is an important and critical problem in Earth science. Earthquake forecasting is one such example and is a difficult task due to the complexity of the occurrence of earthquakes. Since earthquake forecasting crucially depends on the seismic history of a given seismogenic region, the analysis of the past seismicity plays a critical role in modern statistical seismology. In this respect, the recent three significant mainshocks that occurred in Alaska (the 2002, Mw 7.9 Denali; the 2016, Mw 7.1 Iliamna; the 2018, Mw 7.9 Kodiak, and the 2018, Mw 7.1 Anchorage earthquakes) were analyzed in detail. This included the modelling of the frequency-magnitude statistics of the corresponding aftershock sequences. In addition, the aftershock occurrence rates were modelled using the Omori-Utsu law and the Epidemic Type Aftershock Sequence (ETAS) model. For each sequence, the calculation of the probability to have the largest expected aftershock during a given forecasting time interval was performed using both the extreme value approach and the Bayesian predictive framework. For the Bayesian approach, the Markov Chain Monte Carlo (MCMC) sampling of the posterior distribution was performed to generate the chains of the model parameters. These MCMC chains were used to simulate the models forward in time to compute the predictive distributions. The calculation of the probabilities to have the largest expected aftershock to be above a certain magnitude after a mainshock using the Bayesian predictive framework fully takes into account the uncertainties of the model parameters. Moreover, in order to investigate the credibility of the obtained forecasts, several statistical tests were conducted to compare the performance of the earthquake rate models based on the Omori-Utsu formula and the ETAS models. The results indicate that the Bayesian approach combined with the ETAS model outperformed the standard approach based on the extreme value distribution and the Omori-Utsu law.

QUANTITATIVE ANALYSIS OF PALLADIUM IN CORES SAMPLES USING LASER-INDUCED BREAKDOWN SPECTROSCOPY

Samira Selmani[1], Ismail ELHAMDAOUI[1], Marc Constantin[2], Mohamad Sabsabi[3], Francois Vidal[4]

[1]Énergie, Matériaux et Télécommunications samira.selmani@inrs.ca, [2]Université Laval, [3]CNRC-Boucherville, [4]INRS-VARENNES

The mining industry for precious metals, such as palladium and platinum, needs new methods and tools to meet the challenges posed by declining mineral reserves and increasing discovery costs. One such desired breakthrough technology would be to measure low average platinum group element (PGE) levels in ores in real time and in situ during the various stages of exploration and mine production. Laser-induced breakdown spectroscopy (LIBS) appears to be the most promising technique to achieve this goal. In this study we used the LIBS technique to determine the concentration of palladium in core samples from the Lac des Îles and Raglan mines, both located in Ontario, Canada. Ten reference materials, composed of fine compressed powders of various chemical compositions, with a quasi-homogeneous concentration of palladium varying from 25 to 500 ppm, were used to calibrate the Pd I 348.115 nm emission spectral line. A limits of detection of 0.2-0.3 ppm of Pd was obtained. Then, the palladium concentration of 5, 3-sided, ore core samples was determined by LIBS and then compared to that obtained by conventional laboratory techniques (gravimetry/atomic absorption). LIBS analysis was performed by laser scanning the core sample and the average concentration of palladium was determined using the Pd I 348.115 nm line calibration. In addition, a LIBS sampling strategy consisting of scanning along diagonals oriented transversely to the natural ore layers was evaluated on the same 5 cores samples. This sampling strategy yields palladium concentrations very close to that obtained by scanning the entire rock surface, but with only a small fraction of the number of laser shots.

Keywords: Quantitative; Concentrations; Palladium - Platinum Laser-induced breakdown spectroscopy; scanning.

Investigation of fresh impact crater depths on Titan

Jahnavi Shah[1], Catherine Neish[1], Jason Soderblom[2], Shigeru Wakita[2], Brandon Johnson[3]

[1]University of Western Ontario jshah68@uwo.ca, [2]Massachusetts Institute of Technology, [3]Purdue University

Saturn's largest moon, Titan, is the only planetary body in our solar system, besides Earth, that has liquid on its surface and a thick, nitrogen-rich atmosphere. NASA's Cassini mission mapped the surface of Titan and detected an unusually low number of impact craters. This low count is likely the result of erosion and deposition altering the crater morphologies, such that they are unrecognizable from orbit. Cassini data also shows morphological indicators of fluvial erosion and aeolian infill in Titan's craters. As a result, we don't know the original, 'uneroded' morphology of Titan's impact craters: information that is necessary to constrain the amount of erosion that has occurred since their emplacement. Numerical modeling would allow for an improved understanding of fresh crater morphologies on Titan. A comparison of Titan crater depths to Ganymede craters has already provided evidence of erosional processes on Titan; the impact craters on Titan are hundreds of metres shallower than expected. However, this result is based on the assumption that the initial crater depths on Titan are comparable to similarly sized craters on Ganymede and Callisto. Given the potentially different compositions of their surfaces (methane clathrate vs. water ice) and thermal structures of their interiors, this may be a poor assumption. As a result, we need models of more realistic “fresh” Titan craters. This study will simulate impact crater formation on Titan using the impact-Simplified Arbitrary Lagrangian Eulerian (iSALE) shock physics code. The simulations will explore how varying Titan's crustal properties affects the crater depths over a range of diameters. We will investigate a range of thicknesses for its ice crust (40-100 km), as well as a range of thermal gradients in the ice crust (3-10 K/km). The resulting depths of fresh Titan impact craters will then be compared to the observed depths of craters on Titan, to determine the extent by which erosion has shaped its surface.

Dynamic environmental change at the cusp of the Great Oxidation Event: the Gowganda-Lorrain Fm. transition, northern Cobalt basin, Ontario

Nabil Shawwa[1], Thomas McLoughlin-Coleman[1], Michael Babechuk[2], Amy Parkinson[2], Robert Rainbird[3]

[1]Carleton University Nabil.Shawwa@carleton.ca, [2]Memorial University of Newfoundland, [3]Geological Survey of Canada

Grant Young worked extensively on the Paleoproterozoic (ca. 2.45 to 2.22 Ga) Huron(ian) Supergroup, including detailed sedimentological research on both glacial (Coleman member) and non-glacial, deltaic (Firstbrook member) sedimentary rocks of the Gowganda Formation. The outcrop distribution of the Gowganda Fm. and conformably overlying fluvial strata of the Lorrain Fm. define the Cobalt basin, a large embayment of the Huron basin, extending from Sudbury (Ontario) northeastward to Rouyn-Noranda (Quebec). While the Coleman member represents a predominantly glacio-marine depositional setting, the overlying Firstbrook member defines a deltaic-complex recording a period of rapid climatic warming. This paleoenvironmental transition is documented by a single upward-coarsening progradational succession comprising, (1) prodelta laminated mudstone, (2) delta slope interstratified siltstone and mudstone, with or without sandstone and (3), delta foreslope sandstone and lesser siltstone- transitioning to fluvial sandstone and minor clast-supported conglomerate of the Lorrain Fm. At the southern margin of the Huron basin, the delta complex preserves four, upward-coarsening, cycles. The Gowganda to Lorrain formation transition preserves the earliest appearance of terrestrial red beds on Earth, and thus, the onset of the Great Oxidation Event. The results of this study reveal the interplay between mechanisms that affected sediment accommodation space during the development of the Cobalt basin, which include: (1) delta lobe switching, (2) marine transgression/regression (possibly glacio-eustasy driven), (3) rates of subsidence, and (4) syn-depositional faulting. While repeated upward-coarsening cycles of arenite interstratified with mudstone to siltstone are interpreted as a product of delta lobe switching, new observations in the northern Cobalt basin suggest that intervening periods of sea-level rise occurred during the development of the overall progradational succession. Intervening transgressions are inferred from interlayering of intraformational breccia, conglomerate, and sandstone beds within the delta front strata. The conglomerate beds are interpreted as sediment-gravity flows deposited in deep-marine channels. Since the deltaic to deep-marine strata are affiliated with a possibly global-scale deglaciation event and sudden climatic amelioration, it is possible that glacio-eustasy was responsible for observed cyclicity. However, to properly evaluate this, the observed high variability in thickness of Huronian strata in the northern Cobalt basin needs to be considered. Post-glacial deposits in the basin exceed 1 km in thickness, while thinning to less than 100 metres in both the northern and eastern parts of the basin, suggest that subsidence and possible syn-depositional faulting played a role during deposition. Ultimately, refining the depositional model for the Cobalt basin will aid in answering questions linking climate change to the Great Oxidation Event.

Pyroxene major element trends as an indicator for baddeleyite distribution in basaltic shergottites

Alex Sheen[1], Christopher Herd[1]

[1]University of Alberta asheen@ualberta.ca

Baddeleyite (monoclinic ZrO2) is a common late-stage accessory mineral in some planetary basalts including shergottites, which make up the majority of martian meteorites. Aided by microstructural and chemical mapping, baddeleyite is a robust geochronometer for obtaining U-Pb igneous crystallization ages via in-situ analysis such as secondary ion mass spectrometry (SIMS) and focused ion beam thermal ionization mass spectrometry (FIB-TIMS); these methods offer a less destructive alternative to dissolution isotopic analysis when sample is scarce and preservation should be prioritized. Feasibility for baddeleyite U-Pb analysis relies on the sizes and abundance of baddeleyite grains, which are generally determined using microbeam surveys. This study examines eight basaltic shergottites with the aim to identify petrographic, mineralogical, and geochemical factors that may be used to predict baddeleyite distribution in samples not previously surveyed for baddeleyite. Baddeleyite abundance in the studied samples ranges from 0.5 to 2.0 grains/mm2 (grain length ?1 ?m). Results suggest that the degree of fractional crystallization, as reflected in pyroxene major element trends, controls baddeleyite abundance in shergottites to the first order. Samples with pyroxene major element compositions extending beyond the 1 bar stability boundary generally contain more abundant baddeleyite compared to samples with pyroxene compositions terminating at or before the stability boundary. Pyroxene major element trends also correlate with the petrographic setting in which larger baddeleyite grains tend to occur. In samples which display a high-Ca and a low-Ca pyroxene composition series, the largest baddeleyite grains are generally associated with Fe-Ti oxides. In samples where pyroxene major element compositions form a continuous trend and extend beyond the stability boundary, the largest baddeleyite grains occur in polymineralic late-stage pockets. Bulk high field strength element (HFSE) content and oxygen fugacity (fO2) do not appear to directly influence baddeleyite distribution, although they may be contributing factors. Based on our findings, we propose that pyroxene major element trends are a proxy for baddeleyite distribution in shergottites and may be used 1) as a first-pass assessment of a sample's feasibility for in-situ U-Pb geochronology prior to conducting detailed imaging and 2) as a guide to search specific petrographic assemblages for baddeleyite grains sufficiently large for geochronological analysis.

Shallow-ocean and atmospheric redox signatures preserved in the ca. 1.88 Ga Sokoman iron formation, Labrador Trough, Canada

Gabriel Sindol[1], Michael Babechuk[1], James Conliffe[2], John Slack[3], Carolina Rosca[4], Ronny Schoenberg[4]

[1]Memorial University of Newfoundland gabriel.sindol@mun.ca, [2]Department of Industry, Energy, and Technology, [3]U.S. Geological Survey (Emeritus), [4]Eberhard-Karls University of Tübingen

Major episodes of continental-margin iron formation (IF) deposition temporally coincide with periods of extensive shelf development and enhanced hydrothermal activity in the lead-up to the ca. 2.45–2.32 Ga Great Oxidation Event (GOE) and decline thereafter. However, there is another temporary resurgent peak of IF deposition at ca. 1.88 Ga that includes IFs from the Labrador Trough (Sokoman) and the Animikie Basin (Biwabik, Gunflint). These 1.88 Ga IFs coincide with peaks in crustal growth and volcanogenic massive sulfide (VMS) tonnages, leading many researchers to invoke hydrothermal venting as a primary control on developing the requisite marine ferruginous conditions. Alternatively, other researchers have suggested a drop in atmospheric O2 levels may have hampered oxidative continental weathering, resulting in restricted sulfate delivery into the marine realm and consequent expansion of ferruginous conditions in shallow marine environments. A key aspect to further addressing these hypotheses involves detailed studies that relate their sedimentological and stratigraphic context to the redox structure and microbial ecology of the late Paleoproterozoic ocean.

Shale-normalized REE+Y patterns are a vital tool in reconstructing oceanic redox architecture during IF deposition. Data for ca. 1.88 Ga IFs exhibit both small negative to large positive Ce anomalies, sub- and super-chondritic Y/Ho ratios, and variably sloped overall REE+Y patterns. These features have been interpreted as evidence for primary Fe/Mn-(oxyhydr)oxide-driven element cycling across a redox-stratified ocean, with microbial Fe oxidation playing an eminent role in oxide particle development. However, recent petrographic and textural evidence from the ca. 1.88 Ga Gunflint IF support a secondary origin for the hematite, thereby challenging previous assumptions concerning primary oxide shuttling and related potential implications for interpreting the geochemical signatures in other ca. 1.88 Ga IFs.

Within this context, we present a comprehensive mineralogical and geochemical dataset (incl. the REE+Y, Cr, U, V, Ni, Co, and Zn) from bulk rock IF and extracted chert of the ca. 1.88 Ga Sokoman IF from three localities (Lac Ritchie, Sheps Lake, and Hayot Lake). The integrated geochemical-mineralogical-sedimentological data argue against widespread post-depositional hematite formation and confirm that true Ce anomalies ($0.95 < PrSN/Pr^{*}SN > 1.05$) are not directly coupled with the stratigraphic distribution of hematite. Instead, our data support previous findings that variations in Ce and other REE+Y parameters respond to original seawater Fe/Mn-oxide shuttling across a shallow redoxcline controlled by basin dynamics. Furthermore, we argue that continental fluxes of nutrient-type and redox-sensitive trace elements were strongly controlled by both source lithology and low atmospheric O2 conditions.

Exploration implications of isotopically heavy iron in large gem type IIa diamonds

Evan Smith[1]

[1]Gemological Institute of America evan.smith@gia.edu

Large, high-quality type IIa diamonds such as the Cullinan and the Koh-i-Noor are among the most elusive of mined gem diamonds. These are called CLIPPIR diamonds, an acronym reflecting the distinguishing physical characteristics of this variety of diamonds (Cullinan-like, Large, Inclusion Poor, Pure, Irregular, Resorbed) [1]. There is currently no reliable method to predict the occurrence of CLIPPIR diamonds in a deposit, which remains a hurdle for exploration and mining [2]. Mineral inclusions reveal that these are sublithospheric diamonds [1], which explains why their occurrence is effectively independent from more common eclogitic and peridotitic lithospheric diamonds and their associated indicator minerals. More recently, an analysis of iron isotopes in the metallic inclusions sometimes found in CLIPPIR diamonds has provided additional insight into their formation, which may provide clues for exploration. Three measurements of metallic Fe-Ni-C-S inclusions from two diamonds from the Letseng mine, Lesotho reveal remarkably heavy iron isotopic compositions, ?56Fe = 0.79-0.90‰ [3]. These measurements lie far outside the range of known mantle compositions (near 0‰) or expected reaction products at depth. Instead, the heavy signature is ascribed to subducted iron sourced from magnetite and/or Fe-Ni alloys precipitated during seafloor serpentinization of oceanic peridotite. These metallic inclusions provide physical evidence that traces serpentinite subduction into the mantle transition zone. This finding is a step toward a genetic model for CLIPPIR diamonds. Their formation requires input from deeply subducted serpentinized peridotite. Furthermore, this input may come specifically from cold subducting slabs, whose serpentinized mantle portions can bypass the shallow sub-arc dehydration activity and instead transport serpentinite-derived components such as hydrous minerals and iron-rich phases to the transition zone/uppermost lower mantle [4]. The results suggest that geochemical signatures related to deeply subducted serpentinites may eventually provide a basis for targeting CLIPPIR diamonds in volcanic deposits at surface.

[1] Smith, E. M., S. B. Shirey, F. Nestola, E. S. Bullock, J. Wang, S. H. Richardson, and W. Wang (2016), Large gem diamonds from metallic liquid in Earth's deep mantle, Science, 354(6318), 1403-1405. [2] Gurney, J. J., and H. H. Helmstaedt (2012), The origins of Type IIa diamonds and their enhanced economic significance, 10th International Kimberlite Conference, Extended Abstract No. 10IKC-123, 1-6. [3] Smith, E. M., P. Ni, S. B. Shirey, S. H. Richardson, W. Wang, and A. Shahar (2021), Heavy iron in large gem diamonds traces deep subduction of serpentinized ocean floor, Science Advances, 7(14), eabe9773. [4] Shirey, S. B., L. S. Wagner, M. J. Walter, D. G. Pearson, and P. E. van Keken (2021), Slab Transport of Fluids to Deep Focus Earthquake Depths - Thermal Modeling Constraints and Evidence From Diamonds, AGU Advances, 2(2).

Using epiphytic lichens as biomonitors of atmospheric mercury and arsenic associated with dust at a historical gold mine tailings site in Nova Scotia

Michael Smith[1], Carrie Rickwood[2], Gauri Prabhakar[2], Peter Opra[1], Linda Campbell[1]

[1]Saint Mary's University michael.smith@smu.ca, [2]Natural Resources Canada

Mercury (Hg) and arsenic (As) contaminated gold mining waste (tailings) in Nova Scotia, Canada, poses a significant risk to public and ecosystem health. Between the 1860s and 1940s, over 360 gold mines in 64 formal gold districts in Nova Scotia generated approximately three million tonnes of tailings that were released directly into terrestrial and aquatic environments near mining communities. The tailings have elevated Hg and As concentrations due to losses from Hg amalgamation processes, and presence of arsenopyrite in milled gold-bearing ore, respectively. Many of these mines were abandoned by the 1940s and unremediated, leaving a legacy of environmental contamination. Today, with sparse vegetation cover and under a changing climate, there is the potential for intensified dust emissions from these tailings deposits, leading to the remobilization and distribution of these historical contaminants to surrounding environments. Studies to date have investigated dust chemical speciation and mercury fluxes at the sites, but no work has been done to quantify wind-borne dust and air contamination around the sites. Lichens are widely used in biomonitoring spatial patterns of dust and air quality at contaminated sites due to their ability to accumulate airborne contaminants almost entirely from wet and dry atmospheric deposition. In the summer of 2019, we sampled epiphytic lichens (Platismatia and Usnea spp.) over a series of gridded transects over both tailing and reference areas surrounding the Montague gold mine tailings site near Dartmouth, Nova Scotia. The lichens were split into washed and unwashed subsets, and both analysed for total Hg (THg) and total As (TAs) concentrations along with the rinse water from the washed lichen subset. The concentrations from the unwashed samples were mapped to determine spatial distribution patterns. Seasonal dust and elemental levels were also determined using passive air samplers and rain collectors along a stream-based transect through the main sampling grid. We will report the geographical distribution of Hg and As in lichen and their proximity to historical gold mining sites.

Understanding Permeability in a Canadian Shield Setting

Andrew Snowdon[1], Stefano Normani[1], Jonathan Sykes[1]

[1]University of Waterloo sdnorman@uwaterloo.ca

Over the last fifty years there has been an increased interest in characterizing Precambrian crystalline rock, such as the Canadian Shield, to investigate the feasibility of deep geologic repositories for isolating used nuclear fuel. Permeability in fractured crystalline rock settings can vary by many orders of magnitude and can have a profound influence on groundwater flow and solute transit times. Extensive work has been conducted by many individuals in Canada with a large amount of that work done by Atomic Energy of Canada Limited (AECL). Few peer-reviewed journal articles containing this data have been published, so a large amount of the data, especially data on fracture zones, have until now, been unavailable for modelling and analysis. Through collecting and analyzing over one-hundred technical reports written between 1975 and 1996, it was possible to characterize Precambrian crystalline rock and separate the data into equivalent porous media (EPM), and fracture zones (FZs). A permeability versus depth relationship was developed and a novel logistic function was fit to represent the depth-dependent permeability of crystalline rock in both EPMs and FZs. The crystalline rock permeability database contains over 600 data points from insitu hydraulic testing in boreholes from five AECL sites situated on the Canadian Shield, ranging from Manitoba to Quebec. The rock mass permeability is approximately 2-3 orders of magnitude lower than in the fracture zones, but varies with depth from ground surface. These depth-dependent permeability profiles are then used in numerical models to provide a more comprehensive understanding and characterization of fluid migration in fractured crystalline rock settings.

LiDAR-based quantitative assessment of drumlin to mega-scale glacial lineation continuums and flow of the paleo Seneca-Cayuga paleo-Ice Stream

Shane Sookhan[1], Nick Eyles[1], Syed Bukhari[1], Roger Paulen[2]

[1]University of Toronto Scarborough shane.sookhan@mail.utoronto.ca, [2]Geological Survey of Canada

Shortly after 14,500 ybp during the deglaciation of the Laurentide Ice Sheet in eastern North America, the 80 km wide Seneca-Cayuga paleo ice stream occupied the overdeepened New York State Finger Lake basins. This presentation describes a new methodological framework for evaluating the topography of the former ice stream bed from high-resolution LiDAR DEM data, allowing mapping and analysis of almost four thousand subglacially streamlined bedforms such as drumlins and mega-scale glacial lineations. Qualitative and quantitative techniques were applied to the statistical analysis of bedform elongation ratio and orientation using Natural Neighbour Interpolation and unsupervised machine learning-based data clustering. Analysis reveals a geomorphic continuum of as many as seven morphotypes of streamlined bedforms from drumlins to mega-scale glacial lineations with intermediate 'channeled drumlins' possibly recording erosion of parent drumlins. Spatial analysis using orientation Grouping Analysis identifies several flow-parallel sets of bedforms reflecting the presence of multiple ice flow units in the ice stream up to 10 km wide that were topographically controlled by glacially-overdeepened basins of lakes Canandaigua, Seneca, and Cayuga (-151, -306, -242 below mean sea level respectively). Longitudinal variation in bedform elongation along as much as 60 km length of flow lines is provisionally interpreted as a proxy for ice flow velocities which ranged from steady state flow (drumlins), intermediate velocities (channeled drumlins) to fast flow (mega-scale glacial lineations). Quantitative data also identifies faster axial flow and slower flow along the margins of each ice flow unit. Fast flow was triggered at the grounding lines of flow units terminating in deep (as much as 600 m) proglacial lakes at the southern end of each overdeepened Finger Lake basin and propagated northwards along each flow unit at different rates reflecting the size and depth of frontal waterbodies. Petrographic data from tills derived from distinctive Paleozoic quartzites outcropping in a narrow west-east belt perpendicular to flow of each ice stream identifies extended longitudinal subglacial advection during fast flow consistent with very rapid bedform evolution.

Detrital zircon U-Pb-Hf isotope provenance and quantitative mineralogy of rift and passive margin strata in the Humber zone, western Newfoundland: Implications for Ediacaran to Cambrian paleogeography and development of the northeastern Laurentian margin

Maya Soukup[1], Luke Beranek[1], Stefanie Lode[2]

[1]Memorial University of Newfoundland maya.a.soukup@gmail.com, [2]Geological Survey of Denmark and Greenland (GEUS)

Provenance studies can discern changes in paleogeography and sediment dispersal related to supercontinent breakup. The Humber zone of the western Newfoundland Appalachians contains deep-water strata of the Humber Arm allochthon and shallow-water strata of the parautochthonous Humber platform that record changes to rift margin geometry, paleogeography, and sediment dispersal, and provide an opportunity to test proposed correlations for syn-rift and passive margin deposits along the eastern Laurentian margin. Several competing models are proposed to explain the multi-phase, protracted rifting that took place during the Cryogenian to early Cambrian periods along eastern Laurentia, including depth-dependent extension (low-angle detachment and magma-poor rift margin models) and mantle plume - triple junction models. New field stratigraphic, scanning electron microscopic imaging combined with mineral liberation analysis (SEM-MLA), and high-n (~300 analyses per sample) detrital zircon U-Pb geochronology and Hf isotope geochemical studies were conducted on rift and passive margin strata in the Humber zone to test these models, constrain maximum depositional ages (MDA), and evaluate regional correlation of syn-rift to passive margin units in western Newfoundland. Both, deep- and shallow-marine strata, yield Tonian to early Stenian MDA estimates that are ~400 Myr older than early Cambrian or older biostratigraphic constraints, and contain statistically minor Ediacaran detrital zircon grains. In the platformal Labrador Group, immature strata of the basal Bradore Formation indicate derivation from geographically restricted Grenville basement sources, and suggests syn-rift deposition on an isolated rift shoulder. In contrast, mature strata of the overlying Hawke Bay Formation indicate well-mixed, broad geographic provenance in a post-rift setting and contain recycled constituents originally from the Canadian Shield, Grenville province, and local Ediacaran igneous rocks. SEM-MLA results from the Hawke Bay Formation corroborate polycyclic recycling of zircon grains and the mechanical weathering of Proterozoic sediment. In the distal Curling Group, basal(?) strata of the Blow Me Down Brook Formation and overlying Summerside and Irishtown formations exhibit broad, well-mixed provenance and indicate primary sources from the Canadian Shield, Grenville province, and local Ediacaran rift successions. Detrital zircon U-Pb ages and SEM-MLA data from the Blow Me Down Brook Formation are consistent with syn-rift derivation from adjacent Grenville basement and older, polycyclic Canadian Shield material. Future SEM-MLA imaging will be completed to assess any evidence of local sourcing in the overlying syn- to post-rift lower Cambrian strata. The detrital zircon results, in concert with published geological constraints, corroborate deposition in syn-rift and post-rift settings that were accommodated by depth-dependent extensional processes.

The geochemical evolution of felsic magmatic intrusions in the Yellowknife greenstone belt, NWT: identifying adakites in the Archean

Sarah Speight[1], Jacob Hanley[2], Chris McFarlane[1]

[1]University of New Brunswick sarah.gordon185@gmail.com, [2]Saint Mary's University

The Yellowknife greenstone belt (YGB) hosts two historic high-grade gold deposits, the Con and Giant mines, in the Archean Slave province. Felsic magmatism began with the intrusion of the Ryan Lake Pluton (tonalites and granodiorites), the Defeat Suite and Duckfish granites, and finally host rocks were crosscut by abundant feldspar-quartz porphyry, quartz porphyry, and aplite dikes. Overall, the YGB was built over the course of at least 200 Ma, except for the younger Proterozoic faults. The complex tectono-metamorphic history and pervasive hydrothermal alteration makes studying Archean magmatism challenging. Representative samples were taken of each lithology to compare whole rock geochemistry, focusing on the use of immobile trace elements due to the variable hydrothermal alteration observed. Crosscutting field relationships between the dikes, plutons and host rocks are complicated and their relationship to each other, gold showings, or the overlying volcaniclastics of the Banting Group is unknown. Geochemical data separate into two clusters on granite discrimination diagrams that compare Zr/TiO2 and Zr/Ti to Nb/Y. These diagrams indicate that the tonalites, granodiorites, granites, and proximal dikes are sub-alkaline and follow a fractionation trend from andesite-basalts through to rhyolites and dacites. The second data cluster are alkaline and more enriched in Nb/Y, identifying the Duckfish granite and related aplites to be trachy-andesite to trachytes. Despite the physical and petrological similarities, there are geochemical differences between two sets of aplite dikes and are associated with different plutons. The first set of aplites are proximal to the Ryan Lake Pluton and Defeat

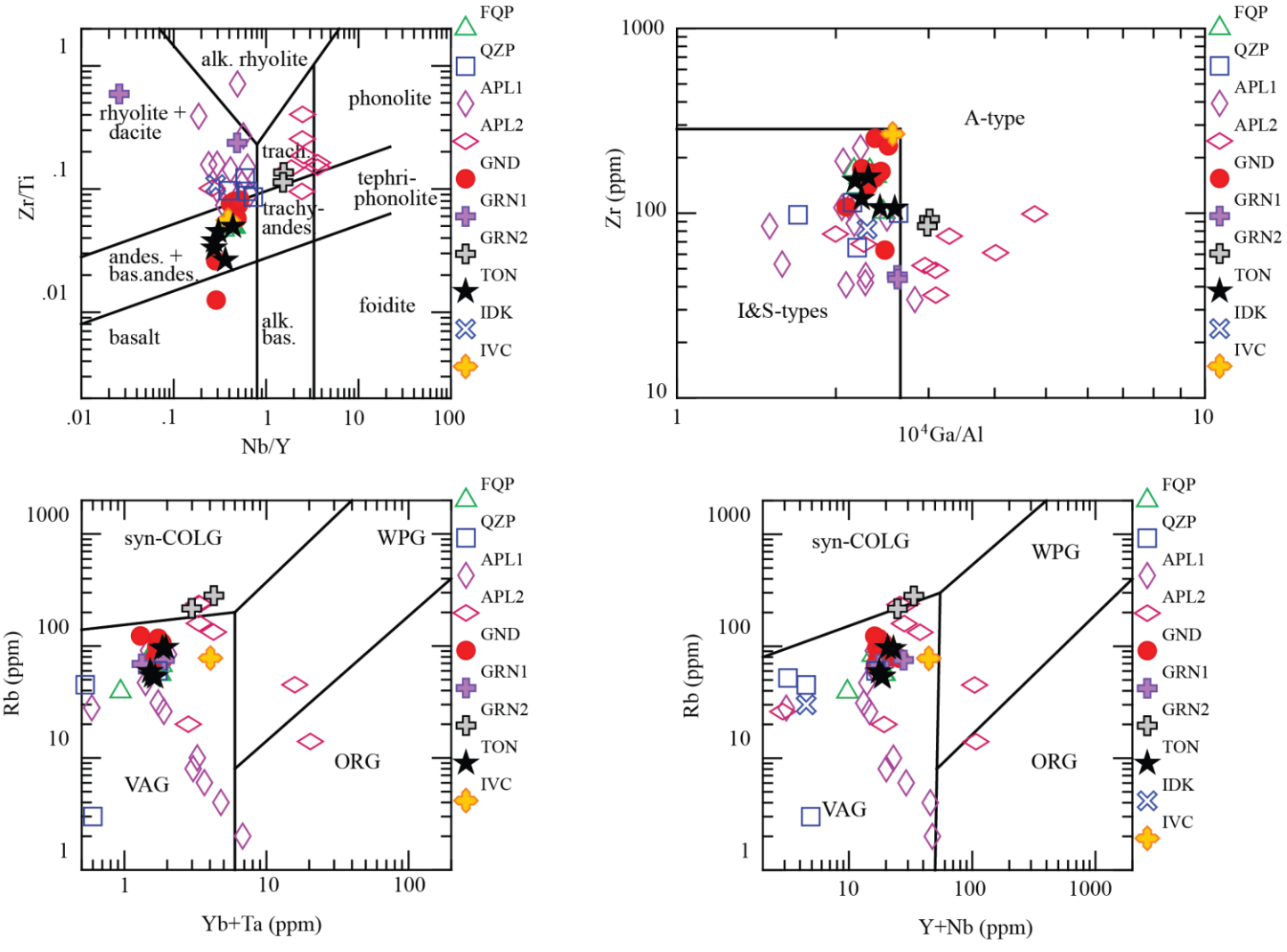

Suite and the second group of aplites are related to the Duckfish Granite. There are several tectonic discrimination diagrams that identify at least two fractionation trends, geochemically separating the aplite dikes and their source. Most samples fall within the I- and S-type granite fields but the Duckfish granite and aplite samples cross between that and the A-type granite field, indicating a change in the tectonic regime. This can also be seen in discrimination diagrams that compare Ta, Yb, Nb, Y, and Rb. The Ryan Lake, Defeat Suite and surrounding samples fall in the volcanic arc to syn-collisional granite fields and rarely the orogenic fields, whereas the Duckfish granite and surrounding aplite dikes fall within the syn-collisional to within-plate to orogenic granite fields. In each case the trends can be traced from one field to another suggesting a gradual change in the tectonic environments involved in magma generation. Finally, some samples were found to have an adakitic signature, identified by their high Sr/Y and La/Yb ratios, which has been linked to subduction of young lithosphere. The identification of these rock types in the Archean can place markers on when and where subduction and therefore plate tectonics was active in the Archean.

Evolutionary innovations in early spire-bearing brachiopods from Ordovician Laurentia

Colin Sproat[1], Jessica McLeod[1]

[1]University of Saskatchewan c.sproat@usask.ca

The Great Ordovician Biodiversification Event (GOBE) marked the rise of most Paleozoic brachiopod orders, including the Atrypida. Although perhaps best known from the larger, commonly frilled shells of mid-Paleozoic genera such as its namesake, Atrypa, early atrypides were much smaller with simple ornamentation. Nonetheless, several important innovations evolved early in the evolution of this order that may have been key to its successful recovery following the Late Ordovician Mass Extinction. Most notably, atypides were the first brachiopods to evolve a calcified support structure (spiralia) for their lophophore, a characteristic rare in other brachiopods early in the Paleozoic but one that would become common by the mid-Paleozoic. They were also amongst the first brachiopods with the ability to remodel their hinge as they grew to create a more secure joint between the shells.

The two most common early atrypides in the shallow marine settings of Late Ordovician North America were Anazyga and Zygospira. Formerly, these were classified under the same genus but Anazyga is found only in the early Katian. Anazyga was small, about 1 to 3 mm in width with a biconvex profile and only colonized the carbonate shelf and basins on the edge of the continent. Zygospira evolved later in the Katian and became abundant throughout eastern North America with sporadic occurrences in the epicontinental seas of the interior (Maysvillian to Richmondian) in the Late Ordovician. The genus is markedly larger than Anazyga (up to 1 cm in width) and can be differentiated from the earlier genus based on differences in the orientation and configuration of the spiralia.

Externally, the shells became larger and more coarsely ribbed. Some of the latest Zygospira were up to 10 times larger than early Anazyga and up to 50% larger than early Zygospira species. This mirrors evolutionary trends in other brachiopod lineages from this time, although species in the continental interior remained smaller.

The spiralia also changed shape in these species, shifting from being oriented towards the centreline to being pointed into the dorsal valve. This occurred at the same time as a shift in the structure thought to support the mouth parts of the brachiopod, perhaps indicating a change in the way the organism filtered organic material from the water column. The pressures driving this evolution remain uncertain but it is notable that unlike most other brachiopod lineages, the early atrypides never became common in the continental interior in Ordovician times. Perhaps the high degree of biomineralization required to create spiralia and constantly remodel the shell favoured the more dynamic and nutrient-rich waters of the edge of the continent rather than the more stagnant epicontinental seas near the equator. "

Are peridotitic diamond substrates distinct from diamond-free cratonic peridotites?

Thomas Stachel[1], Herman Grütter[2]

[1]University of Alberta tstachel@ualberta.ca, [2]SRK Consulting (Canada) Inc.

The principal distinction between diamond substrates and the cratonic mantle roots as sampled by garnet peridotite xenoliths is the much higher proportion of harzburgite (-dunite) to lherzolite (-wehrlite) in the former (~85:15 %) compared to the latter (18:82 %). Dunitic mineralogies are common diamond substrates (~38%) but rarely documented in xenoliths (~2 %). Using mineral Mg# as an indicator of source depletion through melt extraction again documents the more depleted character of diamond substrates relative to the cratonic garnet-peridotite xenolith record. On a like-for-like paragenesis level, however, olivine inside and outside of diamond has statistically indistinguishable means in Mg#. This observation implies: (1) that the major element composition of inclusions is imposed largely by the substrate and not by the diamond forming medium and (2) that widespread Fe-rich metasomatism of the lithospheric mantle did not occur subsequent to diamond formation (Paleoarchean to Mesoproterozoic). The latter conclusion precludes neither localized metasomatic shifts in Mg#, nor metasomatism by small melt fractions/fluids subsequent to diamond formation, as such events have low fluid/rock ratios and hence limited impact on bulk rock Mg#. A distinctive feature of inclusions relative to xenolith minerals is the higher Cr/Al of garnet and chromite in diamond. Higher Cr/Al for inclusions is not limited to the harzburgitic-dunitic paragenesis, but also occurs among lherzolitic inclusions. This suggests that the almost exclusive restriction of Cr2O3 contents >13 wt% to inclusion garnets is not a consequence of higher degrees of primary melt depletion being restricted to, or preferentially preserved, in diamond substrates. Instead, the very high Cr contents in a subset of inclusions likely relate to the pressure and temperature dependence of the distribution of Cr between garnet and spinel. Experiments showed inclusion-like high Cr/Al for coexisting Cr-pyrope and Cr-spinel in harzburgite at high pressures and temperatures (>5 GPa and >1200 °C; Girnis and Brey 1999). High Cr/Al inclusion compositions thus likely reflect some diamond growth occurring over a wide range of temperatures, elevated above a cratonic geotherm during high-temperature thermal perturbations. Na and Ti are sensitive indicators of mantle metasomatism. Enrichment of Na and Ti in both inclusion and xenolith minerals is most prominent in the lherzolitic paragenesis and very intense Ti-rich metasomatism is almost entirely restricted to lherzolite xenoliths that resided at temperatures >1130 °C, i.e. above the hydrous solidus. Since equilibration temperatures of >1130 °C are common also for inclusions, the near absence of intense Ti-metasomatism in inclusions likely relates to either a diamond unfriendly character of such metasomatism or an increase in Ti-metasomatic intensity or frequency subsequent to principally Archean-Mesoproterozoic formation of peridotitic diamonds.

Geology Rocks! Inquiry based geoscience education programs from the Oil Museum of Canada

Christina Sydorko[1]

[1]Oil Museum of Canada christina.sydorko@county-lambton.on.ca

The Oil Museum of Canada, National Historic Site in Southwestern Ontario preserves the site of the first commercial oil well and oil field in North America, established in 1858. The museum houses over 9,000 artifacts that interpret the history and influence of the County of Lambton's proud oil heritage. The Oil Museum of Canada is pleased to present its newest Travelling Trunk on geology and coordinating asynchronous learning programs which detail both the history and formation of this natural resource, oil. These programs are geared to grades 4-9. These educational resources provide foundational knowledge for teachers to build on, with their students. The geology programs use a structured inquiry based model where students are encouraged to ask questions, investigate through experiments, hands on tasks, and report their observations. It contains specimens, experiments, lesson plans, worksheets, slideshows, and rubrics. The 'Geology Rocks!' program requires the students' active participation to build the mental constructs for understanding. Students are asked to make connections between their learning and the world around them, to explain concepts to their peers, and to listen to differing viewpoints on oil and geology. This type of educational structure leads to a deeper more internalized understanding of Southern Ontario's Paleozoic lithography. The Oil Museum of Canada's virtual programs are accessed through our website and the physical kit can be rented from the museum. We encourage the programs to be used together but each version can be used independently to support student learning.

Using Atom Probe Tomography to study native gold in geological end members

Kim Tait[1], Evan Hastie[2], Brian Langelier[3], Joseph Petrus[4], Harold Gibson[4], David Crabtree[2], Ross Sherlock?, Lee White[1]

[1]Royal Ontario Museum kimtait@gmail.com, [2]Ontario Geological Survey, [3]McMaster University, [4]Laurentian University

Constraining the formation history of native gold and the elemental mobility associated with gold is critical for understanding high-grade gold deposit formation and source, as well as improving our understanding of gold for metallurgical processing. Due to the high value of gold, the typical size range and complexity of the metal, most gold deposit research has utilized mineralogical proxies for gold, rather than gold itself to infer its source, transport and deposition. The outstanding questions for native gold are what major and trace elements are associated with gold from different deposit types and how are they distributed within gold grains. Are associated elements distinct nanophases, or are they substituting into crystallographic sites within the gold structure? Are the elemental distributions zoned, clustered or homogenous? To answer this, we use a novel combination of quantitative chemistry from the electron microprobe with 3D atomic-scale elemental distribution from atom probe tomography (APT) to compare the elemental distribution and chemistry of gold from a highly deformed and metamorphosed Archean orogenic gold deposit (Preston mine) with a relatively primary, young epithermal gold deposit (McLaughlin mine). These are end members of native gold both in terms of deposit type and geologic time. Our results provide new insights into the complementary roles of fluid and crystallization processes in the formation of gold that can be applied to other gold deposits. The samples selected for this study are part of a much larger multi-year Gold Fingerprinting project with the Ontario Geological Survey (OGS), the Royal Ontario Museum (ROM) and Metal Earth (Laurentian University).

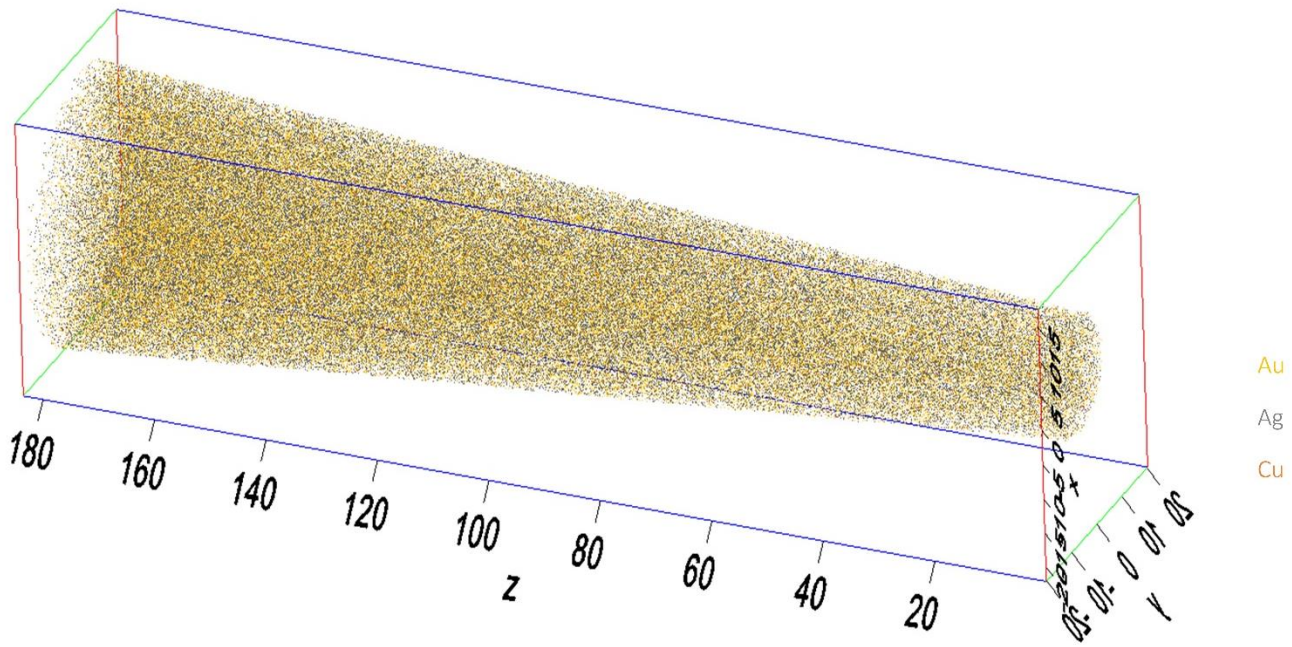

Formation of the Ament Bay Metasedimentary Assemblage in the easternmost Western Wabigoon Terrane: Implications for gold exploration in Timiskaming-type basins

Michael Tamosauskas[1], Chong Ma[1], Rasmus Haugaard[1], Robert Lodge[1], Ross Sherlock[1]

[1]Laurentian University mtamosauskas@laurentian.ca

The Neoarchean Sturgeon Lake greenstone belt (SLGB) makes up the easternmost portion of the western Wabigoon terrane of the Superior craton, and is comprised of mostly mafic- to- felsic volcanic and plutonic rocks and minor late-stage clastic assemblages. The Ament Bay Metasedimentary Assemblage (ABMA) is the youngest supracrustal assemblage of the SLGB, consists of dominantly arkosic- to- lithic arenites and wackes as well as polymictic conglomerates, and is surrounded by the 2721-2718 Ma Central Sturgeon Assemblage, the youngest volcanic unit in the SLGB. The sedimentary facies of the ABMA resembles a Timiskaming-type basin, which are associated with gold mineralization in the Abitibi greenstone belt. The ABMA and typical Timiskaming-type basins consist of mostly immature clastic rocks derived in fluvial-alluvial environments, are coeval with alkalic magmatism, and represent the final supracrustal depositional stage in a greenstone belt. However, clast compositions, detrital zircon provenances, and interlayering relations between the AMBA and surrounding volcanic rocks across contact zones, jointly suggest that the ABMA is conformable with the Central Sturgeon Assemblage and represents a syn- to late-volcanic sedimentary sequence. This is in contrast to Timiskaming-type basins, which are underlain by a regional unconformity. Similar occurrences to ABMA may be applicable to other Neoarchean basins, implying it is crucial to determine contact relationships when exploring for gold-endowed Timiskaming-type basins.

Delineation of the Medora-Waskada Buried Aquifer near Souris, Manitoba using time-domain electromagnetics

Steven Taniguchi[1], Ian Ferguson[1] ij_ferguson@umanitoba.ca

[1]University of Manitoba

Ground time-domain electromagnetic (TEM) methods were used to image the Medora-Waskada buried valley aquifer. The intent of the study was to confirm the location of the valley at a location east of Souris, Manitoba, image the shales at the base of the valley, map the lateral variation in the valley fill, and to examine the viability of TEM to image buried valleys. A total of eleven TEM sites were set up along a north-south profile on Hebron Road 11.5 km east of Souris Manitoba. Six of the sites deployed 80 x 80 and 20 x 20 m transmitter loops while the remaining five sites used a 20 x 20 m loop only. Inversion of the averaged and edited TEM response from each site revealed a three-layer valley structure at the deeper western portion of the buried valley and a four-layer valley structure at the shallower eastern portion of the buried valley. The first layer was resolved across all sites and was interpreted as surficial glacial deposits ranging in thickness from 2.2 to 6.7 m and with resistivity ranging from 4.8 to 12.2 Ω.m. The second layer was interpreted to be the glacial fill deposited over multiple fill events. The depth to the base of this layer ranged from 20 m outside of the valley to 65 m in the deepest part of the valley. The third layer was interpreted to be the Odanah Member shale which was absent in three of the sites where the valley was cut deepest. The resistivity of the Odanah Member ranged from 7 to 14.5 Ω.m. The final layer was interpreted to be the Millwood Member shale with a resistivity ranging from 3.1 to 6.4 Ω.m. The imaged buried valley east of Souris was consistent with being the northern extension of the Medora-Waskada valley which had previously been imaged geophysically only to the southwest, between Medora and Waskada, Manitoba.

Living the low life: Ediacaran reclining organisms at Mistaken Point

Rod Taylor[1], Jenna Neville[1], Duncan McIlroy[1]

[1]Memorial University of Newfoundland rodt@mun.ca

The Ediacaran fossils found in eastern Newfoundland's Mistaken Point Ecological Reserve represent the world's oldest known complex body fossils, dating as far back as 576 million years. These Ediacaran organisms were preserved through rapid burial of organisms that were attached to the seafloor at the time of burial, effectively obrution deposits. Conventional wisdom tells us that many of these organisms - e.g., *Charniodiscus procerus*, *Hapsidophyllas flexibilis*, *Charnia masoni* - were attached to the seafloor via a stalk, disc and/or stolon but were held upright in the water column, possibly garnering nutrition through filter feeding and/or osmotrophy. Other Ediacaran organisms lived a reclining lifestyle, with one side of the body in direct contact with the seafloor. Such epifaunal organisms must have developed adaptations to allow them to survive on the Ediacaran seafloor: maintaining contact with seafloor sediments would have reduced or eliminated water flow, resulting in the build-up of porewater sulphide through the growth of sulphate-reducing bacteria. These epifaunal organisms may have actively transported oxygenated water to their lower surfaces, enabling the growth of chemosynthetic sulphur oxidizing bacteria that could have prevented the build-up of sulphide in a simple form of symbiosis. Recent research suggests that this epifaunal lifestyle was more common on the Ediacaran seafloor than has previously been recognized. *Fractofusus misrai* (Fig. 1a) and *F. andersoni* have long been recognized as having lived an epifaunal lifestyle, with the complete body lying in contact with (and probably displacing) seafloor sediments immediately beneath the microbial mat that covered most of the Ediacaran seafloor in the area. *Beothukis mistakensis* (Fig. 1b) is a rare organism from Mistaken Point that was, until recently, synonymised with the genus *Culmofrons*; while *Culmofrons* possessed a stem and disc that anchored it to the seafloor (and probably lived with its frond held upwards into the water column), *B. mistakensis* possessed neither stem nor disc and was almost certainly epifaunal. *Gigarimaneta samsoni* (Fig. 1c), a newly described morphologically complex organism from Mistaken Point, also lay in direct contact with seafloor sediments and could reach sizes considerably larger than *Fractofusus* or *Beothukis*. Other taxa generally accepted as having lived upright in the water column show evidence that suggests they too may have lived epifaunal lifestyles. The unrecognised abundance of epifaunal taxa would directly impact currently accepted models of community ecological structure for the Mistaken Point biotas and our understanding of Ediacaran palaeoecology. Figure 1. Reclining organisms from Mistaken Point: a, *Fractofusus misrai*, E surface; b, *Beothukis mistakensis*, E surface; c, *Gigarimaneta samsoni*, F surface (scale bars: a, b = 1 cm; c = 8 cm).

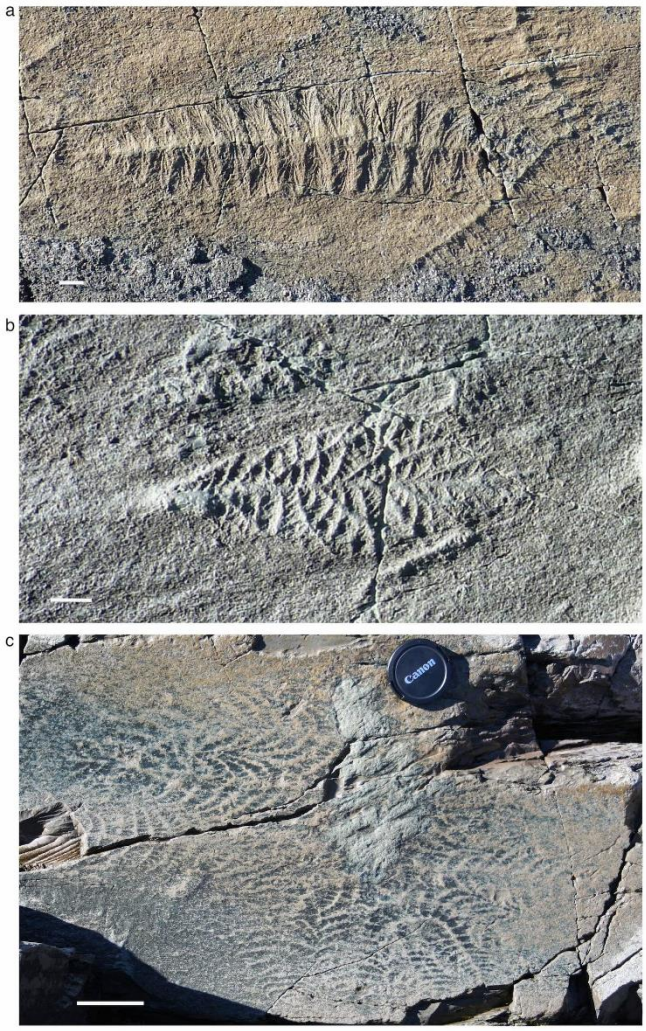

An analysis of lunar impact craters with radar-dark haloes

Ashka Thaker[1], Catherine Neish[1], David Blewett[2], Yong-chun Zheng[3]

[1]The University of Western Ontario athaker@uwo.ca, [2]JHU/APL, [3]National Astronomical Observatories of China

The lunar regolith is a layer of unconsolidated material covering the lunar surface. The physical properties of the regolith play a significant role in understanding many aspects of lunar geology, including its history and evolution over time. Using satellite imagery, we can analyze these physical properties. Passive microwave radiometry and radar imaging are well suited for observing the physical properties of lunar surface and sub-surface at varying depths due to their greater penetration range compared to optical and near-infrared wavelengths. In this study, we use previously calibrated brightness temperature (TB) maps from the Microwave Radiometer (MRM) on CSNA's Chang'E-2 (CE-2) orbiter along with other complimentary datasets such as P-band (70 cm) Arecibo radar data, S-band (12.6 cm) radar data from Arecibo and the Miniature Radio Frequency (Mini-RF) radar on NASA's Lunar Reconnaissance Orbiter (LRO), and LRO Diviner rock abundance data. Our aim is to investigate the regolith properties of distinctive low-return, radar-dark, ring-shaped structures surrounding certain lunar impact craters. Such craters are known as 'radar-dark halo craters'. The origin of these haloes remains a mystery, but previous work suggests that these haloes represent an ejecta layer depleted in decimeter- to meter-sized blocks. In this work, we seek to improve our knowledge of scatterer distribution in these haloes and understand their evolution over time by conducting a multiwavelength analysis. In addition to observing radar-dark halo craters of different geological ages, we will compare the regolith characteristics of radar-dark halo craters with those of non-radar-dark halo craters of similar sizes. We aim to find any similarities or differences in their regolith characteristics in order to constrain their formation mechanism.

Key words: Impact craters, Microwave Radiometry, Radar Observations, Moon.

Evaluating anomalous palaeomagnetic field behaviour in the Ediacaran with new palaeointensity data from Laurentia

Daniele Thallner[1], Andrew Biggin[1], Mimi Hill[1], Henry Halls[2], Phil McCausland[3]

[1]University of Liverpool daniele.thallner@liverpool.ac.uk, [2]University of Toronto at Missisauga, [3]University of Western Ontario

Long-term variations in geomagnetic field behaviour contain essential information on deep Earth processes through geological time. A topic of long-standing debate has been the age of the onset of Earth's inner core nucleation, as uncertainty in the value of thermal conductivity of the core allows for a wide range in age estimates, but a late Neoproterozoic age has recently been inferred from an ultra-weak palaeointensity estimate at ~565 Ma. Palaeomagnetic investigations from this time are known to give anomalous results, showing ambiguous apparent polar wander paths in a hyper-reversing field. However, full characterisation of the geomagnetic field in the Ediacaran period (635-538 Ma) has been prevented by a paucity of field strength estimates. To reduce this data gap, multi-method palaeointensity determinations have been performed on rocks from six dykes of the Grenville dyke swarm (SE Canada, 584-598 Ma) and volcanic rocks of the Skinner Cove formation (Newfoundland, 550.5 Ma). These results confirm that the field was exceptionally weak, with virtual dipole moments between 0.3 and 1.5 x1022Am2. These extremely low values suggest that the geomagnetic field has been remarkably weak over a much longer time period than previously seen from palaeointensity data, and starts to increase in strength at the Ediacaran-Cambrian transition. These results could correspond to considerably lower field strengths predicted by geodynamo simulations for fields with low dipolarity before the onset of nucleation of the solid inner core. However, the context of these extremely weak palaeointensities is still unclear and different causes such as a reconfiguration of convective patterns in the outer core due to unusual core-mantle heat flow patterns cannot be ruled out, as field strengths are still mostly unexplored for the time periods that encompass the Ediacaran, highlighting the ubiquitous need for additional high quality palaeointensity data.

Colour and Multispectral Analysis of Mars with the Colour and Stereo Surface Imaging System (CaSSIS) onboard the ExoMars 2016 Trace Gas Orbiter (TGO)

Livio Tornabene[1], Vidhya Rangarajan[1], Eric Pilles[1], James Burley[1], Anthony Dicecca[1], Nicolas Thomas[2], Gabriele Cremonese[3]

[1]University of Western Ontario ltornabe@uwo.ca, [2]University of Bern, [3]University of Padua

The Colour and Stereo Surface Imaging System (CaSSIS) is a full-colour visible to near-infrared (VNIR) bi-directional pushframe stereo camera onboard the ExoMars 2016 Trace Gas Orbiter (TGO). TGO reached its science orbit in April of 2018 and CaSSIS continues to provide multispectral images with four broadband colour filters optimized for Mars photometry. The CaSSIS filters are (Name [centre wavelength/bandwidth - both in nm]): BLU [497.5/134.3], PAN [677.4/231.5], RED [835.4/98.0] and NIR [940.2/120.6]. Images are nominally ~9.5 km wide and up to 50 framelets or ~50 km long; a scale of ~4.6 m/px is achieved from TGO at a nearly circular ~360 x 420 km orbit and is resampled to 4 m/px during geometric processing. TGO is not sun-synchronous due to an orbital inclination of 74°. This enables imaging of the surface at different local solar times (LSTs) and a wider range of observation geometries than most previous Mars imagers, including very low incidence/phase observations providing optimal surface colour and spectral contrast. The fixed pointing at ~10° off nadir combined with a rotation mechanism enable stereo image acquisitions over a single orbital pass. TGO is currently permitted to roll up to a maximum of 5° to facilitate the targeting of key locations on the surface enabling complete imaging and validation of landing sites. During an earlier phase of the mission, a data transfer rate restriction was determined to limit the total number of pixels that can be transferred within the time between the acquisition of the individual framelets that comprise a single CaSSIS image. At the current nominal TGO altitude range, and resulting ground track velocity, a down-selection is required to balance the framing rate and the read-out caused by this "bottleneck" issue. Thus, planners must reduce the swath-width from the maximum value of 2048 px and/or choose to either switch off colour filters to reduce the read-out to a rate that can be handled. Hence, most CaSSIS images are planned with only 3 filters (>60%), with fewer narrower 4-filter images taken (~20%). These choices result in several image modes; however, only some are useful for colour and multispectral analysis. Besides images with all 4 filters, these useful image modes include: 4 combinations of 3 filters (in order of most to least common: NPB, RPB, NRB and NRP) and a simulated true colour ("RGB") derived product, which is based on only two filters (PAN and BLU). Here we will present a summary of how the CaSSIS may be used for geologic and atmospheric investigations of Mars through colour and multispectral analysis. Band ratios, and other spectral parameters, are devised to identify surface materials and atmospheric phenomena and have been adjusted to accommodate the variety of image modes CaSSIS provides. An empirical technique for minimizing contributions from atmospheric scatterers in the VNIR, through the dark subtraction method effectively augments surface investigations by enabling comparisons with mineral and phase reference spectra, including spectra from hyperspectral datasets.

Evaluating the Corrosion of Used Fuel Containers in Canadian Crystalline and Sedimentary Environments for the Long Term Storage of Used Nuclear Fuel

Claire Tully[1], Emilie Spasov[2], Wilfred Binns[3], Katja Engel[2], Dmitrij Zagidulin[1], Josh Neufeld[2], James Noel[1]

[1]Western University ctully3@uwo.ca, [2]University of Waterloo, [3]Nuclear Waste Management Organization

The internationally accepted best practice for managing used nuclear fuel (UNF) is to isolate and contain it within a multiple-barrier system underground in a deep geological repository (DGR). The Nuclear Waste Management Organization (NWMO) is responsible for the long-term management of UNF in Canada. Since 2007, the NWMO has been conducting site investigation studies to find a suitable host site for a DGR including a willing and informed host community. This search has narrowed to two potential host sites in Ontario, the communities of South Bruce (sedimentary rock) and Ignace (crystalline rock). To facilitate selection of a final DGR host site the NWMO Site Investigations team is currently conducting a borehole drilling campaign in both communities to properly characterize the geospheres. In the proposed DGR design, used fuel bundles will be sealed in copper-coated carbon steel used fuel containers (UFC), encased in blocks of highly compacted bentonite clay, and emplaced approximately 500 m below ground in the DGR. However, in order to receive the required regulatory approvals for the construction of a DGR, it will be necessary to demonstrate the long-term integrity of the copper canister materials in compacted bentonite clay in DGR relevant conditions. While the NWMO has extensive copper corrosion and bentonite-based microbiology research programs the NWMO borehole campaign provides a unique opportunity to examine the behaviour of the multiple barrier system in a potential host site. To investigate how the canister material will fare under repository-like conditions, canister materials embedded in bentonite clay are encapsulated in a permeable module and lowered to approximately repository depth in an NWMO borehole. The interval containing the modules will be sealed above and below the test segment using pressurized plugs where they will remain for up to eight years. Modules will be extracted periodically and undergo petrophysical evaluation, microbial culturing and profiling of the bentonite clay, and surface analysis of the copper coupons. This work will help to inform the NWMO's detailed site characterization work once a final host site is chosen. Work leading up to borehole module experiments has been extensive, a portion of this work has focused on canister materials embedded in bentonite clay exposed to saline water, similar to that of sedimentary ground water salinity at various oxygen concentrations. To achieve these conditions, modules similar to the borehole modules were placed in the Pacific Ocean at depths of 90 and 2000 m for 6 months and two years, respectively. Examination of the ocean modules showed uniform corrosion on the embedded canister material, with the dominate corrosion product being copper (I) oxide, copper chloride species were detected migrating into the bentonite clay. Overall, low average corrosion rates of the coper material were observed indicating suitable material selection for the environmental factors.

Organic compound analyses of two recent meteorite falls of the CM2 Aguas Zarcas and C2 ungrouped Tarda carbonaceous chondrites: Methods for differentiating between terrestrial and extraterrestrial organics

Libby Tunney[1], Patrick Hill[1], Christopher Herd[1], Robert Hilts[2], Miranda Holt[1]

[1]University of Alberta ltunney@ualberta.ca, [2]MacEwan University

Once meteorites fall to the Earth's surface, the pristine extraterrestrial organic matter they may contain is readily compromised by terrestrial organic compounds (contaminants). Terrestrial contaminants can obscure extraterrestrial signatures and complicate organic matter analyses on astromaterials, especially carbonaceous chondrites due to their high carbon content. Since studies of organic matter in astromaterials can yield clues to the chemistry and processes within the solar system, contamination needs to be well documented, understood, and minimized to the best of our abilities. Two recent meteorite falls have presented a unique opportunity to develop methods to best differentiate terrestrial organic compounds from those of an extraterrestrial origin with fresh meteoritic material. The Aguas Zarcas CM2 carbonaceous chondrite fell on April 23, 2019, in San Carlos county, Alajuela province, Costa Rica. Approximately 11 kg of Aguas Zarcas stones were collected prior to the first rainfall (pre-rain) whereas another 16 kg were collected post-rain. The Tarda C2 ungrouped carbonaceous chondrite fell on August 25, 2020 in Morocco. In our studies, 5 stones of Aguas Zarcas (4 pre-rain and 1 post-rain), 2 stones of Tarda, and a sand sample from Tarda's fall site were subsampled, powdered, and extracted with dichloromethane (DCM) and subsequently with water using MTBSTFA as the derivatizing agent. Laboratory surfaces and materials were swabbed and extracted with DCM to determine if any contaminants were transferred from the laboratory to the meteorites themselves. All extractions were analyzed by gas chromatography-mass spectrometry (GC-MS), with any detectable organic compounds identified using the NIST database. The Aguas Zarcas and Tarda stones contained one or both allotropes of sulfur (S6 and S8), with Aguas Zarcas stones also containing various polycyclic aromatic hydrocarbons (PAHs) in the DCM extractions. The water extractions detected intrinsic amino acids, alcohols, and carboxylic acids in both Aguas Zarcas and Tarda. These compounds are commonly found in other carbonaceous chondrites and rare at the Earth's surface, thus these are intrinsic to the meteorites. This conclusion is further confirmed in Tarda as these proposed intrinsic compounds are absent in the sand sample. No contaminants found in the laboratory during subsampling and processing were detected in the meteorite extracts, again supporting that any contamination is likely due to the terrestrial surface. The majority of the terrestrial organics in the DCM and hot water extracts, which make up about 50-75% of the total compounds detected, fit in to one of four common source categories: agricultural products, fuels, pharmaceuticals, and polymers. Our study advocates for the documentation of potential contamination histories of freshly fallen meteorites by ground truthing with samples from both the terrestrial surface and laboratory environments.

Analysis of Vertical Electrical Sounding (VES) Data over a prospective geothermal area in Turkey

Fethi Turanli[1], Alison Leitch[1]

[1]Department of Earth Sciences, Memorial University of Newfoundland ftturanli@mun.ca

Geophysical methods are one of the important disciplines to delineate geothermal resources. Among the geophysical methods, geophysical electrical methods play a vital role by determining the resistivity, which depends on temperature and fluid content and is therefore a key variable in geothermal systems. In this study, data from 384 Vertical Electrical Soundings (VES) were analysed, to determine heat sources and structure of the geothermal area in the Afyon-Sandikli graben, Turkey. This study applied 1D and 2D inversion techniques in an effort to generate resistivity models of geothermal system. Prior to inversion, the raw resistivity data was characterized in terms of elevation changes in the study area, smoothness of the resistivity sounding curves, consistency between neighbouring sounding curves and their nearness to faults. Considering all these criteria, 1D resistivity models were obtained. Many of the soundings were arranged at even intervals along lines. Such linear arrangements of soundings were used for 2D inversion. The resulting models are compared and discussed in terms of resistivity distribution in the geothermal system.

Effect of FeHEDTA on Magnetic Properties of Soils

Smita Tyagi[1], Maria Cioppa[1]

[1]University of Windsor tyagi6@uwindsor.ca

Industrial, agricultural and urban activities may induce anthropogenic pollutants into the local, regional and/or global environment. Soils can accumulate these pollutants and therefore soil monitoring can be used in environmental assessments. Geophysical methods provide rapid, nondestructive, and diagnostic soil monitoring, and one of the most common geophysical methods used is magnetism. Given that environmental magnetic studies of soils have been used to model climate variations and soil forming processes in addition to anthropogenic effects, this study aimed to examine the effects of a common iron based herbicide (iron hydroxylethylenediaminetriacetic acid aka FeHEDTA) on soil magnetic properties. The magnetic properties of FeHEDTA control samples in varying concentrations (5-50% by weight in gypsum powder), untreated specimens from soils of Windsor-Essex County (Ontario Canada) and FeHEDTA-treated specimens from the same soils were examined. Magnetic susceptibility, frequency-dependent magnetic susceptibility, artificial remanence analysis (isothermal and anhysteretic), and hysteresis measurements were used to determine the extent of the FeHEDTA effects through comparison of untreated soil specimens and FeHEDTA treated soil specimens. The results indicate that: 1) FeHEDTA additions of >26% by weight to the gypsum powder resulted in a magnetic signature characteristic of superparamagnetic magnetite; 2) the strongest effect of FeHEDTA on the clay rich soil specimen was an increase in frequency dependence of susceptibility suggesting that the FeHEDTA was reacting with clay minerals to increase the magnetic concentration in treated soil samples; and, 3) the effect of FeHEDTA is most evident in soils with comparatively lower initial magnetic mineral concentrations. The results suggest that the standard application dose of FeHEDTA for weed-killing would have negligible effects on soil; however, over application or direct application to soil could result in a small measurable effect.

Thermodynamic modelling of deep crustal fluids: The compositions of fluids involved in ruby formation in Southwest Greenland

Vincent van Hinsberg[1], Chris Yakymchuk[2], Christopher Kirkland[3], Kristoffer Szilas?

[1]McGill University vincent.vanhinsberg@mcgill.ca, [2]University of Waterloo, [3]Curtin University, ?University of Copenhagen

Thermodynamic modelling of mineral stability and mineral-fluid equilibria provides a powerful means to constrain the compositions of deep crustal fluids, and to understand the role of these fluids in mobilizing and redistribution elements in the crust. The element transporting capacity of fluids critically depends on the physical conditions, including P, T, fO2 and pH, and the types and concentrations of ligands. Solubility experiments show that element solubilities vary by orders of magnitude depending on the pertinent physico-chemical conditions, and tight constraints on these conditions are therefore required for meaningful thermodynamic modelling. Here, we present results that constrain the compositions of the fluids involved in ruby formation in the Archaean North Atlantic Craton of southern Greenland. Ruby occurs due to fluid-induced interaction among high-grade metamorphic lithologies of contrasting chemistry. We use mineral stability relations and mineral compositions to constrain the P-T conditions, fO2 and X(CO2) of the metasomatising fluid, as well as its ligand concentrations. These constraints subsequently allow for estimating fluid cation concentrations from thermodynamic modelling of mineral-fluid equilibria. Results show that metasomatism took place at 650 to 725°C and 7 kbar involving a boron-rich, graphite-saturated, acidic fluid of low fO2 and low X(CO2). Aqueous aluminium concentrations are low and indicate that ruby saturation is the result of residual enrichment rather than aluminium mobilisation. Intrusion of the ca 2.55 Ga Qôrqut granite is the likely source of fluid and boron, and U-Pb dating of rutile inclusions in ruby is consistent with a temporal link between ruby formation and granite emplacement. Interaction with meta-dunite and sulfides modified this magmatic, oxidized fluid, introduced SO4, and led to the reduced high XMg and K-rich fluid as constrained from the ruby-bearing samples. This study highlights the potential of thermodynamic modelling of mineral-fluid equilibria to predictively model deep crustal fluids, and specifically to unravel the complex fluid-rock interplay that takes place in heterogeneous metamorphic lithologies.

Insights into the Ediacaran-Cambrian sedimentary, magmatic, and metamorphic evolution of Ganderia from new U-Pb zircon ages in the Bras d'Or terrane of Cape Breton Island, Nova Scotia, Canada

Deanne Van Rooyen[1], Sandra Barr[2], Chris White[3], James Crowley[4]

[1]Cape Breton University deanne_vanrooyen@cbu.ca, [2]Acadia University, [3]Nova Scotia Department of Energy and Mines, [4]Boise State University

The Bras d'Or terrane of central Cape Breton Island, Nova Scotia, Canada, is a key component in the Appalachian-Caledonide orogen because it contains well preserved evidence for the Ediacaran to Early Cambrian evolution of Ganderia, in contrast to most other Ganderian terranes which preserve mainly their Paleozoic histories. The Bras d'Or terrane consists of a complex assemblage of low- to high-grade metamorphic rocks and voluminous dioritic to granite plutons formed in a late Ediacaran through Terreneuvian subduction zone, probably on the edge of the Amazonian craton. New ages presented here combined with previous ages provide more details of its magmatic history, and show that subduction occurred between ca. 580 Ma and 520 Ma, followed by initiation of extensional magmatism related to rifting from Gondwana and subsequent opening of the Rheic Ocean. New detrital zircon age spectra from the metasedimentary host rocks of the McMillan Flowage Formation show that identification of a characteristic "Ganderian" detrital signature is problematic because detrital zircon populations vary with rock type and samples from different parts of the formation show significant variations in Proterozoic and Ediacaran zircon age spectra. Field relations and regional structures show that younger ages for concordant zircon populations in some samples cannot represent maximum depositional ages for the protoliths of these rocks. We conclude that they have been reset by low-grade metamorphic recrystallization and/or Pb-loss, even though other evidence for such resetting is not apparent in the current dataset with the exception of low Th/U ratios in the majority of the young zircons. Hence that resetting is cryptic and could have led to incorrect assignment of maximum depositional age without other evidence provided by detailed mapping, structural evidence, and ages of cross-cutting plutons. Overall, the data support the correlation of the McMillan Flowage Formation with other low- and high-grade metamorphic rocks in the Bras d'Or terrane and in the Brookville terrane of southern New Brunswick, with sedimentary deposition at ca. 600-580 Ma on the margin of Amazonia, prior to rifting at ca. 515-490 Ma to initiate formation of the Rheic Ocean.

Experimental investigation of the formation and transformation pathways of Ca-Mg-carbonates at low temperatures

Colton Vessey[1], Maija Raudsepp[1], Vasileios Mavromatis[2], Jean-Michel Brazier[3], Yinuo Li[4], Anna Harrison[2], Siobhan Wilson[1]

[1]University of Alberta vessey@ualberta.ca, [2]Géosciences Environnement Toulouse (GET), [3]Institute of Applied Geosciences, [4]Department of Geological Sciences and Geological Engineering

Direct precipitation of dolomite [CaMg(CO3)2] and magnesite (MgCO3) is kinetically inhibited at ambient conditions due to the high energy required to overcome the Mg2+(aq) hydration sphere. As a result, metastable Ca Mg carbonate phases preferentially form and recrystallize over time to thermodynamically more stable phases. For example, amorphous Ca-Mg carbonate (ACMC) that readily precipitates at ambient temperatures is a key precursor phase to the precipitation of low (LMC) and high (HMC) Mg calcite, and very high magnesium calcite (VHMC), which may undergo cation ordering during diagenesis to produce ordered dolomite. Similarly, magnesite formation can proceed through dypingite [Mg5(CO3)4(OH)2 *~5H2O] and hydromagnesite [Mg5(CO3)4(OH)2 *4H2O] precipitation. However, previous studies have not considered the co precipitation, and subsequent transformation, of Mg and Ca Mg carbonates at low temperatures (< 100 °C) that reflect near surface and early diagenetic conditions (e.g., lagoonal, playa, or other evaporative depositional environments). Here, we performed batch experiments at 40, 60 and 80 °C by mixing highly concentrated Na2CO3, MgSO4 and CaCl2 solutions. Initial solutions also contained trace concentrations of Li and Sr. Changes in major and trace elements in fluids and solids, mineralogy, and mol% MgCO3 (XMg) were monitored throughout each experiment for 104 days. At 40 and 60 °C, metastable dypingite and monohydrocalcite (CaCO3*H2O) were present initially but readily transformed into hydromagnesite and HMC, respectively. Reactions at 40 °C were predominantly characterized by the assemblage of VHMC, hydromagnesite, and aragonite (CaCO3). In contrast, the abundance of VHMC decreases with increasing temperature between 60 and 80 °C, and hydromagnesite transforms to magnesite. Interestingly, two compositionally distinct types of magnesite formed at 60 and 80 °C -- high Ca (71 < XMg < 82 mol%) and low Ca magnesite (XMg > 85 mol%). The high Ca magnesite formed earlier in the reaction than low Ca magnesite and both were commonly found together in samples. Liquid-solid partition coefficients for Li and Sr significantly decrease in magnitude over time and as reaction temperature increases from 40 to 80 °C. Overall, our work describes the geochemical evolution of Mg and Ca Mg-carbonate precipitation and transformation pathways with varying temperature. These results have implications for cycling of Mg in saline environments that may lead to dolomitization over time and fractionation of trace metals (Li and Sr) used as indicators of paleoenvironmental conditions.

Processing and Combining Electromagnetic Datasets at the M'Deek Geothermal Field

Zoë Vestrum[1], Martyn Unsworth[1], Benjamin Lee[1], Fred Heikkinen[2], Megan Eyre[2], Danial Alonso Torres[2], Tim Thompson[2], Alison Thompson[2]

[1]University of Alberta zvestrum@ualberta.ca, [2]Borealis GeoPower Inc

Electromagnetic (EM) geophysical methods are commonly utilized in the exploration of geothermal resources as electrical resistivity is dependent on both fluid content and temperature. However, using these methods in areas with existing infrastructure and conductive near-surface lithologies proves technically challenging. In this study we will combine multiple EM methods to constrain the conductive near-surface features as well as implement robust time series processing to accommodate noise created by existing electrical infrastructure. The M'deek Geothermal Field is located near the city of Terrace in northwest British Colombia. It is located within the Stikine Volcanic Zone which feeds the Mt Layton Hot Springs, Canada's hottest hot springs whose First Nations' use is recorded in oral history. Previously, several studies have been conducted in the area, however the roots of the geothermal field have been unexplored till recently. Kitselas Geothermal Inc., a First Nations-majority owned corporation, conducted a diverse geoscientific study to characterize the M'deek Geothermal Field in 2019 and 2020. Two of these datasets are used in this study: airborne time domain EM (VTEM) and ground based magnetotelluric (MT). The VTEM survey was flown over the geothermal field in 2019. The following year 39 MT stations were acquired in an irregular 3D pattern within the VTEM survey area. We combined these datasets to create a more reliable resistivity model of the M'deek Geothermal Field to a depth of 10 km. Our model was created by first correcting for the cultural noise, such as powerlines, transformers, or pipelines located in the City of Terrace, by applying robust time series processing as well as remote referencing to the MT data. Then, the resistivity model (<500 m depth) from the VTEM data was interpolated onto the inversion mesh for the MT data which is used as an initial model for the inversion. The MT data were then inverted to find a 3D resistivity model which is consistent with the VTEM resistivity model, allowing us to better incorporate near-surface conductors. In this study, we will highlight a range of approaches used in noise reduction, 3D inversion, and interpretation of EM datasets of the M'deek Geothermal Field.

Seismic Full Wave Imaging at Larder Lake

Brian Villamizar[1], R. Gerhard Pratt[1], Mostafa Naghizadeh[2]

[1]University of Western Ontario bvillami@uwo.ca, [2]Laurentian University

For many decades, the mining industry has been successfully able to mine shallow mineral deposits. However, these near-surface deposits are becoming increasingly difficult to find. There is a pressing need for exploration methods that can find deeper mining prospects more reliably. This requires mapping the distribution of ore deposits at depth. Subsurface imaging methods can provide solutions for these exploration campaigns. The imaging of structures in sedimentary basins has typically been carried out using conventional seismic reflection techniques. In complex geological architectures, such as those within the Superior Province in Canada, conventional seismic imaging yields suboptimal results due to factors stemming from complex energy scattering and crooked seismic geometries. Full-waveform inversion (FWI) is a nonlinear inverse technique capable of retrieving quantitative images of velocity structures. Judicious data preconditioning, and multiscale inversion strategies allow FWI to effectively estimate velocity variations in the first few kilometers of the subsurface. Non-conventional seismic reflection processing, based on azimuthal binning and enhanced migration velocity models, improves energy focusing and imaging quality of structures at depth. We demonstrate that the serious nonlinearity of FWI in Larder Lake is alleviated by implementing a "multiscale layer-stripping" strategy. The strategy uses a i) combination of explosive and vibroseis sources to retrieve low-wavenumber features of the velocity background, ii) hierarchical minimization of logarithmic phase-only and conventional phase-amplitude residuals to mitigate large dynamic variations within the data, and iii) progressive inclusion of higher frequencies and late arrivals to obtain a natural transition between low- and high- wavenumber features. We illustrate that the implementation of optimum binning strategies effectively enhances signal alignment, generating in-phase stacked sections. The final result is an optimal reflectivity image highlighting structural features at depth. With the application of these imaging techniques, we unravel the geometry of prominent structures in structurally controlled mineralized zones. The Larder Lake-Cadillac Deformation Zone (LLCDZ), and the Lincoln-Nipissing Shear Zone (LNSZ), are imaged. The LNSZ is retrieved as a north-dipping fault, extending to depths not previously identified of 8 km. Combining near-surface velocity images with reflectivity images at depth, we were able to fill the gap between surface geology and crustal-scale structures in the Larder Lake mining district. This enables a better understanding of the geometry of mineralized structural conduits in the near surface and their development at depth, increasing mining exploration and production success.

Distinguishing between winged rock inclusions and rootless asymmetric folds in the Ottawa River Gneiss Complex (Ontario portion), western Grenville Province

Dennis Waddington[1], Walfried Schwerdtner[2]

[1]Waddington Consulting dhw@ca.inter.net, [2]University of Toronto

Structural geologists use a number of geological features to determine shear sense, an important part of mapping and interpretation of ductile deformation zones in high grade gneiss terrains. Several of these features are considered here by reference to the Ottawa River Gneiss Complex (ORGC) in the western Grenville Province, Ontario and many years of literature on experimental and field aspects of structural geology in high grade gneissic terrains.

Boudin-like rock inclusions with mirror-symmetric curved wings, a common variety of winged inclusion, are rotated pieces of pulled-apart competent layers widely used as shear-sense indicators in ductile deformation zones. But winged inclusions can closely resemble rootless S-Z folds in shape so care must be taken to distinguish between them in the field. Rootless S-Z folds consist mainly of a distorted short limb and two pinched-out long limbs (Carter et al., 2020. GSA Abstracts with Programs, vol. 52, no. 6). Many rootless S-Z folds are akin to oblique folds described by Passchier et al. (Field Geology of High-Grade Gneiss Terrains, Springer-Verlag, 1990, pp. 39, 40, 62), cylindrical isoclinal features initiated by local kinematic perturbations, transient ductile shortening of thin layers oblique to the direction of bulk ductile shearing. The hinge lines rotate into close parallelism with the direction of bulk shearing during progressive ductile deformation reaching very high magnitudes and cease to be reliable indicators of local shear sense. Distinguishing in the field between rootless S-Z folds and winged rock inclusions can often be accomplished near the boundaries of deformation zones, where strain magnitudes are lower and undisrupted trains of tight to isoclinal S-Z folds may be observed.

The ca. 1050-1015 Ma ORGC includes a 1090-1050 Ma thrust-sheet stack, and comprises the lower plate and the southeastern detachment zone of a large metamorphic core complex. During mid-crustal assembly and subsequent vertical thinning of the thrust-sheet stack, its high-grade gneisses were heterogeneously strained and redeformed, producing thrust-induced zones of very high strain with horizontal thicknesses of 1-5 km, exhibiting rootless S-Z folds or their coaxially re-buckled counterparts. Boudin-like inclusions 10-100 cm long with straight or slightly curved wings, potential indicators of the sense of local shearing, occur at a few localities in the ORGC. Rather than a series of codirectional shear increments, however, the curvature of these wings may be due to the passive superposition of two finite deformations: (1) a subhorizontal local shortening incurred during the 1090-1050 Ma thrusting and (2) a horizontal local extension due to the 1050-1015 Ma collapse of the thrust-sheet stack.

It is vitally important to distinguish between rootless S-Z folds and winged rock inclusions in the field, because shear-related solid-body rotations play different roles in their respective deformation paths.

Complexities in Calcite Textures Revealed: A Combined EBSD, XRF, SEM and Raman study of Steen River Impactites

Erin Walton[1], Nicholas Timms[2]

[1]MacEwan University ewalton@ualberta.ca, [2]Curtin University

This study focuses on impactites from the Steen River impact structure in AB, Canada. Target rocks comprised ~1.3 km of Devonian evaporites, limestone and shale overlying Precambrian granite. Previous work on calcite-bearing impactites suggest several generations: (1) cm-size lithic limestone clasts retaining sedimentary structures, (2) mm-size marble-textured calcite recrystallized from limestone, (3) frothy calcite formed by incipient decomposition, (4) calcite crystallized from impact melt, and (5) post-impact, hydrothermal calcite. We investigate calcite in these same breccias using XRF and EBSD mapping. Results and Discussion: S1-921: Impact melt occurs as groundmass-supported clasts, mapped using EBSD (2 ?m step size). One area contains smectite-filled amygdales, with domains of banded calcite aligned with vesicle trains and plagioclase laths. This calcite contains minor MgO; the vug-fill calcite does not. EBSD shows that vug-fill and flow-textured calcite comprise coarse, strain-free, highly crystalline calcite. The grain boundaries of large calcite crystals cut across the flow texture. S3-769.5: This breccia sample contains hydrothermal calcite and entrained andradite-rimmed limestone clasts. One mapped area (4 µm step size), spans a limestone clast / hydrothermal calcite. All calcite domains have random crystallographic orientations and distinct textures delineated by grain sizes quantified by EBSD. A second large area map (step size of 6 µm), illustrates the range of carbonate textures, including coarse hydrothermal calcite, a recrystallized limestone clast, a sulfide-rich limestone clast, and vug-fill calcite within silicate impact melt. Grains within all calcite domains have random crystallographic orientations. XRF mapping shows that the limestone clasts, as well as clasts mapped as carbonate impact melt, are low in Sr and Mn-rich, whereas textures identified as hydrothermal calcite are Sr-rich and Mn-poor. S3-703A: This sample contains a cm-size, fossil-bearing limestone clast with a dark rim showing Mn-enrichment and Sr-depletion from XRF. Grains contacting the breccia groundmass are frothy. Impact melt occurs as fluidal-textured silicate glass and calcite-bearing clasts. A fluidal calcite-rich clast was mapped at 8 µm and 1 µm step sizes. The calcite grains are coarse, strain-free, twin-free and grow across the vesicles. EBSD maps of frothy calcite show these grains comprise a single crystal orientation. Mn-rich vesicle-free rims yield strong EBSD patterns. Conclusion: Our results demonstrate that the geological history from calcite texture and composition is complex. Fluidal textures in BSE images, consistent with calcite crystallized from a molten state and attributed to impact melting, may be replacement textures, revealed by EBSD mapping. This is likely due to the solubility of calcite in the post-impact hydrothermal environment and that impact products may be in in metastable states that are susceptible to repacement.

Geology of the Western Part of the Porphyry Zone, Douay Gold Deposit: Genesis of Archean ?syenite-associated? mineralization in the Northern Abitibi Greenstone Belt

Taylor Wasuita[1], Lucie Mathieu[1], Ross Sherlock[2], Benoît Dubé[3], Fred Speidel?

[1]Université du Québec à Chicoutimi twasu898@mtroyal.ca, [2]Laurentian University, [3]Geological Survey of Canada, ?Maple Gold Mines Ltd.

In the Abitibi greenstone belt, the role played by the alkaline intrusions in the formation of syenite-associated gold deposits remains debated. This lack of consensus affects exploration strategies based on the metallogenic model for intrusion-related gold systems (IRGS). This project will also evaluate if Archean alkaline magmas have the potential to contribute significant amounts of gold-bearing fluids to Neoarchean mineralizing systems. This study focuses on the geological characteristics of the western portion of the Porphyry Zone of the Douay Gold deposit in order to provide constraints on the timing and genesis of the deposit and to test the IRGS metallogenic model. The Douay deposit is an Archean syenite-associated gold system, located in the northern part of the Abitibi greenstone belt, 55 km southwest of Matagami, Québec. The deposit is owned by Maple Gold Mines Ltd. and contains 8.6 Mt of indicated mineral resources at an average grade of 1.52 g/t Au, and 71.2 Mt of inferred mineral resources at an average grade of 1.03 g/t Au. The Douay deposit is an example of an exploration project established on the basis of a debated metallogenic model, i.e., gold mineralization is spatially associated with the Douay syenite and may correspond to an IRGS, but the deposit is also structurally-controlled and may correspond to an intrusion-hosted orogenic gold system. This deposit is located within close proximity to the Casa Berardi Tectonic Zone and of the following lithologies: Cartwright Hills Group (ca. 2.721 Ma), Taibi Group (<2.969 Ma), and the Douay Alkaline Intrusive Complex (ca. 2,676 Ma) that is spatially associated with gold mineralization. Field work and observations performed on drill core samples was used to document the main types of hydrothermal alteration, which correspond to potassic, carbonatization, sericitization, and hematization. Furthermore, mineral chemistry (pyrite and alteration minerals) determined using LA-ICP-MS will be used to evaluate the relative importance of magmatic (IRGS) and metamorphic (orogenic gold system) fluids input in the Douay area. This study will contribute to a better understanding of ancient mineralizing systems and will have implications for exploration strategies and for our understanding of Neoarchean upper crustal fertilizing processes.

Progress on the appraisal and definition of the proposed Anthropocene Epoch/Series

Colin Waters[1], Martin Head[2], Simon Turner[3], Jan Zalasiewicz[1]

[1]University of Leicester cw398@leicester.ac.uk, [2]Brock University, [3]University College London

The Anthropocene Working Group (AWG) of the Subcommission on Quaternary Stratigraphy (SQS) has been tasked since 2009 with gathering evidence to assess the Anthropocene as a potential new formal Epoch/Series and corresponding Age/Stage. In a binding vote in 2019, the AWG agreed by supermajority that the Anthropocene should be treated as a chronostratigraphic unit defined by a Global boundary Stratotype Section and Point (GSSP) that coincides with one of the stratigraphic guides at around the mid-20th century. Anthropogenic influence on geological signals commenced thousands of years ago, but the mid-20th century provides the most pronounced shift in most global trends, reflecting surges in human population, energy consumption (especially hydrocarbons), technological innovation and international trade. Evidence includes the appearance and rapid dispersal of more than 200,000 new mineral-like forms, fuel ash and plastic polymers, artificial rock types (e.g. concrete) and deposits associated with mineral extraction and urban development. There is also profound modification of sedimentary processes through increased erosion rates due to agricultural expansion and deforestation and reduced sediment fluxes due to damming of rivers. Biological evidence includes the irreversible consequences of extinctions (considered to be on a trajectory towards the sixth mass extinction event), and unprecedented trans-continental species transfers and the dominance of humans plus domesticated species (now >95% of terrestrial vertebrate biomass). Recent climate and sea level trends are outside the trajectory of the Holocene Epoch, with global temperatures now warmest for 125,000 years. Chemical signals

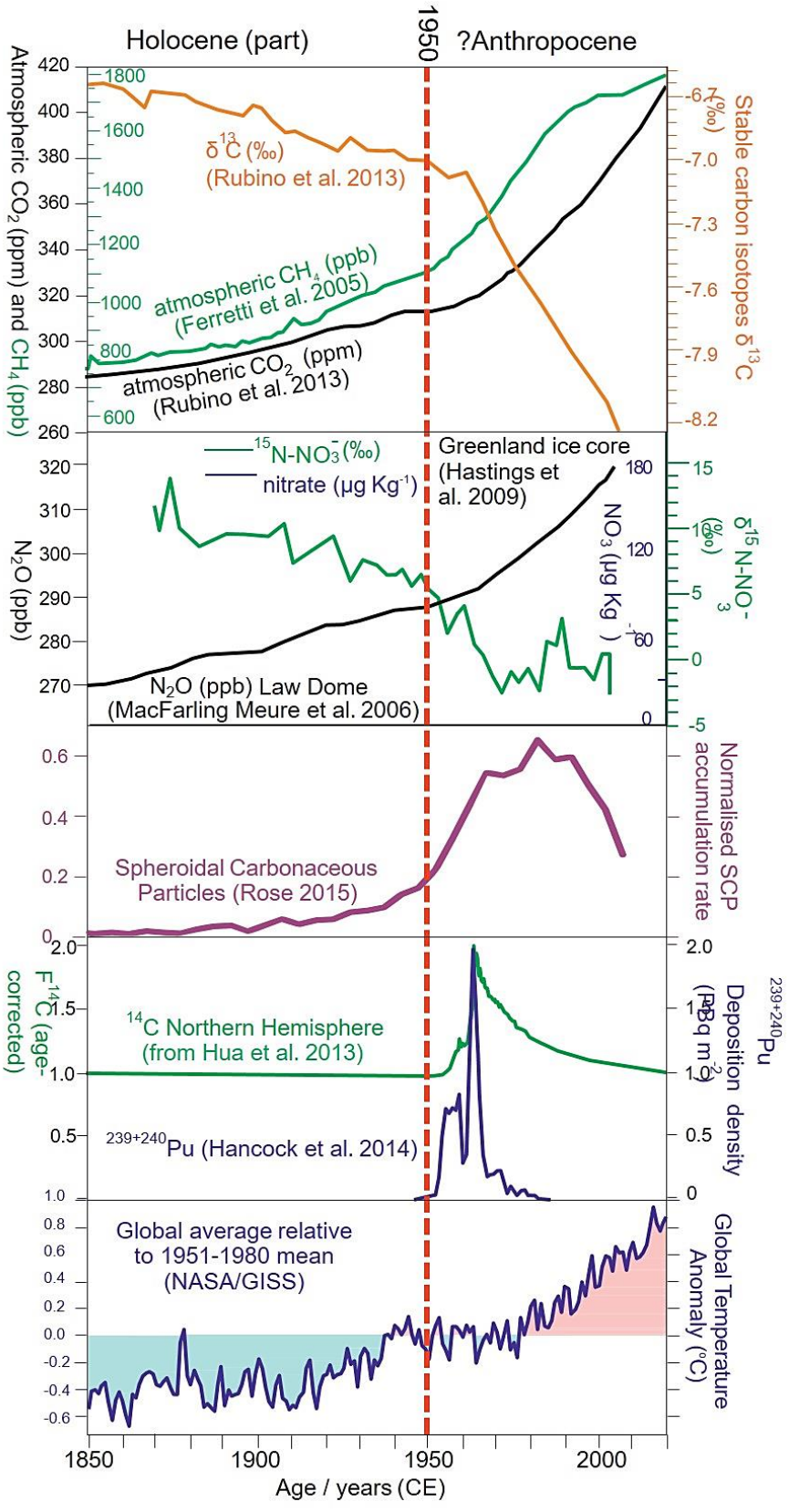

include isotope patterns reflecting unprecedented perturbations to the carbon and nitrogen cycles, driven by burning fossil fuels and use of artificial fertilizers. Many disseminated metal and persistent organic pollutants form novel signatures, and a global radionuclide 'bomb-spike' reflects atmospheric testing of thermonuclear devices mainly between 1952 and 1963. Work is in progress to assess 11 sites from diverse environments (two anoxic marine sediments, three lakes, estuarine deposits, a peat, two corals, a speleothem and a glacial icesheet) from five continents (four sites in N. America) as potential candidate GSSPs. The results are expected to be published in 2022 and will form the basis of a formal submission that will require recommendation of one GSSP candidate by AWG, endorsement by SQS and approval by the International Commission on Stratigraphy. If finally ratified by the International Union of Geological Sciences Executive Committee, this would be the first such unit that directly reflects a pervasive shift in the Earth System due to human activities. Graphical abstract: Shifts in a number of key stratigraphic guides coincide with the mid-20th century (see Zalasiewicz et al. 2020. The Anthropocene. Geologic Time Scale 2020. Cambridge Univ. Press).

Anatomy of a Cambrian trilobite extinction event, Honey Creek Formation, Wichita Mountains region, Oklahoma

Stephen Westrop[1], Sean Blackwell[1]

[1]University of Oklahoma swestrop@ou.edu

At least five major trilobite extinction events are recorded in the Upper Cambrian-Lower Ordovician succession in Laurentian North America. One of these, at the base of Cambrian Sunwaptan Stage, is expressed in the Honey Creek Formation of the Wichita Mountains region. The Honey Creek was deposited in an archipelago of rhyolite islands during a period of rising sea level and onlap of the Carlton Rhyolite. Sharp lateral facies changes, from sandstone rich to carbonate dominated, occur over distances of less than a kilometer, reflecting the influence of local sources of siliciclastics. The extinction occurs through a stratigraphic interval of about four meters, with turnover at the base and the top of the Irvingella major Zone; there is little associated change in sedimentary facies. The base of the zone is marked by the replacement of a diverse fauna of the Elvinia Zone with a low diversity trilobite biofacies dominated by Irvingella and Comanchia. Orthid brachiopods also appear in abundance in the extinction interval, and the succession comprises stacked brachiopod and trilobite shell beds. A further drop in diversity occurs at the top of zone, where Irvingella and Comanchia are replaced by Parabolinoides, which occurs in mixed trilobite-brachiopod shell beds. Diversity remains low through an interval of about 10 meters of strata that is marked by the appearance of the trilobite genus Taenicephalus, and a decline in the abundance of orthids. The data from the Honey Creek Formation demonstrate the extinction was a multistep event with both turnover and immigration of trilobites and a "bloom" of rhynchonelliform brachiopods. The abundance of the latter indicates unusual ecological conditions, as rhynchonelliform brachiopods are generally rare components of marine paleocommunities of the Cambrian of Laurentia.

Paradoxical mid-crustal displacements and stratigraphic continuity: tectonic evolution of the Paleoproterozoic Amer Group, Nunavut, Canada

Joseph White[1], Lydia Calhoun[1], Charles Jefferson[2]

[1]University of New Brunswick clancy@unb.ca, [2]Geological Survery of Canada (Ret'd)

The Paleoproterozoic Amer Group, central Nunavut, comprises four dominantly sedimentary sequences (Ps1 through Ps4) deposited unconformably on Archean basement of the Rae structural sub-province. A major historical distraction in correlation of this belt with temporally related sequences has been an underlying acceptance of minimal internal disruption. Overall, the continuity of the stratigraphic sequence in light of the intense deformation produces a distinct tectonic paradox. The difficulties of dealing with this poly-deformed terrane are exacerbated by the absence of exposure in critical areas. This problem has been addressed by integrating detailed outcrop examination with high-resolution aeromagnetic data, as well as legacy drill hole data and legacy samples and thin sections. The final analysis is dependent on the distinct magnetic responses of the magnetite-bearing Three Lakes and Showing Lakes formations that, in preserved stratigraphic sequences are separated by the Oora Lake Fm. The aforesaid approach has enabled identification of a consistent, yet distinctly different geometry for the Amer Group "basins". Notwithstanding the recognized lithostratigraphy sequence, intense deformation and crustal thickening occurred as three events. D1 produced the most intense tectonic fabrics through isoclinal folding, multiple transposition (three generations of folds) and displacement along discrete detachments resulting in sub-horizontal axial surfaces and tectono-stratigraphy. The most intense displacements occur within the initially shale-dominated units (e.g. Resort Lake Fm., Three Lakes Fm.) which also exhibit the most explicit evidence for fluid flow. Basement gneisses exhibit comparable sub-horizontal fabrics over extensive regions (100's of km) indicative of horizontal mid-crustal flow. D2 generated the regional, generally upright synclinoria, and is separated from D1 by the Ps3-Ps4 unconformity. Although this is the most obvious tectonic event, its effect on the units is considerably less than D1. Late D3 folds with sub-horizontal axial surfaces are rare and the region is transected by arrays of ENE- and NW- trending faults. In contrast to the apparent straightforward structure of the regional D2 synclinoria, the D1 tectono-stratigraphy forms large, regional recumbent structures, but for which evidence occurs at all scales and within separate data sets i.e. outcrop, geophysics, drill hole. The occurrence of elongate "cigar-shaped" mineralized zones reflects concentration by intense fluid flow within D1 hinge zones coaxially overprinted by D2. The heterogeneity of deformation throughout this mid-crustal section emphasizes the intrinsic importance of rheological partitioning (mechanical stratigraphy) in sustaining lithological sequences during continental crust evolution.

Evaluating the Earthquake Risk Pool in Canada

Khris A Wilhelm[1], Bohan Li[1], Katsuichiro Goda[2], Paul Kovacs[1]

[1]Institute for Catastrophic Loss Reduction kwilhel2@uwo.ca, [2]Western University

Earthquakes pose significant risks to homeowners in British Columbia, Quebec, and eastern Ontario. Many homeowners in these areas do not have earthquake insurance for their properties, and recent surveys suggest Quebec homeowners are unaware that their general insurance policies do not include earthquake coverage. If a devastating earthquake were to occur in one of these regions, homeowners would be left vulnerable, and very frustrated. A general earthquake insurance pool is one way to rectify this current problem. In this risk pool scheme, if earthquake loss occurs, the Government would cover a portion of the losses less than a certain amount (in our case $100,000) and then the insurance companies would insure losses above the threshold. This is different to the current practice of the homeowner paying a deductible and then the insurance companies paying out the rest of the losses. Throughout the duration of this project, we have used two earthquake loss models that quantify the loss experienced by all stakeholders, should an earthquake event occur. The first model quantifies the loss to the average home in Canada, considering different insurance parameters. These parameters include the deductible, take-up rates, and loss amounts that the government and private insurers will cover. The second loss model quantifies losses to stakeholders in worst case scenario events. These events include ground motion events in affecting Western Quebec, Victoria, and Vancouver. The purpose of the creation of these two models is to determine whether an insurance risk pool would be an adequate solution to the risks that earthquakes pose. Through comparing different insurance schemes, we have found that the homeowners' predicted losses with the risk pool is significantly less than the homeowners' predicted losses with the current scheme in place. Specifically, in Quebec, we found the owner loss under the current scheme with the current 100% take-up to be $48.9 Million, while the owner losses with the risk pool were only $7.8 Million. We have also found that even with 100 percent take-up rates, the insurers' predicted losses are comparable in both the risk pool situation ($96 Million) and current scheme ($142 Million). Therefore, we believe that the earthquake risk pool is beneficial for homeowners and insurers in Canada.

Planetary scale change to the biosphere recorded in the fossil record can be used to identify the Anthropocene

Mark Williams[1], Reinhold Leinfelder[2], Anthony Barnosky[3], Martin Head[4], Francine McCarthy[4], Alejandro Cearreta[5], Kristine DeLong[5], Stephen Himson[1], Rachael Holmes[1], Jens Zinke[1]

[1]University of Leicester mri@leicester.ac.uk, [2]Freie Universitaet, [3]Stanford University, [4]Brock University, [4]Universidad del País Vasco UPV/EHU, [5]Louisiana State University

The fossil record of anthropogenic changes to the biosphere is examined to assess its utility in identifying a formal Anthropocene Series. We examine three distinctive biostratigraphic signatures of humans associated with: 1) hunter-gatherers, 2) domestication and settlement, and 3) globalisation. For each, we determine its utility for recognising the Anthropocene. All three signatures have significant biostratigraphic records of regional importance that can sometimes be correlated inter-regionally and help understand the developing pattern of human expansion and appropriation of resources, but none has individual species that provide a globally synchronous marker. All three signatures overlap stratigraphically, in that they are part of a continuum of change, with complex regional patterns, rather than time-limited events. However, in contrast to earlier palaeontological signals of humans, we find that the mid to late 20th century palaeontological record of globalisation can be used to build a chain of palaeontological correlation using introduced species, which dovetails with other stratigraphic markers of the Anthropocene to provide sound recognition of its lower boundary. This boundary would also be a proxy of accelerating species extinction in the 20th century and of a state shift in the biosphere. The expression of the basal Anthropocene - from a palaeontological perspective - is similar to that of other series boundaries from deeper time. We note that chains of correlation, because of their precise chronology, could be linked with other disciplinary-based time scales, none having more importance than the others, but when correlated together providing a more comprehensive approach to understanding Earth System change. Graphical abstract: Image credit, Stephen Himson. The mollusc assemblage of the River Thames near Teddington Lock, Richmond-upon-Thames, UK. Two species of non-native molluscs dominate the river in this area: the zebra mussel, Dreissena polymorpha, and the Asian clam, Corbicula fluminea. C. fluminea was introduced to Europe in 1980 (it entered the Thames in 2004). D. polymorpha was widespread in Europe from the 19th century, but only introduced to North America in 1986. Therefore, the first occurrence of D. polymorpha in North America, and the first co-occurrence of C. fluminea with D. polymorpha in Europe, illustrate a potential late 20th century chain of correlation. Many other species can be used in this way.

Beyond the red dot: Mapping gossans as vectors to hydrothermal deposits in the High Arctic Large Igneous Province

Marie-Claude Williamson[1], Ashley Abraham[1], Rick McNeil[1], Stephen Day[1], Benoit Saumur[2], Jeanne Percival[1], Derek Wilton[3], Myriam Lemelin[4]

[1]Geological Survey of Canada marie-claude.williamson@canada.ca, [2]Université du Québec à Montréal, [3]Memorial University of Newfoundland, [4]Université de Sherbrooke

Gossans are surficial deposits that result from the oxidation and weathering of sulphide and oxide minerals in the host bedrock. In some important cases, gossans are associated with an ore deposit (e.g., Voisey's Bay, Labrador). Most gossans are small (a few tens of metres to less than 1 to 2 km in length) and they are routinely noted by a single point on geological maps. In sparsely-vegetated areas of the Canadian Arctic, distinctive colours of the oxide cap allow for remote predictive mapping (RPM) in the visible-near-infrared (VNIR) and short-wave infrared (SWIR) portions of the electromagnetic spectrum. Research carried out by the Geological Survey of Canada over the past decade has led to new insights on the mapping, morphology, stratigraphy, mineralogy, and geochemistry of gossans that form in a permafrost environment. In one of the study areas located on Axel Heiberg Island, Nunavut, steep and irregular topography reveal 3D structural relationships between evaporite diapirs and igneous bedrock. Detailed mapping, sampling and laboratory studies of the gossans, bedrock and stream sediments revealed geochemical anomalies that potentially link the gossans and hydrothermal deposits within Expedition Fiord. Our results provide geological constraints on the magmatic and/or hydrothermal processes that could lead to the formation of ore deposits in large igneous provinces. The study area is located on the north shore of Strand Bay, western Axel Heiberg Island (Figure 1A). In this part of the Sverdrup Basin, the bedrock consists of the Lower Cretaceous Isachsen Formation sedimentary-volcanic succession, Upper Cretaceous Strand Fiord Formation basalt and feeder dykes, and some minor exposures of the Aptian-Albian Christopher Formation shales. The entire stratigraphic succession is intruded by evaporite structures (anhydrite and gypsum). Diapirs host many gossans that formed by fluids circulating through local conduits in brecciated basaltic rafts within the diapirs, which resulted in the precipitation of sulphide mounds. Breccias and chaotic terrain at the periphery of diapirs are interpreted by dynamic uplift. The first evidence for mineral potential came from the results of a stream sediment survey at 21 sites (Figure 1A). Heavy mineral concentrates (HMC) yielded remarkably high concentrations of chalcopyrite from local sources. In addition, some stream sediment samples showed anomalous concentrations of Pb, Zn, Ag, and Cd. In this area, gossans are clearly associated with volcanic rocks (Figure 1B), sills (Figure 1C; circle shows geologist for scale), and rafted igneous rocks mixed with evaporite. We present a comparative study of the mineralogy and geochemistry of bedrock, gossans and stream sediments that highlights the role of evaporite domes as a focus for the circulation of hydrothermal fluids in the Strand Fiord-Expedition Fiord region.

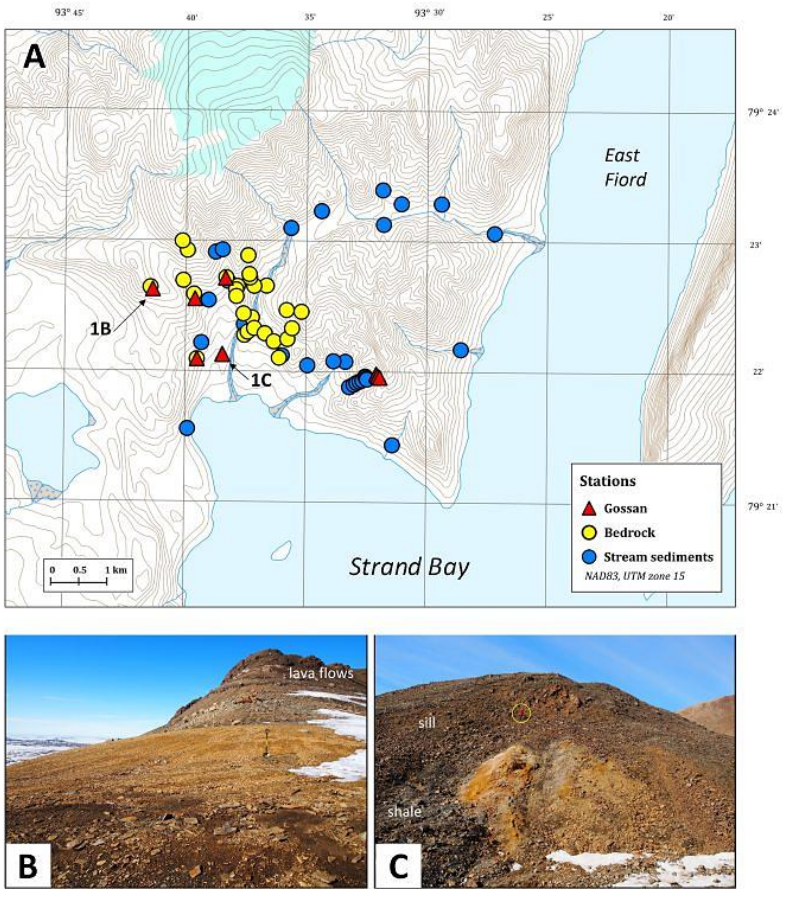

Zircon morphology and chemistry reveal multi-stage metasomatic Zr mineralization in the world-class Baerzhe REE-Nb-Zr-Be deposit

MINGQIAN WU[1], IAIN SAMSON[1]

[1]University of Windsor aria.wu1990@gmail.com

China's Baerzhe deposit contains large endowments of rare metal mineralization hosted in a peralkaline granitic pluton. This pluton comprises multiple phases, including an unaltered miaskitic granite porphyry, a variably hematized miaskitic granite, and an agpaitic granite that underwent Na metasomatism and hematization. REE-Nb-Be mineralization is present in both the altered miaskitic and agpaitic granites, whereas high-grade Zr mineralization (? 2.5 wt% of ZrO2, mainly in metasomatic zircon) is present only in the agpaitic granite. Previous research identified four types of metasomatic zircon in the agpaitic granite. All metasomatic zircon was suggested to have formed at the same general stage of evolution of the system, prior to REE-Nb-Be mineralization. Raman analyses and back-scattered imaging of these different zircon types suggest that all the metasomatic zircon is not metamict and shows no evidence of alteration, such that they will have retained their original chemistry. Some zircon occurs as inclusions in snowball quartz (poikilitic quartz containing concentrically zoned mineral inclusions). These zircon inclusions display oscillatory zoning under cathodoluminescence (CL), and exhibits chondrite-normalized REE patterns with positive slopes and a large increase of concentrations from Gd to Lu. Zircon also occurs as a replacement after elpidite, which is rare, and in quartz-zircon pseudomorphs, which are abundant. Both of these types are characterized by comparable, irregular zoning in CL images, and exhibit relatively flat chondrite-normalized patterns with concave-down HREE portions. Such features confirm that the pseudomorphs represent replacement of elpidite. A fourth zircon type occurs as replacement of magmatic amphibole, is unzoned in CL, has similar, flat chondrite-normalized patterns to the elpidite-replacement and pseudomorph zircon but has much higher REE concentrations. In addition, the amphibole-replacement type contains high Be concentrations (ca. 200 ppm), more than four times higher than the other types. The data indicate that the inclusion and amphibole-replacement zircon crystallized from two different fluids; the pseudomorph and elpidite-replacement zircon could have crystallized from either of the two fluids. Deuteric and variably altered magmatic zircon from the altered miaskitic granite exhibits different chondrite-normalized REE patterns to zircon from the agpaitic granite described above. This suggests that the fluid responsible for zircon alteration and crystallization in the altered miaskitic granite was neither of the two zircon-forming fluids that affected the agpaitic granite. Although many studies have distinguished magmatic from non-magmatic zircon using textural and chemical features, the Baerzhe data reveal that Zr-rich alkaline rocks can have been affected by complex, multi-stage metasomatic zircon-forming events. This could be one of the reasons that these rocks contain very high Zr concentrations.

Age and provenance of the lithospheric mantle beneath the Chidliak kimberlite province, southern Baffin Island: Implications for the evolution of the North Atlantic Craton

Yong Xu[1], Graham Pearson[2], Garrett Harris[2], Maya Kopylova[3], Jingao Liu[1]

[1]China University of Geosciences (Beijing) jingao@cugb.edu.cn, [2]University of Alberta, [3]University of British Columbia

A suite of peridotite xenoliths from the Chidliak kimberlite province provides an ideal opportunity to assess the age of the mantle lithosphere beneath the eastern Hall Peninsula Block (EHPB) in southern Baffin Island, Nunavut and to provide constraints on the lithospheric architecture of this region. The new dataset comprises highly siderophile element (HSE) abundances and Re-Os isotopic compositions for 32 peridotite xenoliths sampled from four Late Jurassic-Early Cretaceous kimberlite pipes (CH-1, -6, -7, and -44). These peridotites represent strongly depleted mantle residues, with bulk-rock and olivine chemistry denoting melt extraction extents of up to 40%. The vast majority of samples show PPGE (Pt and Pd) depletion relative to IPGE (Os, Ir, and Ru) ((Pt/Ir)N: 0.10-0.96, median = 0.57; (Pd/Ir)N: 0.03-0.79, median = 0.24), coupled with mostly unradiogenic Os isotopic compositions (187Os/188Os = 0.1084-0.1170). These peridotites display strong correlations between 187Os/188Os and melt depletion indicators (such as olivine Mg number and bulk-rock Al2O3, (Pd/Ir)N), suggesting that an ancient (~2.8 Ga) melt depletion event governed the formation of the Chidliak lithosphere. The prominent mode of TRDerupt model ages at ca. 2.8 Ga matches the main crust-building ages of the EHPB, demonstrating temporal crust-mantle coupled in the Meso-Neoarchean. These ancient melt-depletion ages are present throughout the depth of the ~ 200 km thick lithospheric mantle column beneath Chidliak. The Meso-Neoarchean formation age of the EHPB mantle broadly coincides with the timing of stabilization of the lithospheric mantle beneath the Greenlandic portion of the North Atlantic Craton (NAC). This, along with the similarity in modal mineralogy, chemical composition and evolutionary history, indicates that the EHPB, southern Baffin Island was once -contiguous with the Greenlandic NAC. The mantle lithosphere beneath both the EHPB and the NAC show a similar metasomatic history, modified by multiple pulses of metasomatism. These multiple metasomatic events combined to weaken and thin the lithospheric mantle, culminating in the formation of the Labrador Sea and Davis Strait separating the EHPB from the Greenlandic NAC in the Paleocene.

Numerical Simulation of Tectonic Deformation and Thermally Induced Buoyancy in Driving Ore-forming Fluid Flow in Association with the Formation of the Chanziping Uranium Deposit, South China

Jianwen Yang[1]

[1]University of Windsor jianweny@uwindsor.ca

In this study, the software package FLAC is employed to investigate the relative importance of tectonic deformation and thermally induced buoyancy in driving hydrothermal ore-forming fluid flow associated with the formation of the Chanziping uranium deposit. Numerical results indicate that an extensional tectonic deformation in the late Yanshanian causes wide range of downwelling flow in the late Mesozoic Cretaceous red sandstone, leaching uranium minerals from the red basin fill. The oxidizing uranium-rich basinal fluid channels downwards along a regional fault to the Paleozoic Cambrian granitic basement, meeting with the upwelling basement-derived reducing fluid, driven by the buoyancy force, at the intersection of the regional fault and a fracture zone in the Cambrian black shale. This leads to the Chanziping ore genesis in the hanging wall of the regional fault. The tectonic deformation-driven fluid flow overwhelms the buoyancy-driven flow caused by a typical geothermal gradient, even though there is only 1% elongating or shortening. Thermally induced buoyancy cannot essentially alter the fluid flow pattern at the presence of tectonic deformation, but it can slightly enhance (for shortening deformation) or impede (for elongating deformation) the deformation-driven fluid flow regime. Thermally induced buoyancy alone cannot focus ore-forming fluid to the ore genesis site.

Middle Devonian Blue Mountain Granodiorites and associated Benjamin River South porphyry Cu-Mo deposits, northeastern New Brunswick: analysis of adakitic signatures and fertility

Fazilat Yousefi[1], David Lentz[1], James Walker[2]

[1]University of New Brunswick fazilat.yousefi@unb.ca, [2]Department of Natural Resources and Energy Development

Benjamin River South is part of the mid-Paleozoic Appalachian realm of Ganderia, which covers an area of about 80 km2 in northeastern New Brunswick. The hypabyssal Blue Mountain Granodiorite Suite (BMGS) includes several porphyry Cu-Mo deposits, i.e., several cupolas (60 to ~600m diameter), northeast of the Blue Mountian Granodiorite. These mineralized cupolas intrude into two main rock types; the nearby older Benjamin River Intrusive Complex has been dated at 418 +/- 1 Ma (U-Pb zircon) and is cogenetic with the regional rift-related bimodal host volcanic suite. However, these mineralized cupolas were dated by U-Pb zircon (400.7 +/- 0.4 Ma); these Middle Devonian (400 Ma) intrusive tonalitic to granodioritic phases (andesitic) that hosts most of the mineralization are tan coloured, with biotite-hornblende (8-12%) and plagioclase (42-47%) porphyritic with a fine- to medium-grained hypidiomorphic-granular groundmass. The average of copper in the samples with the lowest mineralization (< 200 ppm Cu & < 40 ppm Mo) is 69 ppm Cu and 5 ppm Mo, with an average S = 0.35%. The primary pyrite-chalcopyrite is dominantly disseminated with local stockwork vein-style mineralization within alkalic-type alteration (+/- phyllic) in varying proportions throughout the porphyries, but to a lesser extent in the bimodal volcanic rocks. Pervasive K-feldspathization and biotitization of pre-existing ferromagnesian phases and feldspars is manifested by an increase in K/Na, Fe and S with Cu and Mo. The secondary mineralization is in the form of sulfide-rich pyrite-base-metal veins that cut the disseminated mineralization. Molybdenite commonly occurs in crosscutting quartz-bearing veins. Crosscutting relationships are uncommon, but where present appear to indicate that the secondary sulfide veins were emplaced later than the quartz veins. Weak pervasive propylitic alteration is superimposed on much of the host primary mineralization alteration, although some is vein controlled. Based on Na2O<1 and K2O/Na2O>4, altered and less altered were determined. The less altered porphyries were used to classify these rocks, using major and then trace elements. The BMGS range from diorite to granodiorite. These rocks plot in the alkalic-calcic to calc-alkalic field on the Na2O+K2O-CaO versus SiO2 diagram with A/CNK= 1.0-1.3, magnesian granites, with FeOt/(FeOt+MgO) values increasing with increasing SiO2. This is consistent with their high magnetic susceptibilities, reflecting titanomagnetite and their oxidized nature. The Zr/Ti abundance correlates with the SiO2 contents. The very low Nb (4-5 ppm) vs Y (3-8 ppm) contents are consistent with I-type, ensimatic

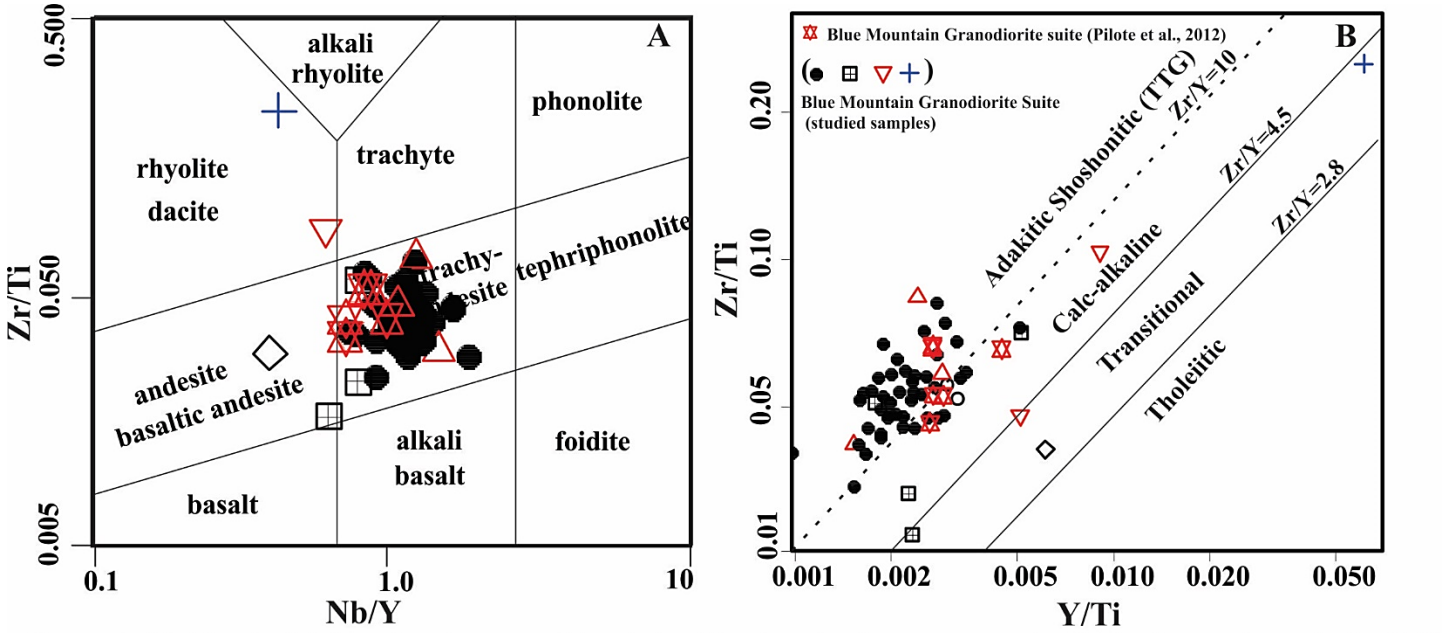

Figure: A. Nb/Y vs. Zr/Ti for volcanic compositional classification; the data erroneously plot in the trachy-andesite field due to their adakitic affinity. B. Zr/Ti vs. Y/Ti (highlighting Zr/Y) for discerning magmatic affinity

volcanic arc signatures. The very low Zr (100-160 ppm) and Th (2-5 ppm) contents, with relatively low Ti and V (with Ti/V >35) support an oxidized calc-alkalic affinity with minimal crustal contamination, consistent with their very low Zr/Y (ave 22), Th/Y (ave 5.0), and Nb/Y (ave 2.0) and high Sr/Y and La/Yb like adakitic systems.

Forces that drive the breakup of supercontinents

Nan Zhang[1]

[1]Peking University nan_zhang@pku.edu.cn

Subduction retreat, mantle plumes, and orogens are all considered important for determining the loci of supercontinent breakup. Our analysis of extensional stress has demonstrated that the plume-push force is more important than the dragging force of subduction retreat during supercontinent break-up, while is less important than the subduction retreat dragging force during the drifting of broken continents right after the break-up. Orogens play another important role in the break-up of supercontinent. Because cratons are generally thicker, stronger and more viscous than orogens, supercontinent breakup generally occur along preexisting orogens. The relative importance during different periods from rifting to drifting requires quantitatively analysis. We built three-dimensional global mantle dynamic model to examine the relative influence of the global subduction zone, the lower mantle large low shear velocity provinces (LLSVPs), and orogens in the breakup of Pangea since 200 Ma. Our model is able to reproduce three phases of plume pulses, corresponding to the CAMP, Karoo and Parana LIPs, respectively. The South Atlantic Ocean started to open along the orogens between Africa and South America. Our model indicates that the opening of central Atlantic resulted from the interaction of the CAMP and the orogens between North America, South America and Africa. The breakup between the Amazon and West African cratons can be divided into two stages. The first stage is weakening of a relatively thick cratonic lithosphere by the CAMP event through a long-term partial melting. During the second stage the breakup migrated from south to north through the interaction between the linear orogens and mantle plumes controlled by the subduction zone and the African LLSVP. Our modelling also shows that the dragging force of subduction retreat is ~3 times larger than the plume pushing force after the South Atlantic break-up.

The deformation and slip response of subglacial tills to overriding ice

Lucas Zoet[1], Dougal Hansen[1], Neal Iverson[2]

[1]University of Wisconsin-Madison lzoet@wisc.edu, [2]Iowa State University

Many fast-moving glaciers sit atop a bed of water-saturated, unconsolidated sediment (till) that can deform in response to the stress applied by overriding ice. The deformation of this sediment has ramifications in both glaciology and glacial geomorphology as its strain accounts for much of the glacier's forward motion and produces some of the most iconic glacial landforms. Despite its fundamental importance in glacial processes, however, the manner in which ice slips atop and deforms till as well as the factors that set till flux are not well understood. Much of this uncertainty stems from the rheological complexity of the ice-bed interface, where ice at its pressure melting point slides over a Coulomb material (till), as well as the enigmatic micromechanics controlling the distribution of strain in an actively deforming till layer. Furthermore, it is difficult to access the ice-bed interface of modern glaciers, which impedes direct study of these processes under realistic conditions. In order to investigate these processes, we use large-diameter, novel ring shear devices to replicate the relevant in-situ conditions. Housed in cold rooms, these devices slide rings of temperate ice over unconsolidated till beds over a range of realistic effective stresses and sliding velocities, while continuously monitoring sediment deformation throughout the experiment. The velocity - shear stress relationship is then determined over a range of speeds for a single effective stress (ice overburden pressure - water pressure). These observations lead to a slip law for deformable-bedded glaciers with a regularized Coulomb form, which depends on the properties of the till as well as on clasts at the ice-bed interface. Deformation of the sediment is recorded by photographing the till bed at regular intervals through clear acrylic walls and then quantifying the displacement that occurred between image pairs using digital image correlation. These observations demonstrate that till flux increases with sliding velocity and that the depth of till deformation shallows with increasing effective stress (~9-170 kPa). Using these results, we directly constrain how these independent variables affect subglacial sediment deformation for use in both glaciology and glacial geomorphology.